

Contributors

Numbers in parentheses indicate the pages on which the authors' contributions begin.

- MIGUEL A. ESTERUELAS (1), Departamento de Química Inorgánica, Instituto de Ciencia de Materiales de Aragón, Universidad de Zaragoza, CSIC, 50009 Zaragoza, Spain
- CARLO FLORIANI (167), Institut de Chimie Minérale et Analytique, BCH 3307, Université de Lausanne, CH-1015 Lausanne, Switzerland
- RITA FLORIANI-MORO (167), Institut de Chimie Minérale et Analytique, BCH 3307, Université de Lausanne, CH-1015 Lausanne, Switzerland
- GREGORY C. FU (101), Department of Chemistry, Massachusetts Institute of Technology, Cambridge, Massachusetts 02139
- SANG OOK KANG (61), Department of Chemistry, Korea University, Chochiwon, Chungnam. 339-700, Korea
- JAEEJUNG KO (61), Department of Chemistry, Korea University, Chochiwon, Chungnam. 339-700, Korea
- RENJI OKAZAKI (121), Department of Chemical and Biological Sciences, Faculty of Science, Japan Women's University, Bunkyo-ku, Tokyo 112-8681, Japan
- LUIS A. ORO (1), Departamento de Química Inorgánica, Instituto de Ciencia de Materiales de Aragón, Universidad de Zaragoza, CSIC, 50009 Zaragoza, Spain
- NORIHIRO TOKITOH (121), Institute for Chemical Research, Kyoto University, Gokasho, Uji, Kyoto 611-0011, Japan
- GREGORY H. ROBINSON (283), Department of Chemistry, The University of Georgia, Athens, Georgia 30605
- ANDREAS SCHNEPF (235), Institut für Anorganische Chemie der Universität Karlsruhe, D-76133 Karlsruhe, Germany
- HANSGEORG SCHNÖCKEL (235), Institut für Anorganische Chemie der Universität Karlsruhe, D-76133 Karlsruhe, Germany

The Chemical and Catalytic Reactions of Hydrido-Chloro-Carbonylbis (triisopropylphosphine)osmium(II) and Its Major Derivatives

MIGUEL A. ESTERUELAS and LUIS A. ORO

*Departamento de Química Inorgánica
Instituto de Ciencia de Materiales de Aragón, Universidad de Zaragoza, CSIC
50009 Zaragoza, Spain*

I. Introduction	2
II. Spectroscopic Features and Coordination Polyhedron of OsHCl(CO)(P ⁱ Pr ₃) ₂	3
III. Addition Reactions to OsHCl(CO)(P ⁱ Pr ₃) ₂ : Formation of Six-Coordinate Hydrido-Chloro-Carbonyl Derivatives	5
IV. Addition of the Os—H Bond of OsHCl(CO)(P ⁱ Pr ₃) ₂ to Carbon—Carbon Triple Bonds: Formation of Alkenyl Derivatives	7
V. Formation of Hydride-Vinylidene Complexes by Addition of Terminal Alkynes to OsHCl(CO)(P ⁱ Pr ₃) ₂	11
VI. Formation of Dienyl Complexes by Reaction of OsHCl(CO)(P ⁱ Pr ₃) ₂ with Enynes	14
VII. Reactions of OsHCl(CO)(P ⁱ Pr ₃) ₂ with Alkynols: Formation of α,β-Unsaturated Carbene Complexes	17
VIII. Reactions of OsHCl(CO)(P ⁱ Pr ₃) ₂ with HX Molecules: Formation of Dihydrogen Derivatives	19
IX. The Complex OsCl ₂ (η ² -H ₂)(CO)(P ⁱ Pr ₃) ₂ as Precursor of Carbene, Alkenyl-Carbene, and μ-Bis-Carbene Derivatives	21
X. Reaction of OsHCl(CO)(P ⁱ Pr ₃) ₂ with <i>n</i> -BuLi: The Chemistry of the Dihydride OsH ₂ (CO)(η ² -CH ₂ =CHEt)(P ⁱ Pr ₃) ₂	24
XI. Reactions of OsH ₂ (η ² -H ₂)(CO)(P ⁱ Pr ₃) ₂ with Alkynes: Alkynyl and Related Compounds	32
XII. Reaction of OsHCl(CO)(P ⁱ Pr ₃) ₂ with NaBH ₄ : The Chemistry of OsH(η ² -H ₂ BH ₂)(CO)(P ⁱ Pr ₃) ₂	38
XIII. Decomposition of OsH(η ² -H ₂ BH ₂)(CO)(P ⁱ Pr ₃) ₂ in the Presence of Alcohols: Synthesis and Reactions of Hydride-Alkyl Compounds	40
XIV. Reactions of OsHCl(CO)(P ⁱ Pr ₃) ₂ with C ₅ H ₆ and Na[HBpz ₃]: Cyclopentadienyl and Tris(pyrazolyl)borate Compounds	44
XV. Reactions of OsHCl(CO)(P ⁱ Pr ₃) ₂ with NaXR (X=O, S)	46
XVI. Other Metathetical Reactions on the Chloride Ligand of OsHCl(CO)(P ⁱ Pr ₃) ₂	50
XVII. OsHCl(CO)(P ⁱ Pr ₃) ₂ as a Homogeneous Catalyst	51
XVIII. Final Remarks	55
References	56

I

INTRODUCTION

Since Chatt and Davidson^{1a} observed the first clear example of simple oxidative addition of a C—H bond of naphthalene to a ruthenium metal center, $\text{Ru}(\text{dmpe})_2$ ($\text{dmpe} = \text{Me}_2\text{PCH}_2\text{CH}_2\text{PMe}_2$), hydrocarbon activation has been the subject of many transition metal studies.^{1b-c} Sometimes, the efforts in this field have ended in findings different from the initial objectives, which have been the starting point for the development of novel organometallic chemistry.

At the beginning of the 1980's, Werner's group was actively interested in C—H activation processes. They showed that not only the $\text{Ru}(\text{diphosphine})_2$ species are capable of activating C—H bonds of aromatic compounds, but also the related ruthenium(0) and osmium(0) $\text{M}(\text{PR}_4)_4$ ($\text{M} = \text{Ru}, \text{Os}$) fragments containing monodentate basic phosphine ligands. Furthermore, they observed that the reactivity of these systems depends critically on the electronic and steric properties of the phosphine coordinated to the metal. While the fragments $\text{M}(\text{PMe}_3)_4$, generated by reduction of *trans*- $\text{MCl}_2(\text{PMe}_3)_4$ with Na/Hg in benzene, undergo intramolecular C—H activation to afford $\text{MH}\{\text{P}(\text{Me})_2\text{CH}_2\}(\text{PMe}_3)_3$ ($\text{M} = \text{Ru}, \text{Os}$),² the mixed complexes all *trans*- $\text{MCl}_2(\text{PMe}_3)_2\{\text{P}(\text{OMe})_3\}_2$ react under the same conditions by intermolecular addition of benzene to form $\text{MH}(\text{Ph})(\text{PMe}_3)_2\{\text{P}(\text{OMe})_3\}_2$ ($\text{M} = \text{Ru}, \text{Os}$).³ In addition, they showed during investigations of the reactivity of arene-osmium(0) complexes that even a small change in the coordination sphere of the metal can direct the course of the reaction towards either intra- or intermolecular C—H activation.⁴

The need to understand the way in which the properties of the phosphine influence the reactivity of these systems prompted Werner to extend the above mentioned studies to $\text{Ru}-\text{P}^i\text{Pr}_3$ and $\text{Os}-\text{P}^i\text{Pr}_3$ derivatives. It was known from earlier work in the group that arene-ruthenium compounds of the type $\text{RuH}_2(\eta^6\text{-arene})(\text{P}^i\text{Pr}_3)$ react under UV irradiation in hydrocarbon solvents to give either $\text{RuH}\{(\text{P}^i\text{Pr}_2)\text{CH}(\text{Me})\text{CH}_2\}(\eta^6\text{-arene})$ or $\text{RuH}(\text{R})(\eta^6\text{-arene})(\text{P}^i\text{Pr}_3)$ by intra- or intermolecular oxidative addition.⁵ The route first investigating preparation of the $\text{Ru}-\text{P}^i\text{Pr}_3$ and $\text{Os}-\text{P}^i\text{Pr}_3$ derivatives was the ligand displacement starting from $\text{MCl}_2(\text{PPh}_3)_3$ ($\text{M} = \text{Ru}, \text{Os}$). The method was useful to obtain $\text{MCl}_2(\text{PMe}_3)_4$ ($\text{M} = \text{Ru}, \text{Os}$).² However, all attempts during 4 months of hard work were unsuccessful. An alternative method involved treatment of the corresponding $\text{MCl}_3 \cdot x\text{H}_2\text{O}$ with the phosphine, in alcohol. The choice of solvent was critical for the course of the reaction.

In 1961, Vaska and Diluzio⁶ showed that hydride-carbonylphosphine complexes of the formula $\text{MHX}(\text{CO})(\text{PPh}_3)_3$ ($\text{M} = \text{Ru}, \text{Os}$; $\text{X} = \text{Cl}, \text{Br}$) can be directly obtained from the metal halides and triphenylphosphine, using 2-methoxyethanol or ethylene glycol at 120–190°C. In agreement with this, in 1971, Moers⁷ reported the

isolation of the five-coordinate complex $\text{OsHCl}(\text{CO})(\text{PCy}_3)_2$, on boiling a solution of tricyclohexylphosphine and K_2OsCl_6 in 2-methoxyethanol under nitrogen for 48 h, and in 1979, Gill and Shaw⁸ described the synthesis of $\text{RuHCl}(\text{CO})(\text{Pt-Bu}_2\text{R})_2$ ($\text{R} = \text{Me, Et}$) by a similar procedure. In contrast to these observations, in 1966, Stephenson and Wilkinson⁹ reported the preparation of $\text{RuCl}_2(\text{PPh}_3)_3$ by refluxing a methanolic solution of triphenylphosphine and $\text{RuCl}_3 \cdot x\text{H}_2\text{O}$, and in 1975, Hoffman and Caulton¹⁰ described the synthesis of $\text{OsCl}_2(\text{PPh}_3)_3$ by treatment of $(\text{NH}_4)_2\text{OsCl}_6$ with triphenylphosphine in a 2.5:1 mixture of *t*-butyl alcohol and water under reflux. Several dinuclear ruthenium compounds had also been obtained by reaction of $\text{RuCl}_3 \cdot x\text{H}_2\text{O}$ with bulky phosphines in ethanol as solvent.¹¹

In order to obtain chloro complexes related to $\text{MCl}_2(\text{PMe}_3)_4$ or $\text{MCl}_2(\text{PPh}_3)_3$ ($\text{M} = \text{Ru, Os}$), methanol appeared to be an appropriate solvent, according to the previously mentioned precedents. However, the treatment of the corresponding metal halides with triisopropylphosphine in methanol under reflux led to the five-coordinate hydride-carbonyl derivatives $\text{MHCl}(\text{CO})(\text{P}^i\text{Pr}_3)_2$ ($\text{M} = \text{Ru, Os}$).¹² Later, the synthesis of $\text{OsHCl}(\text{CO})(\text{Pt-Bu}_2\text{Me})_2$ by reaction of $\text{OsCl}_3 \cdot x\text{H}_2\text{O}$ with *tert*-butylmethylphosphine in 2-methoxyethanol was reported.¹³

In 1991, the preparation of the six-coordinate osmium(IV) complexes $\text{OsH}_2\text{Cl}_2(\text{PR}_3)_2$ ($\text{PR}_3 = \text{P}^i\text{Pr}_3, \text{Pt-Bu}_2\text{Me}$) was also described.¹⁴ Those compounds are synthesized by reaction of $\text{OsCl}_3 \cdot x\text{H}_2\text{O}$ with the corresponding phosphine in 2-propanol under reflux. Previously, in 1971, Chatt and co-workers¹⁵ had reported the formation of the related seven-coordinate derivatives $\text{OsH}_2\text{Cl}_2(\text{PR}_3)_3$ ($\text{PR}_3 = \text{PEt}_2\text{Ph, PMePh}_2, \text{PEtPh}_2$). Recently, the ruthenium compounds $\text{RuH}_2\text{Cl}_2(\text{PR}_3)_2$ ($\text{PR}_3 = \text{P}^i\text{Pr}_3$,¹⁶ $\text{Pt-Bu}_2\text{Me}$ ¹⁷) have been obtained by treatment of $[\text{RuCl}_2(\text{C}_8\text{H}_{12})]_n$ with the phosphine under hydrogen atmosphere in 2-butanol at 80°C.

Although the initial synthesis of $\text{OsHCl}(\text{CO})(\text{P}^i\text{Pr}_3)_2$ could be considered a fortunate accident, the large number of observed reactions and new organometallic complexes developed in the last 15 years using the title complex as starting point prompt us to consider the complex $\text{OsHCl}(\text{CO})(\text{P}^i\text{Pr}_3)_2$ as one of the cornerstones in the development of modern organometallic osmium chemistry. In the following pages, we revise the most important features of its rich chemistry.

II

SPECTROSCOPIC FEATURES AND COORDINATION POLYHEDRON OF $\text{OsHCl}(\text{CO})(\text{P}^i\text{Pr}_3)_2$

The complex $\text{OsHCl}(\text{CO})(\text{P}^i\text{Pr}_3)_2$ is a red, very air sensitive solid, which is, however, stable for long periods at room temperature if kept under argon. In the IR spectrum in benzene, the most noticeable feature is the presence of a $\nu(\text{CO})$ band at 1886 cm^{-1} . At room temperature the ^1H NMR spectrum in benzene- d_6 shows

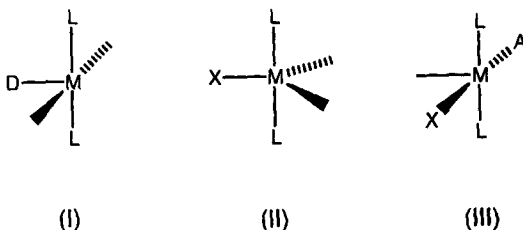
two doublets of virtual triplets at 1.27 and 1.20 ppm for the methyl groups of the triisopropylphosphine ligands. The presence of two signals for these protons, which is a result of the prochirality of the phosphorous atoms, indicates that the structure of the complex is rigid in solution at room temperature, and that the molecule has no mirror plane of symmetry containing the Os—P bonds. In the high field region, the spectrum contains a triplet at -31.92 ppm with a H—P coupling constant of 14 Hz, corresponding to the hydride ligand. The $^{31}\text{P}\{^1\text{H}\}$ NMR spectrum in benzene- d_6 shows a singlet at 47.3 ppm.

These spectroscopic data support a square-pyramidal structure in solution with the phosphines mutually *trans* disposed, the chloride and the carbonyl group occupying the basal sites, and the hydride ligand located at the apex. This structure fully agrees with that found in the solid state, by X-ray diffraction analysis for the related compound $\text{OsHCl}(\text{CO})(\text{PCy}_3)_2$ ¹⁸, and for ab initio DFT (Becke 3LYP) methods for the model complex $\text{OsHCl}(\text{CO})(\text{PH}_3)_2$.¹⁹

Why is the structure square-pyramidal? It has been shown that a diamagnetic $d^6 \text{ML}_5$ complex distorts away from the Jahn–Teller active trigonal bipyramidal structure.²⁰ Two more stable structures are possible: a square pyramid (T) and a distorted trigonal bipyramid (Y). Theoretical studies²¹ have shown that the T and Y structures are very close in energy and that the preference for one over the other comes from a subtle balance of σ and π properties of the ligands.

A T structure with the strongest σ -donor D *trans* to the empty site (I in Scheme 1) is preferred in the case of three pure σ -donor ligands. The presence of a π -acceptor ligand also makes the T structure more stable. When one of the ligands is a π -donor, X, a Y structure of type II (Scheme 1) is observed. This structure permits the formation of a π bond between the empty metal d orbital and the lone pair of X. No such π bond is present in the T structure since all symmetry adapted d orbitals are filled. This partial M—X multiple bond stabilizes Y over T.

In the mixed case—one π -donor and a π -acceptor ligand, as in $\text{OsHCl}(\text{CO})(\text{P}^i\text{Pr}_3)_2$ —the structure III of Scheme 1 (in which the π -donor X ligand and the π -acceptor A ligand are *trans* to each other) is more stable.²² In a T structure, which



SCHEME 1.

is a fragment of an octahedron, the nonbonding orbital(s) is (are) destabilized by the lone pair(s) of X. The π -acceptor ligand can diminish this destabilization by means of back-donation into its empty π^* orbitals. For the best stabilization, the two ligands should be *trans* to each other, yielding a "push-pull" effect.

Why is the complex $\text{OsHCl}(\text{CO})(\text{P}^i\text{Pr}_3)_2$ stable, when it is unsaturated? It has been argued that lone pairs on the alpha atom of a ligand $\text{M}-\text{X}$ (M is a transition metal) can have a major influence on reactivity and structure. If M has empty orbitals of appropriate symmetry, $\text{X} \rightarrow \text{M}$ π donation creates an $\text{M}-\text{X}$ multiple bond, with consequent transfer of electron density to M decreasing its Lewis acidity.²³ The presence of a carbonyl ligand in $\text{OsHCl}(\text{CO})(\text{P}^i\text{Pr}_3)_2$ increases the π -donor capacity of chloro by means of the "push-pull" effect making this molecule not a truly 16-valence electron species.

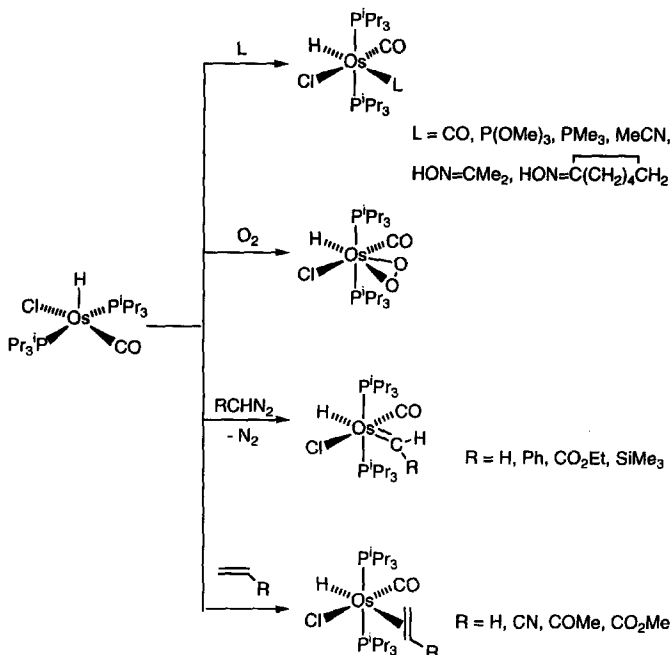
In addition, X-ray diffraction analysis of related molecules reveals that in the sixth (formally unoccupied) position of the octahedron the metallic center is well shielded. Four of the 12 methyl groups of the phosphine ligands surround the metal like an umbrella. As a result of the shielding effect of the methyl groups, a bending of the phosphorus-metal-phosphorus axis is observed.²⁴

III

ADDITION REACTIONS TO $\text{OsHCl}(\text{CO})(\text{P}^i\text{Pr}_3)_2$: FORMATION OF SIX-COORDINATE HYDRIDO-CHLORO-CARBONYL DERIVATIVES

The complex $\text{OsHCl}(\text{CO})(\text{P}^i\text{Pr}_3)_2$ adds Lewis bases that are not too bulky, such as CO, $\text{P}(\text{OMe})_3$, PMe_3 , MeCN , $\text{HON}=\text{CMe}_2$, and $\text{HON}=\text{C}(\text{CH}_2)_4\text{CH}_2$, to afford six-coordinate hydrido-chloro-carbonyl complexes of the type $\text{OsHCl}(\text{CO})(\text{P}^i\text{Pr}_3)_2\text{L}$, where the added ligand lies *trans* to the hydride^{12,25} (Scheme 2). Molecular oxygen also coordinates. Coordination does not involve the breaking of the oxygen-oxygen bond, and the peroxo derivative $\text{OsHCl}(\text{CO})(\text{P}^i\text{Pr}_3)_2(\eta^2\text{-O}_2)$ is formed.²⁶

In contrast to $\text{OsHCl}(\text{CO})(\text{P}^i\text{Pr}_3)_2$, the related complex $\text{OsHCl}(\text{C}=\text{CHPh})(\text{P}^i\text{Pr}_3)_2$, containing a vinylidene ligand instead of a carbonyl group, is capable of activating the oxygen-oxygen double bond of molecular oxygen from the air to give the dioxo compound $\text{OsCl}\{(E)\text{-CH}=\text{CHPh}\}(\text{O})_2(\text{P}^i\text{Pr}_3)_2$.²⁷ This marked difference in behavior appears to be the consequence of electronic differences between $\text{OsHCl}(\text{CO})(\text{P}^i\text{Pr}_3)_2$ and $\text{OsHCl}(\text{C}=\text{CHPh})(\text{P}^i\text{Pr}_3)_2$, which are revealed by the adoption of different coordination polyhedrons. While the complex $\text{OsHCl}(\text{CO})(\text{P}^i\text{Pr}_3)_2$ shows a T structure with a $\text{Cl}-\text{Os}-\text{CO}$ angle of about 160° ,²² the vinylidene derivative has a Y structure with a $\text{Cl}-\text{Os}-\text{vinylidene}$ angle of about 144° .¹⁷ The preference for a Y structure originates from vinylidene being a potent π

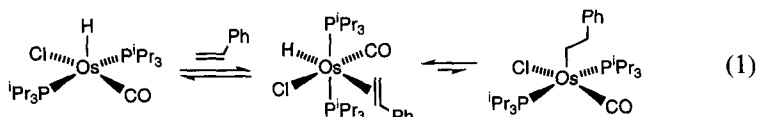


SCHEME 2.

acceptor in the CR_2 plane, but a weak π donor in the orthogonal plane. The donating property of π_{CC} disfavors a *trans* relationship of the $\text{Os}-\text{Cl}$ and vinylidene since this maximizes the overlaps between the occupied orbitals of the metal (d) and the two ligands (π_{CC} and π_{Cl}). Two stabilizing interactions occur when CR_2 lies in the $\text{H}-\text{Os}-\text{Cl}$ plane. In addition to the usual $\text{Os}-\text{Cl}$ π bond characteristic of all Y-shaped $d^6 \text{ML}_5$ species, the x^2-y^2 orbital is back bonding into the $p_{\text{C}\alpha}$ empty orbital.²⁸

The complex $\text{OsHCl(CO)(P}^i\text{Pr}_3)_2$ reacts with diazoalkanes RCHN_2 ($\text{R} = \text{H, Ph, CO}_2\text{Et, SiMe}_3$) at room temperature to give the hydrido-carbene derivatives $\text{OsHCl(CO)(CHR)(P}^i\text{Pr}_3)_2$, also containing the hydride and the carbene ligands in *trans* disposition.²⁹ In benzene, the derivative $\text{OsHCl(CO)(CH}_2\text{)(P}^i\text{Pr}_3)_2$ regenerates the starting material and affords ethylene,³⁰ which under ethylene atmosphere coordinates to the osmium atom to give $\text{OsHCl(CO)(}\eta^2\text{-C}_2\text{H}_4\text{)(P}^i\text{Pr}_3)_2$. Other olefins with electron-withdrawing substituents such as CN , C(O)Me , and CO_2Me also bind to $\text{OsHCl(CO)(P}^i\text{Pr}_3)_2$ to produce octahedral compounds of the formula $\text{OsHCl(CO)(}\eta^2\text{-CH}_2\text{=CHR)(P}^i\text{Pr}_3)_2$ ¹² (Scheme 2). Although a subsequent intramolecular insertion of the olefin into the $\text{Os}-\text{H}$ bond is not observed, the addition of styrene to benzene- d_6 solutions of $\text{OsDCl(CO)(P}^i\text{Pr}_3)_2$ shows $\text{D}-\text{H}$

exchange, suggesting a rapid equilibrium between the species shown in Eq. (1).³¹ Acetone shows a behavior similar to that of styrene.³²



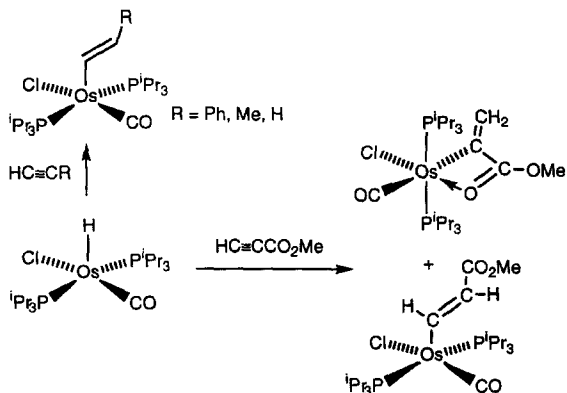
IV

ADDITION OF THE Os—H BOND OF OsHCl(CO)(PⁱPr₃)₂ TO CARBON—CARBON TRIPLE BONDS: FORMATION OF ALKENYL DERIVATIVES

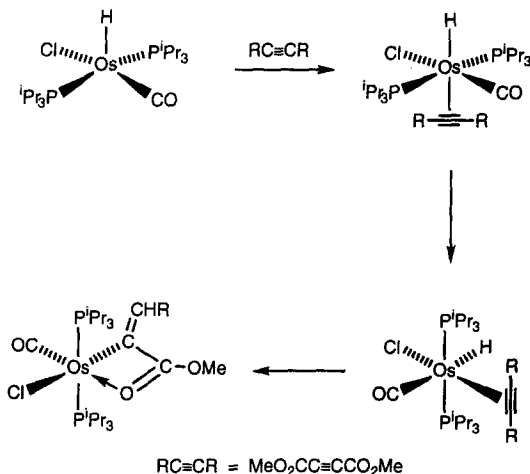
The reactivity of OsHCl(CO)(PⁱPr₃)₂ toward alkynes depends on the type of alkyne used. Whereas phenylacetylene, propyne, and acetylene react by insertion to give the five-coordinate alkenyl derivatives Os{(E)-CH=CHR}Cl(CO)(PⁱPr₃)₂ (R = Ph, Me, H),^{31,33} the reaction with methylpropiolate affords a mixture of Os{C(=CH₂)C(OMe)O}Cl(CO)(PⁱPr₃)₂ and Os{(E)-CH=CHCO₂Me}Cl(CO)(PⁱPr₃)₂³⁴ (Scheme 3), and *tert*-butyl acetylene and diphenylacetylene are inert.

In solution, Os{(E)-CH=CHCO₂Me}Cl(CO)(PⁱPr₃)₂ rearranges quantitatively to form the *Z* isomer Os{CH=CHC(OMe)O}Cl(CO)(PⁱPr₃)₂ in which the alkenyl group behaves as a chelating ligand (Eq. 2).

In contrast to diphenylacetylene, the activated alkyne, ethyne dicarboxylic methyl ester, coordinates to OsHCl(CO)(PⁱPr₃)₂ *trans* to the hydride. Then rearrangement to the *cis*-isomer takes place, followed by insertion to yield the

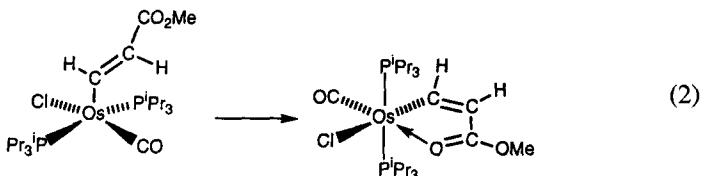


SCHEME 3.

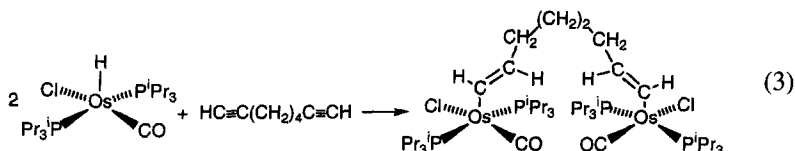


SCHEME 4.

corresponding alkenylosmium compound containing one of the ester units coordinated to the metallic center³¹ (Scheme 4).



The complex $\text{OsHCl(CO)(P}^i\text{Pr}_3)_2$ also reacts with diynes.³⁵ Thus, it has been reported that the treatment of this compound with 0.5 equiv. of 1,7-octadiyne affords, after 6 h at 333 K, the binuclear μ -bis-alkenyl derivative $(\text{P}^i\text{Pr}_3)_2(\text{CO})\text{ClOs}\{\text{CH}=\text{CH}(\text{CH}_2)_4\text{CH}=\text{CH}\}\text{OsCl(CO)(P}^i\text{Pr}_3)_2$ in 83% yield (Eq. 3).

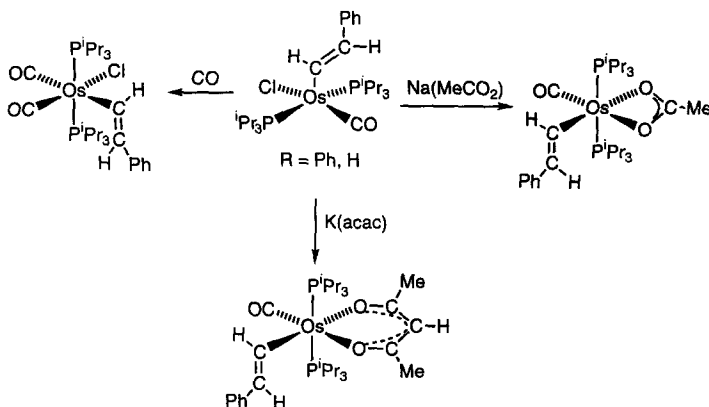


The structure of the styryl derivative $\text{Os}\{(E)\text{-CH}=\text{CHPh}\}\text{Cl(CO)(P}^i\text{Pr}_3)_2$ has been determined by X-ray diffraction analysis.³³ In agreement with $\text{OsHCl(CO)(P}^i\text{Pr}_3)_2$, the coordination polyhedron around the osmium atom can be rationalized as square-pyramidal with the phosphines, mutually *trans* disposed, the chloride and the carbonyl group occupying the basal sites, and the alkenyl located at the

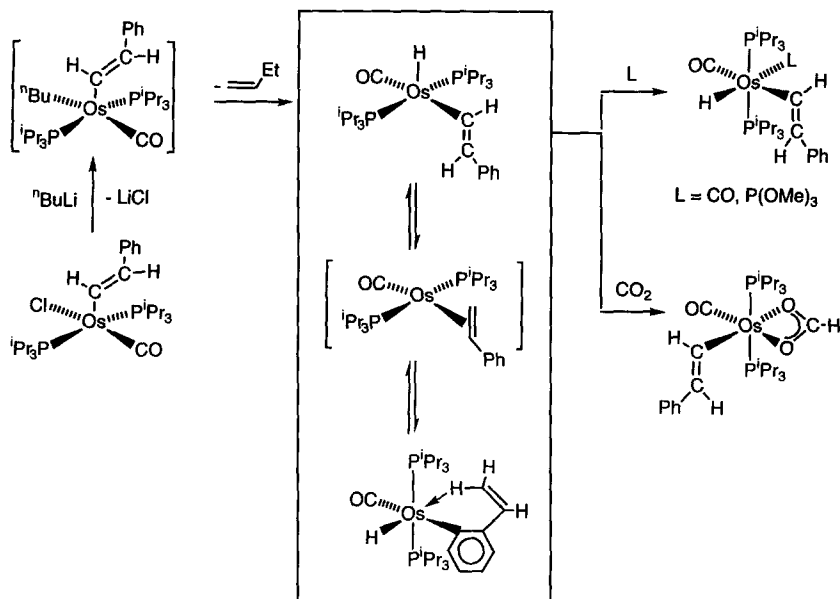
apex. The sixth (formally unoccupied) position of the octahedron is also well shielded by the methyl groups of the phosphines. The shielding effect produces the expected bending of the phosphorus-osmium-phosphorus axis, resulting in a P—Os—P angle of 167.4(1)°. The coordination number six for osmium can be achieved, however, either by addition of carbon monoxide or displacement of the chloride ligand with acetate or acetylacetonate anions (Scheme 5).

The complex $\text{Os}\{(E)\text{-CH=CHPh}\}\text{Cl}(\text{CO})(\text{P}^i\text{Pr}_3)_2$ reacts with *n*-BuLi to give the hydride-aryl derivative $\text{OsH}\{\text{C}_6\text{H}_4(\text{CH=CHH})\}(\text{CO})(\text{P}^i\text{Pr}_3)_2$, which evolves into the hydride-styryl complexes $\text{OsH}\{(E)\text{-CH=CHPh}\}(\text{CO})\text{L}(\text{P}^i\text{Pr}_3)_2$ (L = CO, P(OMe)₃) upon coordination of carbon monoxide and trimethylphosphite, and affords the formato-styryl compound $\text{Os}\{(E)\text{-CH=CHPh}\}(\kappa^2\text{-O}_2\text{CH})(\text{CO})(\text{P}^i\text{Pr}_3)_2$ under CO₂ atmosphere.³⁶

The formation of these compounds has been rationalized according to Scheme 6. The reaction of $\text{Os}\{(E)\text{-CH=CHPh}\}\text{Cl}(\text{CO})(\text{P}^i\text{Pr}_3)_2$ with *n*-BuLi involves replacement of the chloride anion by a butyl group to afford the intermediate $\text{Os}\{(E)\text{-CH=CHPh}\}(n\text{-Bu})(\text{CO})(\text{P}^i\text{Pr}_3)_2$, which by subsequent hydrogen β elimination gives $\text{OsH}\{(E)\text{-CH=CHPh}\}(\text{CO})(\text{P}^i\text{Pr}_3)_2$. The intramolecular reductive elimination of styrene from this compound followed by the C—H activation of the *o*-aryl proton leads to the hydride-aryl species via the styrene-osmium(0) intermediate $\text{Os}\{\eta^2\text{-CH}_2=\text{CHPh}\}(\text{CO})(\text{P}^i\text{Pr}_3)_2$. In spite of the fact that the hydride-aryl complex is the only species detected in solution, the formation of $\text{OsH}\{(E)\text{-CH=CHPh}\}\text{L}(\text{CO})(\text{P}^i\text{Pr}_3)_2$ and $\text{Os}\{(E)\text{-CH=CHPh}\}(\kappa^2\text{-O}_2\text{CH})(\text{CO})(\text{P}^i\text{Pr}_3)_2$ suggests that in solution the hydride-aryl complex is in equilibrium with undetectable concentrations of $\text{OsH}\{(E)\text{-CH=CHPh}\}(\text{CO})(\text{P}^i\text{Pr}_3)_2$. This implies that the olefin-osmium(0) intermediate is easily accessible and can give rise to activation reactions at both the olefinic and the ortho phenyl C—H bonds of the



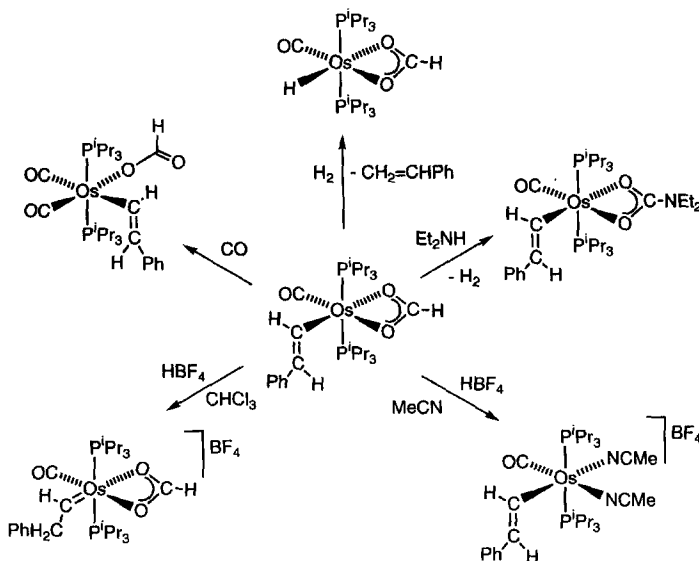
SCHEME 5.



SCHEME 6.

coordinated styrene. Although the product resulting from the phenyl C—H activation is more stable than that resulting of the olefinic C—H activation, the latter is more substitution labile. In addition, it should be pointed out that the olefinic C—H activation is selective; thus only the C—H bond disposed *trans* to the phenyl group is activated.

Carbonylation of the bidentate formate complex $Os\{\kappa^2-(E)\text{-CH=CHPh}\}(\kappa^2\text{-O}_2\text{CH})(CO)(P^iPr_3)_2$ leads to formation of the monodentate formate derivative $Os\{\kappa^2-(E)\text{-CH=CHPh}\}(\kappa^1\text{-OC(O)H})(CO)_2(P^iPr_3)_2$, whereas under hydrogen atmosphere it quantitatively yields styrene and the hydride-formate compound $OsH(\kappa^2\text{-O}_2\text{CH})(CO)(P^iPr_3)_2$. The carbon atom of the formate group of $Os\{\kappa^2-(E)\text{-CH=CHPh}\}(\kappa^2\text{-O}_2\text{CH})(CO)(P^iPr_3)_2$ is susceptible to attack by nucleophiles. Thus, the reaction of this complex with diethylamine leads to the styryl-carbamate derivative $Os\{\kappa^2-(E)\text{-CH=CHPh}\}(\kappa^2\text{-O}_2\text{CNET}_2)(CO)(P^iPr_3)_2$. The reactions of the styryl-formate complex with $HBF_4 \cdot OEt_2$ afford different derivatives depending upon the conditions. In diethyl ether as solvent one of the two oxygen atoms of the formate ligand undergoes electrophilic attack of the proton of the acid to give the unsaturated $[Os\{\kappa^2-(E)\text{-CH=CHPh}\}(CO)(P^iPr_3)_2]^+$ fragment, which can be trapped as $[Os\{\kappa^2-(E)\text{-CH=CHPh}\}(CO)(MeCN)_2(P^iPr_3)_2]BF_4$ in the presence of acetonitrile. In chloroform as solvent, electrophilic attack of the proton takes place at the β -carbon atom of the styryl ligand. In this case the compound formed is the carbene $[Os(\kappa^2\text{-O}_2\text{CH})\{\text{CHCH}_2\text{Ph}\}(CO)(P^iPr_3)_2]BF_4$ (Scheme 7).³⁶

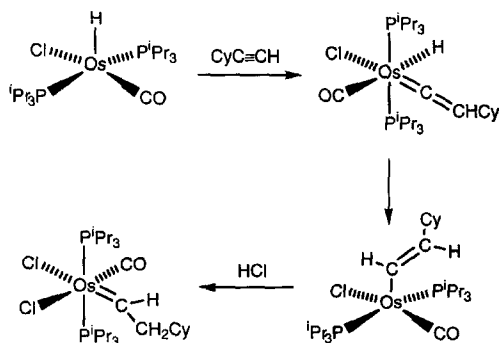


SCHEME 7.

V

FORMATION OF HYDRIDE-VINYLDENE COMPLEXES BY ADDITION OF TERMINAL ALKYNES TO $\text{OsHCl(CO)(P}^i\text{Pr}_3)_2$

In contrast to the reactions shown in Scheme 3, the complex $\text{OsHCl(CO)(P}^i\text{Pr}_3)_2$ reacts with cyclohexylacetylene at room temperature to give the hydride-vinylidene derivative $\text{OsHCl(C}=\text{CHCy)(CO)(P}^i\text{Pr}_3)_2$ in 70% yield (Scheme 8).³⁷ Kinetic measurements yield a second-order rate constant of $(6.0 \pm 0.2) \times 10^{-3} \text{ M}^{-1} \text{ s}^{-1}$ at



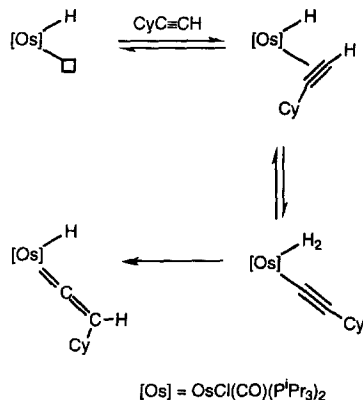
SCHEME 8.

-29°C . When the reaction is carried out using $\text{OsDCI}(\text{CO})(\text{P}^i\text{Pr}_3)_2$ as starting material a 1:1 mixture of the deuterated derivatives $\text{OsHCl}(\text{C}=\text{CDCy})(\text{CO})(\text{P}^i\text{Pr}_3)_2$ and $\text{OsDCI}(\text{C}=\text{CHCy})(\text{CO})(\text{P}^i\text{Pr}_3)_2$ is obtained. H,D-exchange between the deuterated species does not occur. These observations no doubt indicate that the formation of the vinylidene ligand involves a 1,3-hydrogen shift via an alkynyl intermediate. Furthermore, the second-order rate law for the reaction suggests that the 1,3-hydrogen shift is an intramolecular process.

The formation of the alkynyl intermediate should proceed by oxidative addition of the $\text{H}-\text{C}_{\text{sp}}$ alkyne bond to give, at first glance, a dihydride-osmium(IV) species, where both hydride ligands should be nucleophilic centers. In addition, it should be noted that coordination of an acetylide, $[\text{RC}\equiv\text{C}]^-$, to a metal center transfers the nucleophilicity from the α - to the β -carbon atom, and for these systems the transfer is efficient (*vide infra*). Thus, the direct attack of one of the two hydride ligands at the β -carbon atom of the alkynyl group does not seem likely, given the nucleophilicity of these centers. Hence, it can be proposed that the $\text{H}-\text{C}_{\text{sp}}$ activation leads to dihydrogen species. In this way the formation of the hydride-vinylidene compound could be rationalized as the electrophilic attack of an acidic proton of the dihydrogen ligand at the β -carbon atom of the alkynyl group (Scheme 9).

In favor of a dihydrogen intermediate, the following should be noted: (i) the addition of HX molecules to $\text{OsHCl}(\text{CO})(\text{P}^i\text{Pr}_3)_2$ is a useful synthetic route for dihydrogen compounds (*vide infra*), (ii) the electrophilic character of the dihydrogen complexes has been demonstrated,³⁸ and (iii) the addition of electrophiles to metal alkynyl complexes is a general method of preparing vinylidene compounds.³⁹

In toluene at room temperature, the complex $\text{OsHCl}(\text{C}=\text{CHCy})(\text{CO})(\text{P}^i\text{Pr}_3)_2$ evolves after 3 days into the alkenyl derivative $\text{Os}\{(E)\text{-CH}=\text{CHCy}\}\text{Cl}(\text{CO})$

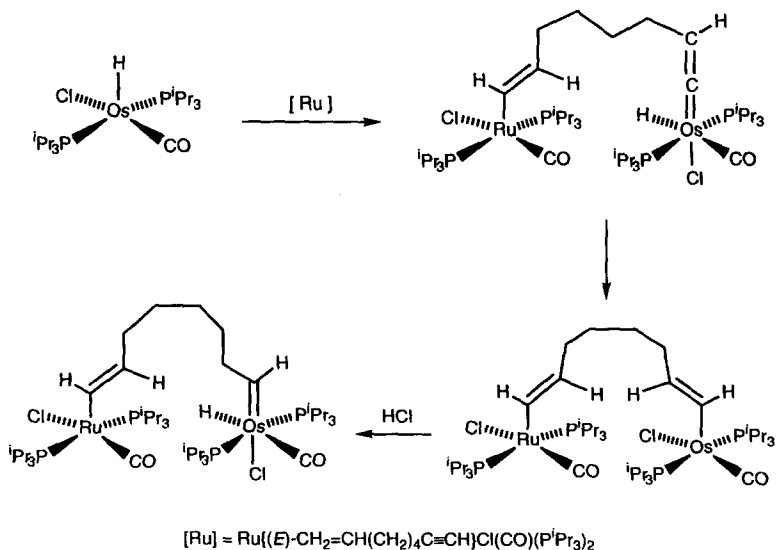


SCHEME 9.

$(P^iPr_3)_2$, which reacts with a stoichiometric amount of a toluene-HCl solution to afford the dichlorocarbene compound $OsCl_2(CHCH_2Cy)(CO)(P^iPr_3)_2$ (Scheme 8).

The metalloalkyne complex $Ru\{(E)-CH=CH(CH_2)_4C\equiv CH\}Cl(CO)(P^iPr_3)_2$ exhibits behavior similar to that of cyclohexylacetylene (Scheme 10).⁴⁰ Thus, it reacts with $OsHCl(CO)(P^iPr_3)_2$ to give the hydride-vinylidene derivative $(P^iPr_3)_2(CO)ClRu\{(E)-CH=CH(CH_2)_4CH=C\}OsHCl(CO)(P^iPr_3)_2$, which evolves in toluene into the heterodinuclear- μ -bisalkenyl complex $(P^iPr_3)_2(CO)ClRu\{(E)-CH=CH(CH_2)_4CH=CH-(E)\}OsCl(CO)(P^iPr_3)_2$. Kinetic measurements between 303 and 343 K yield first-order rate constants, which afford activation parameters of $\Delta H^\ddagger = 22.1 \pm 1.5$, kcal·mol⁻¹ and $\Delta S^\ddagger = -6.1 \pm 2.3$ cal·K⁻¹·mol⁻¹. The slightly negative value of the activation entropy suggests that the insertion of the vinylidene ligand into the Os—H bond is an intramolecular process, which occurs by a concerted mechanism with a geometrically highly oriented transition state.

In agreement with the nucleophilic character shown by the C_β atom of the alkenyl derivative $OsHCl\{(E)-CH=CHCy\}(CO)(P^iPr_3)_2$, the heterodinuclear- μ -bisalkenyl complex $(P^iPr_3)_2(CO)ClRu\{(E)-CH=CH(CH_2)_4CH=CH-(E)\}OsCl(CO)(P^iPr_3)_2$ reacts with HCl. However, interestingly, only the C_β atom of the Os-alkenyl unit is attacked. Thus, the treatment of the μ -bisalkenyl complex with the stoichiometric amount of a toluene HCl solution selectively affords $(P^iPr_3)_2(CO)ClRu\{(E)-CH=CH(CH_2)_5CH\}OsCl_2(CO)(P^iPr_3)_2$ (Scheme 10). This observation proves that under the same conditions, the C_β atom of the alkenyl



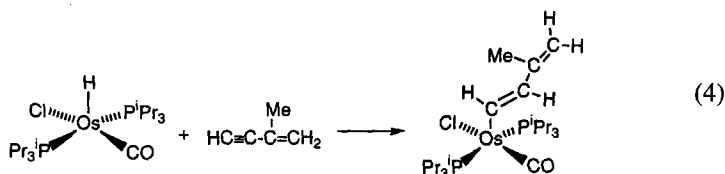
SCHEME 10.

ligands of the osmium-alkenyl complexes has a stronger nucleophilic character than the C_β atom of the alkenyl ligands of ruthenium-alkenyl compounds.

VI

FORMATION OF DIENYL COMPLEXES BY REACTION OF $OsHCl(CO)(P^iPr_3)_2$ WITH ENYNES

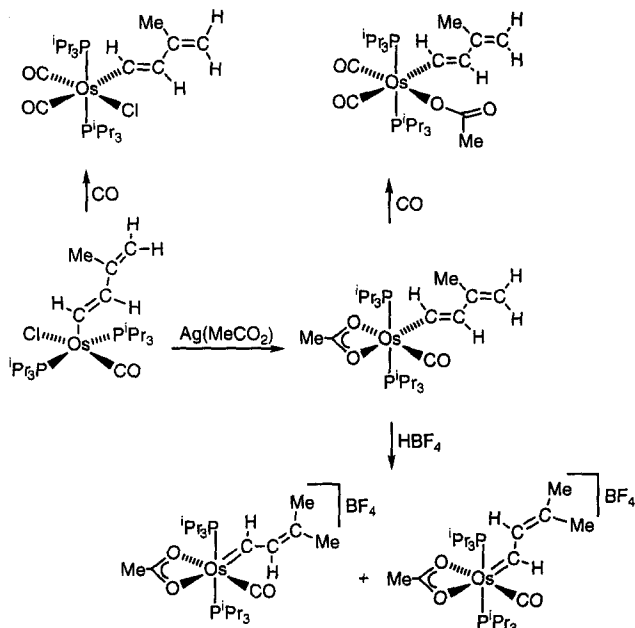
The complex $OsHCl(CO)(P^iPr_3)_2$ reacts with 2-methyl-1-buten-3-yne to give the dienyl derivative $Os\{(E)-CH=CHC(Me)=CH_2\}Cl(CO)(P^iPr_3)_2$ ³⁵ in 86%, which is a result of the selective addition of the $Os-H$ bond of the starting complex to the carbon-carbon triple bond of the enyne (Eq. 4).



Behavior similar to $OsHCl(CO)(P^iPr_3)_2$ has been observed for the five-coordinate monohydrides $RuHCl(CO)(P^iPr_3)_2$ ⁴¹ and $RhH(SnPh_3)(acac)(PCy_3)$.⁴² However, the reaction of $cis-(Me_3Si)CH=CHC\equiv CSiMe_3$ with the six-coordinate $RuHCl(CO)(PPh_3)_3$ gives a stable complex whose molecular structure is formally regarded as the result of either 1,2-addition of the $Ru-H$ to the double bond or 1,4-addition of the $Ru-H$ to the conjugated enyne.⁴³

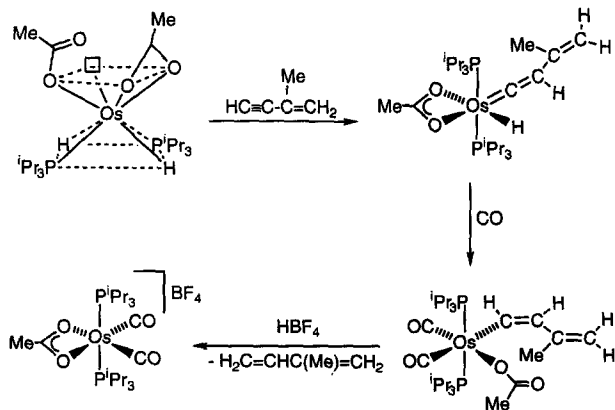
The five-coordinate (*E*)-dienyl compound $Os\{(E)-CH=CHC(Me)=CH_2\}Cl(CO)(P^iPr_3)_2$ reacts with $Ag[MeCO_2]$ in toluene to give $Os\{(E)-CH=CHC(Me)=CH_2\}(\kappa^2-O_2CMe)(CO)(P^iPr_3)_2$. Carbonylation of this complex leads to formation of the monodentate acetate derivative $Os\{(E)-CH=CHC(Me)=CH_2\}\{\kappa^1-OC(O)Me\}(CO)_2(P^iPr_3)_2$. The related chloro complex $Os\{(E)-CH=CHC(Me)=CH_2\}Cl(CO)_2(P^iPr_3)_2$ is similarly prepared starting from $Os\{(E)-CH=CHC(Me)=CH_2\}Cl(CO)(P^iPr_3)_2$. The protonation of $Os\{(E)-CH=CHC(Me)=CH_2\}(\kappa^2-O_2CMe)(CO)(P^iPr_3)_2$ with $HBF_4 \cdot OEt_2$ leads to the α,β -unsaturated carbene $[Os(\kappa^2-O_2CMe)\{CHCH=CMe_2\}(CO)(P^iPr_3)_2]BF_4$, which is isolated as a mixture of the two isomers shown in Scheme 11.⁴⁴

The six-coordinate (*Z*)-dienyl $Os\{(Z)-CH=CHC(Me)=CH_2\}\{\kappa^1-OC(O)Me\}(CO)_2(P^iPr_3)_2$ is also known. It is prepared according to Scheme 12. Treatment of the dihydride $OsH_2(\kappa^2-O_2CMe)\{\kappa^1-OC(O)Me\}(P^iPr_3)_2$ with 1.4 equiv. of 2-methyl-1-buten-3-yne in toluene under reflux gives, after 2 h, the hydride-vinylidene $OsH(\kappa^2-O_2CMe)\{C=CHC(Me)=CH_2\}Cl(P^iPr_3)_2$, which affords $Os\{(Z)-CH=CHC(Me)=CH_2\}\{\kappa^1-OC(O)Me\}(CO)_2(P^iPr_3)_2$ by reaction with carbon

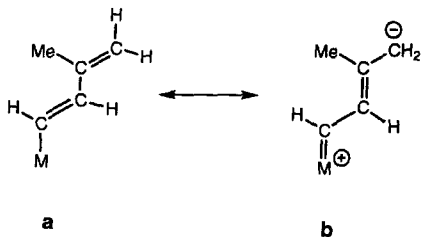


SCHEME 11.

monoxide. The selective formation of the diene ligand with a *Z*-stereochemistry suggests that of the two possible isomers of the hydride-vinylidene only one is present in solution, shown in Scheme 12. In general, however, the (*Z*)-diene complexes are less stable than the corresponding (*E*)-diene complex. In this case *Z* \rightarrow *E* isomerization is not observed. The protonation of $\text{Os}\{(\text{Z})-\text{CH}=\text{CHC}(\text{Me})=\text{CH}_2\}$



SCHEME 12.



SCHEME 13.

$\{\kappa^1\text{-OC(O)Me}\}(\text{CO})_2(\text{P}^i\text{Pr}_3)_2$ with $\text{HBF}_4\cdot\text{OEt}_2$ produces isoprene and the *cis*-dicarbonyl compound $[\text{Os}(\kappa^2\text{-O}_2\text{CMe})(\text{CO})_2(\text{P}^i\text{Pr}_3)_2]\text{BF}_4$ (Scheme 12).

The different behaviors of $\text{Os}\{(E)\text{-CH=CHC(Me)=CH}_2\}(\kappa^2\text{-O}_2\text{CMe})(\text{CO})(\text{P}^i\text{Pr}_3)_2$ and $\text{Os}\{(Z)\text{-CH=CHC(Me)=CH}_2\}\{\kappa^1\text{-OC(O)Me}\}(\text{CO})_2(\text{P}^i\text{Pr}_3)_2$ in the presence of HBF_4 merits attention. X-ray diffraction and reactivity studies on dienyl complexes indicate that for an adequate description of the bonding situation in these types of compounds a second zwitterionic resonance form (**b** in Scheme 13) must be considered. As a result of the significant contribution of the zwitterionic resonance form, the C_8 atoms of the dienyl ligands have a marked nucleophilic character, and their reactions with electrophilic reagents afford α,β -unsaturated carbene derivatives.^{41,45} The behavior of $\text{Os}\{(E)\text{-CH=CHC(Me)=CH}_2\}(\kappa^2\text{-O}_2\text{CMe})(\text{CO})(\text{P}^i\text{Pr}_3)_2$ is in agreement with this. However, the behavior of $\text{Os}\{(Z)\text{-CH=CHC(Me)=CH}_2\}\{\kappa^1\text{-OC(O)Me}\}(\text{CO})_2(\text{P}^i\text{Pr}_3)_2$ markedly differs. The main difference between them is the presence of a carbonyl group, *trans*-disposed to the dienyl ligand in the last compound.

An important contribution of the resonance form **b** requires the donation of electron density from the metal to the dienyl ligand [$\text{M}(\text{d}_\text{M}) \rightarrow \text{C}(\text{p}\pi)$ contribution]. The presence of a carbonyl group (a strong π -acceptor ligand) *trans* to the dienyl reduces the $\text{M}(\text{d}_\text{M}) \rightarrow \text{C}(\text{p}\pi)$ contribution and, therefore, the nucleophilicity of the unsaturated η^1 -carbon ligand. Then the nucleophilic center of the molecule is not the alkenyl ligand but the metallic center, and the protonation at the metal leads to the olefin via reductive elimination from a hydride-dienyl intermediate.²⁴

The *cis-trans* isomerization of alkenyl ligands in transition metal alkenyl compounds is proposed to occur via zwitterionic carbene intermediates.⁴⁶ According to this, the low contribution of the form **b** to the metal-dienyl bond in $\text{Os}\{(Z)\text{-CH=CHC(Me)=CH}_2\}\{\kappa^1\text{-OC(O)Me}\}(\text{CO})_2(\text{P}^i\text{Pr}_3)_2$ could explain why this compound does not evolve into its (*E*)-isomer.

In other words, the nonisomerization of $\text{Os}\{(Z)\text{-CH=CHC(Me)=CH}_2\}\{\kappa^1\text{-OC(O)Me}\}(\text{CO})_2(\text{P}^i\text{Pr}_3)_2$ into $\text{Os}\{(E)\text{-CH=CHC(Me)=CH}_2\}\{\kappa^1\text{-OC(O)Me}\}(\text{CO})_2(\text{P}^i\text{Pr}_3)_2$ and the behavior of the first isomer in the presence of HBF_4

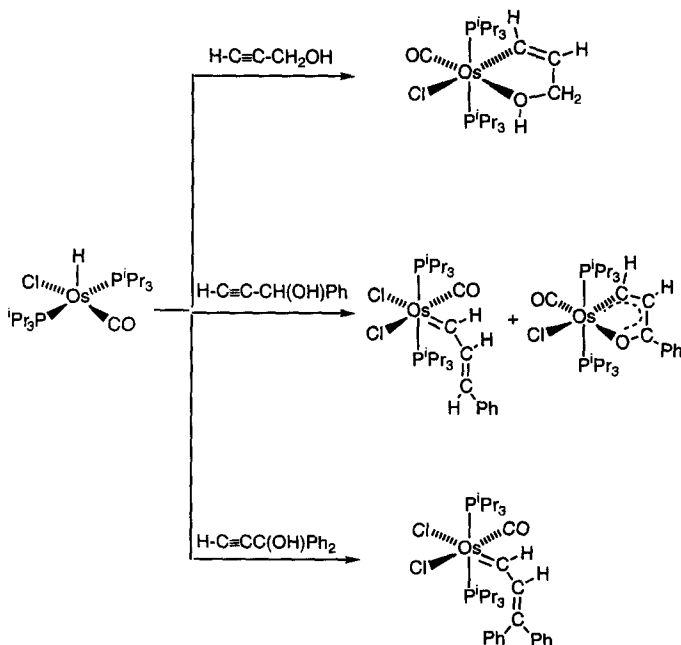
could have the same origin: the presence of a carbonyl group *trans* disposed to the dienyl ligand.

VII

REACTIONS OF $\text{OsHCl}(\text{CO})(\text{P}^i\text{Pr}_3)_2$ WITH ALKYNOLS: FORMATION OF α,β -UNSATURATED CARBENE COMPLEXES

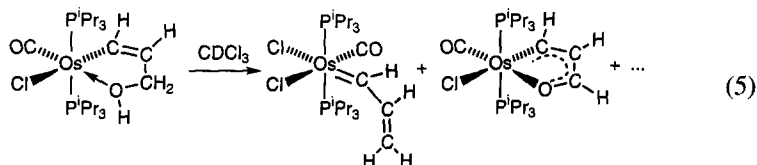
The reactivity of $\text{OsHCl}(\text{CO})(\text{P}^i\text{Pr}_3)_2$ toward alkynols depends on the substituents at the C(OH) carbon atom of the alkynol (Scheme 14).⁴⁷ The reaction with 2-propyn-1-ol initially affords the alkenyl compound $\text{Os}(\text{CH}=\text{CHCH}_2\text{OH})\text{Cl}(\text{CO})(\text{P}^i\text{Pr}_3)_2$ in 85% yield, as a result of the *anti*-addition of the Os—H bond to the carbon-carbon triple bond of the alkynol. In chloroform-*d* solution this complex decomposes to a mixture of products, containing the derivatives $\text{OsCl}_2(\text{CHCH}=\text{CH}_2)(\text{CO})(\text{P}^i\text{Pr}_3)_2$ and $\text{Os}(\text{CHCHCH}\text{O})\text{Cl}(\text{CO})(\text{P}^i\text{Pr}_3)_2$ (Eq. 5).

Compounds related to those shown in Eq. (5), containing at the γ -carbon atom of the corresponding ligands a phenyl group instead of a hydrogen atom, are directly obtained in 41 and 8% yield, respectively, from the reaction with



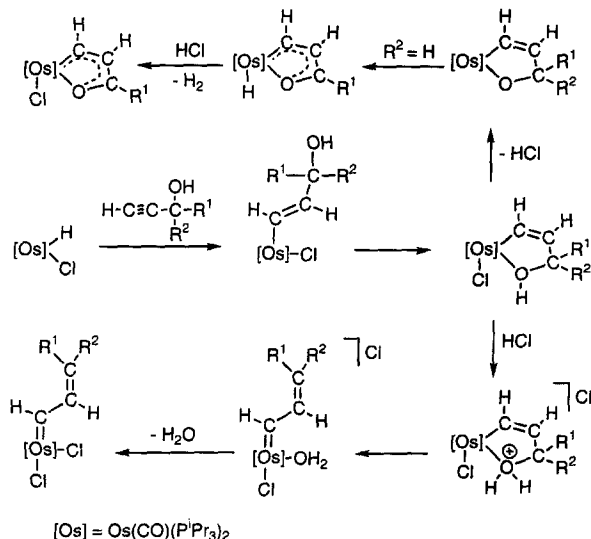
SCHEME 14.

1-phenyl-2-propyn-1-ol. In contrast to the above mentioned cases, the treatment of $\text{OsHCl}(\text{CO})(\text{P}^i\text{Pr}_3)_2$ with 1,1-diphenyl-2-propyn-1-ol leads to the α,β -unsaturated carbene compound $\text{OsCl}_2(\text{CHCH}=\text{CPh}_2)(\text{CO})(\text{P}^i\text{Pr}_3)_2$ in 34% yield.



The formation of the complexes shown in Scheme 14 and Eq. (5) has been rationalized according to Scheme 15. Thus, it has been proposed that the insertion of the $\text{Os}-\text{H}$ bond of $\text{OsHCl}(\text{CO})(\text{P}^i\text{Pr}_3)_2$ into the carbon-carbon triple bond of the alkynol initially gives five-coordinate (*E*)-alkenyl intermediates, which subsequently isomerize into the $\text{Os}\{\text{CH}=\text{CHC}(\text{OH})\text{R}^1\text{R}^2\}$ derivatives. The key to this isomerization is probably the fact that the five-coordinated (*E*)-alkenyl intermediates are 16-electron species, while the $\text{Os}\{\text{CH}=\text{CHC}(\text{OH})\text{R}^1\text{R}^2\}$ derivatives are 18-electron species.

The formation of the complexes $\text{Os}\{\text{CHCHCH}(\text{O})\text{R}^1\}\text{Cl}(\text{CO})(\text{P}^i\text{Pr}_3)_2$ ($\text{R}^1 = \text{Ph}, \text{H}$) from the corresponding $\text{Os}\{\text{CH}=\text{CHC}(\text{OH})\text{R}^1\text{R}^2\}$ species could initially involve the elimination of HCl to give five-coordinate intermediates of the type $\text{Os}\{\text{CH}=\text{CHC}(\text{O})\text{R}^1\text{R}^2\}(\text{CO})(\text{P}^i\text{Pr}_3)_2$, which by a subsequent hydrogen β -elimination ($\text{R}^2 = \text{H}$) should give $\text{Os}\{\text{CHCHCH}(\text{O})\text{R}^1\}\text{H}(\text{CO})(\text{P}^i\text{Pr}_3)_2$. Then the



SCHEME 15.

protonation with HCl of the hydride ligand, followed by displacement of the formed dihydrogen ligand by Cl^- , could give $\text{Os}\{\text{CHCHC}(\text{O})\text{R}^1\}\text{Cl}(\text{CO})(\text{P}^i\text{Pr}_3)_2$ ($\text{R}^1 = \text{Ph}, \text{H}$). In this context, it should be noted that the formation of hydride intermediates from the corresponding $\text{Os}\{\text{CH}=\text{CHC}(\text{OH})\text{R}^1\text{R}^2\}$ species is the result of the dehydrogenation of the alcohol group of the alkenyl ligand. The dehydrogenation of primary and secondary alcohols is a process which plays a main role in the homogeneous catalytic reduction of unsaturated organic substrates.⁴⁸ From a mechanistic point of view, it has been proved that alcohol dehydrogenation proceeds by initial heterolytic activation of the H—O bond, followed by a β -elimination process of hydrogen at the C—H bond of a M—OCHR₂ group. Although the tertiary alcohols can undergo heterolytic activation of the H—O bond, they are not suitable as a source of hydrogen because they do not contain a geminal hydrogen. The process of dehydrogenation of the $\text{Os}\{\text{CH}=\text{CHC}(\text{OH})\text{R}^1\text{R}^2\}$ species, proposed in Scheme 15, involves the same sequence of events as that proposed for the catalytic dehydrogenation of alcohols. In agreement with this, detectable concentrations of $\text{Os}\{\text{CHCHC}(\text{O})\text{Ph}\}\text{Cl}(\text{CO})(\text{P}^i\text{Pr}_3)_2$ are not obtained from the reaction of $\text{OsHCl}(\text{CO})(\text{P}^i\text{Pr}_3)_2$ with 1,1-diphenyl-2-propyn-1-ol.

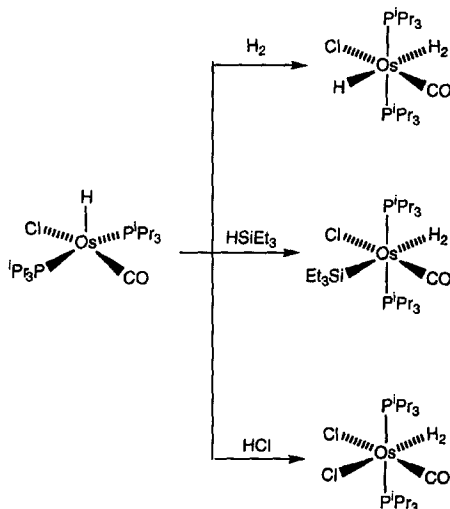
The previously mentioned loss of HCl appears also to be the key to the formation of the dichloro- α,β -unsaturated carbene complexes. The protonation of the OH group of the metallacycle of the remaining amount of the $\text{Os}\{\text{CH}=\text{CHC}(\text{OH})\text{R}^1\text{R}^2\}$ species could afford cationic chloro-aquo- α,β -unsaturated carbene intermediates. Thus, the subsequent displacement of the water molecule by Cl^- should give the dichloro- α,β -unsaturated carbene complexes. In agreement with this proposal, it has been observed that the ruthenium complex $\text{RuHCl}(\text{CO})(\text{P}^i\text{Pr}_3)_2$ reacts with 1-phenyl-2-propyn-1-ol and 1,1-diphenyl-2-propyn-1-ol to give the corresponding (*E*)-alkenyl compounds $\text{Ru}\{(E)\text{-CH}=\text{CHC}(\text{OH})\text{PhR}\}\text{Cl}(\text{CO})(\text{P}^i\text{Pr}_3)_2$, which yield $[\text{RuCl}(\text{CHCH}=\text{CPhR})(\text{CO})(\text{P}^i\text{Pr}_3)_2]\text{BF}_4$ by protonation with $\text{HBF}_4 \cdot \text{OEt}_2$, and that the treatment of these cationic carbene compounds with NaCl affords the dichloro- α,β -unsaturated carbene derivatives $\text{RuCl}_2(\text{CHCH}=\text{CPhR})(\text{CO})(\text{P}^i\text{Pr}_3)_2$ ($\text{R} = \text{Ph}, \text{H}$).⁴⁵

VIII

REACTIONS OF $\text{OsHCl}(\text{CO})(\text{P}^i\text{Pr}_3)_2$ WITH HX MOLECULES: FORMATION OF DIHYDROGEN DERIVATIVES

The complex $\text{OsHCl}(\text{CO})(\text{P}^i\text{Pr}_3)_2$ reacts with HX ($\text{X} = \text{H}, \text{SiEt}_3, \text{Cl}$) molecules to give derivatives of the type $\text{OsXCl}(\eta^2\text{-H}_2)(\text{CO})(\text{P}^i\text{Pr}_3)_2$ ($\text{X} = \text{H}, \text{SiEt}_3, \text{Cl}$), where the hydrogen atoms bonded to the osmium atom undergo nonclassical interaction (Scheme 16).

Under hydrogen atmosphere, the complex $\text{OsHCl}(\text{CO})(\text{P}^i\text{Pr}_3)_2$ is in equilibrium with the *trans*-hydride-dihydrogen compound $\text{OsHCl}(\eta^2\text{-H}_2)(\text{CO})(\text{P}^i\text{Pr}_3)_2$.²⁶



SCHEME 16.

Measurements of the equilibrium constant give thermodynamic parameters of $\Delta H^\circ = -14.1 \pm 0.5 \text{ kcal}\cdot\text{mol}^{-1}$ and $\Delta S^\circ = -30 \pm 1 \text{ cal}\cdot\text{K}^{-1}\cdot\text{mol}^{-1}$, while the activation parameters for the dissociation of the hydrogen molecule are $\Delta H^\ddagger = 14.6 \pm 0.2 \text{ kcal}\cdot\text{mol}^{-1}$ and $\Delta S^\ddagger = 99 \pm 0.5 \text{ cal}\cdot\text{K}^{-1}\cdot\text{mol}^{-1}$. In dissolution the dihydrogen ligand ($r_{\text{H-H}} = 0.8 \text{ \AA}$) is involved in a fast spinning process, and at high temperature, it exchanges the hydrogen atoms with the hydride ligand. The activation parameters for this process are $\Delta H^\ddagger = 17.4 \pm 0.5 \text{ kcal}\cdot\text{mol}^{-1}$ and $\Delta S^\ddagger = 1.3 \pm 1 \text{ cal}\cdot\text{K}^{-1}\cdot\text{mol}^{-1}$.

Ab initio calculations on the model system $\text{OsHCl}(\eta^2\text{-H}_2)(\text{CO})(\text{PH}_3)_2$ confirm that the *trans*-hydride-dihydrogen disposition is the most stable. In addition a *cis*-hydride-dihydrogen isomer ($r_{\text{H-H}} = 0.82 \text{ \AA}$), with a relative energy of $13.8 \text{ kcal}\cdot\text{mol}^{-1}$, occupies a local minimum in the potential hypersurface. In this isomer, the dihydrogen ligand lies *trans* to the carbonyl group.⁴⁹

The reaction of $\text{OsHCl(CO)(P}^i\text{Pr}_3)_2$ with HSiEt_3 leads to the silyl-dihydrogen complex $\text{Os(SiEt}_3\text{)Cl}(\eta^2\text{-H}_2)(\text{CO})(\text{P}^i\text{Pr}_3)_2$ in equilibrium with the dihydride tautomer $\text{OsH}_2(\text{SiEt}_3)\text{Cl(CO)(P}^i\text{Pr}_3)_2$.⁵⁰ Theoretical calculations on the model system $\text{OsCl(CO)(PH}_3)_2\text{"H}_2\text{SiH}_3\text{"}$ suggest the existence of two stable six-coordinate species of very close energy: a dihydrogen complex $\text{Os(SiH}_3\text{)Cl}(\eta^2\text{-H}_2)(\text{CO})(\text{PH}_3)_2$ ($r_{\text{H-H}} = 0.821 \text{ \AA}$), and an $\eta^2\text{-H-SiH}_3$ isomer $\text{OsHCl}(\eta^2\text{-H-SiH}_3)(\text{CO})(\text{PH}_3)_2$ ($r_{\text{H-Si}} = 1.737 \text{ \AA}$). The η^2 -coordination of the H-SiH_3 ligand to the $\text{OsHCl(CO)(PH}_3)_2$ fragment is stronger than that of the dihydrogen ligand by ca. $15 \text{ kcal}\cdot\text{mol}^{-1}$, a value that compensates almost exactly the superior strength of the hydrogen-hydrogen bond with respect to the H-SiH_3 one.⁵¹

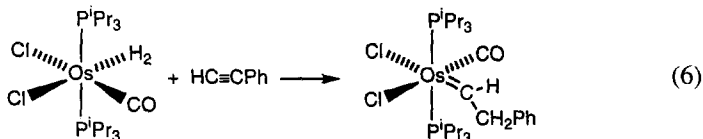
The reaction of $\text{OsHCl}(\text{CO})(\text{P}^i\text{Pr}_3)_2$ with HCl gives the dichloro derivative $\text{OsCl}_2(\eta^2\text{-H}_2)(\text{CO})(\text{P}^i\text{Pr}_3)_2$.³⁵ In solution, this complex is stable under argon for a matter of days. However, the dihydrogen unit is highly activated toward heterolytic cleavage, as demonstrated by deprotonation with NaH and by reactions with carbon monoxide and *tert*-butyl isocyanide, which afford $\text{OsHCl}(\text{CO})\text{L}(\text{P}^i\text{Pr}_3)_2$ ($\text{L} = \text{CO}$, *t*-BuNC) and HCl .

The separation between the hydrogen atoms of $\text{OsCl}_2(\eta^2\text{-H}_2)(\text{CO})(\text{P}^i\text{Pr}_3)_2$ is about 0.3 Å longer than those found in $\text{OsXCl}(\eta^2\text{-H}_2)(\text{CO})(\text{P}^i\text{Pr}_3)_2$ ($\text{X} = \text{H}$, SiEt_3). The value of this parameter, 1.1 Å, lies within the reported range for the so-called elongated dihydrogen compounds. Although these complexes are often seen as frozen structures at various points on the reaction path for the oxidative addition–reductive elimination of molecular hydrogen at the metallic center, their nature is still an open question. High-level *ab initio* calculations performed on the related model compound $\text{OsCl}_2(\eta^2\text{-H}_2)(\text{NH}=\text{CH}_2)(\text{PH}_3)_2$ have led to a new perspective for the understanding of this class of complexes. Instead of species where the oxidative addition–reductive elimination is arrested at some intermediate stage, the picture that emerges from the results is that it is more appropriate to describe them as species containing two hydrogen atoms moving freely in a wide region of the coordination sphere of the metal.⁵²

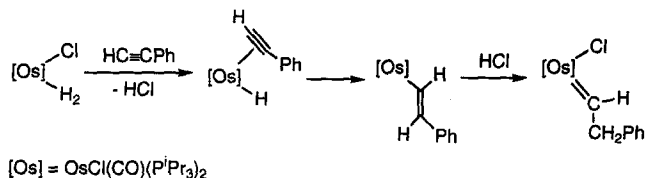
IX

THE COMPLEX $\text{OsCl}_2(\eta^2\text{-H}_2)(\text{CO})(\text{P}^i\text{Pr}_3)_2$ AS PRECURSOR OF CARBENE, ALKENYL-CARBENE, AND μ -BIS-CARBENE DERIVATIVES

The elongated dihydrogen complex $\text{OsCl}_2(\eta^2\text{-H}_2)(\text{CO})(\text{P}^i\text{Pr}_3)_2$ reacts with phenylacetylene to give the dichloro-carbene derivative $\text{OsCl}_2(\text{CHCH}_2\text{Ph})(\text{CO})(\text{P}^i\text{Pr}_3)_2$ (Eq. 6), which has been characterized by X-ray diffraction analysis.³⁵



The formation of this derivative goes by elimination of HCl from the starting material to afford initially a six-coordinated hydride- π -alkyne intermediate, which evolves to the insertion product. Subsequently, the styryl complex undergoes the electrophilic attack of the HCl proton at the β -carbon atom to give a cationic carbene species, followed by the coordination of the chloride anion to the metallic center (Scheme 17). In favor of this proposal, it has been observed not only that the elongated dihydrogen ligand of $\text{OsCl}_2(\eta^2\text{-H}_2)(\text{CO})(\text{P}^i\text{Pr}_3)_2$ is

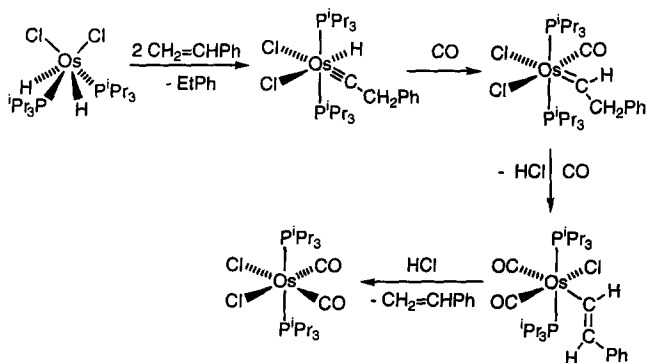


SCHEME 17.

activated toward heterolytic cleavage but also that the styryl complex Os{(E)-CH=CHPh}Cl(CO)(PⁱPr₃)₂ reacts with HCl in a manner similar to Os{(E)-CH=CHR}Cl(CO)(PⁱPr₃)₂ (R = Cy, Ru{(E)-CH=CH(CH₂)₄}Cl(CO)(PⁱPr₃)₂, to give OsCl₂(CHCH₂Ph)(CO)(PⁱPr₃)₂.

Complex OsCl₂(CHCH₂Ph)(CO)(PⁱPr₃)₂ has also been prepared according to Scheme 18.⁵³ The treatment of the complex OsH₂Cl₂(PⁱPr₃)₂ with styrene affords ethylbenzene and the carbyne derivative OsHCl₂(CCH₂Ph)(PⁱPr₃)₂, which is also formed from the reaction of OsH₂Cl₂(PⁱPr₃)₂ with phenylacetylene.⁵⁴ The carbyne compound reacts with carbon monoxide to give OsCl₂(CHCH₂Ph)(CO)(PⁱPr₃)₂, by 1,2-hydride migration from the osmium atom to the α-carbon atom of the carbyne ligand. The same method using propylene as olefin leads to OsCl₂(CHCH₂Me)(CO)(PⁱPr₃)₂,⁵³ whereas the treatment of the hydride carbene OsHCl(CHPh)(CO)(PⁱPr₃)₂ with HCl affords OsCl₂(CHPh)(CO)(PⁱPr₃)₂ and molecular hydrogen.²⁹

The reaction of OsHCl₂(CCH₂Me)(PⁱPr₃)₂ with carbon monoxide takes place within 14 h at 0.036 M and 25°C in dichloromethane-*d*₂. It has been argued that a reaction at this rate cannot occur by a mechanism in which an equilibrium amount of preformed OsCl₂(CHCH₂Me)(PⁱPr₃)₂ is attacked by CO, since DFT calculation of the energy of the optimized structure of the transition state for unimolecular rearrangement between hydride-carbyne and carbene gives an energy of

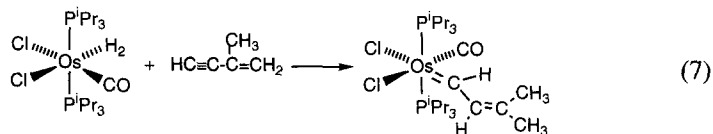


SCHEME 18.

27.2 kcal·mol⁻¹, above the carbyne, which is too large to be consistent with the observed reaction rate to form the carbonylation product. Therefore, the mechanism of this reaction should involve nucleophilic assistance of the hydride-to-carbyne-carbon migration; Os—C bond making will lower the activation energy from its unimolecular value.⁵⁵

Reaction of OsCl₂(CHCH₂Ph)(CO)(P^{*i*}Pr₃)₂ with excess carbon monoxide leads to HCl elimination to form Os{(E)-CH=CHPh}Cl(CO)₂(P^{*i*}Pr₃)₂, which reacts with the liberated HCl at the α-carbon atom to yield styrene and OsCl₂(CO)₂(P^{*i*}Pr₃)₂⁵³ (Scheme 18). The latter is also formed from the reaction of the dimer [(P^{*i*}Pr₃)₂H₂Os(μ-Cl)₃OsH₂(P^{*i*}Pr₃)₂]⁺ with carbon monoxide.⁵⁶ Abstraction of chloride from either OsHCl₂(CCH₂Ph)(P^{*i*}Pr₃)₂ or OsCl₂(CHCH₂Ph)(CO)(P^{*i*}Pr₃)₂ with NaBAR'₄ (Ar' = 3,5-C₆H₃(CF₃)₂) yields the corresponding coordinatively unsaturated carbyne and carbene complexes [OsHCl(CCH₂Ph)(P^{*i*}Pr₃)₂][BAR'₄] and [OsCl(CHCH₂Ph)(CO)(P^{*i*}Pr₃)₂][BAR'₄], respectively. The carbyne [OsHCl(CCH₂Ph)(P^{*i*}Pr₃)₂]⁺ reacts with carbon monoxide to give [OsCl(CHCH₂Ph)(CO)(P^{*i*}Pr₃)₂]⁺ after 1,2-hydride migration to the α-carbon atom of the carbyne ligand. This carbene reacts further, eliminating HCl and undergoing selective protonation, to yield [OsCl(CO)₃(P^{*i*}Pr₃)₂]⁺ and styrene.⁵³

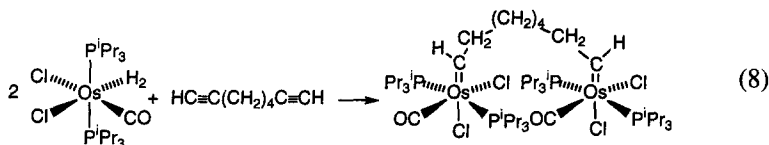
The elongated dihydrogen complex OsCl₂(η²-H₂)(CO)(P^{*i*}Pr₃)₂ also reacts with 2-methyl-1-buten-3-yne. In toluene at room temperature, the reaction affords the alkenylcarbene derivative OsCl₂{CHCH=CMe₂}(CO)(P^{*i*}Pr₃)₂ in 50% yield, after 1 h (Eq. 7).



This alkenyl-carbene complex is also obtained, in a fashion similar to OsCl₂(CHCH₂Ph)(CO)(P^{*i*}Pr₃)₂, by treatment of the dienyl compound Os{(E)-CH=CHC(Me)=CH₂}Cl(CO)(P^{*i*}Pr₃)₂ with a stoichiometric amount of a toluene HCl solution. This reaction has been rationalized as the electrophilic attack of a proton at the δ-carbon atom of the dienyl ligand to afford an unsaturated alkenyl-carbene intermediate, followed by the coordination of a chloride anion. In agreement with these two steps process, it has been observed that the addition of a stoichiometric amount of HBF₄·OEt₂ to a diethyl ether solution of Os{(E)-CH=CHC(Me)=CH₂}Cl(CO)(P^{*i*}Pr₃)₂ gives [OsCl{CHCH=CMe₂}(CO)(P^{*i*}Pr₃)₂][BF₄] in 80% yield, and that the treatment of the latter with NaCl in methanol affords OsCl₂{CHCH=CMe₂}(CO)₂(P^{*i*}Pr₃)₂ in 85% yield.

The unprecedented complex (P^{*i*}Pr₃)₂(CO)Cl₂Os{CH(CH₂)₆CH}OsCl₂(CO)(P^{*i*}Pr₃)₂ has been prepared by similar procedures with 1,7-octadiyne in a 2:1 molar ratio (Eq. 8), and by addition of a stoichiometric amount of a toluene HCl solution

to another toluene solution of $(P^iPr_3)_2(CO)ClOs\{CH=CH(CH_2)_4CH=CH\}OsCl(CO)(P^iPr_3)_2$.³⁵

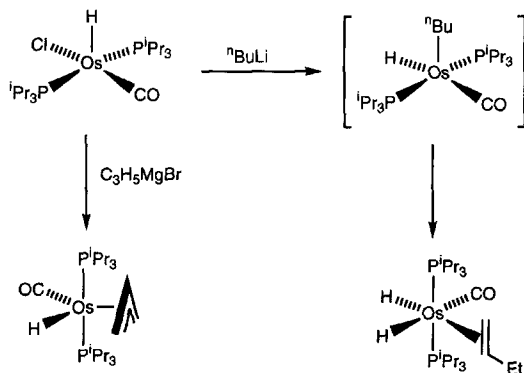


X

REACTION OF $OsHCl(CO)(P^iPr_3)_2$ WITH $n-BuLi$: THE CHEMISTRY OF THE DIHYDRIDE $OsH_2(CO)(\eta^2-CH_2=CHEt)(P^iPr_3)_2$

The complex $OsHCl(CO)(P^iPr_3)_2$ reacts with $n-BuLi$ in hexane at room temperature to give the dihydride $OsH_2(CO)(\eta^2-CH_2=CHEt)(P^iPr_3)_2$, which is isolated as a colorless oil in quantitative yield. The reaction most probably involves the replacement of the Cl^- anion by a butyl group to give $OsH(n-Bu)(CO)(P^iPr_3)_2$, which evolves into the dihydride derivative by a hydrogen β -elimination reaction (Scheme 19).⁵⁷ Treatment of $OsHCl(CO)(P^iPr_3)_2$ with C_3H_5MgBr affords $OsH(\eta^3-C_3H_5)(CO)(P^iPr_3)_2$.⁵⁸

The 1-butene ligand of $OsH_2(CO)(\eta^2-CH_2=CHEt)(P^iPr_3)_2$ can be displaced by Lewis bases. Thus, the addition of 1 equiv. of diphenylphosphine to hexane solutions of the dihydride affords $OsH_2(CO)(PPh_2)(P^iPr_3)_2$.⁵⁹ X-ray diffraction and spectroscopic studies suggest that one of the hydride ligands and the H-P hydrogen atom of the diphenylphosphine interact. The separation between them is about 2.6 Å. Although as a result of the interaction, the $\overline{P-H \cdots H-Os}$ unit forms a



SCHEME 19.

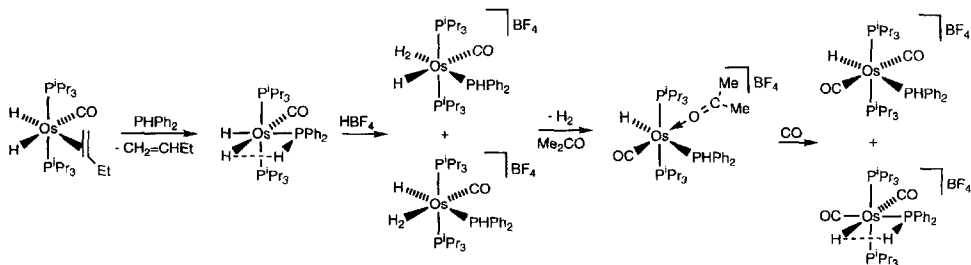
four-membered ring, in solution, the interaction is strong and blocks the free rotation of the diphenylphosphine group around the Os—PPh₂ axis.

The above mentioned interaction is electrostatic in character. As a consequence, it can be broken by addition to the OsH₂(CO)(PPh₂)(P^{*i*}Pr₃)₂ solutions of an acid stronger than the HP hydrogen atom. Thus, the reaction of OsH₂(CO)(PPh₂)(P^{*i*}Pr₃)₂ with HBF₄·OEt₂ in dichloromethane-*d*₂ as solvent gives the *cis*-hydride-dihydrogen derivative [OsH(η²-H₂)(CO)(PPh₂)(P^{*i*}Pr₃)₂]BF₄, which in solution exchanges the relative positions of the hydride and dihydrogen ligands, and does not show H···H interaction between the HP hydrogen atom of the diphenylphosphine group and the hydrogen atoms bonded to the osmium atom (Scheme 20).

The addition of acetone to a dichloromethane-*d*₂ solution of [OsH(η²-H₂)(CO)(PPh₂)(P^{*i*}Pr₃)₂]BF₄ causes the displacement of the dihydrogen ligand and the formation of the solvate complex [OsH{η¹-OCMe₂}(CO)(PPh₂)(P^{*i*}Pr₃)₂]BF₄. By passing a slow stream of carbon monoxide through a dichloromethane solution of this compound, the derivative [OsH(CO)₂(PPh₂)(P^{*i*}Pr₃)₂]BF₄ is obtained as a *ca.* 1:2 mixture of *cis*-dicarbonyl and *trans*-dicarbonyl isomers. In solution, the *trans*-dicarbonyl slowly isomerizes into the *cis* isomer.

An X-ray diffraction study on a single crystal of the *cis*-dicarbonyl derivative reveals that the structure has two crystallographically independent molecules of complex in the asymmetric unit. In both molecules the P—H group lies in quadrants bordered on the hydride ligand. However, in contrast to OsH₂(CO)(PPh₂)(P^{*i*}Pr₃)₂, the four atoms forming the four-membered P—H···H—Os ring are not coplanar. The values of the torsion angle H—Os—P are 66(3)° and −36(2)°. This seems to indicate that although there is also a H···H interaction, it is significantly weaker than that in OsH₂(CO)(PPh₂)(P^{*i*}Pr₃)₂. In agreement with this, the H···H separation in [OsH(CO)₂(PPh₂)(P^{*i*}Pr₃)₂]BF₄ is longer than that in the dihydride derivative (3.04(9) and 2.83 Å versus 2.63(5) Å).

Spectroscopic studies suggest that, in solution, the H···H interaction persists, and although it does not block the motion around the Os—PPh₂ axis, it does reduce

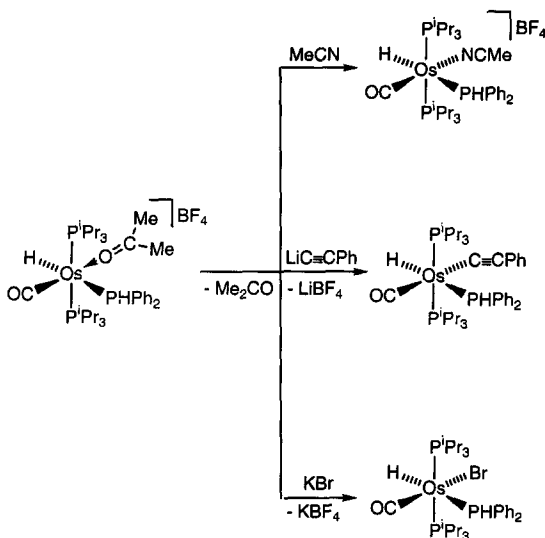


SCHEME 20.

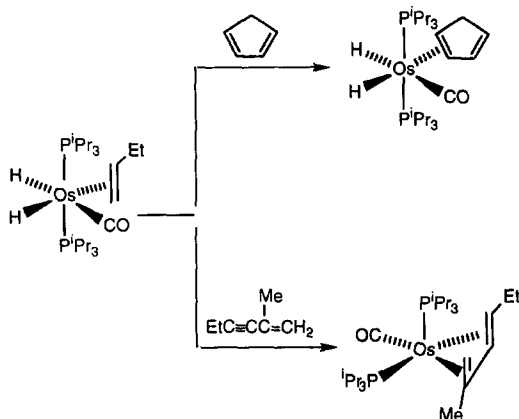
the dynamic properties of the diphenylphosphine ligand. The fluxional process in the *cis*-dicarbonyl isomer consists of an oscillation of the diphenylphosphine group around the Os—PPh₂ axis.

The acetone molecule of [OsH{ η^1 -OCMe₂}](CO)(PPh₂)(P^{*i*}Pr₃)₂]BF₄ can also be displaced by other Lewis bases. Thus, the reactions of the solvate complex with acetonitrile, lithium phenylacetylide, and potassium bromide afford the complexes [OsH(MeCN)(CO)(PPh₂)(P^{*i*}Pr₃)₂]BF₄, OsH(C₂Ph)(CO)(PPh₂)(P^{*i*}Pr₃)₂, and OsHBr(CO)(PPh₂)(P^{*i*}Pr₃)₂, respectively (Scheme 21). In these compounds, the hydride and diphenylphosphine ligand are mutually *trans* disposed, and a H...H interaction is not observed. This suggests that although the H...H interaction can contribute to the stability of a particular complex, it is not sufficient to determine its stereochemistry.

The 1-butene ligand of OsH₂(CO)(η^2 -CH₂=CHEt)(P^{*i*}Pr₃)₂ can be also displaced by cyclopentadiene to yield OsH₂(CO)(η^2 -C₅H₆)(P^{*i*}Pr₃)₂. Although the two hydride ligands and the coordinated carbon-carbon double bond of the cyclopentadiene are in a meridional arrangement around the metal center, which should lead to the rapid hydrogenation of the olefin, this complex does not evolve by hydrogenation of one of the two carbon-carbon double bonds of the diene, even at 60°C. However, the complex OsH₂(CO)(η^2 -CH₂=CHEt)(P^{*i*}Pr₃)₂, in pentane at room temperature, is capable of selectively hydrogenating the carbon-carbon triple bond of 2-methyl-1-hexene-3-yne to afford the methylhexadiene complex Os{ η^4 -CH₂=CMeCH=CHCH₂Me}(CO)(P^{*i*}Pr₃)₂ (Scheme 22).⁶⁰



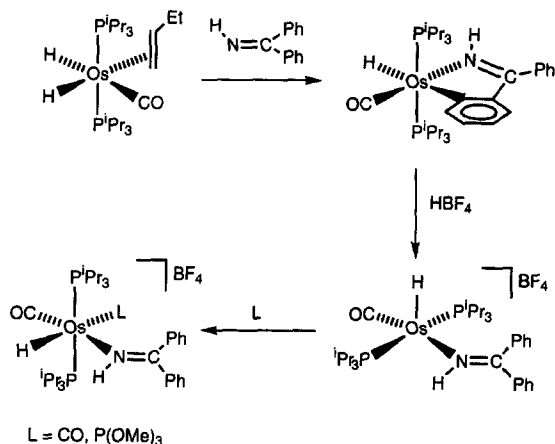
SCHEME 21.



SCHEME 22.

Treatment of the complex $\text{OsH}_2(\text{CO})(\eta^2\text{-CH}_2\text{=CHEt})(\text{P}^i\text{Pr}_3)_2$ with benzophenone imine in a 1:1 ratio in hexane at room temperature leads to the orthometallated compound $\text{OsH}\{\text{NH}=\text{C}(\text{Ph})\text{C}_6\text{H}_4\}(\text{CO})(\text{P}^i\text{Pr}_3)_2$, which is also formed by reaction of the hydride-azavinylidene complex $\text{OsH}(\text{N}=\text{CPh}_2)(\text{CO})(\text{P}^i\text{Pr}_3)_2$ with methanol.⁶¹ The orthometallated compound reacts with one equiv. of $\text{HBF}_4\cdot\text{OEt}_2$ to afford the five-coordinate cationic complex $[\text{OsH}(\text{CO})(\text{NH}=\text{CPh}_2)(\text{P}^i\text{Pr}_3)_2]^+ \text{BF}_4^-$.⁶⁰ Although monodentate nitrogen-bonded imine complexes are rare as a consequence of the weak Lewis basicity of the imine nitrogen atom,⁶² this five-coordinate derivative is relatively stable in the solid state and in solution under argon, and it is a useful starting material to prepare six-coordinate osmium-imine compounds (Scheme 23). The coordination number six for osmium can be achieved by reaction with carbon monoxide and trimethylphosphite. By passing a slow stream of this gas through a dichloromethane solution of $[\text{OsH}(\text{CO})(\text{NH}=\text{CPh}_2)(\text{P}^i\text{Pr}_3)_2] \text{BF}_4$, the *cis*-dicarbonyl complex $[\text{OsH}(\text{CO})_2(\text{NH}=\text{CPh}_2)(\text{P}^i\text{Pr}_3)_2] \text{BF}_4$ is formed, whereas the addition of one equiv. of trimethylphosphite to the five-coordinate imine complex in dichloromethane yields $[\text{OsH}(\text{CO})(\text{NH}=\text{CPh}_2)\{\text{P}(\text{OMe})_3\}(\text{P}^i\text{Pr}_3)_2] \text{BF}_4$.⁶⁰

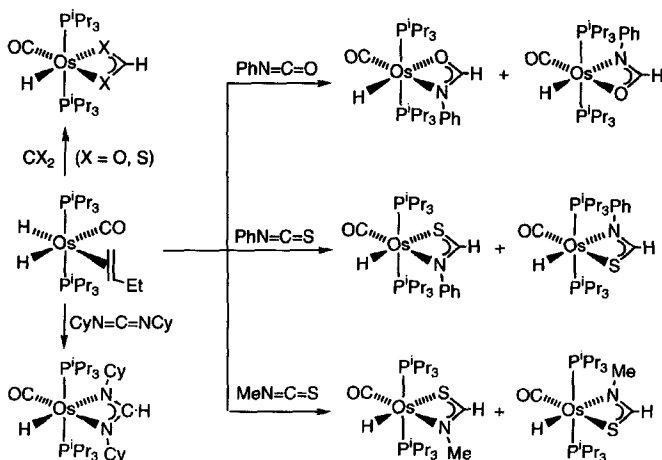
The 1-butene ligand of $\text{OsH}_2(\text{CO})(\eta^2\text{-CH}_2\text{=CHEt})(\text{P}^i\text{Pr}_3)_2$ can also be displaced by heteroallenes. These unsaturated molecules behave as electrophiles. Their δ^+ charged central carbon atom can be attacked not only by conventional nucleophiles but also by metallic bases to form $\text{M}(\eta^2\text{-C}_{\text{heteroallene}})$.⁶³ The stability of these intermediates is mainly determined by the energetics of subsequent reactions. For example, when the metal center binds a hydride ligand, the transfer of the hydride ligand from the metal to the central carbon atom of the heteroallene is generally observed.⁶⁴ In agreement with this, the reactions of $\text{OsH}_2(\text{CO})$



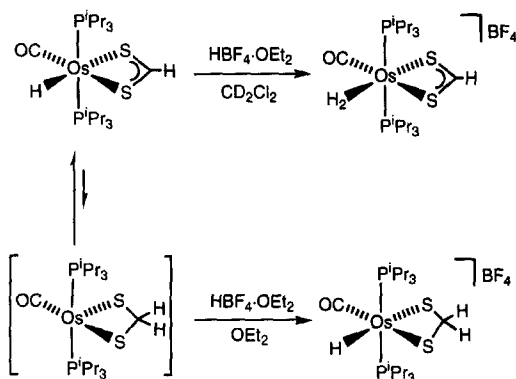
SCHEME 23.

$(\eta^2\text{-CH}_2=\text{CHEt})(\text{P}^i\text{Pr}_3)_2$ with carbon disulfide,⁵⁷ carbon dioxide,³⁶ dicyclohexylcarbodiimide, phenylisocyanate, phenylisothiocyanate, and methylisocyanate⁶⁰ lead to the corresponding insertion products (Scheme 24).

The dithioformato complex $\text{OsH}(\kappa^2\text{-S}_2\text{CH})(\text{CO})(\text{P}^i\text{Pr}_3)_2$ reacts with $\text{HBF}_4\cdot\text{OEt}_2$ to give two different derivatives depending upon the nature of the solvent used (Scheme 25). The addition of one equiv. of $\text{HBF}_4\cdot\text{OEt}_2$ to a solution of the



SCHEME 24.



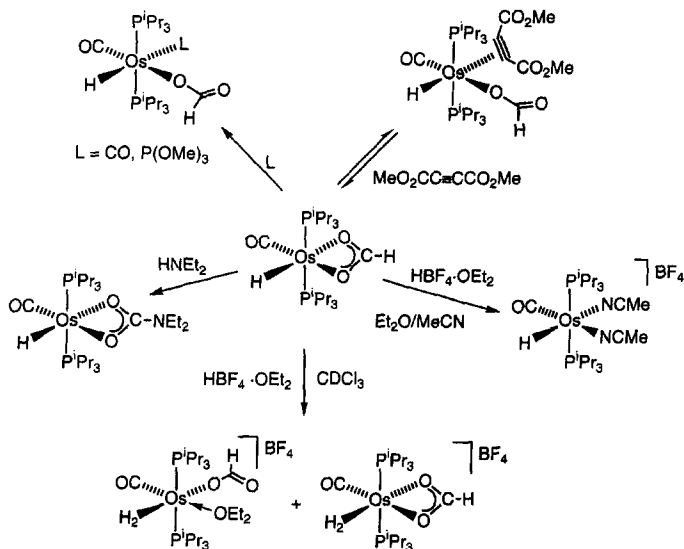
SCHEME 25.

dithioformato complex in dichloromethane-*d*₂ leads, after a few seconds, to the dihydrogen compound [Os(κ²-S₂CH)(η²-H₂)(CO)(PⁱPr₃)₂]BF₄, with a H-H separation of 1.00 Å, while the methanedithiolate derivative [OsH(κ²-S₂CH₂)(CO)(PⁱPr₃)₂]BF₄ is obtained when the reaction is carried out in diethyl ether as solvent.⁵⁷ In this context, it should be mentioned that although the insertion reactions of carbon disulfide into metal-hydride bonds are common, the reduction of carbon disulfide to methanedithiolate has been seen only in a few cases⁶⁵ and, as far as we know, never by reaction of a dithioformato complex with an acid.

Direct attack of the proton at the carbon atom of the dithioformate ligand does not seem likely in view of the electrophilicity of this atom. Hence, it has been proposed that in diethyl ether solution the dithioformato complex is in equilibrium with a nondetected amount of Os(κ²-S₂CH₂)(CO)(PⁱPr₃)₂, which could undergo the attack of the acid. In good agreement with this assumption, Jia *et al.*⁶⁶ have observed that the complex RuH(κ²-S₂CH)(Cyttp) (Cyttp = PhP(CH₂CH₂CH₂PCy₂)₂) is unstable in benzene solution, and slowly isomerizes into Ru(κ²-S₂CH₂)(Cyttp).

The formato complex OsH(κ²-O₂CH)(CO)(PⁱPr₃)₂ has also been prepared by treatment of the hydride-chloro compound OsHCl(CO)(PⁱPr₃)₂ with NaOMe in benzene-methanol under carbon dioxide atmosphere. Under the same conditions, the reaction with carbon disulfide affords OsH(κ²-S₂COMe)(CO)(PⁱPr₃)₂.⁶⁷

The bidentate formate ligand of OsH(κ²-O₂CH)(CO)(PⁱPr₃)₂ is converted into a monodentate group by carbonylation. Thus, the reaction of this compound with carbon monoxide gives OsH{κ¹-OC(O)H}(CO)₂(PⁱPr₃)₂. Similarly, the addition of a stoichiometric amount of trimethylphosphite yields OsH{κ¹-OC(O)H}(CO){P(OMe)₃}(PⁱPr₃)₂, and the addition of a stoichiometric amount of ethyne dicarboxylic methyl ester leads to OsH{κ¹-OC(O)H}(CO)(η²-MeO₂CC≡CCO₂Me)(PⁱPr₃)₂, which in solution partially dissociates the alkyne. As is shown in

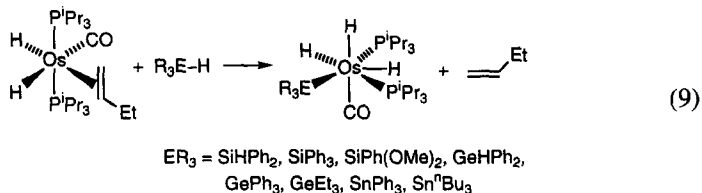


SCHEME 26.

Scheme 26, the reactions of $\text{OsH}(\kappa^2\text{-O}_2\text{CH})(\text{CO})(\text{P}^i\text{Pr}_3)_2$ with $\text{HBF}_4 \cdot \text{OEt}_2$ lead to different derivatives depending upon the conditions. In diethyl ether as solvent the reaction produces a very unsaturated $[\text{OsH}(\text{CO})(\text{P}^i\text{Pr}_3)_2]^+$ fragment, which can be trapped with acetonitrile to give $[\text{OsH}(\text{CO})(\text{MeCN})_2(\text{P}^i\text{Pr}_3)_2]\text{BF}_4$. However, in chloroform-*d*, the electrophilic attack of the proton occurs at the hydride ligand and/or the metal to afford a mixture of products, mainly dihydrogen derivatives. On the basis of theoretical calculations and T_1 measurements, it has been proposed that these derivatives could be the cations $[\text{Os}\{\kappa^2\text{-O}_2\text{CH}\}(\eta^2\text{-H}_2)(\text{CO})(\text{P}^i\text{Pr}_3)_2]^+$ and $[\text{Os}\{\kappa^1\text{-OC(O)H}\}(\eta^2\text{-H}_2)(\text{Et}_2\text{O})(\text{CO})(\text{P}^i\text{Pr}_3)_2]^+$. In addition, it should be mentioned that the carbon atom of the formate ligand of $\text{OsH}(\kappa^2\text{-O}_2\text{CH})(\text{CO})(\text{P}^i\text{Pr}_3)_2$ is the electrophilic center of the molecule, and therefore susceptible to attack by nucleophiles. Thus, the addition of diethyl amine to the solutions of this compound produces the carbamato derivative $\text{OsH}(\kappa^2\text{-O}_2\text{CNEt}_2)(\text{CO})(\text{P}^i\text{Pr}_3)_2$.³⁶

The previously mentioned reactions of $\text{OsH}_2(\text{CO})(\eta^2\text{-CH}_2=\text{CHEt})(\text{P}^i\text{Pr}_3)_2$ indicate that this complex has a high tendency to release the olefin ligand. At the time the resulting unsaturated fragment $\text{OsH}_2(\text{CO})(\text{P}^i\text{Pr}_3)_2$ shows a relatively strong Lewis base character, which becomes apparent in its reactivity with group 14 element hydride compounds. Complex $\text{OsH}_2(\text{CO})(\eta^2\text{-CH}_2=\text{CHEt})(\text{P}^i\text{Pr}_3)_2$ reacts with $\text{R}_3\text{E-H}$ ($\text{R} = \text{Si}, \text{Ge}, \text{Sn}$) by oxidative addition to give the corresponding $\text{OsH}_3(\text{ER}_3)(\text{CO})(\text{P}^i\text{Pr}_3)_2$ (Eq. 9), which can be formulated as derivatives of osmium(IV) with a weak H-E agostic interaction.⁶⁸

X-ray diffraction and spectroscopic studies and theoretical calculations indicate that for the three types of compounds the arrangement of the ligands around the osmium atom is the same. In the solid state and in solution at very low temperatures the coordination polyhedron can be described as a very distorted pentagonal bipyramid with a hydride ligand and the carbonyl group in the axial positions. The other two hydride ligands lie in the equatorial plane, one between the phosphine ligands and the other between the R_3E group and one of the phosphine ligands. In solution at room temperature all compounds are fluxional.



Under hydrogen atmosphere, the complex $\text{OsH}_2(\text{CO})(\eta^2\text{-CH}_2\text{=CHEt})(\text{P}^i\text{Pr}_3)_2$ affords the derivative $\text{OsH}_2(\eta^2\text{-H}_2)(\text{CO})(\text{P}^i\text{Pr}_3)_2$ ⁶⁹ which, in contrast to $\text{OsH}_3(\text{ER}_3)(\text{CO})(\text{P}^i\text{Pr}_3)_2$, shows nonclassical interaction between two of the four hydrogen atoms bonded to the osmium atom. In solution, these atoms exchange their positions giving in the ¹H NMR spectra only one resonance, which has a $T_{1\text{min}}$ of 32 ms at -67°C .⁷⁰

Ab initio DFT calculations on the model compound $\text{OsH}_2(\eta^2\text{-H}_2)(\text{CO})(\text{PH}_3)_2$ indicate that the dihydrogen ligand lies *trans* to a hydride, and that the separation between the hydrogen atoms of the dihydrogen is 0.87 Å. On the basis of separate optimization of the 16-electron $\text{OsH}_2(\text{CO})(\text{PH}_3)_2$ species and free molecular hydrogen, an Os—H₂ bond dissociation energy of 18.9 kcal·mol⁻¹ is calculated. The preferred conformation of the dihydrogen ligand is found to be when the H—H vector eclipses the Os—H bond (i.e., lies in the xz plane). However, the barrier to rotation is calculated to be very small, 0.54 kcal·mol⁻¹. This comes from the fact that back bonding is better in the plane containing the phosphines, since π_{CO}^* in the orthogonal plane stabilizes the d_{xz} orbital. However, the interaction with the *cis* hydride compensates the loss of back bonding in the plane of the carbonyl group and favors the conformation with the lesser back donation. The observed dihydrogen alignment is also sterically favored, especially when considering the additional bulk of the phosphines used experimentally.⁷⁰

Regarding $\text{OsHX}(\eta^2\text{-H}_2)(\text{CO})(\text{P}^i\text{Pr}_3)$ (X = Cl, H), it should be mentioned that the stronger electron-donor halide, when *cis* to the dihydrogen, facilitates loss of molecular hydrogen. The complete absence of π -donor ability (when X = H) renders dihydrogen loss most difficult. However, a π -donor *trans* to the dihydrogen ligand also makes the dihydrogen loss unobservable, as is the case of $\text{OsCl}_2(\eta^2\text{-H}_2)(\text{CO})(\text{P}^i\text{Pr}_3)_2$.⁷⁰

XI

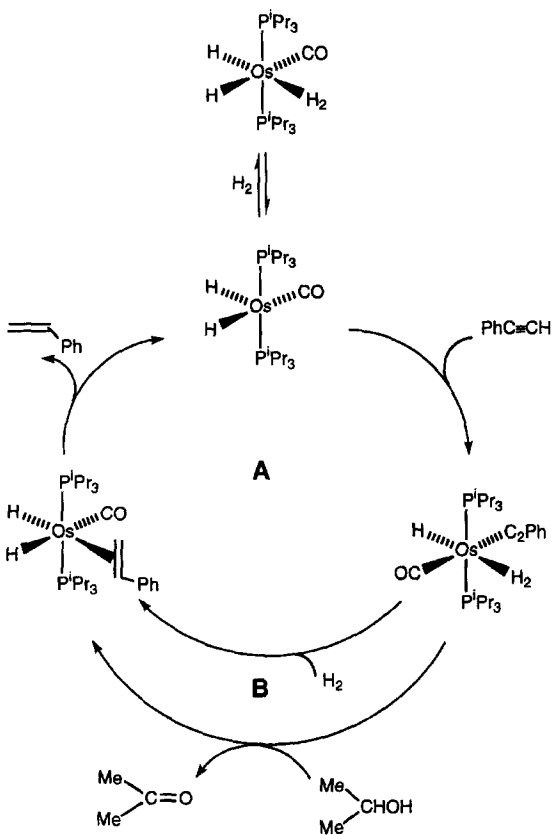
**REACTIONS OF $\text{OsH}_2(\eta^2\text{-H}_2)(\text{CO})(\text{P}^i\text{Pr}_3)_2$ WITH ALKYNES: ALKYNYL
AND RELATED COMPOUNDS**

The reactivity of the dihydride-dihydrogen complex $\text{OsH}_2(\eta^2\text{-H}_2)(\text{CO})(\text{P}^i\text{Pr}_3)_2$ toward alkynes is as expected for the 16-electron dihydride $\text{OsH}_2(\text{CO})(\text{P}^i\text{Pr}_3)_2$, suggesting that in solution the dihydride-dihydrogen complex dissociates the hydrogen molecule. Thus, the reaction of $\text{OsH}_2(\eta^2\text{-H}_2)(\text{CO})(\text{P}^i\text{Pr}_3)_2$ with one equiv. of phenylacetylene affords the alkynyl-hydride-dihydrogen $\text{OsH}_2(\text{C}_2\text{Ph})(\eta^2\text{-H}_2)(\text{CO})(\text{P}^i\text{Pr}_3)_2$, which can be spectroscopically characterized under hydrogen atmosphere. When the hydrogen atmosphere is evacuated and the system refilled with argon, the 16-electron derivative $\text{OsH}_2(\text{C}_2\text{Ph})(\text{CO})(\text{P}^i\text{Pr}_3)_2$ is formed. After several hours under hydrogen atmosphere, the dihydrogen complex is converted into $\text{OsH}_2(\text{CO})(\eta^2\text{-CH}_2=\text{CHPh})(\text{P}^i\text{Pr}_3)_2$, which subsequently evolves into $\text{OsH}_2(\eta^2\text{-H}_2)(\text{CO})(\text{P}^i\text{Pr}_3)_2$ and styrene. Complex $\text{OsH}_2(\text{CO})(\eta^2\text{-CH}_2=\text{CHPh})(\text{P}^i\text{Pr}_3)_2$ can also be formed from $\text{OsH}(\text{C}_2\text{Ph})(\eta^2\text{-H}_2)(\text{CO})(\text{P}^i\text{Pr}_3)_2$ under argon atmosphere by stirring in 2-propanol, which dehydrogenates into acetone.⁷¹ These chemical transformations can be elegantly accommodated by the cycles shown in Scheme 27. Cycle **A** summarizes the stoichiometric reduction of phenylacetylene with molecular hydrogen in the presence of $\text{OsH}_2(\eta^2\text{-H}_2)(\text{CO})(\text{P}^i\text{Pr}_3)_2$, whereas cycle **B** contains the stoichiometric steps for the hydrogen transfer from 2-propanol to phenylacetylene.

Complex $\text{OsH}_2(\eta^2\text{-H}_2)(\text{CO})(\text{P}^i\text{Pr}_3)_2$ reacts with trimethylsilyl acetylene in a manner similar to that of phenylacetylene, giving rise to the related alkynyl-hydride-dihydrogen compound $\text{OsH}(\text{C}_2\text{SiMe}_3)(\eta^2\text{-H}_2)(\text{CO})(\text{P}^i\text{Pr}_3)_2$. Spectroscopic studies indicate that both $\text{OsH}(\text{C}_2\text{R})(\eta^2\text{-H}_2)(\text{CO})(\text{P}^i\text{Pr}_3)_2$ derivatives are not only isoelectronic with $\text{OsHCl}(\eta^2\text{-H}_2)(\text{CO})(\text{P}^i\text{Pr}_3)_2$ but also isostructural, showing a similar reactivity pattern toward Lewis bases. Thus, their reactions with this type of ligand lead to the corresponding six-coordinate alkynyl-hydride derivatives $\text{OsH}(\text{C}_2\text{R})(\text{CO})\text{L}(\text{P}^i\text{Pr}_3)_2$ and molecular hydrogen (Scheme 28).

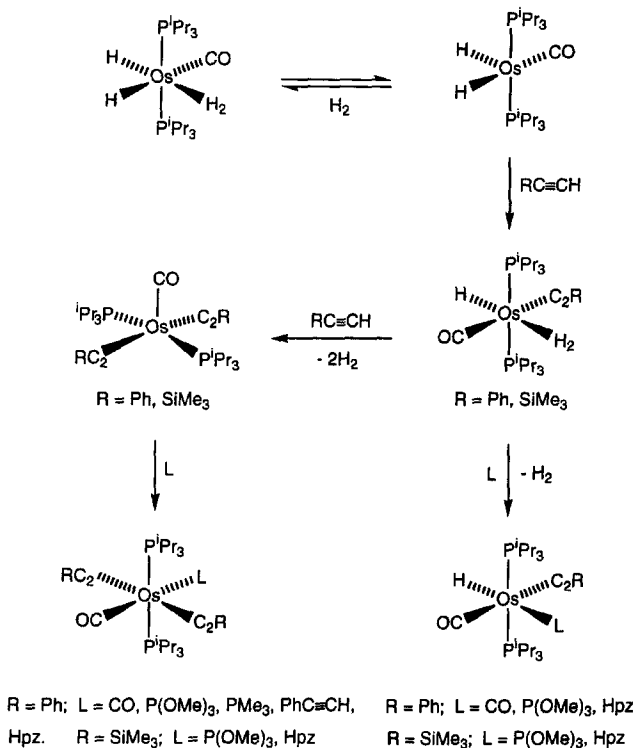
There is, however, a marked difference in reactivity between $\text{OsHCl}(\eta^2\text{-H}_2)(\text{CO})(\text{P}^i\text{Pr}_3)_2$ and $\text{OsH}(\text{C}_2\text{R})(\eta^2\text{-H}_2)(\text{CO})(\text{P}^i\text{Pr}_3)_2$ toward terminal alkynes. While the hydride-chloro compound reacts with phenylacetylene to give $\text{Os}\{(E)\text{-CH=CHPh}\}\text{Cl}(\text{CO})(\text{P}^i\text{Pr}_3)_2$, the alkynyl analogues upon treatment with one equiv. of the corresponding alkynes give molecular hydrogen and the bis-alkynyl compounds $\text{Os}(\text{C}_2\text{R})_2(\text{CO})(\text{P}^i\text{Pr}_3)_2$, which coordinate Lewis bases to afford six-coordinate bis-alkynyl derivatives.^{71,72}

Although the Lewis basicity of the nitrogen atom of imines is weak, the bis-alkynyl complex $\text{Os}(\text{C}_2\text{Ph})_2(\text{CO})(\text{P}^i\text{Pr}_3)_2$ also coordinates benzophenone imine to give the six-coordinate bis-alkynyl complex $\text{Os}(\text{C}_2\text{Ph})_2(\text{CO})(\text{NH=CPh}_2)(\text{P}^i\text{Pr}_3)_2$,



which is isolated as a 1:3 mixture of *cis*-bis-alkynyl and *trans*-bis-alkynyl isomers. In toluene under reflux, the mixture is converted into the *ortho*-metallated compound $\text{Os}(\text{C}_2\text{Ph})\{\text{NH}=\text{C}(\text{Ph})\text{C}_6\text{H}_4\}(\text{CO})(\text{P}^i\text{Pr}_3)$. This complex reacts with $\text{HBF}_4 \cdot \text{OH}_2$ to give phenylacetylene and $[\text{Os}\{\text{NH}=\text{C}(\text{Ph})\text{C}_6\text{H}_4\}(\text{CO})(\text{H}_2\text{O})(\text{P}^i\text{Pr}_3)_2]\text{BF}_4$, which by reaction with MeLi affords $\text{Os}(\text{Me})\{\text{NH}=\text{C}(\text{Ph})\text{C}_6\text{H}_4\}(\text{CO})(\text{P}^i\text{Pr}_3)_2$ (Scheme 29).⁷³

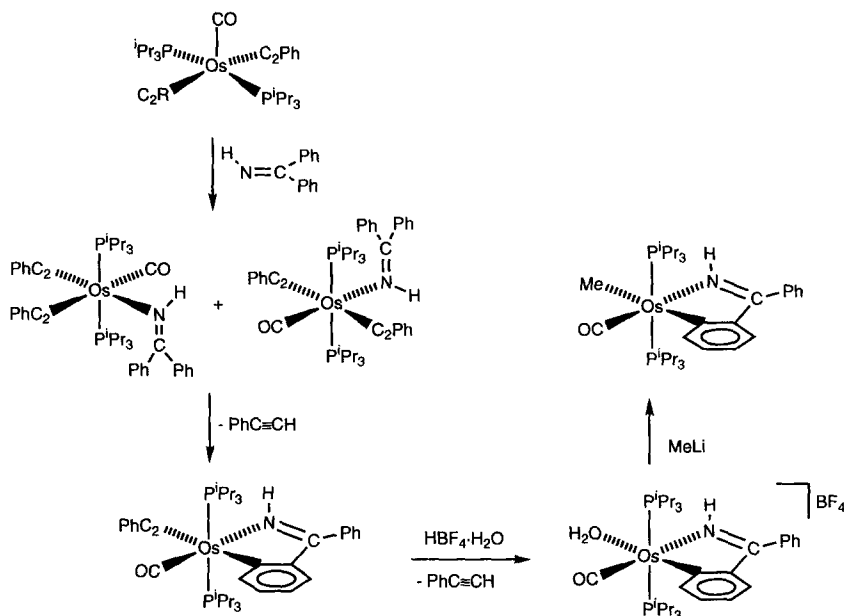
The bis-alkynyl complex $\text{Os}(\text{C}_2\text{Ph})_2(\text{CO})(\text{P}^i\text{Pr}_3)_2$ reacts with molecular hydrogen to give $\text{OsH}(\text{C}_2\text{Ph})(\eta^2\text{-H}_2)(\text{CO})(\text{P}^i\text{Pr}_3)_2$ and styrene. This reaction and that previously mentioned between $\text{OsH}(\text{C}_2\text{Ph})(\eta^2\text{-H}_2)(\text{CO})(\text{P}^i\text{Pr}_3)_2$ and phenylacetylene to give $\text{Os}(\text{C}_2\text{Ph})_2(\text{CO})(\text{P}^i\text{Pr}_3)_2$ can be accommodated by the cycle shown in Scheme 30, which illustrates a new stoichiometric hydrogenation of phenylacetylene to styrene where, visibly, styryl intermediates are not involved.⁷¹



SCHEME 28.

Under argon, in 2-propanol and in the presence of traces of water, the carbon-carbon triple bond of one of the two alkynyl ligands of the complex $\text{Os}(\text{C}_2\text{Ph})_2(\text{CO})(\text{P}^i\text{Pr}_3)_2$ can be broken to give $\text{Os}(\text{CH}_2\text{Ph})(\text{C}_2\text{Ph})(\text{CO})_2(\text{P}^i\text{Pr}_3)_2$. The reaction involves a metal-promoted, hydration disproportionation of the transformed alkynyl ligand catalyzed by the solvent. Thus, the treatment of $\text{Os}(\text{C}_2\text{Ph})_2(\text{CO})(\text{P}^i\text{Pr}_3)_2$ with H_2^{18}O yields $\text{Os}(\text{CH}_2\text{Ph})(\text{C}_2\text{Ph})(\text{C}^{18}\text{O})(\text{CO})(\text{P}^i\text{Pr}_3)_2$, and the reaction of $\text{Os}(\text{C}_2\text{Ph})_2(\text{CO})(\text{P}^i\text{Pr}_3)_2$ with water in the presence of deuterated 2-propanol affords $\text{Os}(\text{CD}_2\text{Ph})(\text{C}_2\text{Ph})(\text{CO})_2(\text{P}^i\text{Pr}_3)_2$ (Scheme 31).⁷⁴

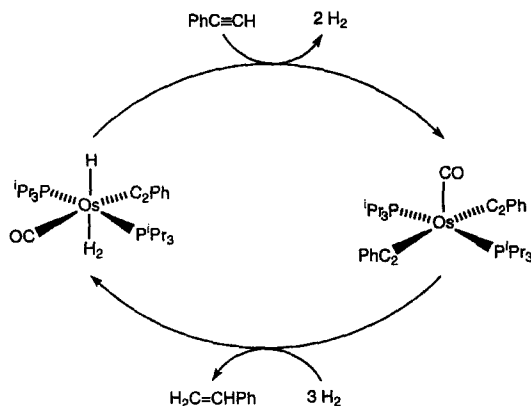
The process has been rationalized according to Scheme 32. The initial step could involve the electrophilic attack of the -OH proton from the alcohol to the β -carbon atom of one of the alkynyl ligands. The alkoxide anion formed should regenerate 2-propanol by water deprotonation. At this stage, the OH^- anion would attack the vinylidene ligand to give an α -hydroxy-alkenyl group. This is in agreement with studies on vinylidene complexes, which have identified the electron deficiency of the vinylidenes at the α -carbon atom.⁷⁵ The reaction of the α -hydroxy-alkenyl species with a second 2-propanol molecule could yield a hydroxy-carbene



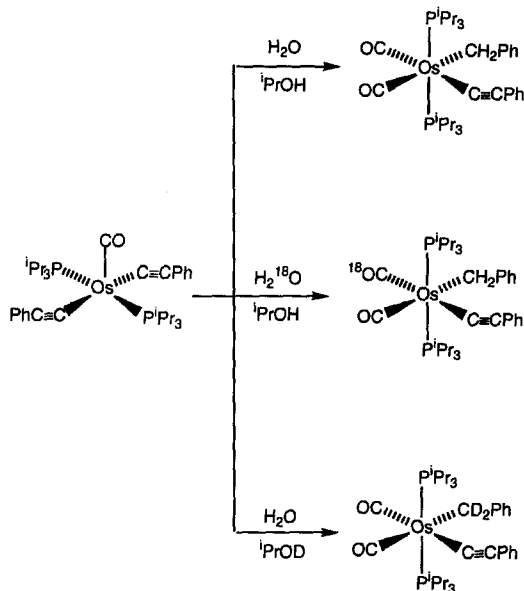
SCHEME 29.

intermediate. The deprotonation of the hydroxy-carbene group by the alkoxide anion formed in the last step should afford an acyl complex. Finally, the CO deinsertion could give $\text{Os}(\text{CH}_2\text{Ph})(\text{C}_2\text{Ph})(\text{CO})_2(\text{P}^i\text{Pr}_3)_2$.

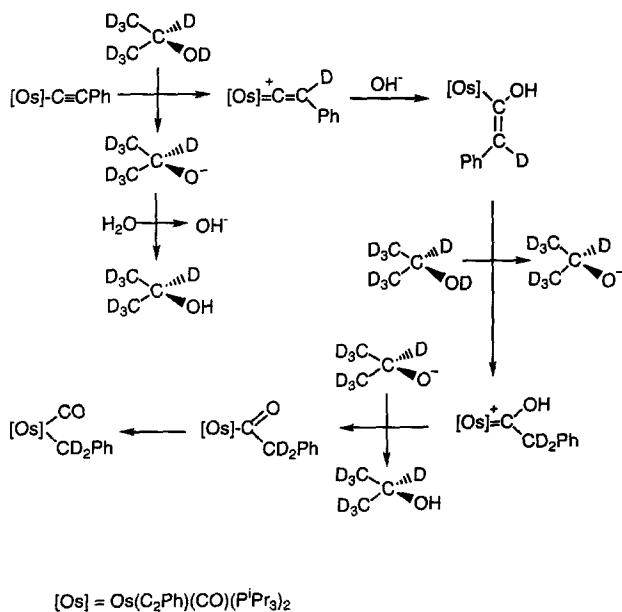
Although a reaction pattern similar to that mentioned for phenylacetylene and trimethylsilylacetylene might be expected for terminal activated alkynes,



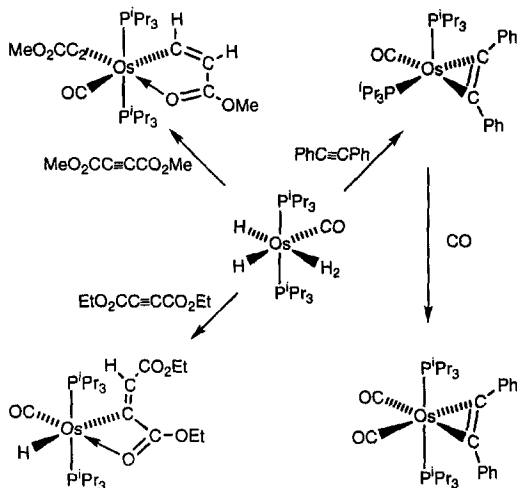
SCHEME 30.



SCHEME 31.



SCHEME 32.

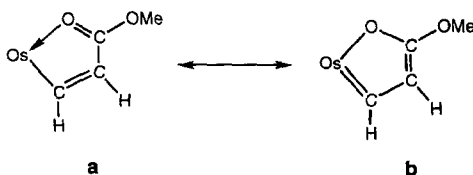


SCHEME 33.

methylpropiolate reacts with $\text{OsH}_2(\eta^2\text{-H}_2)(\text{CO})(\text{P}^i\text{Pr}_3)_2$ to afford the alkynyl-alkenyl derivative $\text{Os}(\text{C}_2\text{CO}_2\text{Me})\{\text{CH}=\text{CHC}(\text{O})\text{OMe}\}(\text{CO})(\text{P}^i\text{Pr}_3)_2$ (Scheme 33).

The molecular structure of this compound determined by X-ray diffraction analysis reveals a significant contribution of the resonance form **b** (Scheme 34) to the osmium alkenyl bond, which is improved by the presence of the carboxyl substituent.⁷¹

The complex $\text{OsH}_2(\eta^2\text{-H}_2)(\text{CO})(\text{P}^i\text{Pr}_3)_2$ also reacts with internal alkynes; the reaction with diphenylacetylene leads to *cis*- and *trans*-stilbene and $\text{Os}(\eta^2\text{-C}_2\text{Ph}_2)(\text{CO})(\text{P}^i\text{Pr}_3)_2$ which has been characterized by X-ray diffraction analysis. The structural analysis reveals a smaller contribution of *sp* hybridization of the acetylenic carbon atoms, and a loss of the acetylenic character of the C_2Ph_2 group. As a result, the $\text{Os}-\text{C}$ bonds are very strong, and the carbonylation of $\text{Os}(\eta^2\text{-C}_2\text{Ph}_2)(\text{CO})(\text{P}^i\text{Pr}_3)_2$ does not produce the displacement of C_2Ph_2 ; the addition of carbon monoxide gives $\text{Os}(\eta^2\text{-C}_2\text{Ph}_2)(\text{CO})_2(\text{P}^i\text{Pr}_3)_2$. The formation of stilbene from the reaction of $\text{OsH}_2(\eta^2\text{-H}_2)(\text{CO})(\text{P}^i\text{Pr}_3)_2$ with diphenylacetylene probably involves hydride-alkenyl species as intermediates. In this context, it should be mentioned that complex $\text{OsH}_2(\eta^2\text{-H}_2)(\text{CO})(\text{P}^i\text{Pr}_3)_2$ reacts with



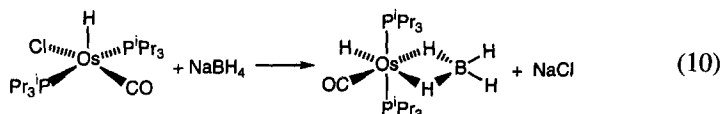
SCHEME 34.

diethylacetylenedicarboxylate to afford the hydride-alkenyl $\overline{\text{OsH}\{\text{C}[\text{C}(\text{O})\text{OEt}]\text{=CHCO}_2\text{Et}\}(\text{CO})(\text{P}^i\text{Pr}_3)_2}$ (Scheme 33).⁷⁶

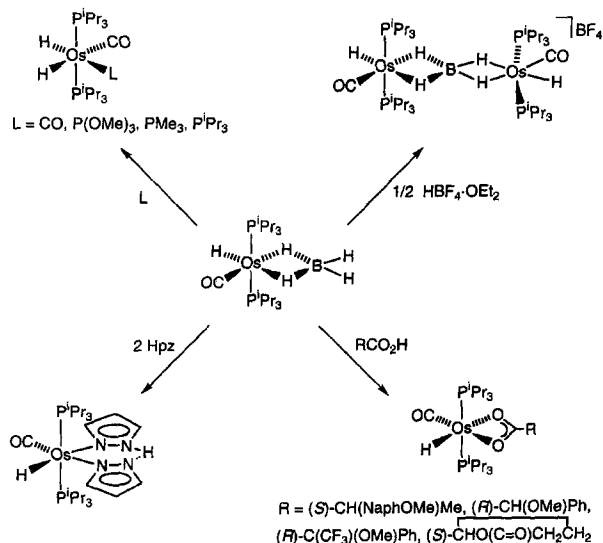
XII

REACTION OF $\text{OsHCl}(\text{CO})(\text{P}^i\text{Pr}_3)_2$ WITH NaBH_4 : THE CHEMISTRY OF $\text{OsH}(\eta^2\text{-H}_2\text{BH}_2)(\text{CO})(\text{P}^i\text{Pr}_3)_2$

The reaction of $\text{OsHCl}(\text{CO})(\text{P}^i\text{Pr}_3)_2$ with NaBH_4 in methanol leads to the octahedral compound $\text{OsH}(\eta^2\text{-H}_2\text{BH}_2)(\text{CO})(\text{P}^i\text{Pr}_3)_2$ (Eq. 10), which has a rigid structure in solution only at low temperatures. Above ca. -30°C an exchange process takes place, which involves the bridging hydrogen atoms and the terminal hydrogens attached to boron but not the metal hydride ligand.¹³



This tetrahydridoborate complex reacts with Lewis bases L such as CO, $\text{P}(\text{OMe})_3$, PMe_3 , and P^iPr_3 to form dihydride-osmium(II) complexes $\text{OsH}_2(\text{CO})\text{L}(\text{P}^i\text{Pr}_3)_2$, whereas the reactions with electrophiles afford monohydride derivatives (Scheme 35). The reaction with $\text{HBF}_4 \cdot \text{OEt}_2$ leads to the binuclear complex $[(\text{P}^i\text{Pr}_3)_2(\text{CO})\text{Hos}(\mu\text{-}\eta^4\text{-H}_2\text{BH}_2)\text{OsH}(\text{CO})(\text{P}^i\text{Pr}_3)_2]\text{BF}_4$, consisting of two OsH

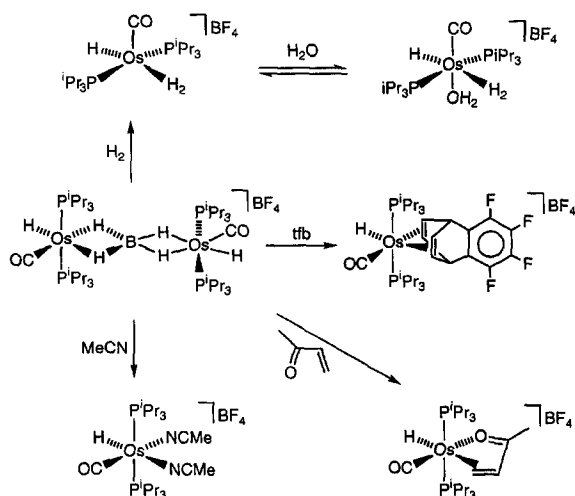


SCHEME 35.

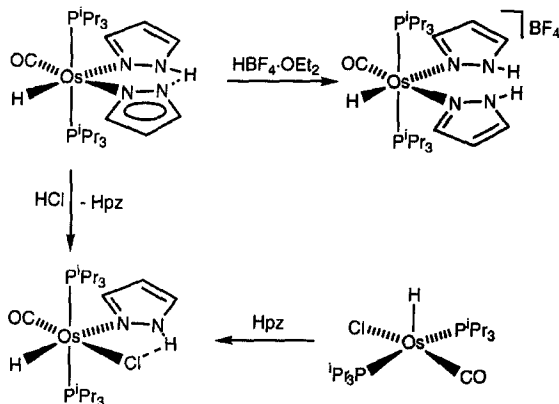
(CO)(PⁱPr₃)₂ fragments bridged by a tetrahedral BH₄ unit. The reactions with carboxylic acids and pyrazole give the mononuclear compounds OsH(κ²-O₂CR)(CO)(PⁱPr₃)₂ and OsH(pz)(CO)(Hpz)(PⁱPr₃)₂, respectively.⁷⁷ It should be pointed out that the N—H hydrogen atom of the pyrazole ligand of OsH(pz)(CO)(Hpz)(PⁱPr₃)₂ lies between this azole group and the pyrazolate forming an intramolecular N...H...N hydrogen bond, as has been proved for the related vinylidene complex OsH(pz)(C=CHPh)(Hpz)(PⁱPr₃)₂ by X-ray diffraction analysis.⁷⁸

The complex [(PⁱPr₃)₂(CO)HOs(μ-η⁴-H₂BH₂)OsH(CO)(PⁱPr₃)₂]BF₄ can be considered to be the result of the stabilization of the unsaturated [OsH(CO)(PⁱPr₃)₂]⁺ fragment by OsH(η²-H₂BH₂)(CO)(PⁱPr₃)₂. So, the mononuclear tetrahydroborate complex is a metalloligand that can be displaced by other coordinating molecules. Thus, under normal conditions (25°C, 1 atm of hydrogen), the binuclear tetrahydridoborate complex reacts with molecular hydrogen to afford the five-coordinate hydride-dihydrogen complex [OsH(η²-H₂)(CO)(PⁱPr₃)₂]BF₄, which coordinates water to give [OsH(η²-H₂)(CO)(H₂O)(PⁱPr₃)₂]BF₄. In chloroform-*d* as solvent, the latter is converted into its precursor by dissociation of the water molecule (ca. 20% in 1 h). Complex OsH(η²-H₂BH₂)(CO)(PⁱPr₃)₂ can also be displaced from [(PⁱPr₃)₂(CO)HOs(μ-η⁴-H₂BH₂)OsH(CO)(PⁱPr₃)₂]BF₄ by tetrafluorobenzobarrelene (tfb), methyl vinyl ketone, and acetonitrile. These displacement reactions lead to [OsH(CO)(tfb)(PⁱPr₃)₂]BF₄, [OsH(CO){π-CH₂=CHC(=O)Me}(PⁱPr₃)₂]BF₄, and [OsH(CO)(MeCN)₂(PⁱPr₃)₂]BF₄, respectively (Scheme 36).⁷⁷

The complex OsH(pz)(CO)(Hpz)(PⁱPr₃)₂ is a useful starting material to prepare new pyrazole compounds. Reaction with HBF₄·OEt₂ leads to the cation



SCHEME 36.



SCHEME 37.

$[\text{OsH}(\text{CO})(\text{Hpz})_2(\text{P}^i\text{Pr}_3)_2]\text{BF}_4$, which can be deprotonated by NaH , while treatment with HCl gives the neutral hydride-chloro complex $\text{OsHCl}(\text{CO})(\text{Hpz})(\text{P}^i\text{Pr}_3)_2$, which can also be prepared by addition of pyrazole to $\text{OsHCl}(\text{CO})(\text{P}^i\text{Pr}_3)_2$ (Scheme 37).⁷⁷

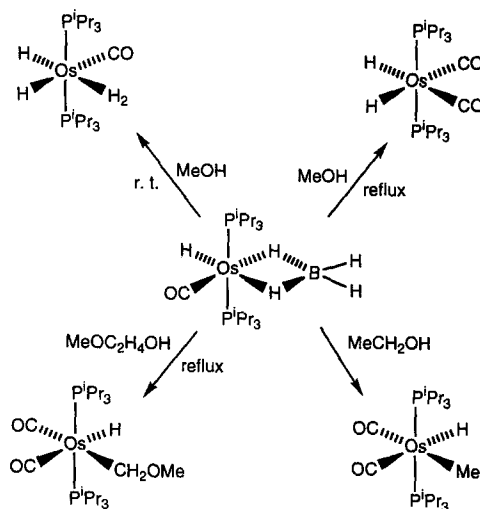
XIII

DECOMPOSITION OF $\text{OsH}(\eta^2\text{-H}_2\text{BH}_2)(\text{CO})(\text{P}^i\text{Pr}_3)_2$ IN THE PRESENCE OF ALCOHOLS: SYNTHESIS AND REACTIONS OF HYDRIDE-ALKYL COMPOUNDS

At room temperature in methanol as solvent, complex $\text{OsH}(\eta^2\text{-H}_2\text{BH}_2)(\text{CO})(\text{P}^i\text{Pr}_3)_2$ decomposes to give the dihydride-dihydrogen compound $\text{OsH}_2(\eta^2\text{-H}_2)(\text{CO})(\text{P}^i\text{Pr}_3)_2$. If the decomposition, however, is carried out under reflux the *cis*-dihydride-*cis*-dicarbonyl derivative $\text{OsH}_2(\text{CO})_2(\text{P}^i\text{Pr}_3)_2$ is formed.¹³

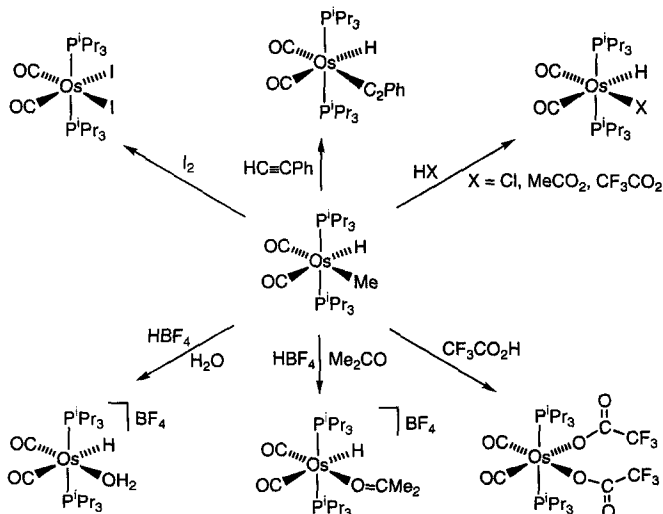
Treatment of $\text{OsH}(\eta^2\text{-H}_2\text{BH}_2)(\text{CO})(\text{P}^i\text{Pr}_3)_2$ with ethanol under reflux does not lead to the formation of $\text{OsH}_2(\text{CO})_2(\text{P}^i\text{Pr}_3)_2$ but instead gives the hydride-methyl osmium(II) compound $\text{OsHMe}(\text{CO})_2(\text{P}^i\text{Pr}_3)_2$ in good yield. 2-Methoxyethanol behaves in a manner similar to ethanol, and the reaction with the tetrahydridoborate complex yields $\text{OsH}(\text{CH}_2\text{OMe})(\text{CO})_2(\text{P}^i\text{Pr}_3)_2$ (Scheme 38).⁷⁹

The hydride-methyl complex $\text{OsH}(\text{Me})(\text{CO})_2(\text{P}^i\text{Pr}_3)_2$ reacts with electrophilic reagents. The reaction products depend on the nature of the reagent (Scheme 39). Whereas the reaction with iodine gives almost quantitatively the diiodide $\text{OsI}_2(\text{CO})_2(\text{P}^i\text{Pr}_3)_2$, the reaction with a five-fold excess of phenylacetylene does not lead to the formation of the previously mentioned bis-alkynyl complex



SCHEME 38.

$\text{Os}(\text{C}_2\text{Ph})_2(\text{CO})_2(\text{P}^i\text{Pr}_3)_2$. It gives instead the hydride-alkynyl $\text{OsH}(\text{C}_2\text{Ph})(\text{CO})_2(\text{P}^i\text{Pr}_3)_2$ in 71% yield. Similarly, upon treatment of $\text{OsH}(\text{Me})(\text{CO})_2(\text{P}^i\text{Pr}_3)_2$ with HCl , MeCO_2H , and $\text{CF}_3\text{CO}_2\text{H}$ the monohydrides $\text{OsHX}(\text{CO})_2(\text{P}^i\text{Pr}_3)_2$ ($\text{X} = \text{Cl}$, MeCO_2 , CF_3CO_2) are obtained. The reaction with excess trifluoroacetic acid in benzene under reflux gives the bis-trifluoroacetate $\text{Os}\{\kappa^1\text{-OC}(\text{O})\text{CF}_3\}_2(\text{CO})_2$

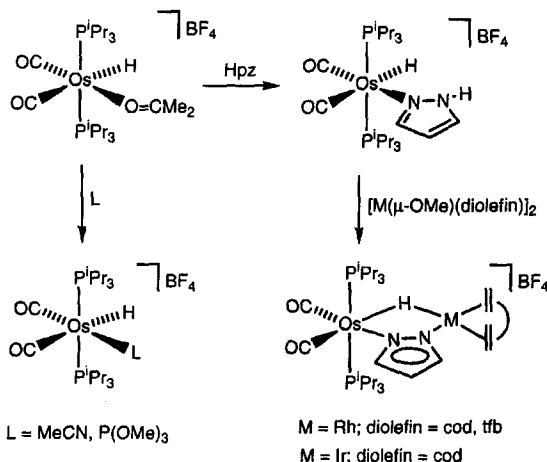


SCHEME 39.

(P^iPr_3)₂. The protonation of $OsHMe(CO)_2(P^iPr_3)_2$ with a diethyl ether solution of HBF_4 in the presence of acetone leads to the quantitative formation of the cationic hydride complex $[OsH(CO)_2\{\eta^1-OCMe_2\}(P^iPr_3)_2]BF_4$. If water instead of acetone is used as a Lewis base, the aquo hydride compound $[OsH(CO)_2(H_2O)(P^iPr_3)_2]BF_4$ is obtained also in excellent yield.

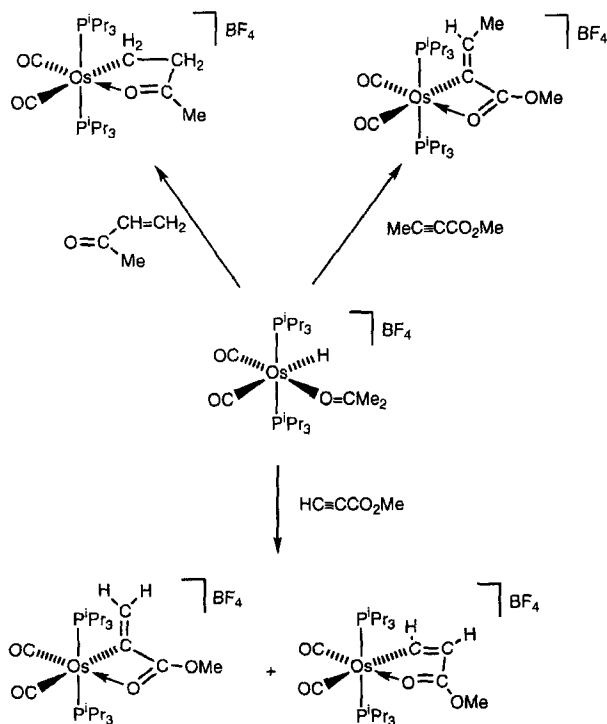
The reactions shown in Scheme 39 indicate that the proton attack preferentially leads to cleavage of the Os—Me and not the Os—H bond. This finding agrees with the assumption⁸⁰ that in compounds of 5d transition metals, M—H bonds are in general more stable (thermodynamically) than their M—C counterparts. The M—H bond causes a higher activation energy for the irreversible H_2 elimination compared with the CH_4 elimination, and thus the observed cleavage of the Os—Me bond in $OsH(Me)(CO)_2(P^iPr_3)_2$ seems to be kinetic in nature.

The acetone ligand of $[OsH(CO)_2\{\eta^1-OCMe_2\}(P^iPr_3)_2]BF_4$ can be readily displaced by acetonitrile, trimethylphosphite, and pyrazole to yield the cationic complexes $[OsH(CO)_2L(P^iPr_3)_2]BF_4$ ($L = MeCN, P(OMe)_3$) and $[OsH(CO)_2(Hpz)(P^iPr_3)_2]BF_4$ (Scheme 40). The substitution is certainly facilitated by the weakness of the Os-acetone bond. The pyrazole ligand in $[OsH(CO)_2(Hpz)(P^iPr_3)_2]BF_4$ contains an acidic NH group which is capable of reacting with the methoxy-bridged dimers $[M(\mu-OMe)(cod)]_2$ ($M = Rh, Ir$; $cod = 1,5$ -cyclooctadiene) and $[Rh(\mu-OMe)(tfb)]_2$ to give the heterobinuclear complexes $[(CO)_2(P^iPr_3)_2 Os(\mu-H)(\mu-pz)M(diolefin)]BF_4$ ($M = Rh, Ir$; diolefin = $cod, M = Rh$; diolefin = tfb).



SCHEME 40.

The acetone ligand in $[\text{OsH}(\text{CO})_2\{\eta^1\text{-OCMe}_2\}(\text{P}^i\text{Pr}_3)_2]\text{BF}_4$ can also be displaced by alkenes and alkynes. Treatment of this complex with methyl vinyl ketone in 1,2-dichloromethane leads, after 14 h under reflux, to $[\text{Os}\{\text{CH}_2\text{CH}_2\text{C}(\text{O})\text{Me}\}(\text{CO})_2(\text{P}^i\text{Pr}_3)_2]\text{BF}_4$ as a result of the insertion of the carbon-carbon double bond of the unsaturated substrate into the Os—H bond of the starting material (Scheme 41). The reaction of $[\text{OsH}(\text{CO})_2\{\kappa^1\text{-OCMe}_2\}(\text{P}^i\text{Pr}_3)_2]\text{BF}_4$ with methyl-2-butyrate leads to $[\text{Os}\{\text{C}[\text{C}(\text{O})\text{OMe}]=\text{CHMe}\}(\text{CO})_2(\text{P}^i\text{Pr}_3)_2]\text{BF}_4$, containing a four-membered ring with an exocyclic carbon-carbon double bond. This complex is the result of the regioselective migration of the hydride ligand from the metal to the $\equiv\text{CMe}$ carbon of the alkyne. This selectivity, however, is not observed for the insertion of the carbon-carbon triple bond of methyl propiolate into the Os—H bond of the acetone complex. The reaction of $[\text{OsH}(\text{CO})_2\{\kappa^1\text{-OCMe}_2\}(\text{P}^i\text{Pr}_3)_2]\text{BF}_4$ with methyl propiolate affords a mixture of the alkenyl derivatives $[\text{Os}\{\text{C}[\text{C}(\text{O})\text{OMe}]=\text{CH}_2\}(\text{CO})_2(\text{P}^i\text{Pr}_3)_2]\text{BF}_4$, and $[\text{Os}\{\text{CH}=\text{CHC}(\text{O})\text{OMe}\}(\text{CO})_2(\text{P}^i\text{Pr}_3)_2]\text{BF}_4$.⁷⁹



SCHEME 41.

XIV

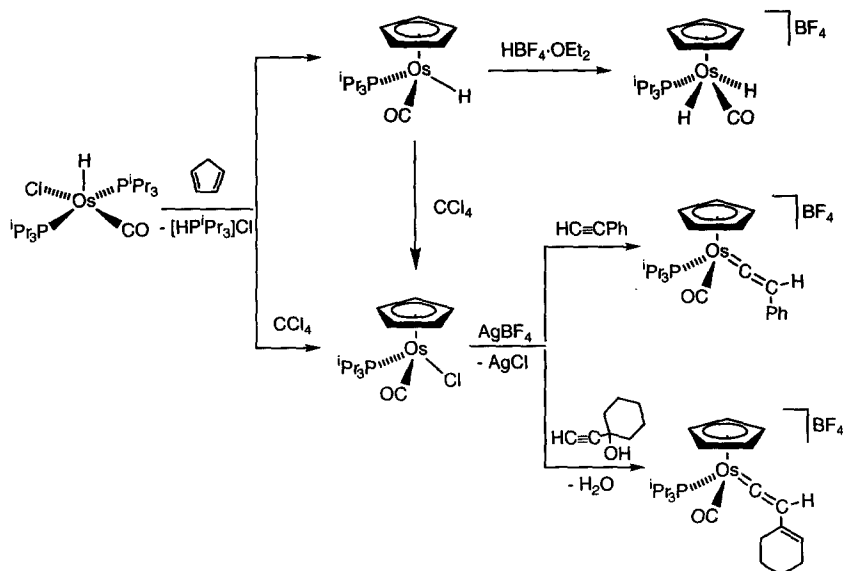
**REACTIONS OF $\text{OsHCl}(\text{CO})(\text{P}^i\text{Pr}_3)_2$ WITH C_5H_6 AND $\text{Na}[\text{HBpz}_3]$:
CYCLOPENTADIENYL AND TRIS(PYRAZOLYL)BORATE COMPOUNDS**

Treatment of a boiling methanol suspension of $\text{OsHCl}(\text{CO})(\text{P}^i\text{Pr}_3)_2$ with freshly distilled cyclopentadiene in a 1:25 molar ratio for 2 days gives $\text{OsH}(\text{cp})(\text{CO})(\text{P}^i\text{Pr}_3)$.⁸¹ In this context, it should be mentioned that the knowledge of cyclopentadienyl-osmium chemistry is rather limited. Certainly, half-sandwich pentamethylcyclopentadienyl- and cyclopentadienyl-ruthenium complexes exhibit a particularly rich and interesting chemistry, which has been very important in the development of the organometallic field.⁸² However, the chemistry of the related half-sandwich osmium complexes has attracted comparatively less attention,⁸³ in particular that containing the $\text{Os}(\text{cp})$ unit.⁸⁴ This is in part due to the lack of convenient osmium synthetic precursors⁸⁵ and the higher kinetic stability of the $\text{Os}(\text{cp})\text{L}_3$ compounds in comparison with the related iron and ruthenium.⁸⁶ The complex $\text{OsH}(\text{cp})(\text{CO})(\text{P}^i\text{Pr}_3)$, which is also prepared by reaction of $\text{OsH}(\text{cp})(\text{P}^i\text{Pr}_3)_2$ ⁸⁷ with carbon monoxide, is a starting point for half-sandwich osmium complexes, including hydride, halide, vinylidene, and alkenyl-vinylidene, derivatives.⁸¹

The complex $\text{OsH}(\text{cp})(\text{CO})(\text{P}^i\text{Pr}_3)$ reacts with $\text{HBF}_4 \cdot \text{OEt}_2$. The reaction leads to the *transoid*-dihydride compound $[\text{OsH}_2(\text{cp})(\text{CO})(\text{P}^i\text{Pr}_3)]\text{BF}_4$. The hydride ligand in $\text{OsH}(\text{cp})(\text{CO})(\text{P}^i\text{Pr}_3)$ is readily replaced by a chlorine ligand by treatment with CCl_4 . The resulting complex $\text{Os}(\text{cp})\text{Cl}(\text{CO})(\text{P}^i\text{Pr}_3)$ reacts with AgBF_4 in the presence of phenylacetylene and 1-ethynyl-1-cyclohexanol to give the stable vinylidene derivatives $[\text{Os}(\text{cp})(\text{CO})(\text{C}=\text{CHPh})(\text{P}^i\text{Pr}_3)]\text{BF}_4$ and $[\text{Os}(\text{cp})(\text{CO})\{\text{C}=\text{CHC}=\text{CH}(\text{CH}_2)_3\text{CH}_2\}(\text{P}^i\text{Pr}_3)]\text{BF}_4$, respectively (Scheme 42).

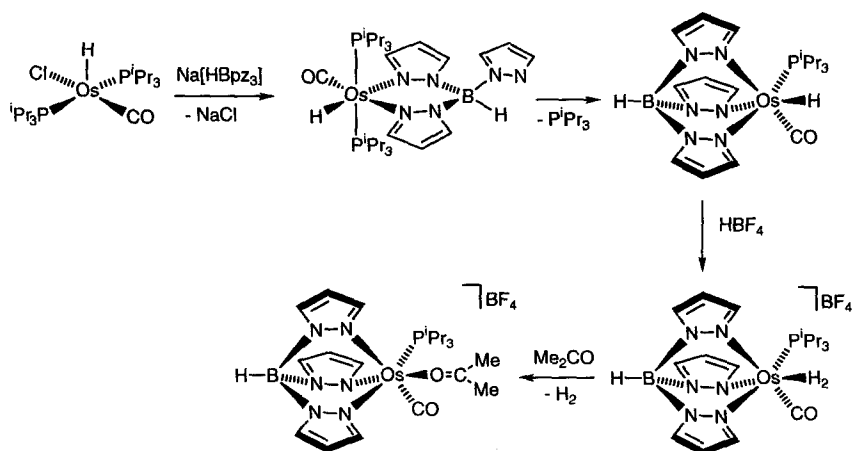
The five-coordinate complex $\text{OsHCl}(\text{CO})(\text{P}^i\text{Pr}_3)_2$ reacts with $\text{Na}[\text{HBpz}_3]$ in methanol at room temperature to give $\text{OsH}(\eta^2\text{-HBpz}_3)(\text{CO})(\text{P}^i\text{Pr}_3)_2$, which in toluene under reflux evolves into $\text{OsH}(\eta^3\text{-HBpz}_3)(\text{CO})(\text{P}^i\text{Pr}_3)$ by dissociation of triisopropylphosphine.⁸⁸ This complex is analogous to the half-sandwich cyclopentadienyl derivative $\text{OsH}(\text{cp})(\text{CO})(\text{P}^i\text{Pr}_3)$. Interestingly, the $\nu(\text{CO})$ vibrations of both compounds are similar (1905 (HBpz_3) and 1900 (cp)), suggesting that the electron-donating abilities of the two ligands are also similar.

In spite of this fact, there is a marked difference in their reactivities toward HBF_4 . While the addition of one equiv. of $\text{HBF}_4 \cdot \text{OEt}_2$ to dichloromethane solutions of $\text{OsH}(\text{cp})(\text{CO})(\text{P}^i\text{Pr}_3)$ affords the dihydride $[\text{OsH}_2(\text{cp})(\text{CO})(\text{P}^i\text{Pr}_3)]\text{BF}_4$, as has been previously mentioned, the reaction of the trispyrazolylborate complex $\text{OsH}(\eta^3\text{-HBpz}_3)(\text{CO})(\text{P}^i\text{Pr}_3)$ with $\text{HBF}_4 \cdot \text{OEt}_2$ leads to the dihydrogen derivative $[\text{Os}(\eta^3\text{-HBpz}_3)(\text{CO})(\eta^2\text{-H}_2)(\text{P}^i\text{Pr}_3)]\text{BF}_4$, with a separation between the hydrogen atoms of the dihydrogen ligand of 0.99 Å, and a pK_a at 213 K of 9.3 on the pseudo-aqueous scale. The dihydrogen ligand can be displaced by acetone to give $[\text{Os}(\eta^3\text{-HBpz}_3)(\text{CO})\{\eta^1\text{-OCMe}_2\}(\text{P}^i\text{Pr}_3)]\text{BF}_4$ (Scheme 43).



SCHEME 42.

The higher tendency of the trispyrazolylborate ligand to stabilize the dihydrogen ligand in comparison with the cyclopentadienyl group merits some additional comment. Often differences in steric and electronic properties as well as differences in symmetry have been argued to explain the tendency of the cyclopentadienyl ligand to afford higher coordination numbers than the trispyrazolylborate.



SCHEME 43.

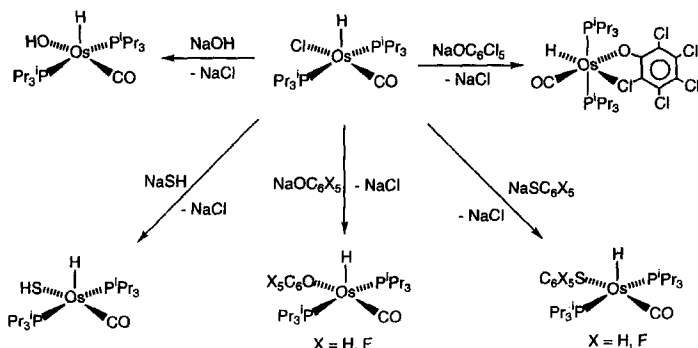
In this case, the electron density of the metallic centers of both systems appears to be similar; therefore, the electronic factors do not appear to play a significant role. Furthermore, it is not reasonable to think that the size of the trispyrazolylborate and cyclopentadienyl groups can affect the coordination mode of the smallest known ligand. However, it should be noted that the symmetry of the $M(\eta^3\text{-HBpz}_3)$ fragment determined by the $N-M-N$ angle (87° for 8 group),⁸⁹ affects the coordination mode of the other ligands of the complex rather than the symmetry of the $M(\text{cp})$ unit. For example, it has been suggested⁹⁰ that the $[\text{Ru}(\eta^3\text{-HBpz}_3)]^+$ unit is strongly hybrid biased to preferentially bind three additional ligands for an octahedral six-coordinate structure to be obtained and maintained. The diffuse electron clouds of the cyclopentadienyl ligand are rather ineffective in promoting strongly directional frontier orbitals. As a consequence, processes involving coordination number increase are less likely for the trispyrazolylborate ligand.

XV

REACTIONS OF $\text{OsHCl}(\text{CO})(\text{P}^i\text{Pr}_3)_2$ WITH NaXR ($X = \text{O}, \text{S}$)

The complex $\text{OsHCl}(\text{CO})(\text{P}^i\text{Pr}_3)_2$ reacts with NaOH , NaSH , phenolates, and thiophenolates to give $\text{OsH}(\text{XR})(\text{CO})(\text{P}^i\text{Pr}_3)_2$ ($X = \text{OH}$,⁹¹ SH ,⁹² OC_6H_5 , OC_6F_5 , SC_6H_5 , SC_6F_5 , OC_6Cl_5 ⁹³) in good to excellent yields. Whereas in the phenolate compounds $\text{OsH}(\text{OC}_6\text{X}_5)(\text{CO})(\text{P}^i\text{Pr}_3)_2$ ($X = \text{H}, \text{F}$) the phenolate group is κ^1 -bonded, in the related pentachlorophenolate derivative, a bidentate coordination mode is present (Scheme 44). This has been confirmed by X-ray diffraction analysis, which reveals a surprisingly short $\text{Os}-\text{Cl}$ distance of $2.574(1) \text{ \AA}$.⁹³

The hydroxo complex $\text{OsH}(\text{OH})(\text{CO})(\text{P}^i\text{Pr}_3)_2$ reacts with dimethyl acetylenedicarboxylate to afford $\text{OsH}\{\text{OC}(\text{OMe})\text{CHC}(\text{CO}_2\text{Me})\text{O}\}(\text{CO})(\text{P}^i\text{Pr}_3)_2$, which has

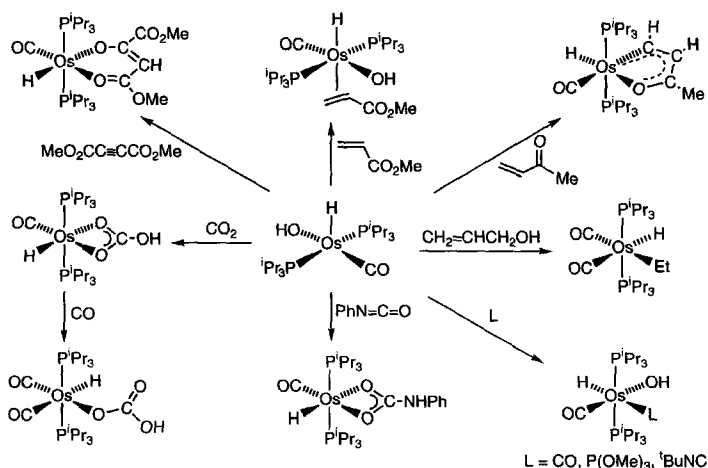


SCHEME 44.

been characterized by X-ray diffraction analysis (Scheme 45).⁹¹ The formation of the κ^2 -O-donor ligand of this compound is the result of the unprecedented *trans* addition of the O—H bond of the starting complex to the carbon-carbon triple bond of the alkyne.

Bergman⁹⁴ has reported the reaction between the saturated hydroxo compound $\text{Ir}(\eta^5\text{-C}_5\text{Me}_5)(\text{Ph})(\text{OH})(\text{PMe}_3)$ and dimethyl acetylenedicarboxylate. In contrast to the above mentioned case, the alkyne undergoes an insertion reaction into the M—O bond to afford the enol complex $\text{Ir}(\eta^5\text{-C}_5\text{Me}_5)(\text{Ph})\{(\text{Z})\text{-C}(\text{CH}_2\text{Me})=\text{C}(\text{CO}_2\text{Me})\text{OH}\}(\text{PMe}_3)$. Similarly, the reactions of the complexes *trans*- $\text{Pd}(\text{C}_6\text{H}_4\text{CH}=\text{NPh})(\text{NHPh})(\text{PMe}_3)_2$ and *trans*- $\text{Pd}(\text{C}_6\text{H}_5)(\text{NHPh})(\text{PMe}_3)_2$ with dimethyl acetylenedicarboxylate result in the insertion of the acetylene into Pd—N bonds.⁹⁵ In addition, we must point out the different behavior of $\text{OsH}(\text{OH})(\text{CO})(\text{P}^i\text{Pr}_3)_2$ and its precursor $\text{OsHCl}(\text{CO})(\text{P}^i\text{Pr}_3)_2$, which reacts with dimethyl acetylenedicarboxylate by insertion of alkyne into the Os—H bond to give the alkenyl derivative $\text{Os}\{\text{C}[\text{C}(\text{O})\text{OMe}]=\text{CHCO}_2\text{Me}\}\text{Cl}(\text{CO})(\text{P}^i\text{Pr}_3)_2$ (Scheme 4).

The complex $\text{OsH}(\text{OH})(\text{CO})(\text{P}^i\text{Pr}_3)_2$ also reacts with methyl acrylate, methyl vinyl ketone, and allyl alcohol.⁹¹ Reaction with methyl acrylate leads to $\text{OsH}(\text{OH})(\text{CO})(\eta^2\text{-CH}_2=\text{CHCO}_2\text{Me})(\text{P}^i\text{Pr}_3)_2$ containing the olefin *trans* to the hydride ligand. In solution, this complex releases the olefin to generate the starting complex. The thermodynamic magnitudes involved in the equilibrium have been determined in toluene- d_8 by $^{31}\text{P}\{^1\text{H}\}$ NMR spectroscopy. The values reported are $\Delta H^\circ = 17.0 \pm 0.5 \text{ kcal}\cdot\text{mol}^{-1}$ and $\Delta S^\circ = 54.0 \pm 1.2 \text{ cal}\cdot\text{K}^{-1}\cdot\text{mol}^{-1}$. In the presence of the methyl vinyl ketone complex $\text{OsH}(\text{OH})(\text{CO})(\text{P}^i\text{Pr}_3)_2$ affords $\text{OsH}\{\text{CHCHC}(\text{O})\text{Me}\}(\text{CO})(\text{P}^i\text{Pr}_3)_2$ and water, whereas in the presence of allyl alcohol the loss of



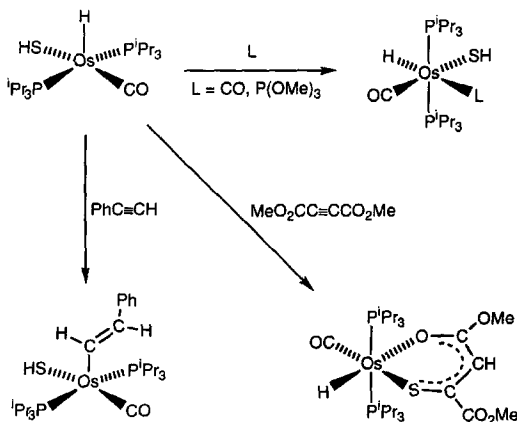
SCHEME 45.

water leads to the hydride-ethyl derivative $\text{OsH}(\text{Et})(\text{CO})_2(\text{P}^i\text{Pr}_3)_2$ (Scheme 45), which is another member of the $\text{OsH}(\text{alkyl})(\text{CO})_2(\text{P}^i\text{Pr}_3)_2$ series (Scheme 38).

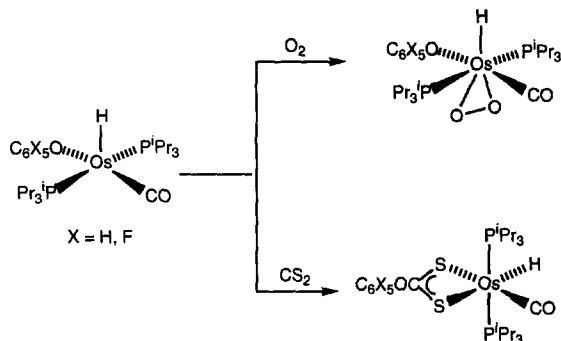
Under a carbon dioxide atmosphere the complex $\text{OsH}(\text{OH})(\text{CO})(\text{P}^i\text{Pr}_3)_2$ gives the bicarbonato derivative $\text{OsH}(\kappa^2\text{-O}_2\text{COH})(\text{CO})(\text{P}^i\text{Pr}_3)_2$, which by carbonylation affords $\text{OsH}\{\kappa^1\text{-OC(O)OH}\}(\text{CO})_2(\text{P}^i\text{Pr}_3)_2$. The complex $\text{OsH}(\text{OH})(\text{CO})(\text{P}^i\text{Pr}_3)_2$ also reacts with phenyl isocyanate to give the carbamato derivative $\text{OsH}(\kappa^2\text{-O}_2\text{CNHPh})(\text{CO})(\text{P}^i\text{Pr}_3)_2$, which is the result of adding the O—H bond of the hydroxo complex to the C=N double bond of the heteroallene. The reactions of $\text{OsH}(\text{OH})(\text{CO})(\text{P}^i\text{Pr}_3)_2$ with Lewis bases that are not bulky such as CO, $\text{P}(\text{OMe})_3$, and *t*-BuNC lead to the corresponding six-coordinate hydride-hydroxo compounds $\text{OsH}(\text{OH})(\text{CO})\text{L}(\text{P}^i\text{Pr}_3)_2$ (Scheme 45).⁹¹

In a manner similar to $\text{OsH}(\text{OH})(\text{CO})(\text{P}^i\text{Pr}_3)_2$, the hydride-metallthiol complex $\text{OsH}(\text{SH})(\text{CO})(\text{P}^i\text{Pr}_3)_2$ adds Lewis bases that are not bulky such as CO and $\text{P}(\text{OMe})_3$ to give the corresponding six-coordinate hydride-metallthiol derivatives $\text{OsH}(\text{SH})(\text{CO})\text{L}(\text{P}^i\text{Pr}_3)_2$ ($\text{L} = \text{CO}, \text{P}(\text{OMe})_3$). $\text{OsH}(\text{OH})(\text{CO})(\text{P}^i\text{Pr}_3)_2$ and $\text{OsH}(\text{SH})(\text{CO})(\text{P}^i\text{Pr}_3)_2$ also show a similar behavior toward dimethyl acetylenedicarboxylate. Treatment of $\text{OsH}(\text{SH})(\text{CO})(\text{P}^i\text{Pr}_3)_2$ with this alkyne affords $\text{OsH}\{\text{SC}(\text{CO}_2\text{Me})\text{CHC}(\text{OMe})\text{O}\}(\text{CO})\text{P}^i\text{Pr}_3)_2$, which is the result of the *trans* addition of the S—H bond to the carbon-carbon triple bond of the alkyne. Phenylacetylene, in contrast to dimethyl acetylenedicarboxylate, reacts with $\text{OsH}(\text{SH})(\text{CO})(\text{P}^i\text{Pr}_3)_2$ by insertion of the carbon-carbon triple bond into the Os—H bond to give the unsaturated alkenyl-metallthiol derivative $\text{Os}\{(\text{E})\text{-CH=CHPh}\}(\text{SH})(\text{CO})(\text{P}^i\text{Pr}_3)_2$, the inorganic counterpart of the organic α,β -unsaturated mercaptans (Scheme 46).⁹²

The hydride-phenolate complexes $\text{OsH}(\text{OC}_6\text{X}_5)(\text{CO})(\text{P}^i\text{Pr}_3)_2$ ($\text{X} = \text{H}, \text{F}$) react with molecular oxygen to give stable 1:1 adducts $\text{OsH}(\text{OC}_6\text{X}_5)(\text{CO})(\eta^2\text{-O}_2)$



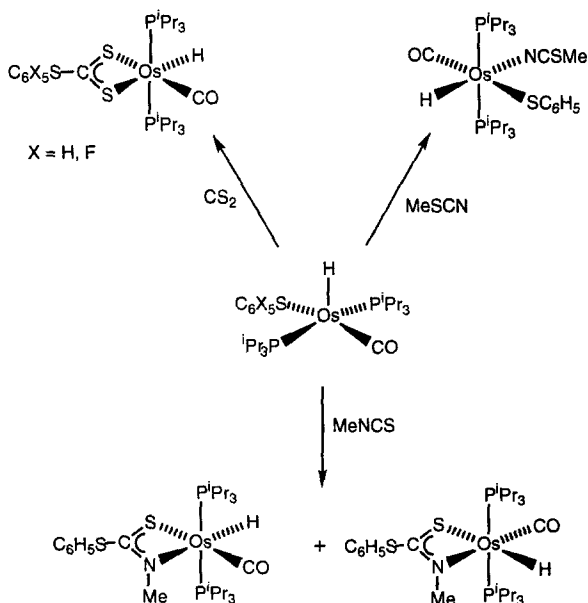
SCHEME 46.



SCHEME 47.

$(\text{P}^i\text{Pr}_3)_2$, and with CS_2 by insertion to yield $\text{OsH}(\kappa^2\text{-S}_2\text{COC}_6\text{X}_5)(\text{CO})(\text{P}^i\text{Pr}_3)_2$ (Scheme 47).⁹³ Similarly, the reactions of the hydride-thiophenolate complexes $\text{OsH}(\text{SC}_6\text{X}_5)(\text{CO})(\text{P}^i\text{Pr}_3)_2$ ($\text{X} = \text{H, F}$) with CS_2 give the trithiocarbonate compound $\text{OsH}(\kappa^2\text{-S}_2\text{CSC}_6\text{X}_5)(\text{CO})(\text{P}^i\text{Pr}_3)_2$ ($\text{X} = \text{H, F}$).

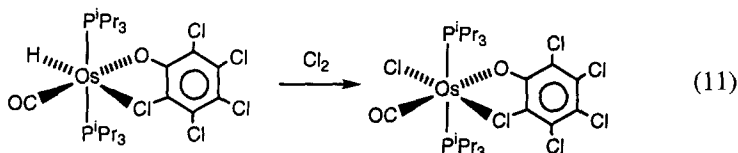
The complex $\text{OsH}(\text{SC}_6\text{H}_5)(\text{CO})(\text{P}^i\text{Pr}_3)_2$ not only reacts with CS_2 but also with MeSCN and the isomer MeNCS (Scheme 48).⁶⁷ Whereas with the thionitrile a



SCHEME 48.

simple addition occurs to give the six-coordinate derivative $\text{OsH}(\text{SC}_6\text{H}_5)(\text{CO})(\text{NCSMe})(\text{P}^i\text{Pr}_3)_2$, the heteroallene undergoes insertion into the $\text{Os}-\text{SC}_6\text{H}_5$ bond to afford $\text{OsH}\{\kappa^5\kappa^1\text{N}-\text{SC}(\text{SC}_6\text{H}_5)\text{NMe}\}(\text{CO})(\text{P}^i\text{Pr}_3)_2$, which is isolated as a mixture of the isomers shown in Scheme 48.

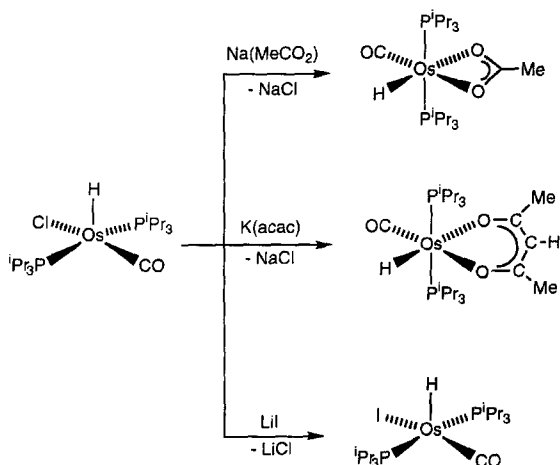
Treatment of $\text{OsH}(\kappa\text{O}, \kappa\text{Cl}-\text{OC}_6\text{Cl}_5)(\text{CO})(\text{P}^i\text{Pr}_3)_2$ with Cl_2 leads to the formation of $\text{OsCl}(\kappa\text{O}, \kappa\text{Cl}-\text{OC}_6\text{Cl}_5)(\text{CO})(\text{P}^i\text{Pr}_3)_2$ by cleavage of the $\text{Os}-\text{H}$ bond (Eq. 11).⁹³



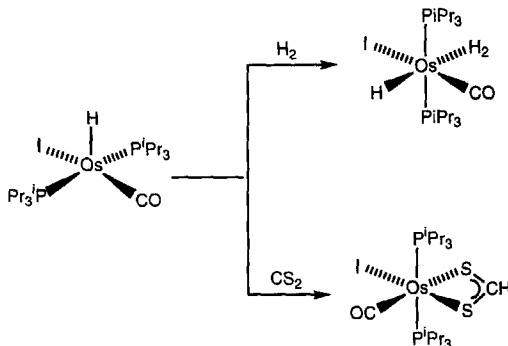
XVI

OTHER METATHETICAL REACTIONS ON THE CHLORIDE LIGAND OF $\text{OsHCl}(\text{CO})(\text{P}^i\text{Pr}_3)_2$

The chloride ligand in $\text{OsHCl}(\text{CO})(\text{P}^i\text{Pr}_3)_2$ can be also replaced by acetate, acetylacetonate, or iodide (Scheme 49). The reactions with the O-donor ligands lead to six-coordinate complexes $\text{OsH}(\kappa^2-\text{O}_2\text{CMe})(\text{CO})(\text{P}^i\text{Pr}_3)_2$ and $\text{OsH}(\text{acac})(\text{CO})(\text{P}^i\text{Pr}_3)_2$,¹² respectively, whereas the treatment of $\text{OsHCl}(\text{CO})(\text{P}^i\text{Pr}_3)_2$ with LiI affords the five-coordinate derivative $\text{OsHI}(\text{CO})(\text{P}^i\text{Pr}_3)_2$.⁶⁷ Complex OsH



SCHEME 49.



SCHEME 50.

$(\kappa^2\text{-O}_2\text{CMe})(\text{CO})(\text{P}^i\text{Pr}_3)_2$ is a further member of the series $\text{OsH}(\kappa^2\text{-O}_2\text{CR})(\text{CO})(\text{P}^i\text{Pr}_3)_2$ (Scheme 35).

In a manner similar to $\text{OsHCl(CO)(P}^i\text{Pr}_3)_2$, the complex $\text{OsHI(CO)(P}^i\text{Pr}_3)_2$ coordinates molecular hydrogen to give the dihydrogen derivative $\text{OsH}_2(\eta^2\text{-H}_2)(\text{CO})(\text{P}^i\text{Pr}_3)_2$, with a separation between the hydrogen atoms of the dihydrogen ligand of 0.97 Å.⁷⁰ The starting hydride-iodo complex also reacts with CS_2 . The reaction quite smoothly affords the dithioformate $\text{OsI}(\kappa^2\text{-S}_2\text{CH})(\text{CO})(\text{P}^i\text{Pr}_3)_2$ by insertion of the heteroallene into the Os-H bond (Scheme 50). Although reaction intermediates have not been isolated, it has been proposed that initially a coordination of the heteroallene to the osmium center occurs which is followed by the hydride migration step. In agreement with this proposal, it has also been observed that the reaction of $\text{OsHCl(CO)(P}^i\text{Pr}_3)_2$ with CS_2 in acetone affords $\text{OsHCl(CO)(}\eta^2\text{-S=CS)(P}^i\text{Pr}_3)_2$, whereas if dichloromethane instead of acetone is used as solvent, the insertion product $\text{OsCl}(\kappa^2\text{-S}_2\text{CH})(\text{CO})(\text{P}^i\text{Pr}_3)_2$ is obtained.⁶⁷

XVII

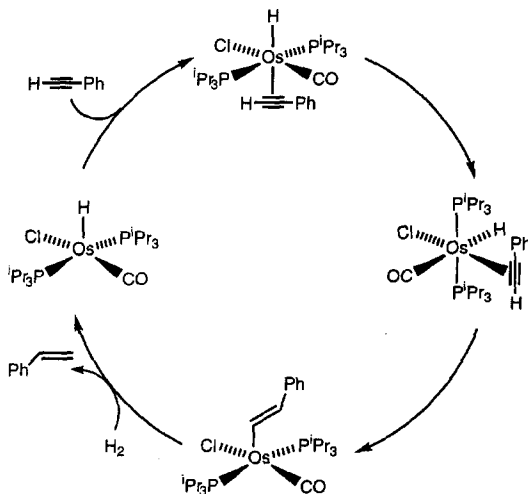
$\text{OsHCl(CO)(P}^i\text{Pr}_3)_2$ AS A HOMOGENEOUS CATALYST

The $\text{OsHCl(CO)(P}^i\text{Pr}_3)_2$ complex is an active catalyst precursor for the hydrogenation of olefins, diolefins, phenylacetylene, or benzylidenacetone.^{26,31,96,97} As expected from the chemistry described in Scheme 3, the formation of the styryl complex $\text{Os}\{(\text{E})\text{-CH=CHPh}\}\text{Cl(CO)(P}^i\text{Pr}_3)_2$ together with its subsequent reaction with hydrogen to regenerate $\text{OsHCl(CO)(P}^i\text{Pr}_3)_2$ constitutes a catalytic cycle for the reduction of phenylacetylene to styrene. At 60°C and atmospheric pressure, selectivities close to 100% are achieved for the hydrogenation of the alkyne to alkene, while reduction of the double bond begins to take place only when most

of the alkyne has been consumed. The catalytic activity depends on the nature of the solvent (benzene, 1,2-dichloroethane, propan-2-ol). Detailed kinetic studies indicate that the rate of formation of styrene is determined by the rate of reaction of alkenyl compounds with hydrogen. The elementary steps involved in the formation of styryl derivative $\text{Os}\{(E)\text{-CH=CHPh}\}\text{Cl}(\text{CO})(\text{P}^i\text{Pr}_3)_2$ are too fast to be observed by spectroscopic methods, but on the basis of the observations collected in Scheme 4 when alkyne dicarboxylic methyl ester is used, the catalytic cycle shown in Scheme 51 has been proposed. The slow step of this catalytic cycle is the reaction of this styryl complex with hydrogen to yield the alkene and regenerate the monohydrides in equilibrium with the dihydrogen complexes (Scheme 51).³¹

Independent studies of the reduction of $\text{C}\equiv\text{C}$ and $\text{C}=\text{C}$ bonds indicate that the latter is kinetically favored. Thus, in the absence of phenylacetylene, the rate of hydrogenation of styrene to ethylbenzene is about one order of magnitude faster than those for $\text{C}\equiv\text{C}$ bond reduction, indicating that the origin of the selectivity cannot be kinetic. The styryl compound represents a thermodynamic sink that causes virtually all the osmium present in solution to be tied up in this form, and therefore the kinetically unfavorable pathway becomes essentially the only one available in the presence of alkyne.³¹

The complex $\text{OsHCl}(\text{CO})(\text{P}^i\text{Pr}_3)_2$ is also an effective catalyst precursor for the selective hydrogenation of benzylideneacetone to 4-phenylbutan-2-one.⁹⁷ In contrast to the hydrogenation of phenylacetylene, kinetic studies on the hydrogenation of benzylideneacetone by $\text{OsHCl}(\text{CO})(\text{P}^i\text{Pr}_3)_2$ show that the reaction is independent of the pressure of hydrogen and first order with respect to the concentration



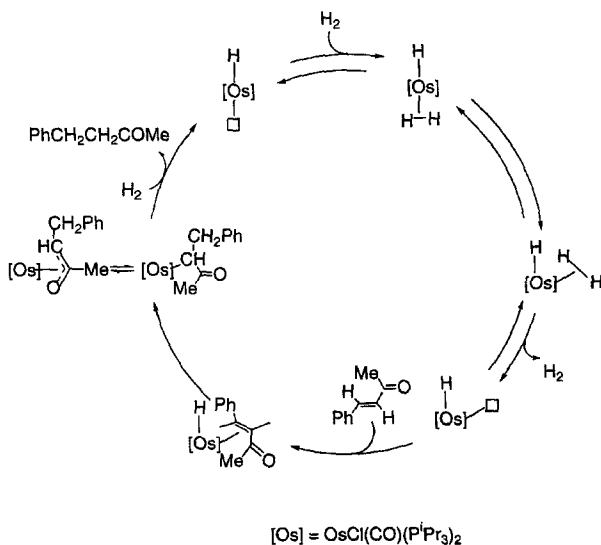
SCHEME 51.

of catalysts and substrate. On the basis of these kinetic data and on spectroscopic observations Scheme 52 has been proposed.

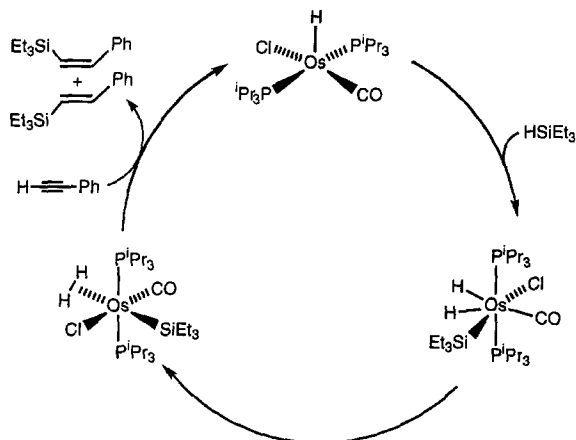
Interestingly, the complex *trans*-hydride-dihydrogen-OsHCl(η^2 -H₂)(CO)(P^{*i*}Pr₃) plays a major role on the process; thus, isomerization to *cis*-hydride-dihydrogen-OsHCl(η^2 -H₂)(CO)(P^{*i*}Pr₃)₂ and subsequent hydrogen dissociation produces a rearrangement to give a new mono-hydride isomer which contains the hydride ligand and the coordination vacancy in a *cis* disposition. Then, coordination of the benzylideneacetone and its subsequent insertion in the Os—H bond must lead to an alkyl intermediate that, by reaction with molecular hydrogen, gives 4-phenylbutan-2-one and regenerates the catalyst.

OsHCl(CO)(P^{*i*}Pr₃)₂ is also a very active and selective catalyst for the addition of triethylsilane to phenylacetylene at 60°C, to yield *trans*- and *cis*-PhHC=CH(SiEt₃).⁵⁰ The reaction of OsHCl(CO)(P^{*i*}Pr₃)₂ with triethylsilane is the rate-determining step. The catalytic reaction proceeds via a silyl dihydrogen intermediate of the formula Os(SiEt₃)Cl(η^2 -H₂)(CO)(P^{*i*}Pr₃)₂ and its dihydride tautomer, OsH₂(SiEt₃)Cl(CO)(P^{*i*}Pr₃)₂ (Scheme 53).

The hydrogenation and hydrosilylation mechanisms using OsHCl(CO)(P^{*i*}Pr₃)₂ as catalyst show significant differences (Schemes 51 and 53). Thus, although the very stable Os{(E)-CH=CHPh}Cl(CO)(P^{*i*}Pr₃)₂ is the only complex observed under catalytic conditions in both cases, the hydrosilylation catalysis proceeds by initial reaction of HSiEt₃ with OsHCl(CO)(P^{*i*}Pr₃)₂. The formation of *cis*-PhHC=CH(SiEt₃) seems to occur by isomerization of a vinyl intermediate formed



SCHEME 52.

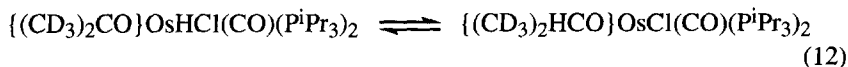


SCHEME 53.

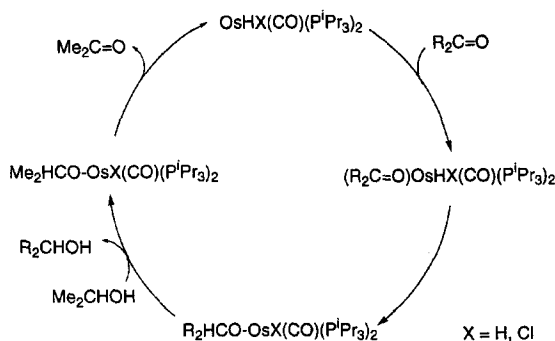
by displacement of the coordinated dihydrogen ligand and subsequent insertion of phenylacetylene into the Os—SiEt₃ bond of Os(SiEt₃)Cl(η²-H₂)(CO)(P^{*i*}Pr₃)₂.⁵⁰ The related RuHCl(CO)(P^{*i*}Pr₃)₂ complex is also an active catalyst and very selective for the hydrosilylation of phenylacetylene, with selective formation of *cis*-PhHC=CH(SiEt₃), most probably through a similar mechanism.⁹⁸

The OsHCl(CO)(P^{*i*}Pr₃)₂ complex is a modest catalyst for the hydrogen transfer from 2-propanol to unsaturated substrates, such as styrene, cyclohexene, cyclohexadienes, ketones, and unsaturated ketones at 83°C.^{96,99} However, the addition of NaBH₄ leads to an important increase of activity due to the initial formation of OsH(η²-H₂BH₂)(CO)(P^{*i*}Pr₃)₂ such that under hydrogen transfer conditions the catalyst precursor OsH₂(η²-H₂)(CO)(P^{*i*}Pr₃)₂,¹³ is formed. It affords OsH₂(CO)(P^{*i*}Pr₃)₂ that acts as the catalyst. Spectroscopic and kinetic studies indicate that the hydrogen transfer from 2-propanol to ketones follows the catalytic cycle shown in Scheme 54.³²

In particular the formation of Os—OCH(CD₃)₂ species by insertion of acetone-d₆ into the Os—H bond has been observed³² (Eq. 12).



Competitive reduction tests for cyclohexanone:styrene, under transfer conditions, show preferential reduction of cyclohexanone; however, under hydrogenation conditions the styrene is reduced exclusively.⁹⁹ It is worth mentioning that the OsH₂(η²-H₂)(CO)(P^{*i*}Pr₃)₂ precatalyst, formed by addition of NaBH₄ to OsHCl(CO)(P^{*i*}Pr₃)₂, rapidly reduces phenylacetylene to styrene, under transfer conditions, but the reaction rate falls progressively due to the formation of Os(C≡CPh)₂(CO)(P^{*i*}Pr₃)₂.⁷² As previously mentioned, an alkynyl-dihydrogen intermediate



SCHEME 54.

$\text{OsH}(\text{C}_2\text{Ph})(\eta^2\text{-H}_2)(\text{CO})(\text{P}^i\text{Pr}_3)_2$ has been isolated by treating $\text{OsH}_2(\eta^2\text{-H}_2)(\text{CO})(\text{P}^i\text{Pr}_3)_2$ with a stoichiometric amount of phenylacetylene.⁷¹ This alkynyl-dihydrogen complex appears to be involved in the catalytic cycles shown in Schemes 27 and 30.⁷¹

The related dihydride-dichloro complex $\text{OsH}_2\text{Cl}_2(\text{P}^i\text{Pr}_3)_2$ is also an active catalyst for the hydrogenation of olefins, diolefins, and α - β -unsaturated ketones,¹⁴ but attempts to hydrogenate phenylacetylene show a rapid deactivation of the catalyst due to formation of a hydride-carbyne complex.⁵⁴

The potential of osmium complexes as homogeneous catalysts has been highlighted in two recent reviews.^{100, 101}

XVIII

FINAL REMARKS

This chapter has discussed the chemical regions opened up by the discovery of $\text{OsHCl}(\text{CO})(\text{P}^i\text{Pr}_3)_2$. The title compound is not only a useful starting material for the preparation of a broad variety of organometallic osmium compounds, but the study of its reactivity has led to the discovery of novel reactions. For example, the addition of HSiEt_3 molecules to give an $\text{Os}(\eta^2\text{-H}_2)$ derivative is a simple route for preparing dihydrogen compounds, alternative to the coordination of molecular hydrogen to unsaturated compounds or to the protonation of saturated hydride complexes. The reaction of $\text{OsCl}_2(\eta^2\text{-H}_2)(\text{CO})(\text{P}^i\text{Pr}_3)_2$ with terminal alkynes to afford carbene derivatives is also a reaction without precedent in organometallic chemistry.

The reactivity of the $\text{OsHCl}(\text{CO})(\text{P}^i\text{Pr}_3)_2$ complex toward terminal alkynes is remarkable and intriguing. Why does the title compound react with cyclohexylacetylene or the metalloalkyne complex $\text{Ru}\{(\text{E})\text{-CH=CH}(\text{CH}_2)_4\text{C}\equiv\text{CH}\}\text{Cl}(\text{CO})(\text{P}^i\text{Pr}_3)_2$

affording vinylidene derivatives before the insertion products? Are π -alkyne intermediates involved in the formation of the vinylidene species? These are some open questions to be answered in the future. The synthesis of the complexes $\text{Os}(\text{cp})\text{Cl}(\text{CO})(\text{P}^i\text{Pr}_3)$ and $\text{Os}(\text{HBpz}_3)\text{Cl}(\text{CO})(\text{P}^i\text{Pr}_3)$ is also noteworthy; these complexes could be appropriate entries for future developments of osmium chemistry.

We have also underlined the potential of the $\text{OsHCl}(\text{CO})(\text{P}^i\text{Pr}_3)_2$ complex in homogeneous catalytic reactions, showing that derived $\text{Os}(\eta^2\text{-H}_2)$ intermediates are formed under catalytic conditions. Stoichiometric and catalytic reactions involving the title complex have advanced together.

In spite of the rich chemistry developed starting from the $\text{OsHCl}(\text{CO})(\text{P}^i\text{Pr}_3)_2$ complex, the presence of a carbonyl group in its coordination sphere is probably a limitation for some subsequent developments. In this context it seems important to mention the encouraging reactivity of the related osmium(IV) complex, $\text{OsH}_2\text{Cl}_2(\text{P}^i\text{Pr}_3)_2$, that in methanol afford $\text{OsHCl}(\text{CO})(\text{P}^i\text{Pr}_3)_2$. We believe that both interrelated osmium complexes present not only a rich chemistry but also a promising future as starting materials in organometallic chemistry.

ACKNOWLEDGMENTS

The authors express their sincere thanks to their co-workers and colleagues, without whose contributions this article could not have been written: their names are cited in the references. Prof. Helmut Werner from Würzburg University, in whose Institute the title complex was initially prepared, is very specially thanked for the intense and exciting chemical cooperation for many years.

REFERENCES

- (1) (a) Chatt, J.; Davidson, J. M. *J. Chem. Soc.* **1965**, 843; (b) Sen, A. *Acc. Chem. Res.* **1998**, *31*, 550; (c) Arndtsen, B. A.; Bergman, R. G.; Mobley, T. A.; Peterson, T. H. *Acc. Chem. Res.* **1995**, *28*, 154.
- (2) Gotzig, J.; Werner, R.; Werner, H. *J. Organomet. Chem.* **1985**, 285, 99.
- (3) Werner, H.; Gotzig, J. *J. Organomet. Chem.* **1985**, 284, 73.
- (4) (a) Werner, R.; Werner, H. *Angew. Chem., Int. Ed. Engl.* **1981**, *20*, 793; (b) Werner, H.; Zenkert, K. *J. Chem. Soc., Chem. Commun.* **1985**, 1607.
- (5) Kletzin, H.; Werner, H. *Angew. Chem., Int. Ed. Engl.* **1983**, *22*, 873.
- (6) Vaska, L.; Diluzio, J. W. *J. Am. Chem. Soc.* **1961**, *83*, 1262.
- (7) Moers, F. G. *J. Chem. Soc., Chem. Commun.* **1971**, 79.
- (8) Gill, D. F.; Shaw, B. L. *Inorg. Chim. Acta* **1979**, *32*, 19.
- (9) Stephenson, T. A.; Wilkinson, G. *J. Inorg. Nucl. Chem.* **1966**, *28*, 945.
- (10) Hoffman, P. R.; Caulton, K. G. *J. Am. Chem. Soc.* **1975**, *97*, 4221.
- (11) Armit, P. W.; Boyd, A. S. F.; Stephenson, T. A. *J. Chem. Soc., Dalton Trans.* **1975**, 1663.
- (12) Esteruelas, M. A.; Werner, H. *J. Organomet. Chem.* **1986**, *303*, 221.
- (13) Werner, H.; Esteruelas, M. A.; Meyer, U.; Wrackmeyer, B. *Chem. Ber.* **1987**, *120*, 11.
- (14) Aracama, M.; Esteruelas, M. A.; Lahoz, F. J.; López, J. A.; Meyer, U.; Oro, L. A.; Werner, H. *Inorg. Chem.* **1991**, *30*, 288.
- (15) Chatt, J.; Melville, D. P.; Richards, R. L. *J. Chem. Soc. A* **1971**, 895.
- (16) Grünwald, C.; Gevert, O.; Woldf, J.; González-Herrero, P.; Werner, H. *Organometallics* **1996**, *15*, 1960.

- (17) Oliván, M.; Clot, E.; Eisenstein, O.; Caulton, K. G. *Organometallics* **1998**, *17*, 3091.
- (18) Moers, F. G.; Noordik, J. H.; Beurskens, P. T. *Cryst. Struct. Comm.* **1981**, *10*, 1149.
- (19) Yandulov, D. V.; Streib, W. E.; Caulton, K. G. *Inorg. Chim. Acta* **1998**, *280*, 125.
- (20) Burdett, J. K.; Perutz, R. N.; Poliakoff, M.; Turner, J. J. *J. Chem. Soc., Chem. Commun.* **1975**, 157.
- (21) (a) Rachidi, E.-I.; Eisenstein, O.; Jean Y. *New J. Chem.* **1990**, *14*, 671 (b) Riehl, J.-F.; Jean, Y.; Eisenstein, O.; Péliissier, M. *Organometallics* **1992**, *11*, 729.
- (22) Poulton, J. T.; Sigalas, M. P.; Foltling, K.; Streib, W. E.; Eisenstein, O.; Caulton, K. G. *Inorg. Chem.* **1994**, *33*, 1476.
- (23) Caulton, K. G. *New J. Chem.* **1994**, *18*, 25.
- (24) Bohanna, C.; Esteruelas, M. A.; Lahoz, F. J.; Oñate, E.; Oro, L. A. *Organometallics* **1995**, *14*, 4685.
- (25) Meyer, U.; Werner, H. *Chem. Ber.* **1990**, *123*, 697.
- (26) Esteruelas, M. A.; Sola, E.; Oro, L. A.; Meyer, U.; Werner, H.; *Angew. Chem., Int. Ed. Engl.* **1988**, *27*, 1563.
- (27) Bourgault, M.; Castillo, A.; Esteruelas, M. A.; Oñate, E.; Ruiz, N. *Organometallics* **1997**, *16*, 636.
- (28) Oliván, M.; Eisenstein, O.; Caulton, K. G. *Organometallics* **1997**, *16*, 2227.
- (29) (a) Werner, H.; Stüer, W.; Laubender, M.; Lehmann, C.; Herbst-Irmer, R. *Organometallics* **1997**, *16*, 2236; (b) Werner, H.; Stüer, W.; Wolf, J.; Laubender, M.; Webernbörfer, B.; Herbst-Irmer, R.; Lehmann, C. *Eur. J. Inorg. Chem.* **1999**, 1889.
- (30) Huang, D.; Spivak, G. J.; Caulton, K. G. *New J. Chem.* **1998**, 1023.
- (31) Andriollo, A.; Esteruelas, M. A.; Meyer, U.; Oro, L. A.; Sánchez-Delgado, R. A.; Sola, E.; Valero, C.; Werner, H. *J. Am. Chem. Soc.* **1989**, *111*, 7431.
- (32) Esteruelas, M. A.; Valero, C.; Oro, L. A.; Meyer, U.; Werner, H. *Inorg. Chem.* **1991**, *30*, 1159.
- (33) Werner, H.; Esteruelas, M. A.; Otto, H. *Organometallics* **1986**, *5*, 2295.
- (34) Werner, H.; Meyer, U.; Peters, K.; von Schnering, H. G. *Chem. Ber.* **1989**, *112*, 2097.
- (35) Esteruelas, M. A.; Lahoz, F. J.; Oñate, E.; Oro, L. A.; Valero, C.; Zeier, B.; *J. Am. Chem. Soc.* **1995**, *117*, 7935.
- (36) Albéniz, M. J.; Esteruelas, M. A.; Lledós, A.; Maseras, F.; Oñate, E.; Oro, L. A.; Sola, E.; Zeier, B. *J. Chem. Soc., Dalton Trans.* **1997**, 181.
- (37) Esteruelas, M. A.; Oro, L. A.; Valero, C. *Organometallics* **1995**, *14*, 3596.
- (38) Jessop, P. G.; Morris, R. H. *Coord. Chem. Rev.* **1992**, *121*, 155.
- (39) Bruce, M. I. *Chem. Rev.* **1991**, *91*, 197.
- (40) Buil, M. L.; Esteruelas, M. A. *Organometallics* **1999**, *18*, 1798.
- (41) Esteruelas, M. A.; Liu, F.; Oñate, E.; Sola, E.; Zeier, B. *Organometallics* **1997**, *16*, 2919.
- (42) Esteruelas, M. A.; Lahoz, F. J.; Oñate, E.; Oro, L. A.; Rodríguez, L. *Organometallics* **1996**, *15*, 3670.
- (43) Wakatsuki, Y.; Yamazaki, H.; Maraguma, Y.; Shimizu, I. *J. Chem. Soc., Chem. Commun.* **1991**, 261.
- (44) Crochet, P.; Esteruelas, M. A.; López, A. M.; Martínez, M.-P.; Oliván, M.; Oñate, E.; Ruiz, N. *Organometallics* **1998**, *17*, 4500.
- (45) Esteruelas, M. A.; Lahoz, F. J.; Oñate, E.; Oro, L. A.; Zeier, B. *Organometallics* **1994**, *13*, 4258.
- (46) Crabtree, R. H. *The Organometallic Chemistry of the Transition Metals*; Wiley: New York, 1988.
- (47) Esteruelas, M. A.; Lahoz, F. J.; Oñate, E.; Oro, L. A.; Zeier, B. *Organometallics* **1994**, *13*, 1662.
- (48) Chaloner, P. A.; Esteruelas, M. A.; Joó, F.; Oro, L. A. *Homogeneous Hydrogenation*; Kluwer Academic Publishers: Dordrecht, 1994; Ch. 3.
- (49) Bakhmutov, V. I.; Bertran, J.; Esteruelas, M. A.; Lledós, A.; Maseras, F.; Modrego, J.; Oro, L. A.; Sola, E.; *Chem. Eur. J.* **1996**, *2*, 815.
- (50) Esteruelas, M. A.; Oro, L. A.; Valero, C. *Organometallics* **1991**, *10*, 463.
- (51) Maseras, F.; Lledós, A. *Organometallics* **1996**, *15*, 1218.

- (52) Barea, G.; Esteruelas, M. A.; Lledós, A.; López, A. M.; Tolosa, J. I. *Inorg. Chem.* **1998**, *37*, 5033.
- (53) Spivak, G. J.; Caulton, K. G. *Organometallics* **1998**, *17*, 5260.
- (54) Espuelas, J.; Esteruelas, M. A.; Lahoz, F. J.; Oro, L. A.; Ruiz, N. *J. Am. Chem. Soc.* **1993**, *115*, 4683.
- (55) Spivak, G. J.; Coalter, J. N.; Oliván, M.; Eisenstein, O.; Caulton, K. G. *Organometallics* **1998**, *17*, 999.
- (56) Kuhlman, R.; Streib, W. E.; Hoffman, J. C.; Caulton, K. G. *J. Am. Chem. Soc.* **1996**, *118*, 6934.
- (57) Albéniz, M. J.; Buil, M. L.; Esteruelas, M. A.; López, A. M.; Oro, L. A.; Zeier, B. *Organometallics* **1994**, *13*, 3746.
- (58) Schlünken, C.; Werner, H. *J. Organomet. Chem.* **1993**, *454*, 243.
- (59) Buil, M. L.; Esteruelas, M. A.; Oñate, E.; Ruiz, N. *Organometallics* **1998**, *17*, 3346.
- (60) Albéniz, M. J.; Buil, M. L.; Esteruelas, M. A.; López, A. M. *J. Organomet. Chem.* **1997**, *545–546*, 495.
- (61) Daniel, T.; Werner, H. *Z. Naturforsch., B* **1992**, *47*, 1707.
- (62) Bohanna, C.; Esteruelas, M. A.; López, A. M.; Oro, L. A. *J. Organomet. Chem.* **1996**, *526*, 73.
- (63) Werner, H. *Coord. Chem. Rev.* **1982**, *43*, 165.
- (64) Yaneff, P. V. *Coord. Chem. Rev.* **1977**, *23*, 183.
- (65) (a) Adams, R. D.; Golembeski, N. M. *J. Am. Chem. Soc.* **1979**, *101*, 1306; (b) Adams, R. D.; Golembeski, N. M.; Selegue, J. P. *J. Am. Chem. Soc.* **1981**, *103*, 546; (c) McKenna, M.; Wright, L. L.; Miller, D. J.; Tanner, L.; Hiltiwanger, R. C.; DuBois, M. R. *J. Am. Chem. Soc.* **1983**, *105*, 5329; (d) Jones, W. D.; Selmeczy, A. D. *Organometallics* **1992**, *11*, 889.
- (66) Jia, G.; Meek, D. W. *Inorg. Chem.* **1991**, *30*, 1953.
- (67) Werner, H.; Tena, M. A.; Mahr, N.; Peters, K.; von Schnering, H.-G. *Chem. Ber.* **1995**, *128*, 41.
- (68) Buil, M. L.; Espinet, P.; Esteruelas, M. A.; Lahoz, F. J.; Lledós, A.; Martínez-Ilarduya, J. M.; Maseras, F.; Modrego, J.; Oñate, E.; Oro, L. A.; Sola, E.; Valero, C. *Inorg. Chem.* **1996**, *35*, 1250.
- (69) Buil, M. L. Ph. D. Dissertation, University of Zaragoza, 1997.
- (70) Gusev, D. G.; Kuhlman, R. L.; Renkema, K. B.; Eisenstein, O.; Caulton, K. G. *Inorg. Chem.* **1996**, *35*, 6775.
- (71) Espuelas, J.; Esteruelas, M. A.; Lahoz, F. J.; Oro, L. A.; Valero, C. *Organometallics* **1993**, *12*, 663.
- (72) Werner, H.; Meyer, U.; Esteruelas, M. A.; Sola, E.; Oro, L. A. *J. Organomet. Chem.* **1989**, *366*, 187.
- (73) Esteruelas, M. A.; Lahoz, F. J.; López, A. M.; Oñate, E.; Oro, L. A. *Organometallics* **1995**, *14*, 2496.
- (74) Buil, M. L.; Esteruelas, M. A.; López, A. M.; Oñate, E. *Organometallics* **1997**, *16*, 3169.
- (75) Kostic, N. M.; Fenske, R. F. *Organometallics* **1982**, *1*, 974.
- (76) Espuelas, J.; Esteruelas, M. A.; Lahoz, F. J.; López, A. M.; Oro, L. A.; Valero, C. *J. Organomet. Chem.* **1994**, *468*, 223.
- (77) Esteruelas, M. A.; García, M. P.; López, A. M.; Oro, L. A.; Ruiz, N.; Schlünken, C.; Valero, C.; Werner, H. *Inorg. Chem.* **1992**, *31*, 5580.
- (78) Esteruelas, M. A.; Oliván, M.; Oñate, E.; Ruiz, N.; Tajada, M. A. *Organometallics* **1999**, *18*, 2953.
- (79) Esteruelas, M. A.; Lahoz, F. J.; López, J. A.; Oro, L. A.; Schlünken, C.; Valero, C.; Werner, H. *Organometallics* **1992**, *11*, 2034.
- (80) (a) Calado, J. C. G.; Dias, A. R.; Salem, M. S.; Marthinho Simoes, J. A. *J. Chem. Soc., Dalton Trans.* **1981**, 1174; (b) Yoneda, G.; Blake, D. M. *Inorg. Chem.* **1981**, *20*, 67.
- (81) Esteruelas, M. A.; Gómez, A. V.; López, A. M.; Oro, L. A. *Organometallics* **1996**, *15*, 878.
- (82) (a) Albers, M. O.; Robinson, D. J.; Singleton, E. *Coord. Chem. Rev.* **1987**, *79*, 1; (b) Davis, S. G.; McNally, J. P.; Smallridge, A. J. *Adv. Organomet. Chem.* **1990**, *30*, 1.

- (83) (a) Hoyano, J.; Graham, W. A. G. *J. Am. Chem. Soc.* **1982**, *104*, 3722; (b) Weber, L.; Bungardt, D. J. *Organomet. Chem.* **1986**, *311*, 269; (c) Pourreau, D. G.; Geoffroy, G. L.; Rheingold, A. L.; Geib, S. J. *Organometallics* **1986**, *5*, 1337; (d) Weber, L.; Reizig, K.; Bungardt, D.; Boese, R. *Organometallics* **1987**, *6*, 110; (e) Johnston, L. J.; Baird, M. C. *Organometallics* **1988**, *7*, 2469; (f) Johnston, L. J.; Baird, M. C. *J. Organomet. Chem.* **1988**, *358*, 405; (g) Gross, Ch. L.; Wilson, S. R.; Girolami, G. S. *J. Am. Chem. Soc.* **1994**, *116*, 10294; (h) Gross, Ch. L.; Girolami, G. S. *Organometallics* **1996**, *15*, 5359; (i) Rink, B.; Scherer, D. J.; Wolmershäuser, G. *Chem. Ber.* **1995**, *128*, 71; (j) Cadierno, V.; Gamasa, M. P.; Gimeno, J.; González-Cueva, M.; Lastra, E.; Borge, J.; García-Granda, S.; Pérez-Carreño, E. *Organometallics* **1996**, *15*, 2137.
- (84) (a) Bruce, M. I.; Wong, F. S. *J. Organomet. Chem.* **1981**, *210*, C5; (b) Hoyano, J. K.; May, C. J.; Graham, W. A. G. *Inorg. Chem.* **1982**, *21*, 3095; (c) Bruce, M. I.; Tomkins, I. B.; Wong, F. S.; Shelton, B. W.; White, A. H. *J. Chem. Soc., Dalton Trans.* **1982**, 687; (d) Wilczewski, T. *J. Organomet. Chem.* **1986**, *317*, 307; (e) Bruce, M. I.; Humphrey, M. G.; Koutsantonis, G. E.; Liddell, M. J. *J. Organomet. Chem.* **1987**, *236*, 247; (f) Bruce, M. I.; Koutsantonis, G. A.; Liddell, M. J.; Nicholson, B. K. *J. Organomet. Chem.* **1987**, *320*, 217; (g) Kowano, Y.; Tobita, H.; Ogino, H. *Organometallics* **1994**, *13*, 3849; (h) Jian, G.; Ng, W. S.; Yao, J.; Lau, C.; Chen, Y. *Organometallics* **1996**, *15*, 5039; (i) Shapley, P. A.; Susta, J. M.; Hunt, J. L. *Organometallics* **1996**, *15*, 1622; (j) Freedman, D. A.; Gill, T. P.; Blough, A. M.; Koefod, R. S.; Mann, K. R. *Inorg. Chem.* **1997**, *36*, 95; (k) Koch, J. L.; Shapley, P. A. *Organometallics* **1999**, *18*, 814.
- (85) Bruce, M. I.; Windsor, N. J. *Aust. J. Chem.* **1977**, *30*, 1601; (b) Herrmann, W. A.; Herdtweck, E.; Schäfer, A. *Chem. Ber.* **1988**, *121*, 1907; (c) Dev, S.; Selegue, J. P. *J. Organomet. Chem.* **1994**, *469*, 107.
- (86) Atwood, J. D. *Inorganic and Organometallic Reaction Mechanisms*; VCH Publishers: New York, 1997; Ch. 3.
- (87) Esteruelas, M. A.; López, A. M.; Ruiz, N.; Tolosa, J. I. *Organometallics* **1997**, *16*, 4653; (b) Crochet, P.; Esteruelas, M. A.; Gutiérrez-Puebla, E. *Organometallics* **1997**, *16*, 4657; (c) Crochet, P.; Esteruelas, M. A.; López, A. M.; Ruiz, N.; Tolosa, J. I. *Organometallics*, **1998**, *17*, 3479; (d) Baya, M.; Crochet, P.; Esteruelas, M. A.; Gutiérrez-Puebla, E.; Ruiz, N. *Organometallics*, **1999**, *18*, 5034; (e) Esteruelas, M. A.; Gutiérrez-Puebla, E.; López, A. M.; Oñate, E.; Tolosa, J. I. *Organometallics*, **2000**, *19*, 275.
- (88) Bohanna, C.; Esteruelas, M. A.; Gómez, A. V.; López, A. M.; Martínez, M.-P. *Organometallics* **1997**, *16*, 4464.
- (89) Allen, F. H.; Kennard, O. *Chem. Des. Automation News* **1993**, *8*, 1, 31–37.
- (90) Gemel, C.; Trimmel, G.; Slugovc, C.; Kremel, S.; Mereiter, K.; Schmidt, R.; Kirchner, K. *Organometallics* **1996**, *15*, 3998.
- (91) Edwards, A. J.; Elipse, S.; Esteruelas, M. A.; Lahoz, F. J.; Oro, L. A.; Valero, C. *Organometallics* **1997**, *16*, 3828.
- (92) Buil, M. L.; Elipse, S.; Esteruelas, M. A.; Oñate, E.; Peinado, E.; Ruiz, N. *Organometallics* **1997**, *16*, 5748.
- (93) Tena, M. A.; Nürnberg, O.; Werner, H. *Chem. Ber.* **1993**, *126*, 1597.
- (94) Woerpel, K. A.; Bergman, R. G. *J. Am. Chem. Soc.* **1993**, *115*, 7888.
- (95) Villanueva, L. A.; Abboud, K. A.; Boncella, J. M. *Organometallics* **1992**, *11*, 2963.
- (96) Esteruelas, M. A.; Sola, E.; Oro, L. A.; Werner, H.; Meyer, U. *J. Mol. Catal.*, **1989**, *53*, 43.
- (97) Esteruelas, M. A.; Oro, L. A.; Valero, C. *Organometallics*, **1992**, *11*, 3362.
- (98) Esteruelas, M. A.; Herrero, J.; Oro, L. A. *Organometallics*, **1993**, *12*, 2377.
- (99) Esteruelas, M. A.; Sola, E.; Oro, L. A.; Werner, H.; Meyer, U. *J. Mol. Catal.*, **1988**, *45*, 1.
- (100) Sánchez-Delgado, R. A.; Rosales, M.; Esteruelas, M. A.; Oro, L. A. *J. Mol. Catal.* **1995**, *96*, 231.
- (101) Esteruelas, M. A.; Oro, L. A. *Chem. Rev.* **1998**, *98*, 577.

Chemistry of *o*-Carboranyl Derivatives

SANG OOK KANG and JAEJUNG KO

Department of Chemistry
Korea University
Chochiwon, Chungnam 339-700, Korea

I. Introduction	61
II. Group IV-B Derivatives (Si, Ge, Sn) of <i>o</i> -Carborane	63
A. Chemistry of Bissilyl and Bistanna <i>o</i> -Carboranyl Derivatives	63
B. Double Silylation Reaction of <i>o</i> -Bis(silyl)carborane	65
C. Reactivity of Strained Compounds, <i>o</i> -Carboranylene-1,2-disilacyclobutene	69
D. Organotin Compounds Containing the C,N-Chelating <i>o</i> -Carboranylamino Ligand	71
E. Metal Complexes Containing the P,Si-Chelating <i>o</i> -Carboranylphosphino Ligand	72
F. Organotin Compounds Containing a C,P-Chelating <i>o</i> -Carboranylphosphino Ligand	75
III. Metal Compounds Containing an X,Y-Carboranyl Chelating Ligand	77
A. Metal Compounds Containing a B,N- or B,P-Carboranyl Chelating Ligand	77
B. Metal Compounds Containing a C,N-Carboranyl Chelating Ligand	80
C. Metal Compounds Containing an S,N- or S,P-Carboranyl Chelating Ligand	81
IV. Metal Compounds Containing a Dithiolato- <i>o</i> -Carborane	83
V. Reactivity of <i>o</i> -Carborane	88
VI. Ligand Design Derived from <i>o</i> -Carborane	93
VII. Concluding Remarks	95
References	97

I

INTRODUCTION

The discovery of polyhedral boranes and polyhedral heteroboranes, which contain at least one atom other than in the cage, initiated a new era in boron chemistry.¹⁻⁴ Most commonly, of the three commercially available isomeric dicarba-*closo*-dodecaborane carboranes(1,2-, 1,7-, and 1,12-), the 1,2-isomer **1** has been used for functionalization and connection to organic molecules. The highly delocalized three-dimensional cage bonding that characterizes these carboranes provides extensive thermal and kinetic stabilization as well as photochemical stability in the ultraviolet and visible regions. The unusual icosahedral geometry of these species provides precise directional control of all exopolyhedral bonds.



The dots represent
carbons; all other
vertices are B-H

1

Although the similarity between benzene, the planar aromatic two-dimensional system, and the icosahedral three-dimensional carboranes may seem remote, there is much the two have in common. The reasons for the overall similarities in stability and reactivity in these two seemingly different molecules probably lie in their comparable molecular orbital systems. Benzene has six π molecular orbitals, three bonding and three antibonding.⁵ The six available π electrons nicely fill the bonding set. *o*-Carborane 1 accommodates 26 electrons in a system of 13 delocalized bonding molecular orbitals and thus resembles its two-dimensional analog benzene.⁶ This similarity in molecular orbital description results in great thermodynamic stability for 1, as well as reactivity reminiscent of benzene.

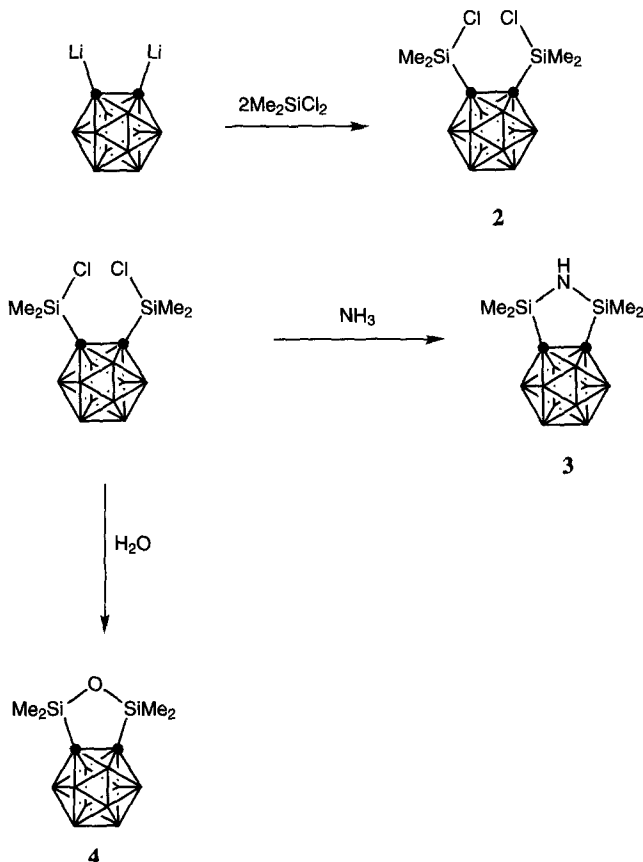
In recent years, the coordination behavior of organometallic compounds containing bidentate aromatic ligands such as 2-[(dimethylamino)methyl]phenyl (HAr^{N}),⁷⁻¹¹ 1,2-benzenedithiol,¹²⁻¹⁴ and *o*-bis(dimethylsilyl)benzene¹⁵⁻¹⁸ has been the focus of extensive studies. The corresponding lithium compounds, LiAr^{N} and $(\text{LiS})_2\text{C}_6\text{H}_4$, are the common starting materials for the preparation of new complexes. Although the HAr^{N} , $\text{C}_6\text{H}_4(\text{SH})_2$, and *o*-bis(SiMe_2H) C_6H_4 ligand system have been used extensively during the past decade as intramolecularly bidentate coordinating ligands for many different metals, the three-dimensional analogues of these interesting compounds containing an *o*-carboranyl unit remain virtually unexplored. Considering the rich chemistry of aryl derivatives and the similarities in stability and reactivity between benzene and *o*-carborane, *o*-carborane may be promising for further transformations as a chelating ligand.

In this account, we give an overview of chemistry of *o*-carboranyl derivatives. The following topics are discussed: (i) group IV-B derivatives (Si, Ge, Sn) of *o*-carborane, (ii) metal compounds containing an X,Y-carboranyl chelating ligand, (iii) metal compounds containing a dithiolato-*o*-carborane, (iv) reactivity of *o*-carborane, and (v) ligand design derived from *o*-carborane. Although numerous works on the chemistry of 7,8-dicarba-*nido*-undecaborate on the coordinating behavior of electron-rich elements such as sulfur and phosphorus¹⁹⁻²² and the C—C bond formation directing for the BNCT²³⁻²⁵ have been well documented, these two areas are beyond the realm of this account.

II

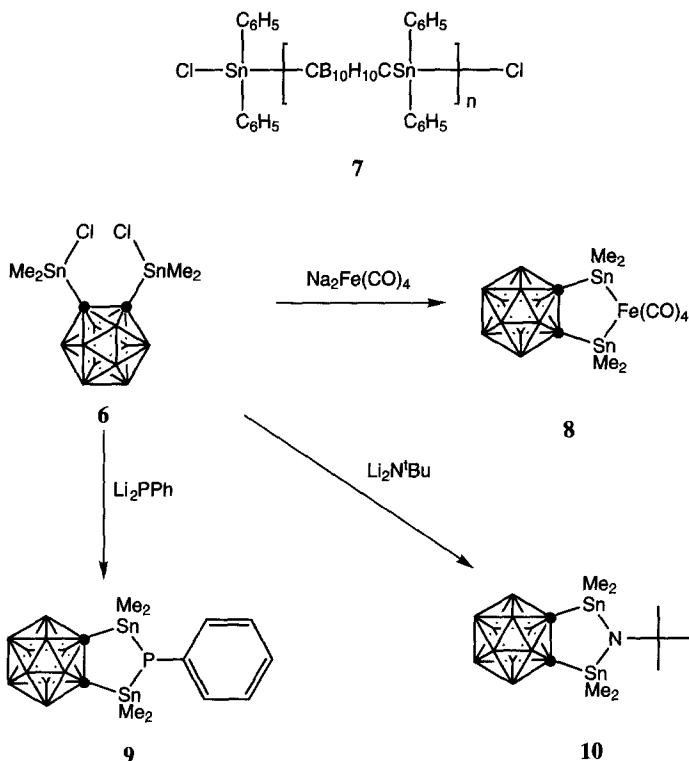
GROUP IV-B DERIVATIVES (Si, Ge, Sn) OF *o*-CARBORANEA. Chemistry of Bissilyl and Bistanna *o*-Carboranyl Derivatives

A primary objective of the syntheses of 1,2-bis(chlorodimethylsilyl)carborane **2** has been the incorporation of the $B_{10}C_2$ carborane nuclei into the backbone of essentially inorganic polymers. Heying *et al.*²⁶ has prepared compound **2** through the reaction of $o\text{-}C_{10}H_{10}C_2Li_2$ and 2 equiv. of Me_2SiCl_2 .



When 1,2-bis(chlorodimethylsilyl)carborane **2** was treated with ammonia, an aminolysis reaction occurred to give the cyclic tetramethyldisilaazane **3**. The ease with which this reaction occurs to form five-membered ring bears notice. Hydrolysis of **2** gives cyclic siloxane compound **4**. Utilization of the same general

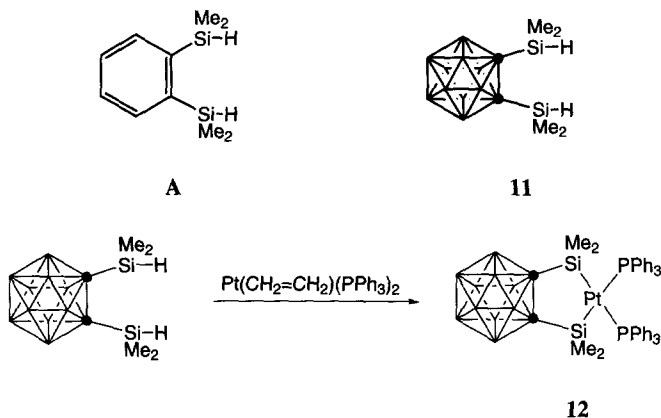
preparative procedure as for **2** has proven quite satisfactory for the preparation of 1,2-bis(chlorodimethylgermyl)carborane **5** and 1,2-bis(chlorodimethyltin)carborane **6**. Employment of an aryl- instead of alkyl-substituted dichlorotin derivatives resulted in a noncyclic and difunctional compound. In the reaction of $(\text{C}_6\text{H}_5)_2\text{Sn}_2\text{Cl}_2$ with $p\text{-B}_{10}\text{H}_{10}\text{C}_2\text{Li}_2$, polymeric material **7** was obtained exclusively.



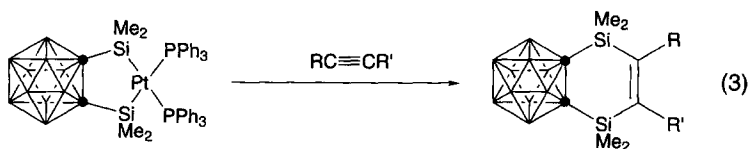
The difunctional 1,2-bis(chlorodimethyltin)carborane **6** is a useful starting material for further reactions. Recently, we²⁷ reported that the compound **6** reacted with $\text{Na}_2\text{Fe}(\text{CO})_4$ to give the orange distannairon compound **8** in high yield. Cyclic distannaphosphane compound **9** has been prepared. Treatment of **6** with $\text{Li}_2\text{N}^t\text{Bu}$ gave the cyclic five-membered product **10**. The X-ray structure analysis of **9** reveals an expected structural feature. The cyclic five-membered configuration $\text{C}_2\text{Sn}_2\text{P}$ is bent, and the phenyl group in P is perpendicular to the bisector of Sn_2C_2 fragment. Analogous to the tin compound, the germanium compound **5** reacted with $\text{Na}_2\text{Fe}(\text{CO})_4$, $\text{Li}_2\text{PC}_6\text{H}_5$, and $\text{Li}_2\text{N}^t\text{Bu}$ to give the digermyliron, phosphane, and azane products, respectively.

B. Double Silylation Reaction of *o*-Bis(silyl)carborane

The double silylation reaction, pioneered by Kumada and co-workers,²⁸ is a convenient synthetic route for obtaining compounds in which two Si—C bonds are created by the addition of two silicon units to unsaturated organic substrates such as alkynes,^{29–31} alkenes,^{32–34} and 1,3-dienes.^{35–37} Platinum and nickel complexes are excellent catalysts for the transformation of silicon-containing linear compounds and for hydrosilylation. Alkynes and olefins underwent dehydrogenative 1,2-double silylation with *o*-bis(dimethylsilyl)benzene **A** in the presence of a catalytic amount of Pt or Ni compounds to afford benzo-1,4-disilacyclohexene. Its congener, 1,2-bis(dimethylsilyl)carborane **11**, remains virtually unexplored. Recently, we^{38–39} reported the cyclic bis(silyl)platinum complex **12** which is a key intermediate in the platinum-catalyzed double silylation of alkynes. The ²⁹Si NMR spectrum of **12** shows the expected pattern of a doublet of doublets (¹J_{Pt–Si} = 1238.6 Hz, ²J_{Si–P(trans)} = 148.8 Hz, ²J_{Si–P(cis)} = 12.8 Hz) from coupling to two different ³¹P nuclei, along with satellites arising from coupling to ¹⁹⁵Pt. The ²⁹Si NMR resonance of 39.6 ppm, a doublet of doublets, strongly resembles the literature values for the *cis*-PtSi₂P₂ complexes.⁴⁰



Complex **12** was found to be a good reactant in the double-silylation reaction. Thus, thermolysis of a toluene solution of **12** and diphenylacetylene at 120°C for 12 h afforded 5,6-carboranylene-1,1,4,4-tetramethyl-2,3-diphenyl-1,4-disilacyclohex-2-ene **13**. When 1-hexyne was employed in the reaction with **12** under the same reaction conditions, the five-membered disila ring compound **18** was isolated. A key feature in the ¹H NMR spectrum of **18** includes a singlet at 6.24 ppm assigned to the vinyl proton. A characteristic high-frequency ¹³C NMR resonance at 138.50 ppm provides evidence for a tethered sp² carbon atom between the two silicon atoms.



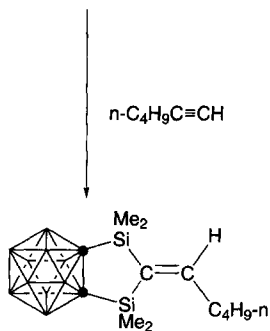
13 $R = R' = Ph$

14 $R = Ph, R' = H$

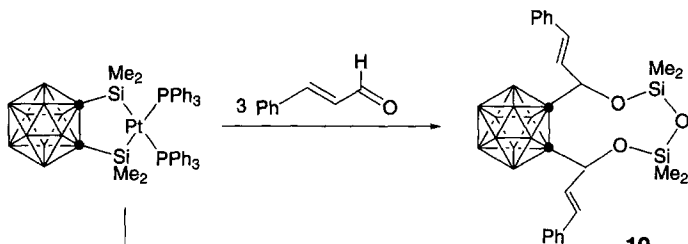
15 $R = R' = Et$

16 $R = R' = Me$

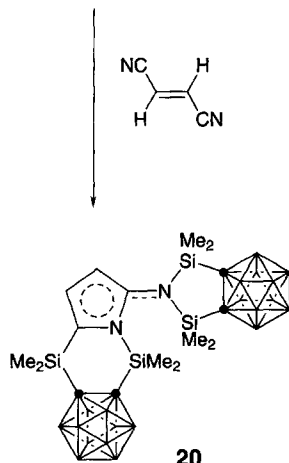
17 $R = R' = COOMe$



18



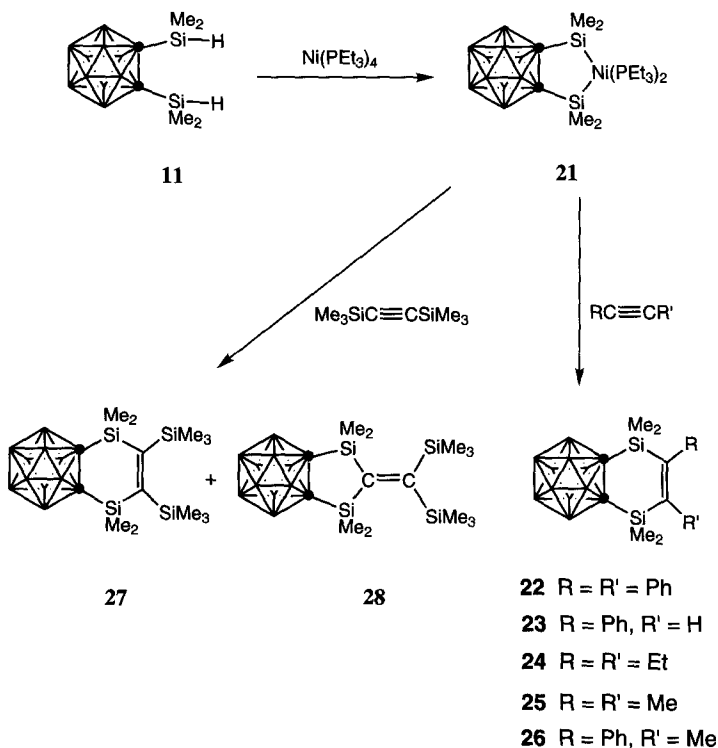
19



20

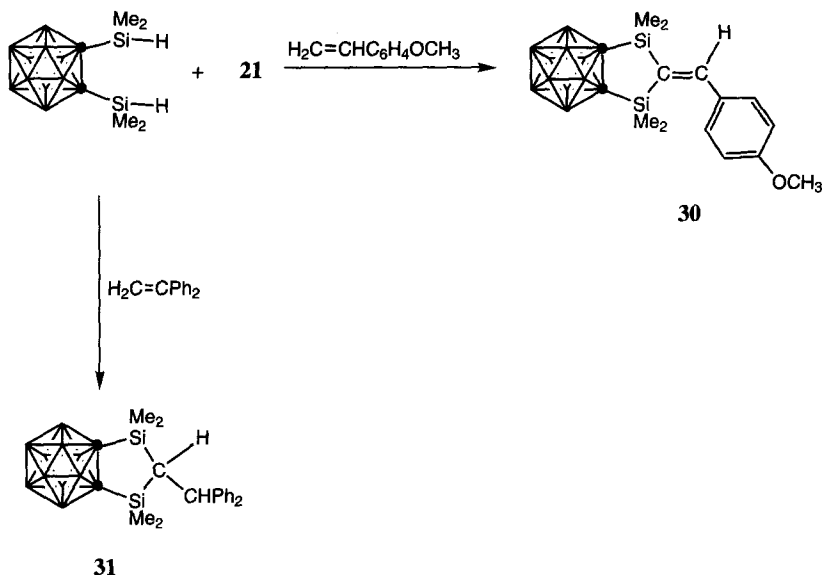
Thermolysis of **12** with *trans*-cinnamaldehyde afforded the insertion compound **19**, formed through the di-insertion of two carbonyl ligands into the C—Si bond of **12**. The reaction of **12** with fumaronitrile yielded the cyclization product **20**. X-ray study revealed **20** to be a cyclization product which contains two types of disilyl moieties, imino and *N,N*-bis(silyl)amino, which are connected by a five-membered ring.

The double silylation reactions of **12** were stoichiometric processes involving reaction of a stable PtSi_2P_2 complex with a variety of unsaturated organic substrates. A catalytic process would be preferred. Recently we⁴¹⁻⁴² have succeeded in the isolation of the bis(silyl)nickel complex that would be suitable as a catalyst. The reaction of 1,2-bis(dimethylsilyl)carborane with $\text{Ni}(\text{PEt}_3)_4$ yielded the cyclic bis(silyl)nickel complex **21**. Complex **21** was found to be a good catalyst for the double silylation reaction of alkynes and alkenes. Thus, the reaction of **1** with $\text{RC}\equiv\text{CR}'$ in the presence of a catalytic amount of **21** afforded the six-membered disilylene ring compounds *o*- $\text{B}_{10}\text{H}_{10}\text{C}_2(\text{SiMe}_2)_2(\text{CR}=\text{CR}')$ **22–26**. In contrast, the reaction of bis(trimethylsilyl)acetylene with **11** in the presence of a catalytic amount of **21** afforded the six-membered disilylene ring compound **27** and the five-membered disilylene ring compound **28**.



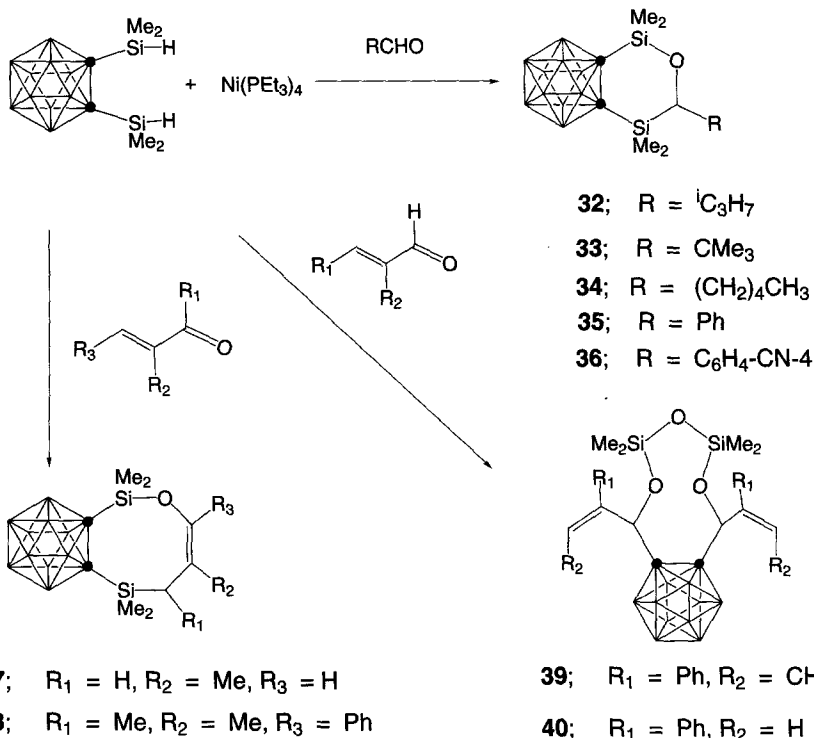
The disilanic nickel compound **21** is not effective in the nickel-catalyzed double silylation reaction with styrene. However, the stoichiometric reaction of **21** with styrene afforded 4,5-carboranylene-1,1,3,3-tetramethyl-2-phenylmethylene-1,3-disilacyclopentane **29**. A key feature in the ^1H NMR spectrum of **29** includes a singlet at 7.71 ppm assigned to the vinyl proton. A characteristic low-frequency ^{13}C NMR resonance at 139.75 ppm provides evidence for a tethered carbon atom of the two silicon moieties. Unambiguous confirmation was provided by X-ray crystallographic analysis of **29**.

The disilanic nickel complex **21** is an effective catalyst for the double silylation of some alkenes. Thus, reaction of **11** with 2 equiv. of 4-vinylanisole in the presence of a catalytic amount of **21** afforded a moderate yield of the five-membered disilylene compound **30**. However, treatment of **11** with 1.2 equiv. of 1,1-diphenylethylene in the presence of a catalytic amount of **21** gave five-membered disilylene ring compound **31**, which contained a saturated side chain.



The disilanic nickel complex **21** was also found to be a good catalyst for the dehydrogenative double silylation of aldehydes. The nickel-catalyzed reactions of 1,2-bis(dimethylsilyl)carborane **11** with aldehydes such as isobutyraldehyde, trimethylacetaldehyde, hexanal, and benzaldehyde afforded 5,6-carboranylene-2-oxa-1,4-disilacyclohexane.^{32,34,36} The dehydrogenative 1,4-double silylation of methacrolein and *trans*-4-phenyl-3-buten-2-one in the presence of a catalytic amount of $\text{Ni}(\text{PEt}_3)_4$ also took place under similar conditions. In contrast, the reaction of **11** with α -methyl-*trans*-cinnamaldehyde and *trans*-cinnamaldehyde under

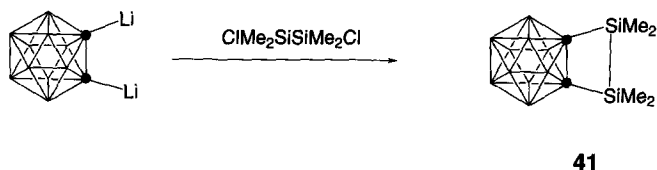
the same reaction conditions yielded products formed via the di-insertion of two carbonyl ligands into the C—Si bond of **11**. The reaction of **21** with diphenylketene yielded the 1,2-adduct across the carbonyl group.



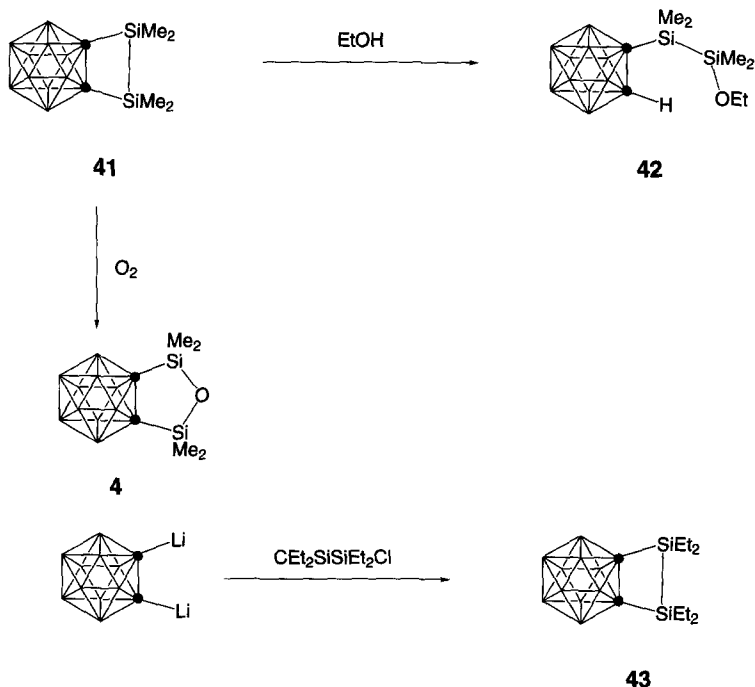
C. Reactivity of Strained Compounds, *o*-Carboranylene-1,2-disilacyclobutene

There exists considerable interest in cyclic molecules containing Si—Si and Si—C bonds because these compounds have been shown to undergo insertion reactions with small molecules, intermolecular ring enlargements, and ring-opening polymerization (ROP) reactions.^{43–44} Concomitantly there has been interest in the incorporation of carboranes into organic and silicon-containing polymers to make advanced thermooxidatively stable materials and ceramic precursors. Recently, Rege *et al.*⁴⁵ reported that the novel strained compound 1,2-(1,1,2,2-tetramethyldisilane-1,2)carborane **41** was synthesized by the reaction of 1,2-dilithiocarborane and dichlorotetramethyldisilane.

In contrast to its organic analog, *o*-(disilanyl)-phenylene,⁴⁶ the reaction of **41** with ethanol leads to cleavage of a Si—C bond rather than a Si—Si bond.

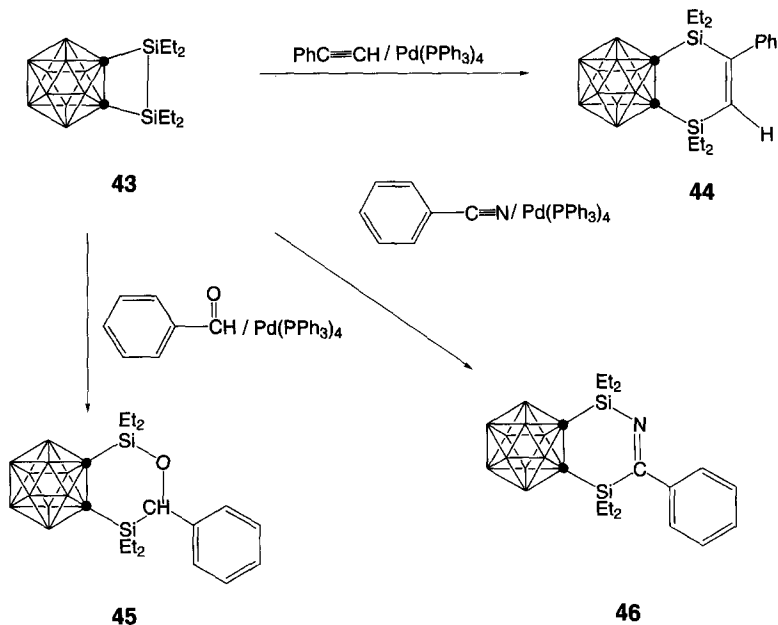


Similar to other cyclic disilanes, exposure of a solution of **41** to oxygen leads to the insertion product of an oxygen into the Si—Si bond. Compound **4** had been made previously by reacting H_2O with 1,2-bis(chlorodimethylsilyl)carborane. Compound **41** does not polymerize spontaneously at room temperature or in the presence of AlCl_3 . The contrast in reactivity between *o*-(disilanyl)phenylene and **41** is presumably due to a lack of significant electron delocalization between the Si atoms and the carborane cage in **41**. Recently, we⁴⁶ reported the synthesis of 1,2-(1,1,2,2-tetraethylidisilane)carborane **43** by the reaction of $\text{B}_{10}\text{H}_{10}\text{C}_2\text{Li}_2$ with tetraethylchlorosilane.



Compound **43** is a colorless solid stable to air and to brief heating to $120 \sim 124^\circ\text{C}$. Similar to its organic analogue, 3,4-benzo-1,1,2,2-tetraethyl-1,2-disilacyclobut-3-one, compound **43** shows interesting chemical behavior. Thermolysis of a toluene

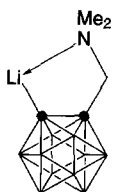
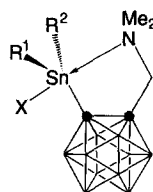
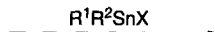
solution of **43** and phenylacetylene in a 1:6 molar ratio at 120°C for 48 h in the presence of a catalytic amount of $\text{Pd}(\text{PPh}_3)_4$ afforded 5,6-carboranylene-1,1,4,4-tetraethyl-2-phenyl-1,4-disilacyclohex-2-ene **44**. The reaction of **43** with benzaldehyde in the presence of a catalytic amount of $\text{Pd}(\text{PPh}_3)_4$ at 140~160°C afforded 5,6-carboranylene-1,1,4,4-tetraethyl-2-oxa-3-phenyl-1,4-disilacyclohexane **45**. Similar nickel-catalyzed reaction of **43** with benzonitrile gave the cyclic six-membered product **46** in 42% yield.



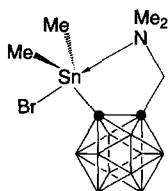
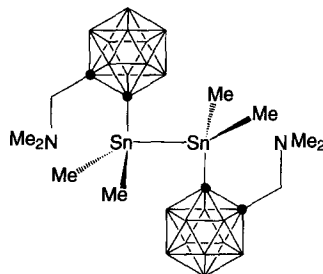
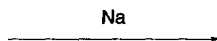
D. Organotin Compounds Containing the C,N-Chelating *o*-Carboranylamino Ligand

Organometallic compounds that have interesting properties and special reactivity can be prepared using C,N-chelating ligands.⁴⁷⁻⁴⁹ These properties are attributable to an extension of their coordination number by intramolecular coordination of a C,N-chelating ligand. Recently, we⁵⁰ have investigated the synthesis of intramolecularly coordinated organotin compounds bearing a bulky *o*-carborane unit that might potentially stabilize the pentacoordinate tin center. Thus, the reaction of $\text{Li Cab}^{\text{C,N}}$ **47** with organotin halides afforded a variety of organotin complexes containing the *o*-carboranylamino ligand. ^1H and ^{119}Sn NMR spectroscopy indicates that the tin center in $(\text{Cab}^{\text{C,N}})\text{SnR}^1\text{R}^2\text{X}$ is pentacoordinate as a result of intramolecular Sn-N coordination. The reaction of 2 equiv. of $(\text{Cab}^{\text{C,N}})\text{SnMe}_3$ with

HgCl₂ results in transmetalation of (Cab^{C,N})SnMe₃, giving the diorganomercury compound (Cab^{C,N})₂Hg **52**.

Li Cab^{C,N}**47**(Cab^{C,N})SnR¹R²X**48**; R¹ = R² = Me, X = Cl**49**; R¹ = R² = Ph, X = Cl**50**; R¹ = R² = Me, X = Br**51**; R¹ = R² = X, X = Cl

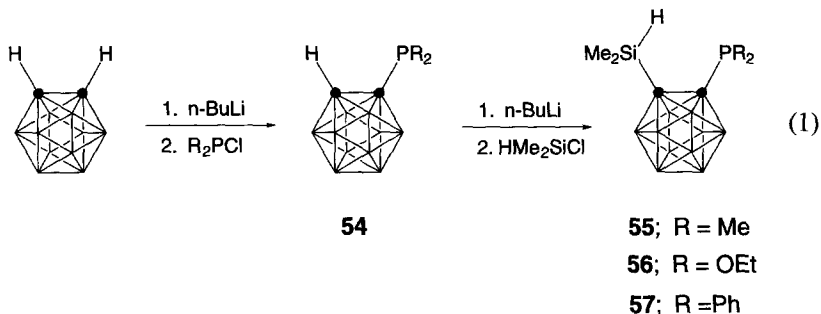
The mercury atom is four-coordinate, both nitrogen atoms being involved in intramolecular coordination. The reaction of (Cab^{C,N})SnMe₂Br with Na afforded the bis(*o*-carboranylamino)distannane [(Cab^{C,N})SnMe₂]₂ **53**. The two tin atoms exhibit approximately trigonal-bipyramidal geometry.

**50****53**

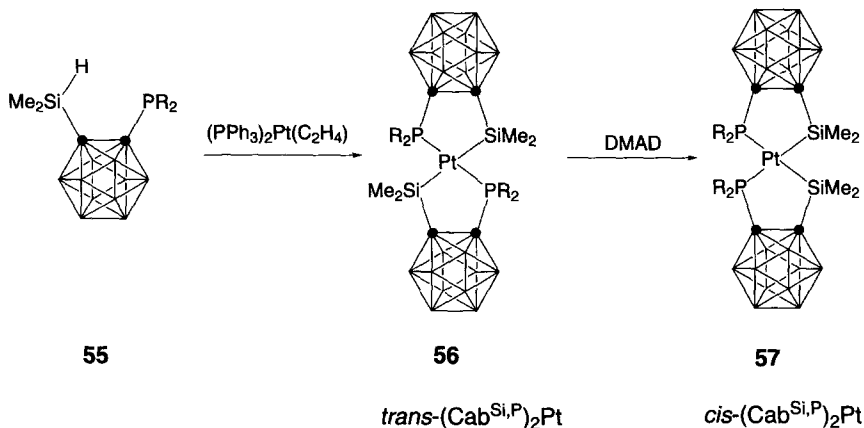
E. Metal Complexes Containing the *P,Si*-Chelating *o*-Carboranylphosphino Ligand

Phosphinoalkylsilanes as chelate ligands with transition metals have been studied, principally to provide a better understanding of metal-catalyzed industrial reactions such as hydrosilylation.⁵¹ Although many examples of bis-chelate metal complexes possessing a *cis*-arrangement of the phosphinoalkylsilyl ligands in a typical square-planar M(II)(M = Pd, Pt) environment have been synthesized,⁵²

few *trans* bis-chelates have received scrutiny due to their inaccessibility. Recently, we⁵³ reported the general synthesis of a new class of stable *trans* bis-chelates with a bulky *o*-carborane. The synthesis of phosphinosilanes **55–57** is shown schematically in Eq. (1).

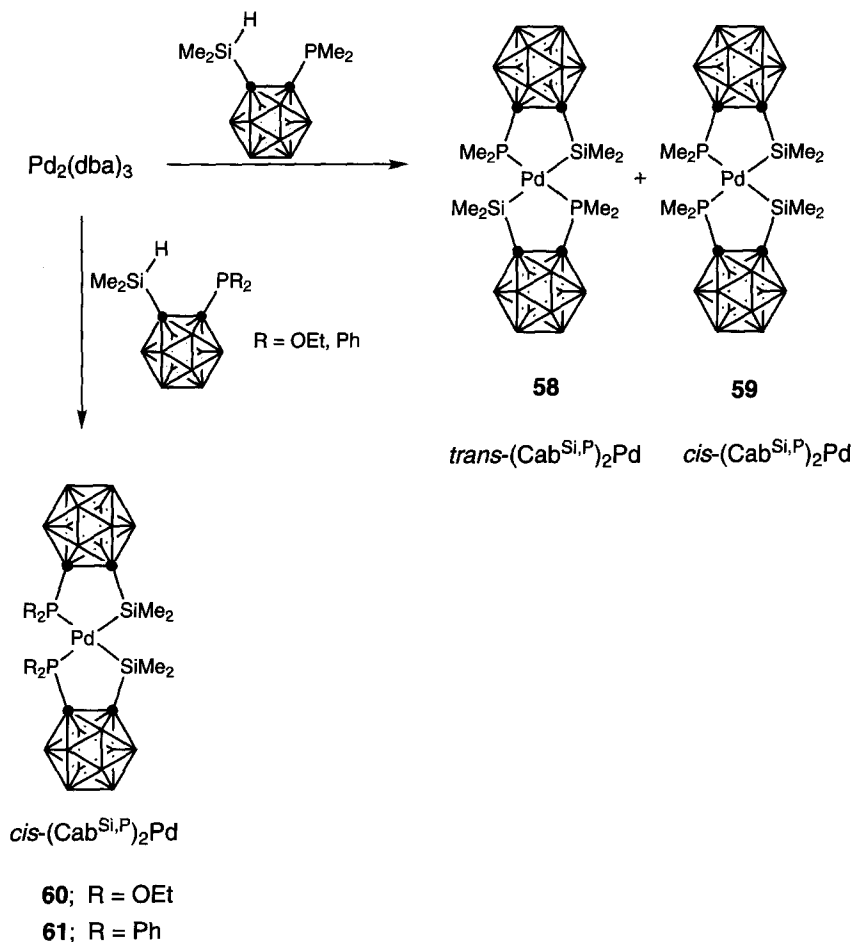


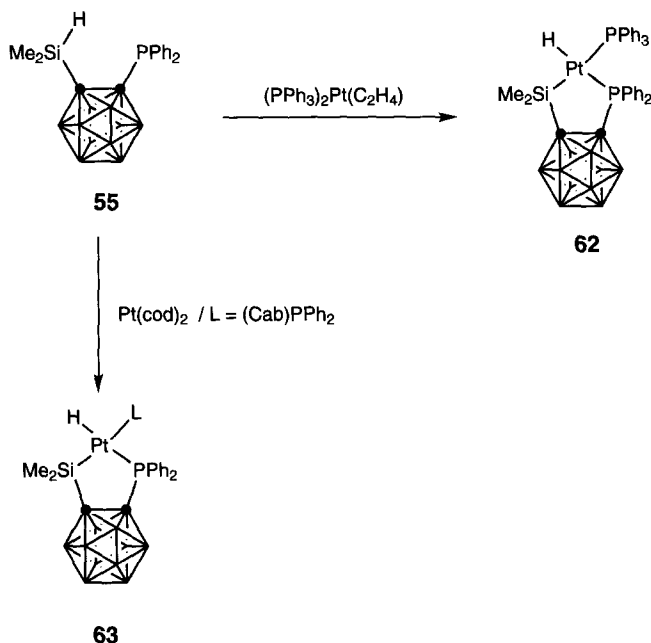
The reaction of $(\text{PPh}_3)_2\text{Pt}(\text{C}_2\text{H}_4)$ and phosphinosilanes **55,56** leads to *trans*-(Cab^{P,Si})₂Pt. A *trans*-arrangement for the phosphinosilyl ligands in a typical square planar Pt(II) environment is proposed by $J_{\text{Pt-P}}$ values in the range of 4049–4055 Hz for compound **56**. This conclusion was substantiated for compound **56** by a single-crystal X-ray study. Initial attempts to isomerize *trans* isomer have been unsuccessful. However, in the presence of dimethyl acetylenedicarboxylate (DMAD) the *trans* isomer **56** cleanly rearranges to the thermodynamically favored *cis* isomer, *cis*-(Cab^{P,Si})₂Pt **57**, at 110°C within an hour.



Other Group 10 metal complexes, such as $\text{Pd}_2(\text{dba})_3$ and $\text{Pt}(\text{cod})_2$, were tested for chelate-assisted oxidative addition of **55**. Use of $\text{Pd}_2(\text{dba})_3$ in the reaction of **55**

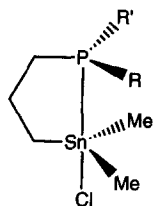
give bis-chelates **58** and **59** in 34% yield with *trans*:*cis* ratio of 2:1. The reaction of $\text{Pd}_2(\text{dba})_3$ with **56** and **57**, on the other hand, is *cis*-selective, producing the compounds **60–61**. These results indicate that the stereoselectivity of the reaction is dependent on the electronic and steric characteristics of the ligands around the metal center. The Pt complex, $(\text{PPh}_3)_2\text{Pt}(\text{C}_2\text{H}_4)$, reacted with **55** to generate the chelating *cis*-Pt(II) hydrido silyl complex $(\text{Cab}^{\text{P,Si}})\text{Pt}(\text{H})(\text{PPh}_3)$ **62**. In a similar fashion, **55** was found to react cleanly with $\text{Pt}(\text{cod})_2$ and $(\text{Cab})\text{PPh}_2$ to provide the sterically encumbered *cis* Pt(II) hydrido silyl complex $(\text{Cab}^{\text{P,Si}})\text{Pt}(\text{H})[(\text{Cab})\text{PPh}_2]$ **63**. Although the hydride ligand was not located by X-ray diffraction, its presence was confirmed by its ^1H NMR resonance operating at around $\delta\text{-1} ({}^1J_{\text{Pt-H}} \sim 1120 \text{ Hz})$.



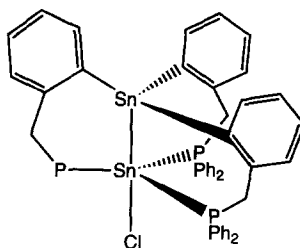


F. Organotin Compounds Containing a C,P-Chelating *o*-Carboranylphosphino Ligand

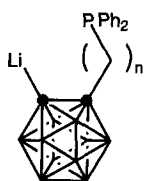
Although triorganotin halides containing a C,Y-chelating ligand in which Y = nitrogen atom or oxygen atom containing substituents have been intensively studied,^{54–56} few compounds^{57–58} containing phosphorus substituents **64–65** have been reported. Recently, we⁵⁹ reported the synthesis of intramolecularly coordinated organotin compounds bearing a bulky *o*-carborane unit and phosphorus unit. The reaction of $\text{LiCab}^{\text{C,P}}$ **66–67** with organotin halides afforded compounds **68–71**. ^1H , ^{31}P , and ^{119}Sn NMR spectroscopy of **68–71** indicates that the tin center is pentacoordinate as a result of intramolecular $\text{Sn} \leftarrow \text{P}$ coordination. The X-ray crystallographic studies of **68** and **70** show that the $\text{Sn} \leftarrow \text{P}$ coordination is relatively weak. Substitution reactions of **68** with NaI , $\text{NaB}(\text{CN})\text{H}_3$, and $\text{NaCpFe}(\text{CO})_2$ readily occur to give the expected products with the moiety intact. The compound **68** also reacted with $\text{Pd}_2(\text{dba})_3$ or $\text{Pt}(\text{cod})_2$ to give the chloro bridged dinuclear complexes. Compound **68** is easily cleaved by donor molecules such as pyridine or triethylphosphine to give the mononuclear compound **74**. In a fashion similar to that of $(\text{Cab}^{\text{C,N}})\text{SnR}^1\text{R}^2\text{X}$, the Wurtz type reaction of **69** with Na afforded the bis(*o*-carboranylphosphino)distannane $[(\text{Cab}^{\text{C,P}})\text{SnMe}_2]_2$ **76**. The



64

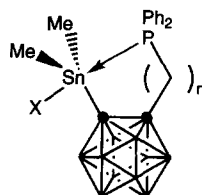


65



66; $n = 0$

67; $n = 1$

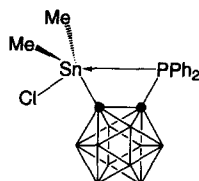


68; $n = 0$, $\text{X} = \text{Cl}$

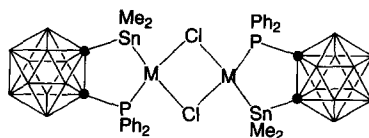
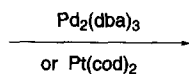
69; $n = 0$, $\text{X} = \text{Br}$

70; $n = 1$, $\text{X} = \text{Cl}$

71; $n = 1$, $\text{X} = \text{Br}$



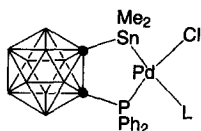
68



72; $\text{M} = \text{Pd}$

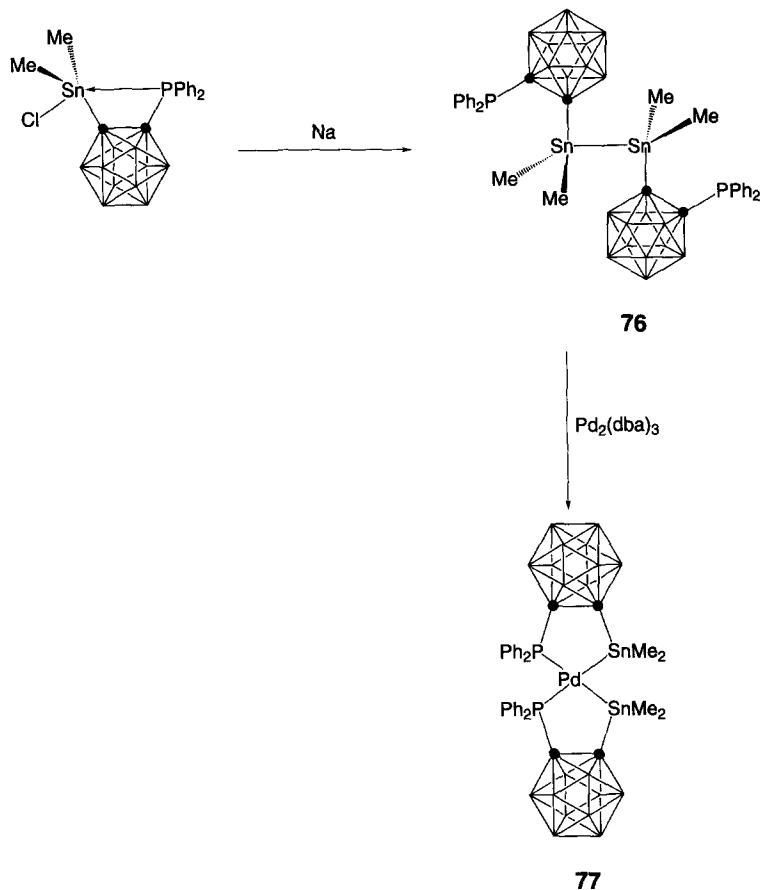
73; $\text{M} = \text{Pt}$

\swarrow $\text{L} = \text{pyridine, PEt}_3$



74; $\text{L} = \text{pyridine}$

75; $\text{L} = \text{PEt}_3$



reaction of **76** with $\text{Pd}_2(\text{dba})_3$ afforded bis-chelate palladium compound **77** in high yield. The structure of **77** was unambiguously determined by single-crystal X-ray crystallography.

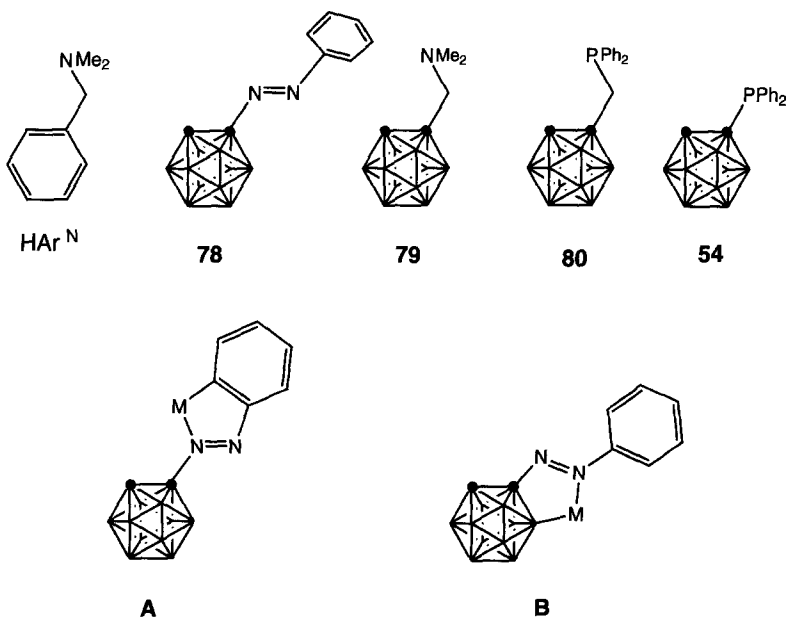
III

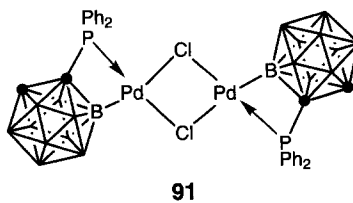
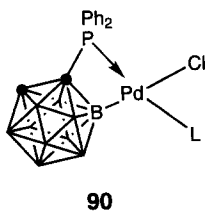
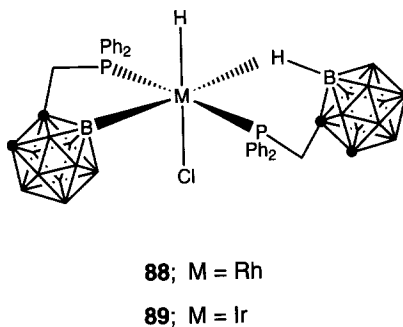
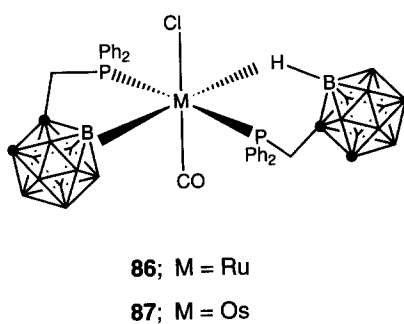
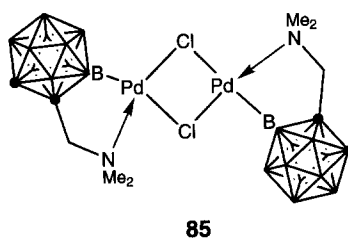
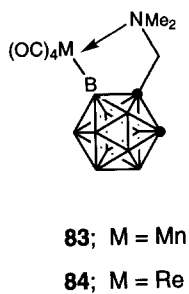
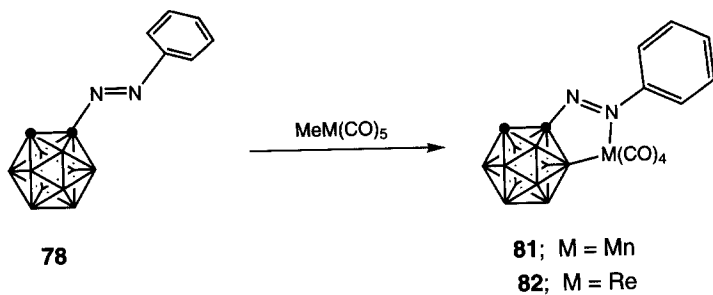
METAL COMPOUNDS CONTAINING AN X,Y-CARBORANYL CHELATING LIGAND

A. Metal Compounds Containing a B,N- or B,P-Carboranyl Chelating Ligand

Organometallic compounds containing the bidentate ligand 2-[(dimethylamino)methyl]phenyl(HAr^{N}) have been extensively studied. Many subclasses of these

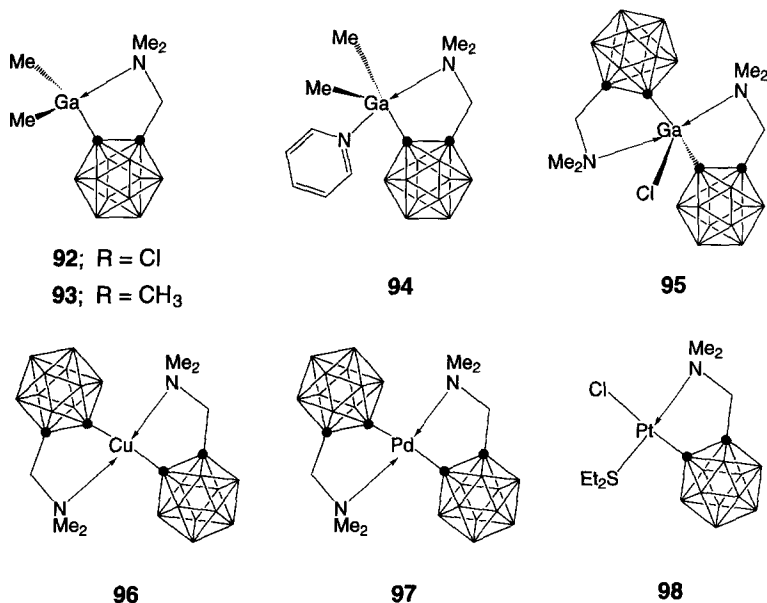
interesting compounds such as phenylazo-, N,N-dialkylamino-, and diphenylphosphino derivatives of *o*-carborane remain virtually unexplored. Recently, Zakharkin and co-workers⁶⁰ have reported the synthesis of such intramolecularly coordinated complexes using ligands **78–80**. The method involves cyclometallation of carboranes containing substituents with a donor atom such as nitrogen or phosphorus. Thus, the reaction of carborane azo-derivative with carbonyl compounds of manganese and rhenium gives rise to the metallation of the carborane nucleus with the formation of *exo*-cyclic derivatives containing the B–M bond stabilized by the intramolecular interaction between the nitrogen and the transition metal atom **A** rather than the metallation of the benzene nucleus to form a benzochelate **B**. Both phenylazo derivative of *o*-carborane and N,N-dialkylaminomethylene carboranes can enter the cyclometallation reaction **83–84** with manganese, rhenium carbonyl complexes, and palladium complex **85**. The diphenylphosphinomethylene carborane **80** reacts with ruthenium or osmium salts under the conditions of reductive carbonylation to form hexa-coordinated complexes **86–87** in which one of the coordinated sites is occupied by the bridged B–H···M bond. Cyclometallation of **80** occurs under the action of Rh(I) complexes in the presence of pyridine as coligands to give stable chelated B- σ -carboranyl compounds. The compound **54** reacts with a bivalent palladium compound to form a donor complex of *trans*-configuration. Heating this complex in toluene gives a mixture of monomeric and dimeric cyclometallated products **90,91**.





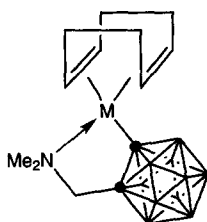
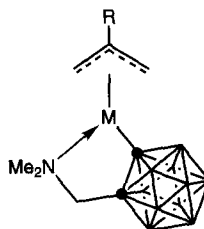
B. Metal Compounds Containing a C,N-Carboranyl Chelating Ligand

Recently, we⁶¹ have developed the possibility of synthesizing intramolecularly coordinated complexes using the HCab^N system. Thus, the reaction of LiCab^N with GaR₂Cl in a 1:1 ratio produced the four-coordinated metallacyclic organogallium compounds Cab^{C,N}GaR₂, in which the gallium atom was stabilized via an intramolecular C,N-coordination. Compound **92** with Lewis acidic character readily reacted with the base pyridine to yield the adduct Cab^NGaCl₂·NC₅H₅ **94**. Reaction of LiCab^N with GaCl₃ in a 2:1 ratio afforded the bis[(dimethylamino)methyl]-*o*-carboranyl]gallium (Cab^N)₂GaCl **95**. The NMR spectra revealed that intramolecular Ga-N coordination occurs in solution, resulting in a pentacoordinate (Cab^N)₂GaCl structure. The trigonal-bipyramidal coordination of the gallium center was confirmed by single-crystal X-ray determination of compound **95**.



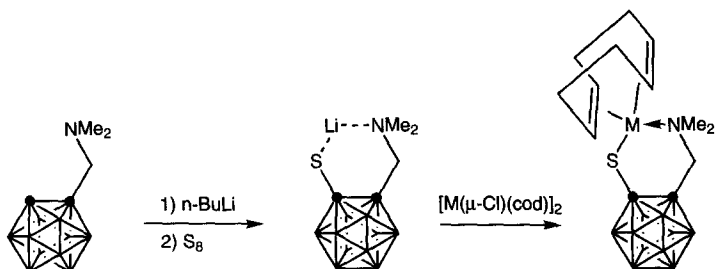
Some five-membered chelated N,N-dialkylaminomethyl derivatives of *o*-carborane, which contain a carbon σ bond with Cu, Pd, and Pt, were reported by Zakharkin *et al.*⁶⁰ The preparation was achieved by the reaction of an N,N-dialkylaminomethyl-*o*-carboranyl lithium with CuCl, (C₆H₅CN)₂PdCl₂, *trans*-(Et₂S)PtCl₂, and (C₆H₅CN)₂PtCl₂. The reaction of 1-lithium-2-N,N-dimethylaminomethyl-*o*-carborane with CuCl gave bis(N,N-dimethylaminomethyl-*o*-carboranyl)copper **96**. The palladium compound **97** was prepared by the reaction of 1-lithium-2-N,N-diethylaminomethyl-*o*-carborane with (C₆H₅CN)₂PdCl₂. Recently, we⁶² prepared the rhodium and iridium compounds chelated by an

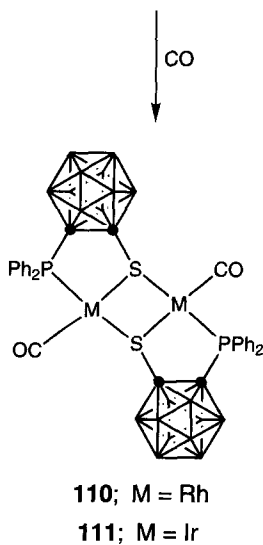
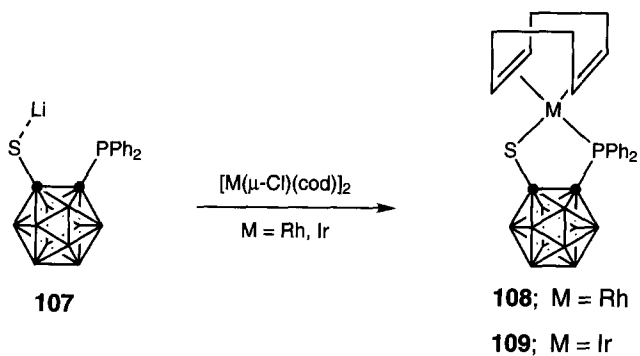
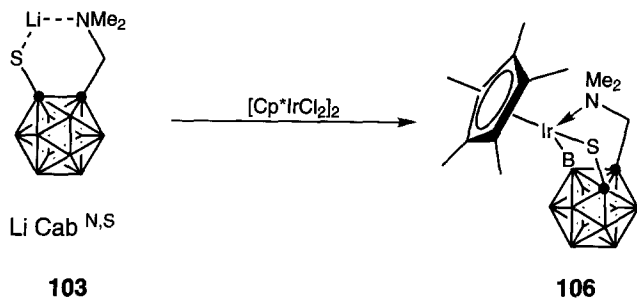
intramolecular C,N-coordination by the reaction of the dimeric metal complexes $[M(\mu\text{-Cl})(\text{cod})]_2$ ($M = \text{Rh}, \text{Ir}$; $\text{cod} = \text{cycloocta-1,5-diene}$) and 2 equiv. of $\text{LiCab}^{\text{C,N}}$. The palladium and platinum compounds **101–102** were obtained by the same synthetic application as for compounds **99–100**.

**99**; $M = \text{Rh}$ **100**; $M = \text{Ir}$ **101**; $M = \text{Pd}$, $R = \text{H}$ **102**; $M = \text{Pt}$, $R = \text{CH}_3$

C. Metal Compounds Containing an *S,N*- or *S,P*-Carboranyl Chelating Ligand

Although transition metal compounds containing an *S,N*-aromatic chelation ligand have been well documented, the analogous compounds containing a carboranyl unit have remained unexplored. Recently, we⁶³ prepared an *ortho*-carboranethiolate ligand with a tertiary amine substituent which can stabilize the metal center by blocking specific coordination sites. Thus, the reaction of $[M(\mu\text{-Cl})(\text{cod})]_2$ ($M = \text{Rh}, \text{Ir}$) with 2 equiv. of 2-(dimethylaminomethyl)-1-(lithiumthiolato)-*ortho*-carborane **103** produced the four-coordinated metallacyclic compounds, $\text{Cab}^{\text{N,S}}\text{M}(\text{cod})$, in which the metal atom was stabilized via intramolecular *N,S*-coordination. The aminothiolo ligand $\text{LiCab}^{\text{N,S}}$ is sterically more demanding than the corresponding thiolato ligand.⁶⁴ Indeed, the reaction of **103** with $[\text{Cp}^*\text{IrCl}_2]_2$ afforded

 $\text{Li Cab}^{\text{N,S}}$ **103****104**; $M = \text{Rh}$ **105**; $M = \text{Ir}$



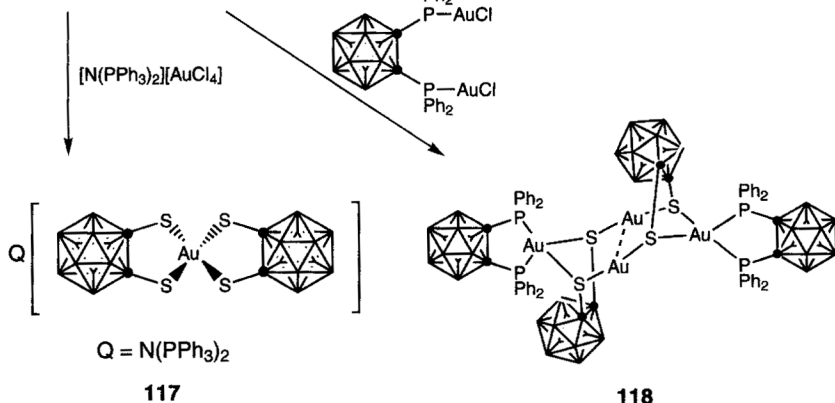
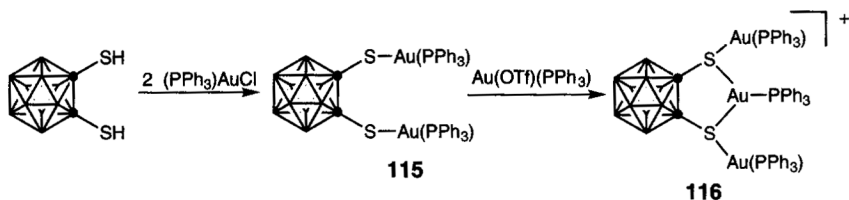
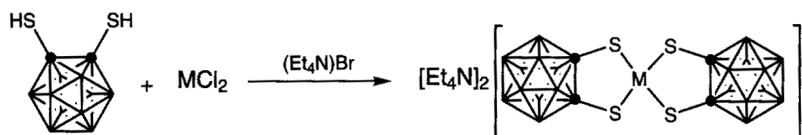
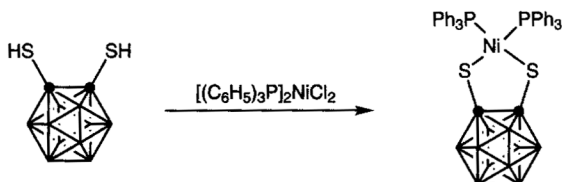
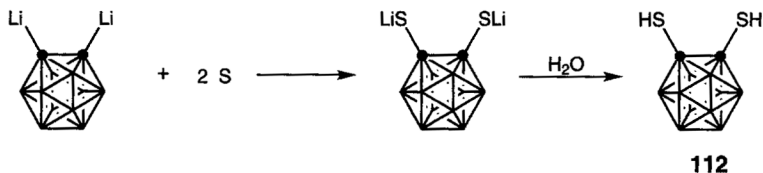
the cyclometalated compound **106** with an intramolecular coordination of the aminomethyl fragment. Intramolecular oxidative addition of the *ortho* B—H bond readily proceeds to give a four-membered ring compound with a thiolato group. The structure of **106** reveals a three-legged piano-stool geometry with the iridium(III) center coordinated by the η^5 -Cp* and an η^3 -[*o*-BC₂B₉H₉S(CH₂NMe₂)-N,S][−] cyclometalated ligand.

The design of new bimetallic complexes involved the use of a newly assembled P,S-chelating ligand containing the bulky *o*-carborane backbone. We⁶⁵ reported that the reaction of [M(μ -Cl)(cod)]₂ (M = Rh, Ir) with 2 equiv. of **107** produced the four-coordinated metallacyclic compounds (Cab^{P,S})M(cod) (M = Rh, Ir) **108–109**. Bubbling carbon monoxide in the compounds **108–109** led to formation of the bimetallic P,S-chelate complexes[(Cab^{P,S})M(CO)]₂ **110–111**. The catalytic activity of the bimetallic rhodium complex **110** was tested for carbonylation of methanol. Complex **110** is much more effective in catalyzing the carbonylation of methanol to acetic acid than the previously known catalyst [RhI₂(CO)₂][−].

IV

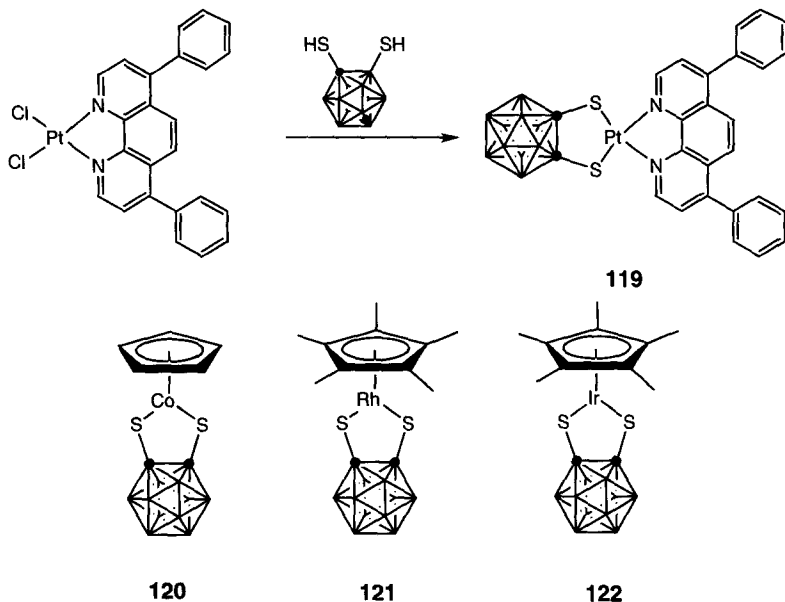
METAL COMPOUNDS CONTAINING A DITHIOLATO-*o*-CARBORANE

The synthesis and study of organometallic complexes possessing an ancillary dithio-*o*-carboranyl ligand have continued to receive attention. In 1,2-dimercapto-*o*-carborane the sulfur donor atom is not only attached to a highly electronegative moiety but also constrained in a system of rigid geometry. This can facilitate the preparation of a variety of transition metal complexes with unusual reactivity and coordination geometry. The ligand can be easily prepared by the reaction of the dilithio carborane with elemental sulfur followed by treatment of the hydrolysis. Smith *et al.*⁶⁶ carried out an extensive investigation of the reaction of the bis(mercapto)carborane **112** with transition metal complexes. The bis(mercapto) compound readily reacted with dichlorobis(triphenylphosphine)nickel(II) to give the cyclic product. Some nickel(II) and cobalt(II) salts have been found to react readily with 1,2-bis(mercapto)-*o*-carborane **112** in the presence of the tetraethylammonium cation to yield square-planar MS₄^{2−} (M = Co, Ni) complexes. The reaction of gold(I) complexes with 1,2-bis(mercapto)-*o*-carborane gave a variety of gold products with unusual coordination geometry. Laguna *et al.*⁶⁷ reported that treatment of 1,2-dimercapto-*o*-carborane with 2 equiv. of PPh₃AuCl in the presence of Na₂CO₃ gave the dinuclear complex [Au₂(μ -S₂C₂B₁₀H₁₀)(PPh₃)₂] **115**. Further reaction of **115** with [Au(OTf)(PPh₃)] leads to the trinuclear species [Au₃(S₂C₂B₁₀H₁₀)(PPh₃)₃](OTf) **116**. On the other hand, the reaction of 1,2-dimercapto-*o*-carborane with [N(PPh₃)₂][AuCl₄] resulted in the formation of the



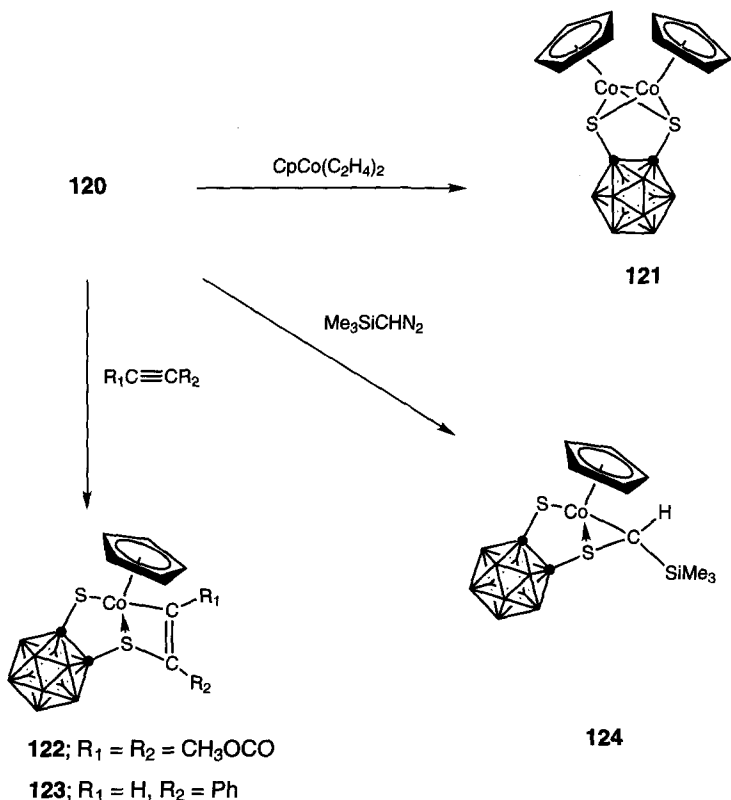
homoleptic gold(III) compound $\text{Q}[\text{Au}(\text{S}_2\text{C}_2\text{B}_{10}\text{H}_{10})_2]$ **117**. Although the most commonly observed geometry for gold(I) is linear two-coordinate, the reaction of **112** with 1,2-bis(diphenylphosphino)-*o*-carborane does not afford the expected complex $[\text{Au}_2\{\mu\text{-(PPh}_3)_2\text{C}_2\text{B}_{10}\text{H}_{10}\}(\mu\text{-S}_2\text{C}_2\text{B}_{10}\text{H}_{10})]$. Instead, a tetranuclear complex **118** is formed; it displays short gold-gold contacts and has two tetrahedrally coordinated gold atoms. This fact could be attributed to the presence of rigid *o*-carborane backbones which should promote chelation.

As an alternative to the conjugated thiol ligands such as toluene 1,2-dithiolate and 1,2-dicyanoethylene-1,2-dithiolate, the compound **119** can be utilized in the synthesis of luminescent square-planar platinum diimine (i.e., phenanthroline and bipyridine) complexes. Grinstaff *et al.*⁶⁸ reported the synthesis of novel diimine dithiolate *o*-carborane platinum(II) complexes that are photochemically stable, soluble in solvents of varying polarities, and potent oxidizing agents in their excited state. 4,7-Diphenyl-1,10-phenanthroline [1,2-dithiolato-1,2-dicarbapcloso-dodecaborane]platinum **119** was synthesized as shown below. These novel platinum diimine thiolate *o*-carborane complexes possess several favorable properties, including an intense visible charge-transfer band, increased solubility, and an energetic excited state.

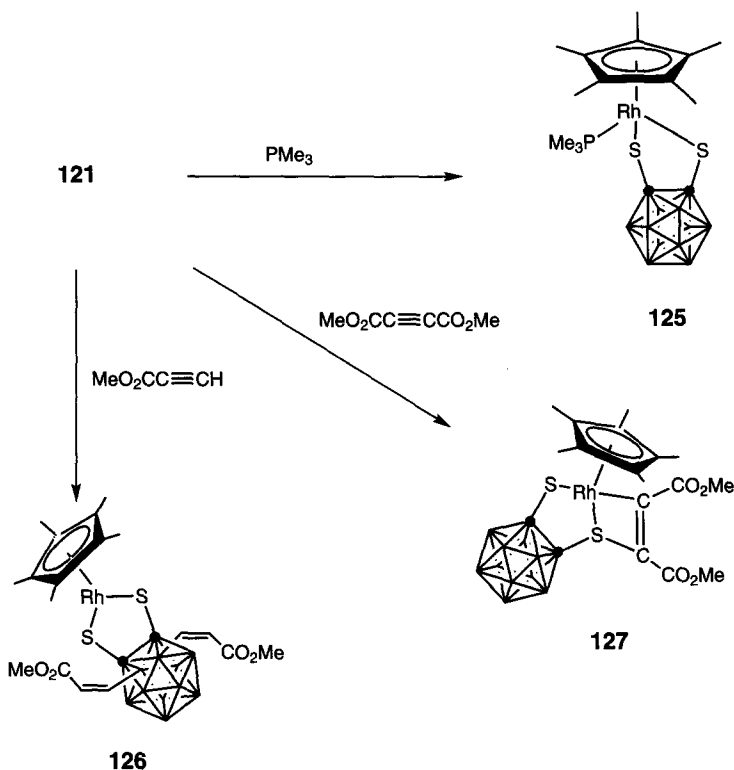


Interest in the synthesis and reactivity of coordinatively unsaturated low-valent metal complexes has led to the use of an *o*-carboranedithiolato ligand in the formation of metalladithiolene ring complexes. Recently, we⁶⁹⁻⁷⁰ and Wrackmeyer *et al.*⁷¹⁻⁷² have reported on the synthesis of the 16e cobalt, rhodium, and iridium

complexes. These complexes may be promising for further transformations owing to the electron deficiency at the metal center, the reactivity of the metal-sulfur bonds, and the potential activation of B-H bonds of the carborane cage at sites close to the metal atom. The mononuclear 16-electron dithio-*o*-carboranylcobalt(III) complex $\text{CpCo}(\text{S}_2\text{C}_2\text{B}_{10}\text{H}_{10})$ **120** was obtained by the reaction of $\text{CpCo}(\text{CO})\text{I}_2$ with dilithium dithio-*o*-carborane. Complex **120** was found to be a good precursor for other addition reactions. It reacts with a variety of substrates such as $\text{CpCo}(\text{C}_2\text{H}_4)_2$, alkynes, and a diazoalkane, generating a new class of dithio-*o*-carboranylcobalt(III) compounds incorporating a CpCo unit and alkene and alkylidene ligands. The reaction of $[\text{Cp}^*\text{RhCl}_2]_2$ with dilithium dithio-*o*-carborane afforded the 16-electron rhodium(III) half-sandwich complex $\text{Cp}^*\text{Rh}[\text{S}_2\text{C}_2(\text{B}_{10}\text{H}_{10})]$ **121**. The 18-electron trimethylphosphine rhodium(III) half-sandwich $\text{Cp}^*\text{Rh}(\text{PMe}_3)[\text{S}_2\text{C}_2(\text{B}_{10}\text{H}_{10})]$ **125** was prepared from the reaction of $\text{Cp}^*\text{RhCl}_2(\text{PMe}_3)$ with the same dichalcogenolate. The complex **125** could also be obtained from the reaction of **121** with trimethylphosphine. Interestingly enough, addition of an alkyne to **121**, followed by insertion into the flexible Rh-S bond, starts a

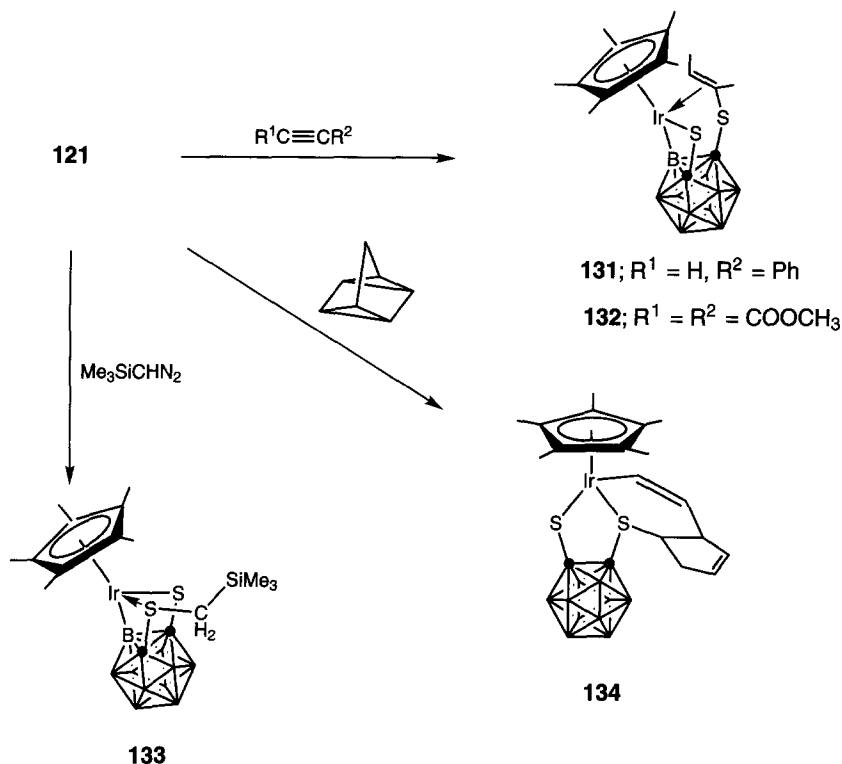


fascinating interplay between 16e and 18e complexes and makes use of all reactive sites. Thus, the reaction of **121** with methyl carboxylate afforded the B(3)/(6)-disubstituted 16e complex **126**. In contrast, the reaction of **121** with acetylene dimethyldicarboxylate gave the 18e complex **127**. The structure of **127** has been confirmed by an X-ray structural study which showed a planar rhodadithiolene five-membered ring, as expected for a 16e species. This electron count is also in agreement with the magnetic deshielding of the ^{103}Rh nucleus ($\delta(^{103}\text{Rh}) = +1210 \pm 5$, close to that of **121** with $\delta(^{103}\text{Rh}) = +1165 \pm 5$).



Complex **122** was prepared similarly to **121**. Subsequent addition reactions of complex **122** with the nucleophiles PMe_3 , CNBu^t , and CO yielded the corresponding complexes $[\text{Cp}^*\text{Ir}(\text{S}_2\text{C}_2\text{B}_{10}\text{H}_{10})(\text{PMe}_3)]$ **128**, $[\text{Cp}^*\text{Ir}(\text{S}_2\text{C}_2\text{B}_{10}\text{H}_{10})(\text{CNBu}^t)]$ **129**, and $[\text{Cp}^*\text{Ir}(\text{S}_2\text{C}_2\text{B}_{10}\text{H}_{10})(\text{CO})]$ **130**. Reaction of **122** with an excess of alkyne resulted in the incorporation of one alkyne molecule, giving $\text{Cp}^*[\text{o-BC}_2\text{B}_9\text{H}_9\text{SS}\{\eta^2\text{-(R}^1\text{C=CR}^2)\}\text{-S}]$ **131–132**, containing a cyclometalated four-membered metallacycle ring of Ir-B-C-S and a coordinating alkenethiol group. Reaction of **121** with (trimethylsilyl)diazomethane resulted in the formation of the bicyclic iridium

metal complex $\text{Cp}^*\text{Ir}[o\text{-BC}_2\text{B}_9\text{H}_9\text{SS}(\text{CH}_2\text{SiMe}_3)\text{-S,S}]$ **133**, in which cyclometallation of a coordinated dithiolato ligand at the iridium(III) metal center has occurred, accompanied by transfer of the methylene group to one end of the sulfur atom of the dithiolato ligand. On the other hand, the reaction of **122** with quadricyclane afforded the addition product $\text{Cp}^*\text{Ir}[\text{C}_2\text{B}_{10}\text{H}_{10}\text{SS}\{\eta^1\text{-(CH=CH)C}_5\text{H}_6\}\text{-S}]$ **134**, formed through the isomerization of a quadricyclane unit.

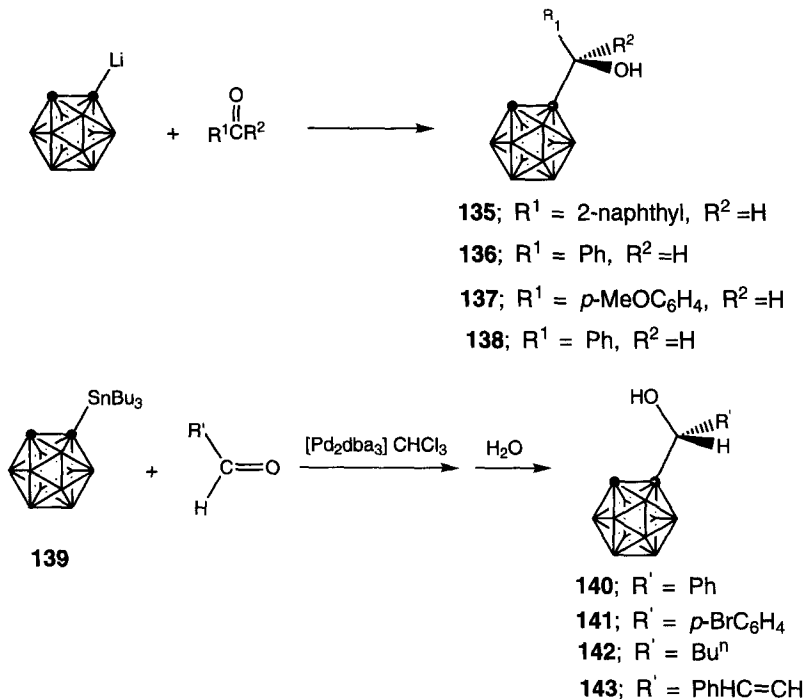


V

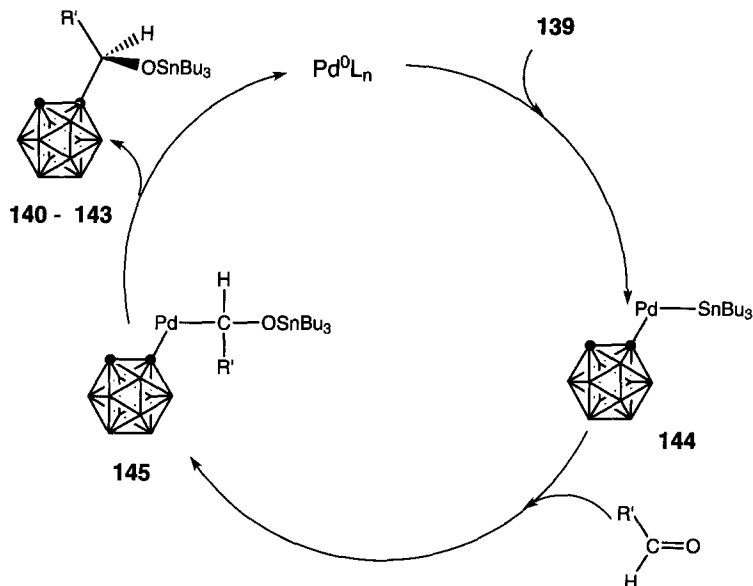
REACTIVITY OF *o*-CARBORANE

The addition of *o*-carborane to electrophiles is one of the most important reactions to synthesize carboranes containing organic functional groups. Lithiocarboranes which are readily prepared from butyllithium with carboranes are widely utilized for C—C bond formation involving various functional groups. Recently, Yamamoto and co-workers have developed addition reactions of lithio-,⁷³

stannyl-,⁷⁴ and silylcarboranes⁷⁵ to various electrophiles, which are potentially useful for synthesizing biologically active functional carboranes. Thus, the functionalized *o*-carboranyl methanols **135–138** can be prepared by the addition of lithiocarborane to carbonyl compounds. The addition of *o*-carboranyltributyltin **139** to aldehydes is catalyzed by $[\text{Pd}_2(\text{dba})_3]\cdot\text{CHCl}_3$ giving the corresponding adducts, 1-(*o*-carboranyl)-1-methanol derivatives **140–143**. The authors presume that the oxidative insertion of Pd_0 into the C—Sn bond of **139** would produce the palladium(II) intermediate **144**, and the addition of **144** to aldehydes would afford **145**, which would give **140–143** via reductive elimination (see Scheme 1). They have also found that Bu_4NF facilitates the reaction of trimethylsilyl-*o*-carborane with aldehydes readily, giving the corresponding alcohols **146–147**. The reaction is highly chemoselective. Thus, functional groups such as nitriles, esters, and nitro groups are tolerated, and the reaction takes place exclusively at the aldehyde group.

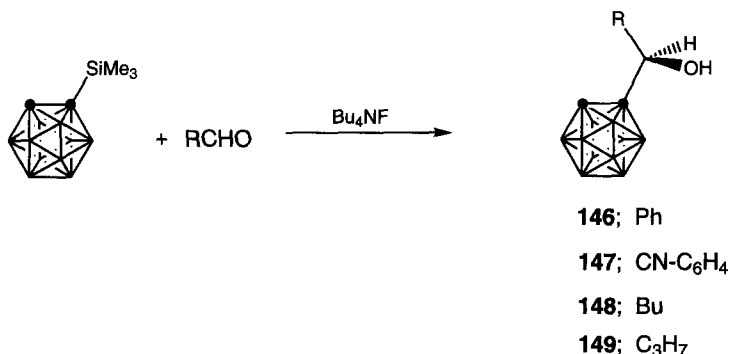


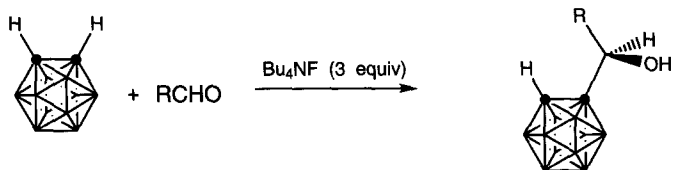
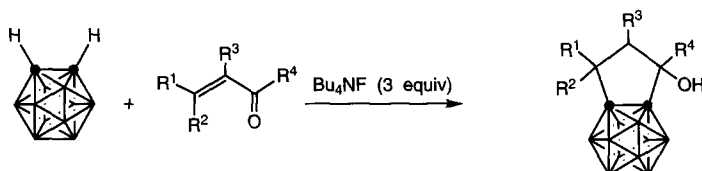
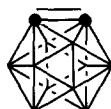
It is known that a carborane framework involves three-center two-electron bonding and is thus an electron-deficient cluster. Shatenshtein⁷⁶ reported that the pK_a value of the C—H proton of carborane is 23. Therefore, a proton attached to the carbon of *o*-carborane could be deprotonated easily by a weak base, and the resulting



SCHEME 1. Mechanism for the palladium catalyzed carboranylation of aldehydes.

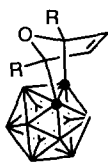
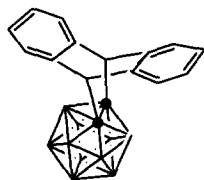
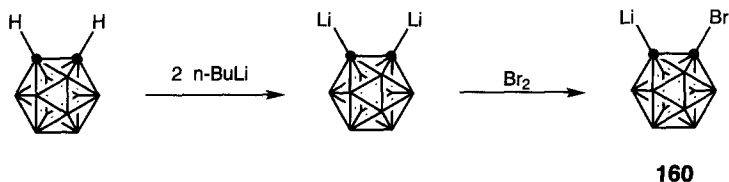
carbanion could react with electrophiles. Yamamoto *et al.*⁷⁷ have found that *o*-carborane undergoes an addition reaction to carbonyl compounds in the presence of TBAF, giving the corresponding *o*-carboranyl carbinols **150–153**. The intramolecular cycloadditions of *o*-carboranes containing carbonyl moieties proceeded by treatment with TBAF to give the corresponding five-, six- and seven-membered carboracycles. *o*-Carborane underwent a facile annulation reaction with various α , β -unsaturated enals and enones in the presence of aqueous TBAF, giving the corresponding five-membered carboracyclic product **154–157**.



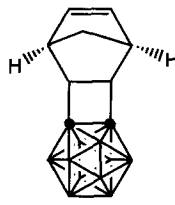
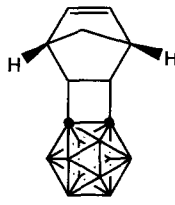
**150**; R = Ph**151**; R = PhCH₂CH₂**152**; R = *i*-Pr**153**; R = Me**154**; R¹ = CH₃, R² = H, R³ = H, R⁴ = H**155**; R¹ = CH₃, R² = CH₃, R³ = H, R⁴ = H**156**; R¹ = Ph, R² = H, R³ = H, R⁴ = H**157**; R¹ = H, R² = H, R³ = H, R⁴ = H**158****159**

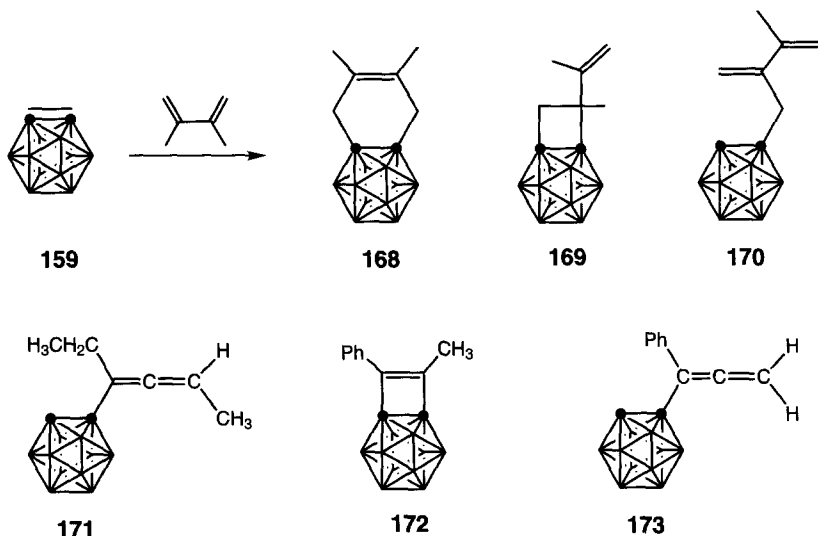
The connection of the three-dimensional carboranes and classical aromatic compounds, the two-dimensional benzenes, has been a fertile area for exploration. 1,2-Dehydrobenzene or benzyne **158** can be trapped by all manner of species. 1,2-Dehydro-*o*-carborane **159** has been shown to undergo many of the same reactions as its two-dimensional relative, 1,2-dehydrobenzene. Although dehydroaromatic molecules can be formed in a variety of ways, synthetic pathways to 1,2-dehydro-*o*-carborane are quite limited. An effective procedure reported so far⁷⁸ first forms the dianion by deprotonation of *o*-carborane with 2 equiv. of butyllithium. Precipitated dilithium carborane is then treated with 1 equiv. of bromine at 0°C to form the soluble bromo anion **160**. Thermolysis of **160** with anthracene, furan, and thiophene as substrates leads to the adducts **161–164**.^{79–80} 1,2-Dehydro-*o*-carborane reacts with norbornadiene to give both homo 2+4 and 2+2 addition, leading to three products **165–167**, in a 7:1 ratio⁷⁹. An acyclic diene, 2,3-dimethyl-1,3-butadiene, gives three products, **168** (4+2 reaction), **169** (2+2 reaction), and

170 (ene reaction), all of which have equivalents in the related chemistry of benzyne.⁸¹ The relative yields of the three kinds of products are comparable for **159** and benzyne **158**. Ene product dominates the reactions of both **159** and benzyne, although for **159** the 2+2 cycloaddition is favored somewhat over 2+4 addition.⁸² Generation of **159** in the presence of 3-hexyne led to a single ene product **171**. The ¹H NMR spectrum of **171** showed single hydrogens attached to the carborane cage (δ 3.72) and to a double bond (δ 5.52). A methyl doublet appeared at δ 1.72, as well as an ethyl group at δ 0.94 and 2.08. Based on the spectroscopic analysis there can be little doubt that the structure of the product is **171**. This provides a quite convenient synthesis of carboranylallenes, but it is clear that no useful amounts of 2+2 adducts are formed. Jones *et al.*⁸² reasoned that a phenyl group would block one possible ene reaction and make the stepwise 2+2 cycloaddition more favorable. In this event, two major products **172** and **173** are formed from the reaction of **159** with methylphenylacetylene in the ratio 3:1. The formation of compound **172** is the first example of a carborane fused to an unsaturated four-membered ring.



163; R = CH₃

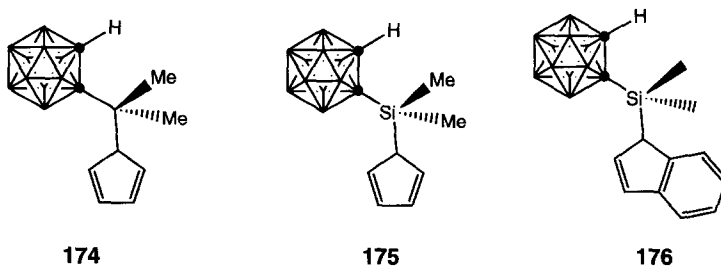


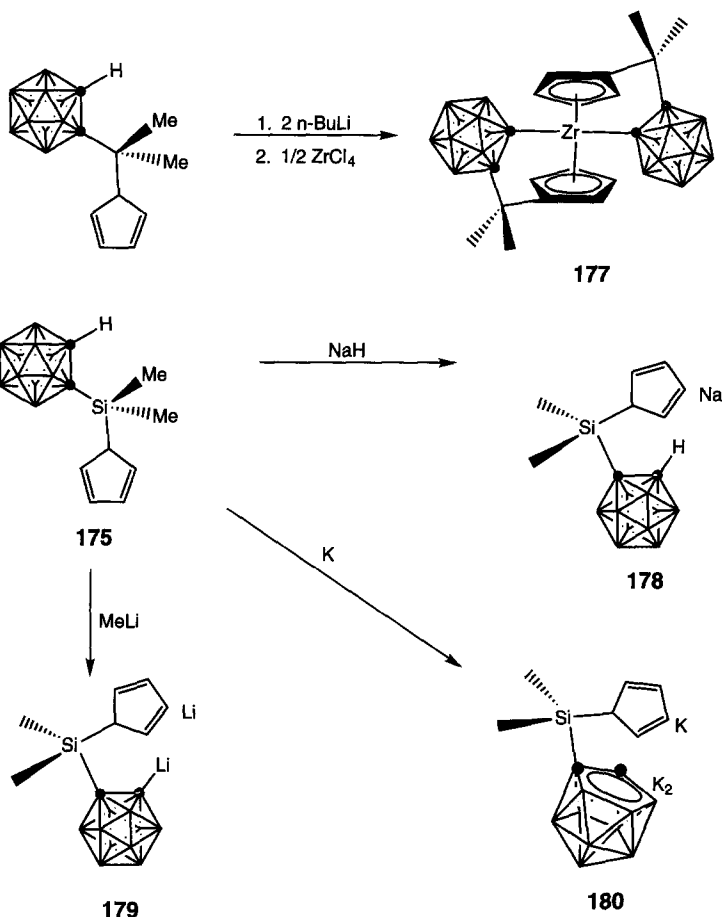


VI

LIGAND DESIGN DERIVED FROM *o*-CARBORANE

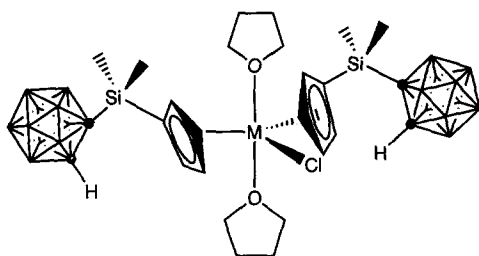
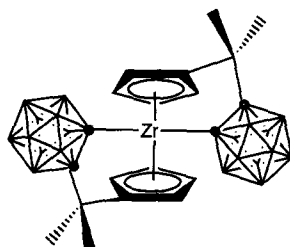
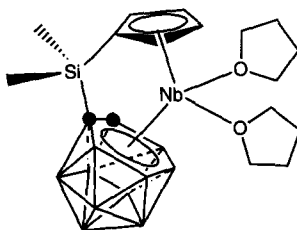
Olefin polymerizations are the most important reactions in the chemical industry. Many catalysts have been developed to make this process more efficient and selective. It is known that bridged ligands have some interesting properties which can control the molecular geometry of the catalysts and afford complexes with solubility, and resistance to ligand redistribution. As a substitute for Cp, *o*-carborane may be a good candidate for the design of new ligands. Recently, Do *et al.*⁸³ reported that the reaction of $\text{Li}_2\text{C}_2\text{B}_{10}\text{H}_{11}$ with 6,6-dimethylfulvene gave the ligand **174**. The ligand **175**, the dimethyl-silyl-bridged analogue of **174**, was prepared from the reaction of $\text{Li}_2\text{C}_2\text{B}_{10}\text{H}_{10}$ and $(\text{C}_5\text{H}_5)\text{SiMe}_2\text{Cl}$ in high yield. Treatment of $\text{Me}_2\text{Si}(\text{C}_9\text{H}_7)\text{Cl}$ with 1 equiv. of $\text{Li}_2\text{C}_2\text{B}_{10}\text{H}_{10}$ gave, after hydrolysis, the ligand $\text{Me}_2\text{Si}(\text{C}_9\text{H}_7)(\text{C}_2\text{B}_{10}\text{H}_{11})$. *rac*- $\text{Zr}(\eta^5\text{-}\eta^1\text{-CpCMe}_2\text{CB}_{10}\text{H}_{10}\text{C})_2$ **177**,





prepared from the reaction of the dilithium salt of the new isopropyl-bridged cyclopentadienyl *o*-carboranyl ligand $\text{CpHMe}_2\text{CB}_{10}\text{H}_{10}\text{CH}$ with ZrCl_4 , catalyzes the formation of syndiotactic poly(methylmethacrylate) in the absence of any alkylating reagent or cationic center generator. Ligand **175** is a versatile ligand which can be easily converted into the monocation **178**, dianion **179**, and trianion **180**, prepared by Xie *et al.*⁸⁴ Reaction of **178** with 0.5 molar equiv. of NdCl_3 generated $[\text{Me}_2\text{Si}(\text{C}_5\text{H}_4)(\text{C}_2\text{B}_{10}\text{H}_{11})]_2\text{NdCl}\cdot 2\text{THF}$ **181**. The X-ray crystal structure of **165** displays a distorted-trigonal-bipyramidal geometry. Treatment of **179** with 1 molar equiv. of NdCl_3 produced the ion-paired complex $[\{\text{Me}_2\text{Si}(\text{C}_5\text{H}_4)(\text{C}_2\text{B}_{10}\text{H}_{10})\}_2\text{Nd}][\text{Li}(\text{THF})_4]$ **183**. The anion adopts a distorted-tetrahedral geometry around the Nd atom, analogous to that of the zirconium compound. Trianion **180** reacted with NdCl_3 in a molar ratio of 1:1 to yield a complex which has been formulated as $[\{\text{Me}_2\text{Si}(\text{C}_5\text{H}_4)(\text{C}_2\text{B}_{10}\text{H}_{11})\}\text{Nd}(\text{THF})_2]_n$ **185**.⁸⁵⁻⁸⁷ The ^1H NMR spectrum of the hydrolysis products of this complex supported the ratio

of two THF molecules per ligand. A versatile compound **176** can be conveniently converted into the monoanion $[\text{Me}_2\text{Si}(\text{C}_9\text{H}_6)(\text{C}_2\text{B}_{10}\text{H}_{11})]\text{Na}$ **186**, the dianion $[\text{Me}_2\text{Si}(\text{C}_9\text{H}_6)(\text{C}_2\text{B}_{10}\text{H}_{10})]\text{Na}_2$ **187**, and the trianion $[\text{Me}_2\text{Si}(\text{C}_9\text{H}_6)(\text{C}_2\text{B}_{10}\text{H}_{11})]\text{K}_3$ **188** by treatment with 1 equiv. or excess amounts of NaH or K metal in THF. Very recently, Xie *et al.*⁸⁷⁻⁸⁸ have reported the synthesis of a variety of organolanthanide compounds from compounds **186-188**. They found that due to the electronic and steric effects of the indenyl group, the resulting organolanthanide complexes show some reactivity patterns different from their cyclopentadienyl analogues.

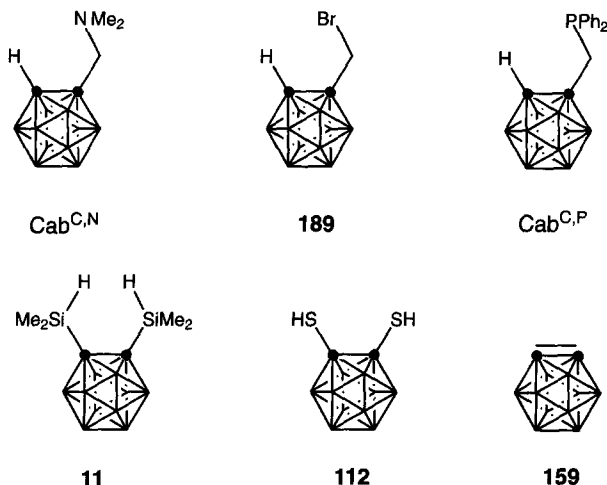
**181**; M = Nb**182**; M = Sm**183**; M = Nb**184**; M = Er**185**

VII

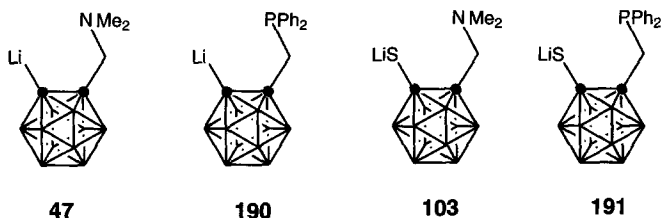
CONCLUDING REMARKS

The concept of intramolecular coordination by the use of C, Y-chelating ligands of aryl units has been well established. However, the analogous chemistry of its cousin, the three-dimensional carborane, remains relatively unexplored. Recently, *o*-carborane has attracted much interest due to its ease of preparation and derivatization, thermal stability, and steric bulk. The easy preparation of *o*-carborane can be utilized for preparing useful compounds similar to the C, Y-chelating ligands of

aryl units. Thus, the use of substituted reactants of *o*-carborane forms a very important preparative method for a huge range of substituted *o*-carborane derivatives. The ligand, Cab^{C,N}, mentioned earlier, and bromomethyl carborane **189** which is a starting material for Cab^{C,P}, can be prepared by the reaction of the corresponding alkynes and decaborane. The ease of synthesis of Cab^{C,N} and Cab^{C,P} makes them highly versatile compounds.



A carborane framework involves three-center two-electron bonding and is thus an electron-deficient cluster. Therefore, the C—H bond of carborane is highly activated. The easy deprotonation of C—H bonds in *o*-carborane with *n*-BuLi makes it applicable to the design of new ligands. Thus, the compounds **11**, **112**, and **159** can be easily prepared by the reaction of dilithio carborane and ClSiMe₂H, the insertion of sulfur into C—Li bonds, and treatment with Br₂, respectively. A proton attached to the carbon of Cab^{C,N} and Cab^{C,P} could be deprotonated easily by *n*-BuLi. The compounds **103** and **161** can be prepared according to the same synthetic procedure as for **112**. As seen in the examples, *o*-carborane may be very promising as a precursor for the design of new ligands. Theoretically, derivatives of the *o*-carboranyl unit will be much like those of an aryl unit. Therefore, it seems that the chemistry of *o*-carboranyl derivatives is just beginning.



ACKNOWLEDGMENTS

Thanks are due to the excellent practical work of a large number of graduate students in our research project. The X-ray crystallographers, Drs. S. W. Lee and S. Cho, are thanked for their continued interest in our studies. The BK-21 project (J. Ko), administered by the Ministry of Education, Korea, is thanked for financial support.

REFERENCES

- (1) Grimes, R. N. *Carboranes*; Academic Press: New York, 1970.
- (2) Muetterties, E. L. *Boron Hydride Chemistry*; Academic Press: New York, 1975.
- (3) Hawthorne, M. F.; Pitochelli, A. R. *J. Am. Chem. Soc.* **1959**, *81*, 5519.
- (4) Miller, H. C.; Miller, N. E.; Muetterties, E. L. *J. Am. Chem. Soc.* **1963**, *85*, 3885.
- (5) Loudon, G. M. *Organic Chemistry*, 2nd ed.; Addison-Wesley: New York, **1988**; Chapter 16.
- (6) Ghosh, T.; Gingrich, H. L.; Kam, C. K.; Mobraaten, E. C.; Jones, M. *J. Am. Chem. Soc.* **1991**, *113*, 1313.
- (7) Jastrzebski, J. T. B. H.; van Koten, G. *Adv. Organomet. Chem.* **1993**, *35*, 241.
- (8) Rippstein, R.; Kickelbick, G.; Schubert, U. *Inorg. Chim. Acta* **1999**, *290*, 100.
- (9) van Koten, G.; Jastrzebski, J. T. B. H.; Noltes, J. G.; Pontenagel, W. M. G. F.; Kroon, J.; Spek, A. L. *J. Am. Chem. Soc.* **1978**, *100*, 5021.
- (10) von Koten, G.; Noltes, J. G. *J. Am. Chem. Soc.* **1976**, *98*, 5393.
- (11) Jastrzebski, J. T. B. H.; Boersma, J.; Esch, P. M.; van Koten, G. *Organometallics*, **1991**, *10*, 930.
- (12) Chan, C. W.; Cheng, L. K.; Che, C. M. *Coord. Chem. Rev.* **1994**, *132*, 87.
- (13) Cummings, S. D.; Eisenberg, R. *J. Am. Chem. Soc.* **1996**, *103*, 1949.
- (14) Vogler, C.; Schwederski, B.; Klein, A.; Kaim, W. *J. Organomet. Chem.* **1992**, *436*, 367.
- (15) Corriu, R. J. P.; Modeau, J. J. E.; Pataud-Sat, M. *J. Organomet. Chem.* **1982**, *228*, 301.
- (16) Eaborn, C.; Metham, T. N.; Pidcock, A. *J. Organomet. Chem.* **1973**, *63*, 107.
- (17) Tanaka, M.; Uchimaru, Y. *Bull. Soc. Chim. Chim. Fr.* **1992**, *129*, 667.
- (18) Fink, W. *Helv. Chim. Acta* **1976**, *59*, 60.
- (19) Viñas, C.; Núñez, R.; Teixidor, F.; Sillanpää, R.; Kivekäs, R. *Organometallics* **1998**, *18*, 4712.
- (20) Teixidor, F.; Flores, M. A.; Viñas, C.; Kivekäs, R.; Sillanpää, R. *Organometallics* **1998**, *17*, 2278.
- (21) Viñas, C.; Flores, M. A.; Núñez, R.; Teixidor, F.; Kivekäs, R.; Sillanpää, R. *Organometallics* **1998**, *17*, 2278.
- (22) Hawthorne, M. F.; Maderna, A. *Chem. Rev.* **1999**, *99*, 3421.
- (23) Soloway, A. H.; Tjarks, W.; Barnum, B. A.; Rong, F. G.; Barth, R. F.; Codogni, I. M.; Wilson, J. G. *Chem. Rev.* **1998**, *98*, 1515.
- (24) Hawthorne, M. F. *Angew. Chem. Int. Ed. Engl.* **1993**, *32*, 950.
- (25) Soloway, A. H.; Tjarks, W.; Barnum, B. A.; Rpmg, F.; Barth, R. F.; Codogni, I. M.; Wilson, J. G. *Chem. Rev.* **1998**, *98*, 1515.
- (26) (a) Papetti, S.; Heying, T. L. *Inorg. Chem.* **1963**, *2*, 1105; (b) Schroeder, H.; Papetti, S.; Alexander, R. P.; Sieckhaus, J. P.; Heying, T. L. *Inorg. Chem.* **1969**, *8*, 2444.
- (27) Lee, J.; Kang, Y.; Kang, S. O.; Ko, J. *Organometallics*, submitted.
- (28) (a) Okinoshima, H.; Yamamoto, K.; Kumada, M. *J. Am. Chem. Soc.* **1972**, *94*, 9263; (b) Kiso, Y.; Tamao, K.; Kumada, M. *J. Organomet. Chem.* **1974**, *76*, 105.
- (29) Sakurai, H.; Kamiyama, Y.; Nakadaira, Y. *J. Am. Chem. Soc.* **1975**, *97*, 931.
- (30) Watanabe, H.; Kobayashi, M.; Saito, M.; Nagai, Y. *J. Organomet. Chem.* **1981**, *216*, 149.
- (31) Naka, A.; Okazaki, S.; Hayashi, M.; Ishikawa, M. *J. Organomet. Chem.* **1995**, *499*, 35.
- (32) Murakami, M.; Anderson, P. G.; Suginome, M.; Ito, Y. *J. Am. Chem. Soc.* **1991**, *113*, 3987.
- (33) Ozawa, F.; Sugawara, M.; Hayashi, T. *Organometallics* **1994**, *13*, 3237.
- (34) Ishikawa, M.; Naka, A.; Ohshita, J. *Organometallics* **1993**, *12*, 4987.

- (35) Carlson, C. W.; West, R. *Organometallics* **1983**, *2*, 1801.
- (36) Obora, Y.; Tsuji, Y.; Kawamura, T. *Organometallics* **1993**, *12*, 2853.
- (37) Tamao, K.; Okazaki, S.; Kumada, M. *J. Organomet. Chem.* **1978**, *146*, 87.
- (38) Kang, Y.; Kang, S. O.; Ko, J. *Organometallics* **1999**, *18*, 1818.
- (39) Kang, Y.; Kang, S. O.; Ko, J. *Organometallics* **2000**, *19*, 1216.
- (40) Pham, E. K.; West, R. *Organometallics* **1990**, *9*, 1517.
- (41) Kang, Y.; Lee, J.; Kong, Y. K.; Kang, S. O.; Ko, J. *Chem. Commun.* **1998**, 2343.
- (42) Kang, Y.; Lee, J.; Kong, Y. K.; Kang, S. O.; Ko, J. *Organometallics* **2000**, *19*, 1722.
- (43) Manners, I. *Angew. Chem., Int. Ed. Engl.* **1996**, *35*, 1602.
- (44) Sita, L. R.; Lyon, S. R. *J. Am. Chem. Soc.* **1993**, *115*, 10374.
- (45) de Rege, F. M.; Kassebaum, J. D.; Scott, B. L.; Abney, K. D.; Balaich, G. J. *Inorg. Chem.* **1999**, *38*, 486.
- (46) Shiina, K. *J. Organomet. Chem.* **1986**, *310*, C57.
- (47) Lee, J.-D.; Kim, S.-J.; Yoo, D.; Ko, J.; Cho, S.; Kang, S. O. *Organometallics* **2000**, *19*, 1695.
- (48) Koten, G. V.; Noltes, J. G. *J. Am. Chem. Soc.* **1976**, *98*, 5393.
- (49) Yoshida, M.; Ueki, T.; Yasuoka, N.; Kasai, N.; Kakudo, M.; Omae, I.; Kikkawa, S.; Matsuda, S. *Bull. Chem. Soc. Jpn* **1968**, *41*, 1113.
- (50) Lee, J.; Kim, S.; Yoo, D.; Ko, J.; Cho, S.; Kang, S. O. *Organometallics* **2000**, *19*, 1695.
- (51) Tsuji, Y.; Obora, Y. *J. Am. Chem. Soc.* **1991**, *407*, 319.
- (52) Murakami, M.; Yoshida, T.; Kawanami, S.; Ito, Y. *J. Am. Chem. Soc.* **1995**, *117*, 6408.
- (53) Lee, Y.-J.; Bae, J.-Y.; Kim, S.-J.; Ko, J.; Choi, M.-G.; Kang, S. O. *Organometallics* **2000**, *19*, 5546.
- (54) Kolb, U.; Dräger, M.; Jousseau, B. *Organometallics* **1991**, *10*, 2737.
- (55) Hartung, H.; Petrick, D.; Schmoll, C.; Weichmann, H. Z. *Anorg. Allg. Chem.* **1987**, *550*, 148.
- (56) Weichmann, H.; Mügge, C.; Grand, A.; Robert, J. B. *J. Organomet. Chem.* **1982**, *238*, 343.
- (57) Jurkschat, K.; Abicht, H. P.; Tzschach, A.; Mahieu, B. *J. Organomet. Chem.* **1986**, *309*, C47.
- (58) Weichmann, H.; Meunier-Piret, J.; van Meersche, M. *J. Organomet. Chem.* **1986**, *309*, 267.
- (59) Lee, T.; Kang, Y.; Lee, S. W.; Kang, S. O.; Ko, J. *Organometallics* **2000**, submitted.
- (60) Kalinen, V. N.; Usatov, A. V.; Zakharkin, L. I. *Proc. Indian Natn. Sci. Acad.*, **1989**, *55*, 293.
- (61) Lee, Y.; Baek, C.; Ko, J.; Park, K.; Cho, S.; Min, S.; Kang, S. O. *Organometallics* **1999**, *18*, 2189.
- (62) Lee, H.; Kang, S. O.; Ko, J. unpublished results.
- (63) Chung, S.; Ko, J.; Park, K.; Cho, S.; Kang, S. O. *Collect. Czech. Chem. Commun.* **1999**, *64*, 883.
- (64) Polo, A.; Claver, C.; Castellón, S.; Ruiz, A. *Organometallics* **1992**, *11*, 3525.
- (65) Lee, H.; Bae, J.; Ko, J.; Kang, Y.; Kim, H. S.; Kang, S. O. *Chem. Lett.* **2000**, 602.
- (66) (a) Smith, H. D.; Obenland, C. O.; Papetti, S. *Inorg. Chem.* **1966**, *5*, 1013.; (b) Smith, H. D.; Robinson, M. A.; Papetti, S. *Inorg. Chem.* **1976**, *6*, 1014.
- (67) (a) Crespo, O.; Gimeno, M. C.; Jones, P. G.; Laguna, A. *J. Chem. Soc., Dalton Trans.*, **1997**, 1099. (b) Crespo, O.; Gimeno, M. C.; Jones, P. G.; Ahrens, B.; Laguna, A. *Inorg. Chem.* **1997**, *36*, 495.
- (68) Base, K.; Grinstaff, M. W. *Inorg. Chem.* **1998**, *37*, 1432.
- (69) Kim, D.; Ko, J.; Park, K.; Cho, S.; Kang, S. O. *Organometallics* **1999**, *18*, 2738.
- (70) (a) Bae, J.; Lee, Y.; Kim, S.; Ko, J.; Cho, S.; Kang, S. O. *Organometallics* **2000**, *19*, 1514. (b) Bae, J.; Park, Y.; Ko, J.; Park, K.; Cho, S.; Kang, S. O. *Inorg. Chim. Acta* **1999**, *289*, 141.
- (71) Herberhold, M.; Jin, G.; Yan, H.; Milius, W.; Wrackmeyer, B. *J. Organomet. Chem.* **1999**, *587*, 252.
- (72) Herberhold, M.; Yan, H.; Milius, W.; Wrackmeyer, B. *Angew. Chem. Int. Ed.* **1999**, *38*, 3689.
- (73) Nakamura, H.; Aoyagi, K.; Yamamoto, Y. *J. Org. Chem.* **1997**, *62*, 780.
- (74) Nakamura, H.; Sadayori, N.; Sekido, M.; Yamamoto, Y. *J. Chem. Soc., Chem. Commun.* **1994**, 2581.
- (75) Cai, J.; Nemoto, H.; Nakamura, H.; Singaram, B.; Yamamoto, Y. *Chem. Lett.* **1996**, 791.

- (76) Shatenshtein, A. L.; Zakharkin, L. L.; Patrov, E. S.; Yakoleva, E. A.; Yakushin, F. S.; Vukmirovich, Z.; Isaeva, G. G.; Kalinin, V. N. *J. Organomet. Chem.* **1970**, *23*, 313.
- (77) Nakamura, H.; Aoyagi, K.; Yamamoto, Y. *J. Am. Chem. Soc.* **1998**, *120*, 1167.
- (78) Gingrich, H. L.; Ghosh, T.; Huang, Q.; Jones, M. *J. Am. Chem. Soc.* **1990**, *112*, 4082.
- (79) Ghosh, T.; Gingrich, H. L.; Kam, C. K.; Mobraaten, E. C.; Jones, M. *J. Am. Chem. Soc.* **1991**, *113*, 1313.
- (80) Barnett-Thamattoor, L.; Zheng, G.; Ho, D. M.; Jones, M. *Inorg. Chem.* **1996**, *35*, 7311.
- (81) Huang, Q.; Gingrich, H. L.; Jones, M. *Inorg. Chem.* **1991**, *30*, 3254.
- (82) Ho, D. M.; Cunningham, R. J.; Brewer, J. A.; Bian, N.; Jones, M. *Inorg. Chem.* **1995**, *34*, 5274.
- (83) Hong, E.; Kim, Y.; Do, Y. *Organometallics* **1998**, *17*, 2933.
- (84) Xie, Z.; Wang, S.; Zhou, Z.; Xue, F.; Mak, T. C. W. *Organometallics* **1998**, *17*, 489.
- (85) Xie, Z.; Wang, S.; Zhou, Z.; Mak, T. C. W. *Organometallics* **1998**, *17*, 1907.
- (86) Xie, Z.; Wang, S.; Zhou, Z.; Mak, T. C. W. *Organometallics* **1999**, *18*, 1641.
- (87) Xie, Z.; Wang, S.; Yang, Q.; Mak, T. C. W. *Organometallics* **1999**, *18*, 2420.
- (88) Wang, S.; Yang, Q.; Mak, T. C. W.; Xie, Z. *Organometallics* **1999**, *18*, 4478.

The Chemistry of Borabenzenes (1986–2000)

GREGORY C. FU

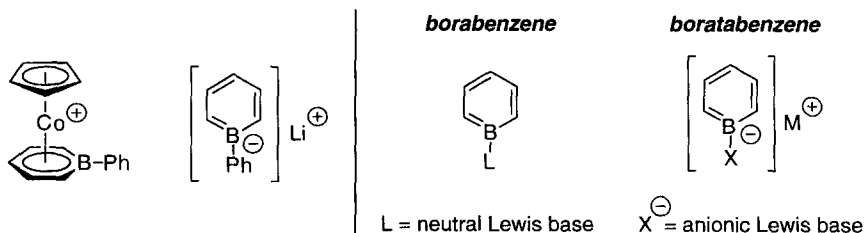
Department of Chemistry
Massachusetts Institute of Technology
Cambridge, Massachusetts 02139

I. Introduction	101
II. Synthesis of Neutral Borabenzene–Ligand Adducts	102
A. General Route	102
B. Specific Adducts	103
C. Approaches to Ligand-Free Borabenzenes	104
III. Synthesis of Anionic Boratabenzenes	105
IV. Boratabenzenes: Structure and Bonding	108
A. Transition Metal-Free Boratabenzenes	108
B. Transition Metal Complexes of Boratabenzenes	110
V. Reactivity of Transition Metal Complexes of Boratabenzenes	113
A. Stoichiometric Reactivity	113
B. Catalytic Reactivity	113
VI. Conclusion	117
References	117

I

INTRODUCTION

Herberich's 1970 report of the synthesis of a cobalt-bound boratabenzene¹ and Ashe's 1971 description of the synthesis of lithium 1-phenylboratabenzene² marked the starting point of the study of borabenzenes, a family of molecules that includes neutral borabenzene–ligand adducts as well as anionic boratabenzenes (Scheme 1).



SCHEME 1.

During the 15 years that followed these pioneering studies, a number of important advances were made in understanding the structure, bonding, and reactivity of borabenzenes, and this early work has been summarized in an excellent review published in 1986.³ The present account provides a progress report of the significant discoveries that have been described during the intervening ~15 years.

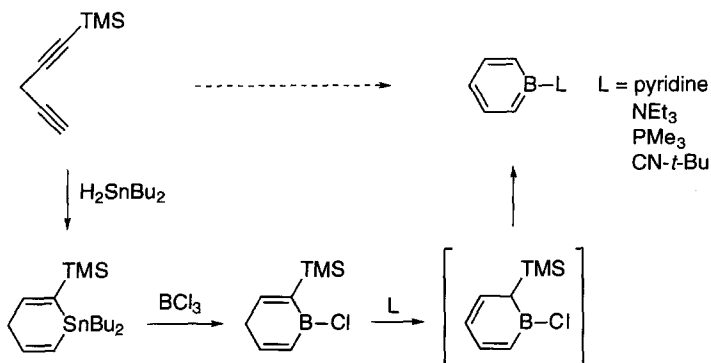
II

SYNTHESIS OF NEUTRAL BORABENZENE-LIGAND ADDUCTS

A. General Route

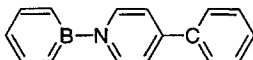
At the time of the 1986 review, only one neutral C_5H_5B-L adduct had been synthesized and fully characterized, C_5H_5B -pyridine.^{4,5} Through a modification of the route employed for the generation of C_5H_5B -pyridine, a wide array of borabenzene-ligand adducts have been synthesized in three steps from commercially available 1-trimethylsilyl-1,4-pentadiyne (Scheme 2).⁶ Thus, reaction of this diyne with H_2SnBu_2 affords a stannacycle that undergoes transmetalation upon treatment with BCl_3 . The resulting boracycle reacts with any of a variety of Lewis bases to produce neutral borabenzene-ligand adducts, presumably via the isomerized boracycle, which has been shown to be both a chemically and a kinetically competent intermediate.

This convenient process has been applied to the synthesis of an interesting heterocyclic analogue of *p*-terphenyl that incorporates three different first-row,



SCHEME 2.

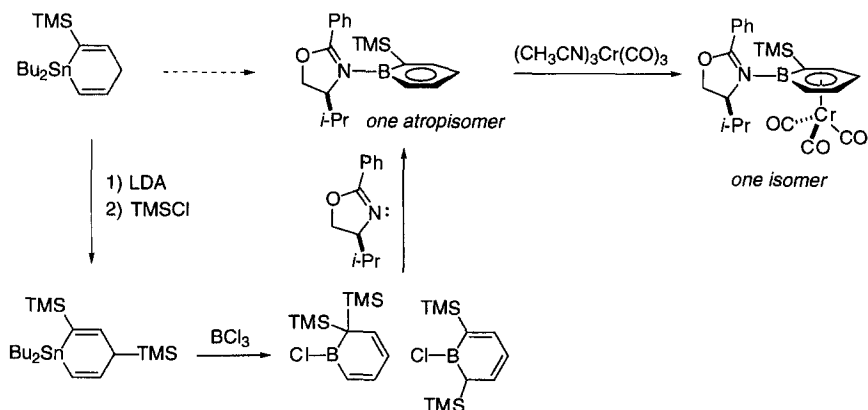
six-membered aromatic systems: a borabenzene, a pyridine, and a benzene ring.⁷ This adduct has been crystallographically characterized.



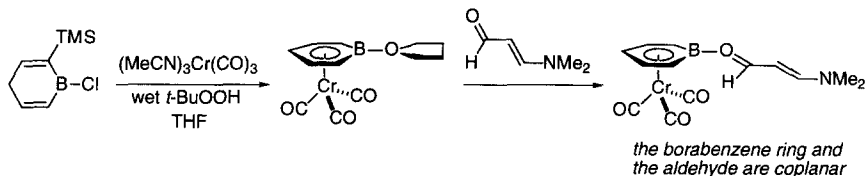
B. Specific Adducts

The stannacycle that is illustrated in Scheme 2 can also serve as a useful intermediate in the synthesis of 2-substituted borabenzene–ligand complexes (Scheme 3).⁸ Thus, deprotonation of the stannacycle, followed by reaction with TMSCl, results in silylation of the 4-position. Treatment of this new stannacycle with BCl_3 leads both to transmetalation and to migration of the newly introduced TMS group. Reaction of the resulting isomeric mixture of boracycles with an enantiopure oxazoline then furnishes a 2-substituted borabenzene–ligand adduct. Due to the steric demand of the Ph, *i*-Pr, and TMS groups, rotation about the B–N bond is hindered at room temperature, and two atropisomers are therefore possible; only the more stable (according to *ab initio* calculations) isomer is produced in this transformation.

The two faces of the borabenzene ring of this borabenzene–oxazoline adduct are inequivalent (diastereotopic), and complexation to $\text{Cr}(\text{CO})_3$ occurs on the less hindered face with high diastereoselectivity (Scheme 3). This work provided the first description of an enantiopure borabenzene and of an enantiopure planar-chiral Lewis acid complex.



SCHEME 3.



SCHEME 4.

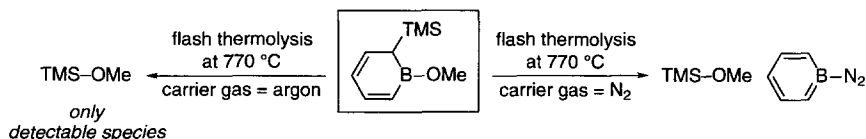
A direct route to a transition metal-bound η^6 -borabenzene complex from a boracyclohexadiene is depicted in Scheme 4.⁹ Treatment of the illustrated boracycle with $(\text{MeCN})_3\text{Cr}(\text{CO})_3$ in THF affords a chromium-bound borabenzene-THF adduct in a single step. This adduct undergoes substitution at boron upon reaction with an electron-rich aldehyde, through an addition-elimination pathway. X-ray crystallographic and NMR studies provide support for significant π -donation from the ligand (THF or aldehyde) to the borabenzene ring. It is suggested that this π -interaction may furnish the basis for a new strategy for the design of a chiral Lewis acid catalyst.

C. Approaches to Ligand-Free Borabenzenes

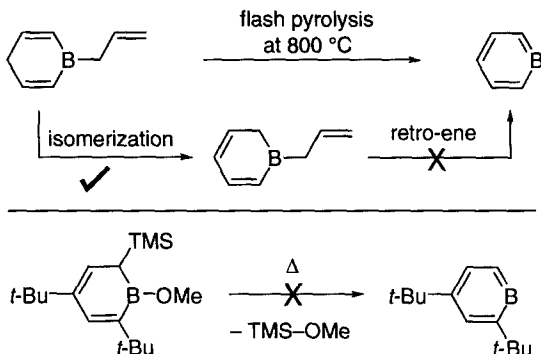
The synthesis of ligand-free, divalent borabenzene ($\text{C}_5\text{H}_5\text{B}$) has been pursued through a variety of routes. For example, flash thermolysis (condensation of the products on a 10 K cold window) of a boracycle precursor has been examined (Scheme 5).¹⁰ With argon as the carrier gas, only TMS-OMe can be identified; on the other hand, with N_2 as the carrier gas, both TMS-OMe and a second compound, which has been assigned as $\text{C}_5\text{H}_5\text{B}-\text{N}_2$ on the basis of IR data,¹¹ are produced. These data provide evidence for the transient formation and high reactivity of $\text{C}_5\text{H}_5\text{B}$.

Attempts to synthesize free borabenzene through an isomerization/retro-ene sequence¹² or to stabilize it through incorporation of a bulky *t*-butyl substituent in the 2-position have been unsuccessful (Scheme 6).¹³

Consistent with experimental observations, computational studies indicate that $\text{C}_5\text{H}_5\text{B}$ should be a highly reactive species.¹⁴



SCHEME 5.



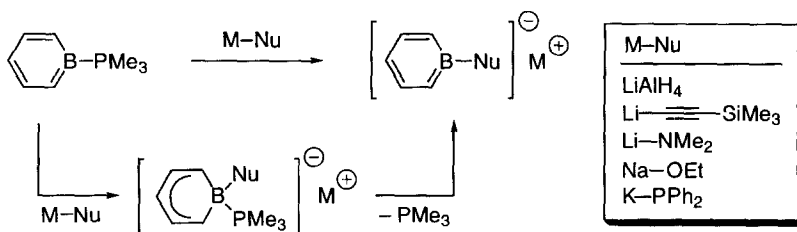
SCHEME 6.

III

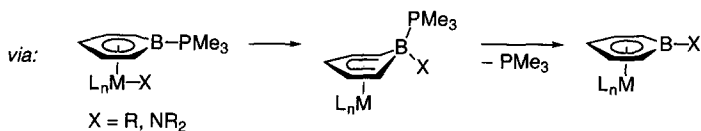
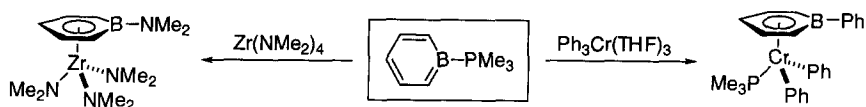
SYNTHESIS OF ANIONIC BORATABENZENES

Neutral borabenzene- PMe_3 , generated through the route described in Scheme 2, reacts with a variety of anionic nucleophiles to furnish *B*-substituted boratabenzenes (Scheme 7).¹⁵ This approach provides efficient access to boratabenzenes that bear a range of boron substituents (H, C, N, O, P) with diverse electronic and steric properties.¹⁶ Mechanistic studies establish that this novel aromatic substitution process follows an addition–elimination pathway.

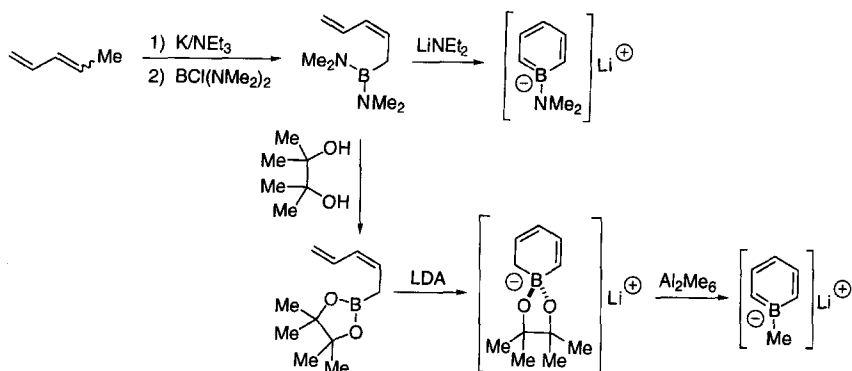
Reaction of the same neutral borabenzene–ligand adduct, $\text{C}_5\text{H}_5\text{B-PMe}_3$, with a transition metal, rather than an alkali, metal alkyl or amide can furnish η^6 -boratabenzene complexes in a single step (Scheme 8).¹⁷ This efficient transformation presumably proceeds through initial π -coordination of $\text{C}_5\text{H}_5\text{B-PMe}_3$ to the transition metal, followed by an intramolecular substitution reaction. In contrast to other approaches to the synthesis of η^6 -boratabenzene complexes, this synthetic route does not have a parallel in η^5 -cyclopentadienyl chemistry.



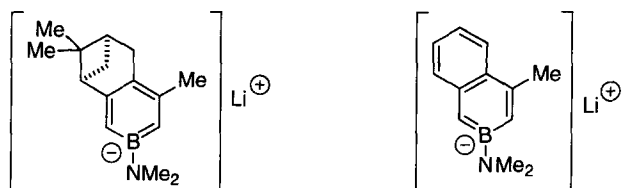
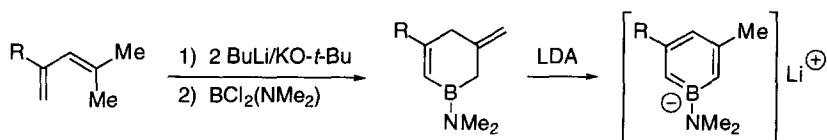
SCHEME 7.



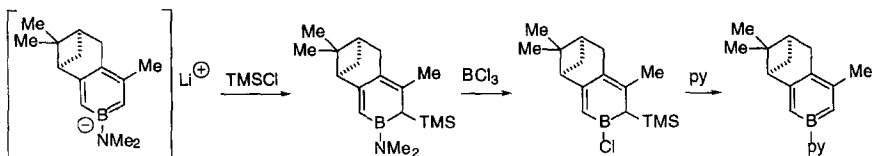
SCHEME 8.



SCHEME 9.



SCHEME 10.



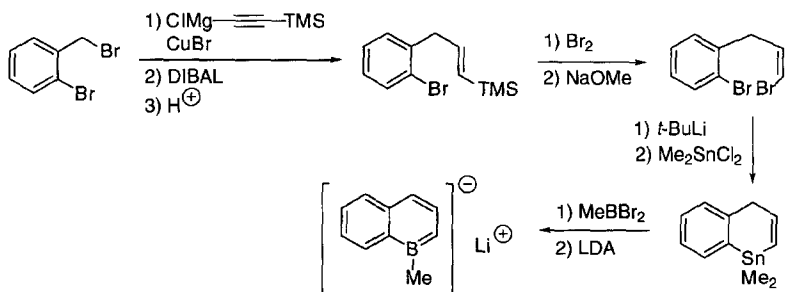
SCHEME 11.

This clever one-step strategy can circumvent reduction problems that sometimes plague reactions of alkali metal boratabenzenes. For example, attempts to synthesize Cr(III)-boratabenzene complexes via treatment of $\text{Cl}_3\text{Cr}(\text{THF})_3$ with $[\text{C}_5\text{H}_5\text{B-Ph}]\text{Li}$ have been unsuccessful, producing instead a Cr(II) complex, $\text{Cr}(\text{C}_5\text{H}_5\text{B-Ph})_2$. In contrast, reaction of $\text{Ph}_3\text{Cr}(\text{THF})_3$ with $\text{C}_5\text{H}_5\text{B-PMe}_3$ furnishes the desired Cr(III) adduct (Scheme 8).^{17b}

An expeditious route to amidoboratabenzenes and alkylboratabenzenes has been developed that starts with commercially available 1,3-pentadiene (Scheme 9).¹⁸ Deprotonation of the diene, followed by quenching with $\text{BCl}(\text{NMe}_2)_2$, affords a 2,4-pentadienylborane. Treatment with LiNEt_2 then leads to ring closure, thereby generating the amidoboratabenzene.

Replacement of the amino groups of the aforementioned 2,4-pentadienylborane (Scheme 9) with pinacol, followed by treatment with base, leads to cyclization to form a boracyclohexadiene.¹⁸ Reaction with Al_2Me_6 then furnishes the target, lithium 1-methylboratabenzene.

A related efficient route to amidoboratabenzenes relies upon *double* metalation of a 1,3-pentadiene and then ring formation via reaction with $\text{BCl}_2(\text{NMe}_2)$ (Scheme 10).¹⁹ Deprotonation of the resulting boracycle produces the desired amidoboratabenzene. This method has been applied to the first synthesis of an enantiopure boratabenzene²⁰ and of a 2-boratanaphthalene²¹ (Scheme 10). The enantiopure boratabenzene has been converted into an enantiopure borabenzene through a silylation–chlorination–elimination sequence (Scheme 11).²²



SCHEME 12.

The first synthesis of a 1-boratanaphthalene has been accomplished via a stannacycle-based route (Scheme 12).²³ The pK_a (dimethylsulfoxide, DMSO) of the conjugate acid of a 1-boratanaphthalene has been determined to be ~ 20 .

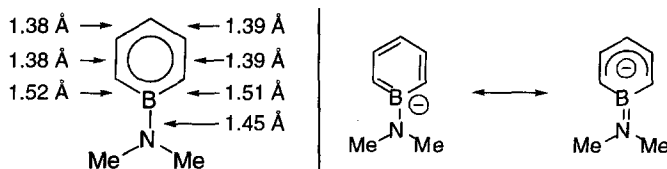
IV

BORATABENZENES: STRUCTURE AND BONDING

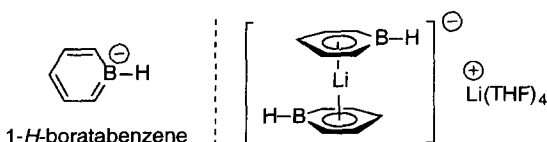
A. Transition Metal-Free Boratabenzenes

The X-ray structure of lithium 1-(dimethylamido)boratabenzene, reported in 1993, provided the first crystallographic characterization of a transition metal-free boratabenzene (Scheme 13).^{18a} The observed bond lengths are consistent with a delocalized anion and with significant B–N double-bond character. In a separate study, the B–N rotational barrier of $[C_5H_5B-NMeBn]Li$ has been determined to be 10.1 kcal/mol, and it has been shown that π -complexation to a transition metal can increase this barrier (e.g., 17.5 kcal/mol for $(C_5H_5B-N(i-Pr)_2)Mn(CO)_3$).²⁴

In 1995, an X-ray crystal structure of an ammonium salt of 1-methylboratabenzene was reported, revealing an almost perfectly planar, symmetrical geometry.^{18b} The same year, the synthesis of lithium 1-*H*-boratabenzene, a boron analogue of benzene, was described.²⁵ A crystallographic study established that it adopts a sandwich structure in the solid state, with a lithium ion positioned at the center of symmetry of two boratabenzene rings (Scheme 14). The rings are planar (all torsion angles are smaller than 1°), and all of the carbon–carbon bond distances are comparable (1.38–1.41 Å). The boron-bound hydrogen of lithium 1-*H*-boratabenzene is hydridic, reacting with D_2O to generate HD, reducing aldehydes to primary alcohols, and reductively cleaving epoxide rings.

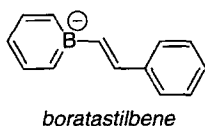


SCHEME 13.



SCHEME 14.

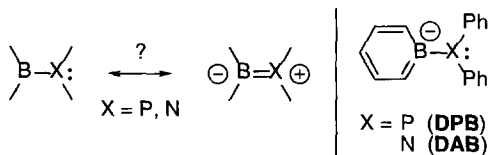
Boratastilbene has recently been synthesized and structurally characterized.²⁶ A study of the consequence of the isoelectronic B[−] for C substitution on the photophysics/photochemistry led to the conclusion that, due to intramolecular charge transfer arising from the inequivalent charge density of the two aromatic rings, nonaggregated boratastilbene is highly emissive relative to stilbene.



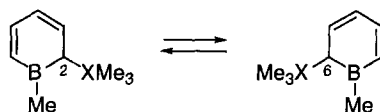
The relative propensity of phosphorus and nitrogen to engage in π -bonding with an adjacent trivalent boron atom has been a topic of long-standing interest (Scheme 15).²⁷ Prior to 1997 there had been no direct structural comparisons of B–P/B–N molecules that differ only in the Group 15 atom. The substitution chemistry outlined in Scheme 7 has been applied to the synthesis of 1-(diphenylphosphido)boratabenzene (DPB) and 1-(diphenylamido)boratabenzene (DAB), and the potassium salt of each of these complexes has been crystallographically characterized.²⁸ The structures adopted in the solid state are as anticipated—conformations consistent with the presence of a π -interaction between boron and nitrogen, but not between boron and phosphorus. Computational, spectroscopic, and reactivity studies provide further support for significant B–N, but not B–P, π -bonding.

The structure of $\text{MeIn}(\text{C}_5\text{H}_5\text{B-Me})_2$ has been explored, and it has been determined to be fluxional in solution on the NMR time scale, with average C_{2v} symmetry.²⁹ An X-ray crystallographic investigation has revealed “soft structural parameters of the indium-ring coordination,” consistent with the solution studies.

Similarly, an examination of the reaction of $[\text{C}_5\text{H}_5\text{B-Me}]\text{Li}$ with Group 14 electrophiles has shown that, while addition of SiMe_3 , GeMe_3 , SnMe_3 , and PbMe_3 occurs preferentially at the 2-position of the heterocycle, the adducts are fluxional in solution at room temperature, undergoing sigmatropic migrations of the XMe_3 group from C2 to C6 (Scheme 16).³⁰ The capacity of the tin derivative to transfer a boratabenzene moiety to a transition metal should prove useful when there is a need



SCHEME 15.

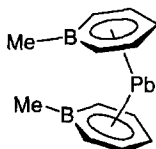


X = Si, Ge, Sn, Pb

SCHEME 16.

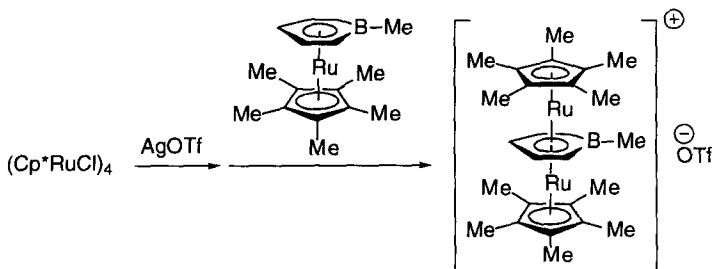
to avoid strongly basic/reducing conditions during the synthesis of a boratabenzene complex.

In contrast to these adducts in which the boratabenzene ring is bound η^1 to the main-group metal, reaction of $[\text{C}_5\text{H}_5\text{B-Me}]\text{Li}$ with PbCl_2 affords a bent-sandwich complex, $\text{Pb}(\eta^6\text{-C}_5\text{H}_5\text{BMe})_2$.³¹ This report provided the first structural characterization of an η^6 -bonding mode to a p-block metal. Reaction of $\text{Pb}(\eta^6\text{-C}_5\text{H}_5\text{BMe})_2$ with a Lewis base such as bipyridine leads to a complex wherein the bipyridine is bound in the pseudoequatorial plane.



B. Transition Metal Complexes of Boratabenzenes

The first triple-deck complexes that contain a bridging boratabenzene have been prepared through treatment of $\text{Cp}^*\text{Ru}(\text{C}_5\text{H}_5\text{B-Me})$ with metallo-electrophiles (Scheme 17).³² The structure of the illustrated adduct has been established by X-ray crystallography.



SCHEME 17.



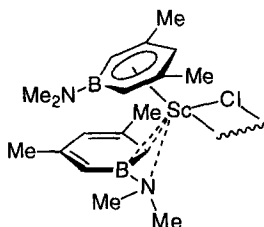
SCHEME 18.

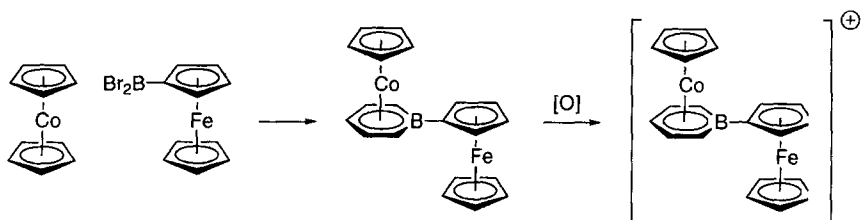
It has been shown that boratabenzenes can provide the framework for a new family of stable, 19-electron iron-sandwich complexes. For example, treatment of (C₆Me₆)FeCp with MeBBBr₂ leads to insertion to furnish the corresponding η⁶-boratabenzene adduct (Scheme 18).³³ The structures, EPR spectra, and reactivity of these boratabenzene complexes are very similar to their well-studied (arene)Fe(cyclopentadienyl) precursors. The unpaired electron resides in an anti-bonding orbital that is largely metal based.

An analogous synthetic route affords (1-ferrocenyl-η⁶-boratabenzene)(η⁵-cyclopentadienyl) cobalt⁺, which has been examined for its potential application as a heterobimetallic nonlinear optic chromophore (Scheme 19).³⁴ This complex exhibits an unexpectedly high first-order hyperpolarizability β. The ferrocenyl substituent serves as an electron-donating group, with the positive charge of the complex being located predominantly on the (boratabenzene)cobalt fragment.

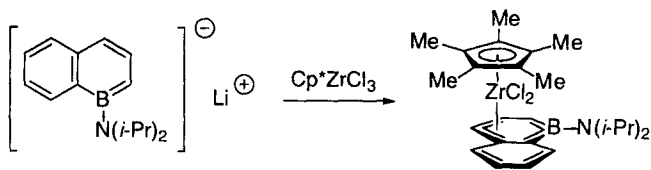
An interesting example of η³ coordination of a boratabenzene to a transition metal has been observed for a Zr(IV)–boratanaphthalene complex (Scheme 20).³⁵ Thus, treatment of the illustrated 1-boratanaphthalene with Cp^{*}ZrCl₃ furnishes an adduct in which the metal–carbon distance for the 3, 4, and 5 positions of the heterocycle (2.53–2.56 Å) is significantly shorter than for the 2 and 6 positions (2.77–2.81 Å). It is suggested that this distorted bonding mode “is the consequence of the high electron demand of Zr(IV), which prefers coordination to the most electron-rich carbon atoms.”

A very different mode of η³ complexation has been observed for the Sc(III)–(bis)boratabenzene complex illustrated below.³⁶ In this instance, a crystallographic study reveals that η³ coordination to one of the boratabenzene rings occurs through the exo nitrogen, the boron, and the 2-carbon. In solution, the complex is fluxional.

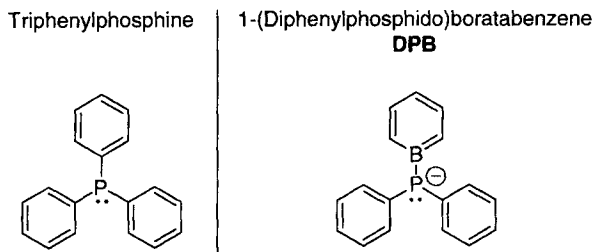




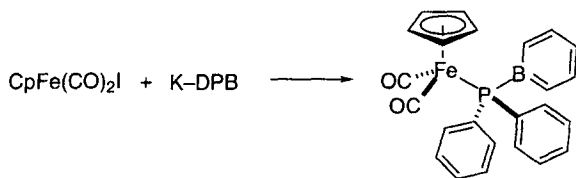
SCHEME 19.



SCHEME 20.



SCHEME 21.



SCHEME 22.

The first metal–boratabenzene complexes in which the boratabenzene is bound through the boron substituent, rather than through the boratabenzene ring, have been described.³⁷ 1-(Diphenylphosphido)boratabenzene, an isosteric and iso-electronic variant of the widely used PPh_3 ligand (Scheme 21), forms σ complexes upon reaction with a variety of transition metal halides (Scheme 22). Spectroscopic and crystallographic data establish that DPB is significantly more electron donating than is PPh_3 . 1-(Diphenylamido)boratabenzene, the nitrogen analogue of DPB, does not form the corresponding nitrogen-bound σ complexes.

V

REACTIVITY OF TRANSITION METAL COMPLEXES OF BORATABENZENES

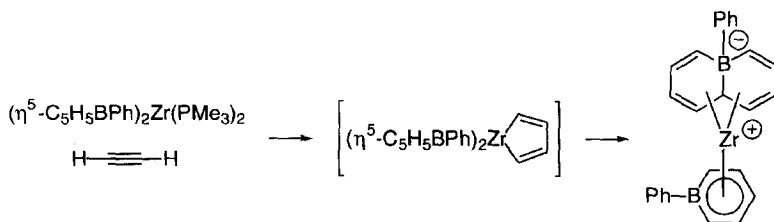
A. Stoichiometric Reactivity

An intriguing annulation has been observed upon treatment of a Zr(II) –boratabenzene complex with an alkyne (Scheme 23).³⁸ This reaction is believed to proceed through generation of the normal metallacyclopentadiene intermediate, followed by migration of the $\text{Zr}-\text{C}$ bond to the electrophilic boron, and then formation of the $\text{C}-\text{C}$ bond. Both the starting Zr(II) complex and the annulation product have been crystallographically characterized.

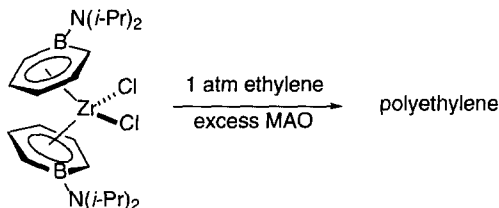
B. Catalytic Reactivity

Among the most exciting frontiers in boratabenzene chemistry is the development of transition metal–boratabenzene complexes as catalysts. As early as 1984, it had been demonstrated that these adducts can accelerate useful reactions—specifically, Bönnemann established that $(\text{C}_5\text{H}_5\text{B}-\text{Ph})\text{Co}(\text{cod})$ serves as a catalyst for pyridine-forming cyclotrimerization reactions of alkynes and nitriles.³⁹

A dozen years later, another breakthrough was reported: the use of Zr(IV) –boratabenzene complexes as catalysts for olefin polymerization (Scheme 24).⁴⁰



SCHEME 23.



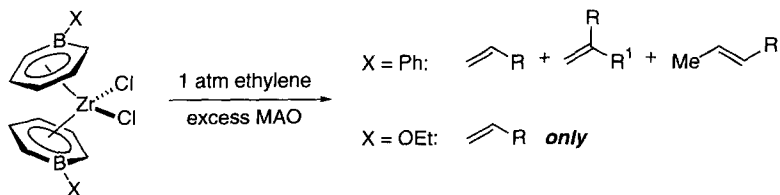
SCHEME 24.

Thus, in the presence of methylaluminoxane (MAO) at 23°C, $(\text{C}_5\text{H}_5\text{B}-\text{N}(\text{i-Pr})_2)_2\text{ZrCl}_2$ polymerizes ethylene with an activity of 105 kg of polyethylene/(h [Zr] mol), similar to that observed with well-studied Cp_2ZrCl_2 as the catalyst. It is believed that MAO is functioning in its usual role in these Ziegler–Natta polymerizations (methylation of Zr and abstraction of methyl to form a highly reactive Zr cation).⁴¹

Prior to this 1996 study, there had been no reports of boratabenzene complexes of early transition metals.⁴² An X-ray crystal structure of the catalyst revealed a C_2 -symmetric geometry that resembles Cp_2Zr -based bent metallocenes. The bond lengths suggest a strong B–N π interaction (rotational barrier measured by NMR: 18 kcal/mol) and a very weak Zr–B interaction ($\sim\eta^5$ coordination of the boratabenzene ring).

In view of the strong electronic interaction between the boron atom and its substituent, it was postulated that the reactivity of the catalyst could be tuned through appropriate choice of this pendant group. Soon after the pioneering initial report, this hypothesis was substantiated. Thus, whereas the $\text{N}(\text{i-Pr})_2$ -substituted catalyst reacts with ethylene to form high-molecular-weight polyethylene (Scheme 24), the corresponding Ph-substituted catalyst furnishes only ethylene oligomers, due to β -hydride elimination.⁴³

Unfortunately, the ethylene oligomers produced by the Ph-substituted catalyst are a complex mixture of 1-alkenes, 2-alkyl-1-alkenes, and 2-alkenes (Scheme 25). In contrast, the OEt-substituted catalyst selectively affords 1-alkenes (average number of inserted ethylene units: 7), due to its relative reluctance to react with olefins other than ethylene.⁴⁴ An X-ray crystal structure of the OEt-substituted



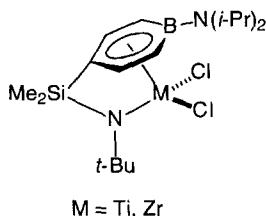
SCHEME 25.

catalyst revealed that the boratabenzene ring is η^6 -bound to zirconium. Other alkoxy-substituted boratabenzene complexes, including the chiral adducts illustrated in Scheme 26, are less selective than the OEt-substituted catalyst for the formation of 1-alkenes.⁴⁵ The synthesis, structure, and polymerization activity of related catalysts, such as (9-phenyl-9-borataanthracene) Cp^*ZrCl_2 , have also been reported.⁴⁶

The OEt-substituted Zr(IV)–boratabenzene complex has been employed in an interesting dual-catalyst approach to the synthesis of branched polyethylene.⁴⁷ Capitalizing on the ability of this boratabenzene complex to generate 1-alkenes (Scheme 25) and the ability of the titanium complex illustrated in Scheme 27 to copolymerize ethylene and 1-alkenes, with a two-catalyst system one can produce branched polyethylene using ethylene as the only monomer (Scheme 27). The structure and properties of the branched polyethylene can be altered by adjusting the reaction conditions.

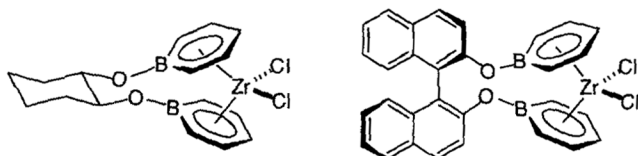
A series of novel, bridged Zr(IV)–boratabenzene complexes have been synthesized and structurally characterized (Scheme 28).⁴⁸ The geometries of these adducts closely resemble those of classical *ansa*-metallocenes. In the presence of excess MAO, these boratabenzene complexes catalyze the polymerization of olefins.

Boratabenzene analogues of commercially significant “constrained geometry” catalysts have also been investigated.⁴⁹ For the MAO-activated copolymerization of ethylene/1-octene, the illustrated Ti(IV)–boratabenzene complex is about four times more active than the Zr(IV) complex. The level of 1-octene incorporation is significantly lower than for the corresponding Cp-derived catalysts, due perhaps to the greater steric demand of the amidoboratabenzene framework.

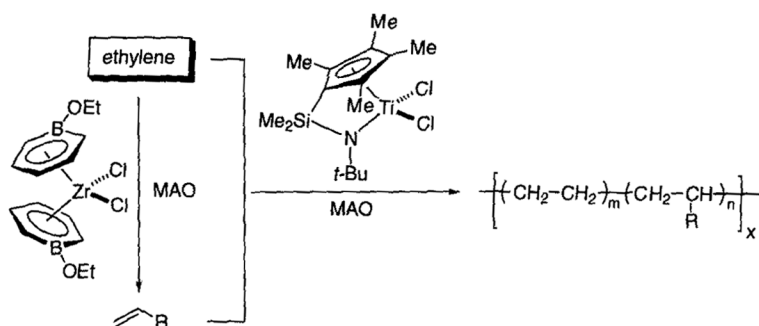
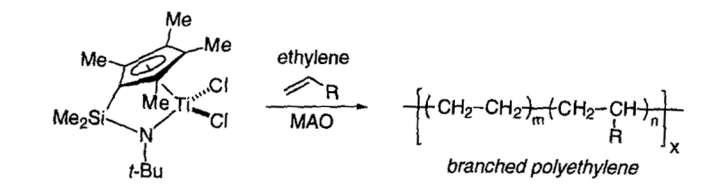


A crystallographically characterized Ti(III)–boratabenzene complex has been found to be ineffective at catalyzing ethylene polymerization.⁵⁰

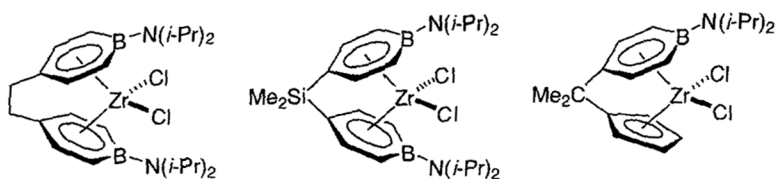
Boratabenzene complexes of Group 3 and Group 6 metals serve as effective catalysts for the oligomerization/polymerization of ethylene. For example, $[(\text{C}_5\text{H}_5\text{BPh})_2\text{ScPh}]_2$, pretreated with H_2 , oligomerizes ethylene to furnish 1-alkenes.^{17a} In the case of a Cr(III)–boratabenzene complex, ethylene is polymerized to afford



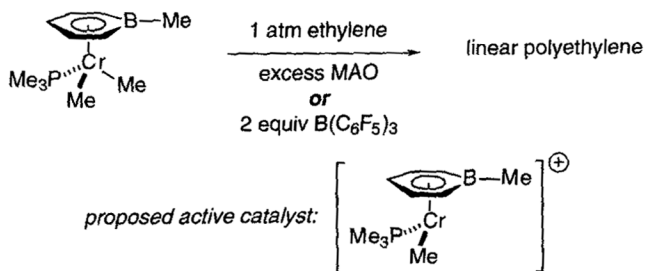
SCHEME 26.



SCHEME 27.



SCHEME 28.



SCHEME 29.

linear polyethylene (Scheme 29).^{17b} The activity of this catalyst is comparable to standard Group 4 metallocenes.

VI

CONCLUSION

The chemistry of borabenzenes and boratabenzenes has advanced considerably since Herberich's comprehensive 1986 review. During the intervening years, efficient new methods for the synthesis of these complexes have been developed, thereby making them readily accessible. Through structural and spectroscopic studies, novel modes of bonding, both to transition metals and to main-group metals, have been discovered. On the reactivity front, transition metal–boratabenzene complexes have been shown to serve as effective catalysts for the polymerization of olefins. The exploitation of metal–bora(ta)benzene complexes as catalysts is a particularly exciting area of research, one that will no doubt continue to prove fruitful during the coming years.

ACKNOWLEDGMENTS

I am grateful to Dr. Jens P. Hildebrand and to Shih-Yuan Liu for proofreading this article.

REFERENCES

- (1) Herberich, G. E.; Greiss, G.; Heil, H. F. *Angew. Chem., Int. Ed. Engl.* **1970**, *9*, 805.
- (2) Ashe, A. J., III; Shu, P. *J. Am. Chem. Soc.* **1971**, *93*, 1804.
- (3) Herberich, G. E.; Ohst, H. *Adv. Organomet. Chem.* **1986**, *25*, 199.
- (4) Boese, R.; Finke, N.; Henkelmann, J.; Maier, G.; Paetzold, P.; Reisenauer, H. P.; Schmid, G. *Chem. Ber.* **1985**, *118*, 1644. See also: Boese, R.; Finke, N.; Keil, T.; Paetzold, P.; Schmid, G. *Z. Naturforsch., B* **1985**, *40*, 1327.
- (5) (a) Pyridine- and triethylamine-2-boranaphthalene: Reference 4; (b) (Dimethyl sulfide)-9-boraanthracene: Jutzi, P. *Angew. Chem., Int. Ed. Engl.* **1971**, *10*, 838.
- (6) Hoic, D. A.; Wolf, J. R.; Davis, W. M.; Fu, G. C. *Organometallics* **1996**, *15*, 1315.
- (7) Qiao, S.; Hoic, D. A.; Fu, G. C. *Organometallics* **1997**, *16*, 1501.
- (8) Tweddell, J.; Hoic, D. A.; Fu, G. C. *J. Org. Chem.* **1997**, *62*, 8286.
- (9) Amendola, M. C.; Stockman, K. E.; Hoic, D. A.; Davis, W. M.; Fu, G. C. *Angew. Chem., Int. Ed. Engl.* **1997**, *36*, 267.
- (10) Maier, G.; Reisenauer, H. P.; Henkelmann, J.; Kliche, C. *Angew. Chem., Int. Ed. Engl.* **1988**, *27*, 295.
- (11) For a computational study of $C_5H_5B-N_2$, see: Cioslowski, J.; Hay, P. J. *J. Am. Chem. Soc.* **1990**, *112*, 1707.
- (12) Maier, G. *Pure Appl. Chem.* **1986**, *58*, 95.
- (13) Maier, G.; Wolf, H.-J.; Boese, R. *Chem. Ber.* **1990**, *123*, 505.

- (14) (a) Raabe, G.; Schleker, W.; Heyne, E.; Fleischhauer, J. *Z. Naturforsch.* **1987**, *42a*, 352; (b) Schulman, J. M.; Disch, R. L. *Organometallics* **1989**, *8*, 733; (c) Cioslowski, J.; Hay, P. J. *J. Am. Chem. Soc.* **1990**, *112*, 1707; (d) Karadakov, P. B.; Ellis, M.; Gerratt, J.; Cooper, D. L.; Raimondi, M. *Int. J. Quantum Chem.* **1997**, *63*, 441.
- (15) Qiao, S.; Hoic, D. A.; Fu, G. C. *J. Am. Chem. Soc.* **1996**, *118*, 6329.
- (16) For the synthesis of certain *B*-alkoxyboratabenzenes, a two-step procedure may be advantageous: Rogers, J. S.; Lachicotte, R. J.; Bazan, G. C. *J. Am. Chem. Soc.* **1999**, *121*, 1288.
- (17) (a) Putzer, M. A.; Rogers, J. S.; Bazan, G. C. *J. Am. Chem. Soc.* **1999**, *121*, 8112; (b) Rogers, J. S.; Bu, X.; Bazan, G. C. *J. Am. Chem. Soc.* **2000**, *122*, 730.
- (18) (a) Herberich, G. E.; Schmidt, B.; Englert, U.; Wagner, T. *Organometallics* **1993**, *12*, 2891; (b) Herberich, G. E.; Schmidt, B.; Englert, U. *Organometallics* **1995**, *14*, 471.
- (19) Herberich, G. E.; Englert, U.; Schmidt, M. U.; Standt, R. *Organometallics* **1996**, *15*, 2707.
- (20) Herberich, G. E.; Ganter, B.; Pons, M. *Organometallics* **1998**, *17*, 1254.
- (21) Herberich, G. E.; Cura, E.; Ni, J. *Inorg. Chem. Commun.* **1999**, *2*, 503.
- (22) Herberich, G. E.; Englert, U.; Ganter, B.; Pons, M.; Wang, R. *Organometallics* **1999**, *18*, 3406.
- (23) Ashe, A. J., III; Fang, X.; Kampf, J. W. *Organometallics* **1999**, *18*, 466.
- (24) Ashe, A. J., III; Kampf, J. W.; Müller, C.; Schneider, M. *Organometallics* **1996**, *15*, 387.
- (25) Hoic, D. A.; Davis, W. M.; Fu, G. C. *J. Am. Chem. Soc.* **1995**, *117*, 8480.
- (26) Lee, B. Y.; Wang, S.; Putzer, M.; Bartholomew, G. P.; Bu, X.; Bazan, G. C. *J. Am. Chem. Soc.* **2000**, *122*, 3969.
- (27) (a) Paine, R. T.; Nöth, H. *Chem. Rev.* **1995**, *95*, 343; (b) Power, P. P. *Angew. Chem., Int. Ed. Engl.* **1990**, *29*, 449.
- (28) Hoic, D. A.; DiMare, M.; Fu, G. C. *J. Am. Chem. Soc.* **1997**, *119*, 7155.
- (29) Englert, U.; Herberich, G. E.; Rosenplänter, J. *Z. Anorg. Allg. Chem.* **1997**, *623*, 1098.
- (30) Herberich, G. E.; Rosenplänter, J.; Schmidt, B.; Englert, U. *Organometallics* **1997**, *16*, 926.
- (31) Herberich, G. E.; Zheng, X.; Rosenplänter, J.; Englert, U. *Organometallics* **1999**, *18*, 4747.
- (32) (a) Herberich, G. E.; Englert, U.; Pubanz, D. *J. Organomet. Chem.* **1993**, *459*, 1; (b) Herberich, G. E.; Englert, U.; Ganter, B.; Lamertz, C. *Organometallics* **1996**, *15*, 5236.
- (33) Herberich, G. E.; Klein, W.; Spaniol, T. P. *Organometallics* **1993**, *12*, 2660.
- (34) Hagenau, U.; Heck, J.; Hendrickx, E.; Persoons, A.; Schuld, T.; Wong, H. *Inorg. Chem.* **1996**, *35*, 7863.
- (35) Ashe, A. J., III; Fang, X.; Kampf, J. W. *Organometallics* **1999**, *18*, 466.
- (36) Herberich, G. E.; Englert, U.; Fischer, A.; Ni, J.; Schmitz, A. *Organometallics* **1999**, *18*, 5496.
- (37) Hoic, D. A.; Davis, W. M.; Fu, G. C. *J. Am. Chem. Soc.* **1996**, *118*, 8176.
- (38) Ashe, A. J., III; Al-Ahmad, S.; Kampf, J. W.; Young, V. G., Jr. *Angew. Chem., Int. Ed. Engl.* **1997**, *36*, 2014. For a related study, see: Ashe, A. J., III; Al-Ahmad, S.; Kampf, J. W. *Organometallics* **1999**, *18*, 4234.
- (39) Bönemann, H.; Brijoux, W.; Brinkmann, R.; Meurers, W. *Helv. Chim. Acta* **1984**, *67*, 1616. See also: Bönemann, H. *Angew. Chem., Int. Ed. Engl.* **1985**, *24*, 248.
- (40) Bazan, G. C.; Rodriguez, G.; Ashe, A. J., III; Al-Ahmad, S.; Müller, C. *J. Am. Chem. Soc.* **1996**, *118*, 2291.
- (41) For a study of the role of alkylaluminum activators, see: Rogers, J. S.; Lachicotte, R. J.; Bazan, G. C. *J. Am. Chem. Soc.* **1999**, *121*, 1288.
- (42) (a) For a more recent study of Group 4–boratabenzene complexes, see: Herberich, G. E.; Englert, U.; Schmitz, A. *Organometallics* **1997**, *16*, 3751; (b) For studies of Ta(V)–boratabenzene complexes, see: Sperry, C. K.; Rodriguez, G.; Bazan, G. C. *J. Organomet. Chem.* **1997**, *548*, 1; (c) Sperry, C. K.; Bazan, G. C.; Cotter, W. D. *J. Am. Chem. Soc.* **1999**, *121*, 1513.
- (43) Bazan, G. C.; Rodriguez, G.; Ashe, A. J., III; Al-Ahmad, S.; Kampf, J. W. *Organometallics* **1997**, *16*, 2492.

- (44) Rogers, J. S.; Bazan, G. C.; Sperry, C. K. *J. Am. Chem. Soc.* **1997**, *119*, 9305.
- (45) Rogers, J. S.; Lachicotte, R. J.; Bazan, G. C. *J. Am. Chem. Soc.* **1999**, *121*, 1288.
- (46) Lee, R. A.; Lachicotte, R. J.; Bazan, G. C. *J. Am. Chem. Soc.* **1998**, *120*, 6037.
- (47) Barnhart, R. W.; Bazan, G. C.; Mourey, T. J. *J. Am. Chem. Soc.* **1998**, *120*, 1082.
- (48) Ashe, A. J., III; Al-Ahmad, S.; Fang, X.; Kampf, J. W. *Organometallics* **1998**, *17*, 3883.
- (49) Ashe, A. J., III; Fang, X.; Kampf, J. W. *Organometallics* **1999**, *18*, 1363.
- (50) Putzer, M. A.; Lachicotte, R. J.; Bazan, G. C. *Inorg. Chem. Commun.* **1999**, *2*, 319.

Recent Advances in the Chemistry of Group 14–Group 16 Double Bond Compounds

NORIIHIRO TOKITOH

*Institute for Chemical Research, Kyoto University
Gokasho, Uji
Kyoto 611-0011, Japan*

RENJI OKAZAKI

*Department of Chemical and Biological Sciences, Faculty of Science
Japan Women's University
Bunkyo-ku, Tokyo 112-8681, Japan*

I. Introduction	121
II. Theoretical Aspects	123
A. Silanone and Silanethione	123
B. Theoretical Calculation of the Bond Energies and Bond Lengths of Heavy Ketones	124
III. Synthetic Methods	127
A. Double Bond Systems Containing a Silicon Atom	127
B. Double Bond Systems Containing a Germanium Atom	140
C. Double Bond Systems Containing a Tin Atom	149
D. Double Bond Systems Containing a Lead Atom	152
IV. Structures and Physical Properties	156
A. X-ray Crystallographic Analysis	156
B. NMR Spectra	158
C. UV-Vis Spectra	159
D. Raman Spectra	160
V. Reactivities	160
VI. Concluding Remarks	162
References	163

I

INTRODUCTION

Low-coordinate species of the main group elements of the second row such as carbenes, olefins, carbonyl compounds (ketones, aldehydes, esters, amides, etc.), aromatic compounds, and azo compounds play very important roles in organic chemistry. Although extensive studies have been devoted to these species not only from the physical organic point of view but also from the standpoints of synthetic chemistry and materials science, the heavier element homologues of these low-coordinate species have been postulated in many reactions only as reactive intermediates, and their chemistry has been undeveloped most probably due to

their high reactivity and instability under ambient conditions. At the beginning of the 20th century all attempts at synthesizing their heavier homologues proved unsuccessful, leading to cyclic oligomers or polymers containing only single covalent bonds. These findings and theoretical works lead to the view that "elements having a principal quantum number greater than two should not be able to form $p\pi-p\pi$ bonds with themselves or with other elements," the so-called "double bond rule."¹ However, this rule was disproved in 1961 by the spectroscopic detection of a compound having a multiple P—C bond.² Furthermore, the isolation of a stable phosphene ($P=C$) was reported in 1978,³ and in 1981 stable diphosphene ($P=P$),⁴ silene ($Si=C$),⁵ and disilene ($Si=Si$)⁶ were successively synthesized by taking advantage of steric protection.

For the stabilization of highly reactive compounds, there are two conceivable methodologies, thermodynamic and kinetic stabilization. The former is defined as stabilization of the ground state by the mesomeric effect of neighboring heteroatoms, attachment of an electron-donating or -withdrawing substituents, or complexation with transition metals. The latter is stabilization resulting from raising the transition state by taking advantage of steric protection with bulky groups, which prevents oligomerization or reactions with other reagents such as oxygen and water. Kinetic stabilization is obviously superior to thermodynamic stabilization since the latter perturbs the intrinsic nature of the species to a greater extent than the former.

As for the heavier element congeners of carbonyl compounds—one of the most important and fundamental functionalities in organic chemistry—earlier works focused on the chemistry of double bonds between a carbon atom and a heavier Group 16 element such as sulfur, selenium, and tellurium. By the middle of 1980s stable thioketones⁷ and selenoketones⁸ and also stable thioaldehydes and selenoaldehydes had been successfully synthesized and isolated using kinetic and/or thermodynamic stabilization.⁹ Furthermore, in 1993, 1,1,3,3-tetramethylindanetellone, the first example of the heaviest congener of this series, was synthesized as a stable compound.¹⁰ Although no example of a stable telluroaldehyde has been reported yet, most of the structures and properties of these heavier chalcogen analogues of ketones have been systematically elucidated.

In contrast to the chemistry of the above-mentioned heavier chalcogen analogues of ketones, that of heavier congeners of ketones containing a heavier Group 14 element (we coin the expression "heavy ketones" for this family of heavier Group 14 element congeners of ketones) has been much less explored until recently. Probably this is due to the much greater difficulty in the stabilization of such highly reactive heavier double bonds with longer bond lengths than those of the carbon—chalcogen double bonds. Since the protecting groups can be introduced only onto the Group 14 elements and the terminal chalcogen atoms are unfortified, it is inherently difficult to stabilize the heavy ketones using the conventional steric protecting groups. In recent years, however, the development of new types of protecting groups made it possible to synthesize and isolate the heavy ketones as stable compounds. In this

article, the remarkable progress in the chemistry of heavy ketones leading to the systematic comparison of their structures and properties is reviewed, to elucidate the intrinsic nature of heavy ketones.

Although some review articles are now available on the synthesis of heavy ketones,¹¹ they are restricted to dealing with some selected elements, especially silicon and germanium. We delineate here a more general account of the whole chemistry of stable double bonds between heavier Group 14 and Group 16 elements [i.e., $RR' M=X$ ($M = \text{Si, Ge, Sn, Pb}$; $X = \text{O, S, Se, Te}$)].

II

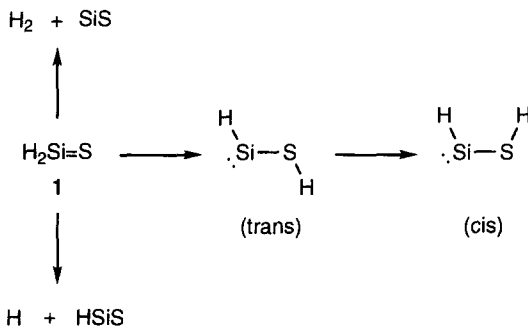
THEORETICAL ASPECTS

A. Silanone and Silanethione

In 1986, Nagase and Kudo reported the theoretical study of silanethione ($\text{H}_2\text{Si}=\text{S}$, **1**) in the ground, excited, and protonated states together with a comparison with silanone ($\text{H}_2\text{Si}=\text{O}$, **2**) and the parent carbonyl system ($\text{H}_2\text{C}=\text{O}$, **3**) by means of *ab initio* calculations including polarization functions and electron correlation.¹² The species and unimolecular reactions pertinent to the stability of $\text{H}_2\text{Si}=\text{S}$ were studied, and the equilibrium structures on the ground singlet potential energy surface of the H_2SiS species and a related silanethiol (H_3SiSH) obtained at HF/6-31G* level were obtained. These authors also described similar theoretical calculations on the geometries of silanone **2**.¹³

The equilibrium structure of $\text{H}_2\text{Si}=\text{S}$ **1** is calculated to be planar with C_{2v} symmetry, as in the case of $\text{H}_2\text{C}=\text{O}$ **2** and $\text{H}_2\text{Si}=\text{O}$ **3**. The Si–S bond length (1.936 Å) in **1** is 0.438 and 0.752 Å longer than the Si–O and C–O bond lengths in **2** and **3**, respectively, but 0.216 Å shorter than the Si–S single bond length (2.152 Å) in $\text{H}_3\text{Si}-\text{SH}$, indicating that there is a certain strength in π bonding between the Si and S atoms. The bond length shortening of 10% from $\text{H}_3\text{Si}-\text{SH}$ to $\text{H}_2\text{Si}=\text{S}$ is comparable to that of 9% from $\text{H}_3\text{Si}-\text{OH}$ to $\text{H}_2\text{Si}=\text{O}$, but it is smaller than that of 15% from $\text{H}_3\text{C}-\text{OH}$ to $\text{H}_2\text{C}=\text{O}$. The smaller shortening of silicon-containing bonds is also found in the ethene analogues: 14% ($\text{H}_2\text{C}=\text{CH}_2$), 10% ($\text{H}_2\text{Si}=\text{CH}_2$), and 9% ($\text{H}_2\text{Si}=\text{SiH}_2$). As a result of calculations, the structure of $\text{H}_2\text{Si}=\text{S}$ is found to be kinetically stable enough toward its unimolecular destruction such as $\text{H}_2\text{Si}=\text{S} \rightarrow \text{H}_2 + \text{SiS}$, $\text{H}_2\text{Si}=\text{S} \rightarrow \text{H} + \text{HSiS}$, and $\text{H}_2\text{Si}=\text{S} \rightarrow \text{H}(\text{HS})\text{Si}$ ·, as in the cases of **2** and **3**. For example, the barrier for the 1,2-H shift in $\text{H}_2\text{Si}=\text{S}$ to $\text{H}(\text{HS})\text{Si}$ · is 54.8 kcal mol⁻¹, suggesting that **1** itself is stable to the unimolecular destruction (Scheme 1).

Furthermore, it was found that $\text{H}_2\text{Si}=\text{S}$ is thermodynamically stable compared with $\text{H}_2\text{Si}=\text{O}$. In an attempt to assess the strength of a silicon–sulfur double bond, a comparison was made of the hydrogenation energies released upon addition of H_2



SCHEME 1.

to **1**, **2**, and **3** at the MP3/6-31G**/6-31G* level.¹² With the calculated hydrogenation energies, the π bond energies $E_\pi(\text{Si}=\text{S})$, $E_\pi(\text{Si}=\text{O})$, and $E_\pi(\text{C}=\text{O})$ are estimated to be 42, 33, and 63 kcal mol⁻¹, respectively. The calculated vibrational frequencies of H₂Si=X (**1** and **2**) at the HF/6-31G* level have been reported [e.g., 682 and 1203 cm⁻¹ (scaled-down frequencies based on the calculation errors) for SiS and SiO stretchings of **1** and **2**, respectively].¹² The proton affinities of **1**, **2**, and **3** were also calculated at several levels of theory.

The zero-point corrected MP3/6-31G**/6-31G* value of 174.7 kcal mol⁻¹ for H₂C=O agrees well with the experimental value of 171.7 kcal mol⁻¹. The proton affinities increase in the order **3** (174.7 kcal mol⁻¹) < **1** (190.5 kcal mol⁻¹) < **2** (208.3 kcal mol⁻¹). This is explained in terms of the predominance of the electrostatic overcharge transfer interactions, because the charge separations in the double bonds increase in the order H₂C^{+0.2}-O^{-0.4} < H₂Si^{+0.7}-S^{-0.4} < H₂Si^{+1.0}-O^{-0.7} while the frontier *n* orbital levels rise in the order **3** (-11.8 eV) \approx **2** (-11.9 eV) < **1** (-9.8 eV).

As a result of comparing the properties of silanethione with silanone and formaldehyde, Nagase and Kudo obtained an important finding that silicon is much less reluctant to form double bonds with sulfur than with oxygen.^{12,13} Thus, silanethione is more stable and less reactive than silanone. They concluded that the major obstacle to the successful isolation of silanethione is its relatively high reactivity.

B. Theoretical Calculation of the Bond Energies and Bond Lengths of Heavy Ketones

The successful synthesis and isolation of a series of heavy ketones (R¹R²M=X; M = Si, Ge, Sn, Pb; X = S, Se, Te) using kinetic stabilization (*vide infra*) and the remarkable progress in the field of theoretical calculations prompted chemists to perform computational calculations on the σ and π bond energies as well as on the single and double bond lengths of H₂M=X at the higher level of theory.¹⁴

TABLE I
BOND ENERGIES (kcal mol⁻¹) AND LENGTHS (Å) FOR M=X CALCULATED AT THE
B3LYP/TZ(d,p) LEVEL

H ₂ M=X	X			
	O	S	'Se	Te
H ₂ C=X				
σ ^a	93.6	73.0	65.1	57.5
π ^b	95.3	54.6	43.2	32.0
d ^c	1.200	1.617	1.758	1.949
Δ ^d	15.5	11.9	11.1	10.1
H ₂ Si=X				
σ ^a	119.7	81.6	73.7	63.2
π ^b	58.5	47.0	40.7	32.9
d ^c	1.514	1.945	2.082	2.288
Δ ^d	8.1	9.4	9.3	8.7
H ₂ Ge=X				
σ ^a	101.5	74.1	67.8	59.1
π ^b	45.9	41.1	36.3	30.3
d ^c	1.634	2.042	2.174	2.373
Δ ^d	8.6	9.5	9.2	8.6
H ₂ Sn=X				
σ ^a	94.8	69.3	64.3	56.4
π ^b	32.8	33.5	30.6	26.3
d ^c	1.802	2.222	2.346	2.543
Δ ^d	7.6	8.9	8.5	8.1
H ₂ Pb=X				
σ ^a	80.9	60.9	57.0	50.3
π ^b	29.0	30.0	27.8	24.4
d ^c	1.853	2.273	2.394	2.590
Δ ^d	8.5	9.2	8.9	8.1

^aσ bond energy.

^bπ bond energy.

^cLength of an M=X double bond.

^dValue of % reduction in a bond length defined as [(single bond length–double bond length)/single bond length] × 100.

The results are shown in Table I, from which one can see the following points of interest pertinent to the intrinsic character of the heavy ketones.

First, a carbon–oxygen double bond is unique in that the σ and π bond energies are almost equal to each other. This is an energetic basis of the well-known reactivity of a carbonyl compound, i.e., the addition–elimination mechanism through a tetrahedral intermediate. On the other hand, in all the other double bonds, the σ bond energy is much greater than the corresponding π bond energy. This

indicates the high reactivity of these double bond compounds toward any kind of addition reaction, because the formation of two new σ bonds on M and X with concurrent cleavage of the π bond results in substantial overall energy gain.

Second, every compound with a Group 14–Group 16 element double bond corresponds to a minimum on the potential energy surface, as confirmed from all positive eigenvalues of the Hessian matrix. This suggests that all the double bond compounds in Table I are synthetically accessible, if one can find an appropriate synthetic methodology.

In addition, the values of percent reduction listed in Table I increase roughly with increasing the π bond energy, although the results for M–O bond compounds are somewhat exceptional. It should be noted that the values except for C=O, C=S, and C=Se are similar to each other, being 8–10% irrespective of the atomic numbers of constitutional elements.

Although σ and π bond energies of $\text{H}_2\text{Si}=\text{S}$ are smaller than those of $\text{H}_2\text{Si}=\text{O}$, the silicon–sulfur double bond compound is considered to be more easily synthesized, since the theoretical calculation predicted¹² that a silicon–sulfur double bond is kinetically more stable than a silicon–oxygen double bond. According to the natural population analysis at the B3LYP/TZ(d,p) level, the double bond ($\text{Si}^{+0.98}\text{S}^{-0.56}$) of $\text{H}_2\text{Si}=\text{S}$ is much less polarized than that ($\text{Si}^{+1.58}\text{O}^{-1.05}$) of $\text{H}_2\text{Si}=\text{O}$, the former being apparently less reactive than the latter. In addition, $\text{H}_2\text{Si}=\text{S}$ is calculated to be $15.0 \text{ kcal mol}^{-1}$ more stable than its divalent isomer, $\text{H}(\text{HS})\text{Si}$, whereas $\text{H}_2\text{Si}=\text{O}$ is only $3.5 \text{ kcal mol}^{-1}$ more stable $\text{H}(\text{HO})\text{Si}$.

Recently, Schleyer and co-workers reported a theoretical study on the stabilities and geometries of a series of carbonyl type compounds, $\text{R}_2\text{M}=\text{O}$ (M = C, Si, Ge, Sn, Pb; R = H, CH_3), and those of carbene type isomers $[\text{R}(\text{RO})\text{M}]$ as shown in Table II.¹⁵ These results show that in $(\text{CH}_3)_2\text{M}=\text{O}$ series the carbene type structure is more stable than the double bond type structure in the case of germanium, tin, and lead, unlike the case of carbon in which the double bond structure is preferred.

TABLE II
CALCULATED RELATIVE ENERGIES (kcal mol^{-1}) FOR R_2MO^a

R	$\text{R}_2\text{M}=\text{O}$		<i>cis</i> -RMOR		<i>trans</i> -RMOR		<i>cyclo</i> ($\text{R}_2\text{M}=\text{O}$) ₃	
	H ^b	CH_3^c	H	CH_3	H	CH_3	H	CH_3
C	0.0	0.0	57.52	72.21	52.16	63.67	−9.73	—
Si	0.0	0.0	−2.06	22.35	−1.81	21.09	−66.92	—
Ge	0.0	0.0	−31.12	−10.17	−30.73	−11.50	−53.73	—
Sn	0.0	0.0	−49.70	−31.00	−48.97	−31.47	−61.70	—
Pb	0.0	0.0	−70.74	−55.34	−69.55	−55.31	−46.90	—

^aB3LYP.

^b6-31++G**.

^c6-31+G*.

On the other hand, the calculation for the relative stabilities of $\text{H}_2\text{Si}=\text{S}$ shows that the silanethione form ($\text{H}_2\text{Si}=\text{S}$, $0.0 \text{ kcal mol}^{-1}$) is more stable than both *s-cis*- HSiSH ($12.0 \text{ kcal mol}^{-1}$) and *s-trans*- HSiSH ($9.3 \text{ kcal mol}^{-1}$) isomers.¹² Thus, the relative stability of heavy ketones to their carbene type isomers is considerably influenced by the combination of the Group 14 and Group 16 elements.

In order to elucidate the systematic stability of lead-containing heavy ketones, theoretical calculation was carried out on the relative stability of a series for carbonyl type compounds, $\text{H}_2\text{Pb}=\text{X}$ ($\text{X} = \text{O}, \text{S}, \text{Se}, \text{and Te}$) versus [*trans*- $\text{H}(\text{HX})\text{Pb}:$].¹⁶ The calculated relative energies for [$\text{H}_2\text{Pb}=\text{X}$] versus [$\text{H}(\text{HX})\text{Pb}:$] are 66.5, 39.4, 32.7, and $27.1 \text{ kcal mol}^{-1}$ for $\text{X}=\text{O}, \text{S}, \text{Se}, \text{and Te}$, respectively. The results indicate that the plumbylene type form [*trans*- $\text{H}(\text{HX})\text{Pb}:$] is more stable than the double bond type structure [$\text{H}_2\text{Pb}=\text{X}$] for all calculated Group 16 element isomers. These results agree with the experimental results that an aryl(arylthio)plumbylene is more stable than a plumbanethione (*vide infra*), though it makes a good contrast with the other lighter Group 14 homologues in which double bond structure is preferred (*vide infra*).

III

SYNTHETIC METHODS

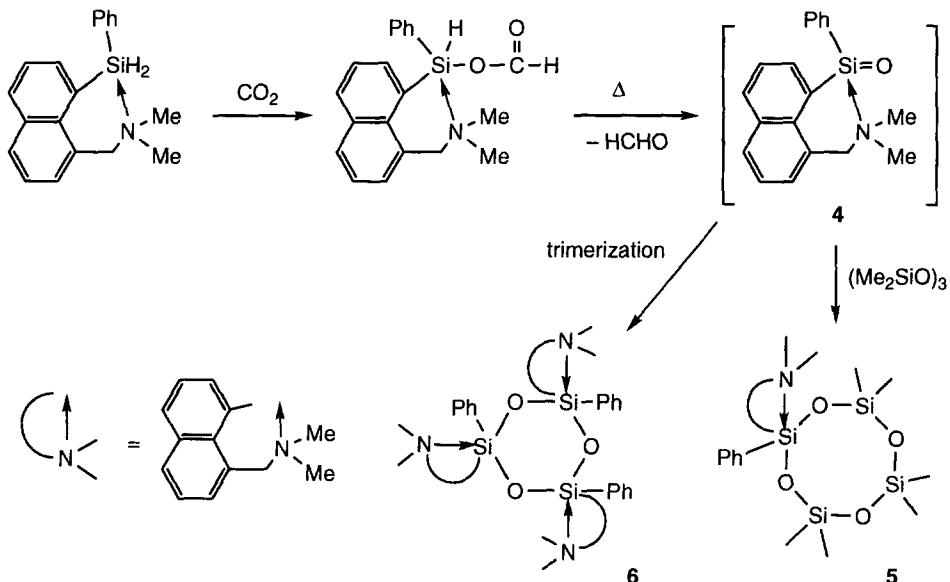
A. Double Bond Systems Containing a Silicon Atom

1. Silicon–Oxygen Double Bond Compounds (Silanones)

In the previous reviews,^{11a,d–f} syntheses of many examples of transient silicon–oxygen double bond compounds such as $\text{MeHSi}=\text{O}$, $\text{Me}_2\text{Si}=\text{O}$, $\text{H}_2\text{Si}=\text{O}$ (**2**), $(\text{HO})\text{HSi}=\text{O}$ (silanoic acid), and $(\text{HO})_2\text{Si}=\text{O}$ (silicic acid) have been described, and they are reportedly isolated as stable species in the low temperature matrices. However, the stabilization of this extremely reactive double bond species is very difficult, and no stable example of silanone ($\text{RR}'\text{Si}=\text{O}$) has been isolated until now even by the methods of thermodynamic or kinetic stabilization.

For example, in the case of intramolecularly base-stabilized silanone **4** it was trapped by excess hexamethylcyclotrisiloxane to give the corresponding insertion product **5** but isolated as a trimer **6** in the absence of such a trapping reagent (Scheme 2).¹⁷

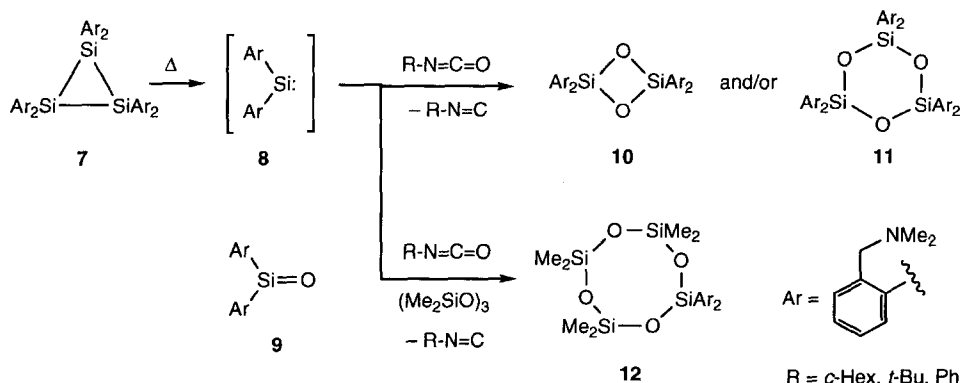
More recently, Belzner *et al.* reported a new type of oxygen transfer reaction from isocyanates to bis[2-(dimethylaminomethyl)phenyl]silylene (**8**)¹⁸ which was thermally generated from the corresponding cyclotrisilane **7**, and they obtained some convincing results of the involvement of silanone **9** (Scheme 3). However, they found that silanone **9** is not stable enough to be isolated. Only cyclic di- and trisiloxanes **10** and **11** (i.e., the cyclic dimer and trimer of the silanone **9**) were obtained together with the corresponding isonitrile as other main products when



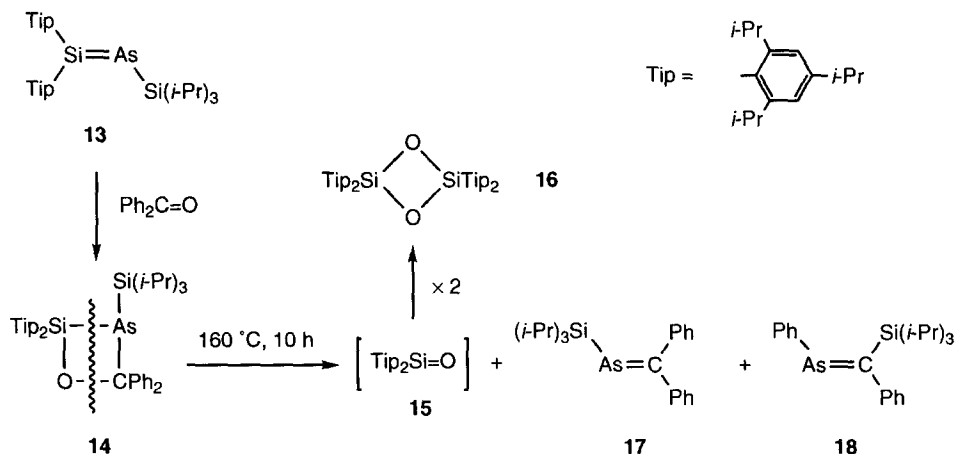
SCHEME 2.

a toluene solution of a mixture of cyclotrisilane **7** and cyclohexyl isocyanate (or *t*-butyl isocyanate) was heated at 70°C (Scheme 3). The intermediacy of silanone **9** was evidenced by the formation of the insertion product **12** in the presence of $(\text{Me}_2\text{SiO})_3$ as in the case of Corriu's silanone **4**.

On the other hand, Driess *et al.* have succeeded in the synthesis and isolation of a stable silicon–arsenic double bond compound (**13**), the first stable arsanilene (arsanilidenesilane),¹⁹ and they found that the arsanilene **13** undergoes ready



SCHEME 3.

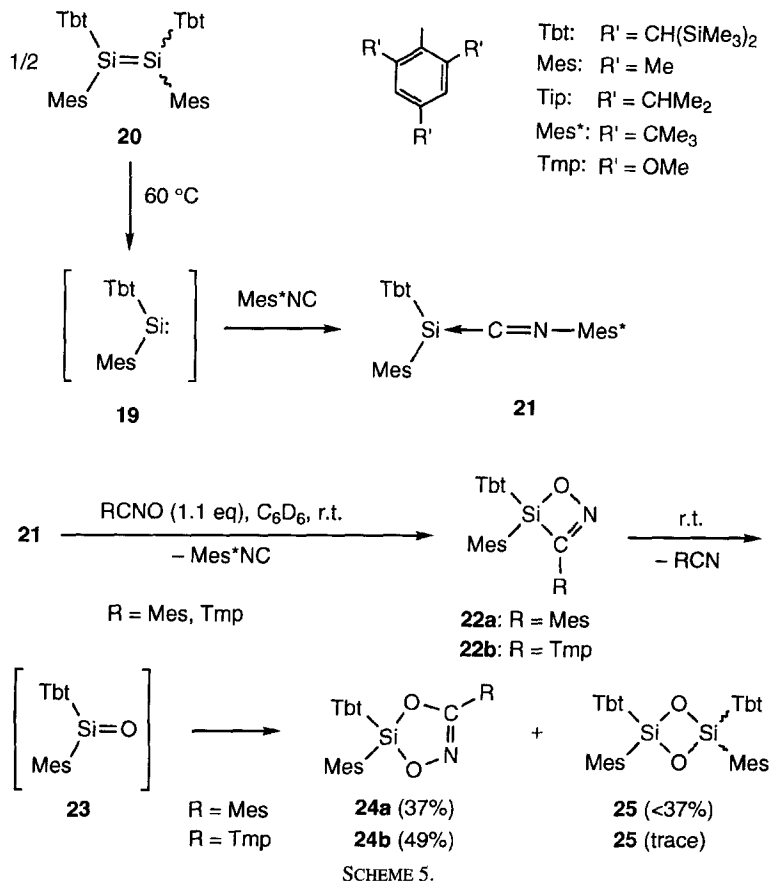


SCHEME 4.

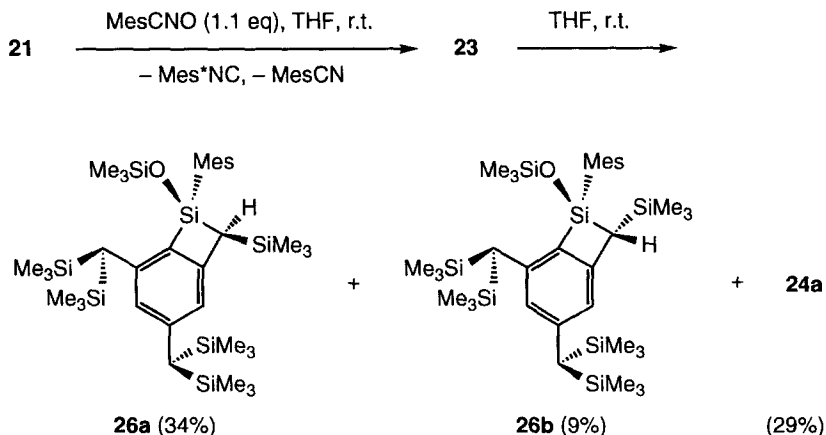
[2+2]cycloaddition reaction with benzophenone to give the four-membered ring product **14** as a stable crystalline compound. Furthermore, the arsenic-containing siloxetane **14** was found to decompose thermally under drastic conditions (160 °C, 10 h) to give the cyclic dimer (**16**) of a silanone, $\text{Tip}_2\text{Si}=\text{O}$ (**15**), together with the arsaalkenes **17** and **18** (Scheme 4).¹⁹ The formation of the dioxadisiletane **16** should be noted as the first example of dimerization of a silanone (in contrast to the common trimerization or tetramerization of less hindered silanones). This metathetical reaction of arsaalkene **13** with benzophenone represents a new approach to arsaalkenes via arsaalkenes by means of a pseudo-Wittig reaction. The authors further extended this type of reaction to the system containing phosphorus and reported the similar formation of silanone dimer starting from analogously substituted phosphasilene.²⁰

Quite recently, another approach²¹ to the kinetically stabilized silanone has been made using an extremely bulky substituent, 2,4,6-tris[bis(trimethylsilyl)methyl]phenyl (Tbt) group, which is very effective in the kinetic stabilization of other heavy ketones (*vide infra*). Extremely congested diarylsilylene, $\text{Tbt}(\text{Mes})\text{Si}:$ (**19**; Mes = mesityl; see Scheme 5) which can be readily generated by the thermal dissociation of the corresponding (*E*)- or (*Z*)-disilene $\text{Tbt}(\text{Mes})\text{Si}=\text{SiTbt}(\text{Mes})$ (**20**),²² reacted with a bulky isocyanide to give a stable silylene–isocyanide complex **21**, and this complex was found to act as a silylene equivalent in solution under very mild conditions.²³

When a C_6D_6 solution of the silylene–isocyanide complex **21** was treated with an equimolar amount of mesitronitrile oxide at room temperature, the blue color of **21** immediately disappeared, and the ²⁹Si and ¹³C NMR spectra of the reaction mixture exhibited characteristic strong signals ($\delta_{\text{Si}} = 26.9$, $\delta_{\text{C}} = 184.3$) assignable to those of compound **22a** having a novel 1,2,4-oxazasilene ring system (Scheme 5). The oxazasilene **22a** was not stable at ambient temperature, and



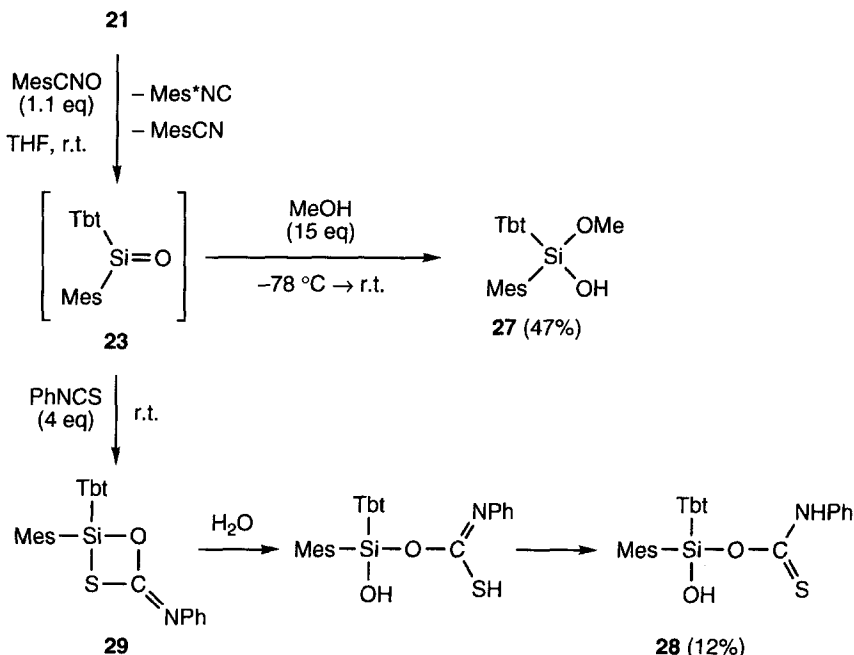
it undergoes further reaction to give 1,3,4,2-dioxazasilole **24a** and (*E*)- and (*Z*)-1,3,2,4-dioxadisiletanes **25** along with the corresponding isocyanide and mesitonitrile. This result can be reasonably explained by the dissociation of oxazasilene **22a** giving silanone **23** and mesitonitrile followed by the [2+3] cycloaddition of intermediary silanone **23** with the nitrile oxide and the head-to-tail dimerization reaction of **23** leading to the formation of **24a** and **25**, respectively (Scheme 5).²¹ Similar results were obtained in the reaction of **21** with TmpCNO (Tmp = 2,4,6-trimethoxyphenyl). The instability of **22** at room temperature is in sharp contrast to the fact that the germanium analogue of **22** is a crystalline compound stable at room temperature.²⁴ This is most likely due to larger steric repulsion among the substituents in **22** as compared to that in the germanium analogue, which is caused by the shorter Si—C bond of the oxazasilene ring than the corresponding Ge—C bond.



SCHEME 6.

The reaction of complex **21** with mesitronitrile oxide in THF differed from that in C_6D_6 . In contrast to the above-mentioned reaction in C_6D_6 giving dimerization products **25**, the reaction in THF gave diastereoisomers of benzosilacyclobutenes, **26a** and **26b**, together with the [2+3] cycloadduct **24a** (Scheme 6). The relative configuration of **26a,b** was definitively determined by X-ray structural analysis.²⁴ The reaction mechanism for formation of **26a,b** is considered to be similar to that for the analogous cyclization reaction of the similarly substituted germanone, $Tbt(Tip)Ge=O$ (*vide infra*).^{24,25} The nucleophilic attack of the oxygen atom in the $Si=O$ double bond of **23** on the silicon atom of the *o*-bis(trimethylsilyl)methyl group, followed by intramolecular cyclization with the C–Si bond formation, affords **26a** and **26b**. The difference in the products between the reactions in C_6D_6 and in THF is probably due to the larger polarization of the $Si=O$ double bond of **23** in THF which is more polar and higher in coordination ability. The fact that the corresponding silanethione $[Tbt(Mes)Si=S]$, the sulfur analogue of silanone **23**, does not give such an intramolecular cyclization product but the corresponding dimerization products even in THF (*vide infra*),²⁶ is in keeping with the higher polarization of the $Si=O$ double bond than the $Si=S$ double bond.^{12,14a}

Although the isolation and spectroscopic observation of silanone **23** has been so far unsuccessful, **23** was intermolecularly trapped by methanol and phenyl isothiocyanate to give the final products methoxysilanol **27** and thiocarbamate **28**, respectively (Scheme 7). In both cases, the competing reaction of silanone **23** with mesitronitrile oxide gave the corresponding [2+3] cycloadduct **24a** in 20 and 36% yields, respectively. The formation of **28** can be rationalized by the initial cycloaddition of **23** with phenyl isothiocyanate giving the corresponding [2+2] cycloadduct, 1,3,2-oxathiasiletane **29**, and its subsequent hydrolysis during separation.



SCHEME 7.

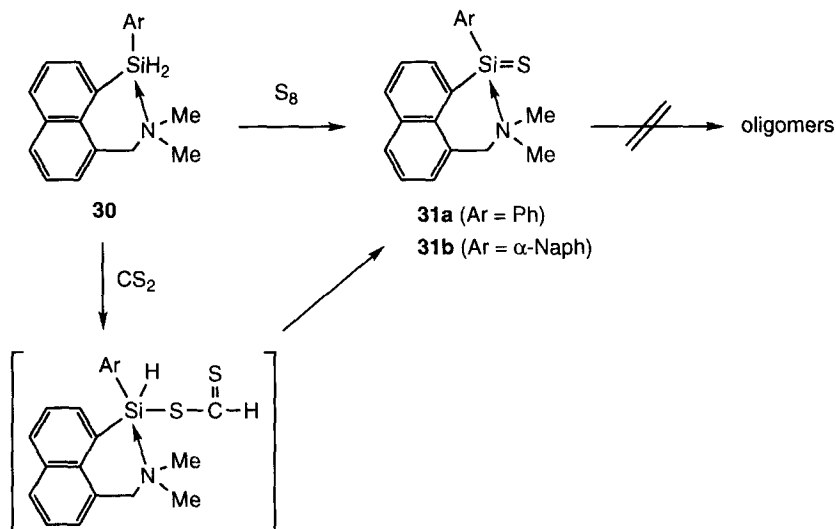
Since the silanone intermediates have been postulated as key intermediates in reports on the synthesis and reactions of organosilicon compounds,²⁷ the isolation of a stable silanone and its characterization should be one of the most fascinating subjects in the future chemistry of low-coordinate organosilicon compounds.

2. Silicon–Sulfur Double Bond Compounds (Silanethiones)

a. Thermodynamically stabilized silanethiones Among the silicon–chalcogen double bond compounds, the silicon–sulfur double bond compound (silanethione) is considered to be most easily synthesized, since it has been predicted by the theoretical calculation that a silicon–sulfur double bond is found to be thermodynamically and kinetically more stable than a silicon–oxygen double bond (silanone).^{12,13}

Although there have been few reports on the chemistry of transient silanethiones,^{11a} some stable examples have been successfully isolated by thermodynamic stabilization. In 1989, Corriu *et al.* reported the first synthesis of an isolable silanethione **31a** (mp 170–171°C) by the reactions of the pentacoordinated functionalized silane **30a** with elemental sulfur or carbon disulfide (Scheme 8).¹⁷

In contrast to the ready trimerization of the silanone **4** having the same ligands, silanethione **31a** was found to be relatively long lived in solution ($t_{1/2}$: 3 d in CDCl_3 at 25°C) as a monomeric species, though extreme precautions must be taken to



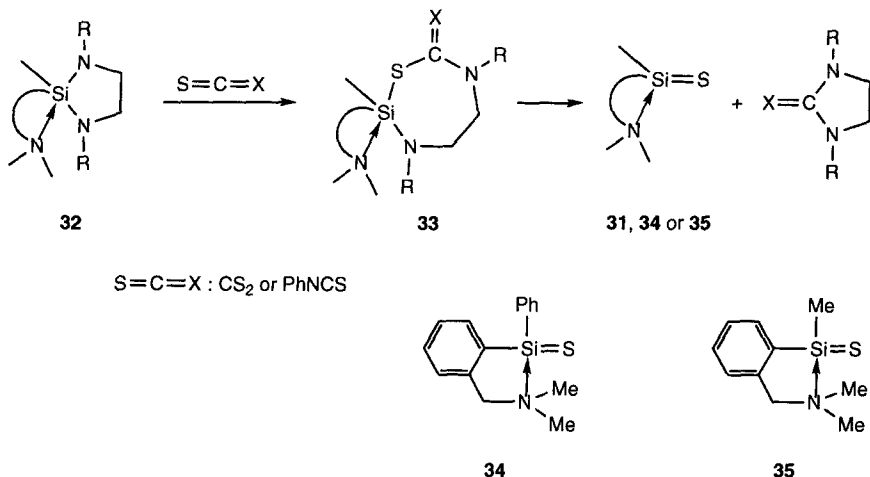
SCHEME 8.

avoid exposure to minute amounts of air. Silanethione **31a** shows its ^{29}Si chemical shift at $\delta +22.3$, suggesting a strong intramolecular coordination of the nitrogen atom. The coordinated silanethione **31a** showed unexpectedly low reactivity with electrophiles and nucleophiles. Phosphanes, phosphites, ketones, epoxides, methyl iodide, and hydrogen chloride are unreactive, as are alkoxyasilanes, siloxanes, and hydrosilanes. Only when **31a** was treated with a large excess of methanol, was the corresponding dimethoxysilane produced. Hydrolysis and oxidation lead to the silanone trimer **6**.

Corriu *et al.* also described an alternative synthetic method for internally coordinated silanethiones starting from the pentacoordinated diaminosilanes.²⁸ As shown in Scheme 9, the pentacoordinated diaminosilanes **32** are allowed to react with sulfur-containing heterocumulenes such as carbon disulfide or phenyl isothiocyanate to give the corresponding insertion products **33**, which undergo thermal decomposition to produce the corresponding silanethiones **31**, **34**, and **35**.²⁸

As in the case of silanone **9**, the reaction of the silylene bis[2-(dimethylamino-methyl): phenyl]silanediyl (**8**) with phenyl isothiocyanate was examined.²⁹ In this reaction the expected silanethione **36** was obtained as a single product; even in the presence of $(\text{Me}_2\text{SiO})_3$, no insertion product of **36** into a $\text{Si}-\text{O}$ bond of $(\text{Me}_2\text{SiO})_3$ was observed (Scheme 10).

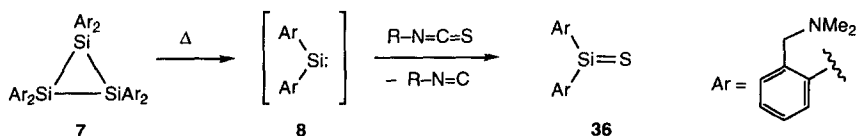
According to the ^{29}Si NMR spectral data (*vide infra*), the silicon center of **36** is assumed to be pentacoordinated due to its intramolecular interaction with both terminal amino groups attached to the substituents. This kind of two-fold coordination of the nucleophilic side arm of the 2-(dimethylaminomethyl)phenyl substituent to



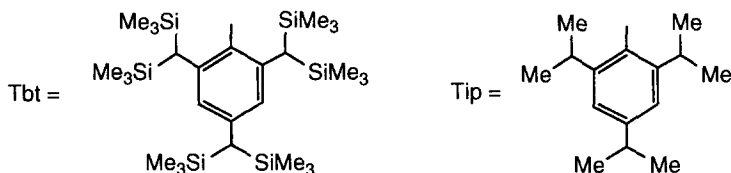
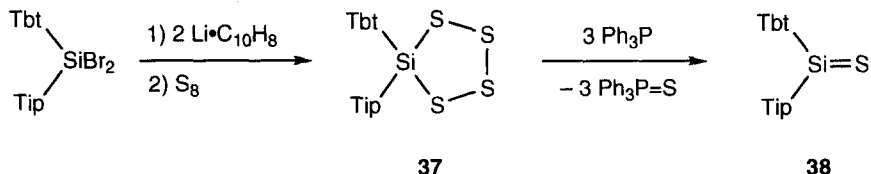
SCHEME 9.

a coordinatively unsaturated silicon center has been proven to be effective in the thermodynamic stabilization of silyl cations as well.³⁰ Although silanethione **36** was reportedly isolated as a white powder [mp 215°C (dec)], there was neither a description of the reactivity nor crystallographic structural analysis of **36**.

b. Kinetically stabilized silanethiones In order to synthesize a stable silanethione, it is important to choose a proper precursor and a suitable methodology, since it can be anticipated that a desired silanethione will be too reactive toward atmospheric oxygen and moisture to be purified with chromatography. Recently, the first kinetically stabilized silanethione **38** was successfully synthesized and isolated using a new and efficient steric protecting group, Tbt group.³¹ The synthetic strategy for this stable silanethione **38** is based on simple desulfurization of the corresponding silicon-containing cyclic polysulfides **37** by a phosphine reagent. Thus, a hexane solution of Tbt- and Tip-substituted tetrathiasilolane **37**^{31b,32} was refluxed in the presence of 3 molar equivalents of triphenylphosphine to produce silanethione **38** together with triphenylphosphine sulfide quantitatively (Scheme 11). Since triphenylphosphine sulfide is almost insoluble in hexane, silanethione **38** was easily separated from the reaction mixture by filtration of the precipitated



SCHEME 10.



SCHEME 11.

phosphine sulfide, and was purified as a yellow crystalline compound (mp 185–189°C) by recrystallization from hexane under argon atmosphere in a glovebox.³¹

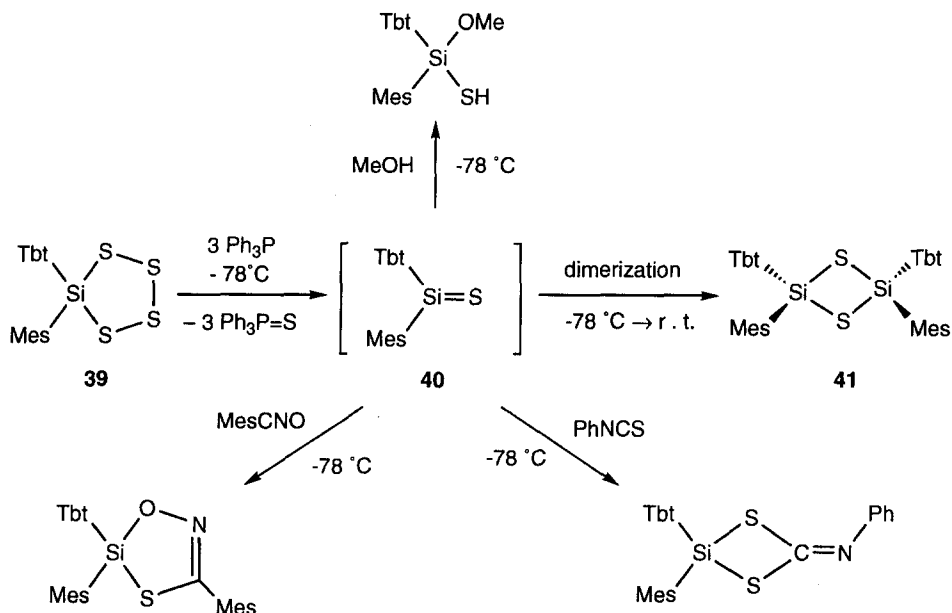
Silanethione **38** was characterized by ¹H, ¹³C, and ²⁹Si NMR, Raman, and UV-vis spectroscopic methods. The ²⁹Si NMR chemical shift of **38** (δ_{Si} 166.56/C₆D₆) for the silathiocarbonyl unit is much downfield shifted from those of the thermodynamically stabilized silanethiones, **31**, **34**, **35**,²⁸ and **36**,²⁹ mentioned in the previous sections, clearly indicating a genuine Si=S double bond in **38** without any intra- or intermolecular coordination. The molecular structure of **38** was successfully established by X-ray crystallographic analysis, and the detailed structural parameters are discussed in the following section.

It should be noted that the combination of the Tbt and Tip groups is found to be indispensable for stabilizing the reactive silicon–sulfur double bond. When a less hindered tetrathiasilolane **39** bearing Tbt and Mes groups on the silicon atom was desulfurized with triphenylphosphine as in the case of **37**, the color of the solution turned yellow at –78°C, suggesting the initial formation of the expected silanethione **40**, but it undergoes ready head-to-tail [2+2] dimerization to give the corresponding 1,3,2,4-dithiadisiletane derivative **41** quantitatively (Scheme 12).³¹

Although it is possible to trap the silanethione **40** by intermolecular addition reactions at –78°C (Scheme 12), the combination of Tbt and Mes groups is not efficient enough to stabilize the silathiocarbonyl unit as stable compounds at ambient temperature.

3. Silicon–Selenium and Silicon–Tellurium Double Bond Compounds (Silaneselones and Silanetellones)

In contrast to the remarkable progress in the chemistry of silanones and silanethiones, very little is known for the chemistry of their heavier chalcogen

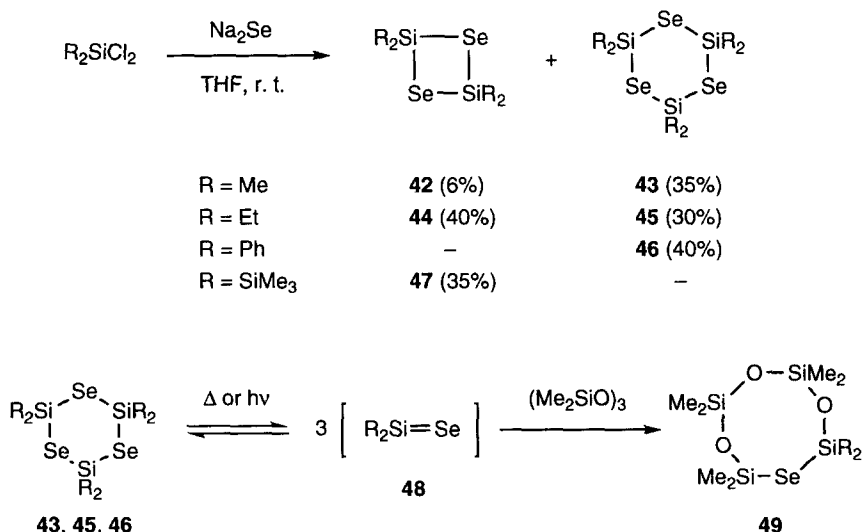


SCHEME 12.

analogues, the silaneselones and silanetellones. However, some developments have been recently reported for these unprecedented heavier congeners.

a. Transient silaneselones For the generation of silaneselones, Boudjouk *et al.* have described the photochemical and thermal fragmentation of cyclosilaseselenanes.³³ Thus, several cyclodisiladiselenanes and cyclotrisilatriseselenanes, $(\text{R}_2\text{SiSe})_n$ (**42–47**; $n = 2, 3$), were prepared from *in situ* generated Na_2Se and the corresponding R_2SiCl_2 (Scheme 13).³⁴ The properties of the cyclosilaseselenanes depend on the groups attached to silicon, ranging from alkyl-substituted systems [e.g., **42** and **43** ($\text{R} = \text{Me}$) and **44** and **45** ($\text{R} = \text{Et}$) are thermally unstable and air-sensitive yellow oils] to a silyl-substituted one **47** ($\text{R} = \text{SiMe}_3$) which was isolated as green crystals stable to air for several days.

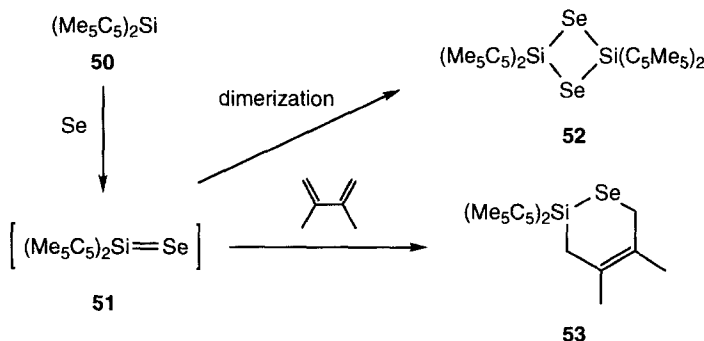
The cyclosilaseselenanes here obtained generate the corresponding silaneselones, $\text{R}_2\text{Si}=\text{Se}$ (**48**), thermally and photochemically when $\text{R} = \text{Me}$, Et and $n = 3$ but only thermally when $\text{R} = \text{Me}$, Et and $n = 2$ (Scheme 13). The silaneselones **48** are easily trapped with $(\text{Me}_2\text{SiO})_3$ to give the insertion product **49**. In the case of $\text{R} = \text{Ph}$, only the six-membered ring product **46** was available as the precursor, which afforded a modest yield of an insertion reaction product of $\text{Ph}_2\text{Si}=\text{Se}$ to $(\text{Me}_2\text{SiO})_3$ under thermal conditions but gave a complex mixture upon photolysis. On the other hand, trimethylsilyl substituted cyclodisiladiselenane **47** was found



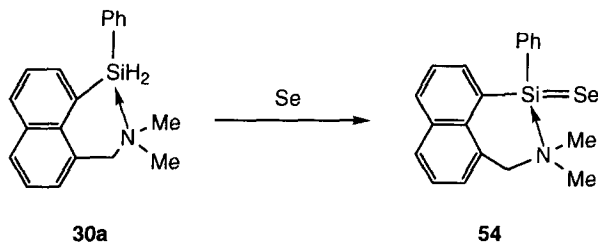
SCHEME 13.

to be reluctant to ring fragmentation either on thermolysis (250°C for 5 days in a sealed tube) or on photolysis.^{33b}

In 1989 Jutzi *et al.* reported the reaction of decamethylsilicocene **50** with tri-*n*-butylphosphine selenide in benzene at room temperature, leading to almost quantitative formation of a 1,3,2,4-diselenadisiletane derivative **52**, a head-to-tail [2+2] cycloaddition reaction product of the initially formed silaneselone **51**.³⁵ The intermediacy of silaneselone **51** was experimentally supported by the reaction in the presence of 2,3-dimethyl-1,3-butadiene resulting in the formation of the corresponding [2+4] cycloaddition reaction product **53** (Scheme 14).



SCHEME 14.



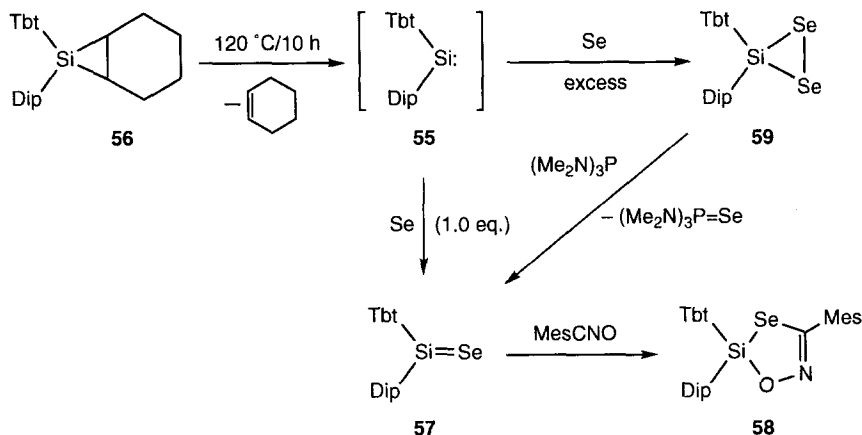
SCHEME 15.

Structural analysis of the reaction products clearly shows that the ligand on silicon undergoes a haptotropic rearrangement from $\eta^5\text{-C}_5\text{Me}_5$ in **50** to $\eta^1\text{-C}_5\text{Me}_5$ in **52** and **53** as in the cases of oxygenation and thionation of **50**.³⁶ Apparently, silaneselone **51** is not kinetically stable enough to be isolated under normal conditions.

b. Thermodynamically stabilized silaneselone The reaction of the pentacoordinated functionalized silane **30** (*vide supra*) with elemental selenium was examined by Corriu *et al.* to give stable silaneselone **54**, which is thermodynamically stabilized by the intramolecular coordination of the nitrogen-containing substituent (Scheme 15).¹⁷ Although the structure of **54** was supported by ^{29}Si and ^{13}C NMR and MS spectra including a downfield ^{29}Si chemical shift ($\delta = +29.4$) and a large coupling constant with ^{77}Se ($J_{\text{SeSi}} = 257$ Hz), neither crystallographic structural analysis nor reactivity of this isolable $\text{Si}=\text{Se}$ compound has been reported.

c. Kinetically stabilized silaneselone As in the case of stable silanethione **38**, kinetic stabilization of a silaneselone was examined using the Tbt group. Since the synthesis and isolation of the cyclic polyselenides Tbt(R)SiSe_4 ($\text{R} = \text{Mes}$ or Tip) were unsuccessful, probably due to the higher instability than that of the corresponding tetrathiasilolanes such as **37** and **39**, the direct selenation of the sterically hindered diarylsilylene Tbt(Dip)Si : (**55**; $\text{Dip} = 2,6\text{-diisopropylphenyl}$) was examined. Thus, the bicyclic silirane derivative (**56**) bearing Tbt and Dip groups on the silicon atom was treated with elemental selenium at 120°C in C_6D_6 (sealed tube) to afford a red solution, suggesting the formation of the corresponding silaneselone **57** (Scheme 16).³⁷

The formation of silaneselone **57** was evidenced by the trapping reaction with mesitonitrile oxide leading to the corresponding cycloadduct **58** and was also supported by the observation of a remarkably downfield ^{29}Si chemical shift ($\delta_{\text{Si}} = 174$) indicative of the $\text{Si}=\text{Se}$ double bond of **57**. Although this direct selenation of silylene **55** with an equimolar amount of selenium was not reproducible, the use of excess amount of elemental selenium resulted in the formation of a new cyclic diselenide, diselenasilirane **59**, as a stable compound ($\delta_{\text{Si}} = -44$ and



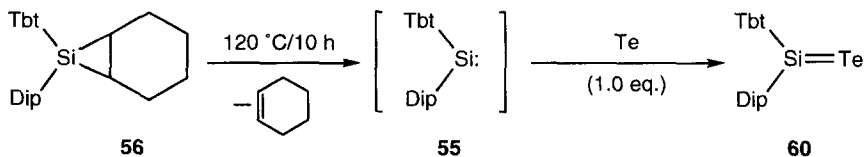
SCHEME 16.

$\delta_{\text{Se}} = -174$). Diselenasilirane **59** was found to be another useful precursor of silaneselone **57** when treated with an equimolar amount of a phosphine reagent (Scheme 16).³⁷

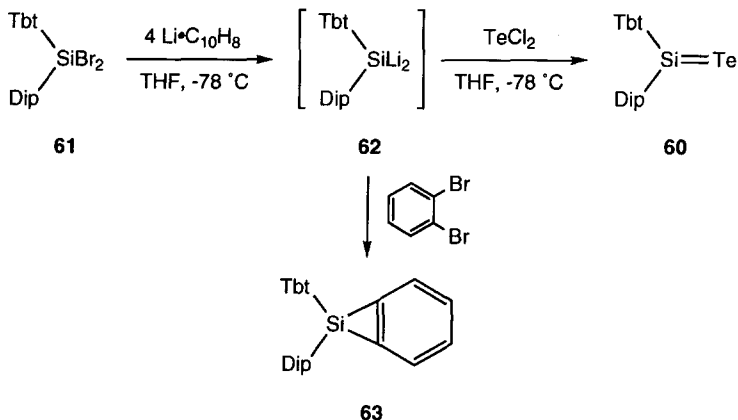
As shown by NMR spectra, silaneselone **57** exists as a stable species in solution at ambient temperature, but its isolation as crystals has not been achieved yet probably due to the low chemical yield in the final step.

d. *Kinetically stabilized silanetellone* The reaction of thermally generated bulky diarylsilylene **55** with elemental tellurium resulted in the formation of the corresponding silicon–tellurium double bond compound, the first example of stable silanetellone Tbt(Dip)Si=Te **60** (Scheme 17).³⁷ The formation of silanetellone **60** was evidenced by the ^{29}Si and ^{125}Te NMR chemical shifts ($\delta_{\text{Si}} = 170.7$ and $\delta_{\text{Te}} = 730.8$) and the characteristic green color ($\lambda_{\text{max}} = 593 \text{ nm}$ in C_6D_6).

In addition to the telluration of a silylene, another unique synthetic route has been developed for the silicon–tellurium double bond system. Recently, it has been reported that the exhaustive reduction of an overcrowded dibromosilane Tbt(Dip)SiBr_2 (**61**) with an excess amount (more than 4 equiv.) of lithium



SCHEME 17.



SCHEME 18.

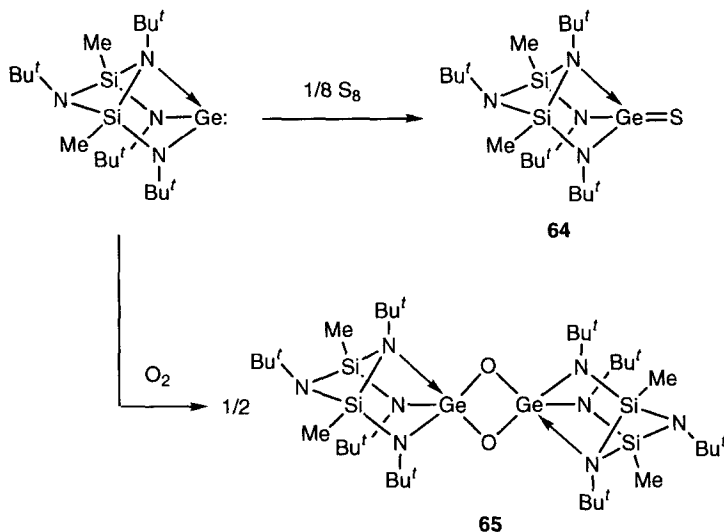
naphthalenide leads to generation of the corresponding diaryldilithiosilane $\text{Tbt}(\text{Dip})\text{-SiLi}_2$ (**62**),³⁸ which was found to be very useful for the synthesis of unprecedented organosilicon compounds such as the first stable silacyclopentabenzene **63** (Scheme 18).³⁹ As a further synthetic application of dilithiosilane **62**, the reaction of **62** with tellurium(II) dichloride was examined in THF at -78°C to give the expected silanetellone **60** (Scheme 18).³⁷ The spectroscopic data of the reaction product were identical with those obtained for the sample prepared by the telluration of the corresponding silylene **55**.

Thus, the synthetic route via dilithiosilane **62** should be noted as an alternative synthetic approach to the heavy ketones. To date, the isolation of silanetellone **60** as stable crystals has not been achieved yet, though **60** was found to be stable in solution at ambient temperature.

B. Double Bond Systems Containing a Germanium Atom

Until recently, there have been only two examples of stable Ge-S double bond compounds and one each for Ge-Se and Ge-Te double bond compounds, but both of them are stabilized by the intramolecular coordination of a nitrogen ligand to the germanium center.

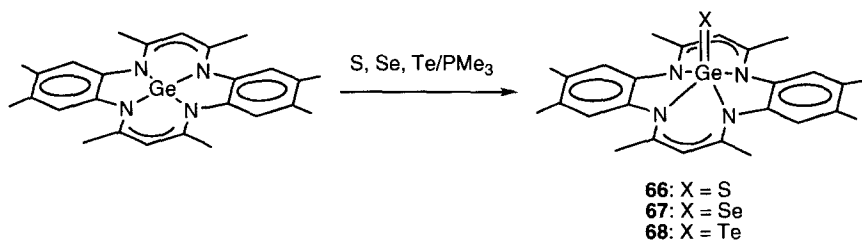
In 1989, Veith and his co-workers reported the synthesis of a base-stabilized Ge-S double bond species **64** (Scheme 19). X-ray structural analysis⁴⁰ shows that the sum of the bond angles around the Ge atom was 355° , which indicates the geometry for the Ge atom can be described as distorted tetrahedral, or better still as trigonal planar with an additional bond ($\text{N}\rightarrow\text{Ge}$). The Ge-S bond distance of $2.063(3) \text{ \AA}$ was about 0.2 \AA shorter than for a Ge-S single bond. ^1H NMR showed three signals assigned to nonequivalent *t*-butyl, also indicating



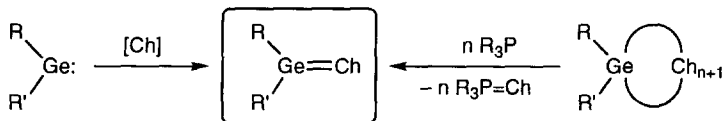
SCHEME 19.

this coordination of the nitrogen atom. The synthesis of a germanone bearing the same substituent was also studied by Veith *et al.* (Scheme 19),^{40a} but the trial was unsuccessful, since it resulted in the formation of **65**, a dimer of the corresponding germanium–oxygen double bond species. This is most likely due to the high polarity of the $\text{Ge}=\text{O}$ bond⁴¹ in spite of thermodynamic stabilization.

Meanwhile, Parkin and his co-workers have also reported the synthesis of a series of terminal chalcogenido complexes of germanium **66**, **67**, and **68** (Scheme 20).⁴² X-ray structural analyses of **66**, **67**, and **68** revealed that they have unique germa-chalcogenourea structures stabilized by the intramolecular coordination of nitrogen atoms. The central $\text{Ge}-\text{X}$ ($\text{X} = \text{S}, \text{Se}, \text{Te}$) bond of **66**, **67**, and **68** should be represented by a resonance structure, $\text{Ge}^+ - \text{X}^- \longleftrightarrow \text{Ge}=\text{X}$, because their bond



SCHEME 20.



Ch = O, S, Se, Te

SCHEME 21.

lengths are somewhat elongated compared to the sums of theoretically predicted double bond covalent radii; 2.110(2) Å for Ge=S (**66**), 2.247(1) Å for Ge=Se (**67**), 2.446(1) Å for Ge=Te (**68**).

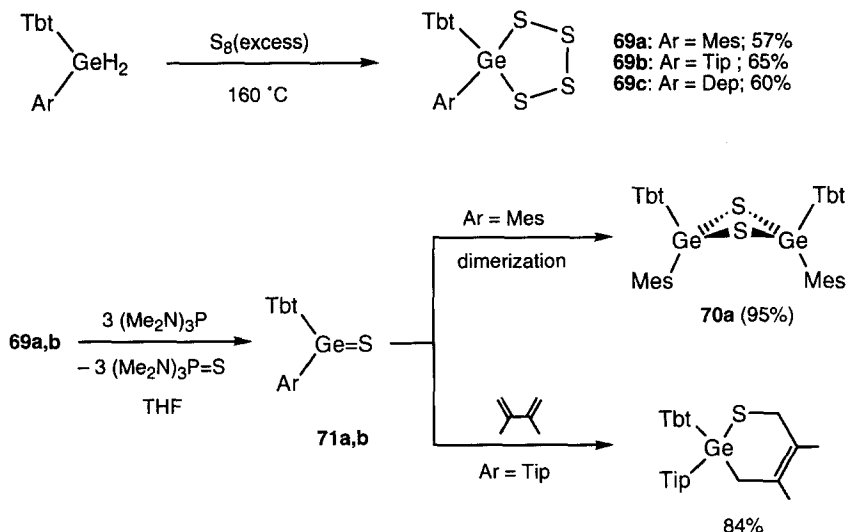
1. Synthetic Strategies for Stable Germanium-Containing Heavy Ketones^{11b,45}

A variety of preparation methods are known for transient germanium–chalcogen double bond species; some of them seemed to be useful also for the synthesis of kinetically stabilized systems. Indeed, the reaction of a germylene with an appropriate chalcogen source was found to be one of the most versatile and general methods for the synthesis of stable germanium-containing heavy ketones (Scheme 21).

As in the case of silanethione **38**, an efficient synthetic method has been developed for stable germanethiones and germaneselones (i.e. germanium–sulfur and germanium–selenium double bond compounds), via dechalcogenation reactions of the corresponding overcrowded germanium-containing cyclic polychalcogenides with a phosphine reagent (Scheme 21). Although this method is much superior to the direct chalcogenation of germylenes in view of the easy separation and isolation of the heavy ketones by simple filtration of the phosphine chalcogenides formed, it cannot be applied to the synthesis of germanones and germanetellones, due to the lack of stable precursors such as cyclic polyoxides and polytellurides.

2. Stable Diaryl-Substituted Germanethione and Germaneselone

a. Synthesis of a stable diarylgermanethione As the precursors for stable germanethiones, a series of overcrowded cyclic polysulfides 1,2,3,4,5-tetrathiagermolanes Tbt(Mes)GeS₄ (**69a**; Mes = mesityl), Tbt(Tip)GeS₄ **69b**, Tbt(Dep)GeS₄ (**69c**; Dep = 2,6-diethylphenyl) bearing two bulky aryl groups have been synthesized.^{32,44} In expectation of synthesizing germanethiones, these cyclic polysulfides were desulfurized with 3 molar amounts of hexamethylphosphorous triamide. But the desulfurization of tetrathiolane **69a** resulted in the formation of 1,3,2,4-dithiadigermetane **70a**, a dimer of germanethione Tbt(Mes)Ge=S **71a**, suggesting the combination of Tbt and Mes groups is not sufficient to stabilize the reactive

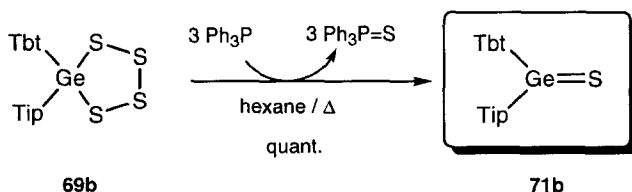


SCHEME 22.

Ge=S double bond of **71a** (Scheme 22).⁴⁵ In contrast, desulfurization of **69b** bearing a bulkier Tip group gave germanethione Tbt(Tip)Ge=S **71b** without forming any dimer **70a**. The generation of germanethione **71b** was confirmed by a trapping reaction with 2,3-dimethyl-1,3-butadiene (Scheme 22).⁴⁶

Although germanethione Tbt(Tip)Ge=S **71b** is highly reactive toward water and oxygen, **71b** can be isolated as orange-yellow crystals quantitatively by filtration of the triphenylphosphine sulfide followed by the careful recrystallization from the hexane solution under argon atmosphere in a glovebox (Scheme 23). It should be noted that **71b** is the first kinetically stabilized isolable germanethione.⁴⁴

Germanethione **71b** is very sensitive toward moisture but thermally quite stable; it melted at 163–165°C without decomposition, and no change was observed even after heating its hexane solution at 160°C for 3 days in a sealed tube. A hexane solution of **71b** was orange-yellow, showing an absorption maximum at 450 nm

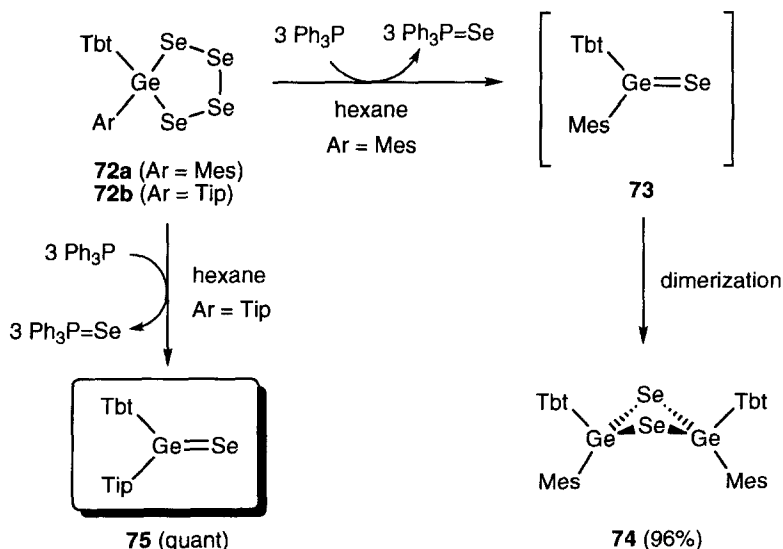


SCHEME 23.

which is attributed to $n-\pi^*$ transition of the $\text{Ge}=\text{S}$ double bond. On the other hand, no change in color was observed throughout the desulfurization of less hindered tetrathiagermolane **69a** leading to **70a**, most probably due to the extremely fast dimerization of **71a**. Similar desulfurization of tetrathiagermolane **69c** bearing a Dep group, medium in size between Mes and Tip, also gave a dimer of the corresponding germanethione $\text{Tbt}(\text{Dep})\text{Ge}=\text{S}$ **71c**.⁴⁷ At the beginning of the reaction, however, the electronic spectrum of the hexane solution showed the appearance of transient absorption at 450 nm, attributable to the intermediary germanethione **71c**. These results can be reasonably interpreted in terms of the bulkiness of protecting groups on the germanium atom, indicating that the combination of Tbt and Tip groups is necessary to isolate a germanethione.⁴⁷

b. Synthesis of a stable diarylgermaneselone When the less hindered tetraselenagermolane $\text{Tbt}(\text{Mes})\text{GeSe}_4$ **72a**^{47,48} was treated with triphenylphosphine in hexane at 90°C in a sealed tube, only 1,3,2,4-diselenadigermetane **74**, a dimer of the corresponding germaneselone $\text{Tbt}(\text{Mes})\text{Ge}=\text{Se}$ (**73**), was obtained even in the presence of an excess amount of 2,3-dimethyl-1,3-butadiene, showing the high reactivity of a germaneselone and the insufficient steric protection by the combination of Tbt and Mes groups (Scheme 24).⁴⁷

By contrast, deselenation of the bulkier precursor $\text{Tbt}(\text{Tip})\text{GeSe}_4$ **72b** with 3 molar amounts of triphenylphosphine in refluxing hexane under argon resulted in the quantitative isolation of the first stable germaneselone $\text{Tbt}(\text{Tip})\text{Ge}=\text{Se}$ **75** as red



SCHEME 24.

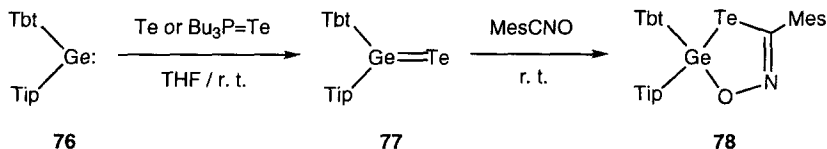
crystals (Scheme 24).^{47,49} Dimerization of **75** was not observed even in refluxing hexane, in spite of the bond distance of Ge=Se being longer than that of Ge=S. Germaneselone **75** was extremely sensitive to moisture but thermally quite stable under inert atmosphere (**75**; mp 191–194°C). One can see that the combination of Tbt and Tip groups is effective to stabilize the reactive germaselenocarbonyl unit of **75**, as in the case of germanethione **71b**.

c. Stable diaryl-substituted germanetellone In contrast to the extensive studies on thiocarbonyl and selenocarbonyl compounds,^{7,8} the chemistry of tellurocarbonyl compounds has been much less studied owing to their instabilities.^{8c,50} The chemistry of a germanetellone, the germanium analogue of a tellone, has also been very little explored. Theoretical calculations for H₂Ge=Te at the B3LYP/TZ(d,p) level have predicted that it has even smaller σ (59.1 kcal mol⁻¹) and π (30.3 kcal mol⁻¹) bond energies than those of the corresponding germanethione and germaneselone, but exists at an energy minimum, suggesting the possibility of its isolation.^{31b} Parkin *et al.* have reported the synthesis and crystallographic structure of gematellurourea **68**, which is stabilized by intramolecular coordination of nitrogen atoms onto the Ge atom,⁴² the only report on the chemistry of germanium–tellurium double bond species.

In view of these situations, synthesis and isolation of a kinetically stabilized germanetellone are significant not only for clarifying the character of the Ge–Te double bond by itself but also for elucidating the properties of germanium-containing heavy ketones systematically.

The successful isolation of stable germanethione **71b** and germaneselone **75** suggests that an overcrowded cyclic polytelluride might be a useful precursor for a germanetellone, if one is available. However, no isolable cyclic polytelluride has been obtained, probably owing to the instability of polytellurides. Therefore, stable diarylgermylene **76** obtained by reduction of the corresponding dibromide with lithium naphthalenide was allowed to react with an equimolar amount of elemental tellurium in THF to synthesize a germanetellone **77** directly. The color of the solution gradually changed over 10 h from blue ($\lambda_{\text{max}} = 581$ nm) due to **76** to green ($\lambda_{\text{max}} = 623$ nm), the red shift of which is indicative of the generation of a germanetellone **77** as compared to the absorption maximum of germaneselone **75** ($\lambda_{\text{max}} = 510$ nm in THF).⁴⁹ The addition of mesitonitrile oxide as a trapping reagent to this green solution resulted in the formation of oxatellurazagermole **78**, the [3+2] cycloadduct of germanetellone Tbt(Tip)Ge=Te **77**, in 37% yield (Scheme 25).^{51,52} This is the first generation and direct observation of a kinetically stabilized germanetellone. The conversion of **75** to germanetellone **77** was, however, considered to be insufficient, judging from the low yield of **78**, which was most likely due to the insolubility of elemental tellurium.

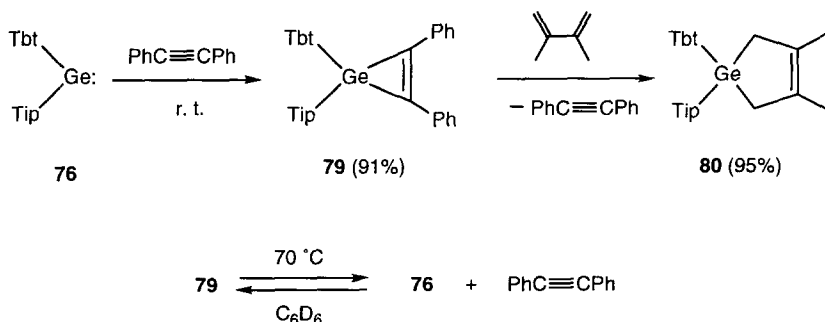
These results suggest the generation of germanetellone **77** which is stable in solution at room temperature, but an alternative synthetic method for **77** was considered to be necessary for its isolation, because the final solution of **77** obtained



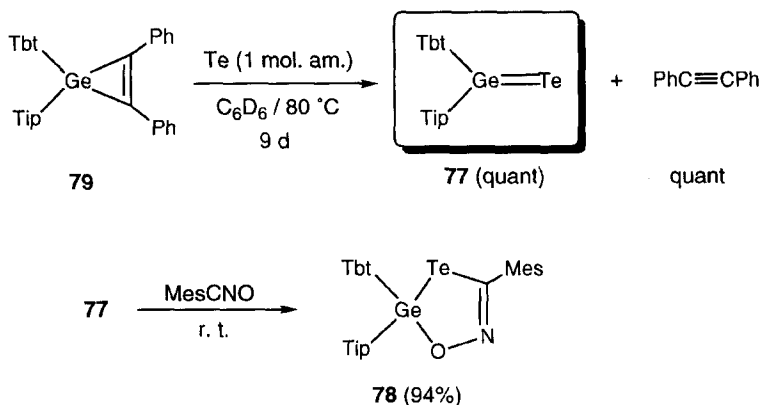
SCHEME 25.

by the above-mentioned reaction should contain inevitable by-products such as naphthalene, tributylphosphine, and lithium bromide.

d. Isolation of a stable germanetellone First, the synthesis of an overcrowded germirene suitable as a precursor of an overcrowded diarylgermylene was examined. Germirene **76** generated from dibromogermene Tbt(Tip)GeBr₂ and lithium naphthalenide was allowed to react with diphenylacetylene to afford germirene **79** in good yield as white crystals (Scheme 26).⁵³ This germirene is kinetically stable owing to the bulky groups, in contrast to the previously reported germirenes⁵⁴ which are known to be hydrolyzed rapidly in air. Since the thermal lability of germirene **79** was indicated by decomposition at 118–120°C in the solid state, a benzene-*d*₆ solution of germirene **79** and 2,3-dimethyl-1,3-butadiene in an NMR tube was heated while the solution was being monitored by ¹H NMR. Only a slight change was observed at 50°C, but heating up to 70°C for 9 h gave germacyclopentene **80** (95%) and diphenylacetylene (100%) with complete consumption of the starting material (Scheme 26). This cheletropic reaction is reversible; in the absence of the trapping reagent, the colorless solution at room temperature turns pale blue at 50°C, showing the regeneration of germirene **76**, and becomes colorless again on cooling. These results indicate that germirene **79** is a useful precursor for diarylgermylene Tbt(Tip)Ge: **76** under neutral conditions without forming any reactive by-products (Scheme 26).⁵³



SCHEME 26.



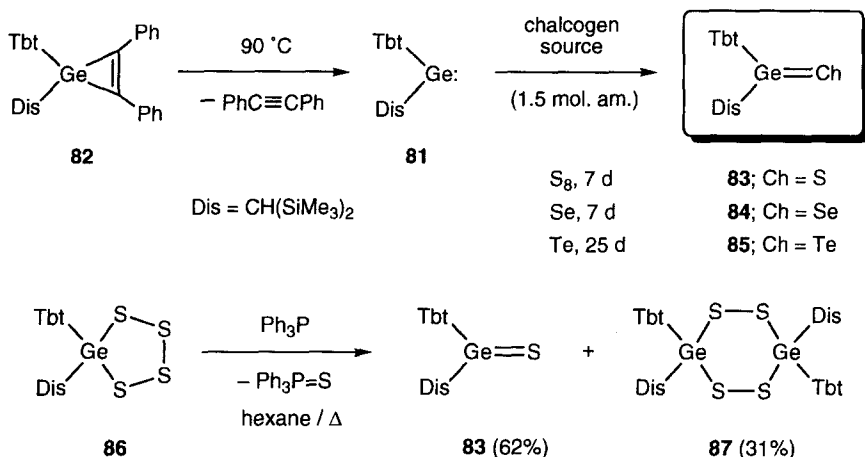
SCHEME 27.

For the synthesis of germanetellone **77**, germirene **79** and an equimolar amount of elemental tellurium were allowed to react in benzene-*d*₆ at 80 °C, and the reaction was monitored by ¹H NMR. Heating for 9 days led to the appearance of new signals along with those of diphenylacetylene at the expense of those assigned to **79**, and the solution turned green. The sealed tube was opened in a glovebox filled with argon, and mesitronitrile oxide was added to the solution to afford [3+2] cycloadduct **78** in 94% yield (Scheme 27).^{51,52} These results clearly showed the almost quantitative generation of germanetellone **77**. Removal of the solvent from the green solution without the addition of mesitronitrile oxide gave germanetellone **77** quantitatively as green crystals (Scheme 27).^{51,52} This is the first isolation of a kinetically stabilized germanetellone. Germanetellone **77** was sensitive to moisture, especially so in solution, but was thermally quite stable; **77** melted at 205–210 °C without decomposition.

3. Synthesis of Alkyl,aryl-Substituted Germanium-Containing Heavy Ketones

For systematic synthesis and isolation of alkyl,aryl-disubstituted germanium-containing heavy ketones, the chalcogenation of an alkyl,aryl-disubstituted germylene, Tbt(Dis)Ge: **81** [Dis = bis(trimethylsilyl)methyl],⁵³ was examined (Scheme 28). Germylene **81** was generated by the cycloreversion of the corresponding germirene **82** under conditions similar to those for diarylgermylene **76**.

Thermal reaction of germirene **82** was performed in the presence of 1/8 molar amount of S₈ to give germanethione Tbt(Dis)Ge=S (**83**) quantitatively, which was isolated as yellow crystals in a glovebox under pure argon (Scheme 28). Similarly, germaneselone Tbt(Dis)Ge=Se (**84**) and germanetellone Tbt(Dis)Ge=Te (**85**) were also synthesized quantitatively and isolated as orange-red and blue-green crystals, respectively (Scheme 28).^{43,51} Although the reactions of germylene



SCHEME 28.

81 with elemental sulfur and selenium are completed after a week, that with tellurium was very slow and needed more than 3 weeks to finish, most likely due to the extremely low solubility of tellurium powder.

Although germanethione **83** can also be synthesized by the desulfurization of the corresponding tetrathiagermolane **86** with triphenylphosphine, the formation of **83** is not exclusive (62%); the 1,2,4,5,3,6-tetrathiadigermacyclohexane derivative **87** was isolated in 31% yield. This result shows that some intermolecular coupling process of the intermediates might be involved in the desulfurization of **86** bearing the less hindered Dis group as compared to the case of Tbt(Tip)GeS₄ (**69b**).⁴³

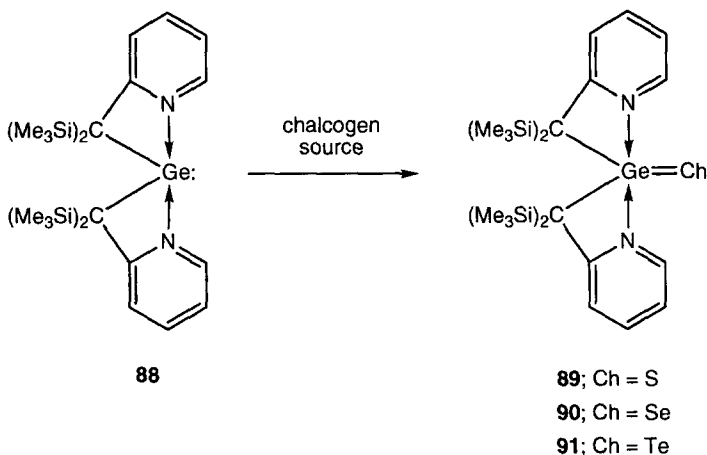
4. Synthesis of Stable Dialkyl-Substituted Germanium-Containing Heavy Ketones

Although there have been no reports so far on the synthesis of kinetically stabilized germanium-containing heavy ketones bearing only alkyl substituents, penta-coordinate germane-chalcogenones **89–91** bearing two alkyl ligands were recently synthesized by the chalcogenation of the corresponding base-stabilized germynes **88** (Scheme 29).⁵⁵

Their crystallographic structural analysis revealed that these pentacoordinate Ge complexes have pseudo-trigonal bipyramidal geometry with a trigonal planar arrangement of the chalcogen and the two carbon atoms around the germanium center. The Ge–chalcogen bond lengths of **89–91** were found to be intermediate between the typical single and double bond lengths (*vide infra*).

5. Heteroatom-Substituted Germanium-Chalcogen Double Bond Compounds

In addition to the extensive studies on Ge-containing heavy ketones, there have been reported several examples of stable germanium–chalcogen double



SCHEME 29.

bonds having two heteroatom substituents **93**,⁵⁶ **95**,⁵⁷ **96**,^{57a} **98a,b**,⁵⁸ and **99a–d** (Scheme 30).⁵⁸

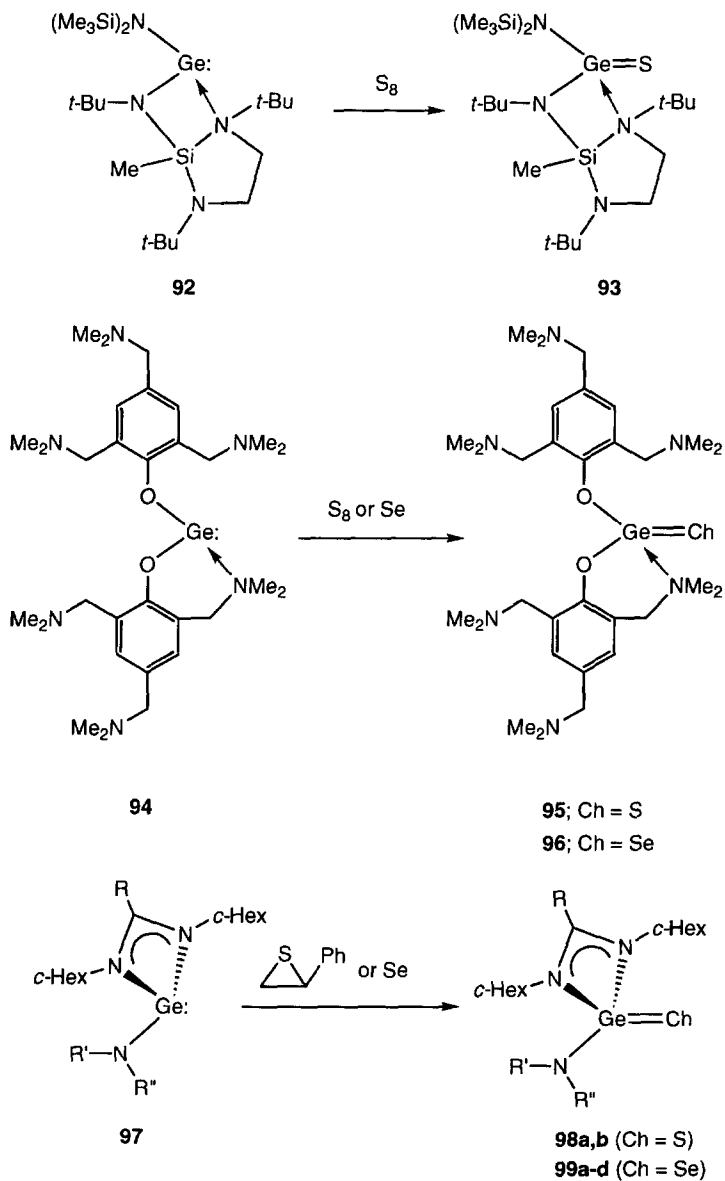
Most of them were prepared by the direct chalcogenation of the corresponding germynes **92**, **94**, and **97** thermodynamically stabilized with the heteroatom substituents.

C. Double Bond Systems Containing a Tin Atom

1. Synthesis of Stable Stannanethiones and Stannaneselones

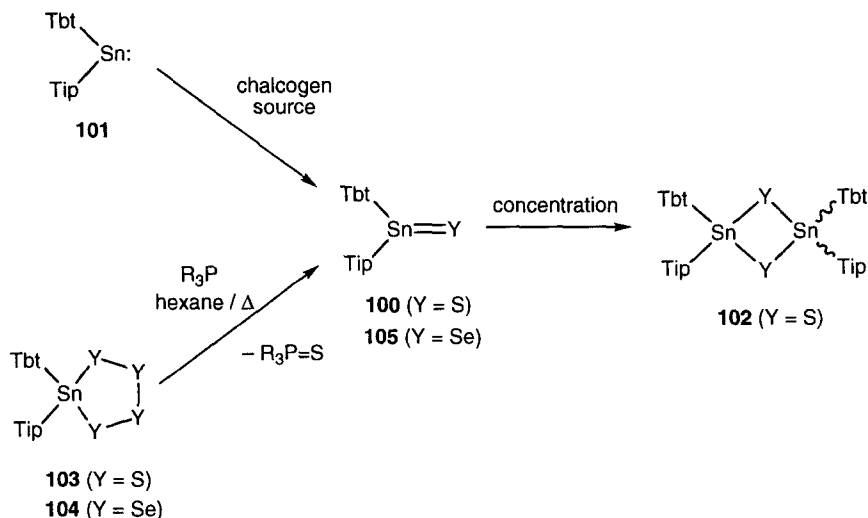
The successful isolation of Si- and Ge-containing heavy ketones naturally provoked the challenge to synthesize and isolate the much heavier congeners, tin–chalcogen double bonds. However, the combination of Tbt and Tip groups is not bulky enough to stabilize the stannanethione Tbt(Tip)Sn=S **100**⁵⁹ in contrast to the lighter analogues such as silanethione **38** and germanethione **71b**.

Although the stability of stannanethione **100**, which was generated in the sulfurization of the corresponding stannylene Tbt(Tip)Sn: (**101**) with elemental sulfur, was evidenced by the characteristic absorption maxima ($\lambda_{\text{max}} = 465 \text{ nm}$) in its electronic spectra, concentration of the reaction mixture resulted in the dimerization of **100** giving the 1,3,2,4-dithiadistannetane derivative **102** (Scheme 31).^{59a,c} Stannanethione **100** can also be formed in the desulfurization of the corresponding tetrathiastannolane **103** with triphenylphosphine, but the formation of **100** has been confirmed only by trapping experiments (*vide infra*),^{59b} and the ¹¹⁹Sn NMR chemical shift for the central tin atom of **100** was not measured. The formation of similarly substituted stannaneselone **105** was also demonstrated by intramolecular



- a:** $R = Me$, $R' = c-Hex$, $R'' = C(Me)=N(c-Hex)$
b: $R = t-Bu$, $R' = c-Hex$, $R'' = C(Me)=N(c-Hex)$
c: $R = Me$, $R' = R'' = SiMe_3$
d: $R = t-Bu$, $R' = R'' = SiMe_3$

SCHEME 30.

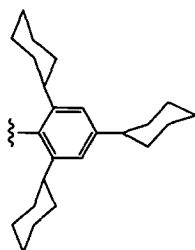
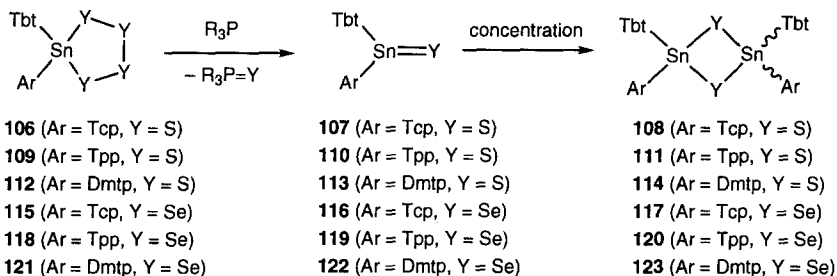
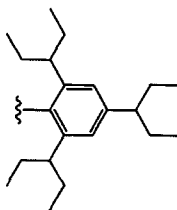


SCHEME 31.

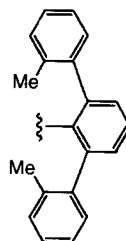
trapping experiments (*vide infra*), but no spectroscopic evidence was obtained (Scheme 31).^{59b,60}

The high reactivity of tin–chalcogen double bonds was somewhat suppressed by the modification of the steric protecting group combined with the Tbt group from Tip group to more hindered ones such as 2,4,6-tricyclohexylphenyl (Tcp), 2,4,6-tris(1-ethylpropyl)phenyl (Tpp), and 2,2''-dimethyl-*m*-terphenyl (Dmtp) groups.^{61,62} Thus, in these bulkier systems, the corresponding stannanethiones (107, 110, and 113) and stannaneselones (116, 119, and 122) showed characteristic orange and red colors, respectively, and all of them showed considerably deshielded ^{119}Sn NMR chemical shifts ($\delta_{\text{Sn}} = 467$ to 643 ppm) at ambient temperature, suggesting the sp^2 character of their tin centers and also their stability in solution (Scheme 32). On concentration of their NMR samples, however, these tin-containing heavy ketones underwent dimerization to give the corresponding dimers (108, 111, 114, 117, 120, and 123), and it was unsuccessful to isolate them as a stable solid or crystallines.

As the final goal of the synthesis and isolation of tin–chalcogen double bond species, further modification of Dmtp group was examined.⁶² Thus, the fine tuning of the side chains of the terphenyl unit of Dmtp (i.e., the use of 2,2''-diisopropyl-*m*-terphenyl (Ditp) group which bears two isopropyl groups instead of methyl groups in 2 and 2'' positions) allowed isolation of the corresponding stannanethione 125 and stannaneselone 127 as stable orange and red crystals, respectively. Both 125 and 127 were synthesized by the dechalcogenation of the corresponding Tbt- and Ditp-substituted tetrachalcogenastannolanes 124 and 126 with three equivalent

Tc_p group

Tpp group



Dmtp group

SCHEME 32.

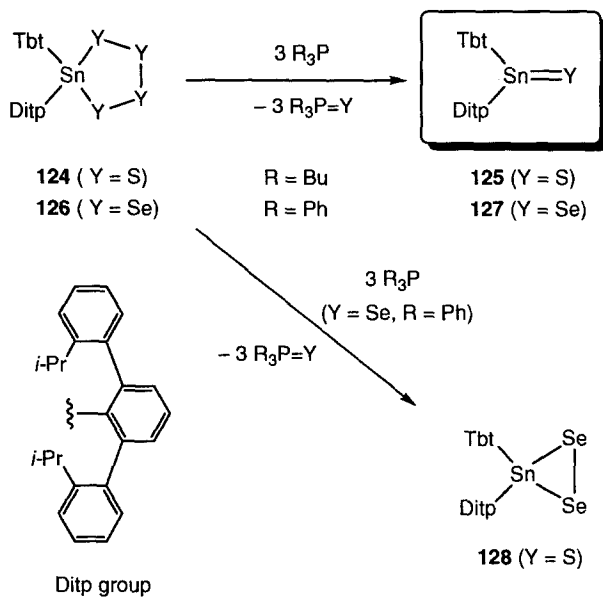
moles of phosphine reagents (Scheme 33).⁶² As judged by ¹¹⁹Sn NMR and electronic spectra, no dimerization was observed for **125** and **127** even after concentration to the solid state, and the molecular geometry of stannaneselone **127** was definitively determined by X-ray crystallographic analysis as shown in Fig. 1.

In addition to the successful isolation of the stable stannaneselone **127**, it should be noted that deselenation of **126** with two equivalent molar amounts of triphenylphosphine resulted in the isolation of a novel tin-containing cyclic diselenide, diselenastannirane **128**, as a stable crystalline compound.⁶⁰

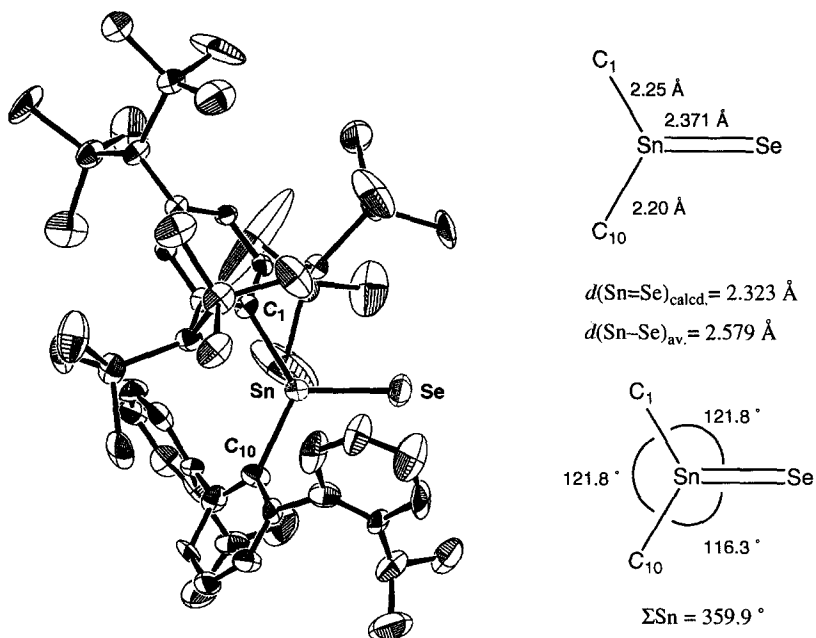
D. Double Bond Systems Containing a Lead Atom¹⁶

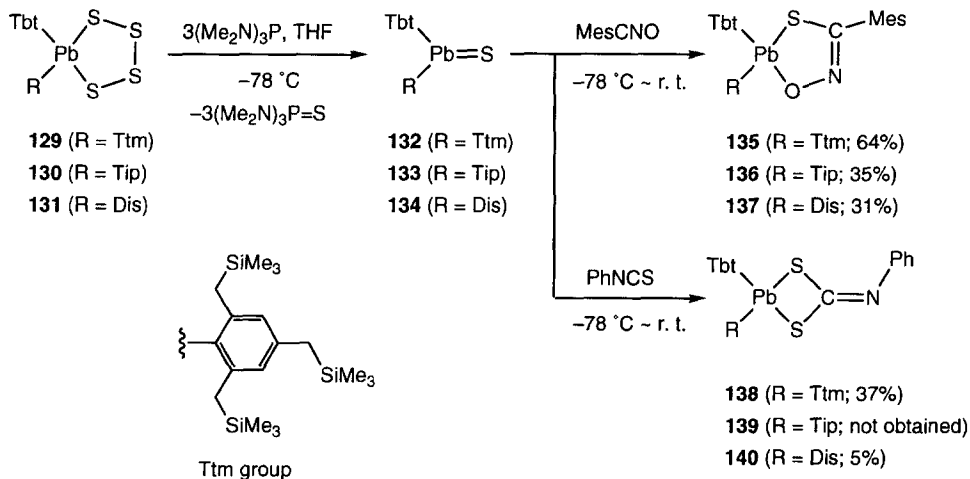
1. Synthesis of Plumbanethiones by Desulfurization of Tetrathiaplumbolanes

In anticipation of kinetic stabilization of a plumbanethione, the heaviest congener of metallanethiones of Group 14 elements, a series of hindered tetrathiaplumbolanes **129**–**131** was desulfurized with 3 equiv. of hexamethylphosphorous triamide at low temperature (−78°C in THF). The color of the reaction solution turned red for **129** and **130** or orange for **131**, indicating the generation of plumbanethiones **132**, **133** or **134**, respectively.^{16,63} Subsequent addition of mesitonitrile oxide to this solution at −78°C gave the corresponding



SCHEME 33.

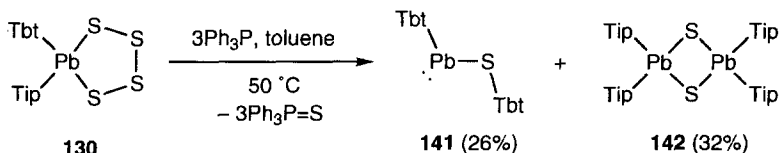
FIG. 1. ORTEP drawing of Tbt(Ditp)Sn=Se (**127**) and some selected bond lengths and angles.



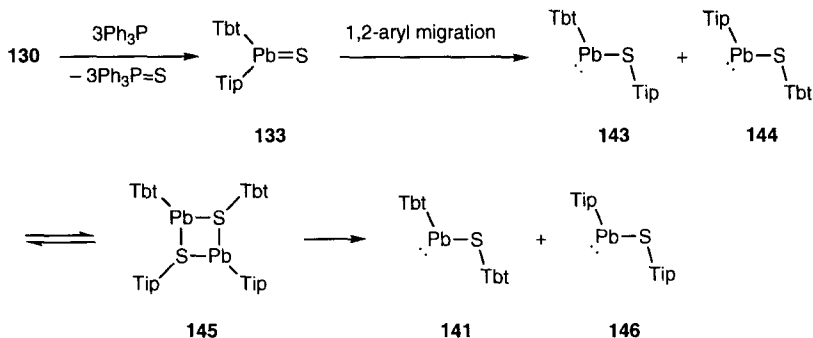
SCHEME 34.

oxathiazaplumbos **135–137**, a [3+2] cycloadduct of plumbanethione **132–134**, in a moderate yield in each case (Scheme 34).^{16,63} Plumbanethiones **132** and **134** were also trapped with phenyl isothiocyanate to give [2+2] cycloaddition products **138** and **140**, respectively, though **133** did not afford such an adduct **139**. The formation of new Pb-containing heterocycles **135–137**, **138**, and **140** is worthy of note as the first examples of the trapping of plumbanethiones. Observation of the color changes of the reaction solution suggests that plumbanethiones **132–134** thus formed are stable in solution at least below -20°C .

In order to elucidate the thermal stability of the plumbanethione **133**, tetrathiaplumbolane **130** was desulfurized at higher temperature. Reaction of **130** with 3 equiv. of triphenylphosphine in toluene at 50°C gave a deep red solution, from which plumbylene **141** was precipitated as pure deep red crystals (Scheme 35).⁶⁴ Besides **141**, 1,3,2,4-dithiadiplumbetane **142** was obtained as another lead-containing main product. It should be noted that the final product **141** bears only Tbt groups while **142** has only Tip groups, though the starting material **130** bears both Tbt and Tip groups on the lead atom.



SCHEME 35.



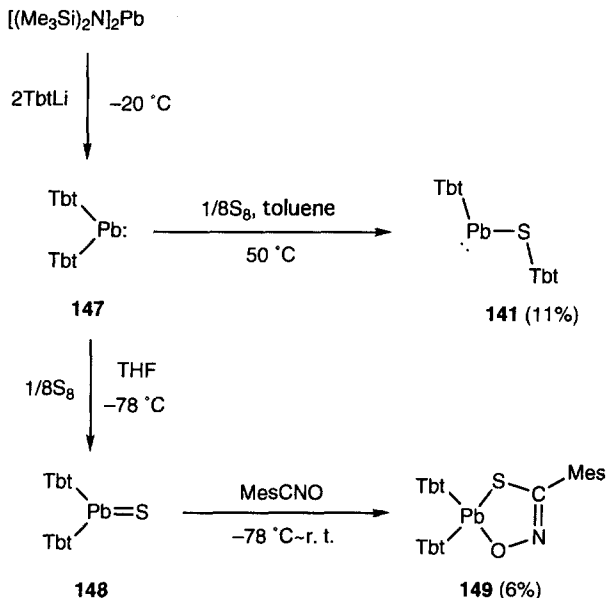
SCHEME 36.

The fact that the final products, plumbylene **141** and dithiadiplymbetane **142**, bear only Tbt and Tip groups, respectively, indicates the presence of some comproportionation process in their formation from **133**. A plausible mechanism is shown in Scheme 36 for the formation of **141** and **142**, though a detailed reaction mechanism is not clear at present.⁶⁴ The tetrathiaplumbolane **130** is first desulfurized to provide plumbanethione **133**, as has been seen in the desulfurization of **130** at low temperature. Plumbanethione **133** might undergo 1,2-aryl migration to give plumbylenes **143** and **144**, which subsequently react to afford an arylsulfido bridged organolead heterocycle **145**, since a less hindered arylthioplumbylene is known to have a tendency to oligomerize forming a cyclic compound.^{65a} The retro [2+2] cycloaddition reaction of **145** affords **141** and **146**. Dithiadiplymbetane **142** may be obtained from the less crowded plumbylene **146**.

X-ray crystallographic analysis reveals that plumbylene **141** exists as a monomer, and there is no intermolecular interaction between the lead and sulfur atoms,^{64a} while other heteroatom-substituted plumbylenes so far known exist as a heteroatom-bridged cyclic oligomer.⁶⁵

2. Synthesis of a Plumbanethione by Sulfurization of a Plumbylene

In order to prove the 1,2-aryl migration process proposed for plumbanethione **133**, the synthesis of plumbanethione **148** by sulfurization of a diarylplumbylene **147** with one atom equivalent of elemental sulfur at low temperature and the successive trapping reaction of **148** with mesitonitrile oxide were carried out (Scheme 37).¹⁶ The formation of cycloadduct **149** indicates the generation of intermediary plumbanethione **148**. Furthermore, the fact that heating of a toluene solution of isolated plumbylene **147** and one atom equivalent of elemental sulfur at 50°C gave **141** clearly demonstrates the occurrence of 1,2-aryl migration in **148** (Scheme 35).¹⁶ The formation of **141** in this experiment is the first demonstration that $\text{R}(\text{RS})\text{Pb}$ is more stable than $\text{R}_2\text{Pb}=\text{S}$.



SCHEME 37.

This interpretation of the experimental results was corroborated by *ab initio* calculations on the relative stabilities of a series of double bond compounds, $[\text{H}_2\text{Pb}=\text{X}]$ and their plumbylene type isomers, $[\text{trans-H-Pb-X-H}]$ and $[\text{cis-H-Pb-X-H}]$ ($\text{X} = \text{O}, \text{S}, \text{Se}, \text{and Te}$) (*vide supra*).¹⁶ The results of the theoretical calculations and experiments for lead-chalcogen double bond species are in sharp contrast to those of the other Group 14 element analogues which do not isomerize to the divalent compounds.^{14b}

IV

STRUCTURES AND PHYSICAL PROPERTIES

A. X-ray Crystallographic Analysis

It should be very important to reveal the structural features of heavy ketones and to make a systematic comparison with those of a carbonyl compound such as the bond shortening and the trigonal planar geometry which result from the sp^2 hybridization between the carbon and oxygen atoms.

First, crystallographic structural analysis of the thermodynamically stabilized silanethione was established for the bulky silanethione **31b** (see Scheme 8).

Although the Si–S bond [2.013(3) Å] in **31b** is shorter than a typical Si–S single bond (2.13–2.16 Å),⁶⁶ suggesting its double bond character to some extent, it is still 0.07 Å longer than the calculated value for the parent silanethione $\text{H}_2\text{Si}=\text{S}$ (**1**). The Si–N distance (1.964 Å) in **31b**, slightly longer than a Si–N σ bond (1.79 Å), supports a very strong coordination of the nitrogen atom of the dimethylaminomethyl group in **31b** to the central silicon atom, which in turn makes the silathiocarbonyl unit of **31b** considerably deviated from the ideal trigonal planar geometry; the sum of the angles around the central silicon atom is 344.9°. The authors concluded that the resonance betaine structure strongly participates in the electronic distribution of the internally coordinated silanethiones **31a,b**.

Therefore, the elucidation of the intrinsic structural parameters of heavy ketones has to be done with kinetically stabilized systems. Most of the heavy ketones synthesized by steric protection with the Tbt group have provided single crystals suitable for X-ray structural analysis. The results for silanethione **38**, germanethione **71b**, germaneselonones **75**, **84**, germanetellones **77**, **85**, and stannaneselone **127**, are summarized in Table III.

The structural parameters of all heavy ketones examined show that they have an almost completely trigonal planar geometry and a distinct double bond nature. The observed double bond lengths and Δ_{obs} [bond shortening (%) compared to the corresponding single bonds] values are in good agreement with calculated values for $\text{H}_2\text{M}=\text{X}$ (*vide supra*, Table I).¹⁴ These findings clearly indicate that heavy ketones have structural features similar to those of a ketone, although their double bond character is lower than that of the corresponding carbon homologues as judged by their Δ_{obs} values.

It should be noted that all the $\text{M}=\text{X}$ bond lengths observed here are significantly shorter than those reported for the corresponding double bond compounds stabilized by intramolecular coordination of heteroatoms. In other words,

TABLE III
STRUCTURAL PARAMETERS OF HEAVY KETONES $\text{Tbt(R)M}=\text{X}$

R	Tip	Tip	Tip	Dis	Tip	Dis	Ditp
M	Si	Ge	Ge	Ge	Ge	Ge	Sn
X	S	S	Se	Se	Te	Te	Se
Compound	38	71b	75	84	77	85	127
$\text{M}-\text{X}$ (Å)	1.948(4)	2.049(3)	2.180(2)	2.173(3)	2.398(1)	2.384(2)	2.375(3)
Δ_{obs} (%) ^a	9	9	9	8	9	8	9
$\Sigma \angle \text{M}(\text{deg})^b$	359.9	359.4	359.3	360.0	359.5	360.0	359.9

^aThe bond shortening (%) compared to the corresponding single bonds.

^bSummation of the bond angles around the M atom.

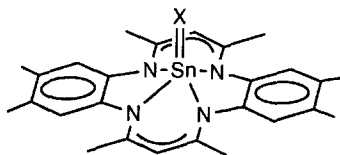
thermodynamically stabilized systems suffer from considerable electronic perturbation by heteroatom substituents.

Although some examples of thermodynamically stabilized double bond systems between Group 14 and Group 16 elements showed trigonal planar geometry due to their structural restriction, almost all of their bond lengths are longer than those kinetically stabilized and theoretically predicted.⁶⁷ These results clearly show that considerable electronic perturbation is inevitably involved in the thermodynamically stabilized systems.

B. NMR Spectra

As in the case of ^{13}C NMR, low-field chemical shifts are characteristic of sp^2 hybridized nuclei in the heavy ketones. For example, the ^{29}Si chemical shifts of silanethione **38** and silaneselone **57** are 167 and 174 ppm, respectively. Silanetellone **60** shows its ^{29}Si NMR signal at 171 ppm. In contrast, the ^{29}Si NMR signals of Corriu's compounds **31a** ($\text{X}=\text{S}$) and **54** ($\text{X}=\text{Se}$) appear at 22.3 and 29.4 ppm, respectively,¹⁷ indicating the high sp^3 nature of the silicon centers in **31a**. The other silanethiones **34** and **35**, not isolated but generated as stable species in solution, are reported to show their characteristic ^{29}Si NMR chemical shifts [34.2 and 41.1 ppm for **34** and **35**, respectively], which are indicative of their intramolecularly coordinated betaine structure as observed in the cases of **31a** and **54**. Silanethione **36** shows a characteristic ^{29}Si NMR chemical shift at δ -21.0, which is apparently upfield shifted compared to that for the noncoordinated, "true" silanethione **38** and at significantly higher field than those of the tetracoordinated silanethiones **31**, **34**, and **35** mentioned above. The characteristic low-field ^{77}Se and ^{125}Te chemical shifts of **57** ($\delta_{\text{Se}} = 635$) and **60** ($\delta_{\text{Te}} = 731$) are also indicative of their sp^2 hybridized chalcogen atoms.

Similarly, stannanethione **125** and stannaneselone **127** kinetically stabilized by Tbt and Ditp groups have ^{119}Sn chemical shifts of 531 and 440 ppm, respectively. Recently, Parkin *et al.* have reported the synthesis of stable terminal chalcogenido complexes of tin **150** (Scheme 38), and the chemical shifts for the central tin atom



150a: $\text{X} = \text{S}$
150b: $\text{X} = \text{Se}$

SCHEME 38.

150 resonate at a much higher field: -303 ppm (**150a**: $X=S$) and -444 ppm (**150b**: $X=Se$).⁶⁸ This clearly shows that the thermodynamically stabilized tin–chalcogen double bonds in **150** ($X=S$, Se) are electronically perturbed to a great extent.

On the other hand, such information is not available for germanium-containing heavy ketones because of difficulty in observing Ge NMR, but the low-field resonating ⁷⁷Se and ¹²⁵Te NMR chemical shifts of germaneselones [$\delta_{se} = 941$ (for **75**) and 872 (for **84**)]^{47,49} and germanetellones [$\delta_{Te} = 1143$ (for **77**) and 1009 (for **85**)]^{43,51} are in keeping with the sp^2 hybridization of these elements as in the cases of silaneselone **57** and silanetellone **60**.

C. UV-Vis Spectra

In Table IV are listed characteristic visible absorptions observed for the heavy ketones kinetically stabilized by Tbt group.

It is known that the $n \rightarrow \pi^*$ absorptions of a series of $R_2C=X$ ($X=O$, S , Se , Te) compounds undergo a systematic red shift on going down the periodic table.¹⁰ A similar tendency is observed for the Si, Ge, and Sn series of $Tbt(R)Si=X$ ($X=S$, Se), $Tbt(R)Ge=X$ ($X=S$, Se , Te), and $Tbt(R)Sn=X$ ($X=S$, Se). In contrast, one can

TABLE IV
ELECTRONIC SPECTRA ($n \rightarrow \pi^*$) OF DOUBLY BONDED COMPOUNDS BETWEEN GROUP 14
ELEMENTS AND CHALCOGENS

	Observed (λ_{max}/nm) ^a			calcd ^b	
	X = S	X = Se		λ_{max}/nm	$\Delta\epsilon n\pi^*/eV^c$
TbtCH=X	587 ^d	792 ^e	H ₂ C=S	460	10.81
Tbt(R)Si=X	396 ^f	456 ^g	H ₂ Si=S	352	10.27
Tbt(R)Ge=X ^h	450 ⁱ	519 ^j	H ₂ Ge=S	367	9.87
Tbt(R)Sn=X	473 ^j	531 ^k	H ₂ Sn=S	381	9.22
			H ₂ Pb=S	373	9.11

^aIn hexane.

^bCIS/TZ(d,p)//B3LYP/TZ(d,p).

^c $\epsilon_{LUMO(\pi^*)} - \epsilon_{HOMO(n)}$.

^dReference 69.

^eReference 73.

^fR = Tip. Reference 22.

^gIn THF. R = Dip.

^hX = Te: R = Tip, λ_{max} 640 nm. Reference 51.

ⁱR = Tip. Reference 47.

^jR = Tip. Reference 59c.

^kR = Ditp. Reference 62.

see a very interesting trend in the absorption maxima of two series, Tbt(R)M=S and Tbt(R)M=Se (M=C, Si, Ge, Sn). In both series their λ_{max} 's are greatly blue-shifted on going from carbon to silicon congeners, whereas λ_{max} 's of silicon, germanium, and tin congeners are red-shifted with increasing atomic number of the Group 14 elements. This trend is also found in calculated values for $\text{H}_2\text{M=S}$ (M=C, Si, Ge, Sn).¹⁴ Since calculated $\Delta\epsilon_{\text{n}\pi^*}$ values increase continuously from $\text{H}_2\text{Sn=S}$ to $\text{H}_2\text{C=S}$, a long wavelength absorption for $\text{H}_2\text{C=S}$ (and hence for TbtCH=S ⁶⁹) most likely results from a large repulsion integral ($J_{\text{n}\pi^*}$) for the carbon-sulfur double bond, as in the case of $\text{H}_2\text{C=O}$ vs $\text{H}_2\text{Si=O}$.⁷⁰

D. Raman Spectra

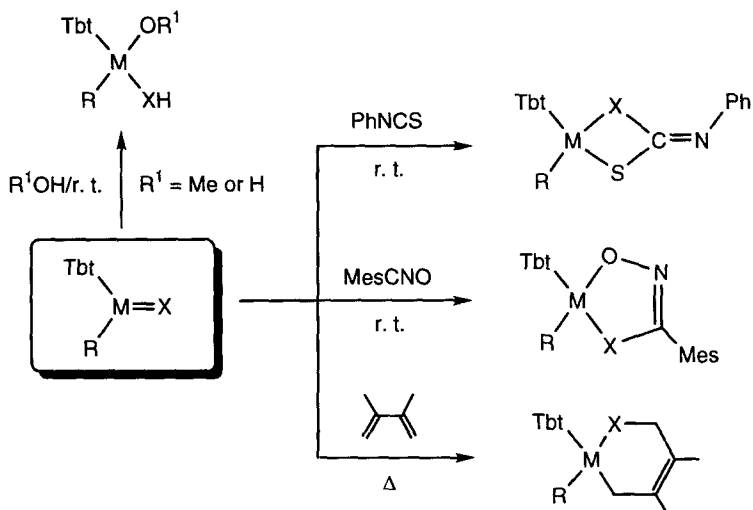
The stretching vibrations of the M=X bond were measured by Raman spectra for silanethione **38** (724 cm^{-1}), germanethiones **71b** (521 cm^{-1}) and **83** (512 cm^{-1}), and germanetellones **77** (381 cm^{-1}) and **85** (386 cm^{-1}). These values are in good accordance with those calculated for $\text{H}_2\text{M=X}$ compounds [723 (Si=S) , 553 (Ge=S) , and $387\text{ (Ge=Te)}\text{ cm}^{-1}$].¹⁴ It is noteworthy that the observed value of Tbt(Tip)Ge=S **71b** is very close to that observed by IR spectroscopy for $\text{Me}_2\text{Ge=S}$ (518 cm^{-1}) in an argon matrix at $17\text{--}18\text{ K}$,⁷¹ indicating similarity in the bond nature of both germanethiones in spite of the great difference in the size and nature of the substituents.

V

REACTIVITIES

As mentioned in the previous sections, heavy ketones undergo ready head-to-tail dimerization (or oligomerization) when the steric protecting groups on the Group 14 element are not bulky enough to suppress their high reactivity. Indeed, Tbt(Mes)M=X ($\text{M = Si, Ge; X = S, Se}$) cannot be isolated at ambient temperature, and instead the dimerization products are obtained. In the cases of tin-containing heavy ketones, the dimerization reactions take place much more easily than in the lighter Group 14 element congeners, and only the combination of Tbt and Ditp groups can stabilize the long and reactive tin-chalcogen double bonds (see Schemes 31–33).

Although the high reactivity of metal-chalcogen double bonds of isolated heavy ketones is somewhat suppressed by the steric protecting groups, Tbt-substituted heavy ketones allow the examination of their intermolecular reactions with relatively small substrates. The most important feature in the reactivity of a carbonyl functionality is reversibility in reactions across its carbon-oxygen double bond (addition-elimination mechanism via a tetracoordinate intermediate) as is observed, for example, in reactions with water and alcohols. The energetic basis



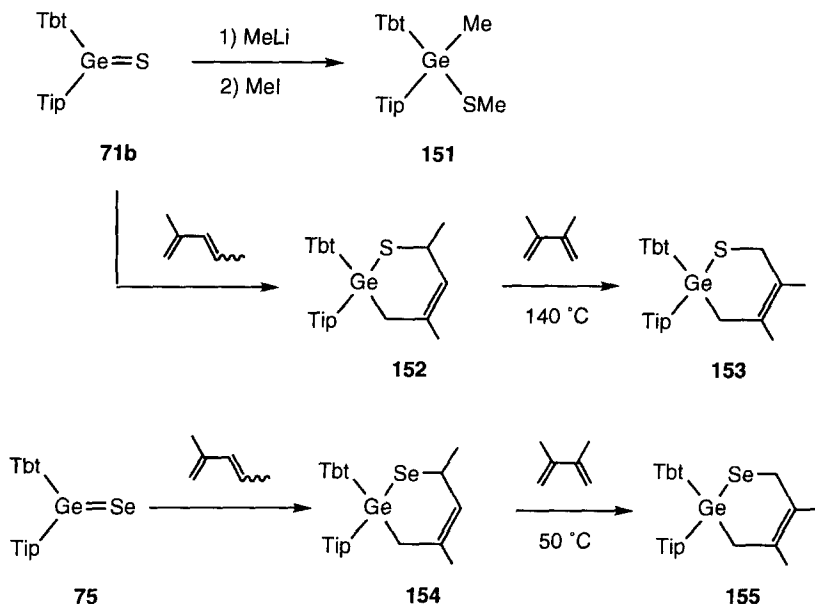
SCHEME 39.

of this reversibility is that there is very little difference in the σ and π bond energies of $\text{C}=\text{O}$ bond (see Table I). In contrast, an addition reaction involving a heavy ketone is highly exothermic and hence essentially irreversible because of its much smaller π bond energy than the corresponding σ bond energy.

All heavy ketones kinetically stabilized by the Tbt group react with water and methanol almost instantaneously to give tetracoordinate adducts (Scheme 39). They also undergo cycloadditions with unsaturated systems such as phenyl isothiocyanate, mesitronitrile oxide, and 2,3-dimethyl-1,3-butadiene to give the corresponding [2+2], [2+3], and [2+4] cycloadducts, respectively (Scheme 39). The former two reactions proceed at room temperature, while the reaction with the diene takes place at higher temperature, with the lighter homologues requiring more severe conditions.

Reaction of **71b** with methyllithium followed by alkylation with methyl iodide gives a germophilic product **151**. The [2+4] cycloaddition of **71b** with 2-methyl-1,3-pentadiene affords **152** regioselectively. When a hexane solution of **152** is heated at 140°C in a sealed tube in the presence of excess 2,3-dimethyl-1,3-butadiene, a dimethylbutadiene adduct **153** is obtained in a high yield, indicating that the Diels–Alder reaction of germanethione **71b** with a diene is reversible, and hence such a diene adduct as **152** or **153** can be a good precursor of germanethione **71b** (Scheme 40).⁴⁷ Similar reactivity was observed for germaneselon **75**, and the retrocycloaddition of **154** takes place at much lower temperature (50°C) than that for **152**, suggesting the weaker $\text{C}-\text{Se}$ bond as compared to $\text{C}-\text{S}$ bond (Scheme 40).

In contrast to the considerable thermal stability of the isolated heavy ketones of silicon, germanium, and tin, a plumbanethione behaves differently. When stable



SCHEME 40.

plumbylene Tbt_2Pb **147**⁷² was sulfurized by 1 molar equiv. of elemental sulfur at 50°C , the heteroleptic plumbylene TbtPbSTbt (**141**) was obtained (Scheme 37)¹⁶ instead of plumbanethione $\text{Tbt}_2\text{Pb}=\text{S}$ **148** which is an expected product in view of the reactivity observed for divalent species of silicon, germanium, and tin (*vide supra*). The formation of **141** is most reasonably explained in terms of 1,2-migration of the Tbt group in the intermediate plumbanethione **148**, and this observation is supporting evidence for the 1,2-aryl migration in plumbanethione **133** proposed in the reaction shown in Scheme 36. This unique 1,2-aryl migration in a plumbanethione is in keeping with a theoretical calculation which reveals that plumbylene $\text{HPb}(\text{SH})$ is about 39 kcal mol^{-1} more stable than plumbanethione $\text{H}_2\text{Pb}=\text{S}$.¹⁶

VI

CONCLUDING REMARKS

Remarkable progress in the chemistry of main group elements enabled us to synthesize and isolate heavy ketones which are capable of existence as stable species if their highly reactive $\text{M}=\text{X}$ bond is adequately protected toward dimerization

by kinetic or thermodynamic stabilization. As can be seen in this article, kinetic stabilization is much superior to thermodynamic stabilization to elucidate the intrinsic nature of the chemical bonding between the heavier Group 14 and Group 16 elements.

Although the structural features of their $M=X$ bonds ($M = \text{Si, Ge, Sn}$; $X =$ chalcogen atom) such as trigonal planar geometry and bond shortening compared to the corresponding $M-X$ single bonds are similar to those of ketones, heavy ketones have much higher reactivity because of their weak π bonds. The systematic study on heavy ketones containing silicon through lead using steric protection with the Tbt group has revealed that unlike lighter congeners, a heavy ketone containing lead, $R_2Pb=X$, is unique in that it is less stable than its isomeric plumbylene $RPb-XR$.

In contrast to the successful isolation and characterization of heavy ketones containing heavier chalcogen atoms such as sulfur, selenium, and tellurium, those containing oxygen are still elusive species and neither their isolation nor spectroscopic detection have been achieved, probably due to their extremely high reactivity caused by their highly polarized structure. Only the stability of germanone $Tbt(Tip)Ge=O$ in solution at room temperature has been indirectly demonstrated by the trapping experiments.^{24, 25} The most fascinating and challenging target molecules in this area should be the stable oxygen-containing heavy ketones.

REFERENCES

- (1) Pitzer, K. S. *J. Am. Chem. Soc.* **1948**, *70*, 2140.
- (2) Gier, T. E. *J. Am. Chem. Soc.* **1961**, *83*, 1769.
- (3) Klebach, T. C.; Lourens, R.; Bickelhaupt, F. J. *Am. Chem. Soc.* **1978**, *100*, 4886.
- (4) Yoshifuji, M.; Shima, I.; Inamoto, N.; Hirotsu, K.; Higuchi, T. *J. Am. Chem. Soc.* **1981**, *103*, 4587.
- (5) Brook, A. G.; Abdesaken, F.; Gutekunst, B.; Gutekunst, G.; Kallury, R. K. *J. Chem. Soc., Chem. Commun.* **1981**, 191.
- (6) West, R.; Fink, M. J.; Michl, J. *Science (Washington DC)*. **1981**, *214*, 1343.
- (7) For reviews, see (a) Duus, F. In *Comprehensive Organic Chemistry*; Barton, D. H. R.; Ollis, W. D., Eds.; Pergamon: Oxford, 1979; Vol. 3, p. 373; (b) Usov, V. A.; Timokhina, L. V.; Voronkov, M. G. *Sulfur Rep.* **1992**, *12*, 95, (c) Voss, J. In *Houben-Weyl Methoden der Organischen Chemie*; Klamann, D., Ed.; George Thieme Verlag: Stuttgart, 1985, Band 11, p. 188; (d) Okazaki, R. *Yuki Gosei Kagaku Kyokai Shi* **1988**, *46*, 1149; (e) McGregor, W. M.; Sherrington, D. C. *Chem. Soc. Rev.* **1993**, 199; (f) Whittingham, W. G. In *Comprehensive Organic Functional Group Transformations*; Katritzky, A. R.; Meth-Cohn, O.; Rees, C. W.; Eds.; Pergamon: Oxford, 1995, Vol. 3, p. 329.
- (8) For reviews, see (a) Magnas, P. D. In *Comprehensive Organic Chemistry*; Barton, D. H. R.; Ollis, W. D.; Eds.; Pergamon: Oxford, 1979, Vol. 3, p. 491; (b) Paulmier, C. In *Selenium Reagents and Intermediates in Organic Synthesis*; Pergamon: Oxford, 1986, p. 58; (c) Guziec, F. S., Jr., In *The Chemistry of Organic Selenium and Tellurium Compounds*; Patai, S. Ed.; Wiley: New York, 1987, Vol. 2, p. 215; (d) Guziec, F.S., Jr.; Guziec, L. J. In *Comprehensive Organic Functional*

- Group Transformations*; Katritzky, A.; Meth-Cohn, O.; Rees, C. W.; Eds.; Pergamon: Oxford, 1995, Vol. 3, p. 381.
- (9) For reviews, see (a) Okazaki, R. In *Organosulfur Chemistry*; Page, P. D. Ed.; Academic Press: London, 1995, Chapter 5, p. 225; (b) Tokitoh, N.; Okazaki, R. *Polish J. Chem.* **1998**, 72, 971.
- (10) Minoura, M.; Kawashima, T.; Okazaki, R. *J. Am. Chem. Soc.* **1993**, 115, 7019.
- (11) (a) For silicon-chalcogen double bonds, see Tokitoh, N.; Okazaki, R. In *The Chemistry of Organosilicon Compounds Vol. 2*; Patai S.; Rappoport, Z., Eds.; Wiley: New York, 1998, Chapt. 17, 1063; (b) For germanium-chalcogen double bonds, see Tokitoh, N.; Matsumoto, T.; Okazaki, R. *Bull. Chem. Soc. Jpn.* **1999**, 72, 1665; (c) For a review on stable doubly bonded compounds of germanium and tin, see Baines, K.M.; Stubbs, W.G. In *Advances in Organometallic Chemistry*; Stone, F.G.; West, R., Eds.; Academic Press: San Diego, **1996**, Vol. 39, 275; (d) Raabe, G.; Michl, J. In *The Chemistry of Organosilicon Compounds Part 2*; Patai, S.; Rappoport, Z., Eds.; Wiley: New York, **1989**, 1015; (e) West, R. *Angew. Chem., Int. Ed. Engl.* **1987**, 26, 1201; (f) Gusel'nikov, L.E.; Nametkin, N.S., *Chem. Rev.* **1979**, 79, 529.
- (12) Kudo, T.; Nagase, S. *Organometallics* **1986**, 5, 1207.
- (13) Kudo, T.; Nagase, S. *J. Phys. Chem.* **1984**, 88, 2833.
- (14) (a) Suzuki, H.; Tokitoh, N.; Okazaki, R.; Nagase, S.; Goto, M. *J. Am. Chem. Soc.* **1998**, 120, 11096; (b) Okazaki, R.; Tokitoh, N. *Acc. Chem. Res.* **2000**, 33, 625.
- (15) Kapp, J.; Remko, M.; Schleyer, P. v. R. *J. Am. Chem. Soc.* **1996**, 118, 5745.
- (16) Kano, N.; Tokitoh, N.; Okazaki, R. *Synthetic Org. Chem. Jpn. (Yuki Gosei Kagaku Kyokai Shi)* **1998**, 56, 919.
- (17) Arya, P.; Boyer, J.; Carré, F.; Corriu, R.; Lanneau, G.; Lapasset, J.; Perrot, M.; Priou, C. *Angew. Chem. Int. Ed. Engl.* **1989**, 28, 1016.
- (18) (a) Belzner, J.; Ihmels, H. *Tetrahedron Lett.* **1993**, 34, 6541; (b) Belzner, J.; Ihmels, H.; Kneisel, B. O.; Gould, R. O.; Herbst-Irmer, R. *Organometallics* **1995**, 14, 305; (c) Corriu, R.; Lanneau, G.; Priou, C.; Soulaïrol, F.; Auner, N.; Probst, R.; Conlin, R.; Tan, C. *J. Organomet. Chem.* **1994**, 466, 55.
- (19) Driess, M.; Pritzkow, H. *Angew. Chem., Int. Ed. Engl.* **1992**, 31, 316.
- (20) Driess, M.; Pritzkow, H.; Rell, S.; Winkler, U. *Organometallics* **1996**, 15, 1845.
- (21) Takeda, N.; Tokitoh, N.; Okazaki, R. *Chem. Lett.* **2000**, 244.
- (22) (a) Suzuki, H.; Tokitoh, N.; Okazaki, R. *J. Am. Chem. Soc.* **1994**, 116, 11572; (b) Suzuki, H.; Tokitoh, N.; Okazaki, R. *Bull. Chem. Soc. Jpn.* **1995**, 68, 2471.
- (23) Takeda, N.; Suzuki, H.; Tokitoh, N.; Okazaki, R.; Nagase, S. *J. Am. Chem. Soc.* **1997**, 119, 1456.
- (24) Matsumoto, T.; Tokitoh, N.; Okazaki, R. *Chem. Commun.* **1997**, 1553.
- (25) Tokitoh, N.; Matsumoto, T.; Okazaki, R. *Chem. Lett.* **1995**, 1087.
- (26) Suzuki, H.; Tokitoh, N.; Okazaki, R. unpublished results.
- (27) (a) Eaborn, C.; Stanczyk, W. A. *J. Chem. Soc., Perkin Trans. 2* **1984**, 2099; (b) Davies, A. G.; Neville, A. G. *J. Organomet. Chem.* **1992**, 436, 255; (c) Goikhman, R.; Aizenberg, M.; Shimon, L. J. W.; Milstein, D. *J. Am. Chem. Soc.* **1996**, 118, 10894.
- (28) Corriu, R. J. P.; Lanneau, G. F.; Mehta, V. D. *J. Organomet. Chem.* **1991**, 419, 9.
- (29) Belzner, J.; Ihmels, H.; Kneisel, B. O.; Herbst-Irmer, R. *Chem. Ber.* **1996**, 129, 125.
- (30) Belzner, J.; Schär, D.; Kneisel, B. O.; Herbst-Irmer, R. *Organometallics* **1994**, 14, 1840.
- (31) (a) Suzuki, H.; Tokitoh, N.; Nagase, S.; Okazaki, R. *J. Am. Chem. Soc.* **1994**, 116, 11578; (b) Suzuki, H.; Tokitoh, N.; Okazaki, R.; Nagase, S.; Goto, M. *J. Am. Chem. Soc.* **1998**, 120, 11096.
- (32) Tokitoh, N.; Suzuki, H.; Matsumoto, T.; Matsuhashi, Y.; Okazaki, R.; Goto, M. *J. Am. Chem. Soc.* **1991**, 113, 7047.
- (33) (a) Thompson, D. P.; Boudjouk, P. *J. Chem. Soc., Chem. Commun.* **1987**, 1466; (b) Boudjouk, P.; Bahr, S. R.; Thompson, D. P. *Organometallics* **1991**, 10, 778.
- (34) Boudjouk, P.; Bahr, S. R.; Thompson, D. P. *Organometallics* **1991**, 10, 778.
- (35) Jutzi, P.; Möhrke, A.; Müller, A.; Bögge, H. *Angew. Chem., Int. Ed. Engl.* **1989**, 28, 1518.

- (36) (a) Jutzi, P.; Möhrke, A. *Angew. Chem., Int. Ed. Engl.* **1989**, 28, 762; (b) Jutzi, P.; Eikenberg, D.; Möhrke, A.; Neumann, B.; Stämmler, H.-G. *Organometallics* **1996**, 15, 753.
- (37) (a) Tokitoh, N.; Sadahiro, T.; Takeda, N.; Okazaki, R. *The 12th International Symposium on Organosilicon Chemistry*, 4A23, Sendai, Japan, 1999; (b) Hatano, K.; Sadahiro, T.; Tokitoh, N.; Okazaki, R. *The 12th International Symposium on Organosilicon Chemistry*, P-85 Sendai, Japan, 1999.
- (38) Tokitoh, N.; Hatano, K.; Sadahiro, T.; Okazaki, R. *Chem. Lett.* **1999**, 931.
- (39) Hatano, K.; Tokitoh, N.; Takagi, N.; Nagase, S. *J. Am. Chem. Soc.* **2000**, 122, 4829.
- (40) (a) Veith, M.; Becker, S.; Huch, V. *Angew. Chem., Int. Ed. Engl.* **1989**, 28, 1237; (b) Veith, M.; Detempe, A.; Huch, V. *Chem. Ber.* **1991**, 124, 1135; (c) Veith, M.; Detempe, A. *Phosphorus, Sulfur, Silicon* **1992**, 65, 17.
- (41) (a) Trinquier, G.; Barthelat, J. C.; Satgé, J. *J. Am. Chem. Soc.* **1982**, 104, 5931; (b) Trinquier, G.; Pelissier, M.; Saint-Roch, B.; Lavayssiere, H. *J. Organomet. Chem.* **1981**, 214, 169.
- (42) Kuchta, M. C.; Parkin, G. *J. Chem. Soc., Chem. Commun.* **1994**, 1351.
- (43) Tokitoh, N.; Okazaki, R. *Main Group Chemistry News* **1995**, 3, 4.
- (44) Matsumoto, T.; Tokitoh, N.; Okazaki, R.; Goto, M. *Organometallics* **1995**, 14, 1008.
- (45) Tokitoh, N.; Matsumoto, T.; Ichida, H.; Okazaki, R. *Tetrahedron Lett.* **1991**, 32, 6877.
- (46) Tokitoh, N.; Matsumoto, T.; Manmaru, K.; Okazaki, R. *J. Am. Chem. Soc.* **1993**, 115, 8855.
- (47) Matsumoto, T.; Tokitoh, N.; Okazaki, R. *J. Am. Chem. Soc.* **1999**, 121, 8811.
- (48) Tokitoh, N.; Matsumoto, T.; Okazaki, R. *Tetrahedron Lett.* **1992**, 33, 2531.
- (49) Matsumoto, T.; Tokitoh, N.; Okazaki, R. *Angew. Chem., Int. Ed. Engl.* **1994**, 33, 2316.
- (50) (a) Erker, G.; Hock, R. *Angew. Chem., Int. Ed. Engl.* **1989**, 28, 179; (b) Segi, M.; Koyama, T.; Tanaka, Y.; Nakajima, T.; Suga, S. *J. Am. Chem. Soc.* **1989**, 111, 8749; (c) Boese, R.; Haas, A.; Limberg, C. *J. Chem. Soc., Chem. Commun.* **1991**, 1378; (d) Haas, A.; Limberg, C. *Chimia* **1992**, 46, 78; (e) Barrett, A. G. M.; Barton, D. H. R.; Read, R. W. *J. Chem. Soc., Chem. Commun.* **1979**, 645; (f) Barrett, A. G. M.; Read, R. W.; Barton, D. H. R. *J. Chem. Soc., Perkin Trans. 1* **1980**, 2191; (g) Severengiz, T.; du Mont, W.-W. *J. Chem. Soc., Chem. Commun.* **1987**, 820; (h) Lerstrup, K. A.; Henriksen, L. *J. Chem. Soc., Chem. Commun.* **1979**, 1102; (i) Lappert, M. F.; Martin, T. R.; McLaughlin, G. M. *J. Chem. Soc., Chem. Commun.* **1980**, 635; (j) Segi, M.; Kojima, A.; Nakajima, T.; Suga, S. *Synlett* **1991**, 2, 105; (k) Minoura, M.; Kawashima, T.; Okazaki, R. *J. Am. Chem. Soc.* **1994**, 115, 7019.
- (51) Tokitoh, N.; Matsumoto, T.; Okazaki, R. *J. Am. Chem. Soc.* **1997**, 119, 2337.
- (52) Tokitoh, N. *Phosphorus, Sulfur, Silicon* **1998**, 136, 137, 138, 123.
- (53) Tokitoh, N.; Kishikawa, K.; Matsumoto, T.; Okazaki, R. *Chem. Lett.* **1995**, 827.
- (54) (a) Krebs, A.; Berndt, J. *Tetrahedron Lett.* **1983**, 24, 4083; (b) Egorov, M. P.; Kolesnikov, S. P.; Struchkov, Yu. T.; Antipin, M. Yu.; Sereda, S. V.; Nefedov, O. M. *J. Organomet. Chem.* **1985**, 290, C27.
- (55) Ossig, G.; Meller, A.; Brönneke, C.; Müller, O.; Schäfer, M.; Herbst-Irmer, R. *Organometallics* **1997**, 16, 2116.
- (56) Veith, M.; Rammo, A. Z. *Anorg. Z. Allg. Chem.* **1997**, 623, 861.
- (57) (a) Barrau, J.; Rima, G.; El Amraoui, T. *J. Organomet. Chem.* **1998**, 570, 163; (b) Barrau, J.; Rima, G.; El Amraoui, T. *Inorg. Chim. Acta* **1996**, 241, 9.
- (58) Foley, S. R.; Bensimon, C.; Richeson, D. S. *J. Am. Chem. Soc.* **1997**, 119, 10359.
- (59) (a) Tokitoh, N.; Saito, M.; Okazaki, R. *J. Am. Chem. Soc.* **1993**, 115, 2065; (b) Matsuhashi, Y.; Tokitoh, N.; Okazaki, R. *Organometallics* **1993**, 12, 2573; (c) Saito, M.; Tokitoh, N.; Okazaki, R. *Organometallics* **1996**, 15, 4531.
- (60) Saito, M.; Tokitoh, N.; Okazaki, R. *J. Organomet. Chem.* **1995**, 499, 43.
- (61) Saito, M.; Ph. D. Thesis, University of Tokyo, **1997**.
- (62) Saito, M.; Tokitoh, N.; Okazaki, R. *J. Am. Chem. Soc.* **1997**, 119, 11124.
- (63) Kano, N.; Tokitoh, N.; Okazaki, R. *Chem. Lett.* **1997**, 277.

- (64) (a) Kano, N.; Tokitoh, N.; Okazaki, R. *Organometallics* **1997**, *16*, 4237; (b) Kano, N.; Tokitoh, N.; Okazaki, R. *Phosphorus, Sulfur, Silicon* **1997**, *124–125*, 517.
- (65) (a) Hitchcock, P. B.; Lappert, M. F.; Samways, B. J.; Weinburg, E. L. *J. Chem. Soc., Chem. Commun.* **1983**, 1492; (b) Goel, S. C.; Chiang, M. Y.; Buhro, W. E. *Inorg. Chem.* **1990**, *29*, 4640; (c) Eaborn, C.; Izod, K.; Hitchcock, P. B.; Sözerli, S. E.; Smith, J. D. *J. Chem. Soc., Chem. Commun.* **1995**, 1829.
- (66) (a) Sheldrick, W. S. In *The Chemistry of Organic Silicon Compound*; Patai, S.; Rappoport, Z.; Eds.; Wiley: New York, Part 1, **1989**, pp. 227–304; (b) see also, Sibao, R. K.; Keder, N. L.; Eckert, H. *Inorg. Chem.* **1990**, *29*, 4163.
- (67) For a recent review, see Escudié, J.; Ranaivonjatovo, H. *Adv. Organomet. Chem.* **1999**, *44*, 113.
- (68) Kuchta, M. C.; Parkin, G. *J. Am. Chem. Soc.* **1994**, *116*, 8372.
- (69) (a) Tokitoh, N.; Takeda, N.; Okazaki, R. *J. Am. Chem. Soc.* **1994**, *116*, 7907; (b) Takeda, N.; Tokitoh, N.; Okazaki, R. *Chem. Eur. J.* **1997**, *3*, 62.
- (70) Kudo, T.; Nagase, S. *Chem. Phys. Lett.* **1986**, *128*, 507.
- (71) Khabashesku, V. N.; Boganov, S. E.; Zuev, P. S.; Nefedov, O. M. *J. Organomet. Chem.* **1991**, *402*, 161.
- (72) Kano, N.; Shibata, K.; Tokitoh, N.; Okazaki, R. *Organometallics* **1999**, *18*, 2999.
- (73) Takeda, N.; Tokitoh, N.; Okazaki, R. *Angew. Chem., Int. Ed. Engl.* **1996**, *35*, 660.

The M–C Bond Functionalities Bonded to an Oxo-Surface Modeled by Calix[4]arenes

CARLO FLORIANI* and RITA FLORIANI-MORO

*Institut de Chimie Minérale et Analytique
BCH 3307 Université de Lausanne
CH-1015 Lausanne, Switzerland*

I. Introductory Remarks: Scope and Limits	167
II. Introduction	168
III. Metalation of Calix[4]arenes and <i>O</i> -Alkylated Calix[4]arenes Using Transition Metals	170
IV. Low-Valent Metalla-Calix[4]arenes	172
A. Metal–Metal Bonded Dimers	172
B. Alkene, Diene, and Alkyne Complexes	178
V. The Organometallic Functionalization of the Metalla-Calix[4]arenes	186
A. The Synthesis and the Chemistry of M–C σ Bonds	186
B. The Synthesis and the Chemistry of Metal-Alkylidene and -Alkylidyne Functionalities	204
C. Outlook	227
References	227

I

INTRODUCTORY REMARKS: SCOPE AND LIMITS

The general purpose of this chapter is to show the potential of calix[4]arenes^{1a,b} as ancillary ligands in coordination and organometallic chemistry of transition metals, in the areas of both metal reactivity and catalysis. Therefore, the main focus will be on the metalation of calix[4]arenes and their *O*-alkylated derivatives, only when it produces compounds potentially useful for exploring the chemical reactivity of the metal centers. A particular emphasis will be placed on modeling studies of the heterogeneous metal-oxo-surfaces using metalla-calix[4]arenes.

The scopes outlined above limit the purpose of this chapter, which will not cover: (1) the transition metal complexation by protonated or functionalized forms of calix[4]arenes; (2) the metalation of calix[4]arenes using non-transition metals; and (3) chemical curiosities derived from the metalation of calix[4]arenes (some recent reviews cover these areas very well).¹ In addition, the authors have been particularly careful to report only those compounds which have a well-established synthesis and a full spectroscopic and structural characterization.

*Tel. +41 21 692 39 02; Fax: +41 21 692 39 05; E-mail: carlo.floriani@icma.unil.ch.

II

INTRODUCTION

Modeling studies of oxo-surfaces² that bind metals appropriate to drive catalytic or stoichiometric reactions date back a very long time.³ An interesting approach foresees the use of a preorganized set of oxygen donor atoms in a quasiplanar arrangement for binding metal ions. In such a context, the calix[4]arene skeleton¹ comes into play,⁴ with a number of unique geometric and electronic peculiarities. Calix[4]arenes have only recently been exploited for binding metals,^{1,4,5} and even more recently as ancillary ligands for supporting reactive metals in organometallic chemistry.¹ In such a role, calix[4]arenes have quite a number of unique attributes. Let us first look at their geometric properties. In the metalladerivatives, calix[4]arenes almost exclusively assume the cone conformation, thus keeping the oxygen set quasiplanar. They usually act as tetraanionic ligands, though the charge of the O₄ set can be tuned by a different degree of alkylation (Chart 1).

The oxygen alkylation enables control of the functionalization degree of the metal and at the same time, using appropriate R substituents, also the steric protection of the metal reactive site. The symmetry of the cone conformation is largely determined by the coordination number of the metal attached to it, and thus, indirectly, by the symmetry of the incoming substrate to the metal. Such geometric features are revealed by the methylene bridging and the Bu^t groups

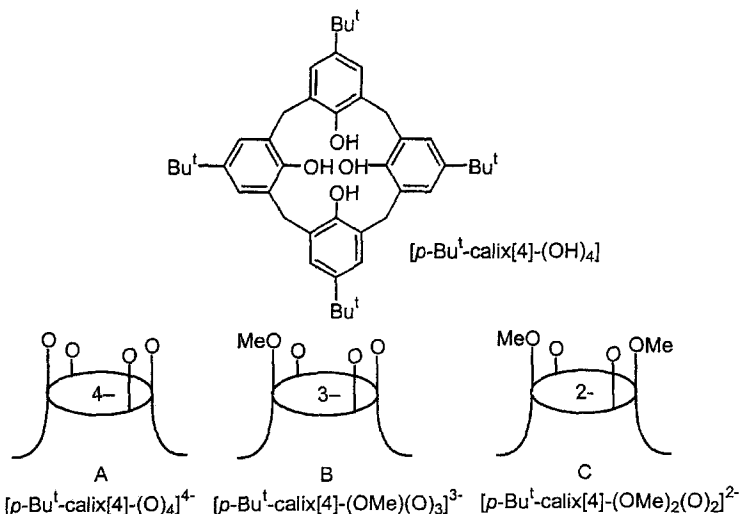


CHART 1. *p*-Bu^t-calix[4]arene and derived anions.

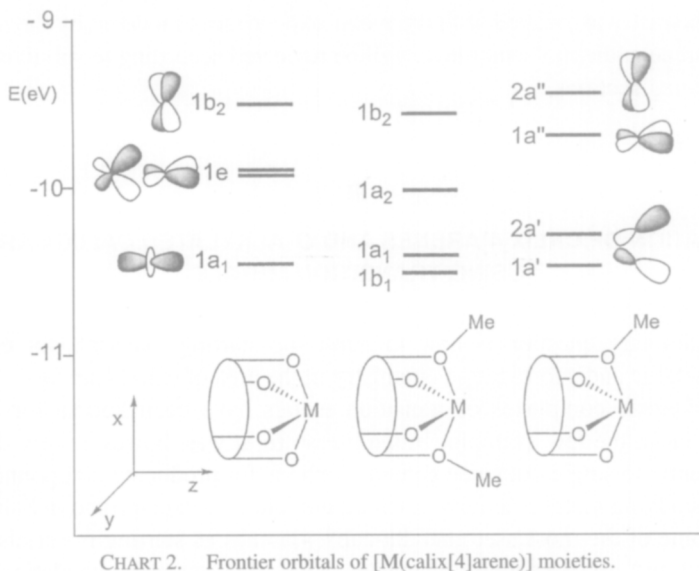


CHART 2. Frontier orbitals of $[M(\text{calix}[4]\text{arene})]$ moieties.

functioning as spectroscopic probes in a ^1H NMR spectrum.⁴ What about the consequences on the frontier orbitals available at the metal due to its binding to the calix[4]arene skeleton? Although in metallacalix[4]arenes the metal anchoring groups are methylene-bridged phenoxo anions, the role of calix[4]arene is different from that of the same number of monomeric phenoxo units.⁴

The four oxygen donor atoms preorganized in a quasiplanar geometry have a major effect in determining the set and relative energy of the frontier orbitals available at the metal for the substrate activation (see Chart 2).

In the calix[4]arene-based fragments the four lowest-lying orbitals, which can accommodate up to eight electrons, lie on two orthogonal planes, thus favoring a facial over a meridional structure when such a fragment is bound to three additional ligands. The facial compared to the meridional arrangement of the three low-lying frontier orbitals favors, among other things, the formation of a metal substrate multiple bond,⁴ that is, stabilization of alkylidenes and alkylidyne, and affects the migration-insertion reactions.⁴

The metal-oxo molecular models outlined above have a quite remarkable potential for studying the metal activity in a quite unusual environment. Some of the possibilities could be: (1) the generation and the chemistry of $\text{M}-\text{C}$, $\text{M}=\text{C}$, $\text{M}\equiv\text{C}$ functionalities; (2) the interaction with alkenes, alkynes, hydrocarbons, and hydrogen; (3) the activation of small molecules like N_2 ⁶ and CO ; (4) the support of metal-metal bonded functionalities; and (5) the generation of highly reactive low-valent metals.

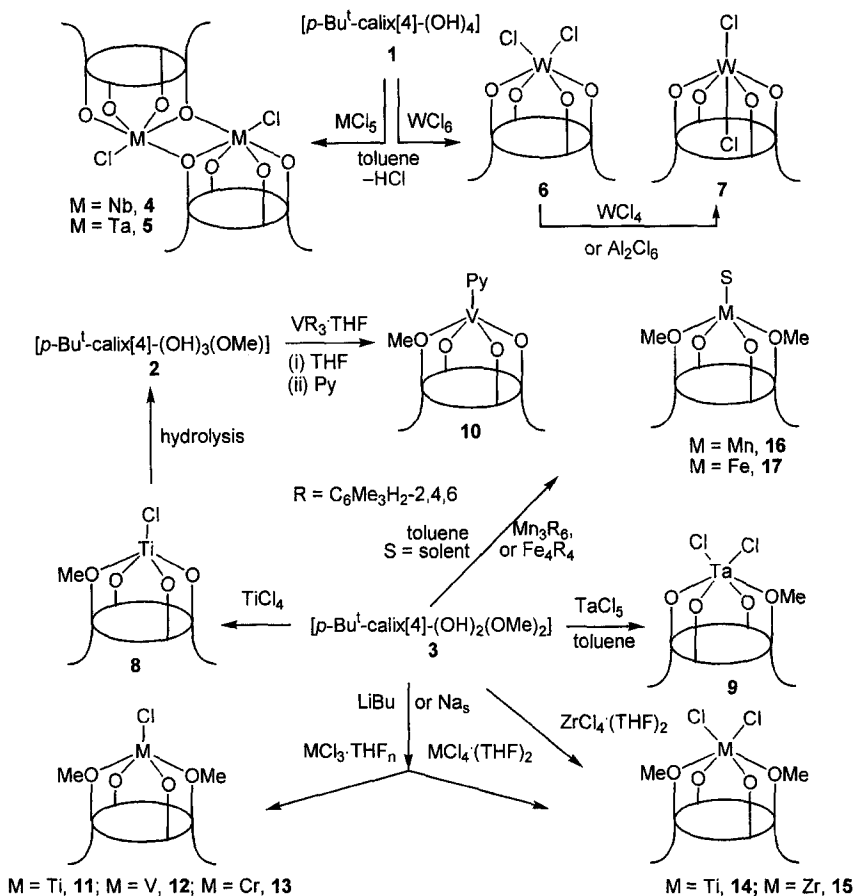
The chemistry associated with the metal-oxo-surfaces modeled by the metalla-calix[4]arene at the molecular level will be reviewed according to subdivisions in the following sections.

III

METALATION OF CALIX[4]ARENES AND *O*-ALKYLATED CALIX[4]ARENES USING TRANSITION METALS

A preliminary question is how to make the starting materials for entering organometallic and coordination chemistry in the area of calix[4]arenes.

Calix[4]arene complexes of transition metals have been known for several years.^{1,5} From the few examples in the literature, it was, however, very difficult until recently to single out some general methods for producing compounds suitable for studying metal reactivity. Each methodology is exemplified in Scheme 1, listing some of the most used metalla-calix[4]arenes as starting materials in coordination and organometallic chemistry. The more versatile metalation methods of calix[4]arene, **1**, mono-*O*-alkylated calix[4]arene, **2**, and bis-*O*-alkylated calix[4]arene, **3** (see A, B, and C in Chart 1)^{1a,b} have been summarized in Scheme 1. The reaction of **1** with metal halides can be pursued in the case of the highest oxidation states of metals like Nb,^{7,8} Ta,^{7,9} and W^{10,11} (see complexes **4–6**). In the latter case, a small excess of WCl₆ or other Lewis acids produces the isomerization to the *trans* derivative **7**.¹¹ When such a method was employed in the metalation of **3** or analogous di-*O*-alkylated calix[4]arenes, the ligand undergoes, except in the case of ZrCl₄ · THF₂, the dealkylation of one of the oxygens, thus producing the corresponding mono-*O*-alkylated calix[4]arene complex. This is, in fact, the best method for the synthesis of **8**¹² and **9**.⁹ In addition, the best synthesis for the mono-*O*-alkylated calix[4]arene, [*p*-Bu^t-calix[4]-(OH)₃(OMe)], goes through the facile hydrolysis of **8**, and the synthesis of **2** can be carried out as a "one pot" reaction.¹² The direct metalation of **1**, **2**, and **3** can be achieved using, when available, homoleptic alkyl-,^{5a,b} aryl-,^{13,14} amido-^{5c} derivatives of transition metals, as exemplified in the synthesis of **10**.¹⁴ Owing to the difficult large-scale synthesis of **2**, it is usually preferable to use the acid-base or oxidative-induced dealkylation of the di-*O*-alkylated derivatives. These latter are obtained as reported in Scheme 1, via a preliminary deprotonation of **3** using LiBu, Na metal, or sodium hydride, followed by the reaction with the corresponding metal halide (see the synthesis of **11**,¹² **12**,¹⁵ **13**,¹⁶ **14**,¹² and **15**¹⁷ in Scheme 1). The alternative synthesis of the bis-*O*-alkylated metalla-calix[4]arene can take advantage of the existing corresponding homoleptic metal(II)-alkyl or -aryl derivatives, as in the case of iron(II)¹³ and manganese(II)¹⁸ complexes. For such metals, the metathesis reaction from the corresponding metal halides is much more difficult. There is a major



SCHEME 1.

difference between the synthetic methods reported above, namely the formation or not of lithium or sodium halides. In many cases, it is quite difficult to free the final complex from these salts, due to the halide binding to the transition metal or the alkali cation being hosted in the calix[4]arene cavity. This latter event depends on how the transition metal shapes the cavity of the calix[4]arene ligand (see below).

At this stage it could be useful to make a comment on the structural features of complexes 4–17. The coordination number of the metal affects strongly the shape of the calix[4]arene fragment. In the case of five-coordinate and, eventually, four-coordinate metals, the calix[4]arene moiety displays a cone, which changes to an elliptical conformation in the case of a six-coordinate metal.^{4,10} Such conformation changes, which appear in the solid state, are also detectable in solution, as in the

case of diamagnetic metals, using ^1H NMR spectroscopy. The resonances of the Bu^t substituents and/or the bridging methylenes probe the two-, four-, and lower symmetries of the calix[4]arene moiety. The synthetic methods mentioned in this section address those metalla-calix[4]arenes which are appropriate for studying the metal reactivity.

It is worth mentioning that the purpose of this chapter is not to provide an exhaustive list of all the metallated calix[4]arenes, which is covered in previous reviews.¹

IV

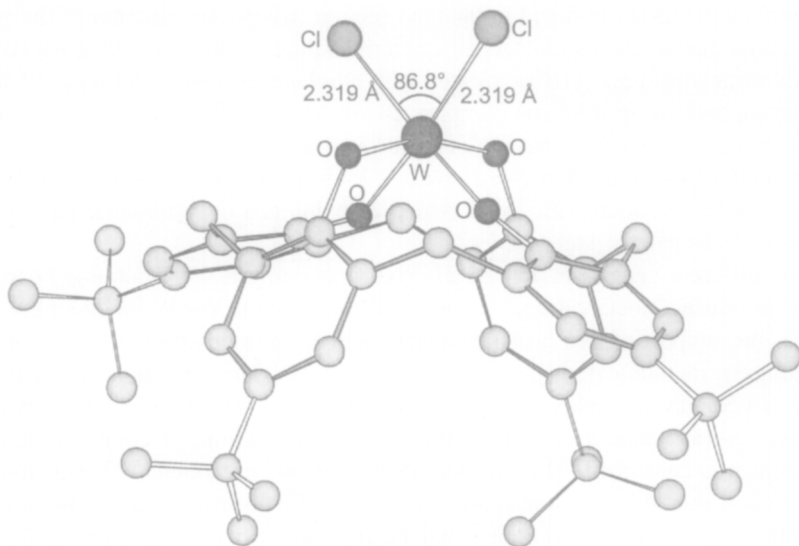
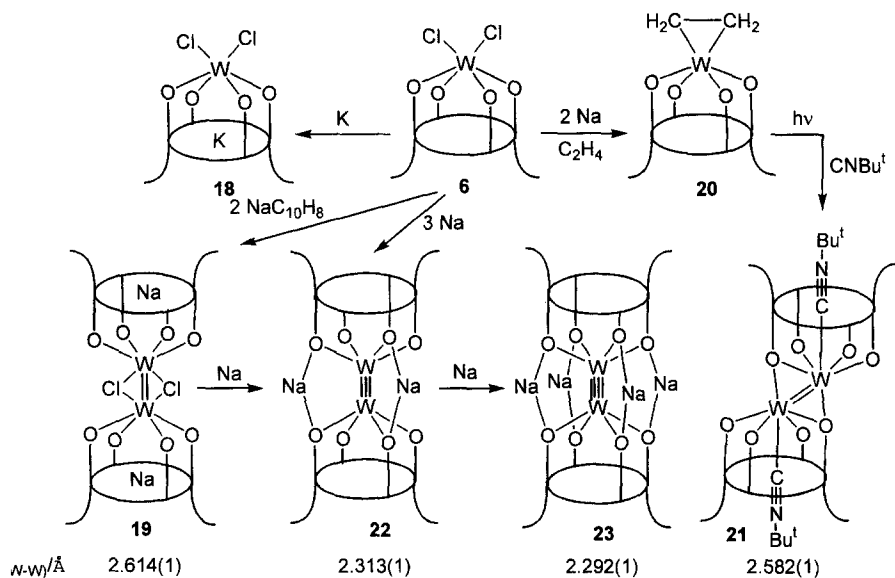
LOW-VALENT METALLA-CALIX[4]ARENES

A. Metal–Metal Bonded Dimers

A set of oxygen donor atoms, providing both σ and π donation to a metal center, is not appropriate to stabilize any low oxidation state of a metal.¹⁹ This is, however, a synthetic advantage since very reactive, unstable, low-valent metalla-calix[4]arenes can be generated *in situ* and intercepted by an appropriate substrate. In the absence of a suitable substrate, the reactive fragment, however, can collapse to form metal–metal bonded dimers. The formation of metal–metal bonds has been, however, so far observed in the case of Group V and VI metals only. The most complete sequence so far reported has been for tungsten, molybdenum, and niobium.

In the case of tungsten,^{11,20} complex **6**, whose structure is displayed in Fig. 1, has been used as starting material. In the absence of any intercepting substrates like olefins, acetylenes, etc. (see the next section), it undergoes controlled reduction (Scheme 2) leading to a number of structurally interesting compounds. When the reduction of **6** was carried out in a K/W 1:1 molar ratio, no salt separation was observed, and the paramagnetic tungsten(V) derivative **18** was obtained. The most interesting structural feature of **18**, overall quite similar to the parent compound **6**, is the unusual complexation inside the calix[4]arene cavity of K^+ , whose solvation is partially provided by η^6 -bonded opposite phenyl rings. A similar solvation mode of K^+ was structurally identified in tantalum-alkali cation calix[4]arene complexes.²¹

Increasing the reducing agent/W ratio and using Na-naphthalenide led to the isolation of the two-electron-reduced, diamagnetic compound **19**. The C_{2v} symmetry of the ^1H NMR spectrum and the X-ray analysis are in agreement with the centrosymmetric structure sketched in Scheme 2 for **19** [$\text{W} = \text{W}$, 2.614(1) Å]. The six-coordination of the metal and the inclusion of the alkali metal cation removes the planarity of the O_4 core and the cone conformation of the calix[4]arene. The sodium cation within the calix[4]arene cavity is η^3 -bonded to two opposite arene rings.

FIG. 1. Crystal structure and selected structural parameters of complex **6**.

SCHEME 2.

As will be discussed in detail in the next section, when the reduction of the parent compound **6** was conducted at low temperature ($-20\text{ }^{\circ}\text{C}$) with 2 equiv. of Na in tetrahydrofuran (THF) saturated with ethylene, complete salt removal was achieved, and the η^2 -ethylene complex **20** was isolated.²² Upon irradiation, the latter released ethylene, behaving as a source of the d^2 $[\text{W}\{p\text{-Bu}^t\text{-calix[4]}-(\text{O})_4\}]$ carbenoid, which coupled to give a new $\text{W}=\text{W}$ dimer $[\text{W}=\text{W}, 2.582(1)\text{ \AA}]$, isolated as the bis- Bu^tNC adduct **21**. In ^1H NMR, **21** exhibits a C_s -symmetric pattern of signals for the calix[4]arene moiety.

The different genesis of **19** and **21**, both containing a $\text{W}=\text{W}$ double bond in an edge-sharing biotetrahedron,²³ clearly indicates that the $\text{W}=\text{W}$ functionality requires the support of two bridging ligands, either chlorides (see **19**) or oxygens of adjacent metalla-calix[4]arene moieties (see **21**). The reduction of **6** with 3 equiv. of Na gave complex **22** (Fig. 2), showing a C_{4v} ^1H NMR spectrum. When excess Na was added to a THF solution of **22**, an additional 1 equiv. of Na per W atom was consumed. The resulting deep blue W^{II} compound, **23**, was found to be diamagnetic in the solid state. The ^1H NMR spectrum of **23** shows a C_{4v} pattern for the calix[4]arene moiety and the diamagnetism of the complex. Among the properties of the electron-rich metalla-calix[4]arene dimers mentioned above,

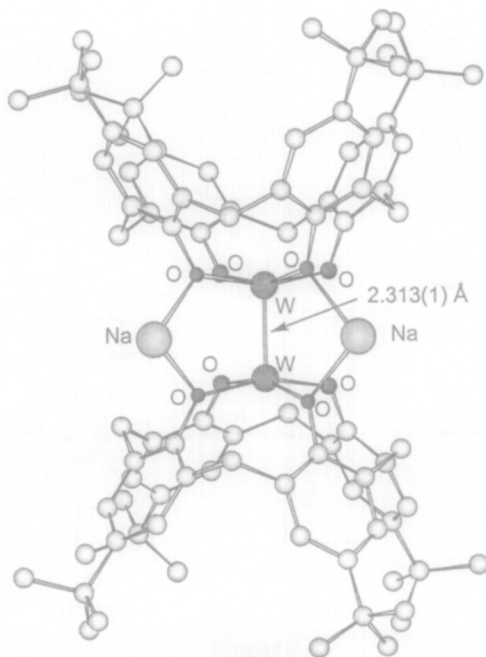


FIG. 2. Crystal structure and selected structural parameter of complex **22**.

their occurrence in the ion-pair form with alkali cations tightly bonded to the calix[4]arene fragments should be emphasized. The alkali metal cations in such structures have very different binding sites, either displaying a bridging bonding mode across the lower rims of two adjacent calix[4]arenes, as in **22** and **23**, or being complexed inside the cavity, as in **18** and **19**, where they experience η^6 or η^3 interactions with the arene rings. Both dimers **22** and **23** contain a tungsten–tungsten multiple bond [2.313(1) and 2.292(1) Å in **22** and **23**, respectively], consistent with a triple bond in **22** and eventually a quadruple bond in **23**.¹¹ The interaction between the two $[\text{W}(\text{calix})]^-$ fragments in **22** is illustrated by the molecular orbital diagram on the right of Chart 3, showing a W–W $\sigma^2\pi^4$ configuration and indicating a metal–metal triple bond character, consistent with the observed metal–metal distance of 2.313(1) Å. For the tetraanionic dimer **23**, which differs from **22** by two more electrons, a formal $\sigma^2\pi^4\delta^2$ configuration with a metal–metal quadruple bond and a shorter W–W bond length is expected, on the basis of the molecular orbital scheme in Chart 3. However, the strong π donation from the oxygen p_π to the tungsten d_{xy} orbitals leads to a significant destabilization of the latter orbitals, involved in the W–W δ bonding. The contribution to metal–metal

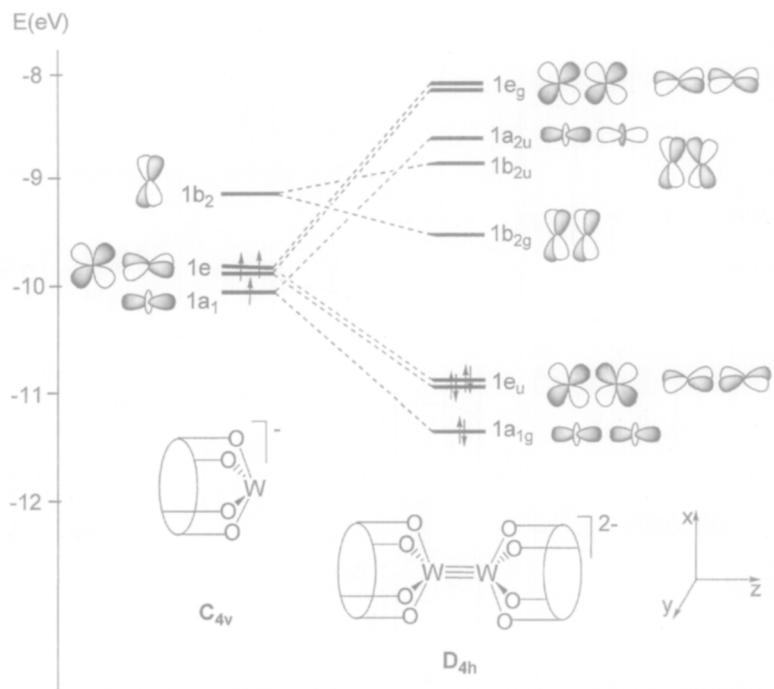
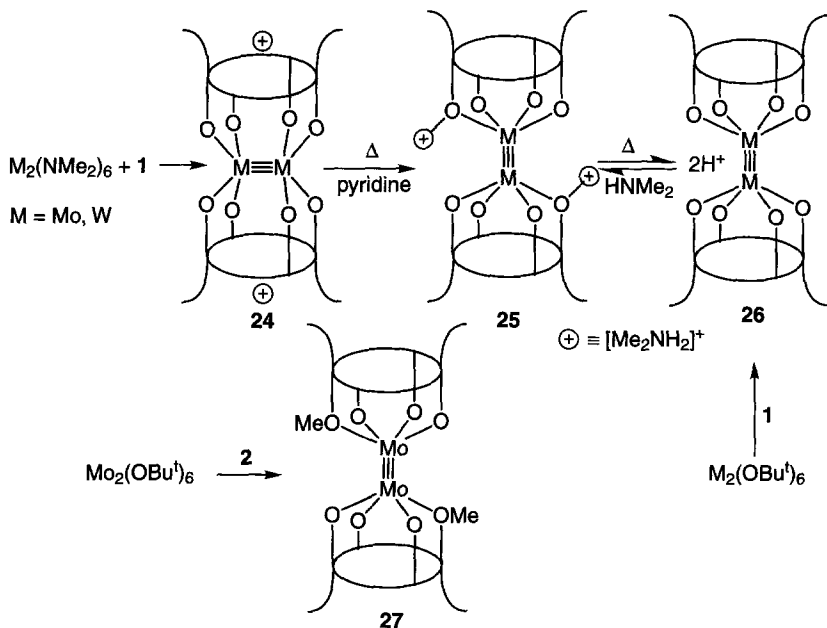


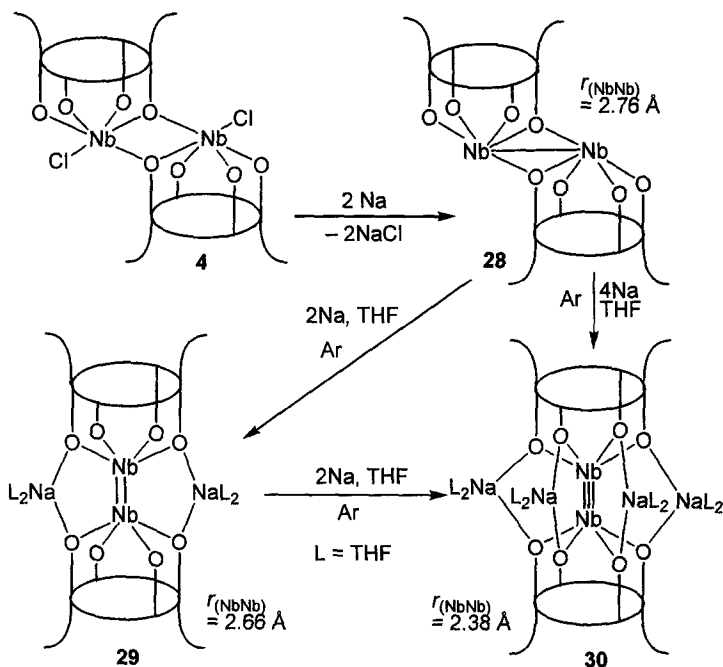
CHART 3. Molecular orbital interaction diagram between the two $[\text{W}(\text{calix})]^-$ fragments in **22**.



SCHEME 3.

molecule of **25** has a center of symmetry, and the Mo₂-calix[4]arene unit has a dumbbell shape [Mo≡Mo bond distance, 2.226(1) Å]. Each Mo atom has four Mo–O phenoxide bonds, one of which is hydrogen bonded to a H₂NMe₂ cation. Heating compound **25** under a dynamic vacuum at 100°C for 3 days forms compounds **26** [Mo≡Mo bonds, 2.226(6) Å]. Compounds **26** are formed directly in the reactions between M₂(OBU^t)₆ compounds and **1** in benzene at room temperature (1 or 2 days). The Mo≡Mo complexation has been observed also in the reaction of **2** with Mo₂(OBU^t)₆, leading to **27**. In neither series of compounds reported above has any particularly interesting reactivity of the M–M bonded functionality been disclosed so far.²⁵

A completely different scenario has been observed in the case of the stepwise reduction of [*p*-Bu^t-calix[4]-(O₄)₂Nb₂(Cl)₂] (see complex **4** in Scheme 1), as reported in Scheme 4.^{8,26,27} Such a reduction has been carried out under argon with a controlled amount at each step of sodium metal. Analogous results have been obtained using other alkali metals,⁶ though the chemistry has been mainly investigated in the case of the sodium derivatives. Complexes **28–30** are all diamagnetic. In the case of **29** [Nb=Nb, 2.659(1) Å], the ¹H NMR spectrum shows a two-fold symmetry in toluene at low temperature, while in coordinating solvents,



SCHEME 4.

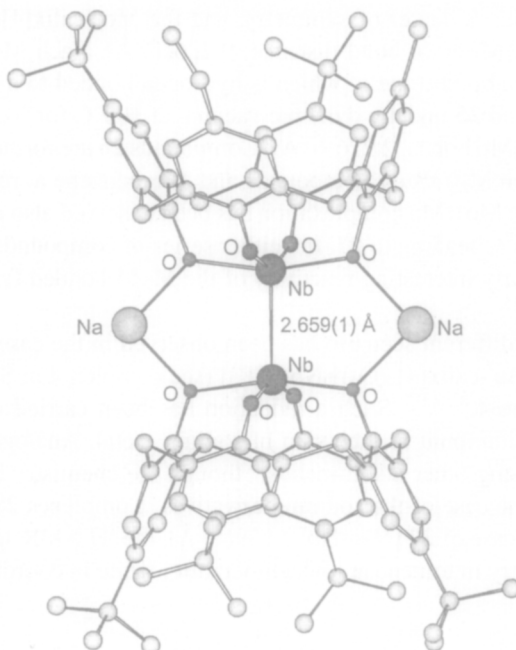


FIG. 3. Crystal structure and selected structural parameter of complex **29**.

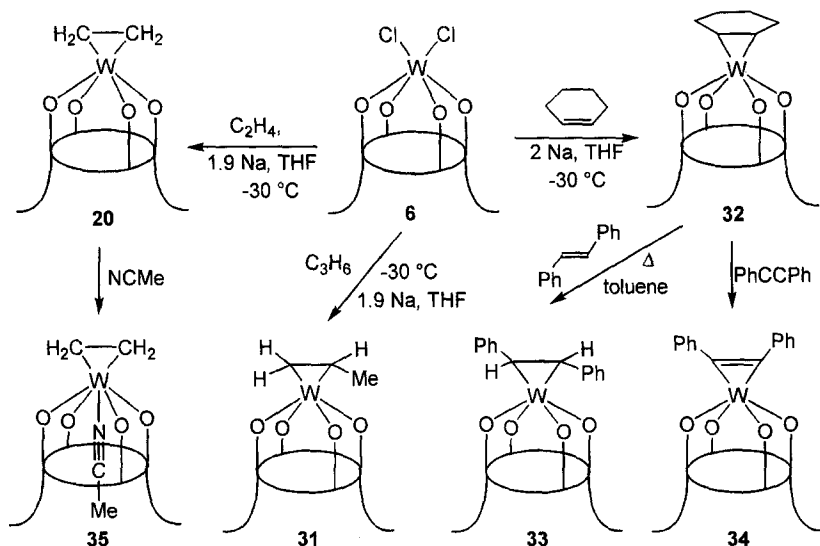
like pyridine, a four-fold symmetry is observed according to the transformation of a tight to a separated ion-pair form.⁶ The structural features of **28–30**^{6,26} are very much similar to those reported for the tungsten derivatives displayed in Scheme 2, though the reactivity is very different. In particular, complex **29** (Fig. 3) reacts with a variety of substrates, like CO, N₂ and alkenes (see below).

B. Alkene, Diene, and Alkyne Complexes

The reduction of a high-valent metalla-calix[4]arene in the presence of olefins, dienes, and acetylenes is probably the best, though not unique, synthetic access to the corresponding complexes. A few significant examples have been so far reported.

As reported in the previous section, the reduction of **6** with alkali metals in THF led to metal-metal bonded species.²² Suitable substrates can intercept the d² [*p*-Bu^t-calix[4]-(O)₄]W fragment, preventing the formation of such dimers, which represent a “thermodynamic sink.”²²

As outlined in Scheme 5, the reduction of **6** below −20°C in THF saturated with ethylene or propylene led to the corresponding η^2 -olefin complexes **20** and



SCHEME 5.

31. The η^2 -cyclohexene complex **32** was obtained by a similar procedure.^{22b,28} The latter exhibits a high thermal lability; new olefin or acetylene complexes can be readily obtained by heating solutions of **32** in toluene (50°C , 12 h) in the presence of a slight excess of the new olefin (provided the desired product is more thermally stable than **32**).^{22b,28} The η^2 -trans-stilbene complex **33** and the diphenylacetylene complex **34** were most conveniently prepared by this route, the direct synthesis being limited by competitive reaction of the free olefin or acetylene with Na.^{22b,28} Attempts to labilize the metal-olefin bond via an additional ligand to the metal was, unexpectedly, unsuccessful. On the contrary, in the case of **20** the addition of MeCN or Bu¹NC led rather to a stabilization of the metal-olefin interaction^{22b} (see complex **35**, Fig. 4). All η^2 -olefin species **20**, **31**–**33** exhibit an effective C_{4v} symmetry in solution (NMR), according to a free rotation of the olefin. The C_2H_4 ligand in **20** gives rise to a single signal both in ^1H NMR and in ^{13}C NMR (at 70 ppm). The W–C [2.124(9) Å] and C–C [1.40 Å] bond distances in complex **31** are in good agreement with the metallacyclop propane formulation.^{22b}

The interactions between the $[\text{W}(\text{calix})]$ metal fragment and the ethylene moiety has been analyzed using the extended Hückel calculations (see Chart 4).^{22b} As supported by the structural parameters of **31**, the d_{xz} is no longer available for π donation from the calixarene oxygens in the xz plane, thus explaining the strong C_{2v} distortion of the $[\{p\text{-Bu}^1\text{-calix[4]}-(\text{O})_4\}\text{W}]$ unit observed in the X-ray structure of **31**, with the two W–O bonds in the metal-ethylene plane ca. 0.2 Å longer than

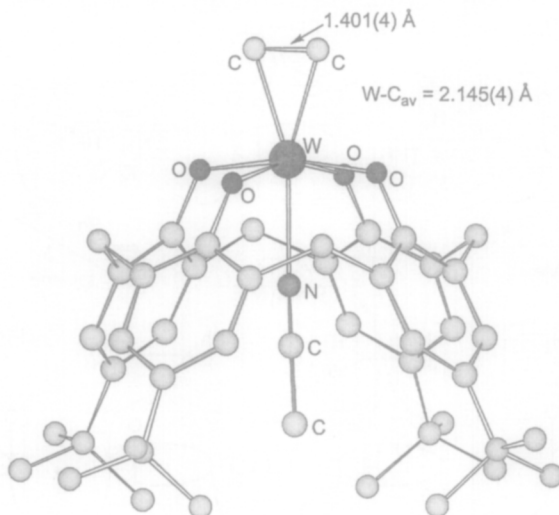


FIG. 4. Crystal structure and selected structural parameters of complex 35.

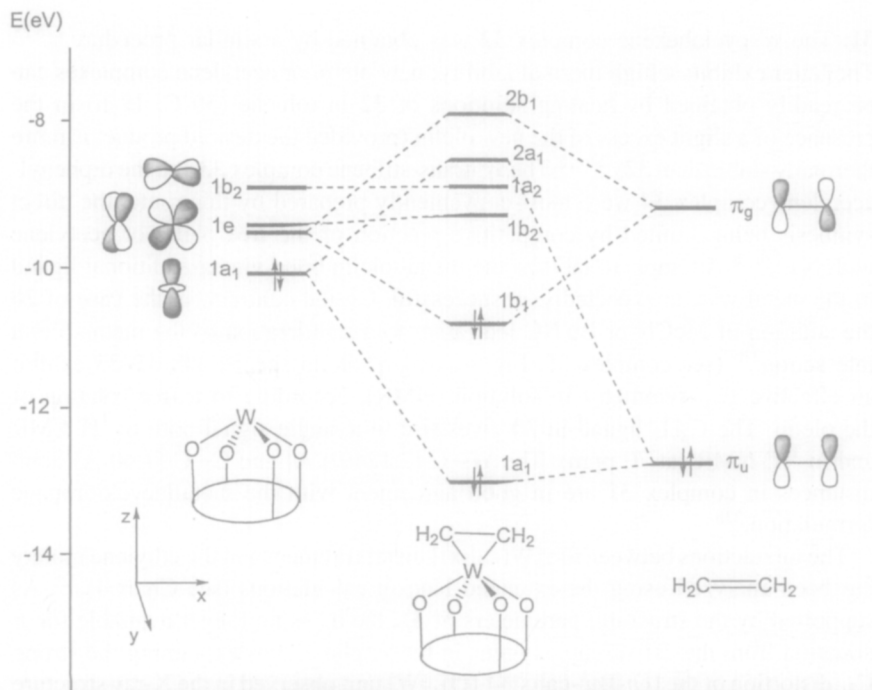
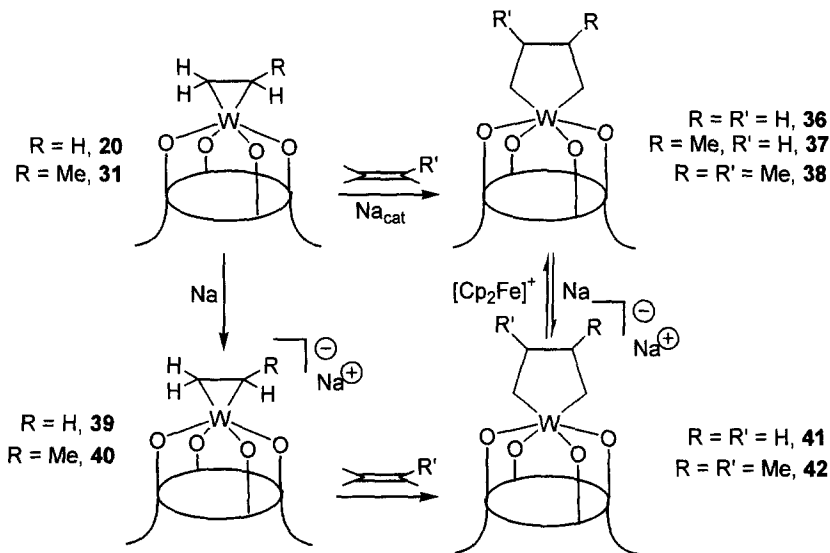


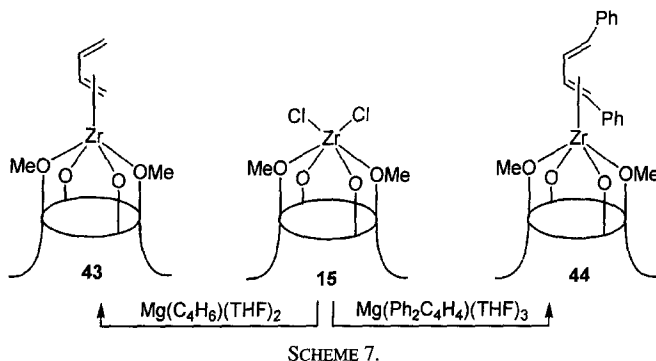
CHART 4. Molecular orbital interaction diagram for 20.



SCHEME 6.

the remaining two W–O bonds in the orthogonal plane.^{22b} The presence of two orthogonal d_{π} orbitals equally available for the interaction with the π system of C_2H_4 suggests a small activation barrier for fragment rotation about the z axis. The calculations on the ethylene complex, with the $C=C$ rotated by 45° with respect to the xz symmetry plane, gave an estimate of the energy barrier of only 3 kcal mol^{-1} . This result suggests an essentially free rotation of the organic fragment and is in good agreement with the 1H NMR of **20** and **31–33**, indicating an apparent C_{4v} symmetry of the calix[4]arene moiety even at low temperatures.^{22b} The metal-assisted olefin chemistry of W-calix[4]arene has another significant peculiarity that justifies the comparison of metalla-calix[4]arenes with a metal-oxo-surface. This is the electron-transfer-catalyzed dimerization of ethylene and propylene to the corresponding metallacyclopentane.^{22b} Unlike many organometallic systems,²⁹ the reductive coupling of an olefin (see Scheme 6) is not a reversible reaction and only occurs in the presence of small amounts of a reducing agent, in our case sodium metal. This led, as a synthetic result, to regiochemically controlled isomers of metallacyclopentanes.

Related results in this area have been reported studying the synthesis and the reactivity of zirconium-butadiene functionality bonded to the p -Bu^t-calix[4]-(O)₂ (OMe)₂ dianion.³⁰ The synthesis of the parent compound used in this study, **43**, is displayed, along with the analogous diphenyl derivative, in Scheme 7, and its structure in Fig. 5.



The reaction can be carried out via the preliminary isolation of **15** or it can be performed *in situ* with the corresponding Mg-butadiene derivative. In the solid state, the bonding mode of the butadiene ligands in both complexes **43** and **44** can be described as π^2, η^4 . A variety of bonding modes of butadiene to zirconium ranging from π^2, η^4 to σ^2, π, η^4 can be found in complexes having subunits other than

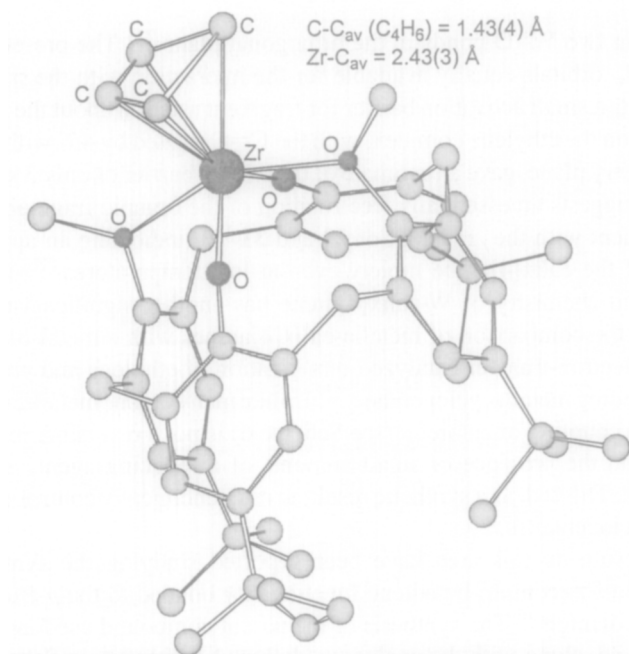
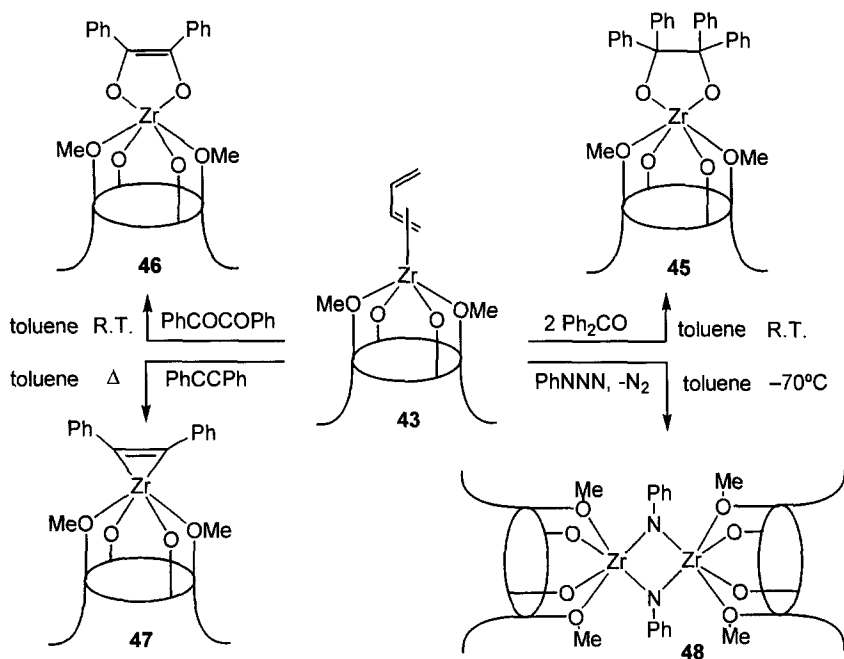


FIG. 5. Crystal structure and selected structural parameters of complex **43**.

[Cp₂Zr].³¹ The structural and spectroscopic characteristics of the Zr-diene fragment in **43** and **44** are more closely related to the [(tmtaa)Zr]³² derivatives [tmtaa = dibenzotetramethyltetraaza[14]annulene dianion] than the corresponding [Cp₂Zr] species. In particular, one can say that the *s-cis* form is the only butadiene conformer detected in the solid state; heating of **43** or **44** did not result in any *cis-trans* isomerization.³³ The Zr-C distances, ranging from 2.398(17)–2.525(16), and the close C–C bond lengths within butadiene, averaging 1.43(2) Å in the structure of **43**, support the π^2, η^4 bonding mode. The plane of the ligand is nearly parallel to the O₄ mean plane. An energy barrier of 20 kcal mol⁻¹ for the rotation of the butadiene unit around the C_{2v} pseudo-axis, leading to a rearrangement between the two possible configurations of the butadiene, has been found, which is compatible with the observed ¹H NMR behavior.³⁰

Scheme 8 displays reactions where **43** behaves as a source of a Zr(II) derivative.³⁰ They can be formally viewed as oxidative additions to the [*p*-Bu^t-calix[4]-(OMe)₂(O)₂Zr] fragment. The main driving force in the case of ketones is the high oxophilicity of the metal, which induces the reductive coupling of benzophenone leading to **45**, or the addition of dibenzoyl causing the formation of the dioxo-metallacycle in **46**, which contain a C–C double bond. It has to be mentioned that

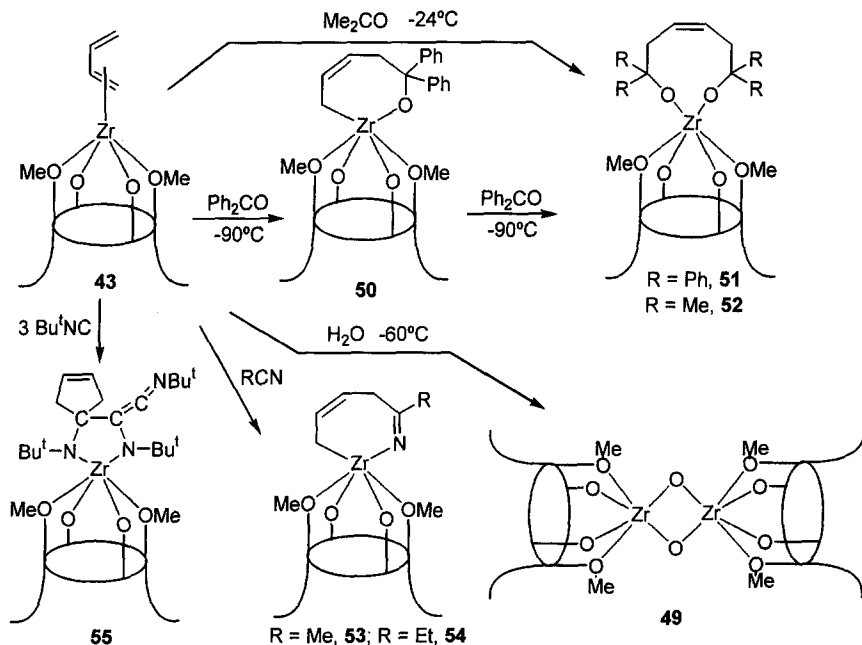


SCHEME 8.

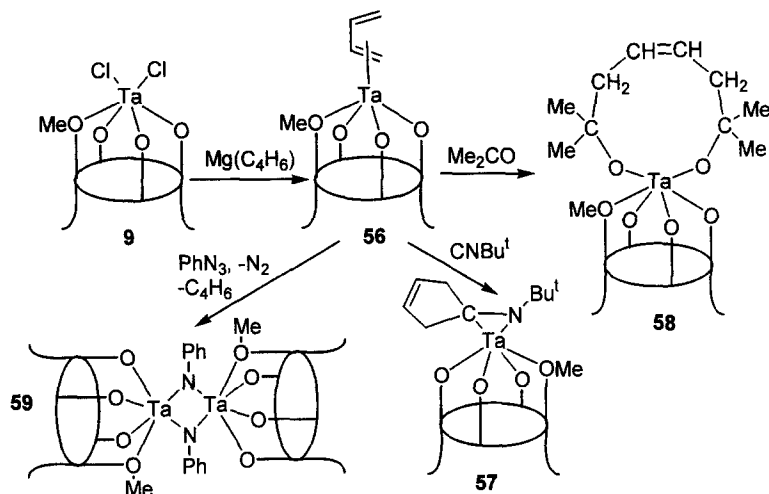
the reaction of **43** with ketones at low temperature (see below) follows a very different pathway and leads to the insertion of the carbonylic group into a Zr–C σ bond. In the reaction with **43**, phenylazide functions as a source of phenylnitrene,^{19b,34} leading to the corresponding Zr(IV)-dimeric phenylimido derivative. Displacement of butadiene with diphenylacetylene³⁵ occurs under more drastic conditions. A complex like **47** has been proposed as an intermediate in the formation of zirconocyclopentadiene coming from the reductive coupling of the diphenylacetylenes and isolated as the PMe_3 adduct.³⁶

Although the bonding mode of butadiene to zirconium is π^2, η^4 , as revealed by X-ray analysis, in a number of reactions and under certain conditions it behaves like a σ^2, π, η^4 butadiene, thus the zirconium–butadiene functionality behaves as though containing two Zr–C σ bonds. This behavior is illustrated in the reactions listed in Scheme 9.

They include the hydrolysis to form the μ -dioxo dimer **49**, and the products derived from the formal insertion of nitriles, ketones, and Bu^tNC into the Zr–C σ bonds. In the case of hydrolysis, butenes have been identified. The occurrence of the zirconyl ("Zr=O") group in a monomeric zirconium compound remains



SCHEME 9.



SCHEME 10.

rather rare.³⁷ The ^1H NMR spectrum of **49** is in agreement with an approximate D_2 symmetry and, thus, shows a singlet for the methoxy groups and a pair of doublets for the bridging methylenes. The reaction of **43** with ketones has a particular dependence on temperature.³⁰ When it was performed at room temperature (see Scheme 8, compounds **45** and **46**), the displacement of butadiene by the incoming substrate was observed. On the contrary, when the reaction was carried out at low temperature and with a 1:1 molar ratio (Scheme 9), the insertion of the ketone unit was observed in one of the two $\text{Zr}-\text{C}$ σ bonds, leading to the seven-member metallacycle in **50**. The reaction then proceeded further with a second mole of Ph_2CO to give **51**.

The tantalum–butadiene derivative **56**, where butadiene displays a $cis-\pi^2, \eta^4$ bonding mode, has been obtained from the reaction of **9** with $[\text{Mg}(\text{C}_4\text{H}_6)]$, in the form of an orange microcrystalline solid (Scheme 10).⁹ The chemistry and structural features of **56** parallel those of the analogous zirconium derivative **43**.³⁰ Different reacting modes have been identified for Bu^tNC , PhN_3 , and Me_2CO . In the reaction with Bu^tNC , the butadiene ligand behaves as though it is bonded to the metal in a σ^2, π, η^4 fashion and affords the imino complex **57**, as a consequence of a double migration such as has been observed for the complexes **114–115** (see Scheme 22). Butadiene behaves in a similar manner in the reaction with acetone, to give the nine-membered dioxo metallacycle, **58**. In the reaction with PhN_3 , complex **56** behaves as a source of the d^2 tantalum(III) fragment [$p\text{-Bu}^t\text{-calix[4]-(OMe)(O)}_3\text{Ta}$] to give a phenylimido derivative (Scheme 10), that is the μ -phenylimido dimer **59** (Fig. 6).

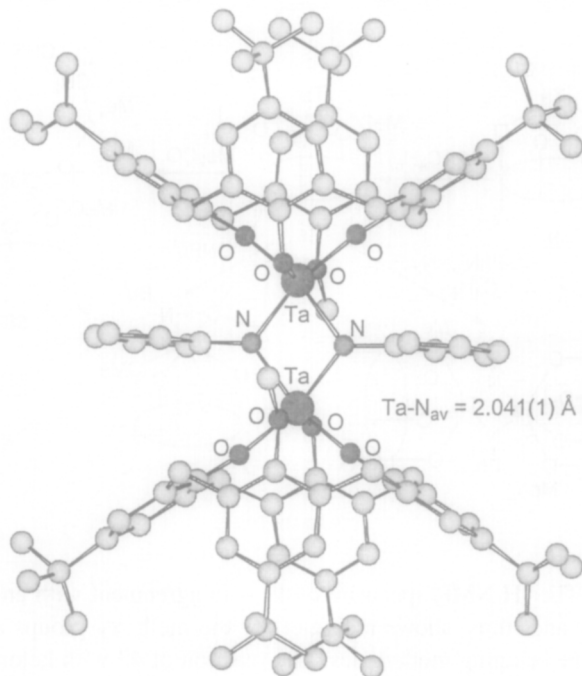


FIG. 6. Crystal structure and selected structural parameter of complex **59**.

V

THE ORGANOMETALLIC FUNCTIONALIZATION OF THE METALLA-CALIX[4]ARENES

A. *The Synthesis and the Chemistry of M—C σ Bonds*

The existence, the properties, and the chemical behavior of the M—C σ bond functionality was largely explored in the case of Group IV and V metals. The starting material used in the case of titanium(III) and titanium(IV) are those reported in Scheme 1, namely **8**, **11**, and **14**.¹² They undergo alkylation or arylation using conventional organometallic methodology. The results are reported in Scheme 11.¹² The organometallic derivatives in Scheme 11 have a basic structure which is exemplified by **62**. Complex **62** has, however, an additional structural peculiarity, since the presence of the *p*-tolyl at the metal gives rise to a very interesting solid state assembly (Fig. 7).¹² It possesses a crystallographically imposed C_2 symmetry, the two-fold axis running through the molecular axis. The most peculiar feature of the structure consists in the columnar chaining

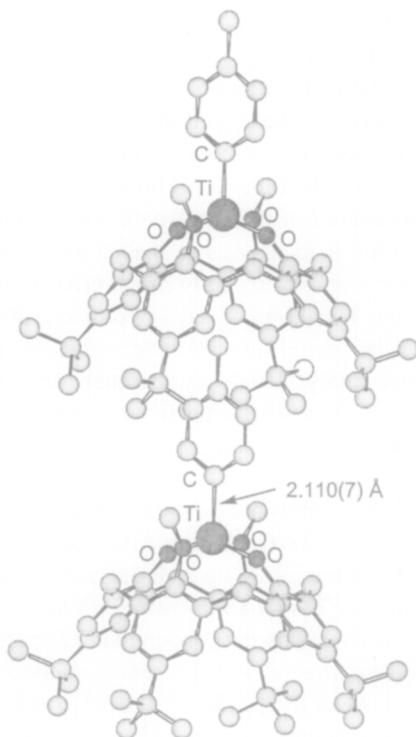
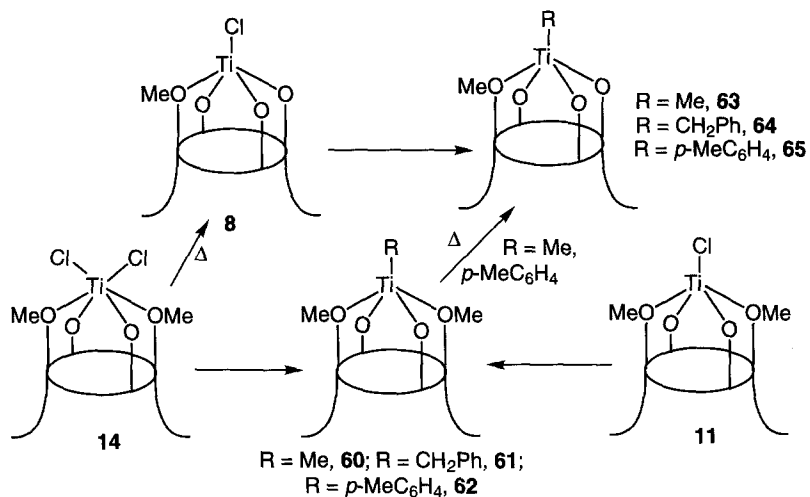
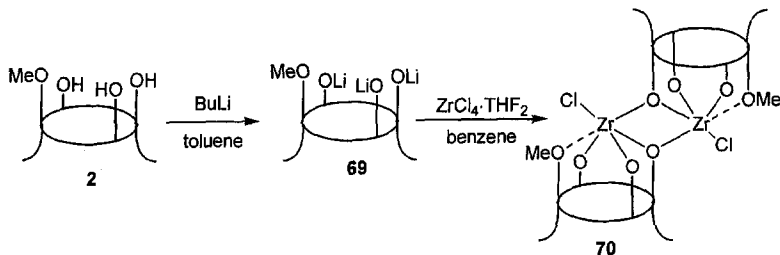


FIG. 7. Crystal structure and selected structural parameter of complex **62**.

of the complex molecules. In all cases the calix[4]arene fragment displays a C_s symmetry in the ^1H NMR spectrum [two pairs of doublets (CH_2); three singlets (Bu^t)].

It has been reported that the trianion **B** in Chart 1 is a suitable ancillary ligand for ensuring stability to the titanium(IV)-carbon functionality, and similarly that the dianion **C** (Chart 1) stabilizes the titanium(III)-carbon functionality. Any attempt to synthesize the $[\text{TiR}_2]$ fragment bonded to the O_4 oxo-matrix via the alkylation of **14** failed, since this reaction proceeds with a preliminary reduction of titanium(IV) to titanium(III). Therefore, due to the different stabilization degree of titanium(IV) and titanium(III) by the trianionic and dianionic forms (**B** and **C** in Chart 1) of the calix[4]arene, a single Ti–C functionality over the O_4 set environment has been identified. All organometallic derivatives **60–65** are particularly appropriate for studying the chemistry of the Ti–C bond in titanium(III) and titanium(IV) derivatives. Some of the more relevant peculiarities of such compounds are: (1) the O_4 set provides an unusual coordination number for titanium in organometallic derivatives, and a quasiplanar oxo-matrix for the metal; (2) the geometric constraints of the calix[4]arene skeleton affects the Ti–O π interaction with the phenoxo groups; (3) the methoxy groups can function as spectator donors. As shown by the different Ti–OMe bond distances in the structures of **8**, **62** (Fig. 7), and **65**,¹² the methoxy group can provide a variable coordination number, as required by the metal along the reaction pathway; (4) the synergism between the ancillary calix[4]arene ligand and the organic functionality. An interesting observation has been made in the context of the latter point. Moderate heating of **60** or **62** did not affect the Ti–C bond, but led to the cleavage of the O–Me bond and the formation of the corresponding titanium(IV) derivatives **63** and **65**, while **11** could not be converted to **8** even under drastic conditions. An important catalytic issue has been recently discovered in titanium-calix[4]arene organometallic chemistry. The $[(\text{DMSC})\text{TiCl}_2]$ complex [$\text{DMSC} = 1,2\text{-alternate dimethylsilyl-bridged } p\text{-Bu}^t\text{-calix[4]arene}$] under reducing conditions is an excellent highly regioselective catalyst for the cyclotrimerization of terminal alkynes³⁸ according to Scheme 12.³⁹ The resting stage in the catalytic cycle is a rare example of a metallanorbornadiene, one Ti–C bond of which is prone to the insertion of aldehydes and ketones.^{39c}

A detailed study has been published on the synthesis, rearrangements, and migration insertion reactions of Zr–C functionalities anchored to a calix[4]arene moiety.⁴⁰ This approach has been developed through the synthesis and the organometallic functionalization of **70** and **15** (Schemes 13 and 14), which give rise to two classes of derivatives related by the base-induced demethylation of one of the methoxy groups. The experimental and theoretical studies reported emphasized the major differences between the $[\text{O}_4\text{Zr}]^{2+}$, $[\text{O}_4\text{Zr}]^+$, and the $[\text{Cp}_2\text{Zr}]^{2+}$ [$\text{Cp} = \eta^5\text{-C}_5\text{H}_5$] fragments.⁴⁰ The parent compound **15**, which serves as starting material

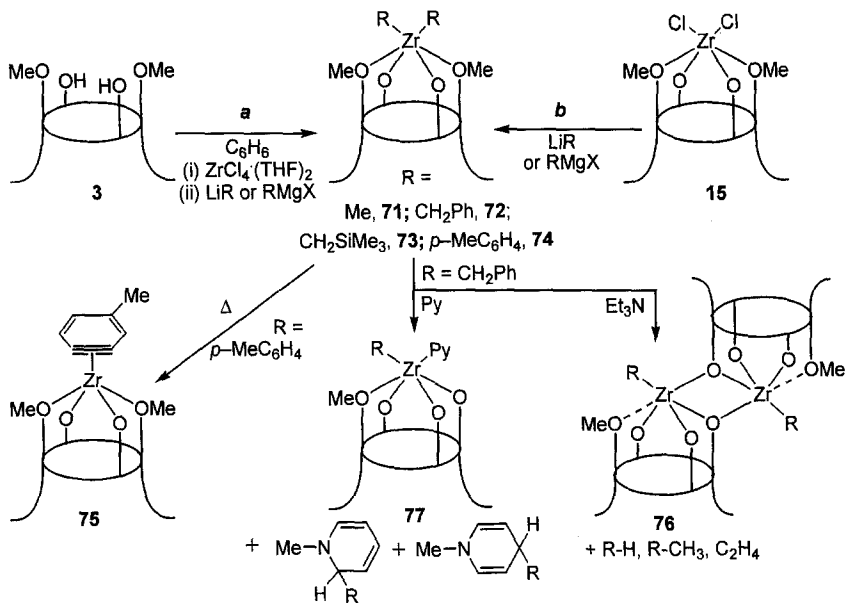


SCHEME 14.

for the organometallic derivatization of zirconium-calix[4]arene, has been prepared according to the two procedures outlined in Scheme 13.⁴⁰

The synthesis avoiding the use of any alkali salt is preferred in this kind of chemistry because the alkali salt very often remains complexed by the ensuing calix[4]arene moiety,²¹ while that passing through the intermediate **68** gives higher yields, when carried out *in situ*. The demethylation of **3**¹² led to an appropriate synthetic approach to the monochlorozirconium(IV)-calix[4]arene, **70**, which can be an attractive parent compound for organometallic functionalization. The synthetic procedure is shown in Scheme 14.⁴⁰

The alkylation of **15** (path *b*, Scheme 15)⁴⁰ has been performed according to conventional procedures using lithium or Grignard reagents. The preliminary isolation of **15** is not essential; thus, the synthesis of the zirconium alkyl or aryl derivatives can be carried out *in situ* directly from **3** (path *a*, Scheme 15). The ¹H NMR spectra of **71–74** all imply *C*_{2v} symmetry, as revealed by the CH₂ (one pair of doublets), Bu^t (two singlets), and MeO (one singlet) patterns. All the alkyl derivatives **71–73** are thermally stable up to 80°C in C₆D₆. The aryl derivative **74** is more thermally sensitive than the corresponding alkyl compounds **71–73**, and refluxing in benzene for 36 h gave the corresponding benzyne derivative,⁴¹ **75** (Fig. 8), via toluene elimination.⁴⁰ The structure of **75**⁴⁰ shows a symmetric bonding mode to the metal, the Zr–C bond distances being very close. Their mean value [2.173(5) Å] is remarkably shorter than those found for Zr–C σ bonds. The C–C bond distances within the benzyne ring are very close without alternation of short and long bond lengths, and they range from 1.386(8) to 1.407(7) Å. Such a trend of structural data is quite close to that observed in [Cp₂Zr(η⁶-C₆H₄)(PMe₃)].^{41c} The plane of the η²-bonded atoms is nearly perpendicular to the mean plane through the O₄ core. The α-elimination, leading to the corresponding alkylidene,⁴² has never been observed in the case of the attempted thermal decomposition of **71–73**. The reactivity study on **71–74** should take into account the base-induced demethylation of one of the methoxy groups when they are treated with a relatively strong base, as established by the transformation of **72** to **76** induced by Et₃N. Complex **76** has also been obtained from the alkylation of **70**



SCHEME 15.

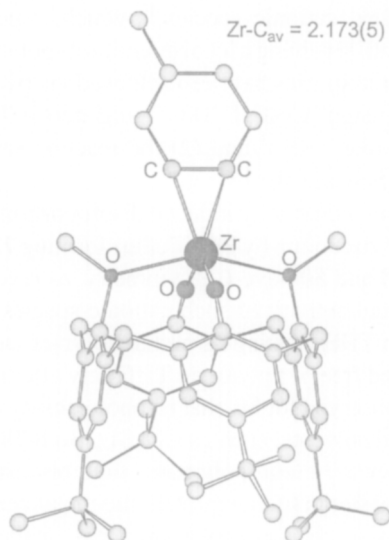
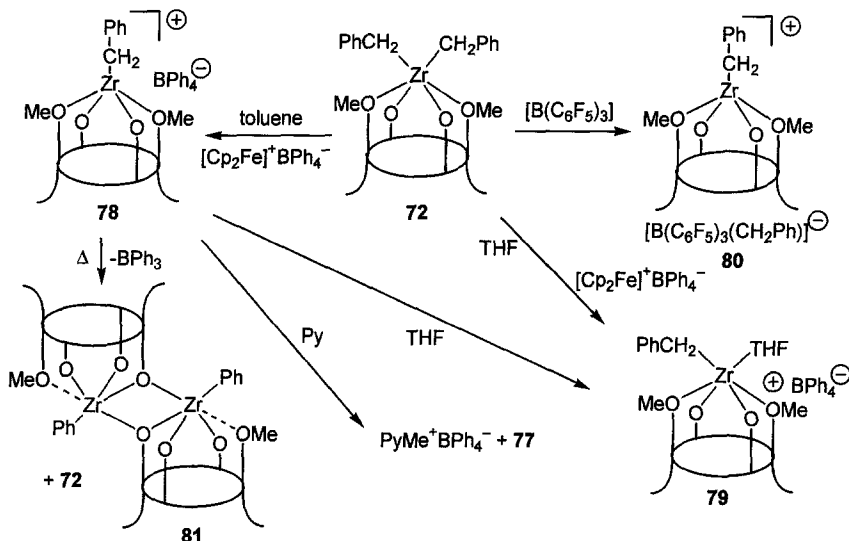


FIG. 8. Crystal structure and selected structural parameter of complex 75.

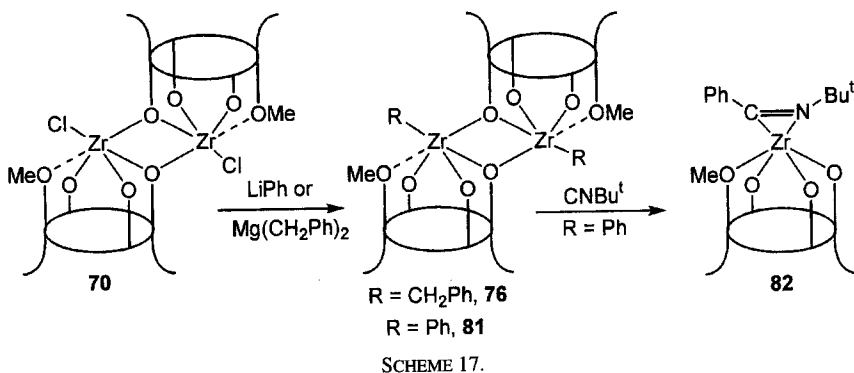


SCHEME 16.

(Scheme 14). The reaction of **72** with pyridine causes the dealkylation both at the methoxy group and at the metal leading to **77** and to the organic products shown in Scheme 15.

Compounds **71–74** are particularly appropriate precursors (Scheme 16) for the corresponding mono-alkyl cationic species,⁴⁰ which, especially in the case of $[\text{Cp}_2\text{Zr}]$ chemistry, are still receiving a lot of attention as polymerization catalysts.⁴³ The generation of cationic species has been achieved via two major routes: (1) the one-electron oxidation using $[\text{Cp}_2\text{Fe}]^+\text{BPh}_4^-$ to generate **78** in toluene, or **79** in a coordinating solvent like THF,⁴³ and (2) the reaction with a Lewis acid, like $[\text{B}(\text{C}_6\text{F}_5)_3]$, to give **80** (Scheme 16).^{43,44}

Complex **78** undergoes a thermally induced disproportionation reaction with simultaneous arylation of zirconium by BPh_4^- , thus forming **72** and **81** (Scheme 16). The cationic species **78** and **80** have C_{2v} symmetry, as revealed by the ^1H NMR spectrum. The Lewis acid activity of such cationic species is not easily defined. Complex **78** reacts with THF, causing its partial polymerization, as is the case for **79**, which can be isolated free of polymeric THF only after recrystallization. Similar behavior has been observed for **80**, that is, photolability and degradation in the presence of halogenated solvents, such as CH_2Cl_2 . Both **78** and **80** did not show, however, any activity toward olefin polymerization, because in such compounds the two methoxy groups sterically overprotect the metal center.⁴⁰ The reaction of **78** with pyridine emphasizes the action of a strong base in the demethylation of one



of the methoxy groups. The pyridine functions as the acceptor of the methyl cation and thus forms **77** and $\text{PyMe}^+\text{BPh}_4^-$. Under basic conditions, the Lewis-acidic zirconium assists the demethylation of one of the methoxy groups.

A better synthetic approach to the organometallic derivatives of the mono-methoxy-calix[4]arene-zirconium fragment is in Scheme 17.⁴⁰ The reaction of **70** with LiPh gave the phenyl derivative **81**, which behaves as expected in the insertion reaction with Bu^tNC ,⁴⁵ leading to a η^2 -iminoacyl, **82** (Fig. 9). The reaction causes the cleavage of the dimer into two monomeric units (see Scheme 17). The results mentioned above show the variety of the Zr-C bonds which have been built up over a calix[4]arene oxo-surface (i.e., Zr-C σ functionalities in $[\text{ZrR}_2]$, $[\text{ZrR}]$, and $[\text{ZrR}]^+$), and a π functionality in $[\text{Zr-aryne}]$. The O_4 -macrocycle is a unique chemical environment for such Zr-C fragments, for a number of reasons: (1) the topology of the O_4 -Zr moiety is approximately square-pyramidal, with the metal out of the " O_4 " plane; (2) the metal orbitals available for binding functionalities or assisting their transformations are located on the free face of the $[\text{ZrO}_4]$ hemisandwich; (3) the partial methylation of the phenoxo groups not only provides a variable range of charges for an O_4 set, but allows one to tune the ratio between strong σ , π donor (the phenoxo) and weak σ donor oxygens (the methoxy); and (4) the competition for the same orbitals by the O_4 set and the organometallic functionalities would be an important factor for their reactivity. For a better understanding of the basic chemical behavior of the $[\text{ZrO}_4]^{n+}$ [$n = 0, 1, 2$] core in binding and assisting the chemistry of organometallic functionalities, extended Hückel calculations on the fragments in Chart 5 have been carried out,⁴⁰ with the aim of studying their frontier orbitals (Chart 6) and comparing them with those of other well-known organometallic fragments, such as $[\text{Cp}_2\text{Zr}]^{2+}$.⁴⁶

In order to emphasize the peculiar role of calix[4]arene as a supporting ligand compared to cyclopentadienyl and phenoxo anions, a detailed investigation has

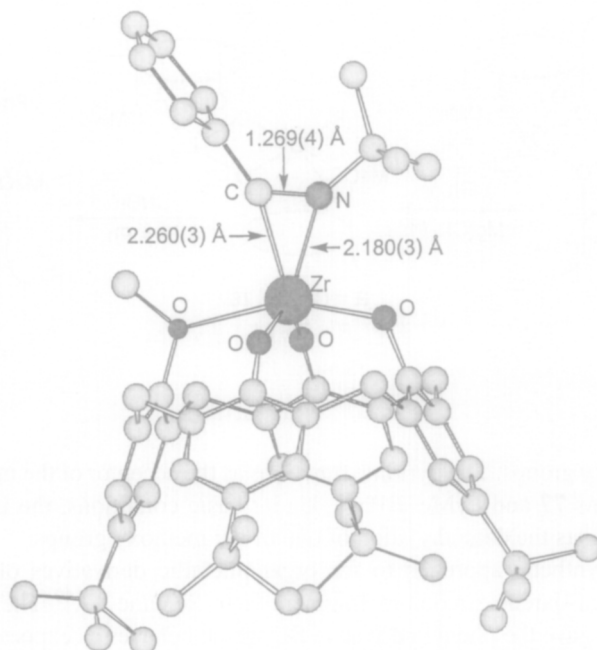


FIG. 9. Crystal structure and selected structural parameters of complex **82**.

been carried out on the migratory insertion of carbon monoxide and isocyanides in the Zr–C σ bonds.⁴⁷ The starting materials of this study are the dialkyl and diaryl derivatives, **71**, **72**, and **74** (Scheme 18). They undergo a sequential series of insertion reactions occurring with the formation of C–C bonds and giving organic fragments which remain bonded to the calix[4]arene-zirconium moiety. Scheme 18 displays the migratory insertion of carbon monoxide into the Zr–C bonds in **71**, **72**, and **74**, and the further migratory aptitude of the resulting Zr–C functionalities to ketones and isocyanides.

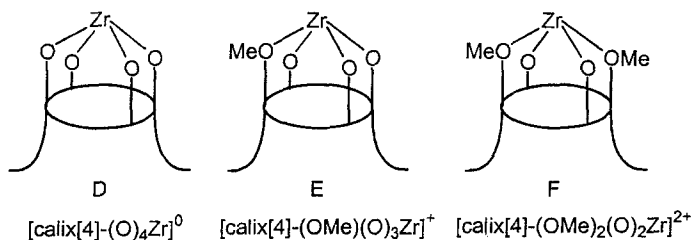


CHART 5. [Zr-calix[4]arene] fragments.

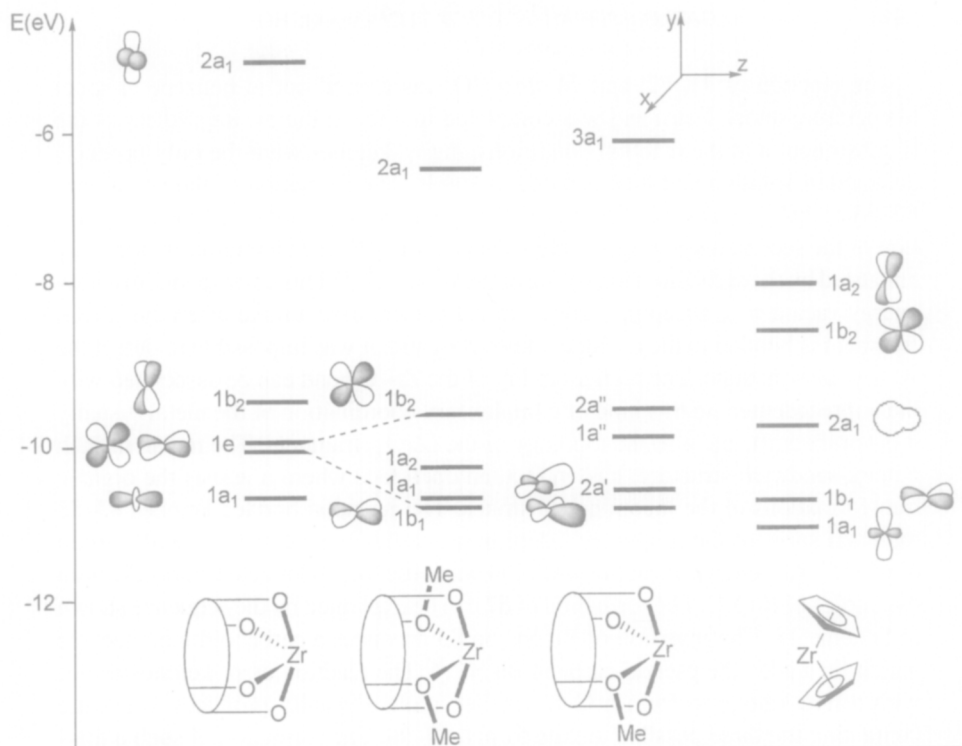
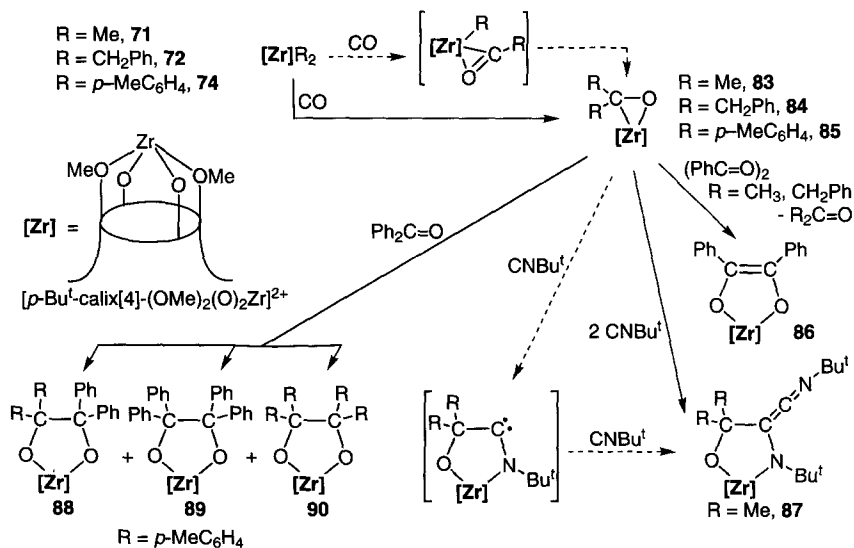


CHART 6. Frontier orbitals of [Zr-calix[4]arene] and zirconocene fragments.

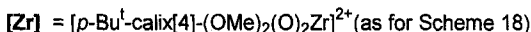
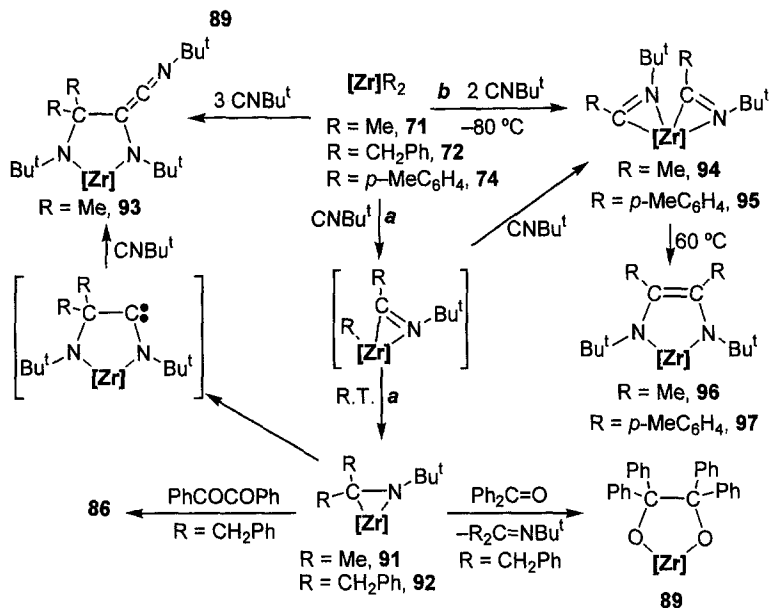


SCHEME 18.

The reaction of **71**, **72**, and **74** with CO was carried out in benzene at room temperature under 1 atm and was completed in a few minutes. Regardless of the R substituent and the reaction conditions, the η^2 -ketones were the only products detected in solution and then isolated as solids. The formation of the η^2 -ketones **83–85** probably occurs via the intermediacy of an η^2 -acyl, followed by the migration of the second alkyl group to the η^2 -acyl carbon.⁴⁵ Such a migration is greatly enhanced by the carbenium ion nature of the η^2 -acyl.^{46,48} This corresponds to a low-energy vacant π^*_{co} accepting orbital. In the present case, unlike when the $[\text{ZrR}_2]$ fragment is bonded to the cyclopentadienyl ligand, it was impossible to detect the η^2 -acyl intermediate. The higher lability of the Zr–C bond can be associated with the unprecedented, in this kind of complex, six-coordination of the metal (usually it is tetrahedral), and also the topology of the $[\text{ZrO}_4]$ fragment. The metal, in such a hemi-sandwich structure, has, in fact, an open face where it assists the organic transformations of the incoming substrates. The η^2 -metal bonded ketones **83–85** maintain some of the migratory insertion properties typical of the metal–carbon σ -bond.⁴⁹ Although no reaction with CO was observed, **83** reacted smoothly with two moles of Bu^1NC . The formation of **87** can be explained by the sequence shown in Scheme 18. The insertion of Bu^1NC on **83** produces a carbenoid metallacycle which then adds the pseudo-carbene Bu^1NC .⁵⁰ The reaction of η^2 -ketone species with a free ketone to form a C–C coupled diolate usually produces a mixture containing the three possible diolate forms, **88–90**. The formation of such a mixture requires that the η^2 -metal bonded ketone be replaced at an early stage by an incoming ketone $[\text{R}'_2\text{CO}]$, so that both reacting species $[\text{Zr}(\eta^2\text{-R}_2\text{CO})]$ and $[\text{Zr}(\eta^2\text{-R}'_2\text{Co})]$ can produce the observed mixture. At this stage two results, which have rare precedents in the literature, should be emphasized: (1) the reactivity of the metal–carbon bond in the η^2 -metal bonded ketones **83–85** toward inserting groups,⁴⁹ a reaction which can be of synthetic utility, and (2) the potential use of **83–85** as a source of zirconium(II) in displacement reactions with appropriate substrates.

In the absence of an excessive driving force derived, as in the case of CO, from the oxophilicity of the metal, the reaction with Bu^1NC allowed one to better single out almost all of the steps of the migratory insertion of the isocyanide into the Zr–C bonds, as shown in Scheme 19.⁴⁷

The reaction of **71**, **72**, and **74** with Bu^1NC exemplifies the migratory aptitude of the alkyl and aryl groups bonded to zirconium. A complete range of migratory insertion pathways has been observed as a function of temperature and the nature of the alkyl or aryl substituent. However, only in the case of **71** was it possible to select a specific pathway using temperature exclusively as the controlling factor.⁴⁷ The reaction of **71** and **72** with Bu^1NC at room temperature (Scheme 19, path *a*) using a 1:1 Zr : Bu^1NC molar ratio led to the η^2 -imine complexes **91** and **92** via the intermediacy of the corresponding η^2 -iminoacyl.^{45,51} The migration of the second alkyl group to the η^2 -iminoacyl carbon was inferred in the case of **71** and **72**, via the isolation of the corresponding η^2 -imine. The metal–carbon bond in



SCHEME 19.

91 can still participate in migratory insertion reactions, similar to those observed in the case of the η^2 -metal bonded ketones in **83–85**. The reaction of **91** with an excess of Bu^tNC or, more simply, the reaction of **71** with 3 moles of Bu^tNC at room temperature led to **93**. This reaction implies the preliminary insertion of an isocyanide into the Zr–C bond of the Zr-imine, **91**, to form the carbenoid intermediate which then adds a further mole of isocyanide to give **93**.⁵⁰ Attempts to insert a ketone into the zirconium–carbon σ bond of the imine **91** resulted, instead, in the displacement of the imine by the ketone, as a consequence of the high oxophilicity of zirconium. The resulting η^2 -metal bonded ketone readily inserts a further molecule of ketone, thus forming the C–C coupled product **89** (see Scheme 18). The proposed displacement of the η^2 -metal bonded imine⁵² in **91** and **92** is supported by the identification of the free imine and by the reaction of **92** with PhCOCOPh , leading, as in the case of **83** and **84**, to **86**. These results suggest a possible synthetic utility of **91** and **92** as a source of the $[\text{calix[4]-(OMe)}_2(\text{O})_2\text{Zr}]^0$ fragment, formally containing a zirconium(II), more available than in the case of **83** and **84**, being devoid of strongly bonded oxygen donor atoms.

The competitive pathway (Scheme 19, path *b*), which has been singled out at low temperature for **71** and **74**, shows the preferential migration of the second

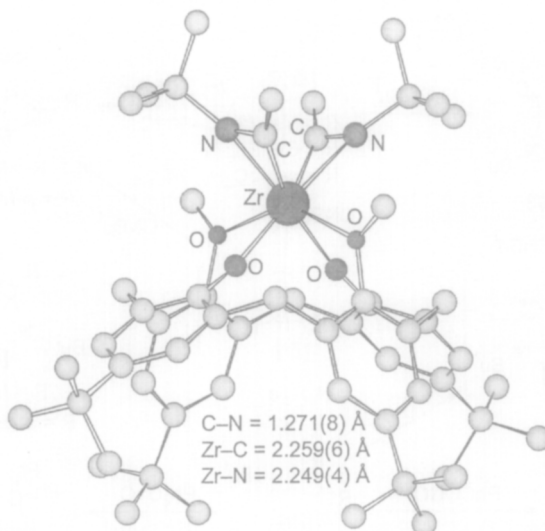


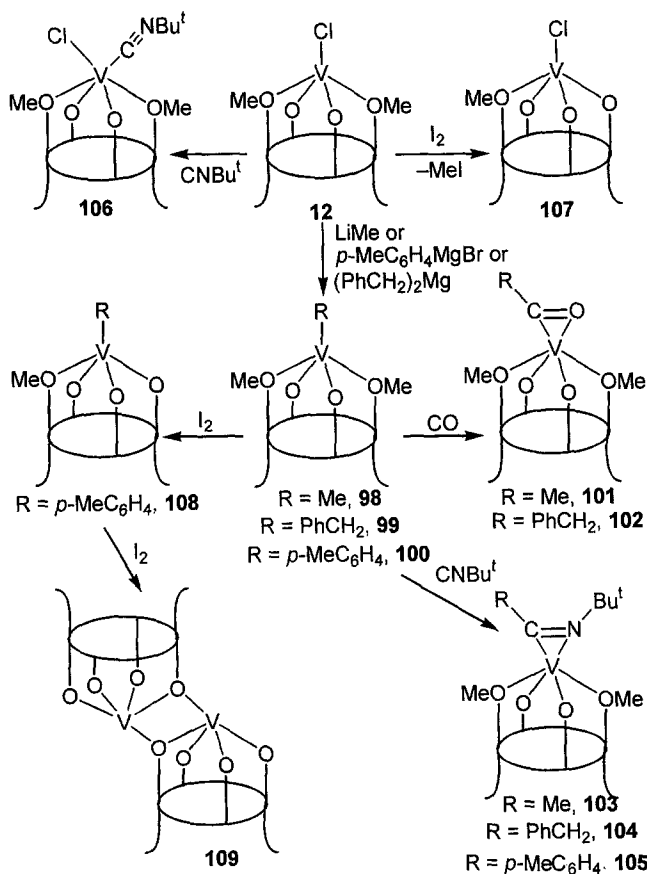
FIG. 10. Crystal structure and selected structural parameters of complex **94**.

alkyl group to an incoming Bu^tNC ,⁵¹ to give bis- η^2 -iminoacyl **94** (Fig. 10) and **95**. Regardless of the $\text{Zr}:\text{Bu}^t\text{NC}$ stoichiometric ratio, the reaction proceeds via pathway *b* at low temperature for **71** and **74**, while in the case of **72**, which is unreactive at low temperature, the only compound formed at room temperature, via the pathway *a*, is always **92**. In the case of the *p*-tolyl substituent, pathway *b* is preferred since only very limited formation of the η^2 -imine is observed, even under forcing conditions. Gentle heating (60°C) induces the intramolecular coupling⁵³ of the two η^2 -iminoacyl derivatives **94** and **95** to the corresponding ene-diamido complexes, **96** and **97**. The intramolecular coupling followed first-order kinetics in both cases. The activation parameters [ΔH^\ddagger ($\text{kJ} \cdot \text{mol}^{-1}$), E_a ($\text{kJ} \cdot \text{mol}^{-1}$)] obtained from the kinetic measurements are 106 ± 2 , 109 ± 2 for complex **94** and 113 ± 8 , 116 ± 8 for complex **95**.⁴⁷

All the reactions displayed in Schemes 18 and 19 belong to four general classes, namely: (1) the migratory insertion of carbon monoxide or isocyanides into a metal-alkyl bond with the consequent formation of η^2 -acyl or η^2 -iminoacyl functionalities; (2) the alkyl-aryl migration to an η^2 -acyl or η^2 -iminoacyl metal-bonded moiety, leading to the corresponding η^2 -ketone or η^2 -imine; (3) the intramolecular coupling of two η^2 -iminoacyls to an ene-diamido ligand; and (4) the migratory insertion of ketones and isocyanides into the $\text{M}-\text{C}$ bond of η^2 -metal bonded ketones and imines.

Although the oxygen atom environment is common in vanadium chemistry⁵⁴ it is rarely used to support the $\text{V}-\text{C}$ functionality.⁵⁵ Two significant exceptions in

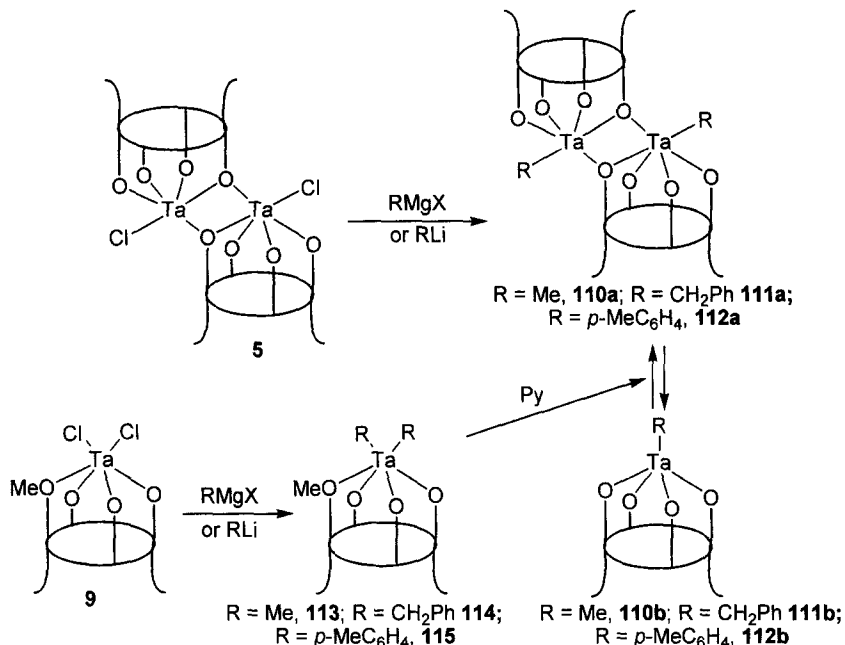
this context are the recent impact that silica-supported vanadium catalysts have had in olefin polymerization⁵⁶ and the work of Feher who used silasesquioxanes as ancillary ligands to better understand the nature of the active silica-supported vanadium species.^{3,57} An interesting relationship between the use of calix[4]arene as an ancillary ligand and other oxygen-supported organometallic functionalities has been found.^{3,4} In the case of vanadium-calix[4]arene derivatives the genesis and reactivity of the V-C functionality anchored to the dimethoxy-*p*-Bu^t-calix[4]arene dianion (C in Chart 1) and the oxidative demethylation of the ligand as an entry into the analogous vanadium (IV) organometallic chemistry have been reported.¹⁵ An overview of this chemistry is reported in Scheme 20. The parent compound **12** can be considered a useful entry point into the organometallic chemistry of



SCHEME 20.

vanadium bonded to the oxo-matrix defined by the calix[4]arene skeleton. It was prepared by reacting **3**, pretreated with BuLi, with $\text{VCl}_3 \cdot \text{THF}_3$. Complex **12** is a yellow-green crystalline solid with the paramagnetism expected for a d^2 high-spin compound ($\mu_{\text{eff}} = 2.69 \mu_{\text{B}}$ at 300 K). Complex **12** undergoes alkylation to the corresponding paramagnetic vanadium(III) derivatives **98–100** using either a lithium or a Grignard reagent (Scheme 20). They have been isolated as thermally stable organometallic derivatives, though they undergo facile oxidative transformations (see below). The reactions in Scheme 20 also emphasize the migratory ability of the alkyl and aryl groups at the metal in insertion reactions with carbon monoxide and Bu^tNC leading to the corresponding η^2 -acyls, **101** and **102**, and η^2 -iminoacyls, **103** and **105**. The precoordination of Bu^tNC at the metal is modeled by the formation of **106** from **12**. The vanadium(III) complexes so far mentioned display interesting redox behavior. Compounds **12** and **100** treated with 1 equiv. of iodine led to the corresponding vanadium(IV) derivatives **107** and **108**, respectively. The oxidation with I_2 is particularly remarkable in the reaction of **100** to **108** since the V–C bond is not affected by the oxidation process. The reaction occurs with the simultaneous loss of MeI. Extended Hückel calculations have been carried out, thus defining the frontier orbitals of the $[\text{calix[4]}-(\text{OMe})_2(\text{O})_2\text{V}]$ fragment engaged in the transformation of the V–C bonds and in the conversion of vanadium(III) to vanadium(IV) organometallics. The oxidation involves the removal of one electron from an essentially pure d orbital, that is $1a_2$. In the resulting vanadium (IV) cationic complex, the strong nucleophile I^- removes the methyl group from a methoxy substituent activated by the relatively high metal oxidation state. The methoxy group not only functions as a weakly binding group, but it can also undergo an acid- or redox-assisted conversion into the corresponding anion. The synthetic relevance of the reaction of **12** and **100** with iodine should also be emphasized, since complexes **107** and **108** would be hardly accessible from a different route. In the case of an excess of I_2 being used in the oxidation of **100** to **108**, the reaction proceeds further with the cleavage of the V–C bond and the complete demethylation of the calix[4]arene **109**. The reaction may proceed via the intermediacy of the corresponding vanadium(IV)-monoiodide derivative, which transfers I^- to the methyl of the residual methoxy group.

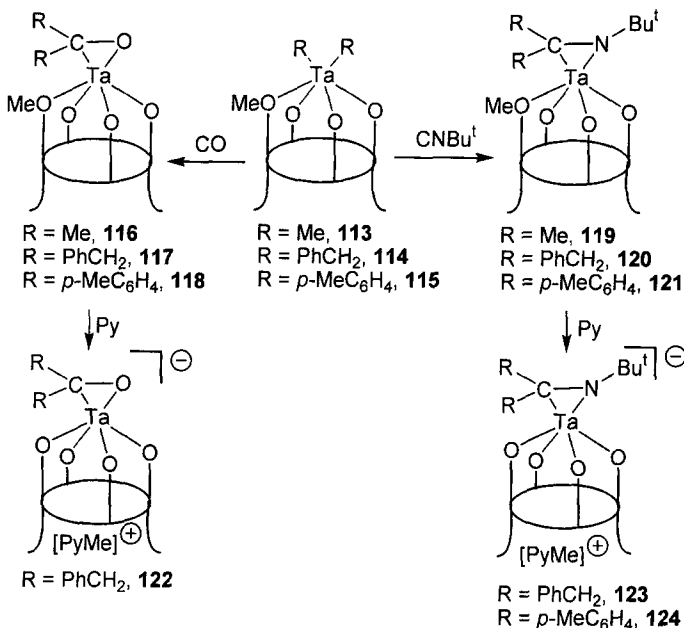
The most rich chemistry of the metal–carbon σ bond has been developed in the case of tantalum(V) anchored to the tetraoxo matrix, as defined by either calix[4]arene tetraanion or the monomethoxy calix[4]arene trianion (A and B, respectively, in Chart 1).⁹ In particular, the synthesis and the chemical reactivity of tantalum σ - and π -bonded to organic fragments are described, including the base-induced demethylation of the methoxy-calix[4]arene. This reaction allows the transfer from one model ligand to the other one without affecting the organic functionality bonded to tantalum. The alkylation pathway of the parent compounds of this chemistry is displayed in Scheme 21. The alkylation of **5** furnished the corresponding alkyl/aryl derivatives, which have been obtained as light-yellow,



SCHEME 21.

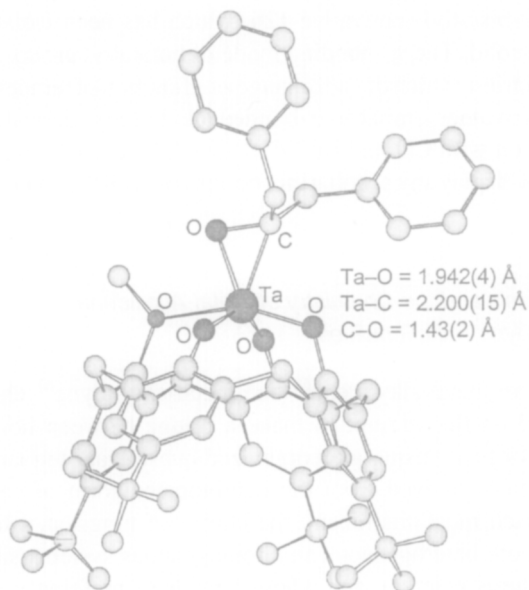
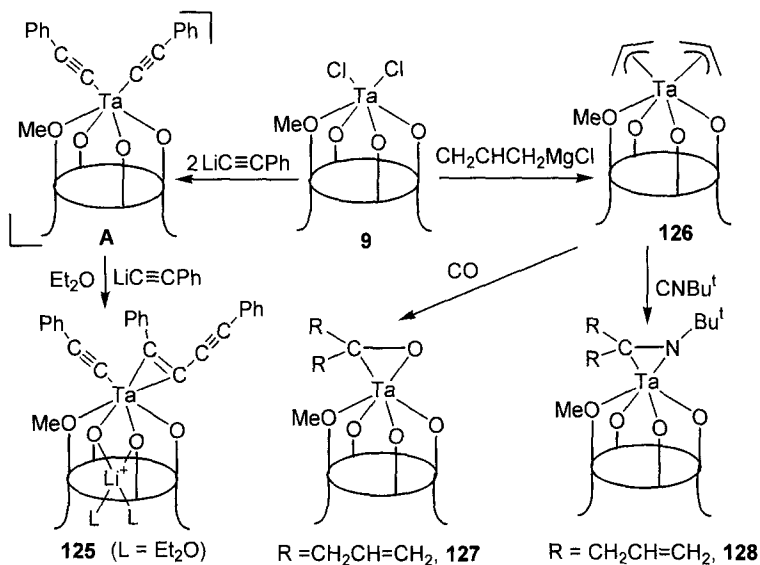
thermally stable, crystalline solids. Although the solid-state structure of **111** and **112** (see below) reveals their dimeric nature, solutions of compounds **110–112** are in equilibrium with their corresponding monomeric form. As can be judged from the ^1H NMR spectrum, such an equilibrium is completely shifted to the right in the case of **111**, while in the case of **110** and **112** both forms are equally present in solution. Reaction of **9** with Grignard reagents led to **113–115**, which are all equally thermally stable in boiling benzene for 24 h. However, depending on the R substituent, they display different reactivities under various conditions. All of them undergo demethylation to **110–112** in the presence of pyridine. The by-products of the reaction are the R–R coupled hydrocarbons and a mixture of alkylated pyridines. The benzyl derivative **114** undergoes demethylation quite readily in the presence of light or under an atmosphere of H_2 .

The migratory insertion reactions of the Ta–C functionalities in complexes **113–115** are presented in Scheme 22.⁹ In the reaction of **113–115** with both CO or Bu^tNC , the migration, under mild conditions (i.e., room temperature), of both alkyl or aryl groups to form η^2 -ketones **116–118** and η^2 -imino derivatives, **119–121**, has been observed. Unlike the case of $[\text{Cp}_2\text{M}]$ or polyphenoxo derivatives of Ta, migration of the second alkyl or aryl group to the intermediate η^2 -acyl or η^2 -iminoacyl derivatives is very fast, which prevents the interception of the



SCHEME 22.

precursor.^{45,53,58} As with the $[(\eta^8\text{-C}_8\text{H}_8)\text{ZrR}_2]$ derivatives,⁵⁹ such a pathway is assisted by the presence on the metal of the three facial frontier orbitals. An extended Hückel analysis was carried out on the migratory insertion reaction of CO and RNC into the Ta–C σ bonds, thus modeling in detail the reactions in Scheme 22. Both classes of compounds **116–118** and **119–121** are particularly thermally stable, and the M–C bond does not undergo a further insertion reaction. They can be quite sensitive to the presence of a base which causes demethylation and formation of the corresponding anionic species, as illustrated by the reaction of **117** (Fig. 11), **120** and **121** with pyridine. Complex **9** can also be used as starting material to synthesize complexes which contain unsaturated carbon functionalities that are bonded to the metal (Scheme 23). Very probably, the reaction with $\text{LiC}\equiv\text{CPh}$ proceeds through the formation of a bis(phenylacetylide) derivative **A**, which then reacts with a third equivalent of $\text{LiC}\equiv\text{CPh}$ by an attack of the α -carbon of one of the acetylide ligands to form **125**. Complex **125** contains a σ -bonded acetylide and an η^2 -bonded 1,4-diphenylbutadiyne, $\text{Ph}-\text{C}\equiv\text{C}-\text{C}\equiv\text{C}-\text{Ph}$. The addition of yet a further equivalent of $\text{LiC}\equiv\text{CPh}$ is, very probably, prevented by the existence of only three available frontier orbitals on the $[\text{calix}[\mathbf{4}]-(\text{OMe})(\text{O})_3\text{Ta}]$ fragment; the fourth orbital is only available for nonbonding electrons (see below). Reaction of **9** with allyl-MgCl led to the complete replacement of both chlorides and to the

FIG. 11. Crystal structure and selected structural parameters of complex **117**.

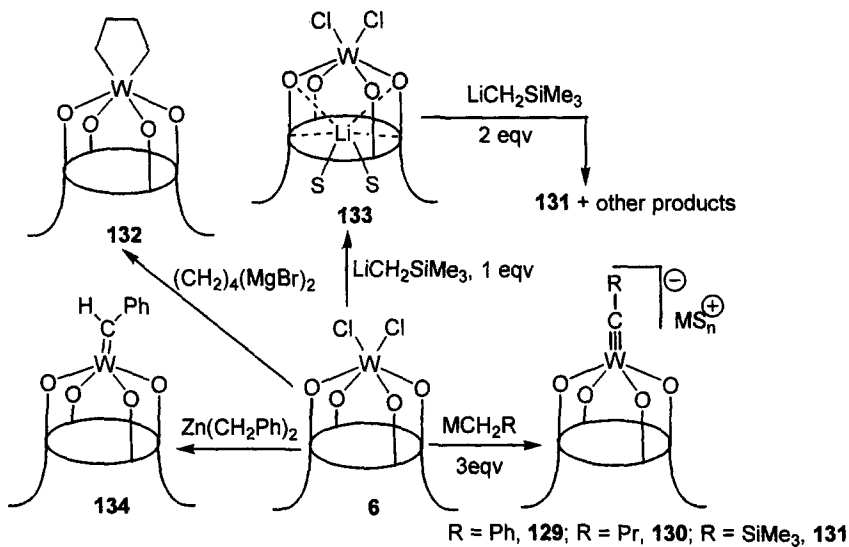
SCHEME 23.

formation of the bis(allyl) derivative **126**, which has been isolated as a yellow microcrystalline solid. The η^3 -bonding mode of both allyl groups is supported by the ^1H NMR spectrum, which did not change as a function of temperature. Complex **126** behaves in a manner similar to σ -bonded alkyl or aryl derivatives undergoing migratory insertion with CO and Bu^tNC to give **127** and **128**, respectively. They apparently do not display any peculiarities compared with the analogous derivatives **116–121**.

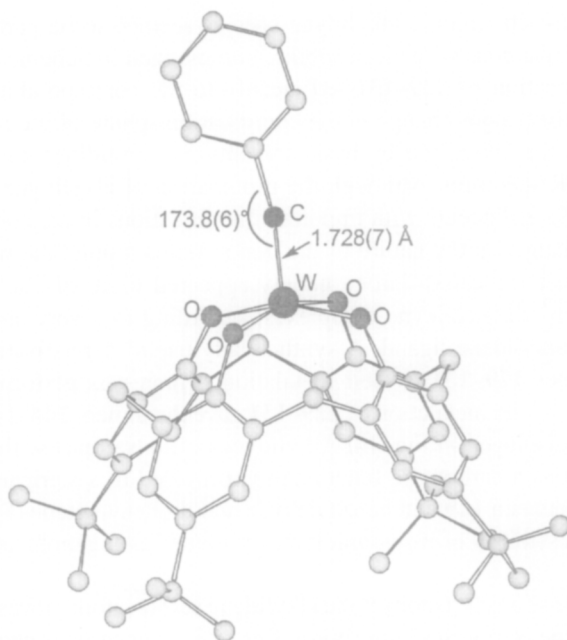
B. *The Synthesis and the Chemistry of Metal-Alkylidene and -Alkylidyne Functionalities*

The approach to metal-alkylidene⁶⁰ and metal-alkylidyne⁶¹ chemistry has essentially focused on the attempt to make a bridge between homogeneous and heterogeneous systems⁶² using a preorganized quasiplanar tetraanionic O_4 set of oxygen donor atoms derived from the deprotonated form of calix[4]arene. To make this approach most significant, the choice of tungsten, which has played a major role in both heterogeneous and homogeneous systems since the discovery of the metathesis reaction, and whose ligands of preference contain oxygen donor atoms,^{60c,d} was considered almost compulsory.⁶³ One might wonder what might be the consequence of using the calix[4]arene as ancillary ligand in metal-alkylidene and metal-alkylidyne chemistry. The metal bonded to the nearly planar calix[4]arene skeleton in its cone conformation displays three frontier orbitals, one σ and two π , particularly appropriate for stabilizing the M–C multiple bond functionality, so that alkylidenes and alkylidynes may form spontaneously from conventional alkylation reactions. The other unique role of calix[4]arene, which makes comparisons with the heterogeneous metal–oxide systems² valuable, is the basic surrounding of the metal where the oxygen donor atoms can assist the protonation–deprotonation of alkylidynes and, in general, their reaction with electrophiles. The so-called macrocyclic stabilization⁶⁴ helped greatly in keeping the metal-calix[4]arene fragment resistant to protic acids and strong electrophiles. The use of a tetraanionic macrocycle led to anionic alkylidynes, thus providing the best entry to functionalized alkylidenes. Anionic alkylidynes would also allow one to set up a novel redox chemistry in the field. Within the scheme outlined above, there has been a report⁶³ on: (1) the genesis of W-anionic alkylidynes; (2) their reversible protonation and deprotonation reactions; (3) their metallation with carbophilic metals leading to dimetallic alkylidenes; (4) their unusual transformation into functionalized alkylidenes using appropriate electrophiles; and (5) their oxidative coupling to μ^2 - η^2 : η^2 -acetylene derivatives.⁶³

The attempts to obtain alkyl derivatives of **6** in the reaction with 1 or 2 equiv. of Li or Mg alkylating agents did not lead to the expected products (Scheme 24). On the other hand, when a 3 : 1 molar ratio was used, alkylidyne derivatives **129–131** (Fig. 12) were readily obtained (Scheme 24). The reaction went well also when



SCHEME 24.

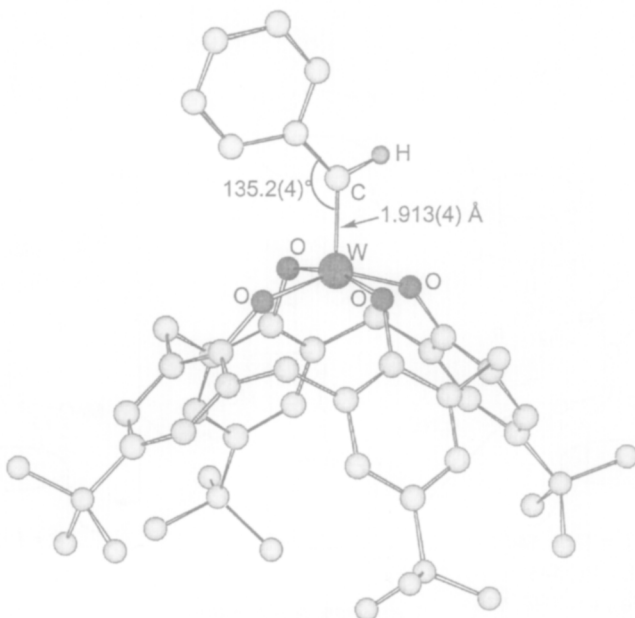
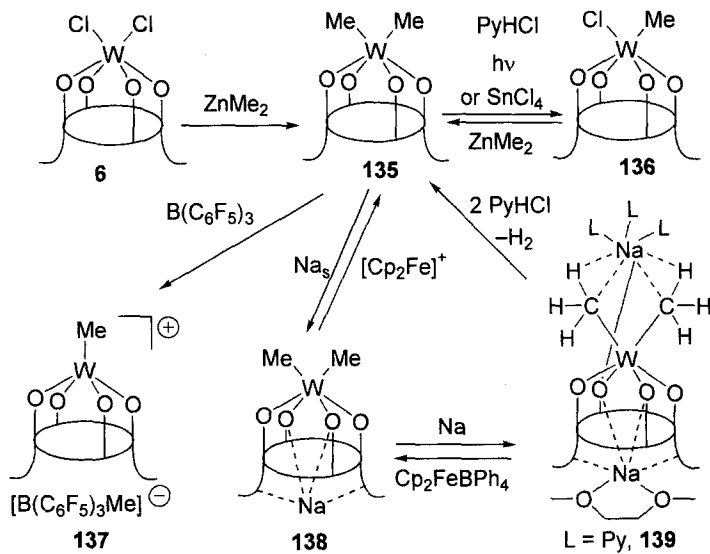
FIG. 12. Crystal structure and selected structural parameters of complex **129**.

β -hydrogens were present, as in the case of **130**. The reaction solvents played an important role both in the selection of the reaction path (α elimination vs reduction) and in the separation of Mg and Li halides. The best results were obtained at low temperature in toluene.⁶³

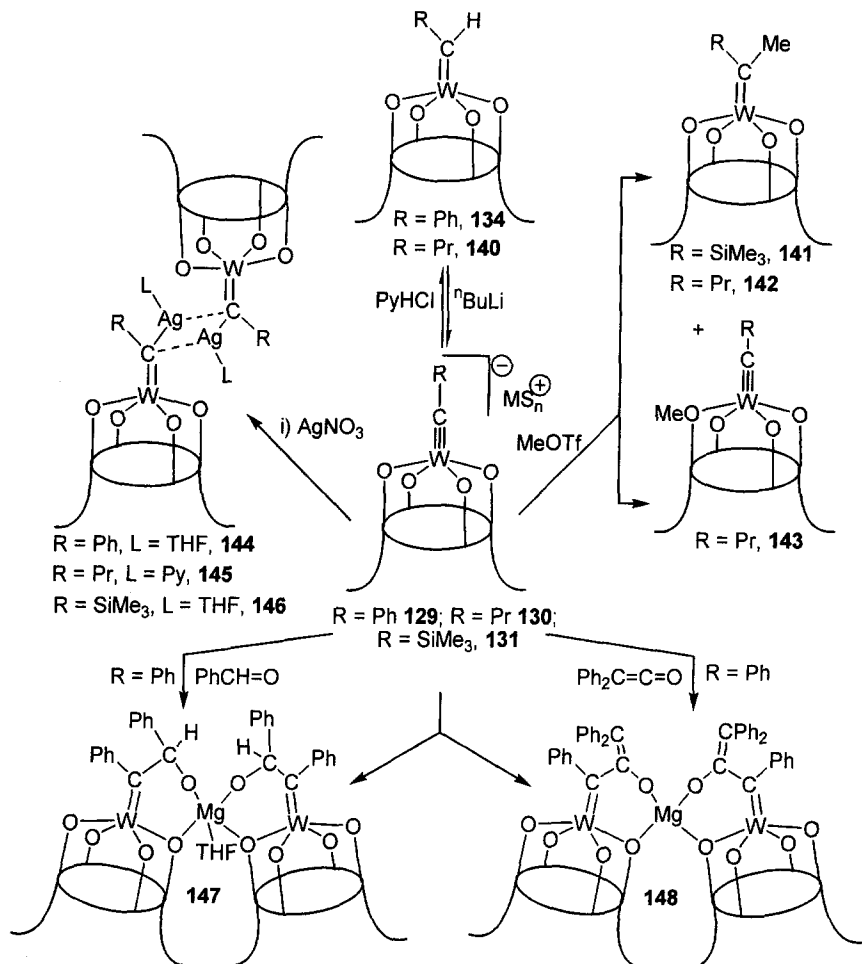
Recent work by Schrock gave evidence of the possibility of obtaining $M\equiv C$ functionalities by loss of H_2 from W(IV) primary alkyls.⁶⁵ This raised the question of the actual mechanism of the direct generation of alkylidyne species described above, especially considering the fact that using 1 or 2 equiv. of MCH_2R ($M = Li, Mg$; $R = Ph, SiMe_3, Bu^n$), reduced, rather than alkylated, species were obtained. The reaction of **6** with $LiCH_2SiMe_3$ was studied in some detail and led to the conclusion that alkylation is an alternative to the reduction path.⁶⁶ Using less reducing alkylating agents in a 2 : 1 ratio, dialkyls/alkylidenes could be prepared. Reacting **6** with butyl-1,4 di-Grignard in a 1 : 1 molar ratio, the dialkyl species **132** was obtained, without the formation of any paramagnetic species.⁶³ The reaction of **6** with $Zn(CH_2Ph)_2$ led to the phenyl alkylidene **134** (Fig. 13). The reaction of **6** with $ZnMe_2$ led to the clean formation of the dimethyl derivative **135**, whose synthesis, acid-base (see complexes **136** and **137**), and redox chemistry (see complexes **138** and **139**) are summarized in Scheme 25.⁶⁷ Complexes **129–131** were found to be thermally and photochemically very stable. Their NMR spectra in coordinating solvents showed a C_{4v} symmetric calix[4]arene moiety. The alkylidyne carbon gave a signal at 260–300 ppm in ^{13}C NMR spectra.

The electron-rich, anionic alkylidyne species seemed to be particularly good candidates for reactions with electrophiles, summarized in Scheme 26.⁶³ The (reversible) protonation of **129–131** led cleanly to the corresponding alkylidenes without any other major change in the coordination sphere of the metal. The deprotonation of the alkylidene by basic solvents (i.e., pyridine), can be followed in the 1H NMR spectrum. Although the protonation of alkylidynes is known, it is not reversible and occurs with important modifications in the coordination geometry and changes in the nature of the donor atoms around the metal.⁶⁸ In the 1H NMR spectra the calix[4]arene moiety appeared to be of C_{4v} symmetry, as in the related η^2 -alkene/alkyne complexes, according to a very small rotational barrier of the alkylidene ligand. A synthetically useful derivatization of the anionic alkylidynes **129–131** is their metalation, which was performed using the carbophilic Ag^+ . The metalation of **129–131** gave the dimers **144–146**. The structure of **145** is displayed in Fig. 14. Alkylidynes can also react with neutral electrophiles, such as a carbonylic functionality, provided it is sterically accessible. The reaction between **129** and benzaldehyde and diphenylketene (Scheme 26) illustrates the possibility of using anionic alkylidynes as organometallic Grignard reagents.⁶³

The presence of a heteroatom at the alkylidene carbon atom moves properties of metal-alkylidene complexes to the borderline of Fischer carbene chemistry.⁶⁹ The

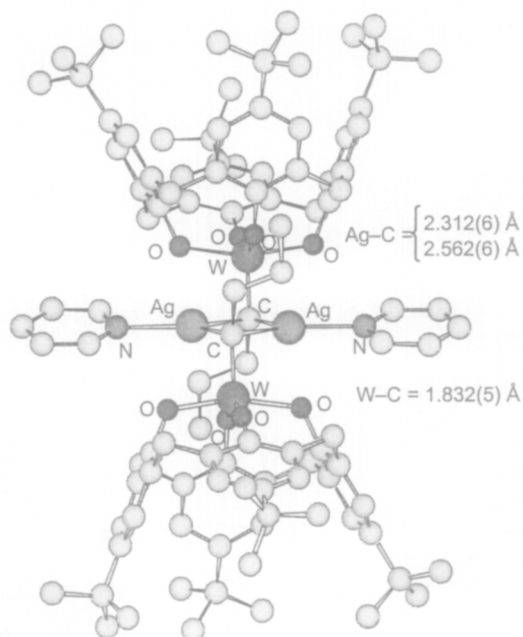
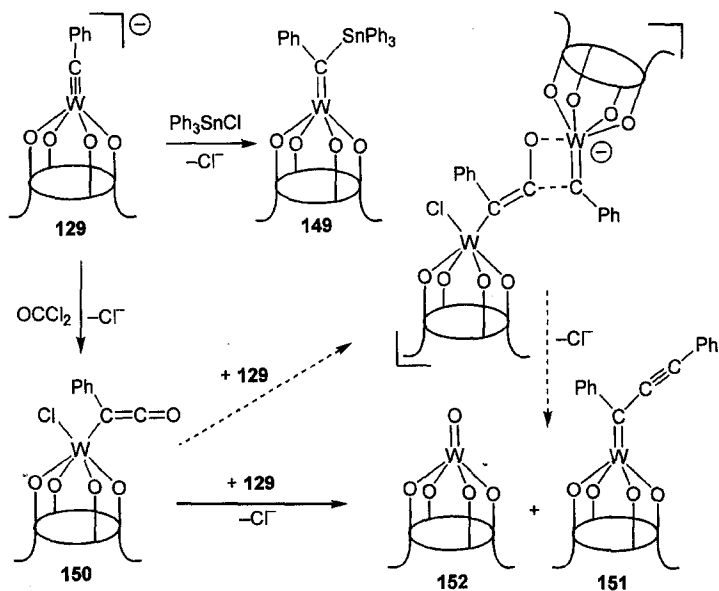
FIG. 13. Crystal structure and selected structural parameters of complex **134**.

SCHEME 25.

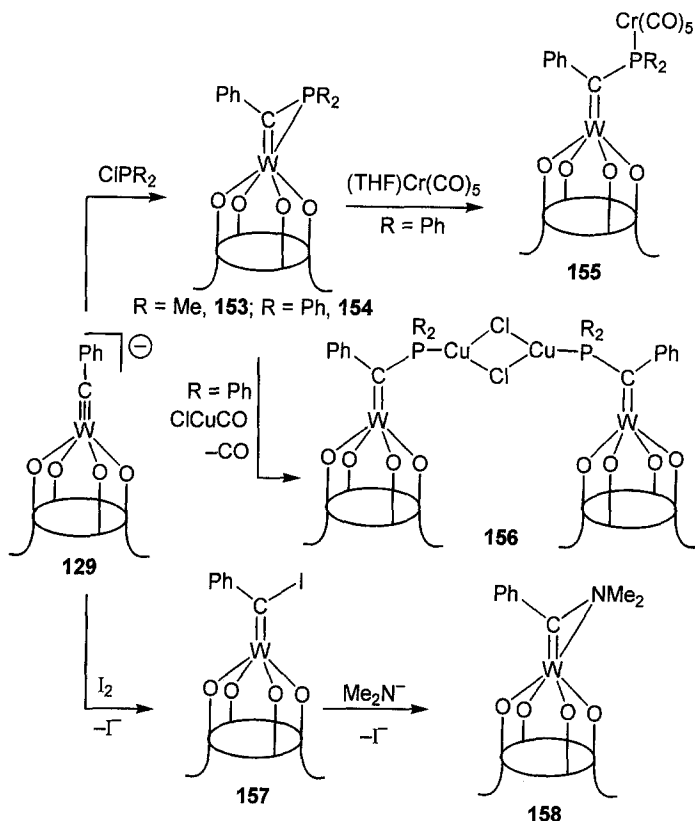


SCHEME 26.

changes in the $\text{M}=\text{C}$ bond polarization caused by the heteroatom and the introduction of functional groups increase the possible use of the metal-alkylidene⁶⁰ synthon both in organic and organometallic synthesis. Anionic tungsten-alkylidene derivatives, exemplified by complex **129**⁶³ in Scheme 27, are the appropriate starting materials for entering the area of functionalized metal-alkylidenes.^{70,71} Two major complementary synthetic routes have been devised for this purpose.⁷² The first is the reaction of **129** with a variety of electrophiles (see Schemes 27 and 28), such as Ph_3SnCl (see complex **149** in Scheme 27), COCl_2 (see complexes **150** and **151** in Scheme 27), ClPR_2 (see complexes **153** and **154** in Scheme 28).

FIG. 14. Crystal structure and selected structural parameters of complex **145**.

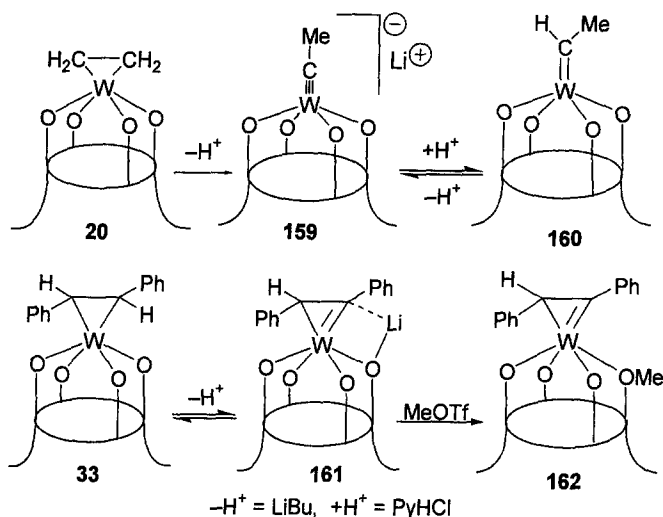
SCHEME 27.



SCHEME 28.

The structure of **151**, along with some structural parameters, is displayed in Fig. 15. Another interesting approach⁷² to functionalized alkylidenes is reported in Scheme 28, and resembles the methodology leading to functionalized carbenes via nucleophilic substitution at halocarbene ligands, developed by Roper.⁷³ Oxidation of **129** with I_2 led to **157**,^{63,72} where iodine can be potentially replaced by a number of organic or organometallic nucleophiles. The donor atoms introduced into the alkylidene functionality have been used for metal complexation (see complexes **155** and **156** in Scheme 28).

Another quite relevant synthetic methodology leading to metal-alkylidenes and alkylidynes has been discovered studying the olefin rearrangement assisted by the metal-oxo-surface modeled by tungsten(IV)-calix[4]arene.²² Once more, advantage is taken of the metal having the appropriate frontier orbitals for establishing a σ and two π bonds along the axial direction. This study addressed a few



SCHEME 29.

The electron-deficient nature of calixarene-supported tungsten(VI) makes α -carbon atoms susceptible to proton abstraction, the resulting carbanion being stabilized by donation to the metal and charge delocalization onto the oxygen atoms.¹⁹ The reaction of complex **33** with BuLi in toluene at low temperature (-80°C) led to the clean deprotonation of the 1,2-disubstituted η^2 -olefin to give the anionic 1-metallacyclopropene, **161** (Scheme 29). The attempted deprotonation of the terminal olefin in **20** led to the alkylidyne **159**, most likely via an anionic 1-metallacyclopropene intermediate, analogous to **161**, undergoing an irreversible 1,2 proton shift. Protonation (PyHCl) of **159** gave the corresponding alkylidene **160**. Complexes **159** and **160** were identified by their characteristic spectroscopic features: a signal at 283.7 ppm, with a $J_{\text{CW}} = 283.7$ Hz, in the ^{13}C NMR spectrum of **159**, and a quartet at 9.93 ppm ($J = 7.8$ Hz, 1H) in the ^1H NMR of **160**. The outcome of this deprotonation–protonation sequence is the isomerization of an η^2 -olefin to an alkylidene. Such a rearrangement, which was proposed⁷⁴ to occur in heterogeneous systems, was seldom observed in solution.⁷⁵ More common are examples of the reverse rearrangement.⁷⁶

A fundamental point in both molecular and surface chemistry concerns the involvement of donor atoms (from the ancillary ligand or the surface) in acid/base reactions.⁷⁷ The reaction of H^+ (from PyHCl) and Me^+ (from MeOTf) with the anionic 1-metallacyclopropene **161** (Scheme 29) has been investigated. Although protonation gave back the starting material as the only product observed in solution (^1H NMR), the reaction with MeOTf led to the neutral 1-metallacyclopropene, **162**,

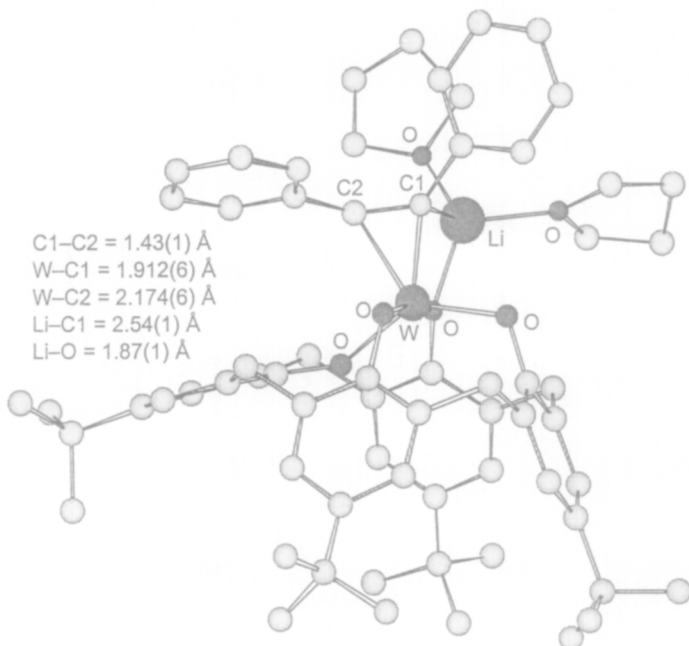
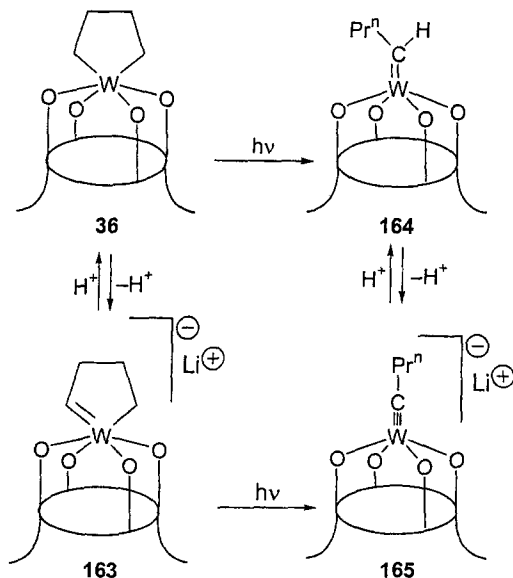


FIG. 16. Crystal structure and selected structural parameters of complex **161**.

alkylated at the oxygen and not at the carbon center (at least when performing the reaction at -80°C in toluene). This suggests that the oxygen atoms are the preferred site of attack of electrophiles on **161** under kinetic control. It can be supposed that protonation also occurs first on oxygen atoms, and that the resulting protonated analogue of **162**, due to the high mobility of H^{+} , readily rearranges to the observed product. The structure of **161**²⁸ in Fig. 16, showing the binding of the lithium cation to both the calix[4]arene oxygen and the carbon of the metallacyclopentene, exemplifies the assistance of the oxygens from calix[4]arene in the reactions with protons and electrophiles.

The metallacycle **36** (see Scheme 6) undergoes, under mild conditions, some remarkable transformations, such as the deprotonation (LiBu) to the 1-metallacyclopentene **163**, which can be reversibly protonated (PyHCl) back to the starting material (Scheme 30).²² Both acid-base interrelated metallacycles **36** and **163**, which are thermally stable, rearrange when irradiated (Xe lamp) to the alkylidene **164** and alkylidyne **165**, respectively.²² Although the photochemical generation of alkylidenes from dialkyls is well established,⁷⁸ it has never been observed on a metallacycle, where such a reaction constitutes an isomerization. More interesting still is the rearrangement of **163** to **165**, which represents the first



SCHEME 30.

example of the photochemical generation of an alkylidyne. It should be noted that this photochemical path represents the best synthetic approach to both **164** and **165**.²²

Although the generation of $\text{M}-\text{C}$, $\text{M}=\text{C}$, and $\text{M}\equiv\text{C}$ functionalities directly from hydrocarbons has been recognized for a long time as a superior feature of heterogeneous over homogeneous catalysts, the investigation of the chemistry of the $\text{d}^2\text{-}[\{p\text{-Bu}^t\text{-calix[4]-(O)}_4\}\text{W}]$ fragment, and in particular of η^2 -olefin species, led to the discovery of a variety of olefin rearrangements which are very close to those supposed to occur on metal oxides or other active surfaces (Chart 8).

Such rearrangements are driven by light, acids, and bases, or occur under reducing conditions. This means that they can be controlled and, in perspective, used to generate *in situ* active species from inert precursors. These rearrangements lead to metallacycles, alkylidenes, and alkylidyne, where the organometallic fragment derives from one of the cheapest building blocks of chemistry, ethylene. The protonation-deprotonation of alkylidene and alkylidyne, respectively, beyond their synthetic value as a means to modify the ligand and as an access to new complexes, has shed new light on the underestimated role of coordinated donor atoms in acid/base reactions, both in homogeneous and surface chemistry. Although some of these transformations are known for different metal fragments, the occurrence both on a single fragment and on a metal-oxo-surface is unique and unprecedented (see Chart 8).

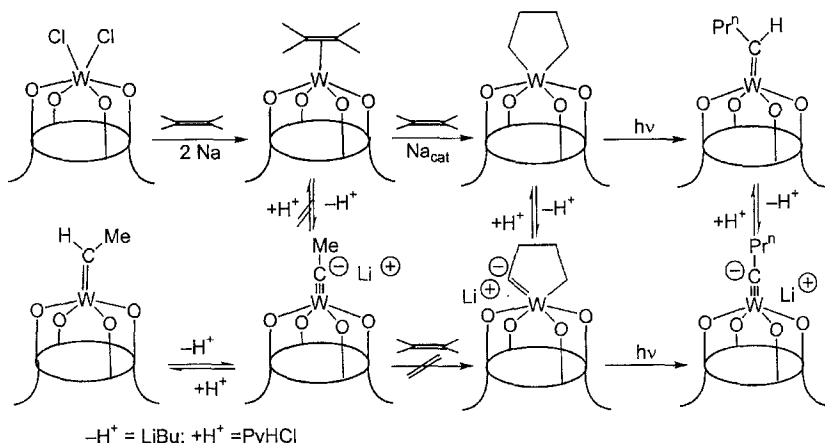


CHART 8. Ethylene rearrangements over a W-oxo surface modeled by W-calix[4]arene.

Following the study on the olefin rearrangements^{22b} over a tungsten-calixarene oxo surface, attention then focused on the possibility of discovering a synthetic methodology for intercepting the 1-metallacyclopropene, which paves the way to metal-alkylidenes,⁶⁰ or other related species.^{79,80} A recent report²⁸ discusses the general synthesis of alkene and alkyne complexes of W(IV)-calix[4]arene, which have been converted into anionic 1-metallacyclopropene by either deprotonation of the alkene or addition of hydrides to the alkyne. By the use of suitably substituted alkenes and alkynes, 1-metallacycloprenes have been isolated in stable forms, which do not rearrange to the corresponding alkylidynes. They have been used for studying the reactivity toward electrophiles and one-electron oxidizing agents.

The alkene-W complexes used in this study are complexes **33**, **166**, and **168** (Schemes 5 and 31). The deprotonation of the W-alkene functionality has been carried out on **166**, which has three methyl substituents at the C=C bond, in order to prevent any rearrangement of the 1-metallacyclopropene to the corresponding alkylidyne.^{22b} The reaction of **166** with LiBu led to the 1-metallacyclopropene **169** (Scheme 32), which was isolated in quite good yield. The alkylidene **169**, a very stable compound, was characterized both in solution and in the solid state.²⁸ The ¹H NMR spectrum shows a four-fold symmetry calixarene skeleton, while the ¹³C NMR spectrum contains a resonance at 271.0 ppm for the alkylidene carbon.

Complex **169** is very susceptible to electrophilic attack, as shown in Scheme 32. The protonation of **169** with PyHCl gave back **166**. In this reaction, the assistance of one of the oxygens as the primary site of the protonation cannot be excluded. The alkylation with MeOTf, unlike in the case of **161** (see Scheme 29),²² occurs at the alkylidene carbon as well, forming the 2,3-dimethyl-2-butene-W derivative **167**, which was obtained also by the direct synthesis given in Scheme 31.

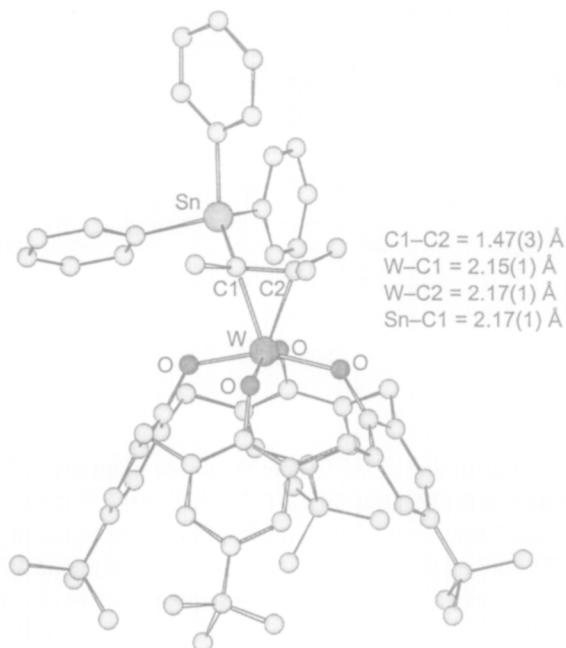
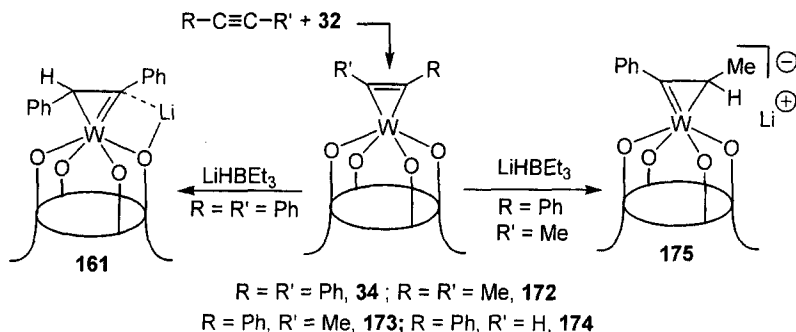


FIG. 17. Crystal structure and selected structural parameters of complex **170**.

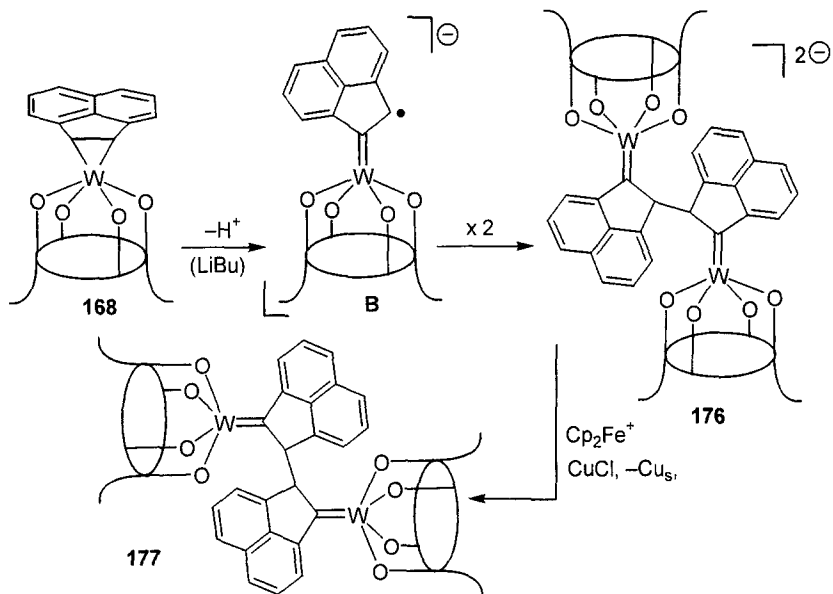
The metallation with Ph_3SnCl follows the same pathway leading to the tin derivative **170**, which can be a useful material in transmetallation reactions.²⁸ Its structure is displayed in Fig. 17. The anionic 1-metallacyclopropene **169** undergoes one-electron oxidation by a variety of reagents, the best one being $[\text{CuCOCl}]$. The reaction proceeds with the formation of a copper metal mirror and **171**. The formation of **171** requires the intermediacy of a free radical species like **A** (Scheme 32), preferentially undergoing dimerization rather than hydrogen abstraction from the solvent. There is no evidence of the formation of an alkylidene coming from the latter route, even in trace amount. DFT calculations support that the removal of one electron from **169** gives a free radical-type metallacyclop propane prone to W–C homolytic cleavage at the most substituted carbon.

A different synthetic access to a 1-metallacyclop propene, which can be a versatile organometallic synthon, is displayed in Scheme 33. The mono-alkyne derivatives of W(IV)-calix[4]arene are easily accessible through the thermal displacement of cyclohexene from **32** using the appropriate acetylenes. The reaction led to complexes **34** and **172–174**. The proposed 3-metallacyclop propene has been confirmed from the spectroscopic and the X-ray data. The ^1H NMR data reveal a cone conformation of the calixarene with a four-fold symmetry, for which the



SCHEME 33.

explanation is similar to that given for the W-alkene complexes. The addition of the hydride to **34** via the reaction of LiHBEt_3 led to the 1-metallacycloprenene **161**,^{79,80} which has been reported to form from the deprotonation of the stilbene complex **33**.²² The bond lengths within the metallacycloprenene units (complexes **161** and **169**),²⁸ support the proposed bonding sequence. In all structures, the W–C single bonds are longer than 2.0 Å, though there is a significant difference between the metal binding to sp^3 (complexes **169** and **161**) or sp^2 carbons (complex **34**). The W–C (alkylidene carbon) bond distances in **169** and **161**, 1.916(5) and 1.912(6) Å, respectively, are in agreement with the presence of the 1-metallacycloprenene functionality. The C–C bond length varies from 1.43_{av} Å in **169** and **161** to ca. 1.30 Å in **34**. Although the lithium cation is interacting at a rather short distance [2.541(13) Å] (see Fig. 16) with one of the carbons of the C_2 unit in **161**, this did not affect the structural parameters mentioned above. The structural analysis reported allows comparison between the two isomeric metallacycloprenenes, namely **161** and **34**. There is a distinctive behavioral difference between **161** (Scheme 29) and **169** (Scheme 32) in the reaction with MeOTf , which in the former case led to the alkylation of the calixarene oxygen, while in the case of **169** the methylation occurred at the 1-metallacycloprenene with the formation of **167**. The protonation of **161**, in contrast, proceeds as in the case of **169**, thus generating the *trans*-stilbene derivative, **33**. DFT calculations support the assistance of oxygen as a primary site of the protonation,^{4,22b,63} so that the protonation of anionic 1-metallacycloprenene would occur via the proton transfer from the oxygen to the carbon.²⁸ The regiochemistry of the reaction of nonsymmetric alkyne complexes with hydrides is exemplified in the reaction of **173** with LiHBEt_3 , which leads to **175**. In other cases too, the nucleophilic attack seems to occur at the carbon of the alkyne bearing the most electron donating substituents. Both compounds **161** and **175** have a ^{13}C NMR resonance for the alkylidene carbon at ca. 250 ppm.



SCHEME 34.

The acenaphthylene complex **168**, when submitted to the deprotonation reaction, revealed the consequence on the stability of the 1-metallacyclopropene as a function of the substituent at the olefin functionality, mainly in terms of steric constraints.²⁸ A particular instability is associated with the formation of a 1-metallacyclopropene fused with a C_5 ring. As a matter of fact, the deprotonation of **168** led to the formation of **176**, presumably via the intermediacy of **B**. It is probable that **B** originates from the homolytic cleavage of the W–C single bond of the 1-metallacyclopropene. The dimerization of **B** would lead to the dinuclear W(V) paramagnetic bis-alkylidene shown in Scheme 34. Complex **176** undergoes either a one- or a two-electron oxidation. In the latter case, the reaction, carried out using either CuCl or $\text{Cp}_2\text{FeBPh}_4$, led to the formation of the diamagnetic derivative **177** (Fig. 18). The ^1H and ^{13}C NMR spectra of **177** did not show any peculiarity or major difference in respect to the other W-alkylidene derivatives.⁶³ Complexes **176** and **177** are structurally very similar, notwithstanding the oxidation state of the metal and the presence of two lithium counterions binding at the oxygens of the calixarene in **176**.²⁸ The 1-metallacyclopropene anions in Schemes 32, 33, and 34 should be considered as the electronic equivalent of metalla-alkylidyne anions, to which they rearrange when the substituents at the two carbons are protons. The two related species resemble each other in, among other things, their behavior toward oxidizing agents. Their dimerization can be

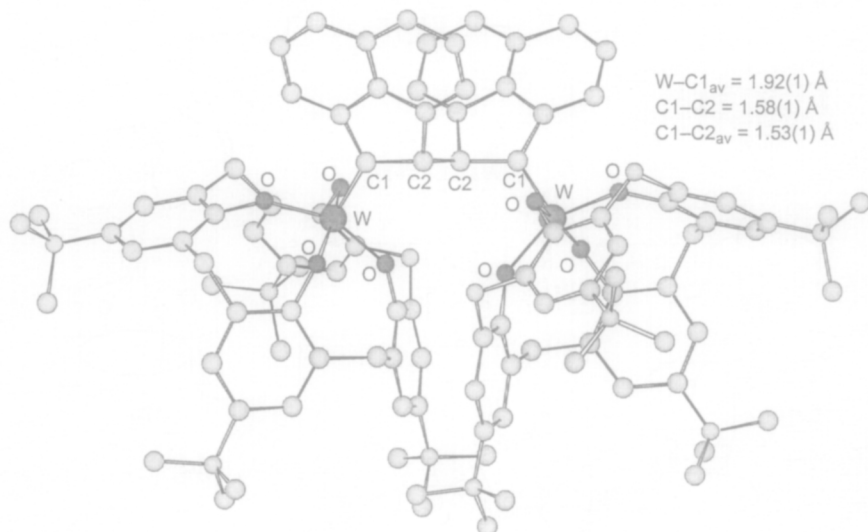


FIG. 18. Crystal structure and selected structural parameters of complex **177**.

achieved by one-electron oxidation. In the case of alkylidynes, their dimerization led to the formation of $\mu : \eta^2 : \eta^2$ acetylene,⁶³ while in Scheme 32 the formation of a dinuclear bis-alkylidene is observed. The alternative synthesis of the latter compounds passes through the deprotonation of strained olefins, which undergo spontaneous evolution to dinuclear alkylidenes. The electronic structure and reactivity pathway of the 1-metallacyclopentene functionality has been analyzed using a DFT approach.²⁸

Although the alkylidene- and alkylidyne-metal functionalities have a very relevant impact on preparative chemistry and catalysis,^{60,61,70} their access is limited to only a few synthetic methodologies. Metalla-calix[4]arenes allowed a direct synthesis of metal-alkylidenes and -alkylidynes from among the most common organic functionalities, namely from olefins, acetylenes (see above), ketones, and aldehydes. This latter entry in the field opens much wider possibilities in the use of such functionalities as synthons in organic synthesis.⁷⁰ In addition, this novel synthetic methodology has been applied to niobium,⁸¹ having a limited number of alkylidene⁸² and alkylidyne⁸³ derivatives, by the use of *p*-Bu^t-calix[4]arene tetraanion as ancillary ligand.⁸ The active compound able to access the chemistry outlined above is a Nb^{III}-calix[4]arene dimer (**29** in Schemes 4 and 35), which contains an Nb=Nb double bond.^{6,8,26,27} This section covers in particular the genesis of Nb-alkylidenes from ketones and aldehydes and their reversible deprotonation–protonation to bridging alkylidynes⁸ along with the use of the [Nb(III)-calix[4]arene] dimer in the McMurry⁸⁴ synthesis of olefins

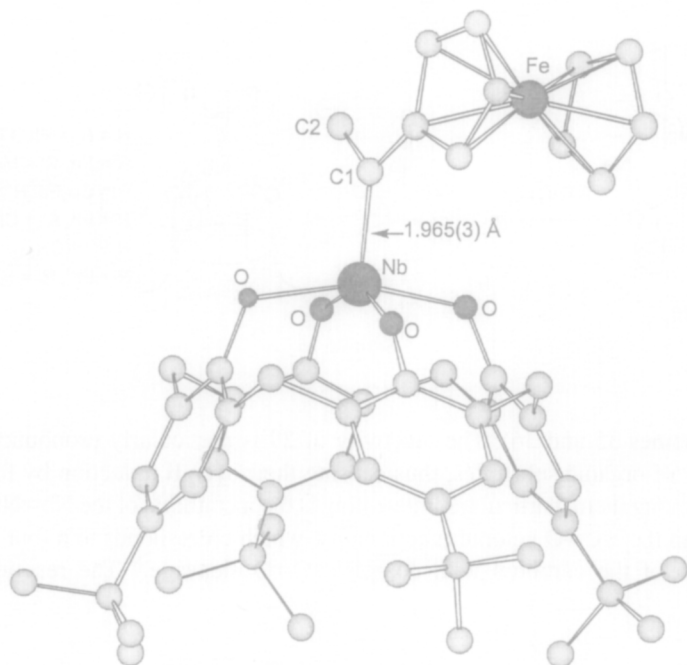
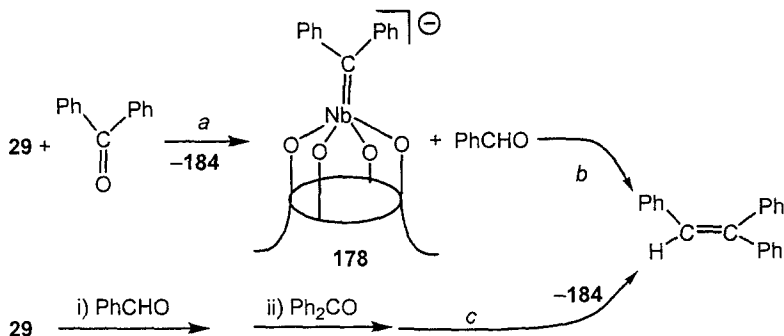


FIG. 19. Crystal structure and selected structural parameter of complex **180**.

proceeds with the formation of the corresponding alkylidenes **178–183** and the oxo-niobium(V) derivative, **184** (Scheme 35). The structure of **180** is displayed in Fig. 19. The reaction has some notable peculiarities. It is not very sensitive to the substituent at the carbonyl functionality, thus occurring equally well with aromatic, mixed, or aliphatic ketones. The synthetic value of the reaction lies in the easy separation of the alkylidene from the corresponding oxo-compound, **184**, thus allowing the introduction of the metal-alkylidene functionality, via the presence of a ketonic group in a variety of organic substrates. Although the reaction with ketones usually led to the formation of the metal-oxo compounds and the corresponding olefin from the coupling,⁸⁵ in the present case the isolation of the intermediate metal-alkylidene was quite easy. Aldehydes usually behave differently and in a more complex manner in their reaction with low-valent metals, while, with the $[\text{Nb}=\text{Nb}]$ bond, the presence of the hydrogen at the carbonyl functionality does not induce a different pathway of reactivity. Unlike previous reports in the field,⁸⁶ the reaction of **29** with aldehydes (see Schemes 35 and 36) leading to **183** and **185** and the corresponding oxo-niobium(V) complex **184** parallels the reactions with ketones. All the Nb-alkylidenes mentioned above possess a very low energy barrier for the rotation of the alkylidene functionality between the two isoenergetic positions for the formation of the metal-C π bonding.⁸ The Nb=C distances

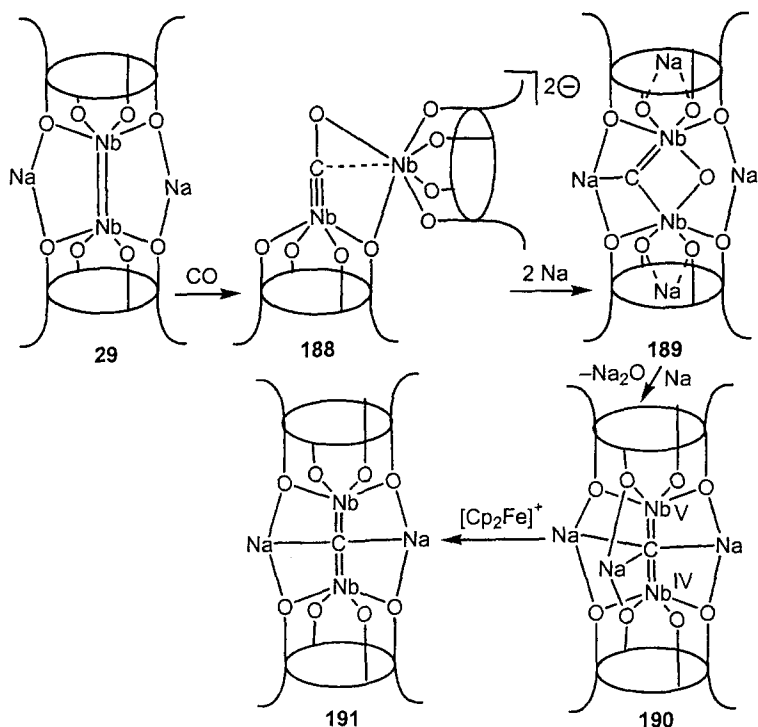


SCHEME 37.

[1.96 Å_{av}] lie in the range of the few Nb-alkylidenes reported.⁸⁷ The protonation of **185** using PyHCl led to the formation of the corresponding benzyl derivative **186**, which was deprotonated back to the alkylidene form using sodium naphthalene. Alkylidene **185** underwent sodium naphthalenide induced deprotonation to the alkylidyne dimer **187**, which can be quite easily protonated back to **185**. An interesting observation in this context is the proton transfer occurring between **186** and **187**, which can be assisted by a quite basic solvent like pyridine and leads to the formation of **185** (Scheme 36). Such a finding is diagnostic of the easy protonation–deprotonation of M–C functionalities bonded to a calix[4]arene moiety.

The synthetic method leading to Nb-alkylidenes and Nb-alkylidyne was particularly successful, due to a quite remarkable difference in the reaction rate of **29** with ketones or aldehydes, vs the subsequent reaction of the alkylidene with ketones and aldehydes (see Scheme 37). The former reaction takes a few minutes at –40°C, while the latter one occurs in hours at room temperature.⁸⁸ The reaction between **178** and benzaldehyde led to triphenylethylene and the niobyl derivative **184**. Due to the difference in reaction rates between *a* and *b* in Scheme 37, it was found that the sequential addition of two different ketones or aldehydes to a THF solution of **29** produced a nonsymmetric olefin in a stepwise McMurry-type reaction.⁸⁴ This is exemplified in the coupling shown in reaction *c* (Scheme 37). The proposed reaction pathway does not involve the intermediacy of a pinacolato ligand and therefore differs from the mechanism of the McMurry reaction and related reductive couplings at activated metal sites.⁸⁹

Taking advantage of the reactivity of the [Nb=Nb] bond in complex **29**, it was possible to achieve the formation of metal-carbido functionalities, related to metal-alkylidenes, directly from carbon monoxide and under very mild conditions.²⁷ The reductive cleavage of carbon monoxide using organometallic fragments represents a discrete homogeneous analogue to the CO dissociation to carbide and oxide on many metal surfaces.⁹⁰ The few existing homogeneous analogues of the CO dissociation, which are mainly due to Wolczanski,⁹¹ Chisholm,⁹² and Cummins,⁹³



SCHEME 38.

often follow convoluted pathways, as is also the case in cluster chemistry.^{90d} Complex **29**, which is able to perform the four-electron reduction of dinitrogen^{6,26} and ketones,⁸ reacts with carbon monoxide (1 atm, -40°C) leading to the oxyalkyldi-dyne dianion **188** (Scheme 38), which occurs in a tetranuclear ion-pair form made up of two dianions bridged by four sodium cations. The structural parameters of the $[\text{Nb}_2\text{CO}]$ fragment in **188** proves the four-electron reduction of carbon monoxide, with the two Nb ions playing completely different roles. The structure and some structural parameters of **188** are shown in Fig. 20. In the aforementioned reduction of CO, one should not disregard the driving force associated with the strong oxygen-alkali cation interactions. The further reduction of **188** using 2 equiv. of sodium metal led to the cleavage of the residual C–O bond and the formation of **189**. The two Nb-calix[4]arene moieties are joined by a μ -carbido and a μ -oxo ligand (Fig. 21). The bent bonding mode of a carbido bridging two transition metal ions in dinuclear complexes is unique.⁹⁴

The two-electron reductive cleavage of C–O from **188** to **189** was followed by the reductive deoxygenation of **189** and the formation of a linear bridging

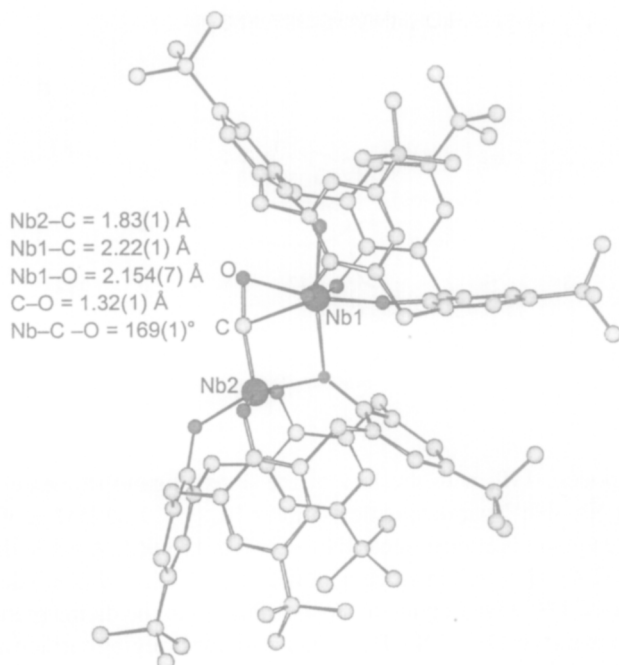


FIG. 20. Crystal structure and selected structural parameters of complex **188**.

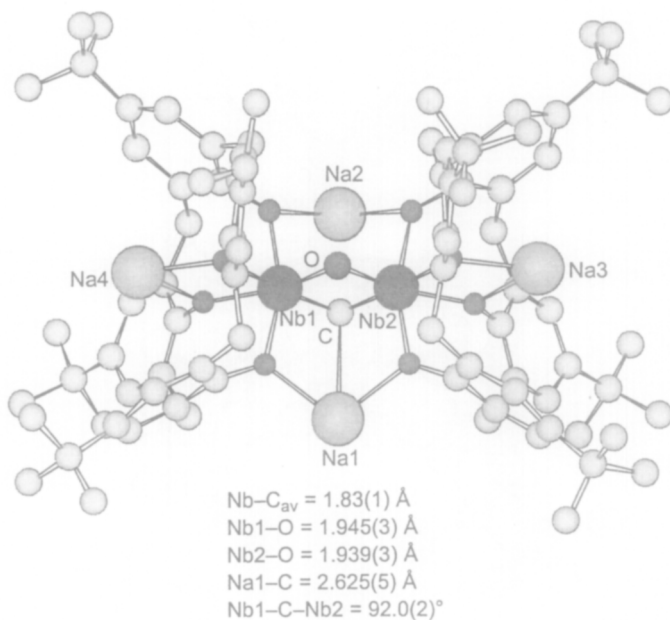
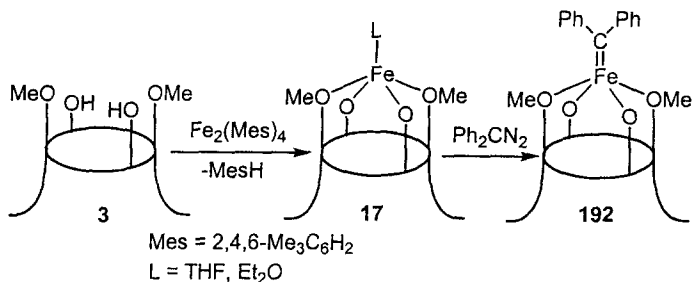
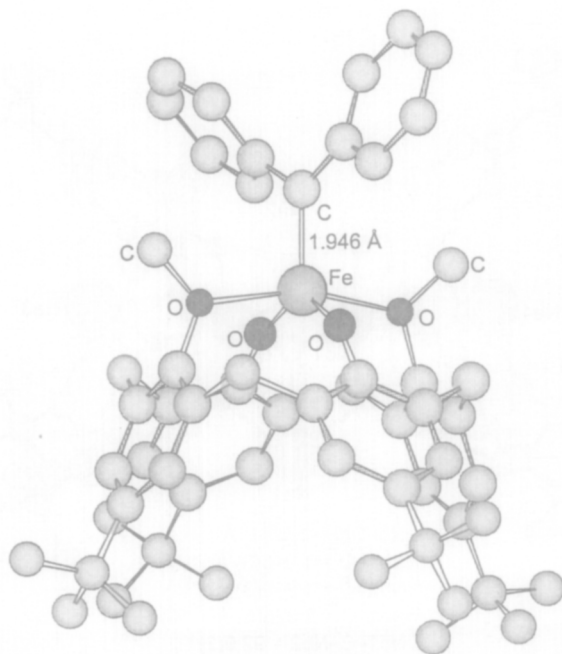


FIG. 21. Crystal structure and selected structural parameters of complex **189**.



SCHEME 39.

carbido compound, **190**, with the loss of the μ -oxo ligand (Scheme 38). Complex **190** is a $\text{Nb}^{\text{V}}\text{-Nb}^{\text{IV}}$ paramagnetic complex [$\mu_{\text{eff}} = 1.65 \text{ BM}$ at 300 K]. The Nb-C-Nb fragment is almost linear [Nb-C-Nb , $173.9(2)^\circ$], while the Nb-C_{av} distance [$1.922(4) \text{ \AA}$] is well in agreement with a $\text{Nb}=\text{C}(\text{alkylidene})$ description.⁸ The oxidation of **190** with 1 equiv. of $\text{Cp}_2\text{FeBPh}_4$ led to the diamagnetic complex **191**, which shows a typical ^{13}C NMR resonance for the bridging carbide at 257 ppm.

FIG. 22. Crystal structure and selected structural parameter of complex **192**.

Other synthetic approaches have been explored for binding an alkylidene functionality to a metalla-calix[4]arene. Among them, the reaction of diazoalkanes with coordinatively unsaturated metalla-calix[4]arenes deserves particular mention. The synthesis of an unusual high-spin (5.2 BM at 292 K) iron(II)-carbene, **192**, is displayed in Scheme 39,¹³ and its structure is shown in Fig. 22.

C. Outlook

A novel generation of organometallic catalysts is expected to come out of the chemistry of metalla-calix[4]arenes. The preorganized oxo-surface of calix[4]arene anions offers a unique opportunity for making molecular model compounds competitive with the well-known heterogeneous oxo-catalysts. They can challenge the heterogeneous systems in assisting the hydrocarbon rearrangements, the polymerization of various types of olefins, and the oxo-transfer processes.

ACKNOWLEDGMENTS

We thank the "Fonds National Suisse de la Recherche Scientifique" (Bern, Switzerland, Grant No. 20-53336.98), Action COST D9 (European Program for Scientific Research, OFES No. C98.008), and Fondation Herbette (University of Lausanne) for financial support.

REFERENCES

- (1) (a) Gutsche, C. D. *Calixarenes*; The Royal Society of Chemistry: Cambridge, U.K., 1989; (b) Gutsche, C. D. *Calixarene Revisited*; The Royal Society of Chemistry: Cambridge, U.K., 1998; (c) *Calixarenes, A Versatile Class of Macrocyclic Compounds*; Vicens, J.; Böhmer, V., Eds.; Kluwer: Dordrecht, 1991; (d) Bohmer, V. *Angew. Chem., Int. Ed. Engl.* **1995**, *34*, 713; (e) Wieser, C.; Dieleman, C. B.; Matt, D. *Coord. Chem. Rev.* **1997**, *165*, 93; (f) Roundhill, D. M. *Progr. Inorg. Chem.* **1995**, 533; (g) Ikeda, A.; Shinkai, S. *Chem. Rev.* **1987**, *97*, 1713.
- (2) (a) Thomas, J. M.; Thomas, W. J. *Principles and Practice of Heterogeneous Catalysis*; VCH: Weinheim, Germany, 1997; (b) *Mechanisms of Reactions of Organometallic Compounds with Surfaces*; Cole-Hamilton, D. J.; Williams, J. O., Eds.; Plenum: New York, 1989; (c) Kung, H. H. *Transition Metal Oxides: Surface Chemistry and Catalysis*; Elsevier: Amsterdam, 1989; (d) Hoffmann, R. *Solid and Surfaces, A Chemist's View of Bonding in Extended Structures*; VCH: Weinheim, Germany; 1988; (e) *Catalyst Design, Progress and Perspectives*; Hegedus, L., Ed., Wiley: New York, 1987; (f) Bond, G. C. *Heterogeneous Catalysis, Principles and Applications, H. Ed.*; Oxford University Press: New York, 1987.
- (3) For related molecular approaches to oxo-surfaces binding organometallic functionalities, see: (a) Chisholm, M. H. *Chemtracts-Inorg. Chem.* **1992**, *4*, 273; (b) Kläui, W. *Angew. Chem., Int. Ed. Engl.* **1990**, *29*, 627; (c) Feher, F. J.; Budzichowski, T. A. *Polyhedron* **1995**, *14*, 3239; (d) Nagata, T.; Pohl, M.; Weiner, H.; Finke, R. G. *Inorg. Chem.* **1997**, *36*, 1366; (e) Pohl, M.; Lyon, D. K.; Mizuno, N.; Nomiy, K.; Finke, R. G. *Inorg. Chem.* **1995**, *34*, 1413.
- (4) Floriani, C. *Chem. Eur. J.* **1999**, *5*, 19.
- (5) (a) Gardiner, M. G.; Lawrence, S. M.; Raston, C. L.; Skelton, B. W.; White, A. H. *Chem. Commun.* **1996**, 2491; (b) Gardiner, M. G.; Koutsantonis, G. A.; Lawrence, S. M.; Nichols,

- P. J.; Raston, C. L. *Chem. Commun.* **1996**, 2035; (c) Gibson, V. C.; Redshaw, C.; Clegg, W.; Elsegood, M. R. *J. J. Chem. Soc. Chem. Commun.* **1995**, 2371; (d) Acho, J. A.; Doerrer, L. H.; Lippard, S. J. *Inorg. Chem.* **1995**, *34*, 2542; (e) Olmstead, M. M.; Sigel, G.; Hope, H.; Xu, X.; Power, P. P. *J. Am. Chem. Soc.* **1985**, *107*, 8087; (f) Delaigue, X.; Hosseini, M. W.; Leize, E.; Kieffer, S.; Van Dorsselaer, A. *Tetrahedron Lett.* **1993**, *34*, 7561; (g) Hajek, F.; Graf, E.; Hosseini, M. W.; De Cian, A.; Fischer, J. *Tetrahedron Lett.* **1997**, *38*, 4555; (h) Atwood, J. L.; Bott, S. G.; Jones, C.; Raston, C. L. *J. Chem. Soc., Chem. Commun.* **1992**, 1349; (i) Atwood, J. L.; Junk, P. C.; Lawrence, S. M.; Raston, C. L. *Supramol. Chem.* **1996**, *7*, 15.
- (6) Caselli, A.; Solari, E.; Scopelliti, R.; Floriani, C.; Re, N.; Rizzoli, C.; Chiesi-Villa, A. *J. Am. Chem. Soc.* **2000**, *122*, 3652.
- (7) Corazza, F.; Floriani, C.; Chiesi-Villa, A.; Guastini, C. *J. Chem. Soc., Chem. Commun.* **1990**, 1083.
- (8) Caselli, A.; Solari, E.; Scopelliti, R.; Floriani, C. *J. Am. Chem. Soc.* **1999**, *121*, 8296.
- (9) Castellano, B.; Solari, E.; Floriani, C.; Re, N.; Chiesi-Villa, A.; Rizzoli, C. *Chem. Eur. J.* **1999**, *5*, 722.
- (10) Corazza, F.; Floriani, C.; Chiesi-Villa, A.; Rizzoli, C. *Inorg. Chem.* **1991**, *30*, 4465.
- (11) Giannini, L.; Solari, E.; Floriani, C.; Re, N.; Chiesi-Villa, A.; Rizzoli, C. *Inorg. Chem.* **1999**, *38*, 1438.
- (12) Zanotti-Gerosa, A.; Solari, E.; Giannini, L.; Floriani, C.; Re, N.; Chiesi-Villa, A.; Rizzoli, C. *Inorg. Chim. Acta* **1998**, *270/1–2*, 298.
- (13) (a) Giusti, M.; Solari, E.; Giannini, L.; Floriani, C.; Chiesi-Villa, A.; Rizzoli, C. *Organometallics* **1997**, *16*, 5610; (b) Esposito, V.; Solari, E.; Floriani, C.; Re, N.; Rizzoli, C.; Chiesi-Villa, A. *Inorg. Chem.* **2000**, *39*, 2604.
- (14) Castellano, B.; Solari, E.; Floriani, C.; Scopelliti, R.; Re, N. *Inorg. Chem.* **1999**, *38*, 3406.
- (15) Castellano, B.; Solari, E.; Floriani, C.; Re, N.; Chiesi-Villa, A.; Rizzoli, C. *Organometallics* **1998**, *17*, 2328.
- (16) Hessenbrouck, J.; Solari, E.; Floriani, C.; Re, N.; Rizzoli, C.; Chiesi-Villa, A. *J. Chem. Soc., Dalton Trans.* **2000**, 191.
- (17) Giannini, L.; Solari, E.; Zanotti-Gerosa, A.; Floriani, C.; Chiesi-Villa, A.; Rizzoli, C. *Angew. Chem., Int. Ed. Engl.* **1996**, *35*, 85.
- (18) Unpublished results.
- (19) (a) *Early Transition Metal Clusters with π -Donor Ligands*; Chisholm, M. H., Ed.; VCH: New York, 1995; (b) Nugent, W. A.; Mayer, J. M. *Metal-Ligand Multiple Bonds*; Wiley: New York, 1988.
- (20) Giannini, L.; Solari, E.; Zanotti-Gerosa, A.; Floriani, C.; Chiesi-Villa, A.; Rizzoli, C. *Angew. Chem., Int. Ed. Engl.* **1997**, *36*, 753.
- (21) Zanotti-Gerosa, A.; Solari, E.; Giannini, L.; Floriani, C.; Chiesi-Villa, A.; Rizzoli, C. *Chem. Commun.* **1997**, 183, and references therein.
- (22) (a) Giannini, L.; Solari, E.; Floriani, C.; Chiesi-Villa, A.; Rizzoli, C. *J. Am. Chem. Soc.* **1998**, *120*, 823; (b) Giannini, L.; Guillemot, G.; Solari, E.; Floriani, C.; Re, N.; Chiesi-Villa, A.; Rizzoli, C. *J. Am. Chem. Soc.* **1999**, *121*, 2797.
- (23) Cotton, F. A.; Walton, R. A. *Multiple Bonds between Metal Atoms, 2nd Ed.*; Oxford University Press: New York, 1993; pp. 597 and 603.
- (24) (a) Chisholm, M. H.; Folting, K.; Huffman, J. C.; Tatz, R. J. *J. Am. Chem. Soc.* **1984**, *106*, 1153; (b) Chisholm, M. H.; Folting, K.; Huffman, J. C.; Putilina, E. F.; Streib, W. E.; Tatz, R. J. *Inorg. Chem.* **1993**, *32*, 3771.
- (25) (a) Chisholm, M. H.; Folting, K.; Streib, W. E.; Wu, D.-D. *Chem. Commun.* **1998**, 379; (b) Chisholm, M. H.; Folting, K.; Streib, W. E.; Wu, D.-D. *Inorg. Chem.* **1999**, *38*, 5219; (c) Acho, J. A.; Ren, T.; Yun, J. W.; Lippard, S. J. *Inorg. Chem.* **1995**, *34*, 5226; (d) Acho, J. A.; Lippard, S. J. *Inorg. Chim. Acta* **1995**, *229*, 5.

- (26) Zanotti-Gerosa, A.; Solari, E.; Giannini, L.; Floriani, C.; Chiesi-Villa, A.; Rizzoli, C. *J. Am. Chem. Soc.* **1998**, *120*, 437.
- (27) Caselli, A.; Solari, E.; Scopelliti, R.; Floriani, C.; Re, N.; Rizzoli, C.; Chiesi-Villa, A. *J. Am. Chem. Soc.* **2000**, *122*, 538.
- (28) Guillemot, G.; Solari, E.; Floriani, C.; Re, N.; Rizzoli, C. *Organometallics* **2000**, *19*, 5218.
- (29) (a) Hill, J. E.; Fanwick, P. E.; Rothwell, I. P. *Organometallics* **1992**, *11*, 1771; (b) Hill, J. E.; Balaich, G. J.; Fanwick, P. E.; Rothwell, I. P. *Organometallics* **1991**, *10*, 3428; (c) Takahashi, T.; Tamura, M.; Saburi, M.; Uchida, Y.; Negishi, E.-I. *J. Chem. Soc. Chem. Commun.* **1989**, 852; (d) Erker, G.; Czisch, P.; Krüger, C.; Wallis, J. M. *Organometallics* **1985**, *4*, 2059; (e) Schrock, R. R.; McLain, S.; Sancho J. *Pure Appl. Chem.* **1980**, *52*, 729; (f) McLain, S.; Wood, C. D.; Schrock, R. R. *J. Am. Chem. Soc.* **1979**, *101*, 4558; (g) Ingrosso, G. In *Reactions of Coordinated Ligands*; Braterman, P. S., Ed.; Plenum: New York, 1986; Vol. 1, Ch. 10.
- (30) Caselli, A.; Giannini, L.; Solari, E.; Floriani, C.; Re, N.; Chiesi-Villa, A.; Rizzoli, C. *Organometallics* **1997**, *16*, 5457.
- (31) (a) Fryzuk, M. D.; Haddad, T. S.; Rettig, S. J. *Organometallics* **1989**, *8*, 1723; (b) Diamond, G. M.; Green, M. L. H.; Walker, N. M.; Howard, J. A. K. *J. Chem. Soc., Dalton Trans.* **1992**, 2641; (c) Blenkins, J.; Hessen, B.; van Bolhuis, F.; Wagner, A. J.; Teuben, J. H. *Organometallics* **1987**, *6*, 459; (d) Yasuda, H.; Nakamura, A. *Angew. Chem., Int. Ed. Engl.* **1987**, *26*, 723.
- (32) Giannini, L.; Solari, E.; Floriani, C.; Chiesi-Villa, A.; Rizzoli, C. *Angew. Chem., Int. Ed. Engl.* **1994**, *33*, 2204.
- (33) (a) Erker, G.; Engel, K.; Korek, U.; Czisch, P.; Berke, H.; Caubère, P.; Vanderesse, R. *Organometallics* **1985**, *4*, 1531; (b) Erker, G.; Wicker, J.; Engel, K.; Krüger, C. *Chem. Ber.* **1982**, *115*, 3300.
- (34) Nugent, W. A.; Haymore, B. L. *Coord. Chem. Rev.* **1980**, *31*, 123.
- (35) (a) Yasuda, H.; Tatsumi, K.; Nakamura, A. *Acc. Chem. Res.* **1985**, *18*, 120; (b) Erker, G.; Lecht, R.; Petersen, J. L.; Bönnemann, H. *Organometallics* **1987**, *6*, 1962; (c) Erker, G.; Aul, R. *Organometallics* **1988**, *7*, 2070; (d) Erker, G.; Sosna, F.; Zwettler, R.; Krüger, C. *Organometallics* **1989**, *8*, 450; (e) Yasuda, H.; Okamoto, T.; Matsuoka, Y.; Nakamura, A.; Kai, Y.; Kanehisa, N.; Kasai, N. *Organometallics* **1989**, *8*, 1139; (f) Erker, G.; Friedrich, S.; Ralf, N. *Chem. Ber.* **1990**, *123*, 821; (g) Erker, G.; Babil, M. *Chem. Ber.* **1990**, *123*, 1327.
- (36) Negishi, E.-I.; Takahashi, T. *Acc. Chem. Res.* **1994**, *27*, 124.
- (37) (a) Lee, S. Y.; Bergman, R. G. *J. Am. Chem. Soc.* **1996**, *118*, 6396; (b) Jacoby, D.; Floriani, C.; Chiesi-Villa, A.; Rizzoli, C. *J. Am. Chem. Soc.* **1993**, *115*, 7025; (c) Howard, W. A.; Waters, M.; Parkin, G. *J. Am. Chem. Soc.* **1993**, *115*, 4917; (d) Carney, M. J.; Walsh, P. J.; Hollander, F. J.; Bergman, R. G. *Organometallics* **1992**, *11*, 761.
- (38) (a) Reetz, M. T. In *Organometallics in Synthesis*; Schlosser, M., Ed.; Wiley: New York, **1994**, Ch. 3; (b) Petasis, N. A.; Fu, D. K. *J. Am. Chem. Soc.* **1993**, *115*, 7208; (c) Buchwald, S. L.; Nielsen, R. B. *Chem. Rev.* **1988**, *88*, 1047; (d) Zambrano, C. H.; Fanwick, P. E.; Rothwell, I. P. *Organometallics* **1994**, *13*, 1174.
- (39) (a) Ozerov, O. V.; Ladipo, F. T.; Patrick, B. O. *J. Am. Chem. Soc.* **1999**, *121*, 7941; (b) Ozerov, O. V.; Patrick, B. O.; Ladipo, F. T. *J. Am. Chem. Soc.* **2000**, *122*, 6423; (c) Ozerov, O. V.; Parkin, S.; Brock, C. P.; Lapido, F. T. *Organometallics* **2000**, *21*, 4188.
- (40) Giannini, L.; Caselli, A.; Solari, E.; Floriani, C.; Chiesi-Villa, A.; Rizzoli, C.; Re, N.; Sgamellotti, A. *J. Am. Chem. Soc.* **1997**, *119*, 9198.
- (41) (a) Buchwald, S. L.; Broene, R. D. In *Comprehensive Organometallic Chemistry II*; Abel, E. W.; Stone, F. G. A.; Wilkinson, G., Eds.; Pergamon: Oxford, 1995, Vol. 12, Ch. 7.4, and references therein; (b) Erker, G.; Albrecht, M.; Krüger, C.; Werner, S. *J. Am. Chem. Soc.* **1992**, *114*, 8531; (c) Buchwald, S. L.; Watson, B. T.; Huffman, J. C. *J. Am. Chem. Soc.* **1986**, *108*, 7411; (d) Buchwald, S. L.; Nielsen, R. B. *Chem. Rev.* **1988**, *88*, 1047.
- (42) Fryzuk, M. D.; Mao, S. S. H. *J. Am. Chem. Soc.* **1993**, *115*, 5336.

- (43) (a) Guram, A. S.; Jordan, R. F. In *Comprehensive Organometallic Chemistry II*; Abel, E. W.; Stone, F. G. A.; Wilkinson, G., Eds.; Pergamon: Oxford, 1995, Vol. 4, Ch. 12; (b) Jordan, R. F.; *Adv. Organomet. Chem.* **1991**, 32, 325.
- (44) Yang, X.; Stern, C. L.; Marks, T. J. *J. Am. Chem. Soc.* **1991**, 113, 3623.
- (45) Durfee, L. D.; Rothwell, I. P. *Chem. Rev.* **1988**, 88, 1059, and references therein.
- (46) Tatsumi, K.; Nakamura, A.; Hofmann, P.; Stauffert, P.; Hoffmann, R. *J. Am. Chem. Soc.* **1985**, 107, 4440.
- (47) Giannini, L.; Caselli, A.; Solari, E.; Floriani, C.; Chiesi-Villa, A.; Rizzoli, C.; Re, N.; Sgamellotti, A. *J. Am. Chem. Soc.* **1997**, 119, 9709.
- (48) (a) Fanwick, P. E.; Kobriger, L. M.; McMullen, A. K.; Rothwell, I. P. *J. Am. Chem. Soc.*, **1986**, 108, 8095; (b) Arnold, J.; Tilley, T. D.; Rheingold, A. L. *J. Am. Chem. Soc.*, **1986**, 108, 5355; (c) Martin, B. D.; Matchett, S. A.; Norton, J. R.; Anderson, O. P.; *J. Am. Chem. Soc.* **1985**, 107, 7952.
- (49) (a) Smuck, S.; Erker, G.; Kotila, S. *J. Organomet. Chem.* **1995**, 502, 75; (b) Bendix, M.; Grehl, M.; Fröhlick, K.; Erker, G. *Organometallics* **1994**, 13, 3366; (c) Erker, G.; Mena, M.; Krüger, C.; Noe, R. *Organometallics* **1991**, 10, 1201.
- (50) (a) Valero, C.; Grehl, M.; Wingbermhühle, D.; Kloppenburg, L.; Carpenetti, D.; Erker, G.; Petersen, J. *Organometallics* **1994**, 13, 415; (b) Scott, M. J.; Lippard, S. J. *J. Am. Chem. Soc.* **1997**, 119, 3411; (c) Ruiz, J.; Vivanco, M.; Floriani, C.; Chiesi-Villa, A.; Rizzoli, C. *Organometallics* **1993**, 12, 1811, and references therein.
- (51) Chamberlain, L. R.; Durfee, L. D.; Fanwick, P. E.; Kobriger, L.; Latesky, S. L.; McMullen, A. K.; Rothwell, I. P.; Folting, K.; Huffman, J. C.; Streib, W. E.; Wang, R. *J. Am. Chem. Soc.* **1987**, 109, 390.
- (52) (a) Durfee, L. D.; Hill, J. E.; Kerschner, J. L.; Fanwick, P. E.; Rothwell, I. P. *Inorg. Chem.* **1989**, 28, 3095; (b) Durfee, L. D.; Fanwick, P. E.; Rothwell, I. P.; Folting, K.; Huffman, J. C. *J. Am. Chem. Soc.* **1987**, 109, 4720.
- (53) Chamberlain, L. R.; Durfee, L. D.; Fanwick, P. E.; Kobriger, L. M.; Latesky, S. L.; McMullen, A. K.; Steffey, B. D.; Rothwell, I. P.; Folting, K.; Huffman, J. C. *J. Am. Chem. Soc.* **1987**, 109, 6068.
- (54) (a) Vilas Boas, L. F.; Costa Pessoa, J. In *Comprehensive Coordination Chemistry*, Wilkinson, G.; Gillard, R. D.; McCleverty, J. A., Eds.; Pergamon: Oxford, 1987; Vol. 3, Ch. 33, p 453; (b) *Vanadium in Biological Systems*; Chasteen, N. D. Ed.; Kluwer: Dordrecht, 1990; (c) Mazzanti, M.; Floriani, C.; Chiesi-Villa, A.; Guastini, C. *J. Chem. Soc., Dalton Trans.* **1989**, 1793; (d) Mazzanti, M.; Floriani, C.; Chiesi-Villa, A.; Guastini, C. *Angew. Chem., Int. Ed. Engl.* **1988**, 27, 576.
- (55) (a) Seidel, W.; Kreisel, G. *Z. Chem.* **1981**, 21, 295; (b) Preuss, F.; Ogger, L. *Z. Naturforsch.* **1982**, 37b, 957; (c) Seangprasertkij, R.; Riechel, T. L. *Inorg. Chem.* **1986**, 25, 3121; (d) Preuss, F.; Becker, H. *Z. Naturforsch.* **1986**, 41b, 185.
- (56) Karol, F. J.; Cann, K.; Wagner, B. E. In *Transition Metals and Organometallics as Catalysts for Olefin Polymerization*; Kaminsky, W., Sinn, H., Eds.; Springer: New York, 1988; pp. 149–161.
- (57) (a) Feher, F. J.; Newman, D. A.; Walzer, J. F. *J. Am. Chem. Soc.* **1989**, 111, 1741; (b) Feher, F. J.; Walzer, J. F. *Inorg. Chem.* **1991**, 30, 1689; (c) Feher, F. J.; Walzer, J. F.; Blanski, R. L. *J. Am. Chem. Soc.* **1991**, 113, 3618; (d) Feher, F. J.; Blanski, R. L. *J. Am. Chem. Soc.* **1992**, 114, 5886; (e) Feher, F. J.; Blanski, R. L. *Organometallics* **1993**, 12, 958.
- (58) Chamberlain, L. R.; Steffey, B. D.; Rothwell, I. P.; Huffman, J. C. *Polyhedron* **1989**, 8, 341.
- (59) Unpublished results.
- (60) (a) Feldman, J.; Schrock, R. R. *Progr. Inorg. Chem.* **1991**, 39, 1; (b) Schrock, R. R. *Alkylidene Complexes of the Earlier Transition Metals in Reaction of Coordinated Ligands*; Braterman, P. S., Ed.; Plenum Press: New York, 1986; Ch. 3; (c) Schrock, R. R. *Acc. Chem. Res.* **1990**, 23, 158; (d) Grubbs, R. H.; Miller, S. J.; Fu, G. C. *Acc. Chem. Res.* **1995**, 28, 446; (e) Buhro, W. E.; Chisholm, M. H. *Adv. Organomet. Chem.* **1987**, 27, 311.

- (61) Fischer, H.; Hofmann, P.; Kreissl, F. R.; Schrock, R. R.; Schubert, U.; Weiss, K. *Carbyne Complexes*; VCH: Weinheim, Germany, 1988.
- (62) (a) Corker, J.; Lefebvre, F.; Lecuyer, C.; Dufaud, V.; Quignard, F.; Choplin, A.; Evans, J.; Basset, J.-M. *Science* **1996**, *271*, 966; (b) Niccolai, G. P.; Basset, J.-M. *Appl. Catal., A*, **1996**, *146*, 145; (c) Vidal, V.; Theolier, A.; Thivolle-Cazat, J.; Basset, J.-M.; Corker, J. *J. Am. Chem. Soc.* **1996**, *118*, 4595.
- (63) Giannini, L.; Solari, E.; Dovesi, S.; Floriani, C.; Re, N.; Chiesi-Villa, A.; Rizzoli, C. *J. Am. Chem. Soc.* **1999**, *121*, 2784.
- (64) (a) *Stereochemistry of Organometallic and Inorganic Compounds*, Volume 2: *Stereochemical and Stereophysical Behaviour of Macrocycles*; Bernal, I., Ed.; Elsevier: Amsterdam, 1987; (b) Dietrich, B.; Viout, P.; Lehn, J.-M. *Macrocyclic Chemistry*; VCH: Weinheim, 1993.
- (65) (a) Shih, K.-Y.; Totland, K.; Seidel, S. W.; Schrock, R. R. *J. Am. Chem. Soc.* **1994**, *116*, 12103; (b) Schrock, R. R.; Seidel, S. W.; Mösch-Zanetti, N.; Dobbs, D. A.; Shih, K.-Y.; Davis, W. M. *Organometallics* **1997**, *16*, 5195; (c) Schrock, R. R. *Acc. Chem. Res.* **1997**, *30*, 9.
- (66) Schrock, R. R.; Clark, D. N.; Wengrovius, J. H.; Rocklage, S. M.; Pedersen, S. F. *Organometallics* **1982**, *1*, 1645, and references therein.
- (67) Giannini, L.; Dovesi, S.; Solari, E.; Floriani, C.; Chiesi-Villa, A.; Rizzoli, C. *Angew. Chem. Int. Ed.* **1999**, *38*, 807.
- (68) (a) Ref. 61, Ch. 4; (b) Ref. 61, Ch. 5; (c) Clark, G. R.; Marsden, K.; Roper, W. R.; Wright, L. J. *J. Am. Chem. Soc.* **1980**, *102*, 6570; (d) Weber, L.; Dembeck, G.; Stammeler, H.-G.; Neumann, B.; Schmidtmann, M.; Müller, A. *Organometallics* **1998**, *17*, 5254; (e) Kim, H. P.; Kim, S.; Jacobson, R. A.; Angelici, R. J. *Organometallics* **1984**, *3*, 1124; (f) Doyle, R. A.; Angelici, R. J. *Organometallics* **1989**, *8*, 2207; (g) Green, M.; Orpen, A. G.; Williams, I. D. *J. Chem. Soc., Chem. Commun.* **1982**, 493.
- (69) Dötz, K. H.; Fischer, H.; Hofmann, P.; Kreissl, F. R.; Schubert, U.; Weiss, K. *Transition Metal Carbene Complexes*; VCH: Weinheim, 1983.
- (70) *Comprehensive Organometallic Chemistry*, Vol. 12; Abel, E. W.; Stone, F. G. A.; Wilkinson, G., Eds.; Pergamon: Oxford, 1995; (a) Ch. 5.3; (b) Ch. 5.4; (c) Ch. 5.5.
- (71) (a) Kreissl, F. R.; Ostermeier, J.; Ogric, C. *Chem. Ber.* **1995**, *128*, 289; (b) Lehotkay, Th.; Wurst, K.; Jaitner, P.; Kreissl, F. R. *J. Organometal. Chem.* **1996**, *523*, 105; (c) Schmidt, S.; Sundermeyer, J.; Möller, F. J. *Organometal. Chem.* **1994**, *475*, 157; (d) Jamison, G. M.; White, P. S.; Templeton, J. L. *Organometallics* **1991**, *10*, 1954.
- (72) Dovesi, S.; Solari, E.; Scopelliti, R.; Floriani, C. *Angew. Chem. Int. Ed.* **1999**, *38*, 2388.
- (73) Clark, G. R.; Marsden, K.; Roper, W. R.; Wright, L. J. *J. Am. Chem. Soc.* **1980**, *102*, 6570. For a review of halocarbene complexes see Brothers, P. J.; Roper, W. R., *Chem. Rev.* **1988**, *88*, 1293. For nucleophilic substitution at haloalkylidynes see Desmond, T.; Lalor, F. J.; Ferguson, G.; Parvez, M. *J. Chem. Soc., Chem. Commun.* **1983**, 457.
- (74) Iwasawa, Y.; Hamamura, H. *J. Chem. Soc., Chem. Commun.* **1983**, 130.
- (75) (a) Miller, G. A.; Cooper, N. J. *J. Am. Chem. Soc.* **1985**, *107*, 709; (b) Freundlich, J. S.; Schrock, R. R.; Cummins, C. C.; Davis, W. M. *J. Am. Chem. Soc.* **1994**, *116*, 6476; (c) Freundlich, J. S.; Schrock, R. R.; Davis, W. M. *J. Am. Chem. Soc.* **1996**, *118*, 3643.
- (76) (a) Freudenberg, J. H.; Schrock, R. R. *Organometallics* **1985**, *4*, 1937; (b) Hatton, W. G.; Gladysz, J. A. *J. Am. Chem. Soc.* **1983**, *105*, 6157.
- (77) Schrock, R. R.; Seidel, S. W.; Mösch-Zanetti, N. C.; Shih, K.-Y.; O'Donoghue, M. B.; Davis, W. M.; Reiff, W. M. *J. Am. Chem. Soc.* **1997**, *119*, 11876.
- (78) (a) Van der Schaaf, P. A.; Hafner, A.; Mühlebach, A. *Angew. Chem., Int. Ed. Engl.* **1996**, *35*, 1845; (b) Chamberlain, L. R.; Rothwell, I. P.; Folting, K.; Huffman, J. C. *J. Chem. Soc., Dalton Trans.* **1987**, 155; (c) Chamberlain, L. R.; Rothwell, I. P. *J. Chem. Soc. Dalton Trans.* **1987**, 163; (d) Chamberlain, L. R.; Rothwell, A. P.; Rothwell, I. P. *J. Am. Chem. Soc.* **1984**, *106*, 1847.

- (79) (a) Casey, C. P.; Brady, J. T.; Boller, T. M.; Weinhold, F.; Hayashi, R. K. *J. Am. Chem. Soc.* **1998**, *120*, 12,500, and references therein; (b) Casey, C. P.; Brady, J. T. *Organometallics* **1998**, *17*, 4620.
- (80) (a) Frohnapfel, D. S.; White, P. S.; Templeton, J. L. *Organometallics* **2000**, *19*, 1497; (b) Frohnapfel, D. S.; Enriquez, A. E.; Templeton, J. L. *Organometallics* **2000**, *19*, 221, and references therein; (c) Legzdins, P.; Lumb, S. A.; Rettig, S. J. *Organometallics* **1999**, *18*, 3128.
- (81) Wigley, D. E.; Gray, S. D. In *Comprehensive Organometallic Chemistry II*; Abel, E. W.; Stone, F. G. A.; Wilkinson, G., Eds.; Pergamon: Oxford, 1995; Vol. 2, Ch. 2.
- (82) (a) Schrock, R. R.; Fellmann, J. D. *J. Am. Chem. Soc.* **1978**, *100*, 3359; (b) Schrock, R. R.; Messerle, L. W.; Wood, C. D.; Guggenberger, L. J. *J. Am. Chem. Soc.* **1978**, *100*, 3793; (c) Rupprecht, G. A.; Messerle, L. W.; Fellmann, J. D.; Schrock, R. R. *J. Am. Chem. Soc.* **1980**, *102*, 6236; (d) Cockcroft, J. K.; Gibson, V. C.; Howard, J. A. K.; Poole, A. D.; Siemeling, U.; Wilson, C. *J. Chem. Soc., Chem. Commun.* **1992**, 1668; (e) De Castro, I.; De La Mata, J.; Gomez, M.; Gomez-Sal, P.; Royo, P.; Selas, J. M. *Polyhedron* **1992**, *11*, 1023; (f) Biasotto, F.; Etienne, M.; Dahan, F. *Organometallics* **1995**, *14*, 1870; (g) Antiñolo, A.; Otero, A.; Fajardo, M.; García-Yebra, C.; Gil-Sanz, R.; López-Mardomingo, C.; Martín, A.; Gomez-Sal, P. *Organometallics* **1994**, *13*, 4679; (h) Kleckley, T. S.; Bennett, J. L.; Wolczanski, P. T.; Lobkovsky, E. B.; *J. Am. Chem. Soc.* **1997**, *119*, 247.
- (83) (a) Vrtis, R. N.; Rao, C. P.; Warner, S.; Lippard, S. J. *J. Am. Chem. Soc.* **1988**, *110*, 2669; (b) Vrtis, R. N.; Shuncheng, L.; Rao, C. P.; Bott, S. G.; Lippard, S. J. *Organometallics* **1991**, *10*, 275; (c) Carnahan, E. M.; Lippard, S. J. *J. Am. Chem. Soc.* **1992**, *114*, 4166; (d) Riley, P. N.; Profflet, R. D.; Fanwick, P. E.; Rothwell, I. P. *Organometallics* **1996**, *15*, 5502, and references therein; (e) Huq, F.; Mowat, W.; Skapski, A. C.; Wilkinson, G. *J. Chem. Soc., Chem. Commun.* **1971**, 1477; (f) Mowat, W.; Wilkinson, G. *J. Chem. Soc., Dalton Trans.* **1973**, 1120; (g) Ogilvy, A. E.; Fanwick, P. E.; Rothwell, I. P. *Organometallics* **1987**, *6*, 73.
- (84) McMurry, J. E. *Acc. Chem. Res.* **1983**, *16*, 405.
- (85) For the reductive cleavage of C-O of ketones see Chisholm, M. H.; Folting, C.; Klang, J. A. *Organometallics* **1990**, *9*, 602 and 609, and references therein.
- (86) Chisholm, M. H.; Huffman, J. C.; Lucas, E. A.; Sousa, A.; Streib, W. E. *J. Am. Chem. Soc.* **1992**, *114*, 2710.
- (87) Bryan, J. C.; Mayer, J. M. *J. Am. Chem. Soc.* **1990**, *112*, 2298.
- (88) The reaction between an early transition metal-alkylidene and a ketone to yield a metal-oxo group and an olefin was first noted by Schrock: Schrock, R. R. *J. Am. Chem. Soc.* **1976**, *98*, 5399.
- (89) Villiers, C.; Ephritikhine, M. *Angew. Chem., Int. Ed. Engl.* **1997**, *36*, 2380, and references therein.
- (90) (a) Low, G. G.; Bell, A. T. *J. Catal.* **1979**, *57*, 397; (b) Roberts, M. W. *Chem. Soc. Rev.* **1977**, *6*, 373; (c) Brodén, G.; Rhodin, T. N.; Brucker, C.; Benbow, R.; Hurych, Z. *Surf. Sci.* **1976**, *59*, 593; (d) Horowitz, C. P.; Shriver, D. F. *Adv. Organomet. Chem.* **1984**, *23*, 219; (e) Bradley, J. S. *Adv. Organomet. Chem.* **1983**, *22*, 1; (f) Muetterties, E. L.; Stein, J. *Chem. Rev.* **1979**, *79*, 479; (g) Tachikawa, M.; Muetterties, E. L. *Progr. Inorg. Chem.* **1981**, *28*, 203; (h) Shriver, D. F.; Sailor, M. J. *Acc. Chem. Res.* **1988**, *21*, 374; (i) Horwitz, C. P.; Shriver, D. F. *J. Am. Chem. Soc.* **1985**, *107*, 8147; (j) Gates, B. C. *Angew. Chem., Int. Ed. Engl.* **1993**, *32*, 228; (k) Colaianni, M. L.; Chen, J. G.; Weinberg, W. H.; Yates, J. T., Jr. *J. Am. Chem. Soc.* **1992**, *114*, 3735; (l) Hermann, W. A.; Biersack, H.; Ziegler, M. L.; Weidenhammer, K.; Siegel, R.; Rehder, D. *J. Am. Chem. Soc.* **1981**, *103*, 1692.
- (91) (a) Miller, R. L.; Wolczanski, P. T.; Rheingold, A. L. *J. Am. Chem. Soc.* **1993**, *115*, 10,422; (b) Neithamer, D. R.; LaPointe, R. E.; Wheeler, R. A.; Richeson, D. S.; Van Duyne, G. D.; Wolczanski, P. T. *J. Am. Chem. Soc.* **1989**, *111*, 9056.
- (92) Chisholm, M. H.; Hammond, C. E.; Johnston, V. J.; Streib, W. E.; Huffman, J. C. *J. Am. Chem. Soc.* **1992**, *114*, 7056, and references therein.

- (93) (a) Peters, J. C.; Odom, A. L.; Cummins, C. C. *Chem. Commun.* **1997**, 1995, and references therein; (b) Cummins, C. C. *Chem. Commun.* **1998**, 1777.
- (94) (a) Mansuy, D.; Lecomte, J.-P.; Chottard, J.-C.; Bartoli, J.-F. *Inorg. Chem.* **1981**, 20, 3119; (b) Goedken, V. L.; Deakin, M. R.; Bottomley, L. A. *J. Chem. Soc., Chem. Commun.* **1982**, 607; (c) Latesky, S. L.; Selegue, J. P. *J. Am. Chem. Soc.* **1987**, 109, 4731; (d) Etienne, M.; White, P. S.; Templeton, J. L. *J. Am. Chem. Soc.* **1991**, 113, 2324.

From AlX/GaX Monohalide Molecules to Metalloid Aluminum and Gallium Clusters

HANSGEORG SCHNÖCKEL and ANDREAS SCHNEPF

Institut für Anorganische Chemie der Universität Karlsruhe
D-76133 Karlsruhe, Germany

I. Introduction	235
II. Cocondensation Technique and Synthesis of Metastable AlX or GaX Solutions	237
III. Metalloid Al Clusters	241
A. $\text{Al}_7[\text{N}(\text{SiMe}_3)_2]_6^-$ Cluster 1	241
B. $\text{Al}_{12}[\text{N}(\text{SiMe}_3)_2]_8^-$ Cluster 2	243
C. $\text{Al}_{14}[\text{N}(\text{SiMe}_3)_2]_6]^{2-}$ Cluster 3	245
D. $\text{Al}_{77}[\text{N}(\text{SiMe}_3)_2]_{20}^{2-}$ Cluster 4	248
E. $\text{Al}_{12}(\text{AlBr}_2)_{10} \cdot 12(\text{THF})$ Cluster 6	252
F. Conclusion	254
IV. Metalloid Ga Clusters	255
A. Solid-State Modifications of Elemental Gallium	255
B. Synthetic Routes to Metalloid Gallium Clusters	260
C. $[\text{Ga}_6(\text{SiPh}_2\text{Me})_8]^{2-}$ Cluster 7	261
D. $\text{Ga}_8[\text{C}(\text{SiMe}_3)_3]_6$ Cluster 8	261
E. $[\text{Ga}_{12}(\text{C}_{13}\text{H}_9)_{10}]^{2-}$ Cluster 9	263
F. $\text{Ga}_{18}(\text{Si}^t\text{Bu}_3)_8$ Cluster 10	265
G. $[\text{Ga}_{19}\{\text{C}(\text{SiMe}_3)_3\}_6]^-$ Cluster 11	265
H. Ga_{22}R_8 Clusters ($\text{R} = \text{Si}(\text{SiMe}_3)_3$ 12 ; $\text{Ge}(\text{SiMe}_3)_3$ 13 ; Si^tBu_3 14)	269
I. $[\text{Ga}_{26}\{\text{Si}(\text{SiMe}_3)_3\}_8]^{2-}$ Cluster 15	271
J. $[\text{Ga}_{84}\{\text{N}(\text{SiMe}_3)_2\}_{20}]^{4-}$ Cluster 16	272
K. Conclusion	277
V. Conclusions and Outlook	277
References	279

I

INTRODUCTION

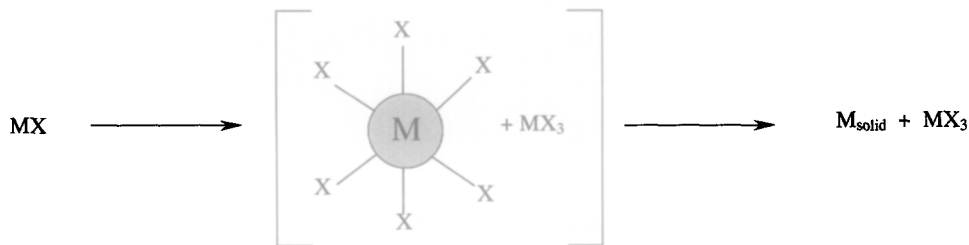
We introduced the term *metalloid cluster* for molecular metal atom clusters¹ in order to limit the very wide-stretched general term *metal cluster* which is based on a definition by Cotton.² According to Cotton's definition, nonmetal atoms are also allowed to take part in a metal cluster, and therefore molecular clusters like $\text{Cu}_{146}\text{Se}_{73}(\text{PPh}_3)_{30}$ ³ should be regarded as metal clusters as well. The prototype of the newly defined class of metalloid clusters is the Au_{55} cluster.⁴ Although all attempts to analyze the structure of this cluster by X-ray diffraction have failed so far, it is generally supposed that it consists of a central Au atom surrounded by two

shells of 12 and 42 further Au atoms. This implies that the Au atoms topologically correspond to the arrangement of atoms within the Au metal. In other words, the idea of the metal structure is contained in a cluster of this kind and fully justifies the term *metalloid* (suffix *-oid* is deduced from the greek εἶδος—idea, prototype).

A few years ago, only a few examples of structurally characterized metalloid clusters were known. For a long period of time, a $\text{Pt}_6\text{Ni}_{38}$ cluster with 6 naked palladium metal atoms (i.e., they do not carry ligands) was considered to be the largest cluster of this type.⁵ Only a year ago, a record within the field of precious metalloid clusters was established with a Pd_{59} cluster containing 11 naked palladium atoms.⁶ Very recently, in November 2000, the largest metalloid cluster formula ever structurally characterized was published.⁷ However, in 1997, it came as a big surprise when our group succeeded—3 years before the Pd_{59} cluster was reported—in synthesizing and structurally analyzing a cluster carrying 57 naked Al atoms.⁸ This $\text{Al}_{77}\text{R}_{20}^{2-}$ cluster [$\text{R} = \text{N}(\text{SiMe}_3)_2$] showed that, when analyzed in detail, packing of the Al atoms is significantly different from the packing in Al metal; the coordination numbers diminish from the cluster center to the outside, and consequently the Al–Al distances become shorter in the same direction. Thus the common idea of these clusters as small ligand-protected metal parts had to be revised, at least for the metalloid clusters discussed within this paper. However, this extremely important result almost escaped notice in a recently published monograph dealing with metal clusters,⁹ as well as in the publication about a Pd_{59} and a Pd_{145} cluster.^{6,7} Obviously, the structure as well as the unconventional synthesis of the Al_{77} cluster were regarded as being an exception, a curiosity.

Herein, we will show that the Al_{77} cluster does in fact *not* constitute an exception but is only one of the achievements of a new synthesis technique which made possible the synthesis and structural characterization of a multitude of further metalloid clusters, all formally representing intermediates on the way to metal formation. Such intermediates on the way to metal formation can help to improve our understanding of the mechanism of one of the oldest chemical processes in the history of chemistry, since metalloid clusters are likely to be formed as intermediates during the precipitation of metals and during metal dissolution. Both reactions can be followed by recording either the cluster size (number of naked metal atoms) or the median oxidation number which drops (e.g., to 0.23) for the Al_{77} cluster. Intermediates containing such “metal-near” oxidation states are best accessible starting from compounds with metals in oxidation states as low as possible and as unstable as possible. The use of metastable $\text{Al}(\text{I})$ - or $\text{Ga}(\text{I})$ solutions which can be transformed under mild conditions by disproportionation to metal and an $\text{Al}(\text{III})$ - or $\text{Ga}(\text{III})$ compound is based on this idea (Scheme 1).^{10,11} During these disproportionation reactions on the way to the metal, metalloid cluster compounds can be trapped, if suitable conditions are applied.

This approach to the formation of metalloid molecular cluster compounds shows clearly the difference from Zintl-like phases which lately have been successfully



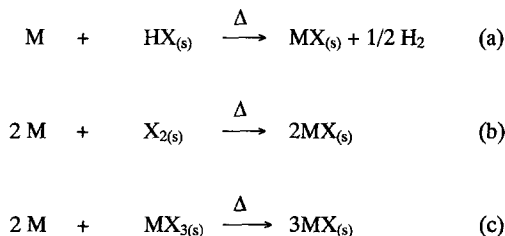
SCHEME 1. Metalloid M_xX_y clusters ($x > y$) as intermediates during the disproportionation reaction of MX solutions ($M = \text{Al, Ga}$; $X = \text{Cl, Br, I}$).

investigated by Corbett.¹² Although there is a certain topological similarity to metalloid clusters as described herein, these metal cluster units carry high negative charges (no electron deficiency!) which are stabilized in a “bath” of positive cations. The preparation method established for these compounds starts from the metal elements by reduction with strong electropositive metals (mostly alkali metals), leading to the “extraction” of small parts out of the infinite crystal lattice structure of metals. This process is responsible for the negative values of the median oxidation state of the clusters, which excludes the presence of electron-deficient bonding, typical for polyhedral and metalloid cluster compounds.¹³ Thus, combined with the cations located in the immediate vicinity, physical properties¹⁴ are observed for these phases that differ significantly from the molecular ligand-protected metalloid clusters representing typical electron-deficient compounds. These Zintl-analogous clusters are not included in the following account.

II

COCONDENSATION TECHNIQUE AND SYNTHESIS OF METASTABLE AlX OR GaX SOLUTIONS

In the last decades, a considerable number of high temperature molecules like the metal mono-, -di-, or trihalogenides were generated and characterized using the matrix isolation technique.¹⁵ In a matrix isolation experiment, the reactive species is embedded in a cage of a solid inert gas (typically a noble gas), kept at a temperature of about -260°C , and can then be characterized spectroscopically without the risk of reactions such as aggregation or disproportionation, which are common for these species under normal conditions.¹⁶ In the past, we have investigated first the properties of AlX and GaX molecules ($X = \text{F, Cl, Br}$) alone, and then the reactivity of these species under matrix conditions, by cocondensation together with reactants such as another AlX, O atoms or HX (e.g., $\text{AlX} + \text{AlX} \rightarrow (\text{AlX})_2$;¹⁷ $\text{AlX} + \text{O} \rightarrow \text{O}=\text{AlX}$;¹⁸ $\text{AlX} + \text{HX} \rightarrow \text{HAlX}_2$).¹⁹



SCHEME 2.

Spectroscopic measurements were used to identify and structurally characterize these species which are generated in microgram scale in the matrix, and the experimental results were compared with the results of quantum-chemical calculations.²⁰ On the basis of these analyses and on earlier work by Peter Timms,²¹ we started about 10 years ago to prepare AlX and GaX in the synthesis scale (1–5 g).¹¹

Special synthetic routes are necessary to gain access to the metastable monohalides of Al and Ga, since they are thermodynamically unstable at room temperature toward disproportionation into Al metal and AlX₃ or Ga metal and GaX₃. First, the gaseous MX species, that are thermodynamically stable at high temperatures,²² have to be synthesized. A variety of methods are available for their preparation, some of which are shown in equations (a)–(c) of Scheme 2.

To suppress as much as possible the disproportionation reaction which is preferred at low temperatures, the process has to be done at relatively high temperatures (800–1000°C). The gaseous MX species thus formed have subsequently to be quenched at low temperatures in order to prevent disproportionation once again, which occurs on slow cooling.¹¹

The preparation of MX_(g) (M = Al, Ga) from reaction of HX_(g) with liquid Al or Ga has already been proved possible in the matrix experiments mentioned above. The matrix experiments also have the advantage that the effect of different HX gas streams on the MX concentration can be tested until optimal conditions are found. These optimized conditions were then also used for the synthesis of these species in larger scales using the apparatus depicted in Fig. 1.

The set-up of the synthesis experiments as shown in Fig. 1 is, in principle, comparable to the experimental set-up used by Timms²³ for the preparation of other high-temperature molecules (e.g., BF). Similar apparatus has been in use for some time now for metal vapor syntheses.²⁴ The reaction between metal and hydrogen halide (HCl, HBr, or HI) takes place in a graphite cell, which is typically positioned in a 30-L stainless steel vessel, and in a vacuum of approximately 5×10^{-5} mbar. Under these conditions, a gaseous equilibrium mixture is formed which—depending on M, HX, and the particular reaction conditions—consists of between 90 and 100% MX and H₂. The gaseous monohalides continuously streaming out of the graphite cell are condensed at 77 K together with a suitable

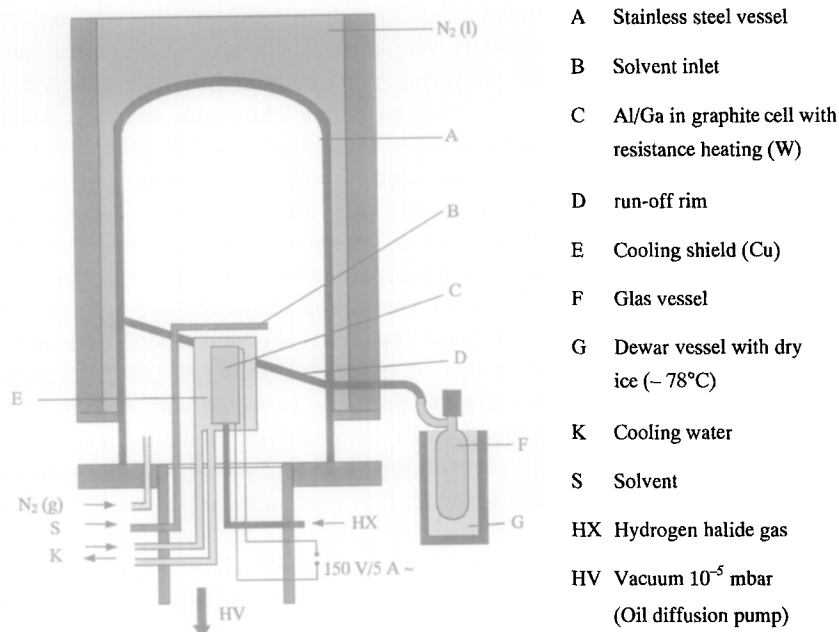


FIG. 1. Schematic picture of the cocondensation-high-vacuum system for the generation of gaseous MX species and their trapping in a matrix of an organic solvent.

solvent on the inner surface of the stainless steel vessel while the hydrogen that emerges from reaction (a) is removed continuously by a high-performance pump system. Typical experiments yield approximately 45 mmol of MX over a period of about 2 h. The coolant is subsequently removed and the melting condensate collected in a Schlenk vessel located under the run-off rim. The solution thus obtained can be studied with conventional techniques. To prevent disproportionation of the MX species once the condensate starts to melt, solvents have to be added which are capable of stabilizing these metastable compounds. The choice of solvents that may be used in this process is very much limited, especially since protic solvents and halogenated hydrocarbons must be ruled out because of their high reactivity with respect to MX. Further limitations result from the requirements of the solvent used with regard to its physical properties; e.g., the solvent must be readily volatile and should have good solvating properties even at extremely low temperatures.

Initial attempts to stabilize AlCl were carried out using pentane as solvent. The dark red condensate obtained at 77 K spontaneously turned black on warming above approximately 170 K due to the formation of aluminum as a result of disproportionation reaction ($3\text{AlCl} \rightarrow 2\text{Al} + \text{AlCl}_3$), and no subvalent Al species

was found in the resulting solutions. Experiments in which pentane was replaced by toluene or other aromatic solvents were also unsuccessful. On the other hand, the use of THF appeared at first promising. After melting the condensate, a deep red solution was obtained at -78°C that reacted violently with water, producing hydrogen gas. The initial euphoria quickly gave place to sobriety, however, because the color of the THF solution vanished several hours after the solution was brought to room temperature. It turned out that this observation was a consequence of ether cleavage reactions,²⁵ which are also known to occur in solutions of boron halides. These undesired reactions can easily be avoided if a less reactive ether such as diethyl ether is used or if only small proportions of THF are added to the mixture. Furthermore, it also became apparent that toluene had to be added to the latter to guarantee that the condensed species becomes fully dissolved upon warming. The deep red solution thus obtained can be stored without significant changes for several weeks at about -50°C . An analysis of the elemental ratio of Al to Cl and the amount of hydrogen produced on hydrolysis of the solution ($\text{Al}^+ + 2\text{H}^+ \rightarrow \text{Al}^{3+} + \text{H}_2$) is in agreement to the existence of solvated "AlCl" in these solutions.¹⁰

Recent studies confirm that "AlBr," "AlI," and "GaX" ($\text{X} = \text{Cl}, \text{Br}, \text{I}$) can be stabilized analogously.²⁶ As expected, the MX compounds become more stable with respect to disproportionation with increasing atomic numbers of M and X, and the example "AlBr" shows that the solvent combination toluene/diethyl ether can be replaced by other nucleophilic solvents in some cases. The thermal stability of the solution increases with increasing Lewis basicity of the solvent. The addition of an aromatic component leads to a further increase of the thermal stability. The number and properties of species contained in these solutions have been the subject of intensive research.²⁷ Exact analysis of these solutions has proved difficult since they tend to undergo disproportionation reactions with progressing time leading to metal and the trihalogenide. Nevertheless, we succeeded in a few rare cases to synthesize crystalline AlX and GaX species from these primary solutions, almost all of which were compounds with classical 2c2e bonds, e.g., $\text{Al}_4\text{Br}_4 \cdot 4(\text{NEt}_3)$ ²⁸ or $\text{Ga}_8\text{I}_8 \cdot 6(\text{PEt}_3)$ ²⁹ (Fig. 2).

These and other subhalogenides, such as $\text{Ga}_5\text{Cl}_7 \cdot 5(\text{Et}_2\text{O})$ ³⁰ and $\text{Al}_5\text{Br}_7 \cdot 5(\text{THF})$,³¹ have been discussed in detail previously³² and will generally not be considered here, because they show no or nearly no parallels to metalloid species; the only exception being $\text{Al}_{12}\text{Br}_{20} \cdot 12(\text{THF})$.³³ With respect to structural systematization, they were the first molecular $\text{Al}^{\text{I}}\text{X}$ or $\text{Ga}^{\text{I}}\text{X}$ species to be structurally characterized; these subhalogenides themselves attract considerable interest. They are also starting points for the synthesis of cluster compounds. Thus, by metathesis reactions we were able to synthesize a series of AlR_n and GaR_n clusters; among these were the first Al(I)-organic compound AlCp^* ³⁴ as well as the analogous GaCp^* ³⁵ compound. However, they will not be discussed here and were only mentioned in order to mark the different bonding properties in comparison to the metalloid clusters.



FIG. 2. Molecular structure of $\text{Ga}_8\text{I}_8 \cdot 6(\text{PEt}_3)$ and $\text{Al}_4\text{Br}_4 \cdot 4(\text{NEt}_3)$ (ethyl groups are omitted for clarity).

III

METALLOID Al CLUSTERS

As indicated above, Al-rich metalloid clusters are generated as intermediates during the disproportionation of AlX solutions. This disproportionation reaction becomes visible by a metal mirror coating and happens even under mild conditions (room temperature); that is, the reactions proceed to the thermodynamically stable final products AlX_3 and Al. We suggested using this Al film formation for technical applications, such as in the metallization of electrical isolation and also for porous materials.³⁶ The Al mirror coating growing on the glass vessel following the disproportionation reaction has yet to be examined regarding the possible formation of nanostructured Al species on a glass surface.

Keeping in mind the tendency of pure subhalides to disproportionation, we tried to slow down the disproportionation process by substituting the halogenide ligands with bulky groups. The use of the $\text{N}(\text{SiMe}_3)_2$ ligand proved to be especially fruitful and we were able to synthesize the following species, each of which will be presented in more detail in the following sections: $[\text{Al}_7\text{R}_6]^-$,³⁷ $[\text{Al}_{12}\text{R}_8]^-$,³⁸ $[\text{Al}_{14}\text{R}_6\text{X}_6]^{2-}$,³⁹ $[\text{Al}_{69}\text{R}_{18}]^{3-}$,⁴⁰ and $[\text{Al}_{77}\text{R}_{20}]^{2-}$ ⁸ ($\text{R} = \text{N}(\text{SiMe}_3)_2$).

A. $[\text{Al}_7\text{N}(\text{SiMe}_3)_2]_6^-$ Cluster **1**³⁷

A metastable solution of xylene/diethyl ether reacts in the temperature range -78 to 30°C with solid $\text{LiN}(\text{SiMe}_3)_3$ to give black crystals identified as $[\text{Al}_7\{\text{N}(\text{SiMe}_3)_2\}_6]^- [\text{Li}(\text{OEt}_2)_3]^+$. The central Al atom of the anion **1** (Fig. 3) is surrounded by a distorted octahedron of six further Al atoms, each of which is bonded to one NR_2 ligand.

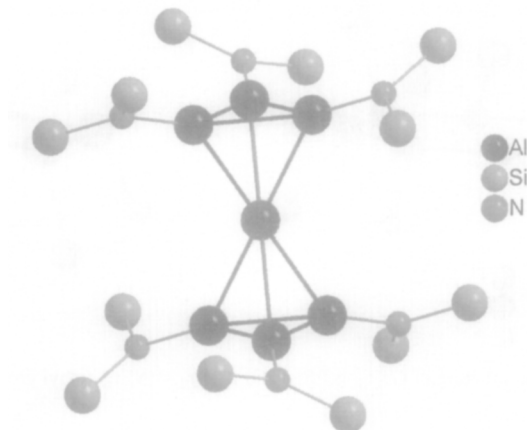


FIG. 3. Molecular structure of $[\text{Al}_7\{\text{N}(\text{SiMe}_3)_2\}_6]^-$ **1** (methyl groups are omitted for clarity).

The distance from the six-coordinate central atom to its Al neighbors is 273 pm, and is thus in between that of Al–Al bonds (266 pm) in typical molecular Al compounds⁴¹ and in Al metal (286 pm). On the other hand, the Al–Al bond connecting the Al atoms within the two Al_3R_3 groups is somewhat shorter (254 pm). The arrangement of the seven Al atoms is unusual, since we are not aware of any other example of two metal atom tetrahedra (exhibiting pure, nonbridged metal–metal bonding) that are vertex connected through a mutual “naked” metal atom. This special arrangement of atoms can be regarded as a primary configuration on the way to close packing, since the addition of only six further Al atoms, arranged around the central atom in the plane between the three-membered rings, leads to a cuboctahedral coordination sphere (Fig. 4).

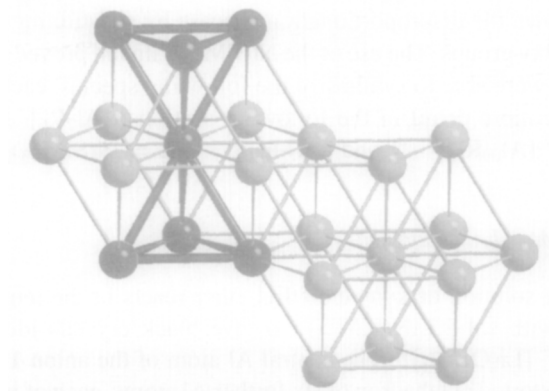


FIG. 4. Section of the cubic close packing of Al-metal. The Al_7 unit of **1** is marked.

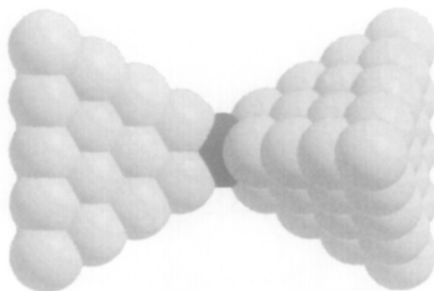
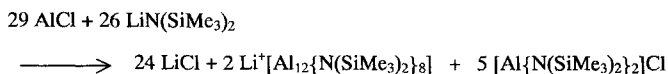


FIG. 5. Geometric model for, e.g., conductivity measurements via a single atom contact.

The interpretation of **1** as an Al^{3+} -center surrounded by two $\text{Al}_3\text{R}_3^{2-42}$ units can be excluded because of the lack of any ^{27}Al NMR signal with an appropriate high-field shift (as observed for AlCp^{*2+}).⁴³ However, the calculated NMR shift for the model compound $\text{Al}_7(\text{NH}_2)_6^-$ is +801 ppm, which is halfway to the position observed for aluminum metal,⁴⁴ and thus the central Al atom in its special coordination sphere appears to be similar to atoms in solid aluminum. A comparison with small anionic Al clusters (e.g., an Al_{13}^- species)⁴⁵ in which a high-field shift for the central Al atom is predicted ($\delta = -195.2$), seems not to be adequate, since the electronic situation on the central Al atoms is obviously completely different from that on the central atom, e.g., in the Al_7R_6^- group, in which the negative charge is localized primarily on the ligands and a slightly positive charge placed equally on the six outer Al atoms. On the basis of these theoretically obtained NMR shifts of the central Al atoms, the Al_7R_6^- clusters and *not* clusters like Al_{13}^- should be regarded as intermediates on the way to the bulk Al metal. It is therefore conceivable that compounds like Al_7R_6^- with well-defined environments around the naked Al atom center can be of interest for the physical characterization of single metal atoms using other methods, for example in nanotechnology⁴⁶ (Fig. 5). All measurements of this type to date were carried out on samples in which the contact between single Al atoms and the atoms of the bulk was not precisely defined.

B. $\text{Al}_{12}[\text{N}(\text{SiMe}_3)_2]_8^-$ Cluster **2**³⁸

If the above mentioned solution of AlCl_3 and $\text{LiN}(\text{SiMe}_3)_2$ is heated to 60°C for a short period of time and then cooled back to room temperature, black crystals of $\text{Li}(\text{OEt})_3^+[\text{Al}_{12}\{\text{N}(\text{SiMe}_3)_2\}_8]^-$ begin to grow within a few days (Scheme 3).



SCHEME 3. Reaction scheme showing the formation of **2**.

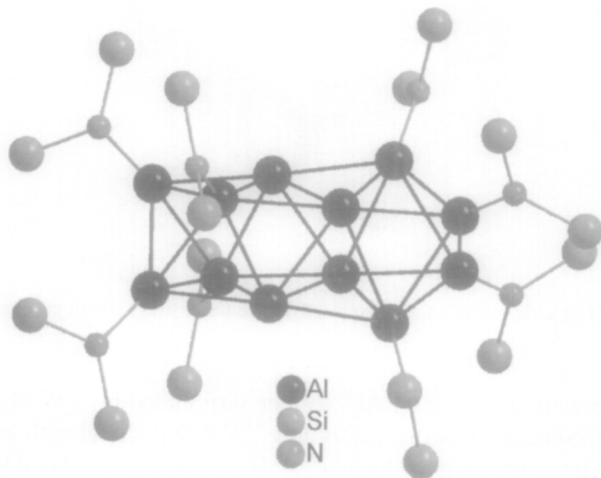


FIG. 6. Molecular structure of $[\text{Al}_{12}\{\text{N}(\text{SiMe}_3)_2\}_8]^{2-}$ **2** (methyl groups are omitted for clarity).

In contrast to the Al_{12} cluster **2**, the Al_7 cluster **1** is formed under milder conditions (24 h at 20°C and several weeks at -25°C) if the same educts are used. The X-ray structure of the anion **2** is shown in Fig. 6.

The structure of the $\text{Al}_{12}[\text{N}(\text{SiMe}_3)_2]_8^{2-}$ anion is similar to that of a neutral In_{12}R_8 cluster compound ($\text{R} = \text{Si}^i\text{Bu}_3$), as published recently by Wiberg *et al.*⁴⁷ The EPR spectra of a solid sample of **2** confirmed the radical character of the anion. Like the In_{12} cluster, the anion of **2** can be regarded as a section of the metallic lattice (Fig. 7).

In order to clarify the bonding properties of **2**, we performed density functional theory (DFT) calculations on the model compounds $\text{Al}_{12}\text{H}_8^{2-}$ and $\text{Al}_{12}(\text{NH}_2)_8^{2-}$; the results of these calculations are in pleasing agreement with the experimental values, and the same was found for the neutral $\text{In}_{12}\text{R}_{12}$ species.

There are 20 triangular faces in **2**, and this structural type also applies for the well-known species $\text{Al}_{12}\text{R}_{12}^{2-}$ ($\text{R} = \text{Si}^i\text{Bu}_3$)⁴⁸ with icosahedral symmetry. The *closo* type $\text{Al}_{12}\text{R}_{12}^{2-}$ anion may be one of the primary intermediates during the formation of **2**. If two R^- groups are removed from such an intermediate, an $\text{Al}_{12}\text{R}_{10}$ species is formed (Scheme 4) which is in principle similar to the distorted icosahedral $\text{Al}_{12}(\text{AlBr}_2)_{10}$ that we reported recently.³³

Further reduction to $\text{Al}_{12}\text{R}_{10}^{2-}$ and dissociation of two additional R^- ligands should lead to an Al_{12}R_8 molecule or the corresponding anion, and indeed this is found in experiments. Since similar cluster compounds are obtained for Al and In ($[\text{Al}_{12}\{\text{N}(\text{SiMe}_3)_2\}_8]^{2-}$ and $\text{In}_{12}(\text{Si}^i\text{Bu}_3)_8$), it is plausible that the proposed mechanism represents a general pathway during reduction processes leading to the bulk metal. Therefore, intermediates similar to **2** are also expected to occur for other

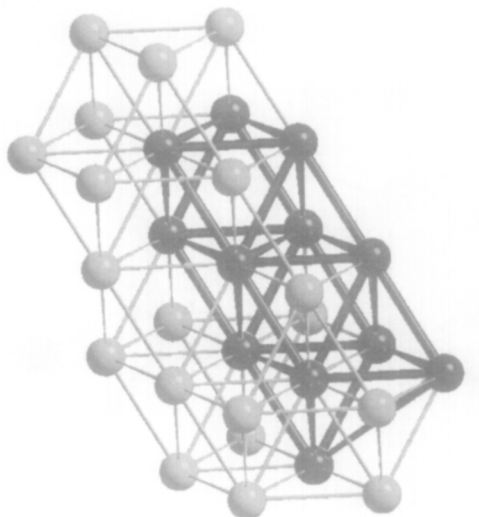
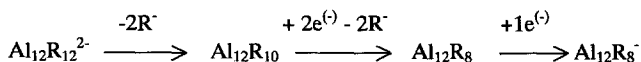


FIG. 7. Section of the cubic close packing of Al-metal. The Al_{12} unit of **2** is marked.

metals. Limitations arise from the size of the metal atoms which must be compatible with the size of the ligands. On this basis, the large supersilyl (Si^tBu_3) ligands are suitable for protecting the large In_{12} cluster, whereas the smaller $\text{N}(\text{SiMe}_2)_2$ groups match the smaller Al_{12} cluster.

C. $\text{Al}_{14}[\text{N}(\text{SiMe}_3)_2]_6\text{I}_6^{2-}$ Cluster **3**³⁹

In order to find optimal reaction conditions for the synthesis of the $\text{Al}_{77}\text{R}_{20}^{2-}$ cluster (see below), we repeatedly heated the reaction solution of AlI_3 in Et_2O and toluene with solid $\text{LiN}(\text{SiMe}_2)_2$ for a short period of time to 55°C . This treatment, followed by cooling the solution back to $+7^\circ\text{C}$, results in dark brown crystalline platelets of **3**, representing the first partially substituted Al subhalogenide compound. Obviously the substitution proceeds significantly slower for iodide than for chloride, and this difference is responsible for the observation that the completely substituted clusters Al_7R_6^- and $\text{Al}_{12}\text{R}_8^-$ are formed starting from AlCl_3 , but not from AlI_3 .



SCHEME 4. Hypothetical reaction scheme for the formation of **2** starting from an icosahedral Al_{12} compound.

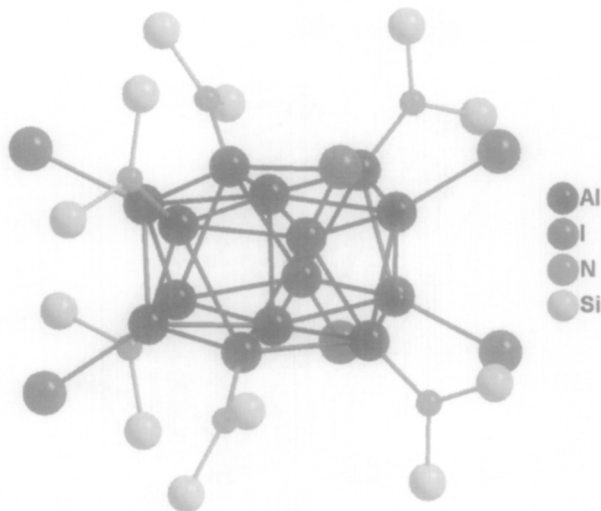


FIG. 8. Molecular structure of $\text{Al}_{14}[\text{N}(\text{SiMe}_3)_2]_6\text{I}_6^{2-}$ **3** (methyl groups are omitted for clarity).

Figure 8 demonstrates the X-ray structure of the cluster dianion **3**. The main structural unit is best described by two staggered, approximately Al-centered Al_6 rings. The central Al atoms deviate somewhat from the planes of the rings and are separated by 272.8 pm. All other Al–Al distances range from 257.0 pm (i.e., between Al atoms with iodine ligands) to 291.0 pm (i.e., between Al atoms with $\text{N}(\text{SiMe}_3)_2$ ligands) and thus lie in the range typical for polyhedral or metalloid Al clusters.

The average oxidation state of the Al atoms in the Al_7R_6^- cluster **1** and in **3** is 0.71, distinctly higher than the value of 0.23 found in the Al_{77} cluster (see below). The disproportionation of the initially monovalent Al species to aluminum metal seems to be therefore equally far advanced for **3** and for **1**. To discuss appropriately the bonding properties in the two species with aluminum in the same average oxidation state, we carried out DFT calculations on the model compounds Al_7R_6^- (**1a**; $\text{R} = \text{NH}_2$) and $\text{Al}_{14}\text{R}_{12}^{2-}$ (**3a**; $\text{R} = \text{NH}_2$).

These calculations indicated that the dimerization process **1a** \rightarrow **3a** is exothermic ($-275 \text{ kJ} \cdot \text{mol}^{-1}$). The bond distances in **1a** and **3a**, which are included in Fig. 9, correspond at a first glance to the experimentally determined values for **1** and **3**. Additional calculations were carried out on the isomer **3b**, the results of which are also included in Fig. 9. In this case, the central Al–Al distance is highly elongated (490.3 pm), and an approximately polyhedral structure results, similar to that found for M_{14} Frank–Kasper polyhedra (e.g., $\text{Mg}_{23}(\text{Al}, \text{Zn})_{49}$),⁴⁹ the only important difference being that the central atom is missing in **3b**.

Although the polyhedral structure of **3b** seems to point to a bonding situation as described by Wade for a *precloso* or *nido* structure,¹³ the calculations

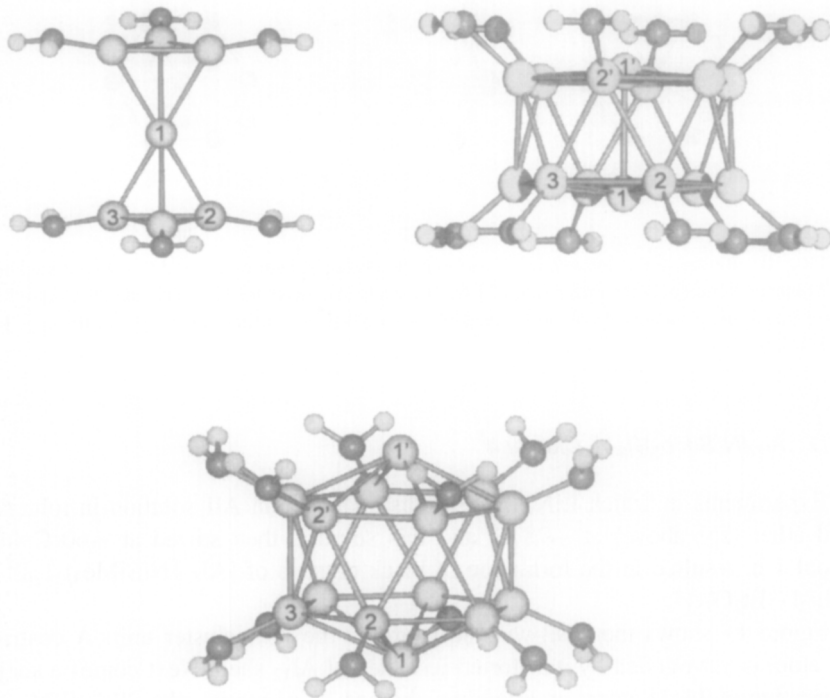


FIG. 9. Calculated structure of the model compounds $\text{Al}_7(\text{NH}_2)_6^-$ (**1a**), $\text{Al}_{14}(\text{NH}_2)_{12}^{2-}$ (**3a**), and polyhedral $\text{Al}_{14}(\text{NH}_2)_{12}^{2-}$ (**3b**). Selected Al–Al distances [pm]: **1a**: Al1–Al2: 276.0, Al2–Al3: 254.3; **3a**: Al1–Al2: 272.1, Al2–Al3: 271.3, Al2–Al2': 269.0, Al1–Al1': 269.3; **3b**: Al1–Al2: 290.8, Al2–Al3: 263.8, Al2–Al2': 280.8, Al1–Al1': 490.3.

showed that **3b** is clearly destabilized with respect to **3a** ($+123 \text{ kJ} \cdot \text{mol}^{-1}$). This implies that for Al_n clusters a metalloid cluster is energetically favored over a polyhedral cluster.⁵⁰ As already discussed for other metalloid clusters (Al_7 , Al_{12} , Al_{77}), the experimental and theoretical findings presented for **3** confirm that Wade's rules are in general not appropriate to describe bonding situations of this type.

To improve our understanding of the exceptional bonding situation in **1** and **3**, we calculated the²⁷ Al NMR shifts for the central (**1a**, **3a**) and apical Al atoms (**3b**). The results for **1a** ($\delta = 652$), **3a** ($\delta = 358$), and **3b** ($\delta = -313$) show—as already discussed for **1**—that for **1a** and **3a**, but not for polyhedral **3b**, the central Al atoms approach the bonding situation found in aluminum metal ($\delta = 1640$).⁴⁴ These theoretical findings confirm the arguments based on the structural properties. The geometry of the partially preformed metal structure becomes evident in the metalloid cluster **3** rationalized in Fig. 10. Close packing as in the metal structure results from rotation by 30° followed by translation.

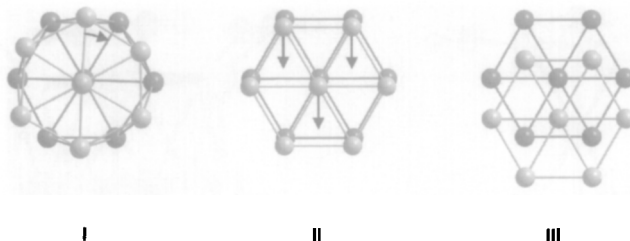


FIG. 10. Illustration of the similarity between the cluster structure of **3** and the closest packing in Al metal: Rotation of the upper ring of **I** by 30° leads to a structure **II**, which can then easily be transformed into a section of the closest packing of Al metal by shifting in the layer of the page by $(1/4, 1/4, 0)$.

D. $\text{Al}_{77}[\text{N}(\text{SiMe}_3)_2]_{20}^{2-}$ Cluster **4**⁸

Experiments in which $\text{LiN}(\text{SiMe}_3)_2$ was added to an AlI solution in toluene and ether (see above) at -78°C , and this solution then stirred at $+60^\circ\text{C}$ for about 1 h, resulted in the formation of black crystals of $[\text{Al}_{77}\{\text{N}(\text{SiMe}_3)_2\}_{20}]^{2-} 2[\text{Li}_2\text{I} \cdot (\text{Et}_2\text{O})_5]^+$.

Figure 11 shows the shell-wise structure of the Al_{77} cluster unit: A central Al atom is surrounded by a distorted icosahedral Al_{12} shell. Next comes a shell consisting of 44 Al atoms and finally a shell of 20 Al atoms with 20 $\text{N}(\text{SiMe}_3)_2$ groups attached through strong $2e2c\text{-AlN}$ bonds. The structural differences of this cluster with respect to clusters of precious metals will be discussed in detail in Section V of this report. It is remarkable that topologically only the central Al atom with its coordination number of 12 is close to the geometric environment of an Al atom in the Al metal. Toward the exterior of the cluster the coordination numbers decrease and the Al–Al bond lengths get correspondingly shorter. The relation between coordination numbers and Al–Al distances is summarized in Table I.

It is not a surprise that the bonds become more localized (molecular) with increasing distance from the cluster center. Although the central Al atom in the cluster has the same coordination number as the Al atoms in the Al bulk metal, the cluster exterior induces a change of the geometry of the neighboring Al atoms which form an icosahedron in the case of the cluster compound instead of the cuboctahedron found in the Al metal. At the same time, the Al–Al distances become shorter (286 pm in the metal vs 277 pm in the cluster). The negative charge of the Al_{77} clusters is neutralized by two $\mu(\text{I})$ bridged Li_2 cations in the crystal. The $\text{Al}_{77}\text{R}_{20}^{2-}$ clusters are packed in a distorted hexagonal primitive symmetry (Fig. 12) with a coordination number of $8 + 12$ (i.e., 8^* (21.7–23.1 Å) and 12^* (26.9–32.7 Å)).

Unfortunately all crystals of $\text{Al}_{77}\text{R}_{20}^{2-}$ that exist so far proved to be too small and too reactive to measure their electrical conductivity or other important physical properties. It should be mentioned that the same problems arise in the case of

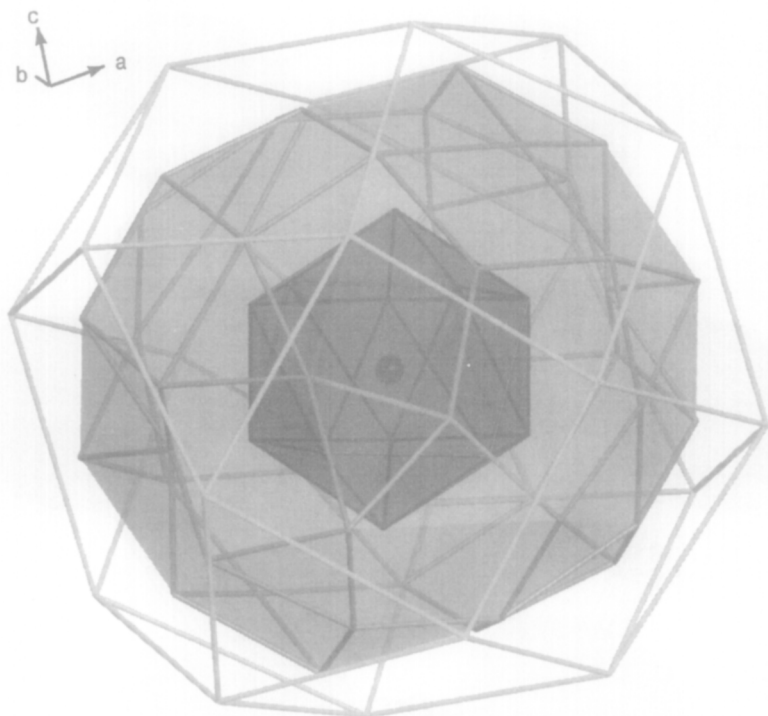


FIG. 11. Molecular structure of $[\text{Al}_{77}\{\text{N}(\text{SiMe}_3)_2\}_{20}]^{2-}$ **4** $[\text{N}(\text{SiMe}_3)_2]$ ligands are omitted for clarity] showing the order of the Al atoms in shells. The edges within this stick model represent the 77 Al atoms.

TABLE I
Al–Al DISTANCES WITHIN AND BETWEEN THE Al_{77} CLUSTER SHELLS

Shell	Center	1	$1 \rightarrow 2^a$	2	$2 \rightarrow 3$	3
Atoms	1	12		44		20
c. n. ^b	12	9 ^c	4	7 ^d	2	(4) ^e
$d_{\text{minimal}} [\text{\AA}]$	2.674	2.693	2.638	2.564	2.565	(4.905)
$d_{\text{maximal}} [\text{\AA}]$	2.870	2.973	2.991	2.999	2.852	(5.170)
$d_{\text{average}} [\text{\AA}]$	2.762	2.795	2.818	2.756	2.688	(5.019)

Note: Only atoms with a distance between 2.5 and 3.0 Å from a particular atom were counted and considered for the coordination number.

^aCoordination from 1. to 2. shell.

^bc. n., coordination number.

^cc. n. = c. n. 1. shell \rightarrow central atom + c. n. 1. shell + c. n. 1. \rightarrow 2. shell = $1 + 4 + 4 = 9$.

^dc. n. = c. n. 2 \rightarrow 1. shell + c. n. 2. shell + c. n. 2. \rightarrow 3. shell = $1 + 3.75 + 2 = 6.75$.

^eThere is no significant bonding between each pair of Al atoms within the 3. shell.

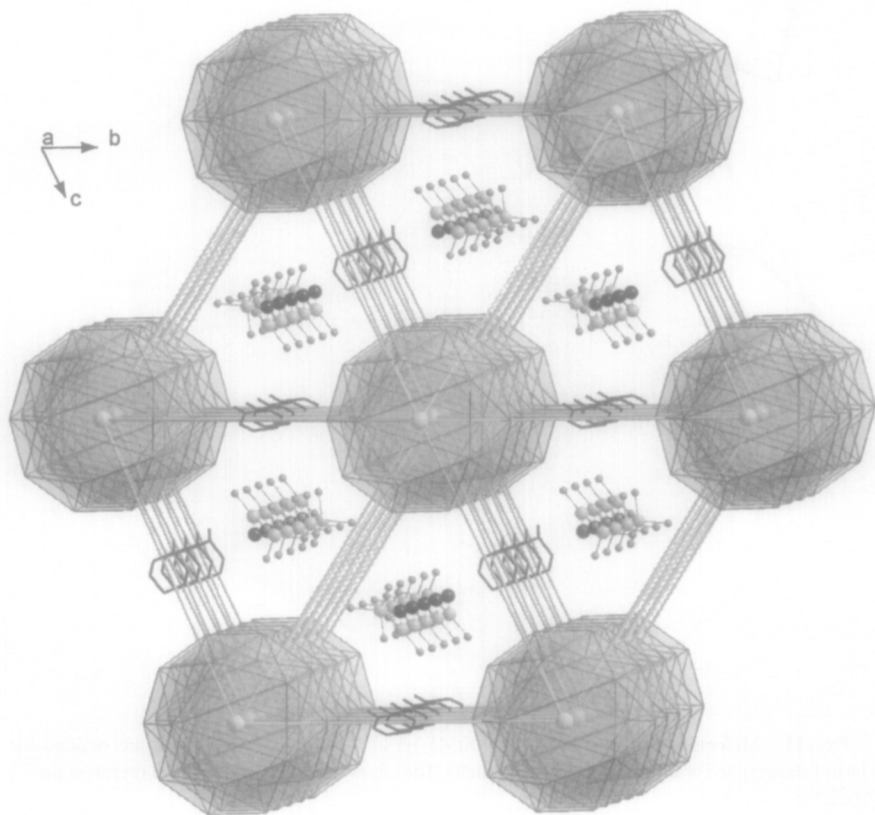


FIG. 12. Arrangement of the $[\text{Al}_{77}\{\text{N}(\text{SiMe}_3)_2\}_{20}]^{2-}$ clusters **4** within the crystal of $[\text{Al}_{77}\{\text{N}(\text{SiMe}_3)_2\}_{20}]^{2-} \cdot 2[\text{Li}_2\text{I} \cdot (\text{Et}_2\text{O})_5]^+ \cdot 2\text{toluene}$.

metalloid clusters of precious metals, and this is the reason why there are only a small number of crystalline, definitely structurally analyzed clusters (see above). So, although this missing tendency for crystallization of metalloid clusters of the precious metals is unsatisfying with respect to their characterization, the easy approach and handling is, together with the relatively poor reactivity (e.g., with O_2 or H_2O), responsible for the many possible applications of the Au_{55} cluster.⁵¹ In contrast to these clusters, the metalloid Al and Ga clusters, which will be discussed below, have an enhanced reactivity; many of them will ignite spontaneously when exposed to air. The same trends in reactivity of metalloid clusters of base and precious metals can be found when the reactivity of main group metals is compared to those of precious metals.

We applied numerous synthesis methods to maximize the yield of the Al_{77} cluster compound whose physical characteristics we wanted to measure. Our most

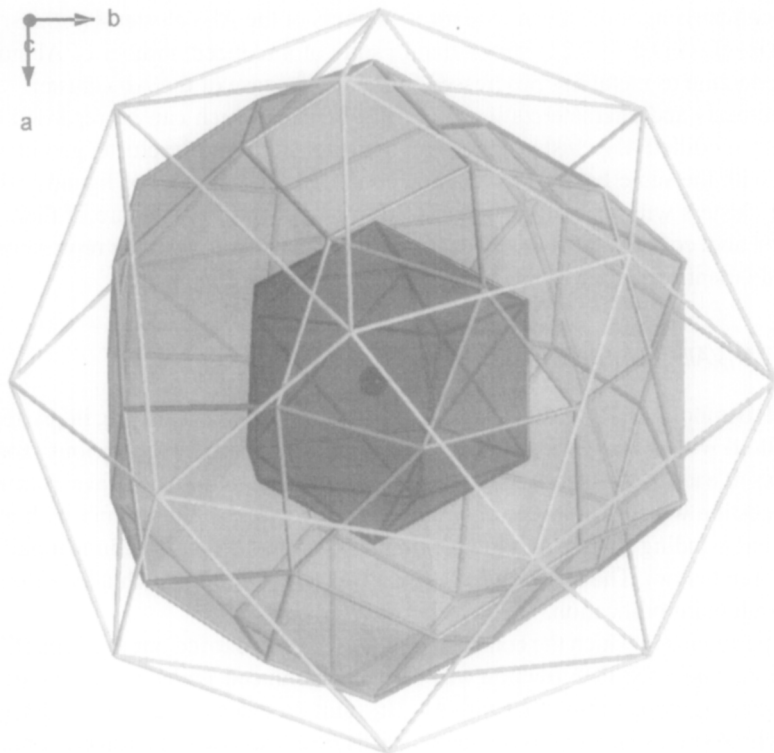


FIG. 13. Molecular structure of $[\text{Al}_{69}\{\text{N}(\text{SiMe}_3)_2\}_{18}]^{3-}$ **5** $[\text{N}(\text{SiMe}_3)_2]$ groups are omitted for clarity] showing the order of the Al atoms in shells. The edges within the stick model represent the 69 Al atoms.

recent experiments, based on a reactive AlCl (toluene/ Et_2O) solution to which solid $\text{LiN}(\text{SiMe}_3)_2$, was added and then heated to 60°C , resulted in dark brown rod-like crystals of the composition $[\text{Al}_{69}\{\text{N}(\text{SiMe}_3)_2\}_{18}]^{3-} \cdot 3[\text{Li} \cdot (\text{Et}_2\text{O})_4]^+$.⁴⁰ The X-ray structure of the Al_{69} nucleus **5** is shown in Fig. 13.

Unlike the Al_{77} cluster, the central Al atom of the Al_{69} nucleus is not surrounded by a distorted icosahedron but a decahedral Al_{12} shell with distorted D_{5h} symmetry. The next shell contains 38 Al atoms, which in turn are surrounded by 18 $\text{Al}[\text{N}(\text{SiMe}_3)_2]$ ligands. Similar to the Al_{77} cluster the coordination numbers decrease and the Al–Al distances shorten in direction from the center to the cluster surface. Although the difference in the structure of this and of the Al_{77} cluster seems at a first to be rather insignificant, the environment of the central Al atom is affected. This shows that a slightest variation on the surface of nanostructured materials can affect the structures in the depth of 1–2 nm toward the core of the nanoparticles. This observation has major implications for catalytic processes.

A comparison of the mean oxidation numbers of the Al_{77} cluster **4** (+0.23) and the Al_{69} clusters **5** (+0.21) shows that in spite of a reduced number of Al atoms, the reduction to metal has progressed further in the case of the Al_{69} cluster.

Synthesis and characterization of an Al_{69} cluster which can be regarded as a slightly modified Al_{77} cluster show the extreme sensitivity of the cluster geometry—even with the same ligand—to reaction conditions and number of ligands. Many more clusters will have to be synthesized to get a consistent picture of their formation and, consequently, the mechanism of metal formation which represents, as already mentioned, one of the oldest chemical processes in history.

E. $\text{Al}_{12}(\text{AlBr}_2)_{10} \cdot 12(\text{THF})$ Cluster **6**³³

All metalloid Al_nR_n clusters discussed in the previous sections are, in principle, metalloid with regard to fcc packed aluminum. Motivated by the various modifications of each of the homologous elements boron and gallium, we have examined the question whether there are also further modifications of aluminum with more covalent bonding of the Al atoms, similar to the boron and gallium modifications (see below). The following analysis gives a first hint for such a hypothetical β -aluminum modification.

Experiments in which the condensation of AlBr was carried out in toluene/THF solution, where the THF fraction was very much reduced, ended not with the Al_x oligomers described above, but with $\text{Al}_{22}\text{Br}_{20}$ units best described as $\text{Al}_{12}(\text{AlBr}_2)_{10} \cdot 12(\text{THF})$ **6** (Fig. 14).⁵² In this compound, a distorted Al_{12} icosahedron is connected

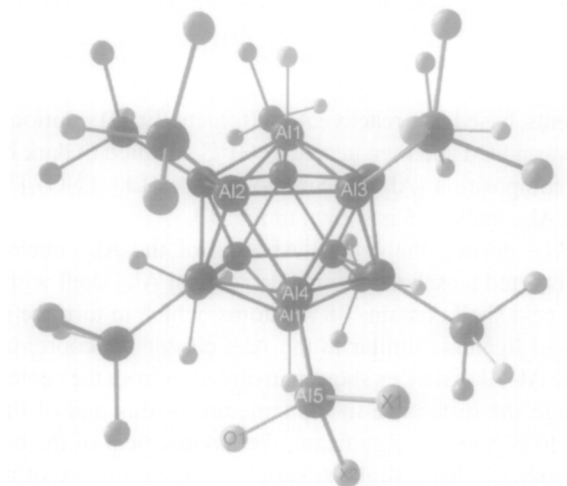


FIG. 14. Molecular structure of $\text{Al}_{12}(\text{AlBr}_2)_{10} \cdot 12(\text{THF})$ **6**. Only the O atoms of the THF molecules are shown.

to a THF molecule at both “peak” ends of the icosahedron. The remaining 10 Al atoms are tied to $\text{AlBr}_2 \cdot \text{THF}$ units via Al–Al bonds. Thus, an internal disproportionation to $12 \text{ Al}^{\pm 0}$ and 10 Al^{2+} species has formally occurred. To our knowledge, such a molecular cluster compound in which the atoms of the icosahedron are linked to atoms of the same species has heretofore been unknown. This finding is even more remarkable, especially regarding the boron modifications, that units of this kind should be embossed, also within molecular species. Up to now, these species did not even exist among the boron subhalogenides, maybe because of the lack of suitable experimental techniques.

The structural similarity of $\text{Al}_{12}\text{Br}_{20} \cdot 12(\text{THF})$ **6** to β -rhombohedral boron with the familiar B_{84} unit raises the question whether another, more covalent, form of aluminum in addition to the metallic α -form exists, similar to the geometry of the Al atoms in the Al_{12} icosahedra of **6**. The mild conditions applied for the synthesis of $\text{Al}_{22}\text{Br}_{20}$ might also favor the formation of such a modification. In order to support this hypothesis, we investigated the structural competition between the fcc and ff-B type for Al by means of *ab initio* full-potential calculations, with the results shown in Fig. 15.⁵²

At a volume corresponding to that of the experimental (fcc) energy minimum modification (V_0), the interatomic distances in the open packed ff-B structure become very short, and the structure is more than $80 \text{ kJ} \cdot \text{mol}^{-1}$ less stable than the fcc close packing. However, when the volume is relaxed the ff-B structure is rapidly stabilized. The optimum volume lies near $V/V_0 = 1.4$, corresponding to an expansion of about 40% with respect to the energy minimum volume. At this volume the Al–Al distances within the Al icosahedra are 264 pm, which compares

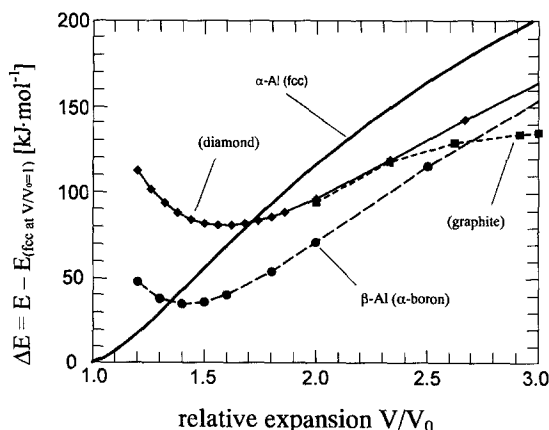


FIG. 15. Structural competition between the fcc and ff-B type of aluminum during expansion (*ab initio* full potential calculation).

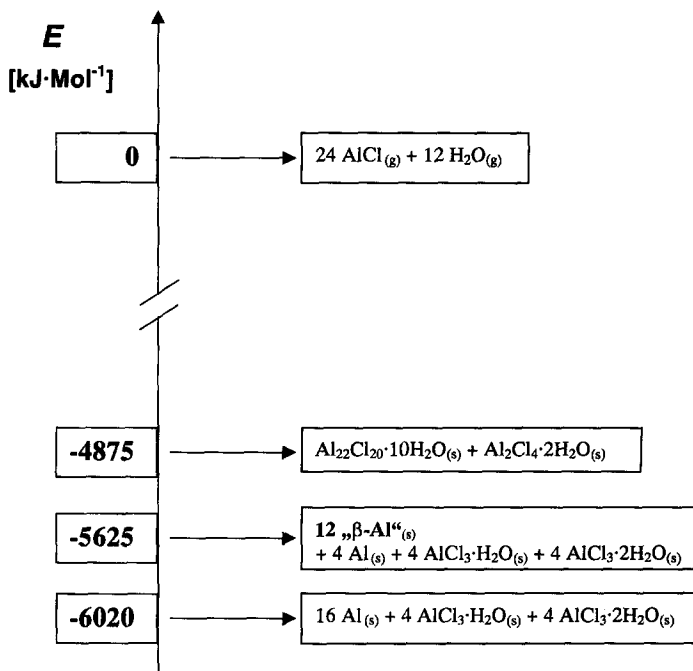


FIG. 16. Energies of **6a** and the hypothetical β -Al relative to the gaseous educts and the thermodynamic end-products.

quite well to the range of distances found within the icosahedra of $\text{Al}_{22}\text{X}_{20}$ units. Additionally, the energy decreases by about $33 \pm 1 \text{ kJ} \cdot \text{mol}^{-1}$ with respect to fcc Al in its energy minimum.

To further explore the energetic situation of the disproportionation product, we calculated the structure and energy of the model system $\text{Al}_{22}\text{Cl}_{20} \cdot 10\text{H}_2\text{O}_{(\text{s})}$ (**6a**) + $\text{Al}_2\text{Cl}_4 \cdot \text{H}_2\text{O}_{(\text{s})}$ in relation to the educts ($24 \text{ AlCl}_{(\text{g})} + 12 \text{ H}_2\text{O}_{(\text{g})}$) and the thermodynamically most stable end products ($16\text{Al}_{(\text{s})} + 4 \text{ AlCl}_3 \cdot \text{H}_2\text{O}_{(\text{s})}$). The energy diagram, shown in Fig. 16, shows that already 81% of the disproportionation energy is liberated when the gaseous educts from solid **6a**.

The hypothetical condensation of the Al_{12} icosahedra of **6a** to ' $\beta\text{-Al}_{12}$ ' is exothermic by a value of $-740 \text{ kJ} \cdot \text{mol}^{-1}$. These considerations show that such a previously unknown elementary structure of aluminum might be stable under the right conditions, leaving the possibility that it is experimentally accessible.

F. Conclusion

The isolation methods and the structures of the metalloid aluminum clusters discussed here have shown the particular suitability of the ligand $\text{N}(\text{SiMe}_3)_2$ for

stabilizing intermediates on the way to the metal (α -Al). In this process, the cluster size depends on the reactivity of the AlX solution and the reaction temperatures. The reactivity of the AlX solutions increases in the order $\text{AlI} < \text{AlBr} < \text{AlCl}$ and thus the cluster size increases in the same order. Low temperatures favor the formation of small clusters (e.g., Al_7R_6^- at -25°C) while relatively high temperatures lead to large clusters (e.g., $\text{Al}_{77}\text{R}_{20}^{2-}$ at $+60^\circ\text{C}$). In all these cases, the clusters can generally be regarded as fragments of the fcc Al metal lattice. However, this conclusion might not be applicable to the $\text{Al}_{22}\text{X}_{20}$ clusters. Formation of icosahedral Al_{12} units and their direct bonding to further AlX₂ groups points to the possible existence of a new Al modification (β -Al). The results of this unconventional molecular chemistry might stimulate new research in solid-state chemistry: this research topic has links to various other areas of chemistry. The consequences of our results for solid-state chemistry become even more evident if we take a closer look at the recently synthesized metalloid gallium compounds, described in the next sections.

IV

METALLOID Ga CLUSTERS

In contrast to aluminum, for which only one solid-state modification is known so far, gallium, the higher homologue of aluminum, has a great variety of solid-state modifications, realized at different pressures and temperatures.⁵³ For metalloid gallium clusters a great variety of structures is expected, too, since these compounds are with respect to their structure in between molecules and solid bulk metal. Therefore it is important for an appropriate discussion to compare the solid-state structure with the structures of the clusters. In the following account, the structures of the different gallium modifications will be summarized first, and then the similarities to the cluster structures will be worked out.

A. Solid-State Modifications of Elemental Gallium

1. α -Gallium⁵⁴

In α -gallium, the thermodynamically stable modification of the element at normal conditions, crystallizing in an independent structure type (Fig. 17), each Ga atom has one neighbor at a distance of 244.8 pm and six further neighbors in duads with distances of 270.2, 272.9, and 279.4 pm. Therefore, the coordination number of each individual gallium atom is best described by the notation $(1 + 6)$. A more detailed analysis of the solid-state structure shows the presence of planar and puckered six-membered rings which are typically only found for Group 14 elements. The Ga–Ga distances in the planar six-membered rings are 244.8 and 270.2 pm; in

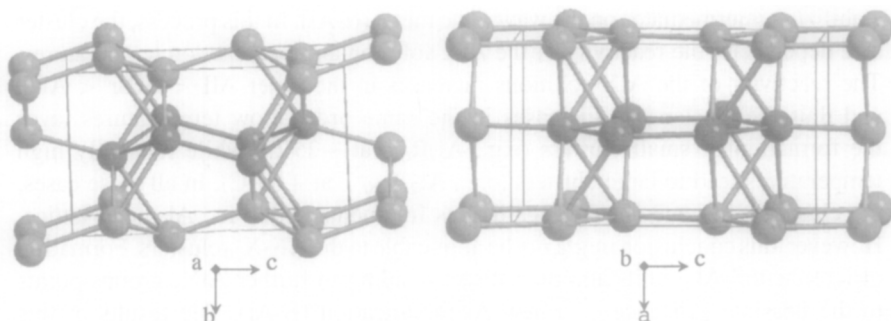


FIG. 17. Section of the solid-state structure of α -gallium. The Ga_6 structural elements are marked.

the puckered six-membered rings they amount to 244.8 and 279.5 pm. Thus, the solid-state structure of α -gallium shows a structure with a complexity unusual for metals, and which contains substructures normally expected for nonmetals rather than metals.

2. β -Gallium⁵⁵

β -Gallium is experimentally accessible by crystallization of liquid gallium at -16.3°C and represents the only modification of elementary gallium which has a certain structural resemblance to the α -phase. Each gallium atom of this structure has eight neighbors arranged in duads with Ga–Ga distances of 268.8, 276.6, 286.4, and 291.9 pm resulting in a $[2 + 2 + 2 + 2]$ coordination. The solid-state structure consists of layers, which themselves consist of twin-threaded ladders, with distances of half a ladder step between two ladders, resulting in a triangle structure between the ladders (see Fig. 18). In the three-dimensional solid-state structure, tubes result (Fig. 18), reminiscent of a cubic primitive structure (α -polonium type).

3. γ -Gallium⁵⁶

The low-temperature phase γ -gallium can be generated by crystallization of liquid gallium at a temperature of -35.6°C . The solid-state structure (Fig. 19) is distinguished by an unusual but highly symmetrical arrangement of gallium atoms which can be described by three different substructures. One of these substructures is a tubular construction of Ga_7 rings. These Ga_7 rings are twisted by 51° to each other so that on the surface of the tubes a triangular pattern develops. Inside the seven-membered rings, the Ga–Ga distances vary in the range of 261.5 to 266.3 pm. Between the seven-membered rings the Ga–Ga distances lie between 291.4 and 296.3 pm. Inside the tubes, a linear arrangement of gallium atoms which can be described as a “one-dimensional Ga wire” is found. The Ga–Ga distances inside

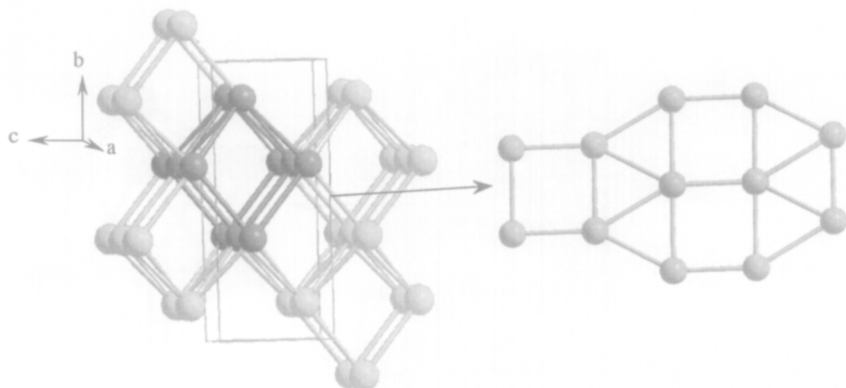


FIG. 18. Section of the solid-state structure of β -gallium. The tubular substructure is marked, and a single layer is pointed out.

this “wire” are 260.2 pm. There is one short distance from the “wire atoms” to the surrounding tube of 291.6 pm and six longer distances with an average value of 305 pm. These two substructures are tied by a third substructure which can be described as a ladder structure. Inside the ladder structure the distances of the Ga atoms are 260.2 and 284.8 pm, whereas there are three bonds to the tubes with an average distance of 277 pm. The extremely variable surroundings of the gallium

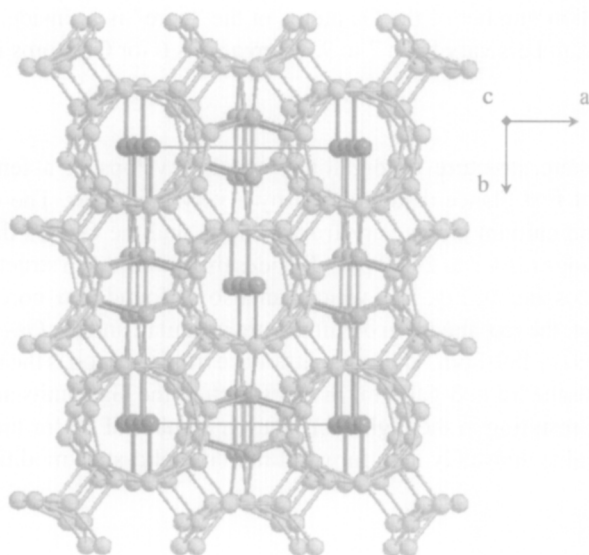


FIG. 19. Section of the solid-state structure of γ -gallium. View along the crystallographic c -axis. The different substructures are marked.

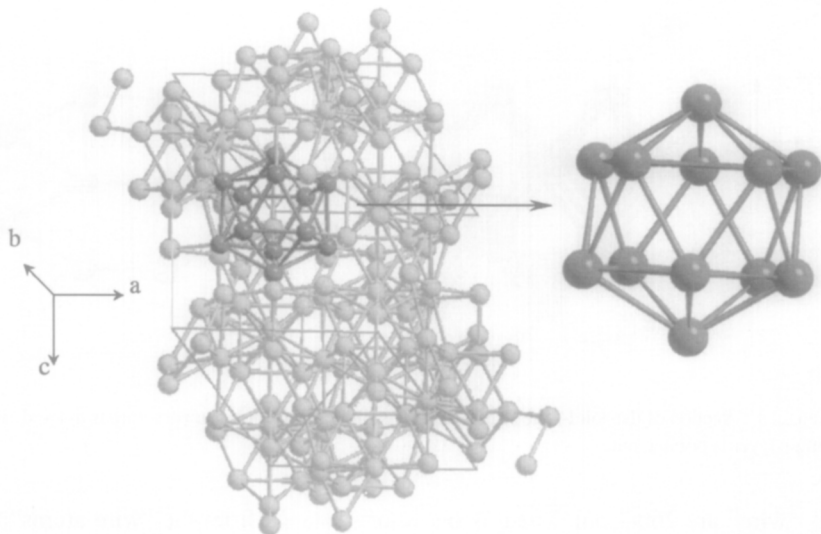


FIG. 20. Section of the solid-state structure of δ -gallium. The icosahedral substructure is marked. A magnification is displayed on the right side.

atoms within these substructures show that γ -gallium contains three different types of gallium atoms which differ, especially regarding their coordination numbers. The coordination number of the Ga atoms in the “wire” is 3. Inside the tube, the coordination numbers vary from 7 to 9, whereas it is 6 for Ga atoms in the ladder.

4. δ -Gallium⁵⁷

The solid-state structure of δ -gallium which develops at a temperature of -19.4°C , is at first glance distinguished by a very low order. The coordination numbers of the gallium atoms vary from 6 to 10, and the Ga–Ga distances also span a large range (254.7 to 292.9 pm). Besides this low order, a structural element exists (Ga_{12} icosahedra; Fig. 20), which can also be found in α -boron. However, unlike α -boron, the icosahedra in δ -gallium are irregular, and the Ga–Ga distances vary from 275.0 to 289.1 pm. The main difference from α -boron is the nonexistence of isolated icosahedra in δ -gallium. In this structure the Ga_{12} units are connected to each other, resulting in the high coordination number of 10 for the connecting Ga atoms, a value unusually high for gallium in its solid-state modifications.

5. Gallium(II)⁵³

Compared to the normal-pressure modifications, the high-pressure modification gallium(II) has a high degree of order. All gallium atoms of this structure have the

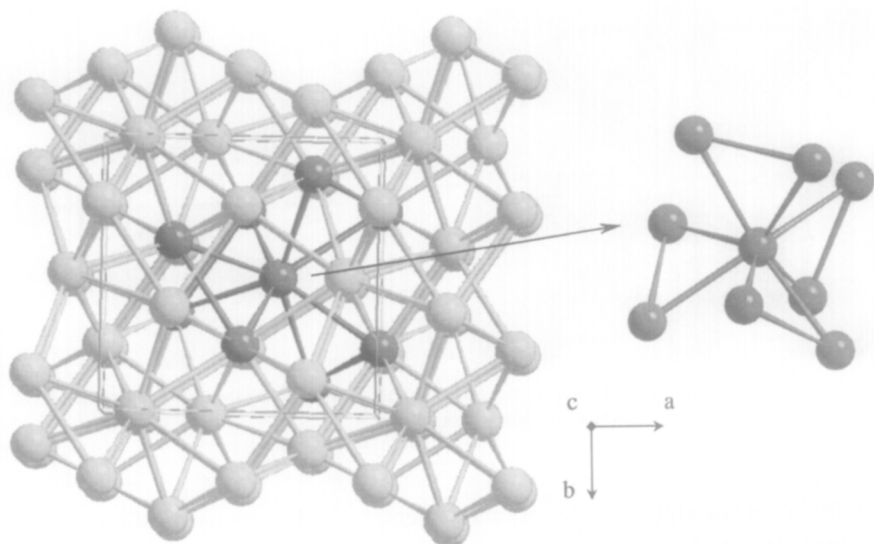


FIG. 21. Section of the solid-state structure of gallium(II). The first coordination sphere is marked and shown separately.

same coordination number of eight, and all Ga–Ga distances are equal (278.3 pm). The first coordination sphere around each gallium atom is best described by four triangles connected by a single atom and whose four bases point to the corners of a tetrahedra (Fig. 21).

6. Gallium(III)⁵³

The high-pressure modification Ga(III), formed at temperatures of about 40°C and under a pressure of 3GPa (the melting point of α -gallium under normal pressure is 30°C), has the highest symmetry of the elemental structures of gallium discovered so far. In Ga(III) each Ga atom has four nearest neighbors at a distance of 281.3 pm and eight neighbors at a longer distance of 298.5 pm. Consequently, each Ga atom has the coordination number 4 + 8 (Fig. 22). Ga(III) is thus the first modification of elemental gallium close to a metal modification with a high coordination number. In full agreement with this, the geometry of the unit cell (tetragonal I) also reflects this trend, and in fact it would transfer into a cubic space-centered cell for $a = b = c$. This variation consequently increases the coordination number from 4 + 8 to 8 + 6, a value similar to the one observed in the metal modification of the tungsten type. An analysis of the first coordination sphere makes the close vicinity to the tungsten type even more obvious (Fig. 22).

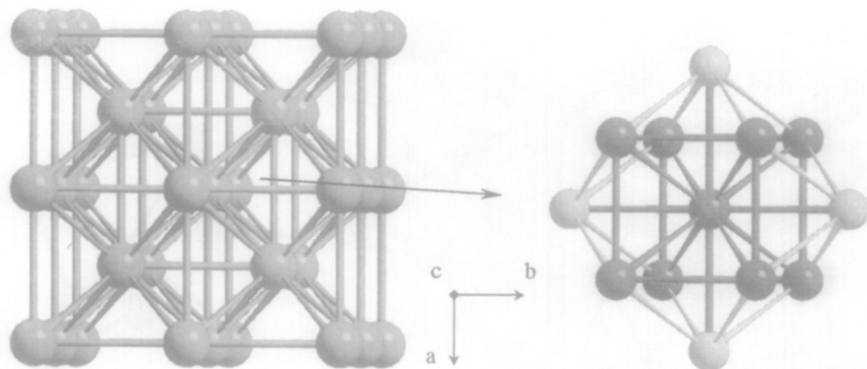


FIG. 22. Section of the solid-state structure of gallium(III). View along the crystallographic *c*-axis. On the right side, the first coordination sphere is shown.

This short description of the various elementary modifications of gallium shows its high structural variety, which also includes structural elements that are atypical for metals. This variety is also reflected in the inner composition of the metalloid gallium clusters, as discussed below.

B. Synthetic Routes to Metalloid Gallium Clusters

Every known synthetic route leading to metalloid clusters proceeds via a metathesis reaction after the disproportionation of a subvalent gallium species into Ga(III) and Ga(0) has started. One has the choice between two different subvalent gallium species as starting materials: A subvalent Ga(I)Br solution generated with the help of the cocondensation technique (see above) or gallium subhalogenides synthesized in the conventional way (e.g., GaI which for the first time was described by Green *et al.*)⁵⁸ In particular, G. Linti and co-workers, were successful in using conventionally synthesized subhalogenides. Using the above mentioned GaI they succeeded in synthesizing a whole series of new gallium cluster compounds: $\text{Ga}_4[\text{Si}(\text{SiMe}_3)_3]_4$,⁵⁹ $[\text{Ga}_4\text{Si}(\text{SiMe}_2)_2\{\text{Si}(\text{SiMe}_3)_3\}_3]^- [\text{Li}(\text{THF})_4]^+$,⁶⁰ $[\text{Ga}_4\text{I}_3\{\text{Si}(\text{SiMe}_3)_3\}_4]^- [\text{Li}(\text{THF})_4]^+$,⁶¹ $\text{Ga}_{22}[\text{Ge}(\text{SiMe}_3)_3]_8$,⁶² and $[\text{Ga}_{26}\{\text{Si}(\text{SiMe}_3)_3\}_8]^{2-} \cdot 2[\text{Li}(\text{THF})_4]^+$.⁶³ However, with the exception of the Ga_{22} and the Ga_{26} cluster, the synthesized compounds are not directly related to metalloid structures, and will therefore not be dealt with here. All other metalloid gallium clusters discussed here were synthesized using a Ga(I)Br solution (toluene/THF) which was produced applying the cocondensation technique as described in Section II. In the following account, the metalloid gallium clusters synthesized so far will be discussed in the order of increasing number of Ga atoms.

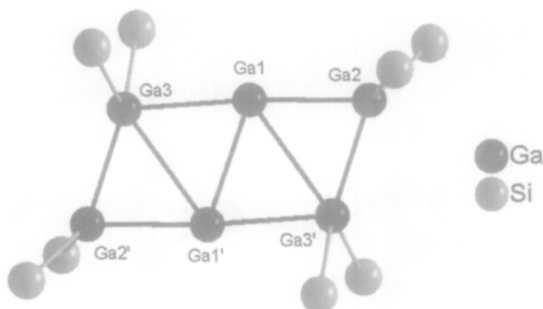


FIG. 23. Molecular structure of $[\text{Ga}_6(\text{SiPh}_2\text{Me})_8]^{2-}$ **7** (methyl and phenyl groups are omitted for clarity). Selected bond lengths [pm]: Ga1-Ga2 = 247.1, Ga1-Ga3 = 260.4, Ga1-Ga1' = 275.7, Ga1-Ga3' = 289.5, Ga2-Ga3 = 252.6.

C. $[\text{Ga}_6(\text{SiPh}_2\text{Me})_8]^{2-}$ Cluster **7**⁶⁴

The $\text{Ga}_6(\text{SiPh}_2\text{Me})_8^{2-}$ **7** anion within the compound $[\text{Ga}_6(\text{SiPh}_2\text{Me})_8]^{2-} \cdot 2[\text{Li}(\text{THF})_4]^+$ represents the smallest metalloid Ga cluster. In this cluster six Ga atoms are arranged ladder-wise in the Ga core (Fig. 23). Four of them are connected to two SiPh_2Me ligands each, with a medium Ga–Si distance of 242 pm. These eight ligands shield the metal core completely from the exterior. The two central Ga atoms are free of ligands and only bonded to other gallium atoms. The extraordinary structure of **7** can be described formally as Ga_6R_6 stabilized by two additional R^- donors, thus posing the question why no octahedral Ga_6R_6 species is formed, analogous to the octahedral aluminum compound $[\text{Al}_6^t\text{Bu}_6]^-$.⁶⁵ For gallium, this option seems to be inconvenient. Instead, two R^- fragments are added to complete the observed structure.

A possible explanation for the formation of this planar ladder structure can be found in the close geometrical similarity of **7** to β -gallium. The relative positions of the Ga atoms in **7** are comparable to those found in β -gallium (see Fig. 18), but as expected, the Ga–Ga distances in **7** are all shorter than in β -gallium due to a more molecular kind of bonding. This means that in **7** the formation of metalloid structures is preferred over the formation of polyhedral structures, which results in the unusual arrangement of the Ga atoms.

D. $\text{Ga}_8[\text{C}(\text{SiMe}_3)_3]_6$ Cluster **8**⁶⁶

The $\text{Ga}_8[\text{C}(\text{SiMe}_3)_3]_6$ **8** cluster, which occurs as an intermediate during the formation of the Ga_{19} cluster (see above), includes the most extraordinary arrangement of gallium atoms in the cluster core of all structures of metalloid gallium clusters

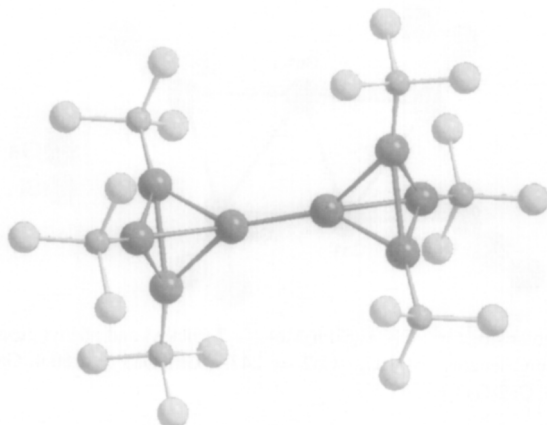


FIG. 24. Molecular structure of $\text{Ga}_8[\text{C}(\text{SiMe}_3)_3]_8$ **8** (methyl groups are omitted for clarity).

known so far. It consists of eight Ga atoms forming two tetrahedra connected at their points through a direct metal–metal bond (Fig. 24).

The Ga–Ga distances in the Ga_8 core vary only slightly (260.5 to 264.8 pm), and therefore the angles within the triangle planes of the tetrahedra differ by not more than 1° from the ideal value of 60° . The ligands are tied to the gallium core with a medium Ga–C distance of 204.5 pm. In **8**, the Ga–Ga bonds as well as the Ga–C bonds are significantly shorter than in tetrahedral $\text{Ga}_4(\text{C}(\text{SiMe}_3)_3)_4$ [$d(\text{Ga–Ga})$: 268.3, $d(\text{Ga–C})$: 207.4 pm].⁶⁷ These data show that the $\text{C}(\text{SiMe}_3)_3$ ligand has a great steric demand, and steric overload will therefore lead to longer distances, as observed in $\text{Ga}_4(\text{C}(\text{SiMe}_3)_3)_4$.⁶⁷

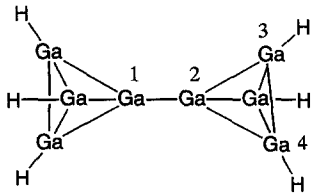
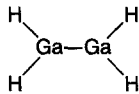
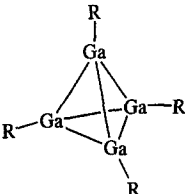
The structural element of two almost ideal tetrahedra which are connected to each other at their tops is completely unknown so far for Group 13 compounds; nor can it be found in the elemental structures, although the central Ga_2 unit is close to the α -phase. However, its coordination number of $4(1 + 3)$ does not reach the coordination number $7(1 + 6)$ of α -gallium.

A structural classification of **8** is difficult due to the fact that an arrangement of metal atoms as in **8** is uncommon in the whole field of molecular metal clusters. For this reason, detailed understanding of the bonding properties in **8** requires quantum chemical calculations. Theoretical analysis seems to be especially applicable to learning more about the bond between the two tetrahedra, which appears at first to be an isolated metal–metal bond between two metal atoms in the formal oxidation state zero.

In order to obtain insight into the bonding properties, DFT calculations on the model compounds Ga_8H_6 **8a**, Ga_2H_4 **8b**, and Ga_4H_4 **8c** were performed, with the results summarized in Table II. The results show that the distances in **8a** exhibit a

TABLE II
Ga–Ga DISTANCES, FORCE CONSTANTS, CHARGES, AND NMR SHIFTS OF THE CALCULATED
MODEL COMPOUNDS **8a**, **8b**, AND **8c**

Compound	Ga–Ga distance (pm)	Force constant (mdyn/Å)	Charge	⁷¹ Ga NMR (ppm)
Ga ₈ H ₆ 8a	d(Ga1–Ga2): 253.8 d(Ga2–Ga3): 259.4 d(Ga3–Ga4): 255.8	0.8 (Ga1–Ga2)	–0.1 (Ga1) 0.0 (Ga3)	1028 (Ga1) 942 (Ga3)
Ga ₂ H ₄ 8b	d(Ga–Ga): 246.2	1.1	0.1	705
Ga ₄ H ₄ 8c	d(Ga–Ga): 256.7	0.6	0.0	986

8a
8b
8c

similar sequence and band width as the distances in **8**. As expected, the charges of the Ga atoms vary; the two central Ga atoms carry a slight negative charge (–0.12; Ga(R): +0.01). In a first approximation, one can talk of a “metallic” metal–metal bond which is for the first time realized in a molecular unit with an almost localized bonding situation, which can be compared to delocalized bonding in metals.

The calculated Ga–Ga distance is close to the value found for Ga₂H₄. Because the stretching force constant of the Ga–Ga bond in the model compound HGaGaH^{2–} (which is a model compound for the so-called Ga–Ga triple bond⁶⁸) is not significantly different from the one in simple bonded Ga–Ga molecules,⁶⁹ a comparison of the force constants is especially interesting. A most detailed analysis indicates that the Ga–Ga bond in Ga₈H₆ **8a** (0.77 mdyn/Å) is weaker than the Ga–Ga bond in Ga₂H₄ **8b** (1.11 mdyn/Å). Obviously, the destabilization of the Ga–Ga bond is caused by the electron shifting within the two Ga₄ tetrahedra. This destabilization is expected to become bigger with increasing coordination numbers of the central Ga atoms, (e.g., two octahedral or icosahedral Ga_n polyhedra connected by a direct Ga–Ga bond). This possibly means that **8** is the first example for a model compound of a contact between particles of this kind, just before they are fused to form a larger cluster.

E. [Ga₁₂(C₁₃H₉)₁₀]^{2–} Cluster **9**⁷⁰

The icosahedral cluster Ga₁₂(C₁₃H₉)₁₀^{2–} **9** within the compound [Ga₁₂(C₁₃H₉)₁₀]^{2–} 2[Li(THF)₄]⁺, which is obtained by the reaction of fluorenyl lithium

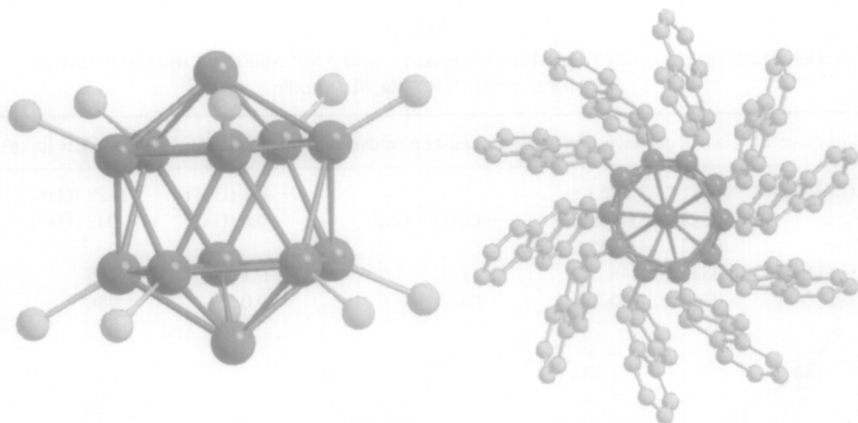


FIG. 25. Molecular structure of $[\text{Ga}_{12}(\text{C}_{13}\text{H}_9)_{10}]^{2-}$ **9**: At left, structure of the Ga_{12} core; at right, view along the axle running through the two naked Ga atoms.

with $\text{Ga}(\text{I})\text{Br}$, can be structurally described as follows: 10 of the 12 Ga atoms which form the icosahedral core structure are each connected to a fluorenyl ligand with a medium Ga–C distance of 205.9 pm. The Ga_{12} icosahedron is slightly expanded in the direction of the two “naked” gallium atoms, so that the longest Ga–Ga distances (268.4 pm) are those between the two Ga_5 rings. The distance between the “naked” Ga atoms and the Ga atoms of their corresponding Ga_5 rings are insignificantly shorter (265.3 pm). The shortest Ga–Ga-distances (258.9 pm) of the icosahedral Ga_{12} lattice are found inside the Ga_5 rings.

Looking along an axis going through both “naked” Ga atoms (Fig. 25) makes it clear that all the fluorenyl ligands are bent by the same angle. This angle can be explained by the hybridization of the carbon atom directly connected to the gallium atom (close to sp^3). The C–C distance to the α -C atoms (150.1 pm) and the C–C distance in the tetrahedral arrangement of the four bonding partners (angular sum of the C atom, $2^\circ \text{Ga-C-C} + \text{C-C-C}$: 330.4) are also in full agreement with this hybridization at the C atom. Due to this geometrical order of the fluorenyl ligands, a paddle wheel-shaped molecule results.

At a first sight, the icosahedral arrangement of the 12 gallium atoms can be described as a closopolyhedron, a structure that is already known from the corresponding boron compounds.⁷¹ However, DFT calculations show that the bonding properties of **9** do not correspond to those found in polyhedral boron compounds. This becomes plausible if one assumes that **9** belongs to the class of metalloid clusters, because **9** can also be described as a fragment of the δ -modification. This becomes obvious if one removes two R^- ligands leading to the neutral compound Ga_{12}R_8 with the same medium oxidation number of the Ga atoms as in **9**.

Consequently, there is a direct relation to the metalloid In_{12}R_8 (see Section III, B) cluster whose inner frame contains metallic partial structures.⁴⁷

The more molecular character of **9** in comparison to δ -gallium is responsible for a decrease of the bond lengths by about 25 pm. These results prove that **9**, considering its synthesis as well as the electronic structure, has to be classified in between polyhedral gallium clusters such as the square antiprismatic cluster $\text{Ga}_8(\text{C}_{13}\text{H}_9)_8^{2-}$ ⁷² and metalloid clusters.

F. $\text{Ga}_{18}(\text{Si}^t\text{Bu}_3)_8$ Cluster **10**⁷³

The core of the metalloid gallium cluster **10** consists of 18 Ga atoms. Eight of the 18 gallium atoms carry a Si^tBu_3 ligand with a medium Ga–Si distance of 246 pm. These 8 gallium atoms form a strongly distorted square antiprism. The gallium core of the cluster is almost completely shielded by the 8 ligands. The Ga–Ga distances within the cluster vary from 250 to 300 pm. Moreover, there is a great structural resemblance of the arrangement of the Ga atoms in the cluster core to the arrangement of the gallium atoms in β -gallium, which can clearly be seen in Fig. 26. This structural proximity to the β -modification might be responsible for the arrangement of the Ga atoms as observed in the cluster core.

G. $[\text{Ga}_{19}\{\text{C}(\text{SiMe}_3)_3\}_6]^-$ Cluster **11**¹

The compound $[\text{Ga}_{19}\{\text{C}(\text{SiMe}_3)_3\}_6]^-[\text{Li}_2\text{Br}(\text{THF})_6]^+$ contains **11**, the smallest metalloid gallium cluster with a shell-like structure discussed here. The gallium core of **11** contains 19 gallium atoms, 6 of which are connected to a trisyl ligand

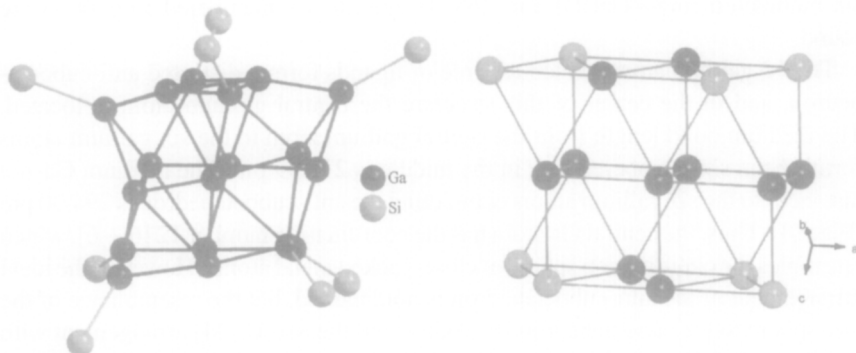


FIG. 26. Molecular structure of $\text{Ga}_{18}(\text{Si}^t\text{Bu}_3)_8$ **10** (^tBu groups are omitted for clarity) and the corresponding section of β -gallium.

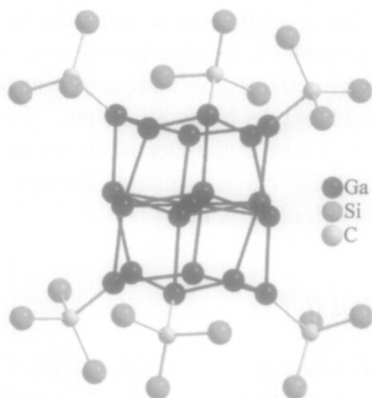


FIG. 27. Molecular structure of $[Ga_{19}\{C(SiMe_3)_3\}_6]^-$ **11** (methyl groups are omitted for clarity).

$C(SiMe_3)_3$ with a medium Ga–C distance of 200.9 pm (Fig. 27). The 19 gallium atoms form three six-membered rings lying on top of each other. The 19th gallium atom is located in the center of the middle six-membered ring. The distances within the middle six-membered ring vary from 277.13 to 279.40 pm, with a medium Ga–Ga-distance of 278.28 pm. The distances within the other two, outer six-membered rings vary from 252.01 to 255.47 pm, which corresponds to a medium value of 253.08 pm. Therefore the Ga–Ga distances within the individual six-membered rings are almost equal. The angles inside the middle six-membered ring vary from 115.97° to 117.05° , thus attaining an almost planar arrangement. The six-membered rings located above and below are puckered. Therefore two different angles within the six-membered rings and also two different Ga–Ga-distances between the six-membered rings of 244.85 (middle six-membered ring—Ga(R)) and 265.30 (middle six-membered ring—Ga) are found.

The 12 gallium atoms which are free of ligands form a distorted anti-cuboctahedron, and in the center of this structure the central gallium atom is located. The medium bond length from the central gallium atom to the six gallium atoms forming the six-membered ring in the middle is 273.99 pm. The medium Ga–Ga distances to the six gallium atoms completing the anti-cuboctahedron is 294.90 pm (Fig. 28). Thus, the central Ga atom has the coordination number 12 $[6 + 6]$, which resembles the coordination sphere of close-packed metal atoms. However, the ideal arrangement of the anti-cuboctahedron is not attained, but the resemblance of the first sphere to the cuboctahedron is striking, and the $M_3-M_6-M_3$ arrangement with widely expanded and moderately twisted M_3 rings in **11** underlines this similarity.

A more detailed analysis of the first sphere of 12 Ga atoms shows that the cluster bears a resemblance not only to the anti-cuboctahedron. In the arrangement

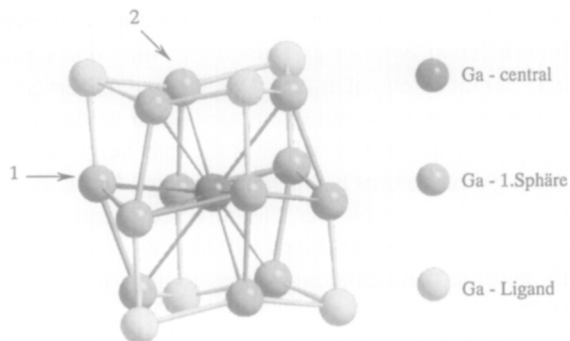


FIG. 28. Molecular structure of the gallium core of $[\text{Ga}_{19}\{\text{C}(\text{SiMe}_3)_3\}_6]^-$ **11**.

illustrated in Fig. 28, one also becomes aware of a similarity to an icosahedral conformation. This icosahedral arrangement is evident in the increase of the angle between the atoms of the central six-membered ring and in the decrease of the Ga–Ga distances within the two three-membered rings, which are additionally twisted with respect to each other. Therefore, the geometric order lies in between anti-cuboctahedron and icosahedron and is thus close to the order found in the first shell of the Al_{177} cluster anion **4** consisting of 12 aluminum atoms.

The six ligand-bearing gallium atoms are connected to three non-ligand-bearing gallium atoms, with a medium bond length of 250.3 pm. In this arrangement, the gallium core is completely shielded by the ligand shell, and this might be responsible for the structure observed in **11**. Upon removal of the $\text{GaC}(\text{SiMe}_3)_3$ fragments—which are stable by themselves⁷⁴—the basic fragment Ga_{13}^- is obtained with a total valence electron number of 40, corresponding to a “stable” Jellium state.⁷⁵ For this reason, in **11** an electronic stabilization also seems plausible. Especially remarkable for **11** is the central gallium atom with the high coordination number 12. The medium bond distance of the central gallium atom to the second shell is 284.45 pm, a value in between the medium bond lengths of the high-pressure modification Ga(II) (278.3 pm) and Ga(III) (292.77 pm), underlining the “metallic character” of the central Ga atom. The fact that the coordination number in **11** is 12 (6 + 6) rather than 8 [Ga(II)] or 4 + 8 [Ga(III)] indicates that gallium, even in the solid state, might be stable in a metallic configuration which is still unknown, most likely because the right conditions for its formation have not yet been found.

Among all the clusters synthesized so far, **11** represents an exception, because it is soluble in THF and thus allows characterization using NMR spectroscopy for the first time for a metalloid gallium cluster. The highly symmetric environment of the central gallium atom should lead to a relatively narrow ^{71}Ga NMR signal—in contrast to the usually broad ^{71}Ga NMR signals common for other

gallium compounds.⁷⁶ In the experiments, from the four expected ⁷¹Ga NMR signals of the four different types of gallium atoms, only one signal at $\delta^{71}\text{Ga} = -134$ with a half height width of $h_{1/2} = 191$ Hz was observed. The low half height width lies in the same magnitude as the signal of the high symmetrical $[\text{GaBr}_4]^-$ species ($h_{1/2} = 185$ Hz⁷⁷), whereas the half height width in low symmetrical substituted gallium atoms is much higher (e.g., $\text{GaBr} \cdot \text{Et}_2\text{O}$ $h_{1/2} = 7000$ Hz⁷⁸). Therefore it seems plausible that the observed signal belongs to the central gallium atom. There is no significant difference between the ¹H, ¹³C, and ²⁹Si NMR shifts and the corresponding values found for tetrakisyltetragallane $\text{Ga}_4[\text{C}(\text{SiMe}_3)_3]_4$.⁶⁷

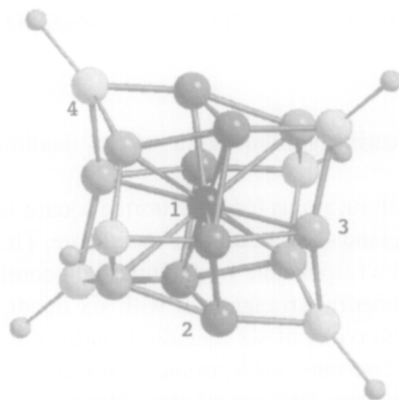
Because there is so far no experimental sign of any ⁷¹Ga NMR resonances of a highly coordinated "metallic" gallium atom, the obtained NMR shift of $\delta^{71}\text{Ga} = -134$ represents a value of great importance with which the shifts of similar species have to be compared in future research, once other soluble compounds of this sort are discovered. However, to gain a first insight into the electronic situation in **11**, NMR shifts for the individual gallium atoms of the model compounds $\text{Ga}_{13}(\text{GaR})_6^-$ ($\text{R} = \text{H}$ (**11(I)**), CH_3 (**11(II)**), $\text{C}(\text{SiH}_3)_3$ (**11(III)**)), were calculated and compared to the experimental value. The results (⁷¹Ga NMR shifts and Ga–Ga distances) are summarized in Table III and show that variation of the ligand causes dramatic changes in the NMR shifts, although the geometry is only slightly affected by this variation.

Comparing the calculated NMR shifts to the observed signal of **11** shows that the methyl compound **11(II)** comes closest to the experimentally observed signal of $\delta^{71}\text{Ga} = -134$ and therefore best matches the description of **11**.

In additional calculations, the NMR shifts of the different Ga atoms in the hypothetical species Ga_{13}^- **11(IV)** ($\delta^{71}\text{Ga} = -603$) were calculated to allow a better comparison of the experimental results with those of hypothetical "naked" metal clusters. **11(IV)** has an icosahedral geometry which is stable by 88 kJ with respect to the cuboctahedral conformation (Table III).⁷⁹ The comparison of the results for the Ga_{13} core of the $\text{Ga}_{13}(\text{GaR})_6^-$ species with the results obtained for the "naked" Ga_{13}^- species shows a striking difference in the NMR shifts. This significant difference between the NMR signal observed for **11** ($\delta^{71}\text{Ga} = -134$) and the calculated signal of the "naked" Ga_{13}^- cluster **11(IV)** ($\delta^{71}\text{Ga} = -603$) demonstrates that the bonding in the calculated "naked" clusters is different from those of experimentally isolated ligand shielded metalloid clusters⁴⁵ and thus does not provide a better understanding of the bonding properties or electronic characteristics of these compounds. The results rather show that the electronic characteristics of metalloid clusters are influenced by the ligands. We are not aware of any appropriate discussion of these observations in the literature to date, although these findings are of great general importance for the electronic tuning of cluster compounds.

TABLE III
 ^{71}Ga NMR SHIFTS CALCULATED BY DFT METHODS AND GEOMETRICAL DATA FOR
 THE MODEL COMPOUNDS^a

Compound	$\text{Ga}_{19}\text{H}_6^-$ 11(I)	$\text{Ga}_{19}(\text{CH}_3)_6^-$ 11(II)	$\text{Ga}_{19}(\text{C}(\text{SiH}_3)_3)_6^-$ 11(III)	Ga_{13}^- 11(IV)	Experiment 11
r(Ga(1)-Ga(2))	283.7	284.1	284.3	270	274.0
r(Ga(1)-Ga(3))	295.9	295.7	298.8	270	295.5
r(Ga(3)-Ga(4))	254.4	255.5	254.5	—	253.1
$\delta^{71}\text{Ga}(1)$	-6	-109	-231	-603	-134
$\delta^{71}\text{Ga}(2)$	156	152	177	-842	—
$\delta^{71}\text{Ga}(3)$	-183	-242	-301	-842	—
$\delta^{71}\text{Ga}(4)$	620	697	651	—	—



^a $\text{Ga}_{13}(\text{GaR})_6^-$ ($\text{R} = \text{H}$ (11(I)), CH_3 (11(II)), $\text{C}(\text{SiH}_3)_3$ (11(III))); the “naked” metal atom cluster Ga_{13}^- 11(IV), and the experimental values for 11 (Ga–Ga distances in pm)

H. Ga_{22}R_8 Clusters ($\text{R} = \text{Si}(\text{SiMe}_3)_3$ **12**; $\text{Ge}(\text{SiMe}_3)_3$ **13**; Si^iBu_3 **14**)^{62,73,80}

In principle, all synthetic routes to the various Ga_{22} clusters $\text{Ga}_{22}[\text{Si}(\text{SiMe}_3)_3]_8$ **12**, $\text{Ga}_{22}[\text{Ge}(\text{SiMe}_3)_3]_8$ **13**, $\text{Ga}_{22}(\text{Si}^i\text{Bu}_3)_8$ **14** are similar, although the techniques differ. The gallium core of the clusters (Fig. 29) can be described as a central gallium atom surrounded by 13 further gallium atoms, with quite long distances (medium value 293.5 pm) between the center atom and its neighbors. The shell of 13 gallium atoms, in which the Ga atoms are separated by a medium Ga–Ga distance of 284.3 pm, is almost identical to the cuboctahedral order (KdZ 12) of metals ($\text{M}_3\text{--M}_6\text{--M}_3$). In the case of the Ga_{22} clusters, one of the planar M_3 triangles is replaced by a planar Ga_4 square (Fig. 30). Due to this variation in the shell of 13 Ga atoms, eight squares are formed, each of which is

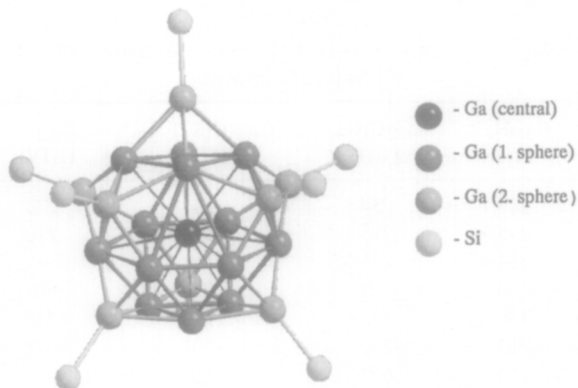


FIG. 29. Molecular structure of the Ga_{22} cluster $\text{Ga}_{22}[\text{Si}(\text{SiMe}_3)_3]_8$ **12** (SiMe_3 groups are omitted for clarity).

capped by a ligand bearing gallium atom with a medium Ga–Ga-distance of 261.9 pm.

The eight exterior gallium atoms form a distorted square antiprism, and the eight ligands form a closed ligand shell around the metal core. This complete protection of the metal core may be responsible for the unusual coordination number of 13. The alternative cuboctahedral arrangement with six quadrangular planes would only form an incomplete cover of six ligands. Besides this description, which is primarily based on steric reasons, an electronic stabilization has to be considered, as is the case for the Ga_{19} cluster. DFT calculations for the naked cluster Ga_{22}^{8+} show that 20 energetically low-lying valence MOs are grouped in such a way that they can be described by the Jellium model.⁷⁵ The number of valence electrons is also a first indication for such an electronic stabilization; if the eight exterior gallium

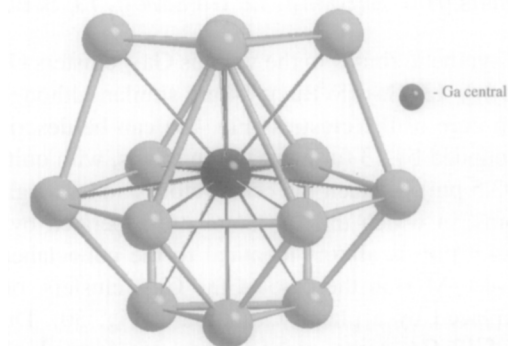


FIG. 30. First coordination sphere with central gallium atom of the Ga_{22} clusters **12**, **13**, and **14**.

atoms are counted as Ga^1 , a total of 58 electrons ($14 \times 3 + 8 \times 2 = 58$) (i.e., a “stable” Jellium state) results. Especially remarkable in **12**, **13**, and **14** is the coordination number of the central gallium atom which is “forced” into a “metallic” coordination of 13 further gallium atoms with long distances. To date, there is no example for a high coordination number for gallium in its solid state. For this reason, a classification of **12**, **13**, and **14** is difficult. However, the arrangement with a gallium atom in the center can be compared to the close packing of the gallium atoms in Ga(III) .

1. $[\text{Ga}_{26}\{\text{Si}(\text{SiMe}_3)_3\}_8]^{2-}$ Cluster **15**⁶³

The third and largest representative of metalloid gallium clusters with a metal atom core shielded by eight ligands is the anion **15** in the compound $[\text{Ga}_{26}\{\text{Si}(\text{SiMe}_3)_3\}_8]^{2-} \cdot 2[\text{Li}(\text{THF})_4]^+$, which is obtained via the GaI route reported by Linti *et al.* In the case of **15** the ligand bearing gallium atoms form a quadrangular antiprism as observed in the Ga_{18} - **10** and the Ga_{22} clusters **12**, **13**, and **14** with a medium Ga–Si distance of 243.9 pm. The metal core of the cluster can be described as follows: A central gallium atom is surrounded by a distorted square prism of eight gallium atoms. The Ga–Ga-distances vary in the range of 278.5 to 286.6 pm. Three of the square planes of the prism are capped with a gallium atom with a medium Ga–Ga-distance from the atoms in the square to this gallium atom of 310 pm. One square is capped with a Ga_2 unit by an average Ga–Ga-distance of 345.8 pm. The gallium atoms in this Ga_2 unit are separated by 260.9 pm. Therefore a nearly cuboctahedral environment of the central gallium atom results, formed by 11 gallium atoms and the center of the Ga_2 - unit. This arrangement leads again to a high coordination number for the central gallium atom in **15** with long Ga–Ga-distances to its neighbors. The arrangement of the gallium atoms in the cluster core of **15** can be regarded as a fragment of the modification Ga(III) . However, the similarities are limited since the environment of the central atom in **15** can be described as a coordination of $8 + 3 + 2$, whereas in Ga(III) the coordination is $4 + 8$ (see Fig. 31). The existence of three metalloid gallium cluster types Ga_{18} **10**, Ga_{22} **12**, and Ga_{26} **15**, which are of the same size and protected on the exterior by the same number of ligands, is most interesting with respect to the question of why the clusters exhibit a different inner framework. A comparison of the two metalloid clusters **10** and **12** shows that the most obvious difference is that the geometric arrangement of the Ga atoms in the Ga_{18} cluster **10** is close to the β -modification, whereas the Ga_{22} cluster **12** is close to the high-pressure modification Ga(III) .

To further explore possible similarities between the corresponding modifications, we have compared the changes of the atom volumes of the compounds or states in question. For the model compounds Ga_{18}H_8 and Ga_{22}H_8 the molecular

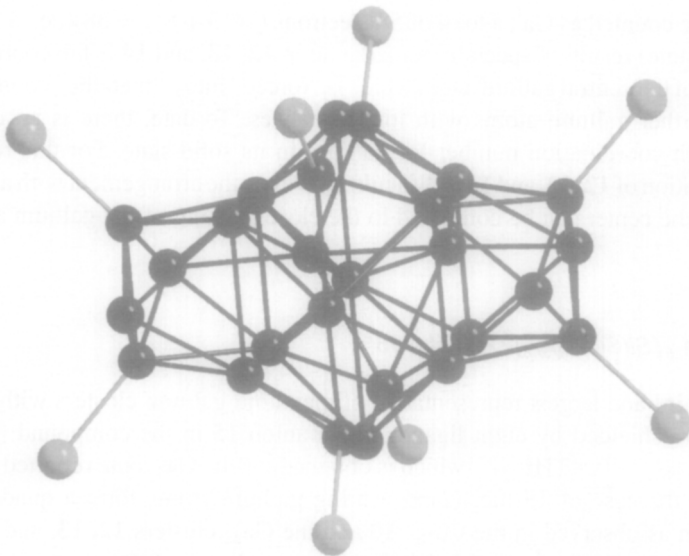


FIG. 31. Molecular structure of $[\text{Ga}_{26}\{\text{Si}(\text{SiMe}_3)_3\}_8]^{2-}$ **15** (SiMe_3 groups are omitted for clarity).

volumes were calculated and atom volumes of 29.9 \AA^3 and 28.8 \AA^3 resulted.⁷³ This means that the atom volume of the gallium atoms in the Ga_{22} cluster decreases by 4.7% compared to the Ga_{18} cluster. A similar volume contraction of 5.1% is also found for the transition of β -gallium to $\text{Ga}(\text{III})$. This wide conformity supports the classification of the different clusters into the same classes as the different solid-state modifications of elementary gallium, which is now not only based on topology but also on other results as discussed above. The conformity also shows that the approximation to the various solid-state modifications of elementary gallium is an important criterion during the formation of these clusters. Another significant criterion in the formation is the almost closed ligand cover. As gallium—in contrast to its lighter homologue aluminum—exists in a variety of different solid-state modifications, a prognosis of the arrangement of metal atoms in the cluster core for a given cluster size (close ligand shell) is difficult. This becomes clear in the discussion of the Ga_{84} cluster, the largest metalloid cluster synthesized and characterized so far, which has an unexpected inner structure but nevertheless can be classified among the solid-state modifications.

J. $[\text{Ga}_{84}\{\text{N}(\text{SiMe}_3)_2\}_{20}]^{4-}$ Cluster **16**⁸¹

As already mentioned, **16** is the largest metalloid gallium cluster structurally analyzed so far. In addition to the 84 gallium atoms, the cluster consists of 20 $\text{N}(\text{SiMe}_3)_2$ ligands. Thus, the number of ligands is identical to that found for the

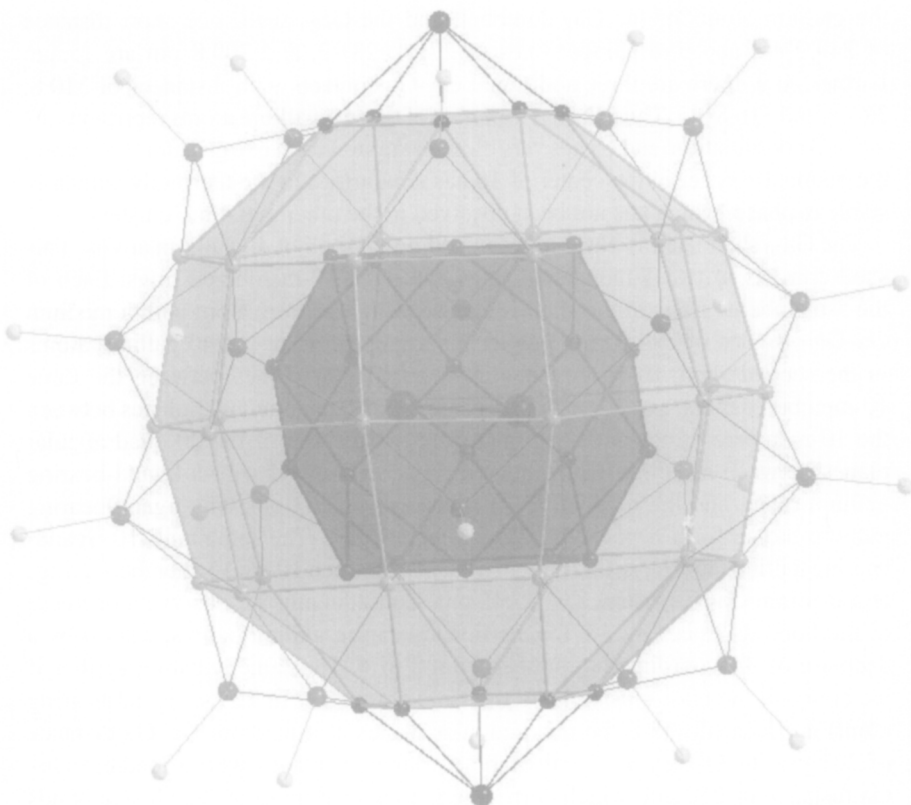


FIG. 32. Molecular structure of $[\text{Ga}_{84}\{\text{N}(\text{SiMe}_3)_2\}_{20}]^{4-}$ **16** (SiMe₃ groups are omitted for clarity) showing the order to the gallium atoms in shells.

Al₇₇ cluster anion **4**. At first glance, the geometric arrangement of the ligands around the cluster core is also the same as in the Al₇₇ cluster compound. However, considering the fact that Ga–Ga bonds are somewhat shorter than Al–Al bonds,⁸² **16** hosts 84 metal atoms instead of 77 within the same ligand cover (Fig. 32). The gallium core of the Ga₈₄ cluster **16** can be described as follows: In the cluster center, a dumbbell of two Ga atoms is located. The Ga–Ga distance of this Ga₂ dumbbell is 234 pm, a value corresponding to the shortest Ga–Ga bond between two gallium atoms in the oxidation state zero, since the Ga–Ga distance of the characteristic Ga₂ unit in α-gallium is 244.8 pm. Moreover, the Ga–Ga bond of the dumbbell in **16** of 234 pm is almost as short as the Ga–Ga bond (232 pm) in Ga₂R₂²⁻ (R = (2,4,6-*i*-Pr₃C₆H₂)₂C₆H₃).^{68,69} The Ga₂ dumbbell is surrounded by a shell of 20 gallium atoms. The Ga₂₀ shell consists of two parallel five-membered rings in antiposition, connected by 10 gallium atoms which can be described as a puckered 10-membered ring. The medium Ga–Ga distance within the Ga₂₀ shell is 274.6 pm. Between

the gallium atoms of the Ga_2 dumbbell and the Ga_{20} shell, one short distance of 249.0 pm and three longer ones of 271.4, 281.2, and 299.8 pm are found. Furthermore, there are three additional Ga–Ga contacts with distances of 310.8, 313.2, and 316.8 pm. Thus, the environment of the two gallium atoms represents a $2 + 3 + 3$ coordination, and comes very close to the structure in α -gallium. Therefore, the geometric order in the center of **16** has similarities to the thermodynamically stable α -phase, which has not been observed in the other metalloid clusters.

The Ga_{20} shell itself is covered by an additional shell of 40 gallium atoms. This shell consists of two 5-membered rings and three 10-membered rings. Each of the 5-membered rings of the shell is capped with a gallium atom with a medium Ga–Ga distance of 280.6 pm. Due to this arrangement of the 40 gallium atoms in the second shell, its surface has 20 quadrangular planes between the three 10-membered rings, and 10 triangular planes and 10 quadrangular planes between the 10-membered rings and the 5-membered rings. Ten of the 20 quadrangular planes between the three 10-membered rings are capped with a ligand-bearing gallium atom, and the medium Ga–Ga distance is 263 pm. The ligand-bearing gallium atoms form a puckered 10-membered ring. The remaining 10 ligand-bearing gallium atoms cap all triangular planes between 10- and 5-membered rings at a medium Ga–Ga distance of 255.2 pm. Consequently we observe a decrease of the bond distances by 3% for the ligand-bearing gallium atoms, caused by a decrease of the coordination number from 5 to 4. The same situation applies if we compare the Ga_{22} cluster **12** to the Ga_{19} cluster **11**. In **12** the ligand-bearing atoms are located above the quadrangular planes at a medium Ga–Ga distance of 267 pm; in **11** they are located above triangular planes with a medium Ga–Ga distance of 250 pm, which corresponds to a shortening of the Ga–Ga bonds by 6%.

This discussion, however, seems not to describe satisfactorily the bonding properties of the cluster, because within the shell of 40 atoms Ga–Ga-distances up to 367.5 pm have to be considered, which is unusually long for gallium. In contrast to this, the Ga–Ga distances between the five-membered rings of the shell of 40 and the five-membered rings of the shell of 20 atoms is only 279.2 pm. On the basis of this result, the five-membered ring of the 40 atom shell has rather to be associated with the 20 atom shell. This implies that the above described shell model is not appropriate to explain the bonding properties of the cluster. By considering only Ga–Ga distances below 300 pm we will obtain a different description of the cluster (see Fig. 33).

In this description, which refers to the bond length, the Ga_2 dumbbell is located within a Ga_{32} subunit whose shape has a strong resemblance to a rugby ball. The medium Ga–Ga distance in the Ga_{32} subunit is 274.3 pm. The remaining 30 gallium atoms cover this subunit in a meandering way, with a medium Ga–Ga distance of 275.6 pm. The Ga_{32} subunit shown in Fig. 33 can be described as two icosahedral Ga_{11} units connected through a puckered 10-membered ring. These

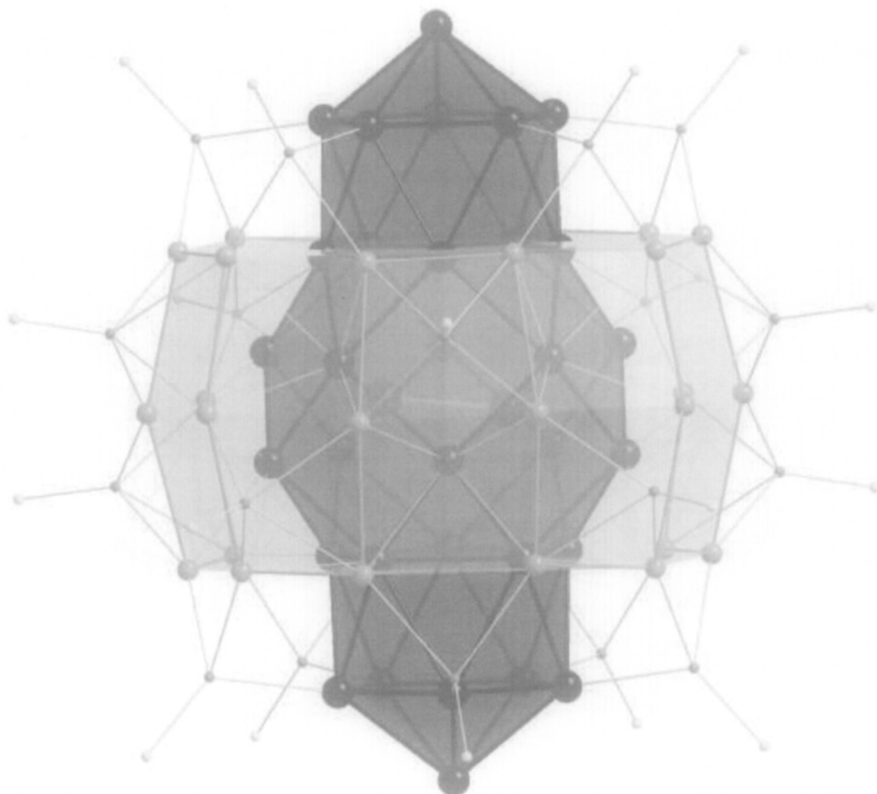


FIG. 33. Molecular structure of $[\text{Ga}_{84}\{\text{N}(\text{SiMe}_3)_2\}_{20}]^{4-}$ **16** (SiMe_3 groups are omitted for clarity) with highlighted Ga_{32} subunit. Ga–Ga distances below 300 pm are shown.

icosahedral Ga_{11} units with Ga–Ga distances varying from 261.6 to 281.4 pm have many similarities to the icosahedral substructure of δ -gallium, the similarities being not limited to the geometry: there are also similar bond lengths (δ -gallium: 275–289 pm). Thus, in addition to the above mentioned resemblance to α -gallium, there is also a relationship to the δ -phase of elementary gallium.

The extraordinary bonding properties in **16** can also be seen in a diagram of **16** (Fig. 34). In **16**, an almost perfect five-numbered axis is attained, distorted only by the central Ga_2 unit. This is the first time that a symmetry close to the five-numbered symmetry is observed for molecular metalloid clusters. A few solid-state modifications with five-numbered symmetry have, however, been found for compounds involving Group 13 elements. Because there is no crystallographic space group with a five-numbered axis, these compounds are summarized under the collective name “quasi-crystals”.⁸³ For a better understanding of quasi-crystals,

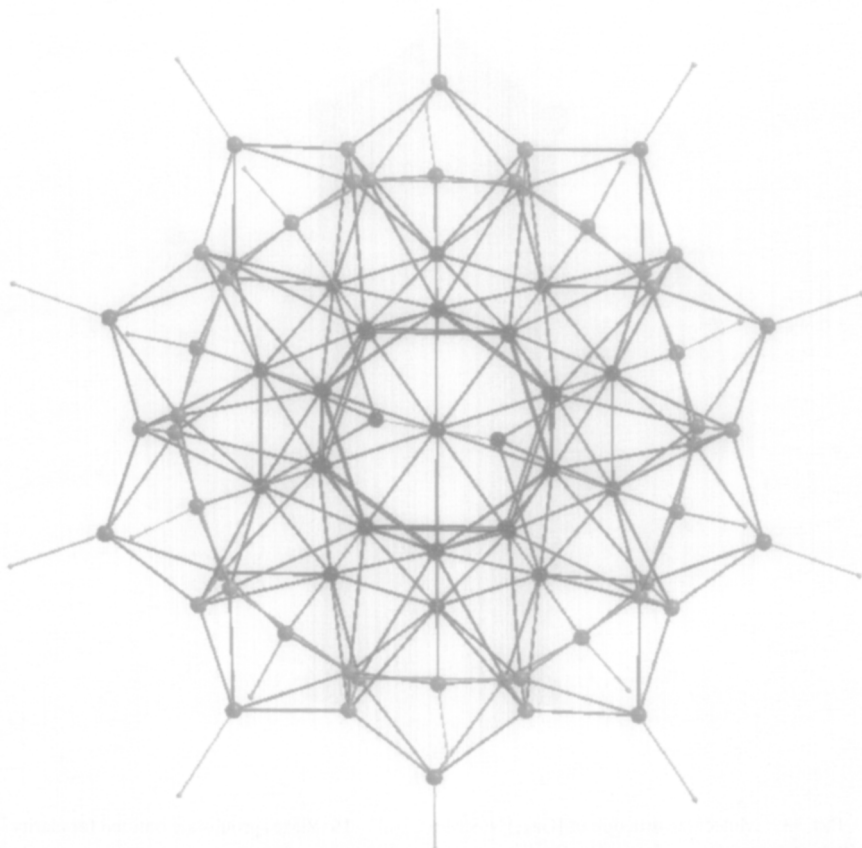


FIG. 34. Molecular structure of $[\text{Ga}_{84}\{\text{N}(\text{SiMe}_3)_2\}_{20}]^{4-}$ **16** (SiMe_3 groups are omitted for clarity).

the relation between the existence of quasi-crystals in compounds of the third main group (e.g., in composition metals of the Al/Mn system) and the distorted C_5 symmetry might be of fundamental importance. The view of the solid-state structure along the distorted five-membered axis shows that in this direction the individual clusters exhibit a tube-like arrangement (Fig. 35). So far, it is unknown whether this cluster arrangement with toluene molecules has an effect on physical properties such as the conductivity of the solid material.

The idea of electronic conductivity in the crystals of this cluster is stimulated by the metallic reflectance of the crystals. A potential conductivity is expected to be anisotropic because of the anisotropic order of the clusters inside the crystal. As a consequence, the electric resistance is expected to be smaller in the direction of the tubes than in the vertical direction where there is no "graphite-like" bridging between the clusters.

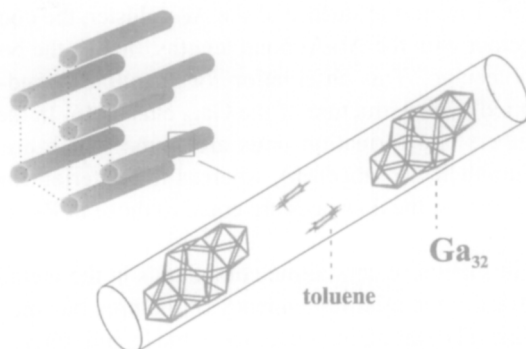


FIG. 35. Arrangement of the $[\text{Ga}_{84}\{\text{N}(\text{SiMe}_3)_2\}_{20}]^{4-}$ clusters **16** (only the Ga_{32} subunits are shown) within the crystal.

K. Conclusion

This survey of the inner structures of the metalloid gallium clusters synthesized so far shows that, as expected, there is a great variety of possible arrangements of gallium atoms in the cluster core. The formation of these clusters in metathesis reactions during the disproportionation reaction of a metastable GaX species is made possible by the full protection of the cluster core, and this protection from the exterior by the ligand shell applies to all these clusters, with exception of the Ga_{84} cluster **16**. The fewer gallium atoms the cluster has, the smaller its size becomes. With the same number of ligands, the steric interaction between the ligands becomes an important factor, showing once more the subtle influence the ligand sphere has on the cluster geometry. Furthermore, electronic aspects could also have a certain influence. This becomes especially evident in the Ga_{22} clusters which, according to the Jellium model, have the advantage of a stable electronic configuration.

V

CONCLUSIONS AND OUTLOOK

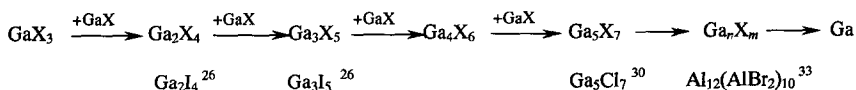
Following the classification of the characterized structures reported here, it is necessary to draw a borderline between these and the metalloid precious metal clusters. Experimental results obtained with microscopic techniques as well as theoretical considerations concerning this metalloid cluster group show that, as a rule, the geometry of the metal atoms represents a fragment of the crystalline material.⁴ On the other hand, the shell-like structure of the Al_{77} cluster **4** indicates that the coordination number 12 which is expected for the close packing, is found only for the central Al atom. The ideal anti-cuboctahedral arrangement is not

realized here either. Toward the surface of the Al_{77} cluster, the coordination numbers decrease together with the Al–Al bond lengths, that is, the bonding relations become more “molecular.” This observation for metalloid ligand-protected clusters is also supported by the structure of the Ga_{84} cluster **16**. In the cluster center, coordination numbers and formation units are found which are typical for α - and δ -gallium (dumbbell, icosahedron), whereas the exterior Ga–Ga bonds are more “molecular,” that is, the distances are equal to those in R_2GaGaR_2 or Ga_4R_4 species.⁸⁴

Moreover, the formation of crystalline compounds in the metalloid Al and Ga clusters is in contrast to the missing tendency of the precious metal cluster compounds to crystallize. The stabilizing influence of the ligand sphere, which is firmly attached to some of the metal atoms by 2e–2c bonds (AlN and GaN) is responsible for this difference. The metal clusters formed from transition metal elements possess a more flexible ligand cover due to σ -donor and π -acceptor bonds to the cluster core (e.g., for CO, PR_3 , and SR_2 ligands) with, to some extent, bridging properties. As a consequence, this will lead to stationary balances with a few energetically nearly identical species. This is the reason that a sufficiently high concentration of a uniform species, which is prerequisite for the synthesis of crystalline samples, is formed only occasionally.

There is also a difference in the mechanism of the Al and Ga cluster formation. A crucial point for reactive species like MX ($\text{M} = \text{Al}, \text{Ga}$; $\text{X} = \text{halogenide}$ or organic substituent) is the disproportionation process which proceeds slowly enough to trap intermediate steps before finally the thermodynamically stable bulk metal and the M^{III} species are formed. A stepwise insertion of the surplus MX units and splitting off of MX_3 species leads to cluster growth (Scheme 5), which can be influenced by varying either the temperature, the donor, the halogenide, or the organic substituent. Thus simply, varying the temperature in the same chemical environment leads to the formation of different clusters like Al_7 **1**, Al_{12} **2**, Al_{14} **3**, or Al_{77} **4**. The same applies to gallium where, by simple variation of the steric demand of the substituted ligand, either a Ga_8 **8**, Ga_{12} **9**, Ga_{18} **10**, Ga_{19} **11**, Ga_{22} **12**, **13**, **14**, or a Ga_{84} cluster **16** is obtained.

The last step, the formation of metal, takes place if in the reducing atmosphere (MX excess) a critical cluster size is reached (e.g., by heating the solution to more than 100°C), thus forming a giant cluster whose metal core is nearly identical to the bulk material and which can disproportionate to metal and M^{III} species without any further significant change of its bondings.



SCHEME 5. Hypothetical reaction scheme for the insertion reaction of MX into MX bonds leading to a cluster compound.

ACKNOWLEDGMENTS

We thank the Deutsche Forschungsgemeinschaft and the Fonds der Chemischen Industrie for financial support, H. J. Himmel for revision of the English text, E. Möllhausen and T. Stiffel for association concerning graphical questions, and I. Krossing, C. Klemp, A. Donchev, H. Köhnlein, G. Stöber, R. Köppe, and E. Baum for helpful discussions.

REFERENCES

- (1) Schnepf, A.; Stöber, G.; Schnöckel, H. *J. Am. Chem. Soc.* **2000**, *122*, 9178.
- (2) Cotton, F. A. *Quart. Rev. Chem. Soc.* **1966**, *20*, 397.
- (3) Krautscheid, H.; Fenske, D.; Baum, G.; Semmelmann, M. *Angew. Chem.* **1993**, *103*, 1364; *Angew. Chem., Int. Ed. Engl.* **1993**, *32*, 1303.
- (4) Schmid, G. (Ed) *Cluster and Colloides*; VCH: Weinheim, New York, 1994.
- (5) Ceriotti, A.; Demartin, F.; Longoni, G.; Manassero, M.; Marchionna, M.; Piva, G.; Sansoni, M. *Angew. Chem.* **1985**, *97*, 708. *Angew. Chem., Int. Ed. Engl.* **1985**, *24*, 697.
- (6) Tran, N. T.; Kawano, M.; Powell, D. R.; Dahl, L. F. *J. Am. Chem. Soc.* **1998**, *120*, 10,986.
- (7) Tran, N. T.; Powell, D. R.; Dahl, L. F. *Angew. Chem. Int. Ed.* **2000**, *39*, 4121.
- (8) Ecker, A.; Weckert, E.; Schnöckel, H. *Nature* **1997**, *387*, 379.
- (9) Braunstein, P.; Oro, L. A.; Raithby, P. R. *Metal Clusters in Chemistry*; VCH: Weinheim, New York, 1999.
- (10) Tacke, M.; Schnöckel, H. *Inorg. Chem.* **1989**, *28*, 2895.
- (11) Dohmeier, C.; Loos, D.; Schnöckel, H. *Angew. Chem.* **1996**, *108*, 141; *Angew. Chem., Int. Ed. Engl.* **1996**, *35*, 129.
- (12) Corbett, J. D. *Angew. Chem.* **2000**, *112*, 682; *Angew. Chem., Int. Ed.* **2000**, *39*, 692.
- (13) Wade, K. *Adv. Inorg. Chem. Radiochem.* **1976**, *18*, 1; Mingos, D. M. P. *Nature* **1972**, *336*, 99; Mingos, D. M. P. *Acc. Chem. Res.* **1984**, *17*, 311.
- (14) Corbett, J. D. In *Chemistry, Structure and Bonding of Zintl Phases and Ions*; VCH: New York, 1996.
- (15) Almond, M. J.; Downs, A. J. In *Advances in Spectroscopy*, Wiley: New York, 1989.
- (16) Schnöckel, H.; Schunk, S. *Chemie in Unserer Zeit* **1987**, *21*, 73.
- (17) Schnöckel, H.; Mehner, T.; Plitt, H. S.; Schunk, S. *J. Am. Chem. Soc.* **1989**, *111*, 4578.
- (18) Schnöckel, H. *J. Mol. Struct.* **1978**, *50*, 267.
- (19) Schnöckel, H. *J. Mol. Struct.* **1978**, *50*, 275; Köppe, R.; Tacke, M.; Schnöckel, H. *Z. Anorg. Allg. Chem.* **1991**, *605*, 35; Köppe, R.; Schnöckel, H. *J. Chem. Soc. Dalton Trans.* **1992**, 3393.
- (20) Junker, M.; Friesen, M.; Schnöckel, H. *J. Chem. Phys.* **2000**, *112*, 1444.
- (21) Timms, P. L. *Adv. Inorg. Chem. Radiochem.* **1972**, *14*, 142.
- (22) Chase, M. W.; Jr.; Davies, C. A.; Downey, J. R.; Jr.; Frurip, D. J.; McDonal, R. A.; Syverend, A. N. *JANNAF-Thermodynamical Tables, 3rd ed.*, Am. Chem. Soc., Am. Inst. of Phys. US National Bureau of Standards, Midland, MI, 1985.
- (23) Timms, P. L. *J. Am. Chem. Soc.* **1967**, *89*, 1629; *ibid.* **1968**, *90*, 4585.
- (24) Zenneck, U. *Angew. Chem.* **1990**, *102*, 171; *Angew. Chem., Int. Ed. Engl.* **1990**, *29*, 138.
- (25) Ecker, A.; Köppe, R.; Üffing, C.; Schnöckel, H. *Z. Anorg. Allg. Chem.* **1998**, *624*, 817.
- (26) For the preparation of subvalent gallium iodide, a simpler sonochemical synthesis based on papers of M. L. H. Green has been established (see IVB); Schnepf, A.; Doriat, C.; Möllhausen, E.; Schnöckel, H. *Chem. Commun.* **1997**, 2111.
- (27) (a) Ecker, A.; Köppe, R.; Üffing, C.; Schnöckel, H. *Z. Anorg. Allg. Chem.* **1998**, *624*, 817; (b) Gauss, J.; Schneider, U.; Ahlrichs, R.; Dohmeier, C.; Schnöckel, H. *J. Am. Chem. Soc.* **1993**, *115*, 2402.

- (28) (a) Mocker, M.; Robl, C.; Schnöckel, H. *Angew. Chem.* **1994**, *106*, 1860; *Angew. Chem. Int. Ed. Engl.* **1994**, *33*, 1754; (b) Ecker, A.; Schnöckel, H. *Z. Anorg. Allg. Chem.* **1996**, *622*, 149.
- (29) Doriat, C. U.; Baum, E.; Ecker, A.; Schnöckel, H. *Angew. Chem.* **1997**, *109*, 2057; *Angew. Chem., Int. Ed. Engl.* **1997**, *36*, 1969.
- (30) Loos, D.; Schnöckel, H.; Fenske, D. *Angew. Chem.* **1993**, *105*, 1124; *Angew. Chem., Int. Ed. Engl.* **1993**, *32*, 1059.
- (31) Klemp, C.; Stöber, G.; Krossing, I.; Schnöckel, H. *Angew. Chem. Int. Ed.* **2000**, *39*, 3691.
- (32) Schnöckel, H.; Klemp, C. In *Inorganic Chemistry Highlights*, Meyer, G.; Naumann, D.; Wesemann, L. (ed.), in press.
- (33) Klemp, C.; Köppe, R.; Weckert, E.; Schnöckel, H. *Angew. Chem.* **1999**, *111*, 1852; *Angew. Chem., Int. Ed. Engl.* **1999**, *38*, 1740.
- (34) Dohmeier, C.; Robl, C.; Tacke, M.; Schnöckel, H. *Angew. Chem.* **1991**, *103*, 594; *Angew. Chem., Int. Ed. Engl.* **1991**, *30*, 564.
- (35) Loos, D.; Baum, E.; Ecker, A.; Schnöckel, H.; Downs, A. *J. Angew. Chem.* **1997**, *109*, 894; *Angew. Chem., Int. Ed. Engl.* **1997**, *36*, 860.
- (36) Schnöckel, H. *Aluminium* **1997**, *73*, 766.
- (37) Purath, A.; Köppe, R.; Schnöckel, H. *Angew. Chem.* **1999**, *111*, 3114; *Angew. Chem., Int. Ed.* **1999**, *38*, 2926.
- (38) Purath, A.; Köppe, R.; Schnöckel, H. *Chem. Commun.* **1999**, 1933.
- (39) Köhnlein, H.; Stöber, G.; Baum, E.; Möllhausen, E.; Huniar, U.; Schnöckel, H. *Angew. Chem.* **112**, 828; *Angew. Chem. Int. Ed.* **2000**, *39*, 799.
- (40) Köhnlein, H.; Stöber, G.; Purath, A.; Klemp, C.; Schnöckel, H. *J. Am. Chem. Soc.*, in preparation.
- (41) Uhl, W. *Angew. Chem.* **1993**, *105*, 1449; *Angew. Chem., Int. Ed. Engl.* **1993**, *32*, 1386.
- (42) The existence of aromatic $\text{Ga}_3\text{R}_3^{2-}$ species has been shown recently; Li, X.-W.; Pennington, W. T.; Robinson, G. H.; *J. Am. Chem. Soc.* **1995**, *117*, 7578; Li, X.-W.; Xie, Y.; Schreiner, P. R.; Gripper, K. D.; Crittendon, R. C.; Campana, C. F.; Schaefer, H. F.; Robinson, G. H. *Organometallics* **1996**, *15*, 3798.
- (43) Dohmeier, C.; Schnöckel, H.; Robl, C.; Schneider, U.; Ahlrichs, R. *Angew. Chem., Int. Ed. Engl.* **1993**, *32*, 1655.
- (44) Faber, S. Dissertation, Saarbrücken, 1996.
- (45) Ahlrichs, R.; Elliot, S. D. *Phys. Chem. Chem. Phys.* **1999**, *1*, 13.
- (46) Scheer, E.; Agraït, N.; Cuevas, J. C.; Yeyati, L. A.; Ludoph, B.; Martin-Rodero, A.; Bollinger, G. R.; van Ruitenbeek, J. M.; Urbina, C. *Nature* **1998**, *394*, 154.
- (47) Wiberg, N.; Blank, T.; Nöth, H.; Ponikvar, W. *Angew. Chem.* **1999**, *111*, 887; *Angew. Chem., Int. Ed. Engl.* **1999**, *38*, 839.
- (48) Hiller, W.; Klinkhammer, K.-W.; Uhl, W.; Wagner, J. *Angew. Chem.* **1991**, *103*, 182; *Angew. Chem., Int. Ed. Engl.* **1991**, *30*, 179.
- (49) Bergman, G.; Wangh, J. L. T.; Pauling, L. *Acta Crystallogr.* **1957**, *10*, 254.
- (50) However, for the corresponding Ga_{14} compound a stabilization for the polyhedral structure of about $+111 \text{ kJ mol}^{-1}$ has been calculated.
- (51) Chi, L. F.; Rakers, S.; Hartig, M.; Gleiche, M.; Fuchs, H.; Schmid, G. *Colloids Surf. A* **2000**, *171*(1-3), 241.
- (52) Further species of this kind have been obtained recently: $\text{Al}_{22}\text{Cl}_{20} \cdot 12\text{THF}$; Klemp, C.; Bruns, M.; Gauss, J.; Häussermann, U.; Stöber, G.; van Wüllen, L.; Jansen, M.; Schnöckel, H. *J. Am. Chem. Soc.*, accepted for publication.
- (53) Bosio, L. *J. Chem. Phys.* **1978**, *68*, 1221.
- (54) Laves, F. *Naturwiss.* **1932**, *20*, 472.
- (55) Bosio, L.; Defrain, A. *Acta Cryst.* **1969**, *B25*, 995.
- (56) Bosio, L.; Curien, H.; Dupont, M.; Rimsky, A. *Acta Cryst.* **1972**, *B28*, 1974.
- (57) Bosio, L.; Curien, H.; Dupont, M.; Rimsky, A. *Acta Cryst.* **1973**, *B29*, 367.

- (58) Green, M. L. H.; Mountford, P.; Smout, G.; Speel, S. *Polyhedron*, **1990**, *22*, 2763.
- (59) Linti, G. *J. Organomet. Chem.* **1996**, *520*, 107.
- (60) Linti, G.; Köstler, W.; Piotrowski, H.; Rodig, A. *Angew. Chem., Int. Ed. Engl.* **1998**, *37*, 2209.
- (61) Köstler, W.; Linti, G. *Angew. Chem.* **1997**, *109*, 2758; *Angew. Chem., Int. Ed. Engl.* **1997**, *36*, 2644.
- (62) Linti, G.; Rodig, A. *Chem. Commun.* **2000**, 127.
- (63) Rodig, A.; Linti, G. *Angew. Chem.* **2000**, *112*, 3076; *Angew. Chem. Int. Ed.* **2000**, *39*, 2952.
- (64) Dochev, A.; Schnepf, A.; Stöber, G.; Baum, E.; Schnöckel, H. *Z. Anorg. Allg. Chem.*, in preparation.
- (65) Dohmeier, C.; Mocker, M.; Schnöckel, H.; Lötze, A.; Schneider, U.; Ahlrichs, R. *Angew. Chem.* **1993**, *105*, 1491; *Angew. Chem., Int. Ed. Engl.* **1993**, *32*, 1428.
- (66) Schnepf, A.; Köppe, R.; Schnöckel, H. *Angew. Chem.* **2001**, *113*, 1287; *Angew. Chem. Int. Ed.* **2001**, *40*, 1287.
- (67) Uhl, W.; Hiller, W.; Layh, M.; Schwarz, W. *Angew. Chem.* **1992**, *104*, 1378; *Angew. Chem., Int. Ed. Engl.* **1992**, *31*, 1364.
- (68) Su, J.; Li, X.-W.; Crittendon, R. C.; Robinson, G. H. *J. Am. Chem. Soc.* **1997**, *119*, 5471.
- (69) Köppe, R.; Schnöckel, H. *Z. Anorg. Allg. Chem.* **2000**, *626*, 1095.
- (70) Schnepf, A.; Stöber, G.; Köppe, R.; Schnöckel, H. *Angew. Chem.* **2000**, *112*, 1709; *Angew. Chem. Int. Ed.* **2000**, *39*, 1637.
- (71) Meuterties, E. L. *The Chemistry of Boron and its Compounds*; Wiley: New York, 1967.
- (72) Schnepf, A.; Stöber, G.; Schnöckel, H. *Z. Anorg. Allg. Chem.* **2000**, *626*, 1676.
- (73) Donchev, A.; Schnepf, A.; Stöber, G.; Baum, E.; Schnöckel, H.; Blank, T.; Wiberg, N. *Chem. Eur. J.* submitted for publication.
- (74) Haaland, A.; Martinsen, K.-G.; Volden, H. V.; Kaim, W.; Waldhör, E.; Uhl, W.; Schütz, U. *Organometallics* **1996**, *15*, 1146.
- (75) Knight, W. D.; Clemenger, K.; deHeer, W. A.; Saunders, W.; Chan, M. Y.; Cohen, M. L. *Phys. Rev. Lett.* **1994**, *52*, 2124.
- (76) Schmidbaur, H. *Angew. Chem.* **1985**, *97*, 893; *Angew. Chem., Int. Ed. Engl.* **1985**, *24*, 893.
- (77) McGarvey, B. R.; Taylor, M. J.; Tuck, D. J. *Inorg. Chem.* **1981**, *20*, 2010.
- (78) Cerný, Z.; Macháček, J.; Fusek, J.; Čásenský, B.; Kriz, O.; Tuck, D. G. *Inorg. Chim. Acta* **1996**, *247*, 119.
- (79) However, latest calculations show that a decahedral isomer of Ga_{13}^- is even more stable; Yi, J. Y. *Phys. Rev. B* **2000**, *61*, 7277.
- (80) Schnepf, A.; Weckert, E.; Linti, G.; Schnöckel, H. *Angew. Chem.* **1999**, *111*, 3578; *Angew. Chem., Int. Ed. Engl.* **1999**, *38*, 3381.
- (81) Schnepf, A.; Schnöckel, H. *Angew. Chem.* **2000**, *113*, 733; *Angew. Chem., Int. Ed.* **2001**, *40*, 711.
- (82) Yu, Q.; Purath, A.; Donchev, A.; Schnöckel, H. *Organometallics* **1999**, *584*, 94.
- (83) Massa, W. *Kristallstrukturbestimmung*; B. G. Teubner: Stuttgart, 1994.
- (84) Uhl, W. *Angew. Chem.*, **1993**, *105*, 1449; *Angew. Chem., Int. Ed. Engl.* **1993**, *32*, 1386.

Multiple Bonds Involving Aluminum and Gallium Atoms

GREGORY H. ROBINSON

*Department of Chemistry
The University of Georgia
Athens, Georgia 30605*

I. Introduction	283
II. Organoaluminum Compounds Containing Multiple Bonds	283
A. The Al-Al One-Electron π -Bond	284
III. Organogallium Compounds Containing Multiple Bonds	286
A. One-Electron Ga-Ga π -Bonds: Initial Evidence of Gallium Multiple Bonds	287
B. Gallium Rings: Cyclogallenes and Metalloaromaticity	288
C. Synthesis and Molecular Structure of a Gallyne: A Case for Gallium-Gallium Triple Bonds	290
IV. Conclusion	293
References	293

I

INTRODUCTION

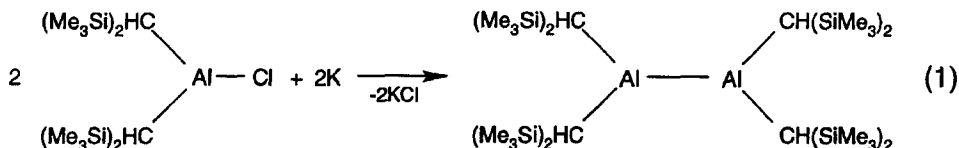
The history of the organometallic chemistry of the Group 13 (III) elements, aluminum, gallium, indium, and thallium, is long and storied. Furthermore, this group constitutes a remarkably diverse collection of elements. Compounds of these elements have found utility in a number of applications from catalytic processes to advanced electronic devices. It is interesting, therefore, that the first compounds containing the M-M bonds (M = Al, Ga, In, or Tl) are a relatively recent development in inorganic chemistry. Few advances in this field have generated more excitement than the concept of multiple bonding relative to these elements. Thus far, however, this promising area has been limited to compounds of aluminum and gallium compounds containing multiple bonds. Just as alkenes and alkynes are intimately associated with their saturated alkane analogs, any discussion of multiple bonding associated with these main group metals should begin with an examination of their single bonded analogs.

II

ORGANOALUMINUM COMPOUNDS CONTAINING MULTIPLE BONDS

While efforts purporting the isolation of organoaluminum compounds containing an Al-Al bond may be traced back to the 1960s,¹⁻⁴ these reports presented

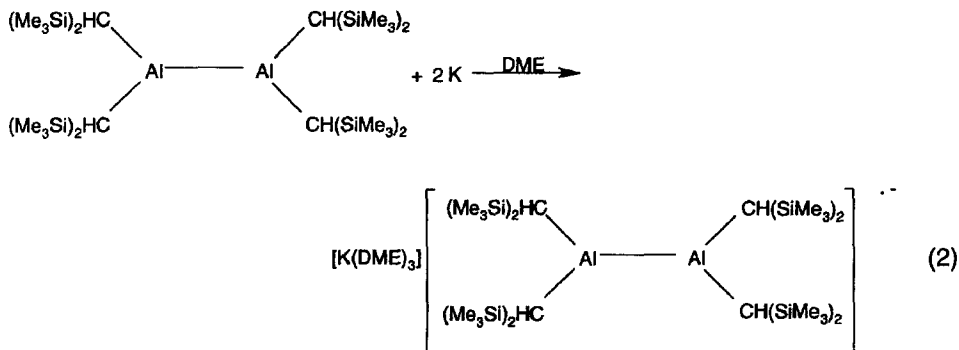
neither compelling structural nor spectroscopic data supporting such a metal-metal interaction. Uhl is credited with unambiguously reporting the first compound containing an Al-Al bond in 1988 with tetrakis[bis(trimethylsilyl)methyl]dialane, $[(\text{Me}_3\text{Si})_2\text{HC}]_2\text{Al}-\text{Al}[\text{CH}(\text{SiMe}_3)_2]_2$, isolated from the potassium metal reduction of bis(trimethylsilyl)methylaluminum chloride (Eq. 1).⁵



The Al-Al bond distance of 2.660(1) Å in this compound served as a benchmark in inorganic chemistry. The fact that the aluminum atoms in $[(\text{Me}_3\text{Si})_2\text{HC}]_2\text{Al}-\text{Al}[\text{CH}(\text{SiMe}_3)_2]_2$ reside in trigonal planar environments about a nearly planar $\text{C}_2\text{Al}-\text{AlC}_2$ core was surprising. An "electronic system delocalized over the Al-Al bond"⁵ was suggested as a factor for the planar $\text{C}_2\text{Al}-\text{AlC}_2$ core. This view will prove important as the concept of π -bonding in Al-Al bonds is embraced (*vide infra*). The significance of the bis(trimethylsilyl)methyl ligand system in the stabilization of this compound was noted as offering desirable steric shielding (thereby preventing disproportionation) and effective electron donating abilities.

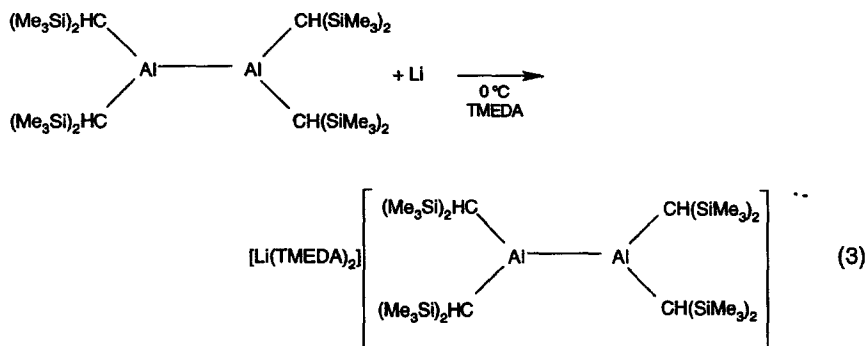
A. The Al-Al One-Electron π -Bond

In an attempt to approach a measure of π -bonding in the Al-Al bond Uhl *et al.* examined the alkali metal reduction of tetrakis[bis(trimethylsilyl)methyl]dialane. Sodium or potassium reduction of $[(\text{Me}_3\text{Si})_2\text{HC}]_2\text{Al}-\text{Al}[\text{CH}(\text{SiMe}_3)_2]_2$ in dimethoxyethane (DME) produced dark blue radical monoanions of $[(\text{Me}_3\text{Si})_2\text{HC}]_2\text{Al}-\text{Al}[\text{CH}(\text{SiMe}_3)_2]_2^-$ (Eq. 2).⁶



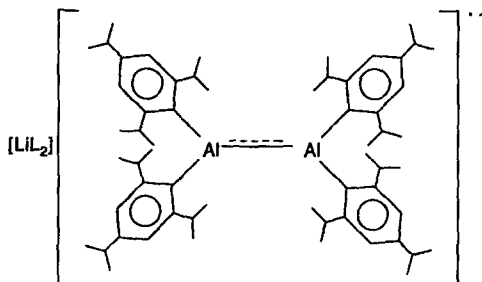
This π -radical, characterized spectroscopically (ESR, UV-Vis, and IR), displayed remarkable stability. In an interesting side note, similar compounds were isolated by these workers by reaction of tetrakis[bis(trimethylsilyl)methyl]dialane with neopentyllithium or trimethylsilylmethylolithium in the presence of tetramethylethylenediamine (TMEDA). Structural data were not reported for this interesting compound.

Coincidentally, another research group was working on the same problem. This team, lead by Pörschke, used lithium in combination with TMEDA to reduce the Al-Al bond in $[(\text{Me}_3\text{Si})_2\text{HC}]_2\text{Al}-\text{Al}[\text{CH}(\text{SiMe}_3)_2]_2$ and afforded an "Al-Al one-electron π -bond" in the radical anion $[(\text{Me}_3\text{Si})_2\text{HC}]_2\text{Al}-\text{Al}[\text{CH}(\text{SiMe}_3)_2]_2^-$ (Eq. 3).⁷



In the presence of TMEDA at 0°C this reaction yields "fine black-violet crystals of the ionic compound." The ESR spectrum confirms the radical anionic character of the species (and appears quite similar to that reported earlier by Uhl).⁶ Importantly, X-ray quality crystals of the compound were obtained, thus allowing unambiguous structural determination. Gross structural features of the radical anion and the neutral dialane are quite similar (i.e., both reside about planar $\text{C}_2\text{Al}-\text{AlC}_2$ trigonal planar cores). However, significant differences between the two are also revealed. For example, the C-Al-C bond angle of $111.9(2)^\circ$ is smaller than that observed in the neutral dialane ($116.7(1)^\circ$). The Al-C bond distances in the radical anion ($2.0420(5) \text{ \AA}$) were lengthened compared to those of the neutral dialane ($1.982(5) \text{ \AA}$). Perhaps most importantly, the Al-Al bond distance in the radical anion of $2.53(1) \text{ \AA}$ is substantially shorter than that observed for the neutral dialane ($2.660(1) \text{ \AA}$). The shortening of 0.13 \AA in the Al-Al bond distance in going from the neutral dialane to the radical anion, the authors state, "is in accord with and Al-Al π -bond of partial multiple bond character."⁶

During this same period another compound was reported claiming an Al-Al π -bond wherein a different ligand system was used: 2,4,6-triisopropylphenyl, $\text{Pr}_3^i\text{C}_6\text{H}_2$. In this work $[\text{Pr}_3^i\text{C}_6\text{H}_2]_2\text{Al}-\text{Al}[\text{C}_6\text{H}_2\text{Pr}_3^i]_2$ was prepared by the potassium



L = TMEDA or 12-crown-4

1

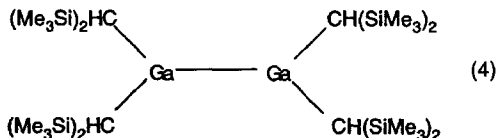
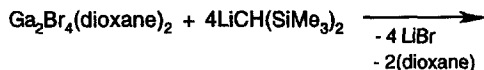
reduction of $[\text{Pr}_3^i\text{C}_6\text{H}_2]_2\text{AlBr}$ in hexane.⁸ The structure of $[\text{Pr}_3^i\text{C}_6\text{H}_2]_2\text{Al-Al}[\text{C}_6\text{H}_2\text{Pr}_3^i]_2$ revealed an Al-Al bond distance of 2.647(3) Å. Moreover, the two C_2Al -trigonal planes of the $\text{C}_2\text{Al-AlC}_2$ core, unlike in the case of $[(\text{Me}_3\text{Si})_2\text{HC}]_2^- \text{Al-Al}[\text{CH}(\text{SiMe}_3)_2]_2$, was shown to be decidedly nonplanar with a torsion angle of 44.8°. Lithium metal reduction of $[\text{Pr}_3^i\text{C}_6\text{H}_2]_2\text{Al-Al}[\text{C}_6\text{H}_2\text{Pr}_3^i]_2$ in the presence of a complexing ligand produced the radical anion $[\text{Pr}_3^i\text{C}_6\text{H}_2]_2\text{Al-Al}[\text{C}_6\text{H}_2\text{Pr}_3^i]_2^{\cdot-}$ (1). Remarkable changes took place upon reduction. The torsion angle between the aluminum planes decreased to an average of 1.4°. Also, the Al-Al bond distance decreased from 2.647(3) Å in the neutral dialane to 2.470(2) Å for the radical anion. The EPR spectrum clearly supported the presence of an unpaired electron as it displayed an 11-line pattern consistent with all of the previously reported radical anions of aluminum. Importantly, considering all of the aluminum-based radical anions reported, the shortest Al-Al bond is observed for $[\text{Pr}_3^i\text{C}_6\text{H}_2]_2\text{Al-Al}[\text{C}_6\text{H}_2\text{Pr}_3^i]_2^{\cdot-}$.

While evidence supporting a one-electron π -bond between two aluminum atoms appears compelling, it is noteworthy that the corresponding two-electron π -bond, $\text{Al}=\text{Al}$ double bond, has yet to be reported.

III

ORGANO gallium COMPOUNDS CONTAINING MULTIPLE BONDS

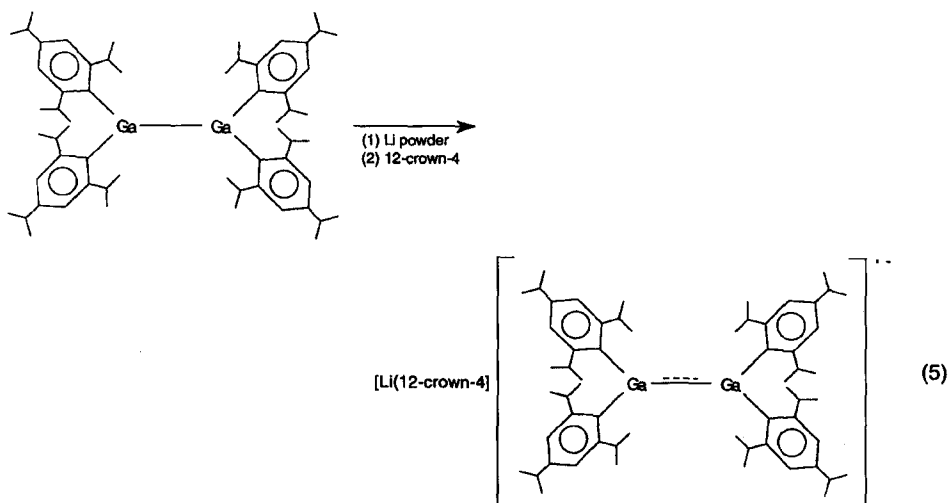
Pivotal in the preparation of the first organometallic gallane is the bis(dioxane) adduct of gallium(II) bromide, $\text{Ga}_2\text{Br}_4(\text{dioxane})_2$ which resides about a Ga-Ga bond at a distance of 2.396(6) Å.⁹ The first organometallic Ga-Ga bonded gallane was reported by Uhl *et al.*, a little more than a decade ago, in the reaction of $\text{Ga}_2\text{Br}_4(\text{dioxane})_2$ with $\text{LiCH}(\text{SiMe}_3)_2$ (Eq. 4).¹⁰



Tetrakis[bis(trimethylsilyl)methyl]digallane, $[(\text{Me}_3\text{Si})_2\text{HC}]_2\text{Ga}-\text{Ga}[\text{CH}(\text{SiMe}_3)_2]_2$, is obtained as yellow crystals. Expectedly, the Ga–Ga bond distance in $[(\text{Me}_3\text{Si})_2\text{HC}]_2\text{Ga}-\text{Ga}[\text{CH}(\text{SiMe}_3)_2]_2$ of 2.541(1) Å is a bit longer (0.146 Å) than that obtained for $\text{Ga}_2\text{Br}_4(\text{dioxane})_2$ (2.395(6) Å). The $\text{C}_2\text{Ga}-\text{GaC}_2$ core, similar to the aluminum analog, is nearly planar.

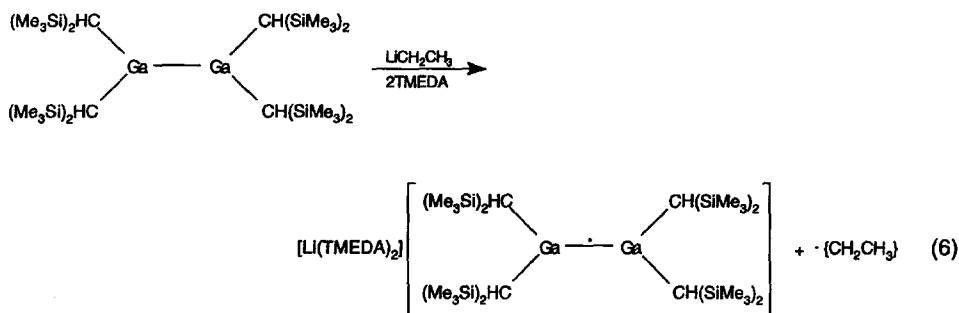
A. One-Electron Ga–Ga π -Bonds: Initial Evidence of Gallium Multiple Bonds

In a similar fashion, gallium(II) chloride bis(dioxane), $\text{Ga}_2\text{Cl}_4(\text{dioxane})_2$ (Ga–Ga: 2.406(1) Å),¹¹ was utilized in the preparation of the first tetraaryldigallane. Reaction of $\text{Ga}_2\text{Cl}_4(\text{dioxane})_2$ with $(\text{Pr}_3^i\text{C}_6\text{H}_2)\text{MgBr}$ yields the $[\text{Pr}_3^i\text{C}_6\text{H}_2]_2\text{Ga}-\text{Ga}[\text{C}_6\text{H}_2\text{Pr}_3^i]_2$ gallane (Ga–Ga: 2.541(1) Å).¹² Again, it is noteworthy that the Ga–Ga bond was elongated in going from the gallium(II) chloride to the gallane. In the same work, the $[\text{Pr}_3^i\text{C}_6\text{H}_2]_2\text{Ga}-\text{Ga}[\text{C}_6\text{H}_2\text{Pr}_3^i]_2$ gallane was treated with an excess of lithium powder to give a dark solution. Upon the addition of 12-crown-4, dark brown-red crystals of $[\text{Li}(12\text{-crown-4})][\text{Pr}_3^i\text{C}_6\text{H}_2]_2\text{Ga}-\text{Ga}[\text{C}_6\text{H}_2\text{Pr}_3^i]_2^-$ were obtained (Eq. 5).



This transformation resulted in a number of striking structural changes. Foremost was a shortening of the Ga–Ga bond distance to 2.343(2) Å and a decrease to 15.5° (from 43.8° in the neutral gallane) in the torsion angle between the GaC₂ planes. It was noted that there was a slight lengthening of the Ga–C bonds to 2.038(3) Å. The authors took these two points as being “consistent with the formation of a one-electron π -bond between the two gallium atoms.”¹² The unpaired electron in this radical anion was manifest in “broad, paramagnetically shifted resonances in the ¹H NMR spectrum.”¹² This position was also supported by a strong EPR signal.

The electron transfer reaction of [(Me₃Si)₂HC]₂Ga–Ga[CH(SiMe₃)₂]₂ with ethyl lithium was reported by Uhl *et al.* to yield thin layers of dark red crystals of the radical anion [(Me₃Si)₂HC]₂Ga–Ga[CH(SiMe₃)₂]₂^{•−} with [Li(TMEDA)₂]⁺, [Li(DME)₃]⁺, or [Li(trimethyltriazinane)₂]⁺ as counter ions (Eq. 6).¹³ ESR spectroscopy displayed temperature-dependent ⁶⁹Ga, ⁷¹Ga, and ²⁹Si hyperfine splitting with significant line broadening. The Ga–Ga bond distance was shown to be 2.401(1) Å—0.14 Å shorter than in the neutral gallane.¹⁰ These data are consistent with a one-electron π -bond.

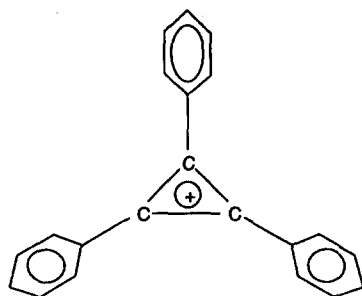


B. Gallium Rings: Cyclogallenes and Metalloaromaticity

The triphenylcyclopropenium cation (2), first prepared by Breslow,¹⁴ is an unusually intriguing species: a 2 π -electron aromatic species constituted by a three-membered carbon ring. In every respect the triphenylcyclopropenium cation displays traditional aromatic behavior, the same as benzene.

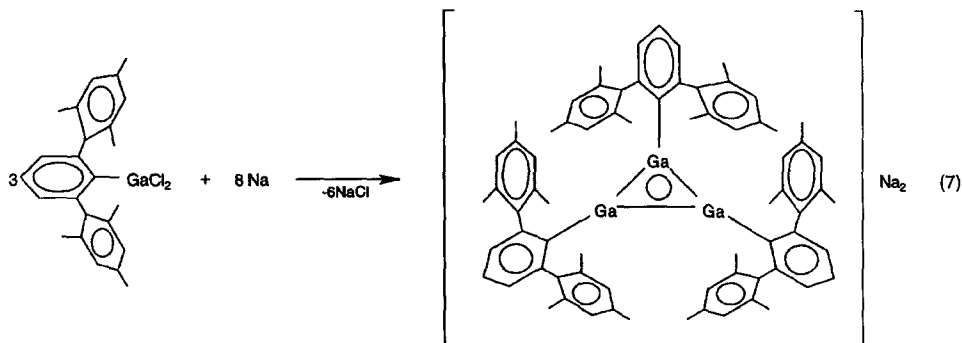
Prior to 1995 no such inorganic compound, save perhaps for borazine, could boast of aromaticity. The utilization of *m*-terphenyl sterically demanding ligands in organogallium chemistry would change this forever.

The sodium metal reduction of [(Me₃C₆H₂)C₆H₃]GaCl₂¹⁵ (Eq. 7) afforded a dark red, almost black, solution from which was obtained similarly colored crystals. This substance was unlike any other that had been prepared in that it existed as



2

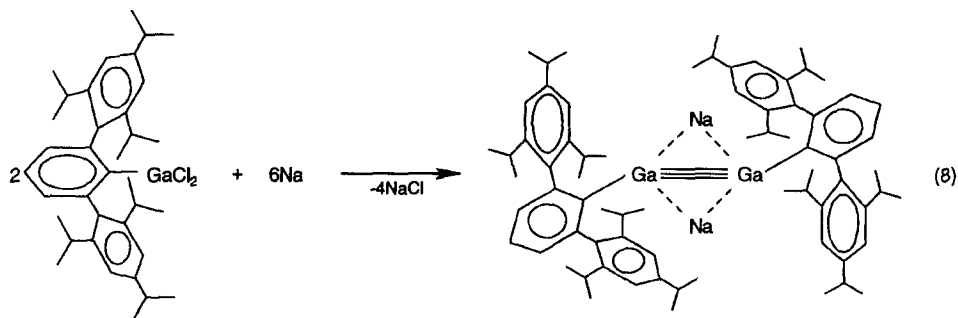
a -Ga-Ga-Ga- three-membered ring with sodium atoms centered above and below the ring. This novel compound, $\text{Na}_2[(\text{Me}_3\text{C}_6\text{H}_2)\text{C}_6\text{H}_3\text{Ga}]_3$,¹⁶ the initial example of a *cyclogallene*, was the first reported of a metallic ring system demonstrating traditional aromatic behavior—metalloaromaticity.^{17–19} Indeed, the metalloaromatic nature of these substances¹⁸ is also supported by the *nucleus independent chemical shifts* (NICS) concept.²⁰



The independent Ga-Ga bond distance in $\text{Na}_2[(\text{Me}_3\text{C}_6\text{H}_2)\text{C}_6\text{H}_3\text{Ga}]_3$ ¹⁶ was determined to be 2.441(1) Å while the Ga-Ga bond distances in the corresponding potassium-based cyclogallene, $\text{K}_2[(\text{Me}_3\text{C}_6\text{H}_2)\text{C}_6\text{H}_3\text{Ga}]_3$,¹⁷ was shown to be slightly shorter at distances of 2.4206(5), 2.4317(5), and 2.4187(5) Å. Cyclogallenes present a credible challenge to borazine as the most important inorganic molecules displaying aromatic behavior. It is important to note that cyclogallenes were the first examples of three-membered ring compounds possessing main group metals.

C. *Synthesis and Molecular Structure of a Gallyne:
A Case for Gallium–Gallium Triple Bonds*

Similar to the situation with aluminum, support for one-electron π -bonds between two gallium atoms is compelling even though a “regular” Ga–Ga two-electron π -bond, a double bond or *gallene*, has not been reported. Thus, a report claiming a Ga–Ga triple bond may initially appear counterintuitive. However, there has been a well-publicized example wherein a $\text{Ga}\equiv\text{Ga}$ triple bond has been reported. The utilization of the sterically demanding ligand has been shown to be quite important in stabilizing unusual organogallium compounds. The *m*-terphenyl ligand system 2,6-dimesitylphenyl has proven particularly beneficial in stabilizing the aforementioned cyclogallenes. In an effort to push the boundaries even further this laboratory sought to examine an even more sterically demanding system with the isopropyl derivative, $[(\text{Pr}^i_3\text{C}_6\text{H}_2)_2\text{C}_6\text{H}_3]$. Reaction of $[(\text{Pr}^i_3\text{C}_6\text{H}_2)_2\text{C}_6\text{H}_3]\text{Li}$ with GaCl_3 affords $[(\text{Pr}^i_3\text{C}_6\text{H}_2)_2\text{C}_6\text{H}_3]\text{GaCl}_2$, which is dimeric in the solid state.²¹ Sodium metal reduction of $[(\text{Pr}^i_3\text{C}_6\text{H}_2)_2\text{C}_6\text{H}_3]\text{GaCl}_2$ yields $\text{Na}_2\{[(\text{Pr}^i_3\text{C}_6\text{H}_2)_2\text{C}_6\text{H}_3]\text{Ga}\equiv\text{Ga}[\text{C}_6\text{H}_3(\text{C}_6\text{H}_2\text{Pr}^i_3)]\}$ as deeply red, almost black, crystals (Eq. 8).¹⁶

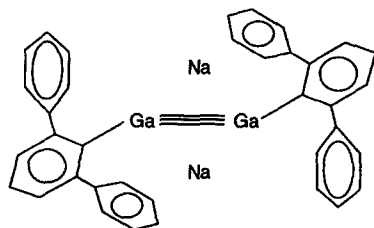


The $\text{Na}_2\{[(\text{Pr}^i_3\text{C}_6\text{H}_2)_2\text{C}_6\text{H}_3]\text{Ga}\equiv\text{Ga}[\text{C}_6\text{H}_3(\text{C}_6\text{H}_2\text{Pr}^i_3)]\}$ compound proved particularly significant as it was reported to contain the first example of a gallium–gallium triple bond, the first *gallyne*. Indeed, a $\text{Ga}\equiv\text{Ga}$ triple bond was suggested even though the angles about the two central gallium atoms in the compound were found to be decidedly nonlinear (with values of $128.5(4)^\circ$ and $133.5(4)^\circ$) coupled with a relatively short Ga–Ga bond ($2.319(3)$ Å). In sum, a triple bond was claimed for a most “unacetylenic” digallium substance. Our interpretation of the bonding in the gallyne has remained unambiguous: The gallium–gallium interaction in this molecule is best described as two donor–acceptor (dative) bonds augmented by one π bond (populated by the two electrons from the two sodium atoms). The two donor–acceptor bond model is consistent with theoretical studies on neutral

R–Ga=Ga–R gallene models.²² This provocative position of a Ga≡Ga triple bond in Na₂[(Prⁱ₃C₆H₂)₂C₆H₃)Ga≡Ga(C₆H₃(C₆H₂Prⁱ₃))] fueled a vigorous debate in the literature.^{23,24} Opposition to the gallyne concept was swift and vigorous, most noticeably from Cotton, Cowley, and Feng (CCF).²⁵ Using density functional theory (DFT), these workers examined a number of main group moieties known to contain multiple bonds and compared those results with the closely related (2,6-diphenyl)phenyl gallyne model, Na₂[(Ph₂C₆H₃)GaGa(C₆H₃Ph₂)]. CCF suggested that the short Ga–Ga bond distance in the gallyne was a consequence of a strong π interaction between the sodium atoms and the substituted phenyl rings of the ligand. The main conclusion of the CCF study regarding the gallyne was that “there can only be a Ga=Ga double bond [one σ bond and one π bond which may be described by two canonical molecular orbitals], namely, Na₂[R–Ga=Ga–R], rather than Na₂[R–GaGa–R]. . .” It is interesting that the CCF effort did not address the concept of bond orders relative to the Ga≡Ga triple bond proposal (*vide infra*).

In an effort to provide a theoretical perspective to the bonding in Na₂[(Prⁱ₃C₆H₂)₂C₆H₃)Ga≡Ga(C₆H₃(C₆H₂Prⁱ₃))], we^{25a} published a study entitled “*The Nature of the Gallium–Gallium Bond*” wherein we utilized DFT on Na₂[H–GaGa–H] and Na₂[Me–GaGa–Me] gallyne model molecules. In this study we observed the same trans-bent geometry in both gallyne models. Moreover, we concluded the bonding in Na₂[H–GaGa–H] and Na₂[Me–GaGa–Me] “to have essentially –Ga≡Ga– triple bonds, composed of two dative and a π bond.”

The concept of bond orders should be discussed in such a debate. It is well known that different methods of calculating bond orders will often result in different bond order values. However, if the same methods are applied to a series of similar molecules, informative trends should emerge. Two methods, Natural Localized Molecular Orbital Natural Population Analysis (NLMO/NPA) and Wiberg Bond Index (WBI), were used in this study. For the [H–Ga≡Ga–H]^{2–} (C_{2h}) model gallyne, we obtained bond order values of 3.02 and 2.36 for NLMO/NPA and WBI, respectively (similar bond order values were obtained for the methyl derivative). However, this study was criticized for using gallyne models which possessed ligands which were too simplistic (i.e., H and Me).²⁴ While we felt confident in the nature of the Ga–Ga interaction with the hydride and methyl model ligands, we were similarly compelled to address this specific criticism in a work entitled “*The Gallium–Gallium Triple Bond in a Realistic Model. A Density Functional Study of Na₂[(C₆H₅)₂GaGaC₆H₃(C₆H₅)₂]*.”²⁶ In this study we utilized a ligand system which lacked only the isopropyl groups (compared to the experimental gallyne), namely 2,6-diphenylphenyl (**3**). The Na₂[(C₆H₅)₂GaGaC₆H₃(C₆H₅)₂] structure was fully optimized with the B3LYP method utilizing a substantial basis of 836 contracted Gaussian functions. As evidenced by a NLMO/NPA bond order of 2.794 for Na₂[(C₆H₅)₂GaGaC₆H₃(C₆H₅)₂], the data obtained were in support of a gallium–gallium triple bond—*albeit a weak Ga–Ga triple bond*. It should be pointed out that the WBI method yields a bond order of only 2.019. However, it is noteworthy



Model Gallyne

3

that the WBI values are frequently smaller than the corresponding formal bond orders. For example, obviously each of the bonds in HF, $\text{H}_3\text{B}-\text{NH}_3$, and H_2O should have a formal bond order of 1.0. However, at the DZP SCF level of theory the WBI bond order value for the H-F bond in HF is 0.67, the B-N bond in $\text{H}_3\text{B}-\text{NH}_3$ is 0.55, and the O-H bond in H_2O is 0.76. Thus, all things considered, a WBI bond order value of 2.019 for the Ga-Ga bond in $\text{Na}_2[(\text{C}_6\text{H}_5)_2\text{GaGaC}_6\text{H}_3(\text{C}_6\text{H}_5)_2]$ is quite reasonable (even as a Ga-Ga triple bond is claimed).

Reports concerning the $\text{Na}_2[(\text{Pr}^i_3\text{C}_6\text{H}_2)_2\text{C}_6\text{H}_3]\text{Ga}\equiv\text{Ga}\{\text{C}_6\text{H}_3(\text{C}_6\text{H}_2\text{Pr}^i_3)\}$ gallyne and the concept of a Ga-Ga triple bond are ever forthcoming. One of the most recent studies concerns topographical analyses of the gallyne using the electron localization function (ELF).²⁷ The ELF method divides triple bonds into two categories: (1) classical or unslipped triple bonds (i.e., acetylene), and (2) non-classical or slipped triple bonds (i.e., the gallyne). Concerning the gallyne, these workers conclude, "*Clearly, this compound has a triple bond!*" In an attempt to confirm their analysis of the triple bond in the gallyne and to rule out a description with two lone pairs at the Ga centers (resulting in a Ga-Ga single bond), the workers examined the bonding in the diphosphene $\text{H}_2\text{P}-\text{PH}_2$ using ELF. The conclusion was unambiguous: "*a P-P single (σ) bond and a lone pair of electrons on each phosphorus atom.*"

Support for a weak Ga-Ga triple bond in the gallyne (aside from studies from our laboratory) may also be garnered from a recent study examining force constants derived from DFT frequency calculations. It is shown that the gallium-gallium bond in $[\text{H}-\text{Ga}\equiv\text{Ga}-\text{H}]^{2-}$ is only slightly strengthened with respect to the Ga-Ga single bond in $[\text{H}_3\text{Ga}-\text{GaH}_3]^{2-}$.²⁸ Moreover, the weakness of the Ga-Ga bond in the gallyne has been addressed in a study entitled "*How Strong Is the Gallium-Gallium Triple Bond.*"²⁹ These workers concluded that the gallium-gallium bond strength (0.87 aJ/\AA^2) in the $\text{Na}_2[\text{H}_2\text{Ga}\equiv\text{GaH}_2]$ gallyne model was calculated to be weaker

than the gallium–gallium double bond ($1.20 \text{ aJ}/\text{\AA}^2$) in the $\text{Na}_2[\text{H}_2\text{Ga}=\text{GaH}_2]$ model gallene. Other workers have also noted the gallyne as having a weak Ga–Ga bond.³⁰ Detailed and critical accounts of the gallyne and the gallium–gallium triple bond debate have recently been published.^{31,32}

IV

CONCLUSION

The concept of aluminum or gallium engaging in multiple bonding is intellectually intriguing and experimentally challenging. Furthermore, this area is of quite recent vintage only coming to the fore in the last decade. With the advent of the one-electron π -bond and the experimental realization of the first gallium–gallium triple bond, this area promises remarkable discoveries in the years to come.

REFERENCES

- (1) Schram, E. P. *Inorg. Chem.* **1966**, *5*, 1291.
- (2) Schram, E. P.; Hall, R. E.; Glore, J. D. *J. Am. Chem. Soc.* **1969**, *91*, 6643.
- (3) Hoberg, H.; Krause, S. *Angew. Chem., Int. Ed. Engl.* **1976**, *15*, 694.
- (4) Hoberg, H.; Krause, S. *Angew. Chem., Int. Ed. Engl.* **1978**, *17*, 949.
- (5) Uhl, W. *Z. Naturforsch.* **1988**, *43b*, 1113.
- (6) Uhl, W.; Vester, A.; Kaim, W.; Poppe, J. *J. Organomet. Chem.* **1993**, *454*, 9.
- (7) Pluta, C.; Pörschke, K.-R.; Kruger, C.; Hildenbrand, K. *Angew. Chem., Int. Ed. Engl.* **1993**, *32*, 388.
- (8) Wehmshulte, R. J.; Ruhlandt-Senge, K.; Olmstead, M. M.; Hope, H.; Sturgeion, B. E.; Power, P. P. *Inorg. Chem.* **1993**, *32*, 2983.
- (9) Small, R. W. H.; Worrall, I. J. *Acta. Cryst.* **1982**, *38*, 250.
- (10) Uhl, W.; Layh, M.; Hildenbrand, T. *J. Organomet. Chem.* **1989**, *364*, 289.
- (11) Beamish, J. C.; Small, R. W. H.; Worrall, I. J. *Inorg. Chem.* **1979**, *18*, 220.
- (12) He, X.; Barlett, R. A.; Olmstead, M. M.; Ruhlandt-Senge, K.; Sturgeon, B. E.; Power, P. P. *Angew. Chem., Int. Ed. Engl.* **1993**, *32*, 717.
- (13) Uhl, W.; Schütz, W.; Kaim, W.; Waldhör, E. *J. Organomet. Chem.* **1995**, *501*, 79.
- (14) Breslow, R. *J. Am. Chem. Soc.* **1957**, *79*, 5318.
- (15) Crittendon, R. C.; Li, X.-W.; Su, J.; Robinson, G. H. *Organometallics* **1997**, *16*, 2443.
- (16) Li, X.-W.; Pennington, W. T.; Robinson, G. H. *J. Am. Chem. Soc.* **1995**, *117*, 7578.
- (17) Li, X.-W.; Xie, Y.; Schreiner, P. R.; Gripper, K. D.; Crittendon, R. C.; Campana, C. F.; Schaefer, H. F.; Robinson, G. H. *Organometallics* **1996**, *15*, 3798.
- (18) Xie, Y.; Schreiner, P. R.; Schaefer, H. F.; Li, X.-W.; Robinson, G. H. *J. Am. Chem. Soc.* **1996**, *118*, 10635.
- (19) Xie, Y.; Schreiner, P. R.; Schaefer, H. F.; Li, X.-W.; Robinson, G. H. *Organometallics* **1998**, *17*, 114.
- (20) Schleyer, P. v. R.; Maerker, C.; Dransfeld, A.; Jiao, H.; Hommes, N. J. R. v. E. *J. Am. Chem. Soc.* **1996**, *118*, 6317.
- (21) Su, J.; Li, X.-W.; Robinson, G. H. *Chem. Commun.* **1998**, 2015.

- (22) Trinquier, G. *J. Am. Chem. Soc.* **1990**, *112*, 2130.
- (23) Dagani, R. *Chem. Eng. News* **1997**, *75* (June 16), 9.
- (24) Dagani, R. *Chem. Eng. News* **1998**, *76* (March 16), 31.
- (25) Cotton, F. A.; Cowley, A. H.; Feng, X. *J. Am. Chem. Soc.* **1998**, *120*, 1795.
- (25a) Xie, Y.; Grev, R. S.; Gu, J.; Schaefer, H. F. III; Schleyer, P. v. R.; Su, J.; Li, X.-W.; Robin G. H. *J. Am. Chem. Soc.* **1998**, *120*, 3773.
- (26) Xie, Y.; Schaefer, H. F.; Robinson, G. H. *Chem. Phys. Lett.* **2000**, *317*, 174.
- (27) Grützmacher, H.; Fässler, T. F. *Chem. Eur. J.* **2000**, *6*, 2317.
- (28) Köppe, R.; Schnöckel, H. *Z. Anorg. Allg. Chem.* **2000**, *626*, 1095.
- (29) Grunenberg, J.; Goldberg, N. *J. Am. Chem. Soc.* **2000**, *122*, 6045.
- (30) Bytheway, I.; Lin, Z. *J. Am. Chem. Soc.* **1998**, *120*, 12133.
- (31) Robinson, G. H. *Acc. Chem. Res.* **1999**, *32*, 773.
- (32) Robinson, G. H. *Chem. Commun.* **2000**, 2175.

Index

A

Ab initio calculations

OsHCl(η -H₂)(CO)(PH₃)₂, 20

OsH₂(η^2 -H₂)(CO)(PH₃)₂, 31

Acenaphthalene complex, 219–220

Alcohols, in OsH(η^2 -H₂BH₂)(CO)(P^{*i*}Pr₃)₂
decomposition, 40–43

Alkali salt, in calix[4]arene synthesis, 190

Alkenes

from alkyne–OsHCl(CO)(P^{*i*}Pr₃)₂ additions,
7–8

–carbene, OsCl₂(η -H₂)(CO)(P^{*i*}Pr₃)₂ as
precursor, 21–24

in metalla-calix[4]arenes, 178–181

in [OsH(CO)₂{ η^1 -OCMe₂}(P^{*i*}Pr₃)₂]BF₄
ligand displacement, 43

–tungsten complexes, 215–217

O-Alkylated calix[4]arenes, metalation,
170–172

Alkylating agents, in metal–alkyl derivatives,
204–206

Alkylidene–metals

from alkylating agents, 204–206

associated chemistry, 204

and Fischer carbene chemistry, 206–210

from metalla-calix[4]arenes, 220

metallacycles, 213–214

from 1-metallacyclopentene, 215

metal-oxo-surface models, 210–211

Nb, synthesis, 223

from protonation, 206

Alkylidyne–metals

from alkylating agents, 204–206

associated chemistry, 204

electrophile reactions, 206

from metalla-calix[4]arenes, 220

metallacycles, 213–214

metal-oxo-surface models, 210–211

Nb, synthesis, 223

Alkyne reactions

with OsHCl(CO)(P^{*i*}Pr₃)₂, 7–14

with [OsH(CO)₂{ η^1 -OCMe₂}(P^{*i*}Pr₃)₂]BF₄,
43

with OsH₂(η^2 -H₂)(CO)(P^{*i*}Pr₃)₂, 32–38

with Zr(II)–boratabenzene complex, 113

Alkynols, OsHCl(CO)(P^{*i*}Pr₃)₂ reactions, 17–19

Allyl alcohol, with OsH(OH)(CO)(P^{*i*}Pr₃)₂, 47

Aluminum

AIX metastable solutions, 237–240

metalloid clusters, *see* Metalloid aluminum
clusters

one-electron Al–Al π -bond, 284–286

Aluminum bromide, 240

Aluminum iodide, 240

Amidoboratabenzenes, 107

Arsasilene, 128

B

Benzophenone reactions, 27

Benzosilacyclobutenes, 130

Benzylideneacetone reactions, 51–53

Benzynes, trapping, 91–92

μ -Bis-carbene derivatives, 21–24

Bis- η^2 -iminoacyl compound, 198

o-Bis(silyl)carborane, 65–69

Bissilyl *o*-carboranyl derivatives, 63–64

Bistanna *o*-carboranyl derivatives, 63–64

Bond energies, Group 14 and 16 double
bonds, 125

Borabenzene

η^6 -borabenzene complex, 104

–ligand adducts, 102–104

ligand-free, 104–105

–oxazoline adduct, ring faces, 103–104

–PMe₃, 105–106

Boracyclohexadiene, 104

Boratabenzenes

anionic, synthesis, 105–108

transition metal complexes, 110–116

transition metal-free compounds, 108–110

1-Boratanaphthalene, 107

Boratastilbene, 109

Butadiene

–Ta compounds, 185

–Zr functionality, 181–184

C

Calix[4]arenes

metalation, 170–172

- as supporting ligand, 193–194
 - synthesis, 190
 - Ta–C σ bond, 200–204
 - Ti–C σ bond, 186–188
 - V–C σ bond, 198–200
 - Zr–C σ bond, 188–198
 - Carbenes
 - $\text{OsCl}_2(\eta^2\text{-H}_2)(\text{CO})(\text{P}^i\text{Pr}_3)_2$ as precursor, 21–24
 - from $\text{OsHCl}(\text{CO})(\text{P}^i\text{Pr}_3)_2$ reactions with alkynols, 17–19
 - Carbon
 - metal functionalities, 214
 - Ta–C σ bond, 200–204
 - Ti–C σ bond, 186–188
 - V–C σ bond, 198–200
 - Zr–C σ bond, 188–198
 - Carbon dioxide, $\text{OsH}(\text{OH})(\text{CO})(\text{P}^i\text{Pr}_3)_2$ reaction, 47
 - Carbon monoxide reactions
 - with $\text{OsCl}_2(\text{CHCH}_2\text{Ph})(\text{CO})(\text{P}^i\text{Pr}_3)_2$, 23
 - with $\text{OsHCl}_2(\text{CCH}_2\text{Me})(\text{P}^i\text{Pr}_3)_2$, 22–23
 - with $\text{OsH}(\text{SH})(\text{CO})(\text{P}^i\text{Pr}_3)_2$, 47–48
 - Carbonylation, $\text{OsHCl}(\text{CO})(\text{P}^i\text{Pr}_3)_2$ complex, 10
 - o*-Carborane
 - o*-bis(silyl)carborane double silylation reaction, 65–69
 - bissilyl *o*-carboranyl derivatives, 63–64
 - bistanna *o*-carboranyl derivatives, 63–64
 - o*-carboranylene-1,2-disilacyclobutene reactivity, 69–71
 - with *P,Si*-chelating *o*-carboranylphosphino ligand, 72–74
 - ligand design from, 93–95
 - organotin compounds, 71–72, 75–77
 - reactivity, 88–92
 - o*-Carboranyl amino ligand, in organotin compounds, 71–72
 - B,N*-Carboranyl chelating ligand, 77–79
 - B,P*-Carboranyl chelating ligand, 77–79
 - C,N*-Carboranyl chelating ligand, 80–81
 - S,N*-Carboranyl chelating ligand, 81–83
 - S,P*-Carboranyl chelating ligand, 81–83
 - o*-Carboranylene-1,2-disilacyclobutene, 69–71
 - o*-Carboranylphosphino ligand
 - P,Si*-chelating, in metal complexes, 72–74
 - C,P*-chelating, organotin compounds with, 75–77
 - o*-Carboranyltributyltin, 89
 - Catalysts, $\text{OsHCl}(\text{CO})(\text{P}^i\text{Pr}_3)_2$ as, 51–55
 - Chlorine, reaction with $\text{OsHCl}(\text{CO})(\text{P}^i\text{Pr}_3)_2$, 19–21
 - Condensation, AlX and GaX solutions, 237–240
 - Coordination polyhedron, $\text{OsHCl}(\text{CO})(\text{P}^i\text{Pr}_3)_2$, 3–5
 - Cr(III)–boratabenzene, 106
 - Cyclogallenes, 288–289
 - Cyclohexadienes, H_2 transfer reactions, 54
 - Cyclohexene, H_2 transfer reactions, 54
 - η^2 -Cyclohexene complex, in metalla-calix[4]arenes, 179
 - Cyclohexylacetylene, addition to $\text{OsHCl}(\text{CO})(\text{P}^i\text{Pr}_3)_2$, 11–12
 - Cyclopentadienes
 - anion as supporting ligand, 193–194
 - $\text{OsHCl}(\text{CO})(\text{P}^i\text{Pr}_3)_2$ reaction, 44–46
 - $\text{OsH}_2(\text{CO})(\eta^2\text{-CH}_2=\text{CHEt})(\text{P}^i\text{Pr}_3)_2$ reaction, 26
- D**
- DAB, *see* 1-(Diphenylamido)boratabenzene
 - Decomposition, $\text{OsH}(\eta^2\text{-H}_2\text{BH}_2)(\text{CO})(\text{P}^i\text{Pr}_3)_2$, 40–43
 - 1,2-Dehydrobenzene, 91–92
 - 1,2-Dehydro-*o*-carborane, 91
 - Desulfurization, tetrathiaplumbolanes, 153–155
 - Diarylgermaneselone, 144–145
 - Diarylgermanethione, 142–144
 - Diaryl-substituted germanetellone, 145
 - Diazoalkanes, $\text{OsHCl}(\text{CO})(\text{P}^i\text{Pr}_3)_2$ reaction, 6–7
 - Dienyl complexes, from enynes, 14–17
 - Dimethyl acetylenedicarboxylate, 47
 - Diolefin reactions
 - $\text{OsHCl}(\text{CO})(\text{P}^i\text{Pr}_3)_2$ as catalyst, 51–52
 - $\text{OsH}_2\text{Cl}_2(\text{P}^i\text{Pr}_3)_2$ as catalyst, 55
 - 1,3,2,4-Dioxadisiletanes, 129
 - 1,3,4,2-Dioxazasilole, 129
 - Diphenylacetylene, 37–38
 - 1-(Diphenylamido)boratabenzene, 109
 - 1-(Diphenylphosphido)boratabenzene σ complex, 112
 - synthesis, 109
 - Disilanickela, in double silylation reaction, 68–69
 - Dithiolato-*o*-carborane, in metal compounds, 83–88
 - Diynes, alkyne– $\text{OsHCl}(\text{CO})(\text{P}^i\text{Pr}_3)_2$ reaction, 8
 - Double bond systems

alkyl,aryl-substituted Ge-containing heavy ketones, 147–148
 dialkyl-substituted Ge-containing heavy ketones, 148
 diarylgermanesellone, 144–145
 diarylgermanethione, 142–144
 diaryl-substituted germanetellone, 145
 with Ge, 140–141
 Ge–chalcogen double bond compounds, 148–149
 Ge-containing heavy ketones, 142
 germanetellone, 146–147
 Group 14 and 16 bond energies, 125
 metal–chalcogen reactivities, 160–161
 plumbanethione, 153–156
 silanesellone, 135–138
 silanetellone, 139–140
 silanethione, 131–135
 silanone, 127–131
 stannaneselones, 149–153
 stannanethiones, 149–153
 Double silylation reaction, *o*-bis(silyl)carborane, 65–69
 DPB, *see* 1-(Diphenylphosphido)boratabenzene

E

Enynes, $\text{OsHCl}(\text{CO})(\text{P}^i\text{Pr}_3)_2$ reactions, 14–17
 Ethanol, $\text{OsH}(\eta^2\text{-H}_2\text{BH}_2)(\text{CO})(\text{P}^i\text{Pr}_3)_2$ treatment, 40
 Ethylene–[W(calix)] fragment interactions, 179–181
 Ethyne dicarboxylic methyl ester, 7–8

F

(1-Ferrocenyl- η^6 -boratabenzene)
 (η^5 -cyclopentadienyl) cobalt⁺, 111
 Fischer carbenes, and metal–alkylidene complexes, 206–210

G

Gallium
 cyclogallenes, 288–289
 Ga–Ga triple bonds, 290–293
 α -gallium, 256
 β -gallium, 256
 γ -gallium, 257–258
 δ -gallium, 258

gallium(II), 258–259
 gallium(III), 260
 GaX metastable solutions, 237–240
 metalloid clusters, *see* Metalloid gallium clusters
 one-electron Ga–Ga π -bonds, 287–288
 ring metalloaromaticity, 288–289
 Gallium bromide, 240
 Gallium chloride, 240
 Gallium iodide, 240
 Gallyne, 290–293
 Germanesellone, diaryl-substituted compound, 144–145
 Germanetellones
 diaryl-substituted, synthesis, 145
 Raman spectroscopy, 160
 synthesis, 146–147
 Germanethiones
 diaryl-substituted compounds, 142–144
 Raman spectroscopy, 160
 Germanium
 alkyl,aryl-substituted systems, 147–148
 –chalcogen double bond compounds, 148–149
 dialkyl-substituted Ge-containing systems, 148
 diarylgermanesellone, 144–145
 diarylgermanethione, 142–144
 diaryl-substituted germanetellone, 145
 double bond systems, 140–141
 germanetellone, 146–147
 heavy ketones containing, 142

H

Heavy ketones
 alkyl,aryl-substituted Ge-containing systems, 147–148
 bond energies, 124–127
 dialkyl-substituted Ge-containing systems, 148
 with Ge, 142
 NMR analysis, 158–159
 Raman spectroscopy, 160
 reactivities, 160–162
 UV–Vis spectroscopy, 159–160
 X-ray crystallographic analysis, 156–158
 Heteroallenes, reaction with
 $\text{OsH}_2(\text{CO})(\eta^2\text{-CH}_2=\text{CHEt})(\text{P}^i\text{Pr}_3)_2$, 27–28

Hydrides

–alkyl compounds, synthesis and reactions, 40–43

–vinylidene complexes, 11–14

Hydrido–chloro–

carbonylbis(isopropylphosphine)osmium(II)

with alkynol, 17–19

with *n*-BuLi, 24–31

with C₃H₆, 44–46

with enyne, 14–17

as homogenous catalyst, 51–55

with HX, 19–21

metathetical reactions, 50–51

with NaBH₄, 38–40

with NaXR, 46–50

with OsHCl(CO)(P^{*i*}Pr₃)₂, 3–14

Hydrogen, molecular

with Os(C₂Ph)₂(CO)(P^{*i*}Pr₃)₂, 33

with OsHCl(CO)(P^{*i*}Pr₃)₂, 19–21

Hydrogen transfer, OsHCl(CO)(P^{*i*}Pr₃)₂ as catalyst, 54

I

Ir(η⁵-C₅Me₅)(Ph)(OH)(PMe₃), 47

Iron-sandwich complexes, 111

Isothiocyanatomethane, with

OsH(SC₆H₅)(CO)(P^{*i*}Pr₃)₂, 49–50

K

Ketones

heavy, *see* Heavy ketones

hydrogen transfer reactions, 54

η²-ketones, 196

methyl vinyl ketones, 43, 47

unsaturated ketones, 54–55

L

Lead, plumbanethione, 153–156

Lewis base reactions

with OsH₂(CO)(η²-CH₂=CHEt)(P^{*i*}Pr₃)₂, 24–25

with [OsHη¹-OCMe₂(CO)(PhPh₂)(P^{*i*}Pr₃)₂]BF₄, 26

with OsH(SH)(CO)(P^{*i*}Pr₃)₂, 47–48

Ligand design, from *o*-carborane, 93–95

Lithium alkylating agents, 204–206

Lithium 1-(dimethylamido)boratabenzene, 108

M

Magnesium alkylating agents, 204–206

Metal–alkylidenes

from alkylating agents, 204–206

associated chemistry, 204

and Fischer carbene chemistry, 206–210

from metalla-calix[4]arenes, 220

metallacycles, 213–214

from 1-metallacyclopropene, 215

metal-oxo-surface models, 210–211

Nb, synthesis, 223

from protonation, 206

Metal–alkylidyne

from alkylating agents, 204–206

associated chemistry, 204

electrophile reactions, 206

from metalla-calix[4]arenes, 220

metallacycles, 213–214

metal-oxo-surface models, 210–211

Nb, synthesis, 223

Metalation

O-alkylated calix[4]arenes, 170–172

calix[4]arenes, 170–172

Metal–carbon σ bond

Ta–C, 200–204

Ti–C, 186–188

V–C, 198–200

Zr–C, 188–198

Metal–chalcogen double bonds, 160–161

Metal complexes

with *B,N*-carboranyl chelating ligand, 77–79

with *B,P*-carboranyl chelating ligand, 77–79

with *C,N*-carboranyl chelating ligand, 80–81

with *S,N*-carboranyl chelating ligand, 81–83

with *S,P*-carboranyl chelating ligand, 81–83

with *P,Si*-chelating *o*-carboranylphosphino ligand, 72–74

with dithiolato-*o*-carborane, 83–88

Metalla-calix[4]arenes

Mb compounds, 176–178

in metal-alkyl complex syntheses, 220

reduction, 178–185

Ta compounds, 200–204

Ti compounds, 186–188

V compounds, 198–200

W compounds, 172–176

Zr compounds, 188–198
 Metallacycles, 213–214
 1-Metallacyclopentene, 213–214
 1-Metallacyclopentene
 and acenaphthalene complex,
 219–220
 synthesis, 212–213, 215
 W(IV)-calix[4]arene route, 217–218
 Metalloaromaticity, Ga rings, 288–289
 Metalloid aluminum clusters
 $\text{Al}_{12}(\text{AlBr}_2)_{10} \cdot 12(\text{THF})$, 252–254
 $\text{Al}_7[\text{N}(\text{SiMe}_3)_2]_6^-$, 241–243
 $\text{Al}_{12}[\text{N}(\text{SiMe}_3)_2]_8^-$, 243–245
 $\text{Al}_{77}[\text{N}(\text{SiMe}_3)_2]_{20}^{2-}$, 248–252
 $\text{Al}_{14}[\text{N}(\text{SiMe}_3)_2]_{616}$, 245–247
 Metalloid gallium clusters
 $[\text{Ga}_{12}(\text{C}_{13}\text{H}_9)_{10}]^{2-}$, 264–265
 $\text{Ga}_8[\text{C}(\text{SiMe}_3)_3]_6$, 262–264
 $[\text{Ga}_{19}\{\text{C}(\text{SiMe}_3)_3\}_6]^-$, 265–269
 $\text{Ga}_{22}[\text{Ge}(\text{SiMe}_3)_3]_8$, 269–271
 $[\text{Ga}_{84}\{\text{N}(\text{SiMe}_3)_2\}_{20}]_4^-$, 273–277
 $\text{Ga}_{18}(\text{Si}^i\text{Bu}_3)_8$, 265
 $\text{Ga}_{22}[\text{Si}^i\text{Bu}_3]_8$, 269–271
 $[\text{Ga}_6(\text{SiPh}_2\text{Me})_8]^-$, 261–262
 $\text{Ga}_{22}[\text{Si}(\text{SiMe}_3)_3]_8$, 269–271
 $[\text{Ga}_{26}\{\text{Si}(\text{SiMe}_3)_3\}_8]^{2-}$, 271–272
 synthetic routes, 260–261
 Metal–metal bonded dimers
 molybdenum, 176–178
 tungsten, 172–176
 Metal-oxo-surface model, 210–211
 Metathetical reactions, on $\text{OsHCl}(\text{CO})(\text{P}^i\text{Pr}_3)_2$
 chloride ligand, 50–51
 Methanedithione, with
 $\text{OsH}(\text{SC}_6\text{H}_5)(\text{CO})(\text{P}^i\text{Pr}_3)_2$, 49–50
 Methyl acrylate, with $\text{OsH}(\text{OH})(\text{CO})(\text{P}^i\text{Pr}_3)_2$,
 47
 1-Methylboratabenzene ammonium salt,
 108–109
 2-Methyl-1-buten-3-yne
 with $\text{OsCl}_2(\eta^2\text{-H}_2)(\text{CO})(\text{P}^i\text{Pr}_3)_2$, 23
 with $\text{OsHCl}(\text{CO})(\text{P}^i\text{Pr}_3)_2$, 14
 Methyl propiolate
 with $[\text{OsH}(\text{CO})_2\{\kappa^1\text{-OCMe}_2\}(\text{P}^i\text{Pr}_3)_2]\text{BF}_4$,
 43
 with $\text{OsH}_2(\eta^2\text{-H}_2)(\text{CO})(\text{P}^i\text{Pr}_3)_2$, 35, 37
 Methyl vinyl ketone
 with $[\text{OsH}(\text{CO})_2\{\eta^1\text{-OCMe}_2\}(\text{P}^i\text{Pr}_3)_2]\text{BF}_4$,
 43
 with $\text{OsH}(\text{OH})(\text{CO})(\text{P}^i\text{Pr}_3)_2$, 47

Molybdenum, metal–metal bonded dimers,
 176–178
 Monochlorozirconium(IV)-calix[4]arene, 190
 Monomethoxy-calix[4]arene-zirconium,
 193

N

Niobium-alkylidenes, 223
 Niobium-alkylidyne, 223
 Niobium(III)-calix[4]arene dimer, 220
 Nuclear magnetic resonance
 heavy ketones, 158–159
 $\text{OsHCl}(\text{CO})(\text{P}^i\text{Pr}_3)_2$, 3–5

O

1,7-Octadiyne, alkyne- $\text{OsHCl}(\text{CO})(\text{P}^i\text{Pr}_3)_2$
 reaction, 8
 Organoaluminum compounds, 283–286
 Organogallium compounds, 287–288
 Organotin compounds, 71–72, 75–77
 Osmium
 $\text{OsCl}_2(\text{CHCH}_2\text{Ph})(\text{CO})(\text{P}^i\text{Pr}_3)_2$, 23
 $\text{OsCl}_2(\eta^2\text{-H}_2)(\text{CO})(\text{P}^i\text{Pr}_3)_2$, 21–24
 $\text{Os}(\text{C}_2\text{Ph})_2(\text{CO})(\text{P}^i\text{Pr}_3)_2$, 33
 Os–H bond, alkyne additions, 7–10
 $\text{OsHCl}_2(\text{CCH}_2\text{Me})(\text{P}^i\text{Pr}_3)_2$, 22–23
 $\text{OsHCl}(\text{C}=\text{CHPh})$, 5–6
 $\text{OsHCl}(\text{CO})(\text{P}^i\text{Pr}_3)_2$, *see* Hydrido–chloro–
 carbonylbis(isopropylphosphine)
 osmium(II)
 $\text{OsHCl}(\eta^2\text{-H}_2)(\text{CO})(\text{PH}_3)_2$, 20
 $\text{OsHCl}(\eta^2\text{-H}_2)(\text{CO})(\text{P}^i\text{Pr}_3)_2$, 32–34
 $\text{OsH}_2\text{Cl}_2(\text{P}^i\text{Pr}_3)_2$, 55
 $\text{OsH}_2(\text{CO})(\eta^2\text{-CH}_2=\text{CHEt})(\text{P}^i\text{Pr}_3)_2$, 24–31
 $[\text{OsH}(\text{CO})_2\{\eta^1\text{-OCMe}_2\}(\text{P}^i\text{Pr}_3)_2]\text{BF}_4$, 42
 $[\text{OsH}(\text{CO})_2\{\kappa^1\text{-OCMe}_2\}(\text{P}^i\text{Pr}_3)_2]\text{BF}_4$, 43
 $\text{OsH}(\text{C}_2\text{R})(\eta^2\text{-H}_2)(\text{CO})(\text{P}^i\text{Pr}_3)_2$, 32–34
 $\text{OsH}(\eta^2\text{-H}_2\text{BH}_2)(\text{CO})(\text{P}^i\text{Pr}_3)_2$, 38–43
 $\text{OsH}_2(\eta^2\text{-H}_2)(\text{CO})(\text{P}^i\text{Pr}_3)_2$, 32–38
 $[\text{OsH}(\eta^2\text{-H}_2)(\text{CO})(\text{P}^i\text{Pr}_3)_2]\text{BF}_4$, 25
 $\text{OsH}(\kappa^2\text{-O}_2\text{CH})(\text{CO})(\text{P}^i\text{Pr}_3)_2$, 29–30
 $\text{OsH}(\kappa^2\text{-S}_2\text{CH})(\text{CO})(\text{P}^i\text{Pr}_3)_2$, 28–29
 $\text{OsH}(\text{OC}_6\text{F}_5)(\text{CO})(\text{P}^i\text{Pr}_3)_2$, 48–49
 $\text{OsH}(\text{OC}_6\text{H}_5)(\text{CO})(\text{P}^i\text{Pr}_3)_2$, 48–49
 $\text{OsH}(\text{OH})(\text{CO})(\text{P}^i\text{Pr}_3)_2$, 47
 $\text{OsH}(\text{SC}_6\text{H}_5)(\text{CO})(\text{P}^i\text{Pr}_3)_2$, 49–50
 $\text{OsH}(\text{SH})(\text{CO})(\text{P}^i\text{Pr}_3)_2$, 47–48
 Oxo-niobium(V) complex, 222

P

- Palladium, $\text{Pd}_2(\text{dba})_3$, 73–74
 Phenolates, with $\text{OsHCl}(\text{CO})(\text{P}^i\text{Pr}_3)_2$, 46–50
 Phenoxo anion, 193–194
 Phenylacetylene
 with $\text{OsHCl}(\text{CO})(\text{P}^i\text{Pr}_3)_2$, 51–52
 triethylsilane addition, 53
 4-Phenylbutan-2-one, 52–53
 1-Phenyl-2-propyn-1-ol, 18
 Phosphinoalkylsilanes, 72–73
 Phosphinosilanes, 73
 π -bonds, one-electron
 Al–Al, 284–286
 Ga–Ga, 287–288
 Platinum, $\text{Pt}(\text{cod})_2$, 73–74
 Plumbanethiones
 by plumbylene sulfurization, 155–156
 reactivities, 161–162
 by tetrathiaplumbolane desulfurization, 153–155
 Plumbylene, sulfurization, 155–156
 Polyethylene, branched, 115
 Polymerization
 MAO-activated, $\text{Ti}(\text{IV})$ -boratabenzene complex in, 116
 olefins, $\text{Zr}(\text{IV})$ -boratabenzenes as catalysts, 114
 $\text{P}(\text{OMe})_3$, with $\text{OsH}(\text{SH})(\text{CO})(\text{P}^i\text{Pr}_3)_2$, 47–48
 $(\text{PPh}_3)_2\text{Pt}(\text{C}_2\text{H}_4)$, 73
 2-Propyn-1-ol, 17
 Protonation
 in metal-alkylidene synthesis, 206
 1-metallacyclopentene, 213–214
 Push-pull effect, in $\text{OsHCl}(\text{CO})(\text{P}^i\text{Pr}_3)_2$, 5
 Pyrazole, 42

S

- Scandium(III)-(bis)boratabenzene complex, 112
 Selenium, silaneselone, 135–138
 σ bonds
 complex from
 1-(diphenylphosphido)boratabenzene, 112
 Ta–C, 200–204
 Ti–C, 186–188
 V–C, 198–200
 Zr–C, 188–198
 Silaneselone, 135–138

- Silane tellone, 139–140
 Silanethione
 kinetically stabilized compounds, 134–135
 Raman spectroscopy, 160
 theoretical study, 123–124
 thermodynamically stabilized compounds, 131–134
 X-ray crystallographic analysis, 156–157
 Silanone
 synthesis, 127–131
 theoretical study, 123–124
 Silicon
 SiEt_3 , reaction with $\text{OsHCl}(\text{CO})(\text{P}^i\text{Pr}_3)_2$, 19–21
 silaneselone, 135–138
 silane tellone, 139–140
 silanethione, 131–135
 silanone, 123–124, 127–131
 synthesis, 127–131
 Silylation reaction, *o*-bis(silyl)carborane, 65–69
 Solid-state structures
 α -gallium, 256
 β -gallium, 256
 γ -gallium, 257–258
 δ -gallium, 258
 gallium(II), 258–259
 Stannacycle, 103
 Stannaneselones, 149–153, 158
 Stannanethiones, 149–153, 158
 Styrene, hydrogen transfer reactions, 54
 Sulfur, silanethione, 131–135
 Sulfurization, plumbylene, 155–156

T

- Tantalum
 -butadiene compounds, 185
 -carbon σ bond, 200–204
 Tellurium, silane tellone, 139–140
 1,2,3,4,5-Tetrathiagermolanes, 142–144
 Tetrathiaplumbolanes, 153–155
 Thiocyanatomethane, with
 $\text{OsH}(\text{SC}_6\text{H}_5)(\text{CO})(\text{P}^i\text{Pr}_3)_2$, 49–50
 Thiophenolates, with $\text{OsHCl}(\text{CO})(\text{P}^i\text{Pr}_3)_2$, 46–50
 Tin
 stannaneselones, 149–153
 stannanethiones, 149–153
 Titanium
 Ti–C σ bond, 186–188

- Ti(IV)-boratabenzene complex, in
MAO-activated copolymerization, 116
- Transition metals
boratabenzenes with, 110–116
boratabenzenes without, 108–110
in calix[4]arenes metalation, 170–172
- Triethylsilane, phenylacetylene addition, 53
- Trimethylphosphite, with
[OsH(CO)₂{ η^1 -OCMe₂}(P^{*i*}Pr₃)₂]BF₄, 42
- Trimethylsilyl acetylene, with
OsH₂(η^2 -H₂)(CO)(P^{*i*}Pr₃)₂, 32
- Tris(pyrazolyl)borate compounds, 44–46
- Tungsten
–alkene complexes, 215–217
–calix fragments, 179–181
metal–metal bonded dimers, 172–176
W(IV), primary alkyls, 206
W(IV)-calix[4]arene, 210–211, 217–218
W(VI)-calix[4]arene, 212
- U
- α,β -Unsaturated carbenes, 17–19
Unsaturated ketones, 54–55
- V
- Vanadium, V–C σ bond, 198–200
- Z
- Zirconium
–butadiene functionality, 181–184
monomethoxy-calix[4]arene-Zr, 193
Zr–C σ bond, 188–198
Zr(II)-boratabenzene complex, 113
Zr(IV)-boratabenzene complex,
114–116
Zr(IV)-boratanaphthalene complex, 112

Cumulative List of Contributors for Volumes 1–36

- Abel, E. W., **5**, 1; **8**, 117
 Aguiló, A., **5**, 321
 Akkerman, O. S., **32**, 147
 Albano, V. G., **14**, 285
 Alper, H., **19**, 183
 Anderson, G. K., **20**, 39; **35**, 1
 Angelici, R. J., **27**, 51
 Aradi, A. A., **30**, 189
 Armitage, D. A., **5**, 1
 Armor, J. N., **19**, 1
 Ash, C. E., **27**, 1
 Ashe, A. J., III, **30**, 77
 Atwell, W. H., **4**, 1
 Baines, K. M., **25**, 1
 Barone, R., **26**, 165
 Bassner, S. L., **28**, 1
 Behrens, H., **18**, 1
 Bennett, M. A., **4**, 353
 Bickelhaupt, F., **32**, 147
 Birmingham, J., **2**, 365
 Blinka, T. A., **23**, 193
 Bockman, T. M., **33**, 51
 Bogdanović, B., **17**, 105
 Bottomley, F., **28**, 339
 Bradley, J. S., **22**, 1
 Brew, S. A., **35**, 135
 Brinckman, F. E., **20**, 313
 Brook, A. G., **7**, 95; **25**, 1
 Bowser, J. R., **36**, 57
 Brown, H. C., **11**, 1
 Brown, T. L., **3**, 365
 Bruce, M. I., **6**, 273; **10**, 273; **11**, 447; **12**, 379;
 22, 59
 Brunner, H., **18**, 151
 Buhro, W. E., **27**, 311
 Byers, P. K., **34**, 1
 Cais, M., **8**, 211
 Calderon, N., **17**, 449
 Callahan, K. P., **14**, 145
 Canty, A. J., **34**, 1
 Cartledge, F. K., **4**, 1
 Chalk, A. J., **6**, 119
 Chanon, M., **26**, 165
 Chatt, J., **12**, 1
 Chini, P., **14**, 285
 Chisholm, M. H., **26**, 97; **27**, 311
 Chiusoli, G. P., **17**, 195
 Chojinowski, J., **30**, 243
 Churchill, M. R., **5**, 93
 Coates, G. E., **9**, 195
 Collman, J. P., **7**, 53
 Compton, N. A., **31**, 91
 Connelly, N. G., **23**, 1; **24**, 87
 Connolly, J. W., **19**, 123
 Corey, J. Y., **13**, 139
 Corriu, R. J. P., **20**, 265
 Courtney, A., **16**, 241
 Coutts, R. S. P., **9**, 135
 Coville, N. J., **36**, 95
 Coyle, T. D., **10**, 237
 Crabtree, R. H., **28**, 299
 Craig, P. J., **11**, 331
 Csuk, R., **28**, 85
 Cullen, W. R., **4**, 145
 Cundy, C. S., **11**, 253
 Curtis, M. D., **19**, 213
 Darensbourg, D. J., **21**, 113; **22**, 129
 Darensbourg, M. Y., **27**, 1
 Davies, S. G., **30**, 1
 Deacon, G. B., **25**, 237
 de Boer, E., **2**, 115
 Deeming, A. J., **26**, 1
 Dessy, R. E., **4**, 267
 Dickson, R. S., **12**, 323
 Dixneuf, P. H., **29**, 163
 Eisch, J. J., **16**, 67
 Ellis, J. E., **31**, 1
 Emerson, G. F., **1**, 1
 Epstein, P. S., **19**, 213
 Erker, G., **24**, 1
 Ernst, C. R., **10**, 79
 Errington, R. J., **31**, 91
 Evans, J., **16**, 319
 Evans, W. J., **24**, 131
 Faller, J. W., **16**, 211
 Farrugia, L. J., **31**, 301

- Faulks, S. J., **25**, 237
 Fehlner, T. P., **21**, 57; **30**, 189
 Fessenden, J. S., **18**, 275
 Fessenden, R. J., **18**, 275
 Fischer, E. O., **14**, 1
 Ford, P. C., **28**, 139
 Forníés, J., **28**, 219
 Forster, D., **17**, 255
 Fraser, P. J., **12**, 323
 Friedrich, H., **36**, 229
 Friedrich, H. B., **33**, 235
 Fritz, H. P., **1**, 239
 Fürstner, A., **28**, 85
 Furukawa, J., **12**, 83
 Fuson, R. C., **1**, 221
 Gallop, M. A., **25**, 121
 Garrou, P. E., **23**, 95
 Geiger, W. E., **23**, 1; **24**, 87
 Geoffroy, G. L., **18**, 207; **24**, 249; **28**, 1
 Gilman, H., **1**, 89; **4**, 1; **7**, 1
 Gladfelter, W. L., **18**, 207; **24**, 41
 Gladysz, J. A., **20**, 1
 Glänzer, B. I., **28**, 85
 Green, M. L. H., **2**, 325
 Grey, R. S., **33**, 125
 Griffith, W. P., **7**, 211
 Grovenstein, E., Jr., **16**, 167
 Gubin, S. P., **10**, 347
 Guerin, C., **20**, 265
 Gysling, H., **9**, 361
 Haiduc, I., **15**, 113
 Halasa, A. F., **18**, 55
 Hamilton, D. G., **28**, 299
 Handwerker, H., **36**, 229
 Harrod, J. F., **6**, 119
 Hart, W. P., **21**, 1
 Hartley, F. H., **15**, 189
 Hawthorne, M. F., **14**, 145
 Heck, R. F., **4**, 243
 Heimbach, P., **8**, 29
 Helmer, B. J., **23**, 193
 Henry, P. M., **13**, 363
 Heppert, J. A., **26**, 97
 Herberich, G. E., **25**, 199
 Herrmann, W. A., **20**, 159
 Hieber, W., **8**, 1
 Hill, A. F., **36**, 131
 Hill, E. A., **16**, 131
 Hoff, C., **19**, 123
 Hoffmeister, H., **32**, 227
 Holzmeier, P., **34**, 67
 Honeyman, R. T., **34**, 1
 Horwitz, C. P., **23**, 219
 Hosmane, N. S., **30**, 99
 Housecroft, C. E., **21**, 57; **33**, 1
 Huang, Y. Z., **20**, 115
 Hughes, R. P., **31**, 183
 Ibers, J. A., **14**, 33
 Ishikawa, M., **19**, 51
 Ittel, S. D., **14**, 33
 Jain, L., **27**, 113
 Jain, V. K., **27**, 113
 James, B. R., **17**, 319
 Janiak, C., **33**, 291
 Jastrzebski, J. T. B. H., **35**, 241
 Jenck, J., **32**, 121
 Jolly, P. W., **8**, 29; **19**, 257
 Jonas, K., **19**, 97
 Jones, M. D., **27**, 279
 Jones, P. R., **15**, 273
 Jordan, R. F., **32**, 325
 Jukes, A. E., **12**, 215
 Jutzi, P., **26**, 217
 Kaesz, H. D., **3**, 1
 Kalck, P., **32**, 121; **34**, 219
 Kaminsky, W., **18**, 99
 Katz, T. J., **16**, 283
 Kawabata, N., **12**, 83
 Kemmitt, R. D. W., **27**, 279
 Kettle, S. F. A., **10**, 199
 Kilner, M., **10**, 115
 Kim, H. P., **27**, 51
 King, R. B., **2**, 157
 Kingston, B. M., **11**, 253
 Kisch, H., **34**, 67
 Kitching, W., **4**, 267
 Kochi, J. K., **33**, 51
 Köster, R., **2**, 257
 Kreiter, C. G., **26**, 297
 Krüger, G., **24**, 1
 Kudaroski, R. A., **22**, 129
 Kühlein, K., **7**, 241
 Kuivila, H. G., **1**, 47
 Kumada, M., **6**, 19; **19**, 51
 Lappert, M. F., **5**, 225; **9**, 397; **11**, 253;
 14, 345
 Lawrence, J. P., **17**, 449
 Le Bozec, H., **29**, 163
 Lendor, P. W., **14**, 345
 Linford, L., **32**, 1

- Longoni, G., **14**, 285
 Luijten, J. G. A., **3**, 397
 Lukehart, C. M., **25**, 45
 Lupin, M. S., **8**, 211
 McGlinchey, M. J., **34**, 285
 McKillop, A., **11**, 147
 McNally, J. P., **30**, 1
 Macomber, D. W., **21**, 1; **25**, 317
 Maddox, M. L., **3**, 1
 Maguire, J. A., **30**, 99
 Maitlis, P. M., **4**, 95
 Mann, B. E., **12**, 135; **28**, 397
 Manuel, T. A., **3**, 181
 Markies, P. R., **32**, 147
 Mason, R., **5**, 93
 Masters, C., **17**, 61
 Matsumura, Y., **14**, 187
 Mayr, A., **32**, 227
 Meister, G., **35**, 41
 Mingos, D. M. P., **15**, 1
 Mochel, V. D., **18**, 55
 Moedritzer, K., **6**, 171
 Molloy, K. C., **33**, 171
 Monteil, F., **34**, 219
 Morgan, G. L., **9**, 195
 Morrison, J. A., **35**, 211
 Moss, J. R., **33**, 235
 Mrowca, J. J., **7**, 157
 Müller, G., **24**, 1
 Mynott, R., **19**, 257
 Nagy, P. L. I., **2**, 325
 Nakamura, A., **14**, 245
 Nesmeyanov, A. N., **10**, 1
 Neumann, W. P., **7**, 241
 Norman, N. C., **31**, 91
 Ofstead, E. A., **17**, 449
 Ohst, H., **25**, 199
 Okawara, R., **5**, 137; **14**, 187
 Oliver, J. P., **8**, 167; **15**, 235; **16**, 111
 Onak, T., **3**, 263
 Oosthuizen, H. E., **22**, 209
 Otsuka, S., **14**, 245
 Pain, G. N., **25**, 237
 Parshall, G. W., **7**, 157
 Paul, I., **10**, 199
 Peres, Y., **32**, 121
 Petrosyan, W. S., **14**, 63
 Pettit, R., **1**, 1
 Pez, G. P., **19**, 1
 Poland, J. S., **9**, 397
 Poliakoff, M., **25**, 277
 Popa, V., **15**, 113
 Pourreau, D. B., **24**, 249
 Powell, P., **26**, 125
 Pratt, J. M., **11**, 331
 Prokai, B., **5**, 225
 Pruett, R. L., **17**, 1
 Rao, G. S., **27**, 113
 Raubenheimer, H. G., **32**, 1
 Rausch, M. D., **21**, 1; **25**, 317
 Reetz, M. T., **16**, 33
 Reutov, O. A., **14**, 63
 Rijkens, F., **3**, 397
 Ritter, J. J., **10**, 237
 Rochow, E. G., **9**, 1
 Rokicki, A., **28**, 139
 Roper, W. R., **7**, 53; **25**, 121
 Roundhill, D. M., **13**, 273
 Rubezhov, A. Z., **10**, 347
 Salerno, G., **17**, 195
 Salter, I. D., **29**, 249
 Satgé, J., **21**, 241
 Schade, C., **27**, 169
 Schaverien, C. J., **36**, 283
 Schmidbaur, H., **9**, 259; **14**, 205
 Schrauzer, G. N., **2**, 1
 Schubert, U., **30**, 151
 Schultz, D. N., **18**, 55
 Schumann, H., **33**, 291
 Schwebke, G. L., **1**, 89
 Seppelt, K., **34**, 207
 Setzer, W. N., **24**, 353
 Seyferth, D., **14**, 97
 Shapakin, S. Yu., **34**, 149
 Shen, Y. C., **20**, 115
 Shriver, D. F., **23**, 219
 Siebert, W., **18**, 301; **35**, 187
 Sikora, D. J., **25**, 317
 Silverthorn, W. E., **13**, 47
 Singleton, E., **22**, 209
 Sinn, H., **18**, 99
 Skinner, H. A., **2**, 49
 Slocum, D. W., **10**, 79
 Smallridge, A. J., **30**, 1
 Smeets, W. J. J., **32**, 147
 Smith, J. D., **13**, 453
 Speier, J. L., **17**, 407
 Spek, A. L., **32**, 147
 Stafford, S. L., **3**, 1
 Stańczyk, W., **30**, 243

- Stone, F. G. A., **1**, 143; **31**, 53; **35**, 135
Su, A. C. L., **17**, 269
Suslick, K. M., **25**, 73
Süss-Fink, G., **35**, 41
Sutin, L., **28**, 339
Swincer, A. G., **22**, 59
Tamao, K., **6**, 19
Tate, D. P., **18**, 55
Taylor, E. C., **11**, 147
Templeton, J. L., **29**, 1
Thayer, J. S., **5**, 169; **13**, 1; **20**, 313
Theodosiou, I., **26**, 165
Timms, P. L., **15**, 53
Todd, L. J., **8**, 87
Touchard, D., **29**, 163
Traven, V. F., **34**, 149
Treichel, P. M., **1**, 143; **11**, 21
Tsuji, J., **17**, 141
Tsutsui, M., **9**, 361; **16**, 241
Turney, T. W., **15**, 53
Tyfield, S. P., **8**, 117
Usón, R., **28**, 219
Vahrenkamp, H., **22**, 169
van der Kerk, G. J. M., **3**, 397
van Koten, G., **21**, 151; **35**, 241
Veith, M., **31**, 269
Vezey, P. N., **15**, 189
von Ragué Schleyer, P., **24**, 353; **27**, 169
Vrieze, K., **21**, 151
Wada, M., **5**, 137
Walton, D. R. M., **13**, 453
Wailles, P. C., **9**, 135
Webster, D. E., **15**, 147
Weitz, E., **25**, 277
West, R., **5**, 169; **16**, 1; **23**, 193
Werner, H., **19**, 155
White, D., **36**, 95
Wiberg, N., **23**, 131; **24**, 179
Wiles, D. R., **11**, 207
Wilke, G., **8**, 29
Williams, R. E., **36**, 1
Winter, M. J., **29**, 101
Wojcicki, A., **11**, 87; **12**, 31
Yamamoto, A., **34**, 111
Yashina, N. S., **14**, 63
Ziegler, K., **6**, 1
Zuckerman, J. J., **9**, 21
Zybill, C., **36**, 229

Cumulative Index for Volumes 37–47

	VOL.	PAGE
Al-Ahmad, Saleem, <i>see</i> Ashe, Arthur J., III		
Andersen, Jo-Ann M., and Moss, John R., <i>Alkyl(pentacarbonyl) Compounds of the Manganese Group Revisited</i>	37	169
Ashe, Arthur J., III, and Al-Ahmad, Saleem, <i>Diheteroferrocenes and Related Derivatives of the Group 15 Elements: Arsenic, Antimony, and Bismuth</i>	39	325
Aumann, Rudolf, <i>(1-Alkynyl)carbene Complexes (= 1-Metalla-1-buten-3-yne)s: Tools for Synthesis</i>	41	165
Baines, K. M., and Stibbs, W. G., <i>Stable Doubly Bonded Compounds of Germanium and Tin</i>	39	275
Baker, Paul K., <i>The Organometallic Chemistry of Halocarbonyl Complexes of Molybdenum(II) and Tungsten(II)</i>	40	45
Belzner, Johannes, and Ihmels, Heiko, <i>Silylenes Coordinated to Lewis Bases</i>	43	1
Berry, Donald H, <i>see</i> Reichl, Jennifer A.	43	197
Bertrand, Guy, <i>see</i> Bourissou, Didier		
Bode, Katrin, and Klingebiel, Uwe, <i>Silylhydrazines: Lithium Derivatives, Isomerism, and Rings</i>	40	1
Bourissou, Didier, and Bertrand, Guy, <i>The Chemistry of Phosphinocarbenes</i>	44	175
Brook, Adrian G., and Brook, Michael A., <i>The Chemistry of Silenes</i>	39	71
Brook, Michael A., <i>see</i> Brook, Adrian G.		
Brothers, Penelope J., and Power, Philip P., <i>Multiple Bonding Involving Heavier Main Group 3 Elements Al, Ga, In, and Tl</i>	39	1
Brothers, Penelope J., <i>Organometallic Chemistry of Transition Metal Porphyrin Complexes</i>	46	223
Carty, Arthur J., <i>see</i> Doherty, Simon		
Chatgililoglu, Chrysostomos, and Newcomb, Martin, <i>Hydrogen Donor Abilities of the Group 14 Hybrides</i>	44	67
Corrigan, John F., <i>see</i> Doherty, Simon		
Cumulative Subject Index for Volumes 1–44	45	1
Doherty, Simon, Corrigan, John F., Carty, Arthur J., and Sappa, Enrico, <i>Homometallic and Heterometallic Transition Metal Allenyl Complexes: Synthesis, Structure, and Reactivity</i>	37	39
Driess, Matthias, <i>Silicon-Phosphorus and Silicon-Arsenic Multiple Bonds</i>	39	193
Dyson, Paul J., <i>Chemistry of Ruthenium–Carbide Clusters Ru₅C(CO)₁₅ and Ru₆C(CO)₁₇</i>	43	43
Eichler, Barrett, and West, Robert, <i>Chemistry of Group 14 Heteroallenes</i>	46	1
Eisch, John J., <i>Boron–Carbon Multiple Bonds</i>	39	355
Escudie, Jean, and Ranaivonjatovo, Henri, <i>Doubly Bonded Derivatives of Germanium</i>	44	113
Esteruelas, Miguel, A., and Oro, Luis, A., <i>The Chemical and Catalytic Reactions of Hydrido-chloro-carbonylbis (triisopropylphosphine) osmium(II) and Its Major Derivatives</i>	47	1
Fleig, Patrick F., <i>see</i> Wojtczak, William A.		

Floriani, Carlo, and Floriani-Moro, Rita, <i>The M–C Bond Functionalities Bonded to an Oxo-Surface Modeled by Calix[4]arenes</i>	47	167
Floriani-Moro, Rita, <i>see</i> Floriani, Carlo		
Fu, Gregory, C., <i>The Chemistry of Borabenzenes (1986–2000)</i>	47	101
Gable, Kevin P., <i>Rhenium and Technetium Oxo Complexes in the Study of Organic Oxidation Mechanisms</i>	41	127
Gauvin, François, Harrod, John F., and Woo, Hee Gweon, <i>Catalytic Dehydrocoupling: A General Strategy for the Formation of Element–Element Bonds</i> ...	42	363
Gibson, Susan E., and Peplow, Mark A., <i>Transition Metal Complexes of Vinylketenes</i>	44	275
Hampden-Smith, Mark J., <i>see</i> Wojtczak, William A.		
Hanusa, Timothy P., <i>see</i> Hays, Melanie L.		
Harrod, John F., <i>see</i> Gauvin, François		
Haubrich, Scott, Power, Philip, and Twamley, Brendan, <i>Element Derivatives of Sterically Encumbering Terphenyl Ligands</i>	44	1
Hays, Melanie L., and Hanusa, Timothy, P., <i>Substituent Effects as Probes of Structure and Bonding in Mononuclear Metallocenes</i>	40	117
Hemme, Ina, <i>see</i> Klingebiel, Uwe		
Hopkins, Michael D., <i>see</i> Manna, Joseph		
Humphrey, Mark G., <i>see</i> Whittall, Ian R.		
Humphrey, Mark G., <i>see</i> Waterman, Susan M.		
Ihmels, Heiko, <i>see</i> Belzner, Johannes	43	1
Jafarpour, Laleh, and Nolan, Steven P., <i>Transition-Metal Systems Bearing a Nucleophilic Carbene Ancillary Ligand: from Thermochemistry to Catalysis</i> ..	46	181
John, Kevin D., <i>see</i> Manna, Joseph		
Jones, William M., and Klosin, Jerzy, <i>Transition-Metal Complexes of Arynes, Strained Cyclic Alkynes, and Strained Cyclic Cumulenes</i>	42	147
Jung, Il Nam, and Yoo, Bok Ryul, <i>Friedel–Crafts Alkylations with Silicon Compounds</i>	46	145
Kang, Sang Ook, and Ko, Jaejung, <i>Chemistry of o-Carboranyl Derivatives</i>	47	61
Kawachi, Atsushi, <i>see</i> Tamao, Kohei		
Klingebiel, Uwe, and Hemme, Ina, <i>Iminosilanes and Related Compounds: Synthesis and Reactions</i>	39	159
Klingebiel, Uwe, <i>see</i> Bode, Katrin		
Klosin, Jerzy, <i>see</i> Jones, William M.		
Ko, Jaejung, <i>see</i> Kang, Sang Ook		
Lotz, Simon, Van Rooyen, Petrus H., and Meyer, Rita, <i>σ, π-Bridging Ligands in Bimetallic and Trimetallic Complexes</i>	37	219
Lucas, Nigel T., <i>see</i> Waterman, Susan M.		
Manna, Joseph, John, Kevin D., and Hopkins, Michael, D., <i>The Bonding of Metal-Alkynyl Complexes</i>	38	79
Manners, Ian, <i>Ring-Opening Polymerization of Metallocenophanes: A New Route to Transition Metal-Based Polymers</i>	37	131
Mathur, Pradeep, <i>Chalcogen-Bridged Metal–Carbonyl Complexes</i>	41	243
McDonagh, Andrew M., <i>see</i> Whittall, Ian R.		
Meyer, Rita, <i>see</i> Lotz, Simon		
Moss, John R., <i>see</i> Andersen, Jo-Ann M.		
Newcomb, Martin <i>see</i> Chatgililoglu, Chrysostomos		
Nienaber, Hubert, <i>see</i> Aumann, Rudolf		
Nolan, Steven P., <i>see</i> Jafarpour, Laleh		

Ogino, Hiroshi, and Tobita, Hiromi, <i>Bridged Silylene and Germylene Complexes</i>	42	223
Okazaki, Renji, <i>see</i> Tokitoh, Norihiro		
Okazaki, Renji, and West, Robert, <i>Chemistry of Stable Disilenes</i>	39	231
Oro, Luis, A., <i>see</i> Esteruelas, Miguel, A.		
Peplow, Mark A., <i>see</i> Gibson, Susan E.		
Power, Philip P., <i>see</i> Brothers, Penelope J.		
Power, Philip, <i>see</i> Haubrich, Scott		
Pülm, Melanie, <i>see</i> Tacke, Reinhold		
Ranaivonjatovo, Henri, <i>see</i> Escudie, Jean		
Reichl, Jenifer A., and Berry, Donald H., <i>Recent Progress in Transition Metal-Catalyzed Reactions of Silicon, Germanium, and Tin</i>	43	197
Robinson, Gregory, H., <i>Multiple Bonds Involving Aluminum and Gallium Atoms</i>	47	283
Roth, Gerhard, <i>see</i> Fischer, Helmut	43	125
Roundhill, D. M., <i>Organotransition-Metal Chemistry and Homogeneous Catalysis in Aqueous Solution</i>	38	155
Sakurai, Hideki, <i>see</i> Sakiguchi, Akira		
Samoc, Marek, <i>see</i> Whittall, Ian R		
Sappa, Enrico, <i>see</i> Doherty, Simon		
Schnepf, Andreas, <i>see</i> Schnöckel, Hansgeorg		
Schnöckel, Hansgeorg, and Schnepf, Andreas, <i>From AlX/GaX Monohalide Molecules to Metalloid Aluminum and Gallium Clusters</i>	47	235
Sekiguchi, Akira, and Sakurai, Hideki, <i>Cage and Cluster Compounds of Silicon, Germanium, and Tin</i>	37	1
Sita, Lawrence R., <i>Structure/Property Relationships of Polystannanes</i>	38	189
Smith, David J., <i>Organometallic Compounds of the Heavier Alkali Metals</i>	43	267
Stibbs, W. G., <i>see</i> Baines, K. M.		
Stumpf, Rüdiger, <i>see</i> Fisher, Helmut	43	125
Sun, Shouheng, and Sweigart, Dwight A., <i>Reactions of 17- and 19-Electron Organometallic Complexes</i>	40	171
Sweigart, Dwight A., <i>see</i> Sun, Shouheng		
Tacke, Reinhold, Pülm, Melanie, and Wagner, Brigitte, <i>Zwitterionic Penta-coordinate Silicon Compounds</i>	44	221
Tamao, Kohei, Kawachi, Atsushi, <i>Silyl Anions</i>	38	1
Thayer, John S., <i>Not for Synthesis Only: The Reactions of Organic Halides with Metal Surfaces</i>	38	59
Tobita, Hiromi, <i>see</i> Ogino, Hiroshi		
Tokitoh, Norihiro, and Okazaki, Renji, <i>Recent Advances in the Chemistry of Group 14–Group 16 Double Bond Compounds</i>	47	121
Twamley, Brendan, <i>see</i> Haubrich, Scott		
Van Rooyen, Petrus H., <i>see</i> Lotz, Simon		
Wagner, Brigitte, <i>see</i> Tacke, Reinhold		
Waterman, Susan M., Lucas, Nigel T., and Humphrey, Mark G., <i>“Very-Mixed”-Metal Carbonyl Clusters</i>	46	47
Weber, Lothar, <i>Transition-Metal Assisted Syntheses of Rings and Cages from Phosphaalkenes and Phosphaalkynes</i>	41	1
Went, Michael J., <i>Synthesis and Reactions of Polynuclear Cobalt–Alkyne Complexes</i>	41	69
West, Robert, <i>see</i> Eichler, Barrett		
West, Robert, <i>see</i> Okazaki, Renji		

Whitmire, Kenton H., <i>Main Group-Transition Metal Cluster Compounds of the Group 15 Elements</i>	42	1
Whittall, Ian R., McDonagh, Andrew M., Humphrey, Mark G., <i>Organometallic Complexes in Nonlinear Optics II: Third-Order Nonlinearities and Optical Limiting Studies</i>	43	349
Whittall, Ian, R., McDonagh, Andrew M., Humphrey, Mark G., and Samoc, Marek, <i>Organometallic Complexes in Nonlinear Optics I: Second-Order Non-linearities</i>	42	291
Wojtczak, William A., Fleig, Patrick F., and Hampden-Smith, Mark J., <i>A Review of Group 2 (Ca, Sr, Ba) Metal-Organic Compounds as Precursors for Chemical Vapor Deposition</i>	40	215
Woo, Hee Gweon, <i>see</i> Gauvin François.....		
Yoo, Bok Ryul, <i>see</i> Jung, Il Nam		

ISBN 0-12-031147-X



9 0065